







Four new species of *Zeugodacus* Hendel (Diptera, Tephritidae, Dacinae, Dacini) and new records of dacines from India

Karamankodu Jacob David¹, Venkateshaiah Abhishek², Ningthoujam Kennedy³,
K. M. Ajaykumara⁴, R. G. Gracy¹, Cheday Bhutia Hissay³

¹ National Bureau of Agricultural Insect Resources, Bengaluru-560024, Karnataka, India

² Keladi Shivappa Nayaka University of Agricultural and Horticultural Sciences, Shivamogga, Karnataka, India

³ College of Post-Graduate Studies in Agricultural Sciences, CAU (Imphal), Umiam-793103, Meghalaya, India

⁴ College of Horticulture and Forestry, CAU (Imphal), Pasighat-791102, Arunachal Pradesh, India

Corresponding author: Karamankodu Jacob David (davidkj.nbaii@gmail.com)

Abstract

Four new species of *Zeugodacus* Hendel are described from India viz., *Zeugodacus mordicae* David & Ajaykumara, **sp. nov.** from Arunachal Pradesh infesting male flower buds of *Momordica dioica*, *Zeugodacus nasivittatus* David & Abhishek, **sp. nov.** from Meghalaya, *Zeugodacus (Sinodacus) sinuvittatus* David & Abhishek, **sp. nov.** from Himachal Pradesh and *Zeugodacus (Zeugodacus) umiam* David & Kennedy, **sp. nov.** from Meghalaya. An illustrated key to all species of *Zeugodacus* from India is also included. *Bactrocera (Parazeugodacus) abbreviata* (Hardy) and *Dacus (Mellesis) vijaysegarani* Drew & Hancock are recorded for the first time from India.

Key words: Arunachal Pradesh, cue lure, dacines, fruit fly, Meghalaya, Shimla, zingerone



Academic editor: Marc De Meyer

Received: 11 October 2023

Accepted: 16 November 2023

Published: 3 January 2024

ZooBank: <https://zoobank.org/54CACA75-91BD-4AFD-8860-2125798B4C15>

Citation: David KJ, Abhishek V, Kennedy N, Ajaykumara KM, Gracy RG, Hissay CB (2024) Four new species of *Zeugodacus* Hendel (Diptera, Tephritidae, Dacinae, Dacini) and new records of dacines from India. ZooKeys 1188: 1–26. <https://doi.org/10.3897/zookeys.1188.114031>

Copyright: © K. J. David et al.

This is an open access article distributed under terms of the Creative Commons Attribution

License (Attribution 4.0 International – CC BY 4.0).

Introduction

Zeugodacus Hendel is a genus in tribe Dacini with 196 species recorded from the world (Doorenweerd et al. 2018) and thirty described species from India (David et al. 2017; David and Ramani 2019). They are characterised by the shallow emargination of sternite 5 in males, posterior lobe of surstylus 5–6× longer than anterior lobe, glans of phallus with patterned acrophallus. Fruit flies of genus *Zeugodacus* Hendel are economically important as several of them are pests of various horticultural crops. *Zeugodacus* was originally treated as a subgenus of *Bactrocera* Macquart, it was elevated to genus level by Virgilio et al. (2015) based on molecular markers which confirmed the findings of Krosch et al. (2012). It was further supported by works by San Jose et al. (2018), Dupuis et al. (2018) and Zhang et al. (2022). Hancock and Drew (2018) consider *Zeugodacus* as a subgenus of *Bactrocera*. David et al. (2017) described *Bactrocera brevipunctata* David and Hancock from Maharashtra which was later transferred to genus *Zeugodacus* by Doorenweerd et al. (2018). David and Ramani (2019) studied the postabdominal structures of 16 species of

Zeugodacus from India and performed a morphology based phylogenetic analysis of tribe Dacini wherein *Bactrocera* and *Dacus* Fabricius were monophyletic and *Zeugodacus* was polyphyletic, which might be due to the reason that only Indian species were included in the phylogenetic analysis. In this paper, four new species of *Zeugodacus* are described with illustrations of postabdominal structures. Two species of dacines, *Bactrocera* (*Parazeugodacus*) *abbreviata* (Hardy) and *Dacus* (*Mellesis*) *vijaysegarani* Drew & Hancock are recorded for the first time from India. An illustrated key to 34 species of *Zeugodacus* from India is also included.

Materials and methods

Specimens deposited in the following museums have been studied: Natural History Museum, London, United Kingdom (**NHM**) and National Insect Museum, ICAR- National Bureau of Agricultural Insect Resources, Bengaluru, India (**NIM**).

Images of specimens, epandrium, and ovipositor were taken using a Leica DFC 420 camera mounted on a Leica M205A stereo zoom microscope; images of glans of phallus, aculeus tip and spicules on eversible membrane were taken using an 8 MP camera temporarily attached to a Leica DM 1000 compound research microscope, Olympus DP 23 attached to BX51 and Olympus SC 50 attached to BX 43; the images were stacked and combined to a single image using Combine ZP (Hadley 2011). Measurements of male and female genitalia were taken using Leica Automontage Software, LAS 3.4. Terminology adopted here follows White et al. (1999) except for wing terminology which follows Cumming and Wood (2017).

One hind leg was removed from one specimen of *Z. momordicae* and used for DNA extraction. The DNA extraction was performed using a DNeasy Blood and Tissue Kit (Qiagen India Pvt. Ltd.) following the manufacturers' instruction. For the molecular study, the standard DNA barcoding region of the mitochondrial COI gene was sequenced, and the PCR was performed using the Universal COI primers (LC01490/HCO2198) (Hebert et al. 2003). The sequence was annotated using NCBI Blast tools and submitted to the NCBI GenBank Database where an accession number was obtained (*Z. momordicae*- OQ353070).

Taxonomic account

Zeugodacus Hendel, 1927

Zeugodacus Hendel, 1927: 26. Raised to genus level by Virgilio et al. 2015: 177.

Type species: *Dacus caudatus* Fabricius, 1805: 276. Type locality: Indonesia, Java.

Diagnosis. Abdominal tergites free, scutum with medial postsutural vitta except for few species in several subgenera including *Parasinodacus* Drew & Romig, *Paradacus* Perkins and some species of *Sinodacus* Zia, sternite 5 of male with shallow/flat posterior emargination. In males, epandrium distinctly

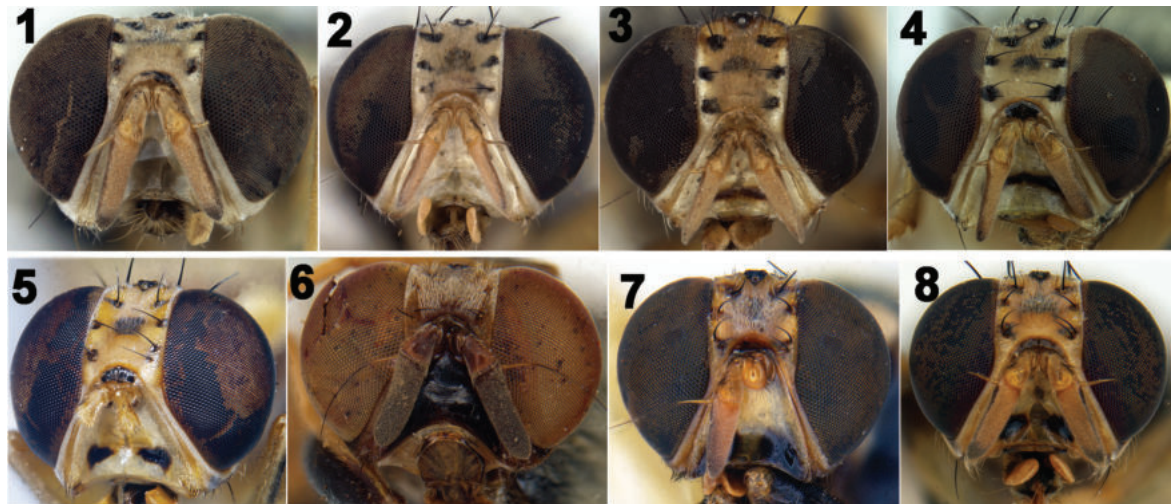
bulb-shaped in posterior view, proctiger hyaline, triangular (when uninflated) smaller than epandrium, lateral surstylus longer than epandrium (profile view); posterior lobe of lateral surstylus 5–6× longer than anterior lobe. Phallus with well-developed acrophallus (single semi-tubular lobe) and patterned/granulated praeputium. Dorsal sclerite of glans without hexagonal pattern. Aculeus dorsoventrally flattened with four pairs of preapical setae (David and Ramani 2019). *Zeugodacus* is similar to *Bactrocera* and *Dacus* in general appearance as they are wasp mimics and are characterised by the presence of reddish-brown to black colour with yellow vittae and markings. It can be differentiated from *Dacus* by the presence of free abdominal tergites and by the presence of four pairs of preapical setae; from *Bactrocera* by the shallow/ flat emargination sternite 5 in males, posterior lobe of lateral surstylus 5–6× longer than anterior lobe and patterned acrophallus.

Key to species of *Zeugodacus* Hendel from India

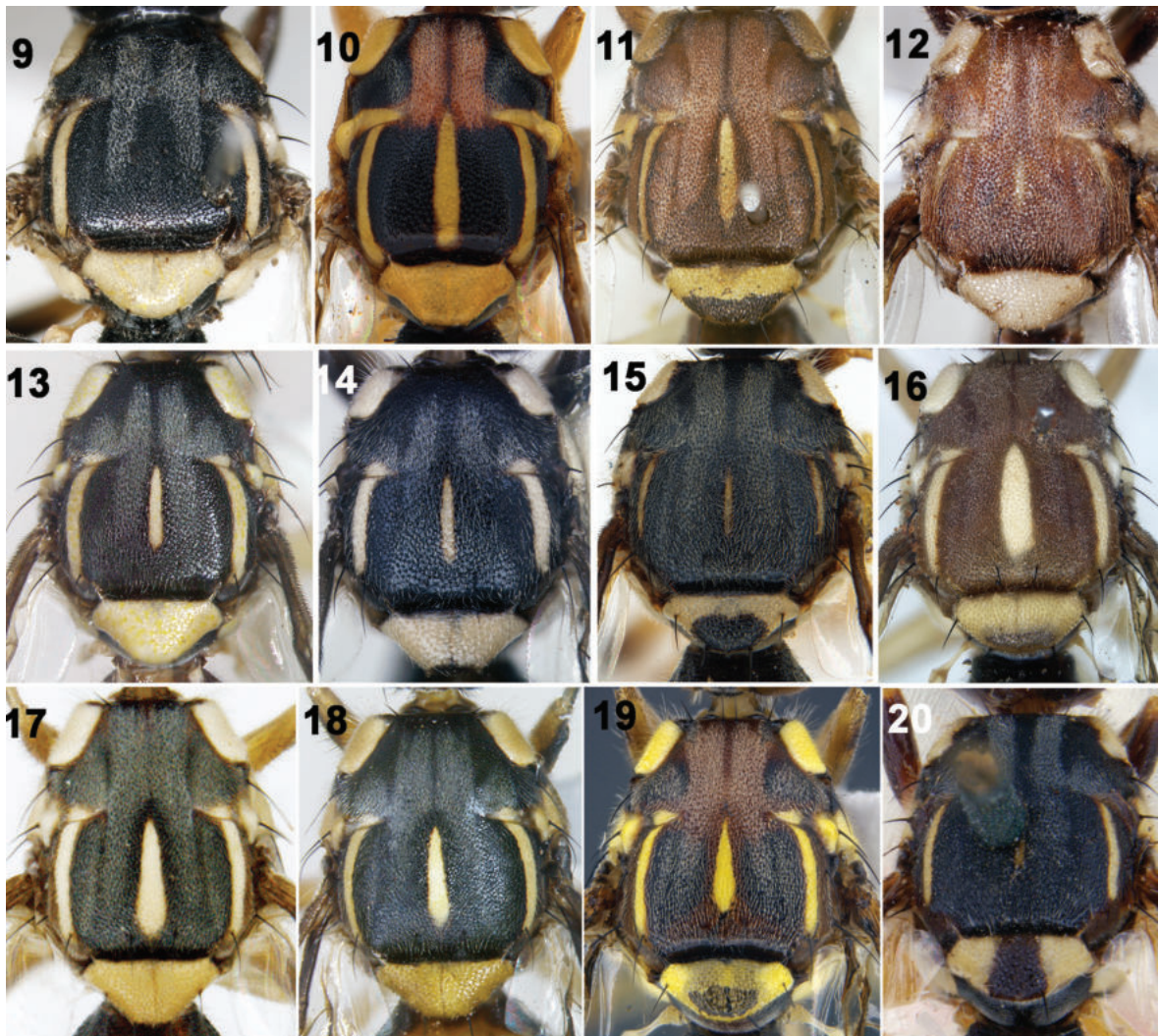
- 1 Medial postsutural vitta present (Figs 10–20) **6**
 - Medial postsutural vitta absent (Fig. 9) **2**
- 2 Scutum black **3**
 - Scutum reddish-brown, lateral postsutural vitta absent (Fig. 86), costal band broad overlapping vein $R_{2+3'}$, expanded into a broad apical spot (Fig. 89) ***Z. sinuvittatus* David & Abhishek, sp. nov.**
- 3 Lateral postsutural vitta absent, costal band overlapping vein R_{2+3} expanded slightly towards apex (Drew and Romig 2013: fig. 282) ***Z. binoyi* Drew**
 - Lateral postsutural vitta present, prescutellar setae present, costal band confluent with vein R_{2+3} **4**
- 4 Forefemur entirely black, 0.75 of mid and hind femur black (Fig. 43) **5**
 - Forefemur fulvous with apical black spot, mid and hind femur fulvous with apical black spots (Fig. 21) ***Z. duplicatus* (Bezzi)**
- 5 Scutum with a yellow spot anterior to notopleural suture, prescutellar acrostichal seta absent ***Z. incisus* (Walker)**
 - Scutum without a yellow spot anterior to notopleural suture, prescutellar acrostichal seta present ***Z. momordicae* David & Ajaykumara, sp. nov.**
- 6 Postsutural supra-alar seta absent (Figs 13, 14) **7**
 - Postsutural supra-alar seta present (Figs 15–20) **9**
- 7 Costal band continuous, confluent with vein $R_{2+3'}$, not expanded into an apical spot (Fig. 36), prescutellar acrostichal seta present **8**
 - Costal band discontinuous with a broad apical spot, prescutellar acrostichal seta absent (Drew and Romig 2013: fig. 9) ***Z. apicalis* (de Meijere)**
- 8 Face fulvous without any markings (Fig. 1), notopleuron yellow (Fig. 13) ***Z. trilineatus* (Hardy)**
 - Face with two separate black spots (Fig. 7), notopleuron black (Fig. 14) ***Z. scutellarius* (Bezzi)**
- 9 Prescutellar acrostichal seta absent (Fig. 12) **10**
 - Prescutellar acrostichal seta present (Figs 15–20) **12**
- 10 Abdomen oval shaped (Fig. 26); apical spot on wing does not cross vein M (Fig. 33) ***Z. havelockiae* Drew & Romig**
 - Abdomen club-shaped (Fig. 25); apical spot on wing crosses vein M **11**

- 11 Yellow spot anterior to transverse suture as broad as notopleuron, lateral postsutural vitta absent, if present, not extending beyond postsutural supra-alar seta, apical spot on wing not reaching apices of vein R_{2+3} and dm-cu crossvein basally (Drew and Romig 2013: fig. 261) **Z. hochii (Zia)**
 - Yellow spot anterior to transverse suture narrower than notopleuron, lateral postsutural vitta prominent and narrows to end before postalar seta (Fig. 12), apical spot broad and reaching apices of vein R_{2+3} and dm-cu (Fig. 29) **Z. brevipunctatus (David & Hancock)**
- 12 Costal band narrow, confluent with vein R_{2+3} , either continuous or discontinuous, not expanded apically (Figs 31, 35, 36) **13**
 - Costal band broad, overlapping vein R_{2+3} , usually expanded into broad apical spot (Figs 30, 33, 34, 37, 38) **26**
- 13 Costal band discontinuous (Fig. 31) **14**
 - Costal band continuous **15**
- 14 Scutellum shining black except for small yellow anterolateral corners (Drew and Romig 2013: fig. 281) **Z. biguttatus (Bezzi)**
 - Scutellum fully yellow without any black markings **Z. freidbergi White**
- 15 Scutum predominantly black with narrow lateral and medial postsutural vittae (Figs 15, 20) **16**
 - Scutum black or brown with broad lateral and medial postsutural vittae (Figs 16–19) **22**
- 16 Scutellum yellow with apical black spot (Fig. 15) or broad black band dividing it into two (Fig. 20) **17**
 - Scutellum predominantly yellow without apical black spot or markings except for a narrow black basal band (Fig. 10) **20**
- 17 Scutellum with broad black band dividing it into two yellow spots (Fig. 20) **Z. assamensis (White)**
 - Scutellum with an apical black spot (Fig. 15) **18**
- 18 Face with two separate black triangular spots (Fig. 8) **Z. scutellaris (Bezzi)**
 - Face either black or with broad black transverse bands connecting spots (Figs 40, 41) **19**
- 19 Medium sized flies (5.4–5.7 mm), face entirely black in males, female with distal half black, abdominal tergites 3–5 fully black **Z. umiam David & Kennedy, sp. nov.**
 - Large sized flies (7–8 mm), face with a transverse band connecting spots, abdominal tergites 3–5 with black markings restricted to lateral regions (Drew and Romig 2013: fig. 309) **Z. hoabinhae Drew & Romig**
- 20 Only apical scutellar setae present **21**
 - Apical and basal scutellar setae present **Z. atrifacies (Perkins)**
- 21 Face entirely black (Fig. 6), forefemur wholly black **Z. diaphorus (Hendel)**
 - Face with black spots, forefemur fuscous, not black (Drew and Romig 2013: fig. 370) **Z. yoshimotoi (Hardy)**
- 22 Anepisternal stripe broad touching postpronotal lobe, katapisternum with a broad yellow transverse marking, anepisternal stripe inverted L-shaped (Fig. 22) **Z. gavisus (Munro)**
 - Anepisternal stripe not touching postpronotal lobe, katapisternum with narrow yellow spot, anepisternal stripe triangular (Figs 23, 24, 79) **23**

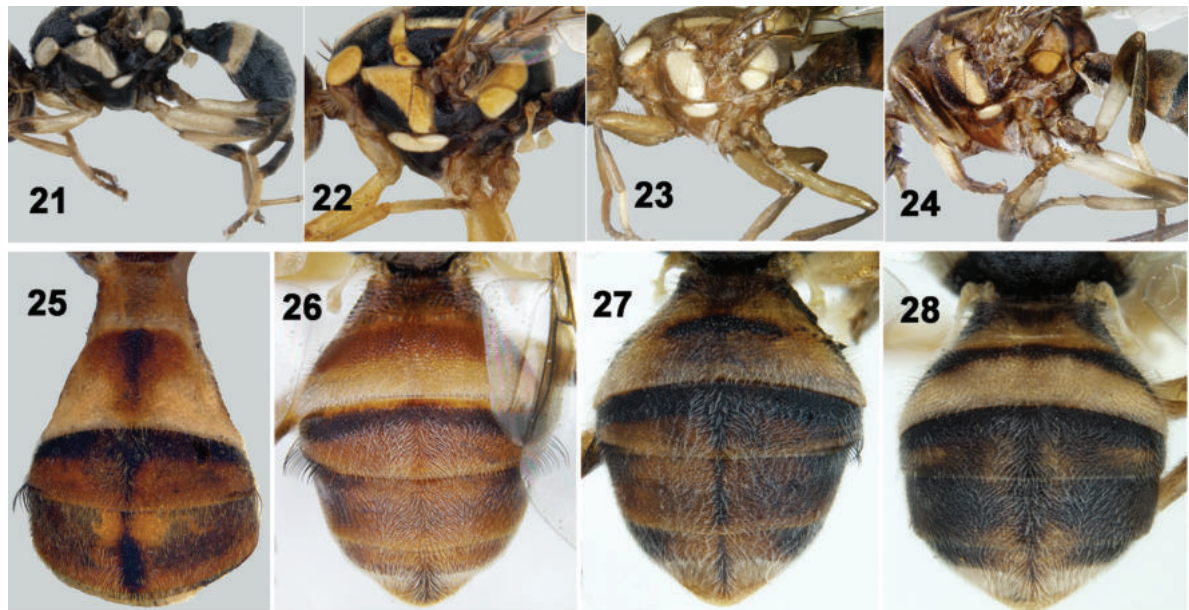
- 23 Abdomen reddish brown without any medial longitudinal band (Fig. 26), face with transverse marking interrupted medially (Fig. 5) **Z. semongokensis** Drew & Romig
- Abdomen yellow with black transverse and longitudinal markings (Figs 27, 28, 80) **24**
- 24 Face fulvous with two separate black spots (Fig. 77), medial postsutural vitta broadened posteriorly (nose-shaped) (Fig. 78), abdomen with medial black longitudinal band interrupted (Fig. 80)..... **Z. nasivittatus** David & Abhishek, sp. nov.
- Face either fulvous or with transverse band (Figs 3, 4), medial postsutural vitta broad or narrow (Figs 17, 18) but not nose shaped, abdomen usually with medial vitta continuous (Figs 27, 28)..... **25**
- 25 Medial postsutural vitta broadened basally and narrowed apically (Fig. 17), pecten of cilia present in male (Fig. 27), face with a black transverse band in both sexes (Fig. 4)..... **Z. caudatus** (Fabricius)
- Medial postsutural vitta narrowed at both ends (Fig. 18), pecten of cilia absent in male (Fig. 28), face fulvous in male (Fig. 2), with a transverse band in female (Fig. 3) **Z. diversus** (Coquillett)
- 26 Costal band broad, confluent with R_{4+5} with or without apical expansion (Figs 30, 32, 34) **27**
- Costal band narrow, not confluent with R_{4+5} ; overlapping vein R_{2+3} or confluent with R_{2+3} (Figs 37, 38)..... **30**
- 27 Wing with prominent subapical band and radial medial band (Fig. 30) **Z. cucurbitae** (Coquillett)
- Wing without subapical band and radial-medial band (Figs 32, 34) **28**
- 28 Scutellum with apical black spot (Figs 11, 16, 19)..... **29**
- Scutellum without apical black spot, costal band broadly confluent with R_{4+5} , not expanded into an apical spot (Drew and Romig 2013: fig. 367) **Z. vultus** (Hardy)
- 29 Postpronotal lobe fuscous (Fig. 11), all femora with fuscous markings (Fig. 24), wing with costal band expanded to broad apical spot (Fig. 34)... **Z. watersi** (Hardy)
- Postpronotal lobe fulvous (Fig. 16), femora yellow (Fig. 23), wing with dark fuscous markings in apical region connected to anal streak (Fig. 32)..... **Z. fuscoalatus** (Drew & Romig)
- 30 Scutellum with apical black spot (Fig. 19)..... **Z. signatus** (Hering)
- Scutellum without apical black spot **31**
- 31 Costal band confluent with vein R_{2+3} (Fig. 37) **32**
- Costal band overlapping vein R_{2+3} (Fig. 38) **33**
- 32 Lateral postsutural vitta parallel sided, not tapering posteriorly **Z. zahadi** (Mahmood)
- Lateral postsutural vitta narrowing posteriorly (Drew and Romig 2013: fig. 363) **Z. trivandrumensis** (Drew & Romig)
- 33 All femora fulvous, anepisternal stripe broad reaching notopleural seta dorsally, supernumerary lobe weak in males (Drew and Romig 2013: fig. 282) **Z. bogorensis** (Drew & Romig)
- All femora with preapical spots, wing in male with well-developed supernumerary lobe **Z. tau** (Walker)



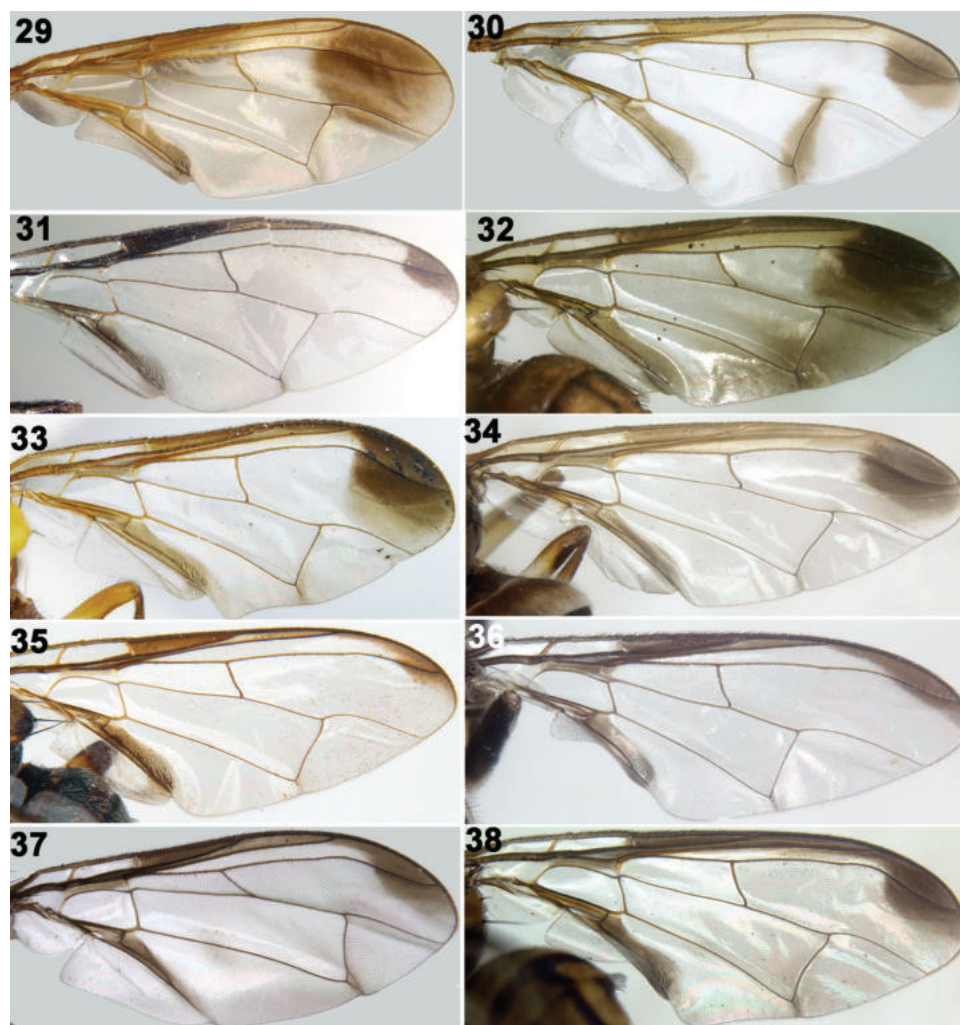
Figures 1–8. Heads of Tephritidae 1 *Z. trilineatus* (Hardy) 2 male of *Z. diversus* (Coquillett) 3 female of *Z. diversus* (Coquillett) 4 *Z. caudatus* (Fabricius) 5 *Z. semongokensis* (Drew & Romig) 6 *Z. diaphorus* (Hendel) 7 *Z. scutellarius* (Bezzi) 8 *Z. scutellaris* (Bezzi).



Figures 9–20. Thorax (dorsal view) of Tephritidae 9 *Z. incisus* (Walker) 10 *Z. gavisus* (Munro) 11 *Z. watersi* (Hardy) 12 *Z. brevipunctatus* (David & Hancock) 13 *Z. trilineatus* (Hardy) 14 *Z. scutellarius* (Bezzi) 15 *Z. scutellaris* (Bezzi) 16 *Z. fuscoalatus* (Drew & Romig) 17 *Z. caudatus* (Fabricius) 18 *Z. diversus* (Coquillett) 19 *Z. signatus* (Hering) 20 *Z. assamensis* (White).



Figures 21–28. 21–24 Thorax (lateral view) and legs 25–28 Abdomen (dorsal view) of Tephritidae 21 *Z. duplicatus* 22 *Z. gavisus* 23 *Z. fuscoalatus* 24 *Z. watersi* 25 *Z. brevipunctatus* 26 *Z. semongokensis* 27 *Z. caudatus* 28 *Z. diversus*.



Figures 29–38. Wings of Tephritidae 29 *Z. brevipunctatus* 30 *Z. cucurbitae* 31 *Z. freidbergi* 32 *Z. fuscoalatus* 33 *Z. have-lockiae* 34 *Z. watersi* 35 *Z. scutellaris* 36 *Z. scutellarius* 37 *Z. zahadi* 38 *Z. tau*.

New species descriptions

Zeugodacus (Parasinodacus) momordicae David & Ajaykumara, sp. nov.

<https://zoobank.org/D8024CC3-CE48-4C83-B2DC-D737D87FD34F>

Figs 39–60

Type locality. INDIA: Arunachal Pradesh, Upper Siang, Padu.

Type material. *Holotype* female, pinned. Original label: "INDIA: Arunachal Pradesh, Upper Siang, Padu, 29. ix. 2022, David, K. J." *Paratypes*. 20♀♀, 3♂♂, INDIA: Arunachal Pradesh, Upper Siang, Padu, 15. ix. 2022, Ajaykumara, K. M.; 15♀♀, 3♂♂, 1 larva, INDIA: Arunachal Pradesh, Upper Siang, Padu, 29. ix. 2022, David, K. J. (deposited at NIM).

Other material examined. 1♀, Formosa, Kagi, 19.08.07, H. Sauter, S. (first label), *Chaetodacus cilifer* Hend.♀ det. M. Hering 1935 (second label) (NHM). 2♀♀, INDIA, Meghalaya, Umiam, 19. v. 2017, Arensungla Pongen (NIM).

Diagnosis. *Zeugodacus momordicae* resembles *Z. incisus* in possessing black scutum, two transverse bands on face, continuous costal band and extensive femoral markings, but can be differentiated by the absence of yellow spot anterior to lateral vittae along transverse suture and presence of prescutellar acrostichal setae. It can be differentiated from *Bactrocera ablepharus* (Bezzi) by the presence of prescutellar acrostichal setae and face with two transverse bands. It can be differentiated from *Z. cilifer* (Figs 61–65, 69) by the aculeus shape and spicules on distal end of eversible membrane as discussed below. Aculeus tip is elongate, parallel sided and not tapering abruptly beyond the preapical conical flange (width of the conical projection- 0.06 mm) and length of aculeus after the preapical flange is 0.21 mm in *Z. cilifer* (Figs 66, 67), whereas in *Z. momordicae*, aculeus is tapering abruptly beyond the preapical conical flange (width of the conical projection -0.08 mm) (Figs 56, 57) and length of aculeus after the preapical flange is 0.15–0.18 mm. Spicules on *Z. cilifer* are conical with single projection with a shorter base (Fig. 68), whereas *Z. momordicae* (Fig. 54) possess broader conical spicules.

Description. Female. Medium sized species (wing length 4.37–5.45 mm), face with two broad black bands. Scutum black with yellow lateral postsutural vitta ending beyond intra-alar seta, anepisternal stripe broad reaching anterior notopleural seta dorsally, continued as a small transverse marking on katepisternum. Wing hyaline with costal band continuous from cell sc to the apex of the wing and confluent with vein R_{2+3} , anal streak well developed. Abdomen predominantly black with a narrow transverse fulvous band on tergites 1 and 2 (in few specimens all tergites black). Females with two spermatheca, aculeus pointed with preapical projection.

Head. Frons fulvous with fuscous markings on anteriomedial hump and around bases of frontal and orbital setae, all setae black; 2 pairs of frontal setae and 1 pair of orbital setae, lunule black. Ocellar triangle and vertex black, ocellar setae vestigial. Face (Figs 40, 41) fulvous with two broad transverse bands (elongate spots in antennal furrow connected by broad transverse band and a broad black band below the antennal sockets). Scape, pedicel fulvous, first flagellomere dark fuscous on outer side and apex, arista non plumose, combined length of pedicel and flagellomere is slightly longer than vertical length of face. Gena fulvous with prominent black patch and a seta. Occiput

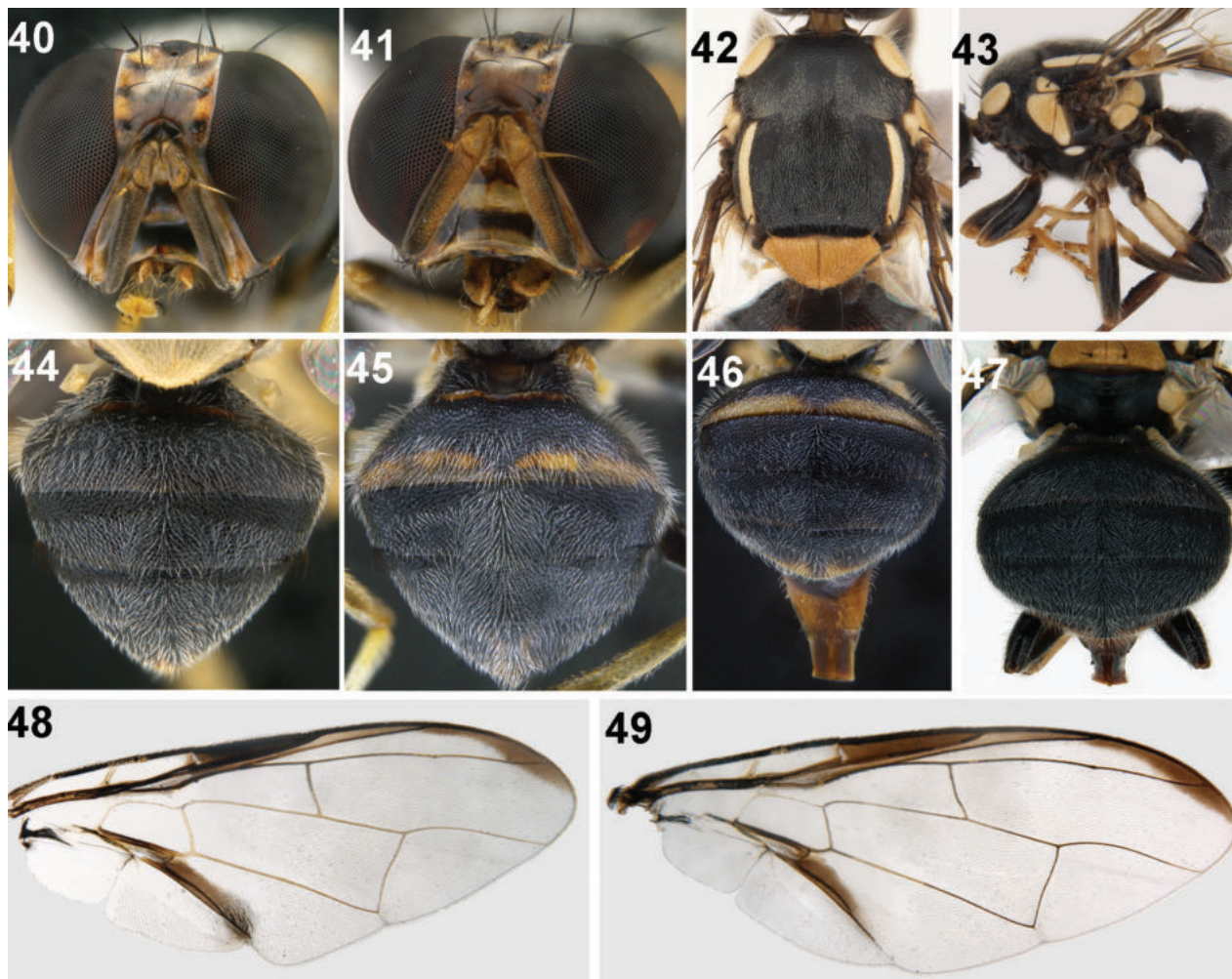
black, fulvous along eye margins; lateral and medial vertical seta present, occipital row without prominent black postocular setae. **Thorax** (Figs 42, 43). wholly black with yellow lateral postsutural vittae extending beyond intra-alar seta, medial vitta lacking; pleura black. Yellow marking as follows; postpronotal lobe, notopleuron, anepisternal stripe (reaching anterior notopleural seta dorsally) continued to katepisternum as a transverse spot; anatergite (posterior apex black); anterior 0.60 of katatergite (remainder black). Scutellum yellow with two scutellar setae. Chaetotaxy: scutellar seta, 1; prescutellar acrostichal seta, 1; intra-alar seta, 1; postsutural supra-alar seta, 1; postalar seta, 1; anepisternal seta, 1; anterior notopleural seta, 1; posterior notopleural seta, 1; scapular setae, 2. Coxa and trochanter black; whole fore femur; 0.75 of mid femur; 0.25 of hind femur black; remainder black. Fore and mid tibiae fulvous/yellow, hind tibia black, all tarsal segments fulvous (Fig. 43). **Wing** (4.37–5.45 mm) predominantly hyaline, cells bc and c hyaline, cell sc dark fuscous, costal band confluent with vein $R_{2+3'}$, slightly expanded apically, anal streak as broad as cell cua_1 , extending till apex of its extension, supernumerary lobe developed (Figs 48, 49). **Abdomen** (Figs 44–47). Abdominal segments entirely black except for a narrow fulvous band on tergite 2 apically (in few specimens all tergites black).

Male. Similar to female except for face (Fig. 40) which is nearly black in few males with a narrow longitudinal fulvous line separating the bands, costal band discontinuous in few male specimens examined, sternite 5 in males black with shallow concavity, pecten present on tergite 3.

Female genitalia. Oviscape conical (Fig. 53), dorsoventrally flattened, basal half dark fuscous, apical half fulvous; eversible membrane twice as long as



Figure 39. Habitus (lateral) of female *Zeugodacus momordicae* David & Ajaykumara, sp. nov.

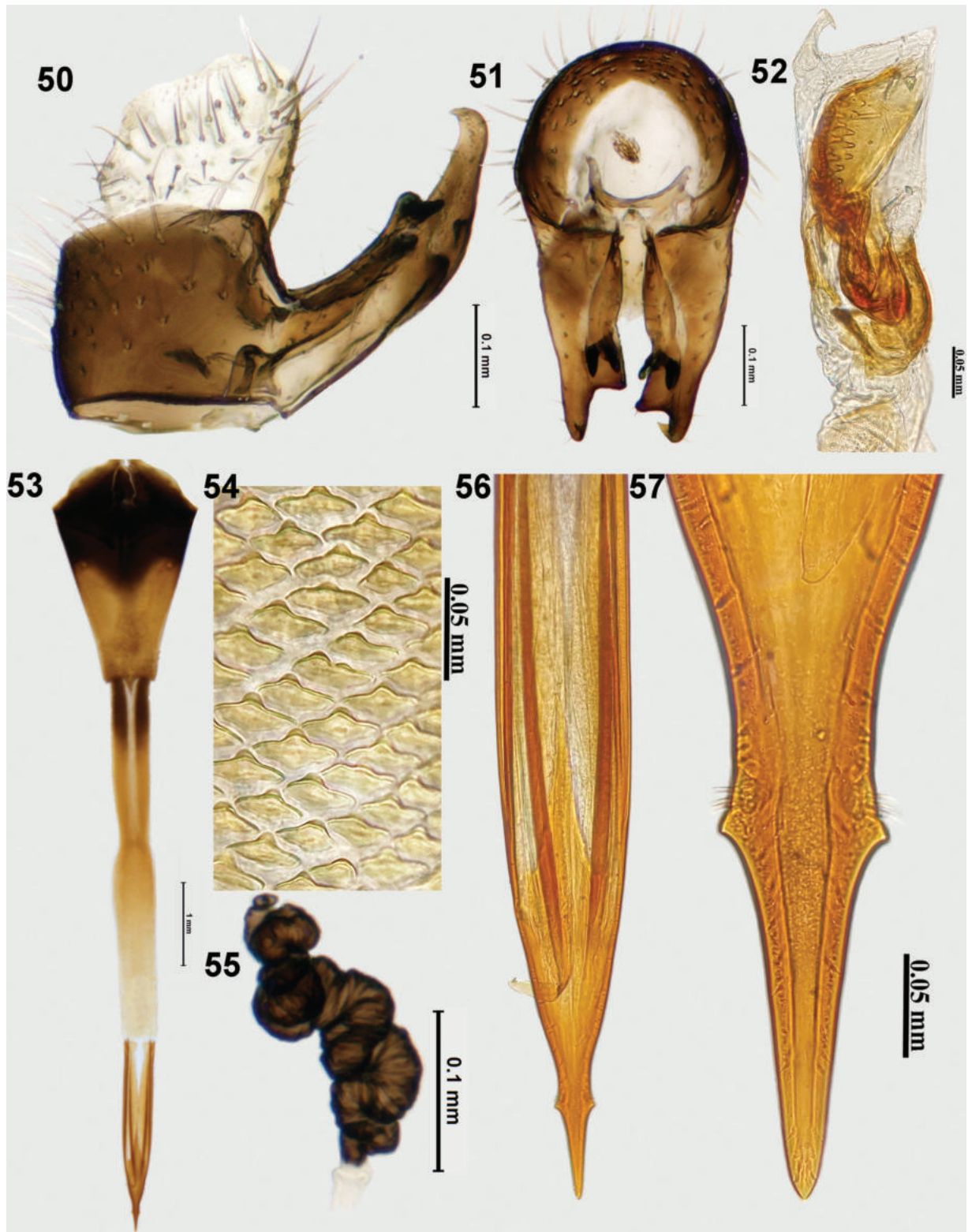


Figures 40–49. *Zeugodacus momordicae* David & Ajaykumara, sp. nov. 40 head frontal view (male) 41 head frontal view (female) 42 scutum 43 thorax (lateral view) and legs 44, 45 male abdomen (dorsal view) 46, 47 female abdomen (dorsal view) 48 wing (male) 49 wing (female).

oviscape (1.69 mm), spicules on distal end of eversible membrane (2.98 mm) with medial conical projection with a wider base (Fig. 54); aculeus (1.36 mm) shorter than eversible membrane with conical preapical flange, needle-shaped aculeus tip (Figs 56, 57); spermatheca dark brown, tightly coiled (Fig. 55).

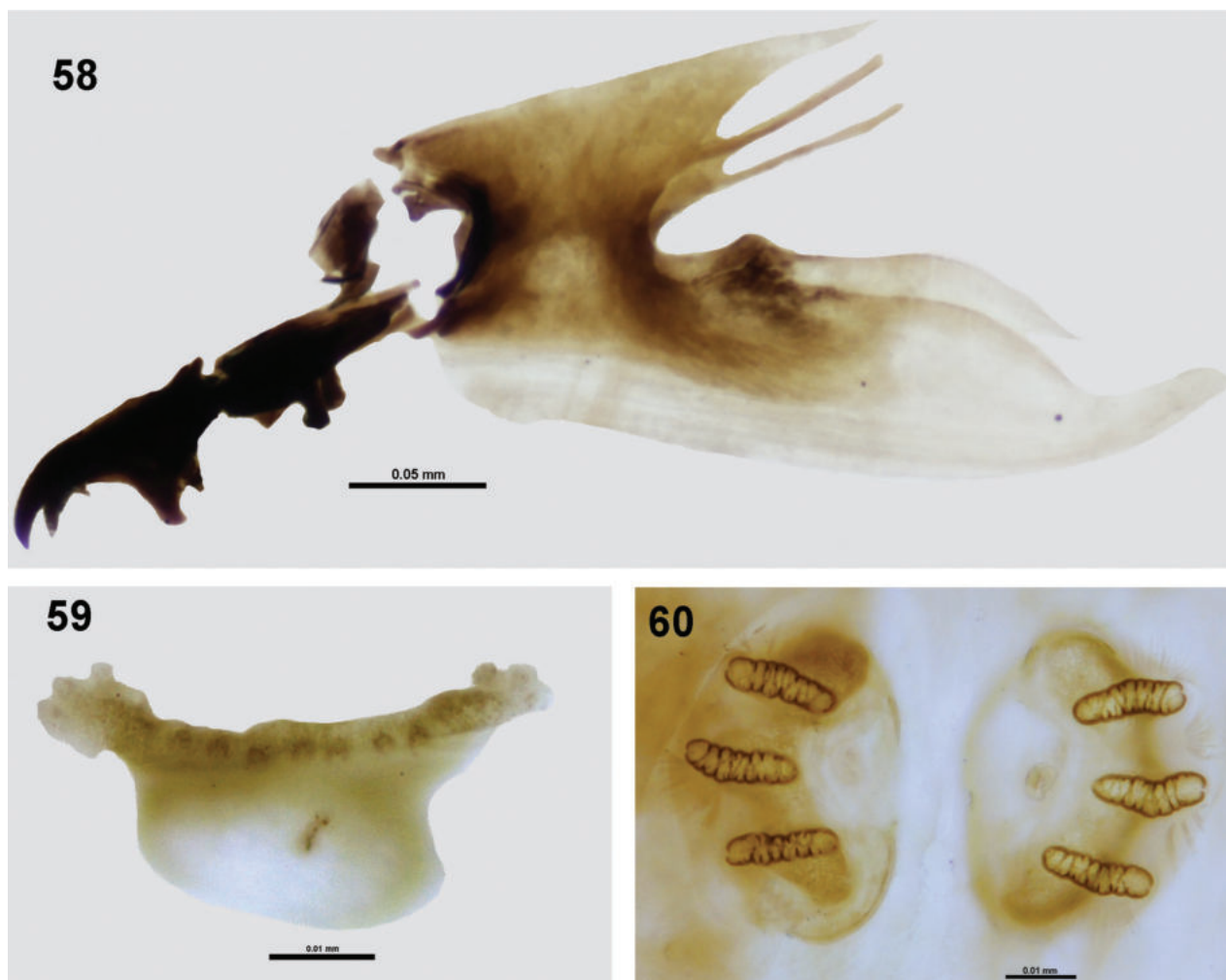
Male genitalia. Epandrium quadrate (profile view), lateral surstylus longer than epandrium; posterior lobe of surstylus 10× longer than anterior lobe (Fig. 50); proctiger hyaline as broad as but, shorter than epandrium; medial surstylus shorter than lateral surstylus with well-developed pair of equal sized prensisetae (Fig. 51). Phallus 3.15 mm long, glans of phallus well sclerotised with 2–3 rows of spine like projections on acrophallus dorsally (Fig. 52), sub-apical lobe T-shaped, preglans lobe present.

III instar larva. Creamy white, tapered anteriorly, blunt posteriorly. Cephalopharyngeal skeleton (Fig. 58): Mandible pointed, with short preapical tooth smaller than apical tooth, ventral apodeme prominent, mandibular neck well developed; hypopharyngeal sclerite shorter than mandible narrowing distally, with well-developed hypopharyngeal bridge in the centre, parastomal bar well developed covering the entire length of hypopharyngeal sclerite, labial sclerite present, anterior sclerite well developed (detached while dissecting); pharyngeal sclerite with



Figures 50–57. Postabdominal structures of *Zeugodacus momordicae* David & Ajaykumara, sp. nov. **50** epandrium and surstyli (lateral view) **51** epandrium and surstyli (posterior view) **52** glans of phallus **53** ovipositor **54** spicules on distal end of eversible membrane **55** spermatheca **56** aculeus **57** aculeus tip.

well-developed dorsal and ventral cornua, ventral bridge lacking. Anterior spiracle with 17 tubules (Fig. 59); slits of posterior spiracle arranged parallel to each other with well-developed dorsal, lateral and ventral spiracular bundles (Fig. 60).



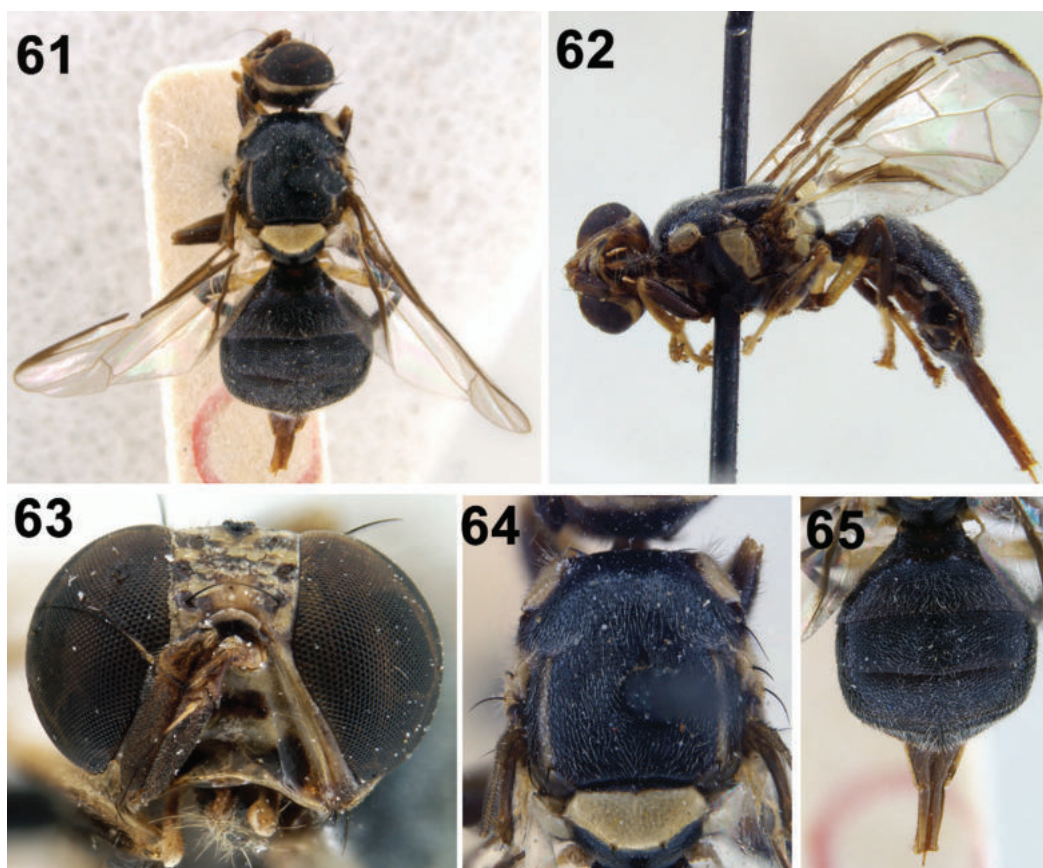
Figures 58–60. Larval morphology of *Zeugodacus momordicae* David & Ajaykumara, sp. nov. **58** cephalopharyngeal skeleton **59** anterior spiracle **60** posterior spiracles.

Etymology. The species name is derived from the genus name *Momordica* in the genitive case.

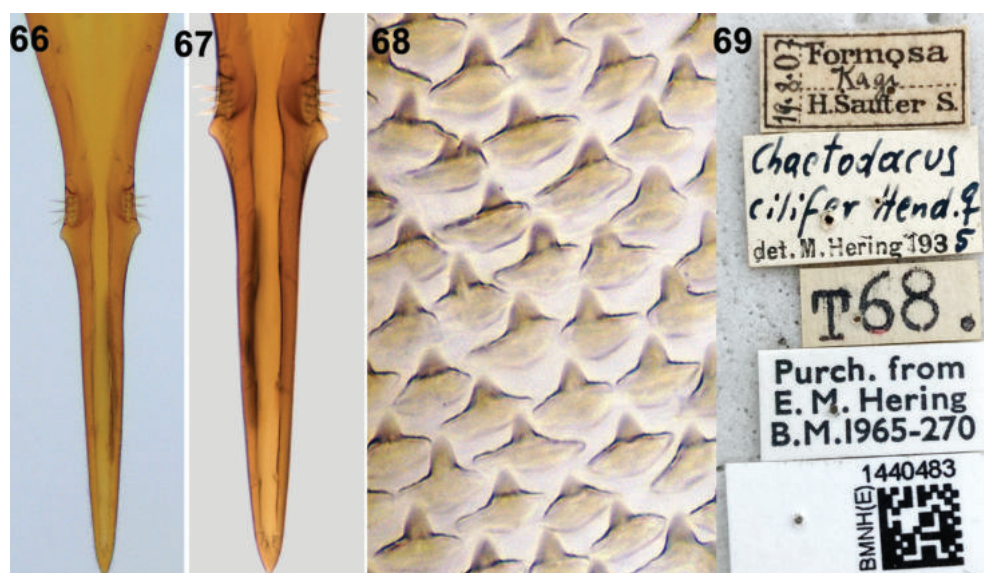
Host plant. Flies were collected on spiny/spine gourd (Figs 70–72); female flies were observed ovipositing inside unopened male flower buds of spiny gourd (Figs 73, 74), *Momordica dioica* Roxb ex Wild. Infested flower buds were having a withered appearance with two or three larvae inside (Figs 75, 76). They were reared up to the adult stage to confirm it as the host.

DNA Barcode. NCBI Accession number OQ353070 (1♀, INDIA: Arunachal Pradesh, Upper Siang, Padu, 29. ix. 2022, David, K.J.). The partial gene sequence of mt-COI of Indian specimen was subjected to similarity search (BLAST-N) in NCBI database which revealed 99% similarity with *Zeugodacus cilifer* reported from Thailand and China, however 97.87% similarity was observed with *Z. cilifer* from Taiwan.

Remarks. Nair et al. (2018; 2021) and Pongen et al. (2023) reported *Zeugodacus cilifer* from Tripura and Meghalaya as a pest of flowers of spiny gourd, respectively. Examination of the postabdominal structure of female of *Z. cilifer* collected from Taiwan (Figs 61–65), the type locality in 1907, deposited at Natural History Museum, London and specimens collected from Pasighat, Arunachal Pradesh and Meghalaya, India revealed that specimens from India are different in the morphology of aculeus and spicules on distal end of evers-

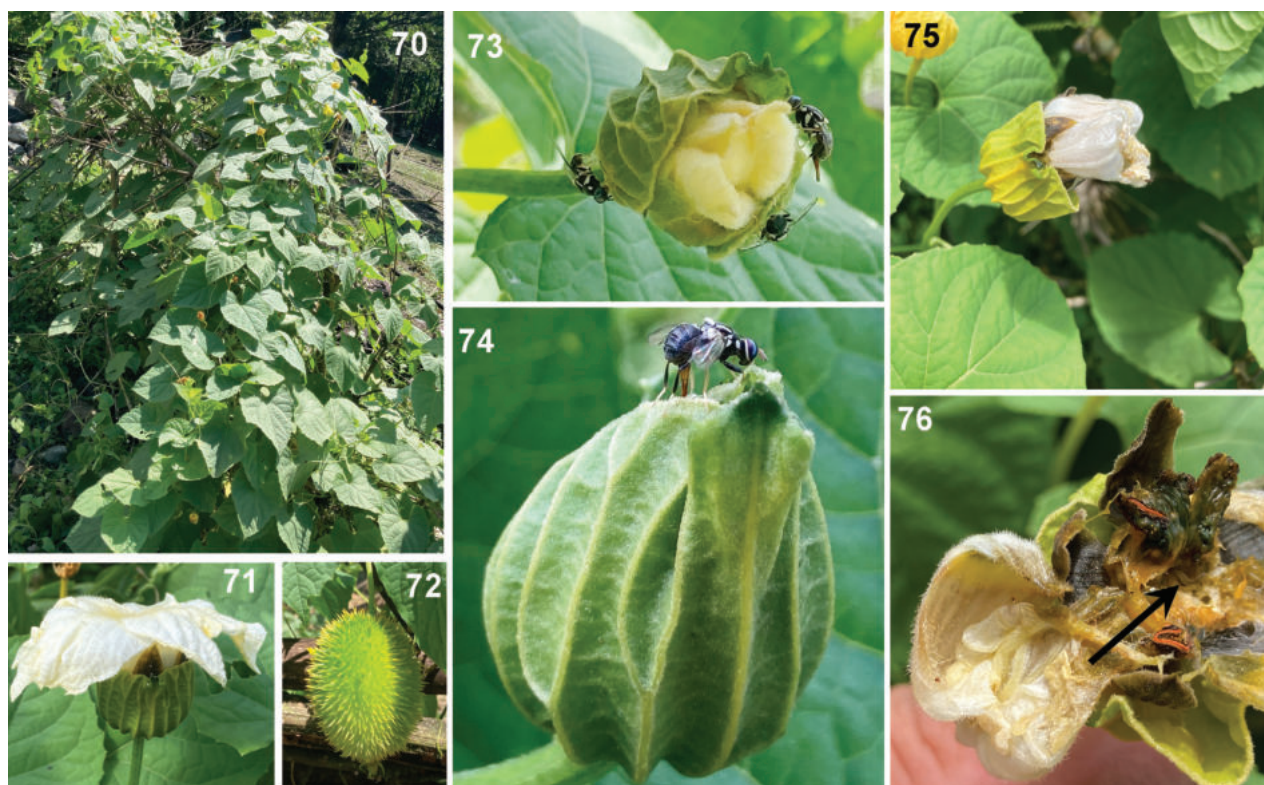


Figures 61–65. *Zeugodacus (Parasinodacus) cilifer* (Hendel) 61 habitus (dorsal) 62 habitus (lateral) 63 head (frontal view) 64 scutum (dorsal view) 65 abdomen.



Figures 66–69. *Zeugodacus (Parasinodacus) cilifer* (Hendel) 66, 67 aculeus tip 68 spicules on distal end of eversible membrane 69 label data.

ible membrane as mentioned in the diagnosis, hence it is here described as a new species. Hence records of *Z. cilifer* by Nair et al. (2018; 2021) and Pongen et al. (2023) are treated as misidentifications of *Z. momordicae*. It is placed in *Zeugodacus* due to shallow/flat posterior emargination of sternite 5 in males,



Figures 70–76. Field infestation of *Zeugodacus (Parasinodacus) momordicae* David & Ajaykumara, sp. nov. **70** habitus of host plant, Spiny gourd, *Momordica dioica* **71** healthy male flower **72** fruit **73** males and females of *Z. momordicae* on male flower bud of spiny gourd **74** female fly of *Z. momordicae* ovipositing into male flower buds **75** infested male flower **76** cut opened infested flower with maggots.

posterior lobe of lateral surstylus much longer than anterior lobe and patterned acrophallus. It is placed in subgenus *Parasinodacus* as it possesses only two scutellar setae and scutum is devoid of medial postsutural vitta.

***Zeugodacus (Zeugodacus) nasivittatus* David & Abhishek, sp. nov.**

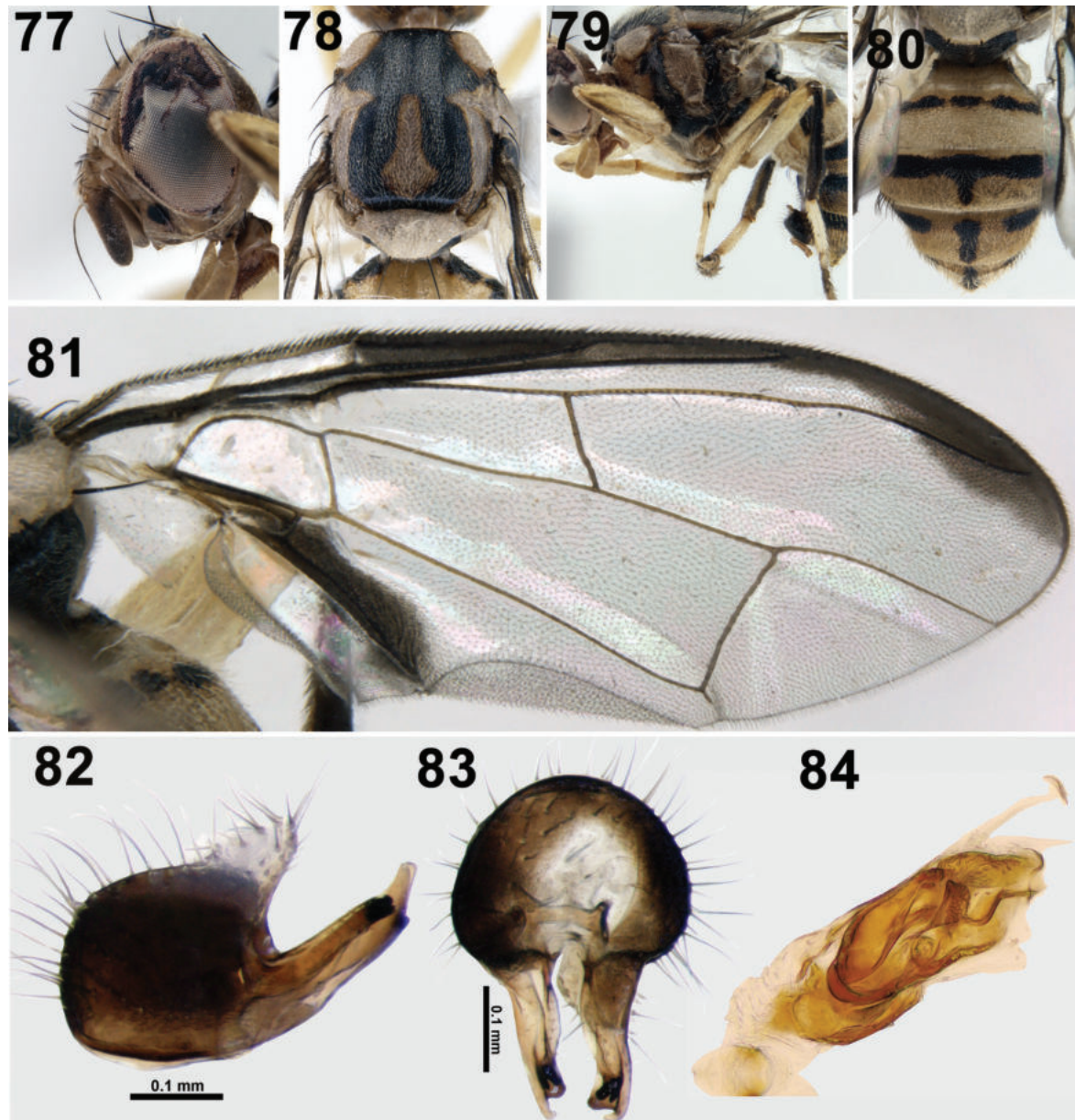
<https://zoobank.org/BA85A422-419F-485A-BCBC-AC73D7BB27C6>

Figs 77–84

Type locality. INDIA, Meghalaya, Umiam.

Type material. *Holotype* male, pinned. Original label: "INDIA, Meghalaya, Umiam, 11.vii.2023, Kennedy N." *Paratype* 1♂, INDIA: Meghalaya, Umiam, 11.vii.2023, Kennedy N., attracted to cue lure (deposited at NIM).

Diagnosis. It is similar to *Zeugodacus hengsawadae* Drew & Romig and *Z. tebeduiae* Drew & Romig in possessing broad medial postsutural vitta and costal band confluent with vein R_{2+3} , but can be easily separated from *Z. hengsawadae* by the entirely fulvous femora without any preapical spots, absence of basal scutellar seta and shape of the medial vitta; from *Z. tebeduiae* by its smaller size (wing length 4.5 mm), absence of elongate narrow facial spots and basal scutellar setae. It can be differentiated from *Z. flavoverticilis* Drew & Romig by the absence of broad transverse marking on katepisternum, presence of slightly expanded costal band towards apex and yellow abdominal tergites with narrow medial and longitudinal bands.



Figures 77–84. *Zeugodacus nasivittatus* David & Abhishek, sp. nov. 77 head (lateral) 78 scutum (dorsal view) 79 thorax (lateral) 80 abdomen 81 wing 82 epandrium (lateral) 83 epandrium (posterior) 84 glans of phallus.

Description. Male. Medium sized species (5.7–5.8 mm); face fulvous with two separate black spots; scutum black colour with a broad lateral postsutural yellow vitta (0.16–0.18 mm wide) ending behind intra-alar seta; notopleuron and postpronotal lobe yellow, prominent yellow spot anterior to notopleural suture; anepisternal stripe reaching anterior notopleural seta dorsally; scutellum without black basal band; wing predominantly hyaline with narrow costal band confluent with R_{2+3} , anal streak wide, dense aggregation of microtrichia around A_1+Cu_2 ; abdominal tergites 3–5, orange-brown with a narrow longitudinal black discontinuous band (0.17 mm), lateral regions of tergites 3–5 with small, fuscous markings.

Head (Fig. 77): Height 1.21 mm. Frons length 1.67× breadth; fulvous with fuscous marking on anteriomedial hump and around bases of frontal and orbital setae, all setae black: three pairs of frontal setae and one pair of orbital setae;

lunule fulvous. Ocellar triangle and vertex black. Face fulvous with two separate black spots (0.16 mm long) on antennal furrows. Scape (0.12 mm long) and pedicel (0.21 mm long) fulvous, first flagellomere (0.51 mm long) dark fuscous on outer side and apex, arista non plumose, combined length of pedicel and flagellomere as long as the vertical length of face. Gena fulvous without a black marking, genal seta present. Occiput light fuscous, fulvous along eye margins; lateral and medial vertical setae present, occipital row without stout black setae. **Thorax** (Figs 78, 79). scutum black (1.75 mm long, 1.74 mm wide) without lanceolate markings. Pleura black in ground colour with red-brown markings anterior to anepisternal stripe, katapisternum and anepimeron. Yellow markings as follows: postpronotal lobe, notopleuron, anepisternal stripe reaching anterior notopleural seta dorsally and continuing to katapisternum as a transverse spot; anatergite (posterior apex black); anterior 3/4 of katatergite (remainder black); broad parallel-sided lateral postsutural vitta ending after intra-alar seta. Medial longitudinal postsutural yellow vitta present (nose shaped). Scutellum yellow without narrow black basal band. Chaetotaxy: scutellar seta, 1; prescutellar acrostichal seta, 1; intra-alar seta, 1; postsutural supra-alar seta, 1; postalar seta, 1; anepisternal seta, 1; anterior notopleural seta, 1; posterior notopleural seta, 1; scapular setae, 2. Coxa fulvous, trochanter light fulvous; all femora fulvous without apical black markings; fore femur without small oval spot, apex of mid femur with faint infuscation; hind femur with prominent black apex. Fore and mid tibiae light fuscous at base, hind tibia dark fuscous, all tarsal segments fulvous. **Wing** (Fig. 81). Length, 4.65 mm, cells bc and c hyaline; microtrichia in outer corner of cell c only; remainder of wing hyaline except dark fuscous cell sc, costal band broad, confluent with R_{2+3} expanded slightly towards apex, extension of cell cua longer than cell cua, base of cell br with microtrichia, anal streak wide covering cell cua, with dense aggregation of microtrichia around A_1+Cu_2 ; supernumerary lobe well developed. **Abdomen** (Fig. 80). 2.81 mm long, 1.66 mm wide, oval, tergites free, tergites 1 and 2 fulvous, tergite 2 with a medial black spot. Tergite 3 reddish brown with a narrow, basal transverse black band. Tergites 3–5 with a narrow, discontinuous medial longitudinal black band and narrow, black lateral markings. Tergite 5 with inconspicuous ceromata, sternite 5 black with shallow concavity and pecten present on tergite 3.

Male genitalia. Epandrium quadrate (profile view), lateral surstylus as long as epandrium; posterior lobe of surstylus 6–7× longer than anterior lobe (Fig. 82); proctiger hyaline, shorter than epandrium; medial surstylus shorter than lateral surstylus with well-developed pair of equal sized prenisetae (Fig. 83). Phallus short, 1.20 mm excluding glans of phallus (0.27 mm), glans of phallus well sclerotised with spine like projections on acrophallus (Fig. 84), subapical lobe T-shaped, preglans lobe present.

Etymology. The species name is derived from Latin words *nasi vitta* which means nose-shaped vitta.

Host plant. Not known.

Male parapheromone. Cue lure.

Remarks. This species is placed in *Zeugodacus* due to the shallow/flat posterior emargination of sternite 5 in males, posterior lobe of lateral surstylus much longer than anterior lobe and patterned acrophallus. It is placed in subgenus *Zeugodacus* as it possesses medial postsutural vitta, postsutural supra-alar, and prescutellar acrostichal seta.

***Zeugodacus (Sinodacus) sinuvittatus* David & Abhishek, sp. nov.**

<https://zoobank.org/424F5A47-0662-4551-A793-238FA7FBF63F>

Figs 85–92

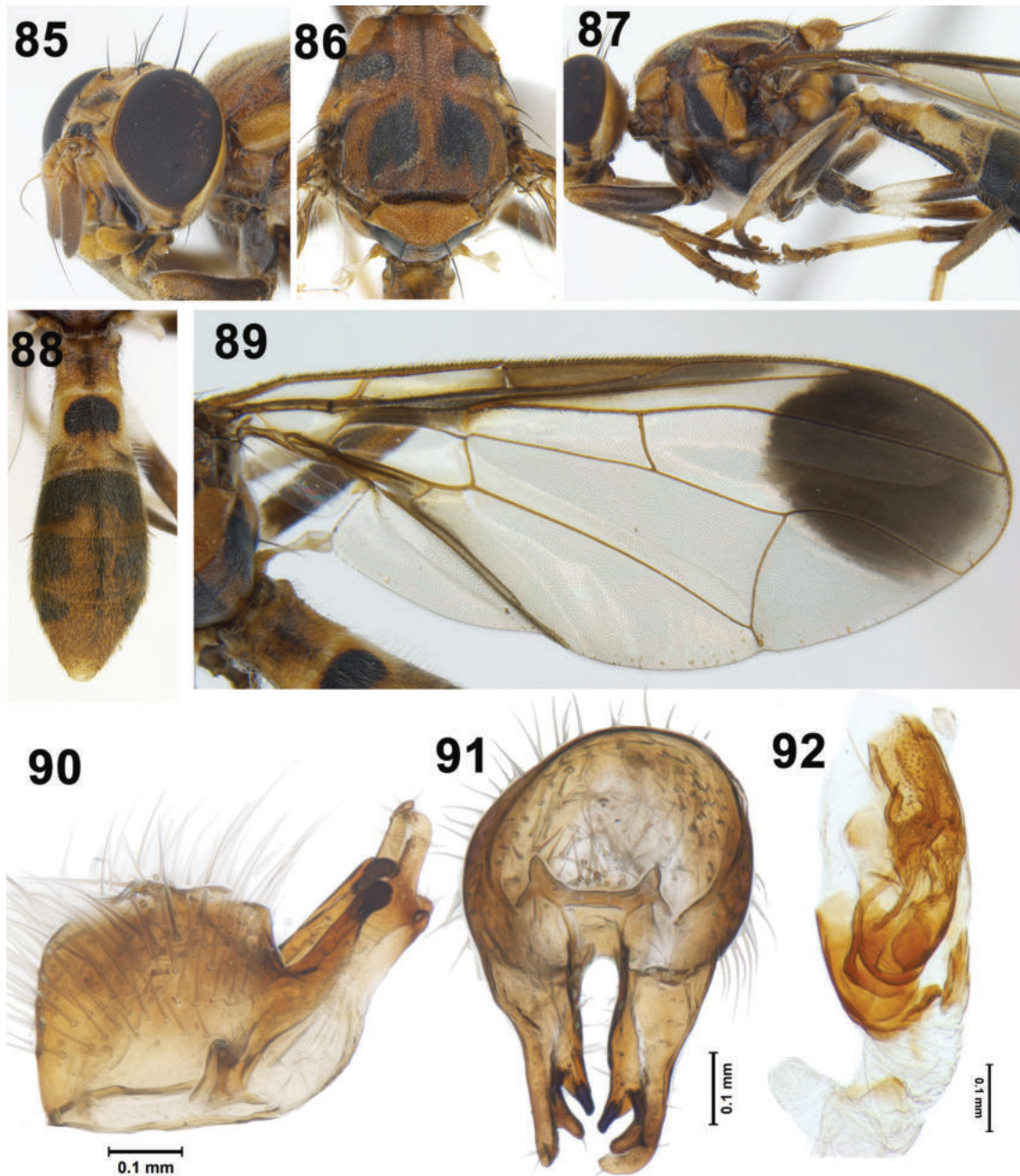
Type locality. INDIA, Himachal Pradesh, Totu, IARI substation, Totu.

Type material. *Holotype* male, pinned. Original label: “INDIA, Himachal Pradesh, Totu, IARI substation, Totu, 18.viii.2019, David, K. J.” (deposited at NIM).

Diagnosis. *Zeugodacus sinuvittatus* is similar to *Z. hochii* (Zia), *Z. infestus* (Enderlein) and *Z. brevipunctatus* David & Hancock in possessing reddish brown scutum, club shaped abdomen and wing with broad apical black spot. It can be differentiated from *Z. hochii* by the absence of medial postsutural vitta, face with separate black spots unlike transverse band, presence of discontinuous costal band slightly overlapping vein R_{2+3} ; from *Z. infestus* and *Z. brevipunctatus* by the absence of lateral and medial postsutural vitta, absence of postsutural supra-alar seta, narrow costal band interrupted in cell r_1 and by the broad apical spot. Unlike *Z. brevipunctatus*, acrophallus of *Z. sinuvittatus* is fully patterned.

Description. Male. Large sized species (wing length 7.05 mm); face fulvous with two elongate black markings in the antennal furrow and a medial longitudinal line; scutum reddish brown in ground colour without lateral and medial vitta, with broad quadrate black patches in presutural and postsutural areas, notopleuron and postpronotal lobe yellow, inconspicuous yellow spot anterior to notopleural suture; anepisternal stripe reaching midway between anterior notopleural seta and notopleuron; scutellum yellow; wing predominantly hyaline with costal band slightly overlapping vein R_{2+3} , discontinuous towards apex of cell r_1 , with a broad apical spot covering the apex of cell r_{2+3} , r_{4+5} and upper one-fourth of cell m , anal streak narrow, no dense aggregation of microtrichia around A_1+Cu_2 ; abdomen club shaped, tergite 2 with a prominent black semicircular spot, tergites 3–5 with dark fuscous lateral markings and a narrow medial longitudinal band.

Head (Fig. 85). Height 1.60 mm. Frons length $1.85\times$ breadth; fulvous with fuscous marking on anteriomedial hump and around bases of frontal and orbital setae, all setae black: two pairs of frontal setae and one pair of orbital setae; lunule black. Ocellar triangle black, vertex yellow. Face fulvous with two separate elongate black markings in antennal furrows and a medial longitudinal black line. Scape (0.23 mm long) and pedicel (0.22 mm long) fulvous, first flagellomere (0.74 mm long) dark fuscous on outer side and apex, arista non plumose, combined length of pedicel and flagellomere longer than the vertical length of face. Gena fulvous with a black marking and a seta. Occiput fulvous; lateral and medial vertical setae present, occipital row with three or four stout black setae. **Thorax** (Figs 86, 87). 2.18 mm long, 2.03 mm wide; scutum red brown with two black quadrate markings one each in presutural and postsutural area. Pleura red-brown in ground colour with black markings anterior to anepisternal stripe, katepisternum and anepimeron. Yellow markings as follows: postpronotal lobe, notopleuron, anepisternal stripe reaching midway between notopleuron and anterior notopleural seta and continuing to katepisternum as a transverse spot; anatergite (posterior apex black); anterior 3/5 of katatergite (remainder black). Scutellum yellow without narrow black basal band, subscutellum red-brown with black lateral margins. Chaetotaxy: scutellar seta, 1; intra-alar seta, 1; postalar seta, 1; anepisternal seta, 1; anterior notopleural seta, 1; posterior notopleural seta, 1; scapular setae, 1. Leg (Fig. 87):



Figures 85–92. *Zeugodacus (Sinodacus) sinuvittatus* David & Abhishek, sp. nov. **85** head (lateral) **86** scutum (dorsal view) **87** thorax (lateral) **88** abdomen **89** wing **90** epandrium (lateral) **91** epandrium (posterior) **92** glands of phallus.

Coxa, trochanter dark fuscous, all femora with extensive fuscous markings; fore femur wholly fuscous, 0.80 of mid femur and 0.60 of hind femur fuscous; fore and hind tibiae fuscous, mid tibia fulvous, tarsal segments slight fuscous. **Wing** (Fig. 89). Length, 7.05 mm, cells bc and c hyaline; microtrichia in outer corner of cell c only; remainder of wing hyaline except dark fuscous cell sc , costal band overlapping vein $R_{2+3'}$ interrupted towards apical one-fourth of cell r_1 and with a broad apical spot covering apex of cell $r_{2+3'}$, r_{4+5} and anterior one fourth of cell m , extension of cell cua longer than cell cua , base of cell br with microtrichia, anal streak narrow, confined to cell cua , lacks dense aggregation of microtrichia around A_1+Cu_2 ; supernumerary lobe weak. **Abdomen** (Fig. 88). 3.69 mm long, 1.92 mm wide, club shaped, tergites free, tergites

1 fulvous, tergite 2 reddish brown with a black semicircular marking, tergite 3 with broad, black basal band and pecten, tergites 4 and 5 with dark lateral margins and a narrow medial longitudinal band. Tergite 5 without prominent shining spots (ceromata).

Male genitalia. Sternite 5 brown with shallow emargination, epandrium quadrate with lateral surstylus as long as epandrium, proctiger membranous, as wide as epandrium, epandrium sclerotised (Figs 90, 91), as long as wide (height 0.3 mm; width 0.34 mm); surstyli as long as epandrium, oblique, 0.38 mm long; posterior lobe of surstylus 6.2× longer than anterior lobe, aedeagus 4.60 mm long with glans of phallus (Fig. 92) 0.625 mm long. Three-quarters of glans heavily sclerotised with well-developed fully patterned acrophallus, praeputium, and subapical lobe.

Etymology. The species name is derived from Latin words *sine* (= without) and *vitta* (= band), as the species lacks lateral and medial poststutural vitta on scutum.

Host plant. Not known, collected by sweep netting on grapevine

Male parapheromone. Not known.

Remarks. This species is placed in *Zeugodacus* due to shallow/flat posterior emargination of sternite 5 in males, posterior lobe of lateral surstylus much longer than anterior lobe and patterned acrophallus. It is placed in subgenus *Sinodacus* as it lacks prescutellar acrostichal seta, basal scutellar seta and due the club-shaped abdomen.

***Zeugodacus (Zeugodacus) umiam* David & Kennedy, sp. nov.**

<https://zoobank.org/3EDCB89D-2BBD-451C-B648-72CAC36605E7>

Figs 93–109

Type locality. INDIA: Meghalaya, Umiam.

Type material. *Holotype* female, pinned. Original label: "INDIA: Meghalaya, Umiam, 06.vii.2021. Kennedy N." *Paratype*, 1♂, INDIA, Meghalaya, Bhoirymbong, Umiam, 10.v.2023, Kennedy N, attracted to cue lure (deposited at NIM).

Diagnosis. *Zeugodacus umiam* is similar to *Z. nigrifacies* (Shiraki) in possessing black face, fore femur entirely black, scutellum with broad black basal band and an apical spot but can be differentiated by the absence of subapical band, band on crossvein r-m and two scutellar setae. It can be distinguished from *Z. menglanus* (Yu, Liu & Yang) by the facial markings (wholly black in male; dorsal half black in female), two scutellar setae and lack of apical expansion in costal band. It is similar to *Z. diaphorus* in possessing apical scutellar spot, two pairs of scutellar setae and black face, but can be separated by the presence of broad black basal band on scutellum, narrow anepisternal stripe not reaching anterior notopleural seta dorsally.

Description. Female. Medium sized, black species (wing length 5.65 mm); face posterior half black; scutum black with narrow yellow lateral postsutural vitta and medial vitta, lateral vitta ending before postalar seta, notopleuron and postpronotal lobe yellow, small yellow spot anterior to notopleural suture, anepisternal stripe not reaching anterior notopleural seta dorsally, scutellum yellow with a broad black basal band, with an apical black spot; wing predominantly hyaline with costal band confluent with vein R_{2+3} , expanded slightly towards apex of cell r_{2+3} and r_{4+5} , anal streak prominent; abdomen oval, all tergites black

except tergite 2 with a broad fulvous band posteriorly, narrow fulvous bands in tergites 3–5.

Head (Fig. 93): Height 1.32 mm. Frons length $1.2\times$ breadth; fuscous, all setae black: two pairs of frontal setae and one pair of orbital setae; lunule black. Ocellar triangle, vertex black, face black in distal half, scape (0.12 mm long) and pedicel (0.14 mm long) fulvous, first flagellomere (0.58 mm long) dark fuscous on outer side and apex, arista non plumose, combined length of pedicel and flagellomere as long as the vertical length of face. Gena fulvous with a black marking and a seta, occiput black; lateral and medial vertical setae present.

Thorax (Figs 94, 95): 2.18 mm long, 2.03 mm wide; scutum black with narrow yellow lateral postsutural vittae ending at postalar seta, medial vitta narrow. Yellow markings as follows: postpronotal lobe, notopleuron, anepisternal stripe reaching midway between notopleuron and anterior notopleural seta and continuing to katapisternum as a small transverse spot; anatergite (posterior apex black); anterior 3/5 of katatergite (remainder black). Scutellum yellow with a black basal band and an apical black spot, subscutellum black. Chaetotaxy: scutellar seta, 1; intra-alar seta, 1; postalar seta, 1; anepisternal seta, 1; anterior notopleural seta, 1; postsutural supra-alar seta, 1; posterior notopleural seta, 1; scapular setae, 1. Leg (Fig. 95): Coxa, trochanter black, all femora with extensive fuscous markings; fore femur wholly black, 0.75 of mid femur and 0.50 of hind femur black; fore, mid and hind tibiae black, tarsal segments fulvous.

Wing (Fig. 97): Length, 5.65 mm, cells bc and c hyaline; microtrichia in outer corner of cell c only; remainder of wing hyaline except dark fuscous cell sc, dark fuscous narrow costal band confluent with vein R_{2+3} expanded slightly towards apex, extension of cell cua as long as cell cua, base of cell br with microtrichia, anal streak prominent confined to cell cua, dense aggregation of microtrichia around A_1+Cu_2 ; supernumerary lobe weak. **Abdomen** (Fig. 96): 2.54 mm long, 2.01 mm wide, oval shaped, tergites free, tergite 1 black, tergite 2 black basally with broad fulvous band, tergites 3–5 black with narrow fulvous markings apically. Tergite 5 with prominent shining spots (ceromata).

Female genitalia. Oviscape dark brown (Fig. 98), conical (1.62 mm), spicules on distal end of eversible membrane (1.42 mm) with six or seven blunt spicules (Fig. 99), aculeus (1.07 mm) with apex trilobed (Fig. 100), spermatheca black, coiled (Fig. 17).

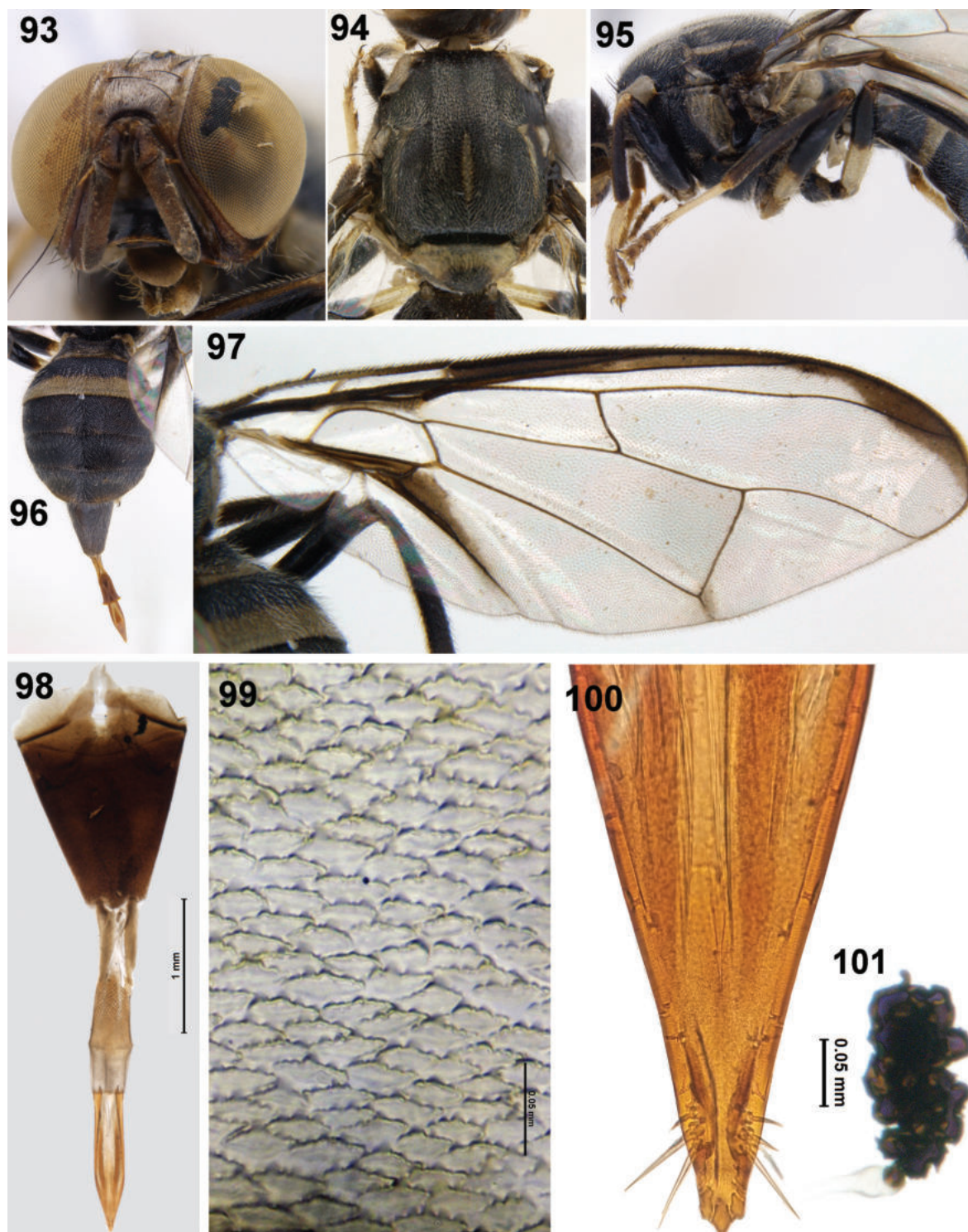
Male (Figs 102–106). Similar to female except for entirely black face, broad basal band on the scutellum, dense aggregation of microtrichia around A_1+Cu_2 , black extensive markings on all femora and pecten on tergite 3.

Male genitalia. Sternite 5 black with shallow emargination, epandrium quadrate with lateral surstylus as long as epandrium, proctiger membranous, not inflated, epandrium sclerotised (Figs 107–108), as long as wide (height 0.31 mm; width 0.28 mm); surstyli slightly shorter than epandrium, oblique, 0.21 mm long; posterior lobe of surstylus $5\times$ longer than anterior lobe, aedeagus 1.93 mm long with glans of phallus (Fig. 109) 0.41 mm long. Three-quarters of glans heavily sclerotised with well-developed patterned acrophallus, praeputium, and subapical lobe.

Etymology. The species name is type locality of the species and is a noun in apposition.

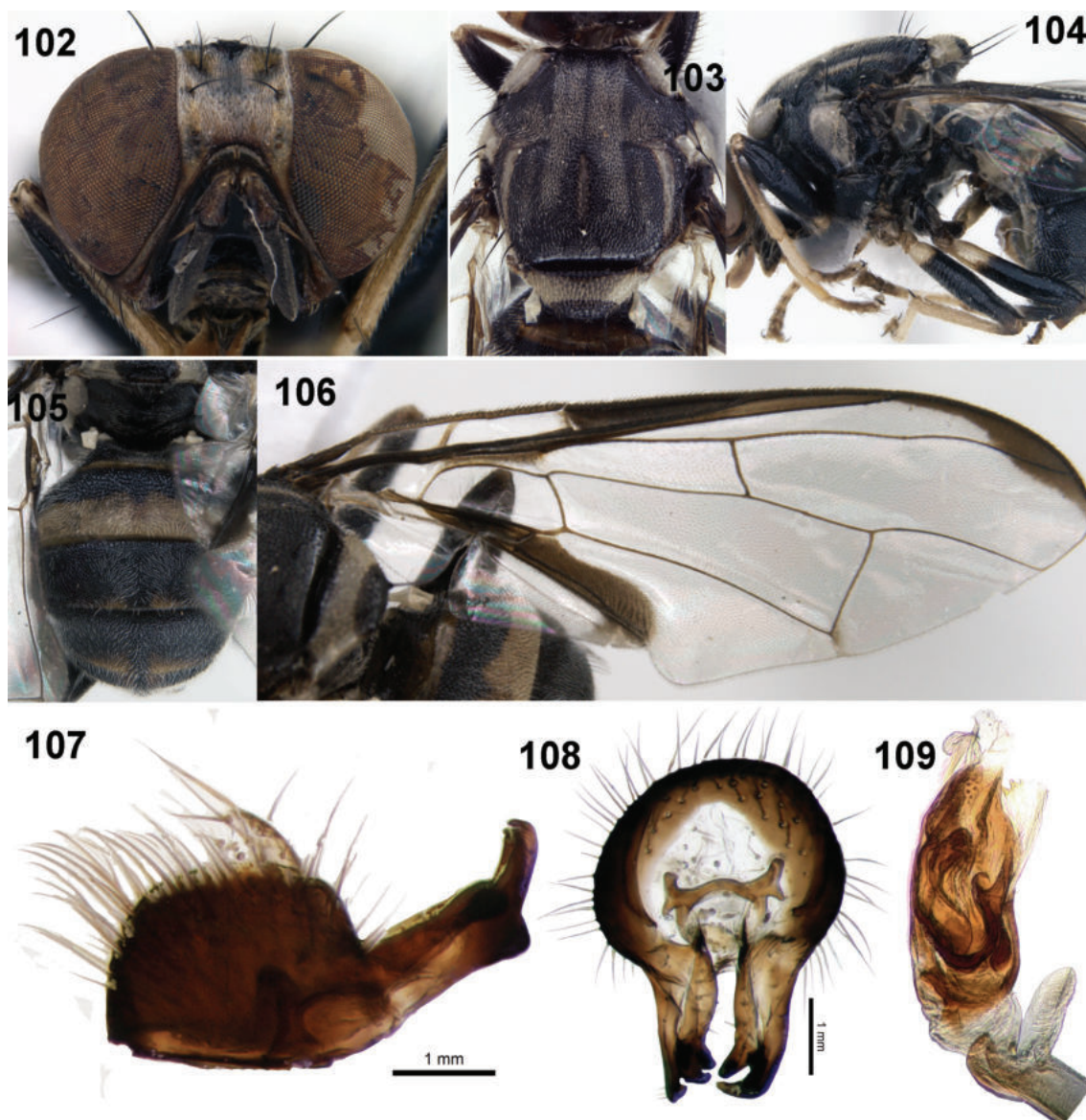
Host plant. Not known.

Male parapheromone. Cue lure.



Figures 93–101. Female of *Zeugodacus umiam* David & Kennedy, sp. nov. **93** head (frontal view) **94** scutum (dorsal view) **95** thorax (lateral view) and legs **96** abdomen **97** wing **98** ovipositor **99** spicules on distal end of eversible membrane **100** aculeus **101** spermatheca.

Remarks. This species is placed in *Zeugodacus* due to shallow/flat posterior emargination of sternite 5 in males, posterior lobe of lateral surstylus much longer than anterior lobe and patterned acrophallus. It is placed in subgenus *Zeugodacus* as it possesses medial postsutural vitta, postsutural supra-alar and prescutellar acrostichal seta.



Figures 102–109. Male of *Zeugodacus umiam* David & Kennedy, sp. nov. **102** head (frontal view) **103** scutum (dorsal view) **104** thorax (lateral view) and legs **105** abdomen **106** wing **107** epandrium and surstyli (lateral view) **108** epandrium and surstyli (posterior view) **109** glans of phallus.

New distributional records

Bactrocera (*Parazeugodacus*) *abbreviata* (Hardy, 1974)

Figs 110–114

Dacus (*Zeugodacus*) *abbreviatus* Hardy, 1974: 44.

Bactrocera (*Zeugodacus*) *abbreviata*: Norrbom et al. 1999: 101.

Bactrocera (*Parazeugodacus*) *abbreviata* (Hardy): Drew and Romig 2016: 243.

Bactrocera abbreviata (Hardy, 1974): Doorenweerd et al. 2018: 23.

Material examined. 1♂, INDIA: Meghalaya, Umiām, 06.07.2021. Kennedy N. (NIM).

Diagnosis. (Figs 29–33): This species has been adequately described by Drew and Romig (2013) except for the postabdominal structures. It resembles *B. bipustulata* in possessing scutellum with a medial black band, hyaline wing with-



Figures 110–114. *Bactrocera* (*Parazeugodacus*) *abbreviata* (Hardy) **110** habitus (dorsal view) **111** habitus (lateral view) **112** epandrium and surstyli (lateral view) **113** epandrium and surstyli (posterior view) **114** glans of phallus (lateral view).

out costal band, short yellow lateral vitta ending at postsutural supra-alar seta, but can be differentiated by the presence of separate black spots on face, all femora fulvous without fuscous/black markings. Male of the species has been examined for genitalia characters. Epandrium quadrate with proctiger smaller than epandrium; posterior lobe of surstylus as long as anterior lobe, epandrium (oval) in posterior view. Glans of phallus with acrophallus patterned; phallus 1.82 mm. This species was originally described from Philippines, distributed across China and Thailand, is being recorded from Meghalaya, India for the first time.

Male attractant. Zingerone.

***Dacus* (*Mellesis*) *vijaysegarani* Drew & Hancock, 1998**

Figs 115–119

Dacus (*Callantra*) *vijaysegarani*: Drew et al. 1998: 636.

Dacus (*Mellesis*) *vijaysegarani*: Drew and Romig 2013: 399.

Dacus vijaysegarani: Dooreenweerd et al. 2018: 43.

Material examined. 1 ♂, INDIA, Meghalaya, Umiam, 29.v.2023, Kennedy N. (NIM).



Figures 115–119. *Dacus (Mellesis) vijaysegarani* Drew & Hancock **115** habitus (dorsal) **116** habitus (lateral) **117** epandrium (lateral view) **118** epandrium (posterior view) **119** glans of phallus.

Diagnosis. This species has been adequately described by Drew et al. (1998) and Drew and Romig (2013) except for postabdominal structures. A male of the fly collected from Meghalaya was dissected to study the postabdominal structures. Epandrium deeply sclerotised, black, lateral surstylus with posterior lobe slightly longer (2–3×) than anterior lobe; epandrium bulbous (in posterior view), glans of phallus elongate (0.7 mm) with patterned aculeus.

Acknowledgments

We are grateful to Dr. Satya Nand Sushil, Director, ICAR-NBAIR for the facilities and support, Dr. David, L. Hancock, United Kingdom for his comments on the identity of the species included in the manuscript, Mr. Nigel P. Wyatt, Department of Life Sciences, Natural History Museum, London for providing specimens of *Z. cilifer* on loan, Dr. S. Salini, Senior Scientist, ICAR-NBAIR for bringing loaned specimens from NHM, Dr. Rumki H. Ch. Sangma, Scientist, ICAR- RC for NEH Region, Umiam, Meghalaya for *Z. momordicae* collected from Meghalaya on loan. The first author acknowledges Mr. M. Maruthi for his support in processing the specimens for dissection.

Additional information

Conflict of interest

The authors have declared that no competing interests exist.

Ethical statement

No ethical statement was reported.

Funding


Page charges for publishing this article was met from Contract Research Project on fruit flies with Godrej Agrovet Pvt. Ltd.

Author contributions

Writing – original draft, preparation of illustrations: DKJ. Review and editing: AV. Molecular characterisation: GR. Resources: KN, AKM, HCB.

Author ORCIDs

Karamankodu Jacob David  <https://orcid.org/0000-0002-5092-141X>

Venkateshaiah Abhishek  <https://orcid.org/0009-0002-7044-3977>

Ningthoujam Kennedy  <https://orcid.org/0000-0002-6709-7252>

K. M. Ajaykumara  <https://orcid.org/0000-0002-4553-3068>

R. G. Gracy  <https://orcid.org/0000-0002-6764-5167>

Cheday Bhutia Hissay  <https://orcid.org/0009-0000-2819-8088>

Data availability

All of the data that support the findings of this study are available in the main text.

References

- Cumming JM, Wood DM (2017) Adult morphology and terminology. In: Kirk-Spriggs AH, Sinclair BJ (Eds) Manual of Afrotropical Diptera (Vol. 1). Introductory Chapters and Keys to Diptera Families. Suricata (Vol. 4). South African National Biodiversity Institute, Pretoria, 89–133.
- David KJ, Ramani S (2019) New species, redescription and phylogenetic revision of tribe Dacini (Diptera: Tephritidae: Dacinae) from India based on morphological characters. Zootaxa 4551(2): 101–146. <https://doi.org/10.11646/zootaxa.4551.2.1>
- David KJ, Hancock DL, Singh SK, Ramani S, Behere GT, Salini S (2017) New species, new records and updated subgeneric key of *Bactrocera* Macquart (Diptera: Tephritidae: Dacinae: Dacini) from India. Zootaxa 4272(3): 386–400. <https://doi.org/10.11646/zootaxa.4272.3.4>
- Drew RAI, Romig MC (2013) Tropical Fruit Flies (Tephritidae: Dacinae) of South-East Asia. CAB International, Wallingford, 653 pp. <https://doi.org/10.1079/9781780640358.0000>
- Drew RAI, Romig MC (2016) Keys to the Tropical fruit flies (Tephritidae: Dacinae) of South-East Asia. CAB International, Wallingford, 487 pp. <https://doi.org/10.1079/9781780644196.0000>
- Drew RAI, Hancock DL, White IM (1998) Revision of the tropical fruit flies (Diptera: Tephritidae: Dacinae) of South East Asia. II. *Dacus* Fabricius. Invertebrate Systematics 12(4): 567–654. <https://doi.org/10.1071/IT96004>

- Doorensweerd C, Leblanc L, Norrbom AL, Jose MS, Rubinoff D (2018) A global checklist of the 932 fruit fly species in the tribe Dacini (Diptera, Tephritidae). *ZooKeys* 730: 17–54. <https://doi.org/10.3897/zookeys.730.21786>
- Dupuis JR, Bremer FT, Kauwe A, Jose MS, Leblanc L, Rubinoff D, Geib SM (2018) HiMAP: Robust phylogenomics from highly multiplexed amplicon sequencing. *Molecular Ecology Resources* 18(5): 1000–1019. <https://doi.org/10.1111/1755-0998.12783>
- Hadley A (2011) Combine ZP. <http://www.hadleyweb.pwp.blueyonder.co.uk/> [Accessed on day month 2019]
- Hancock DL, Drew RAI (2018) A review of the subgenus '*Zeugodacus*' Hendel of '*Bactrocera*' Macquart (Diptera: Tephritidae: Dacinae): an integrative approach. *Australian Entomologist* 45(3): 251–272.
- Hardy DE (1974) The fruit flies of the Philippines (Diptera: Tephritidae). *Pacific Insects Monograph* 32: 1–266.
- Hebert PD, Cywinska A, Ball SL, deWaard JR (2003) Biological identifications through DNA barcodes. *Proceedings of the Royal Society B, Biological Sciences* 270(1512): 313–321. <https://doi.org/10.1098/rspb.2002.2218>
- Krosch MN, Schutze MK, Armstrong KF, Graham GC, Yeates DK, Clarke AR (2012) A molecular phylogeny for the Tribe Dacini (Diptera: Tephritidae): Systematic and biogeographic implications. *Molecular Phylogenetics and Evolution* 64(3): 513–523. <https://doi.org/10.1016/j.ympev.2012.05.006>
- Nair N, Bhattacharjee T, Thangjam B, Giri U, Debnath MR (2018) Species diversity of Dacine fruit flies (Diptera: Tephritidae: Dacinae: Dacini) in Tripura, N.E. India. *Journal of Entomology and Zoology Studies* 6(1): 297–302.
- Nair N, Chatterjee M, Das K, Sehgal M, Meenakshi M (2021) Fruit fly species complex infesting cucurbits in India and their management. *International Journal of Agriculture Environment and Sustainability* 3(2): 8–17.
- Norrbom AL, Carroll LE, Thompson FC, White IM, Freidberg A (1999) Systematic database of names. In: Thompson FC (Ed.) *Fruit fly expert identification system and systematic information database. A resource for identification and information on fruit flies and maggots, with information on their classification, distribution and documentation*. *Myia* 9: 65–251.
- Pongen A, Behere GT, Firake DM, Sharma B, Rajesh T (2023) DNA barcoding of major insect pests and their natural enemies from cucurbitaceous crops in northeast India. *Indian Journal of Entomology* 85(1): 150–154. <https://doi.org/10.55446/IJE.2022.440>
- San Jose M, Doorensweerd C, Leblanc L, Barr N, Geib S, Rubinoff D (2018) Tracking the origins of fly invasions; using mitochondrial haplotype diversity to identify potential source populations in two genetically intertwined fruit fly species (*Bactrocera carambolae* and *Bactrocera dorsalis* [Diptera: Tephritidae]). *Journal of Economic Entomology* 111(6): 2914–2926. <https://doi.org/10.1093/jee/toy272>
- Virgilio M, Jordaens K, Verwimp C, White IM, De Meyer M (2015) Higher phylogeny of frugivorous flies (Diptera, Tephritidae, Dacini): Localised partition conflicts and a novel generic classification. *Molecular Phylogenetics and Evolution* 85: 171–179. <https://doi.org/10.1016/j.ympev.2015.01.007>
- White IM, Headrick DH, Norrbom AL, Carroll LE (1999) Glossary. In: Aluja M, Norrbom AL (Eds) *Fruit Flies (Tephritidae): Phylogeny and Evolution of Behaviour*. CRC Press, Boca Raton, 881–924. <https://doi.org/10.1201/9781420074468.sec8>
- Zhang Q, Dou W, Taning CNT, Yu SS, Yuan GR, Shang F, Smagghe G, Wang JJ (2022) miR-309a is a regulator of ovarian development in the oriental fruit fly *Bactrocera dorsalis*. *PLOS Genetics* 18(9): e1010411. <https://doi.org/10.1371/journal.pgen.1010411>

Revision of the Neotropical genus *Trigava* O'Brien, 1999 (Hemiptera, Fulgoromorpha, Dictyopharidae, Nersiini), with descriptions of two new species from Peru and Brazil

Zhi-Shun Song¹, Lois B. O'Brien², Igor Malenovský^{3,4}, Jürgen Deckert⁵, Charles R. Bartlett⁶

¹ Institute of Insect Resources and Biodiversity, School of Life Sciences, Chemistry & Chemical Engineering, Jiangsu Second Normal University, Nanjing, 210013 China

² Department of Entomology, University of Arizona, Forbes 410, PO Box 210036, Tucson, AZ 85721-0036, USA

³ Department of Botany and Zoology, Faculty of Science, Masaryk University, Kotlářská 2, CZ-611 37, Brno, Czech Republic

⁴ Department of Entomology, Moravian Museum, Zelný trh 6, CZ-659 37, Brno, Czech Republic

⁵ Museum für Naturkunde, Leibniz Institute for Research on Evolution and Biodiversity, Invalidenstraße 43, 10115, Berlin, Germany

⁶ Department of Entomology and Wildlife Ecology, University of Delaware, 250 Townsend Hall, Newark, DE 19716-2160, USA

Corresponding author: Charles R. Bartlett (bartlett@udel.edu)



Academic editor: Mike Wilson

Received: 6 April 2023

Accepted: 6 December 2023

Published: 3 January 2024

ZooBank: <https://zoobank.org/0009E896-5A8F-4522-BE77-B5A25995122F>

Citation: Song Z-S, O'Brien LB, Malenovský I, Deckert J, Bartlett CR (2024) Revision of the Neotropical genus *Trigava* O'Brien, 1999 (Hemiptera, Fulgoromorpha, Dictyopharidae, Nersiini), with descriptions of two new species from Peru and Brazil. ZooKeys 1188: 27–45. <https://doi.org/10.3897/zookeys.1188.89881>

Copyright: © Zhi-Shun Song et al. This is an open access article distributed under terms of the Creative Commons Attribution License ([Attribution 4.0 International – CC BY 4.0](https://creativecommons.org/licenses/by/4.0/)).

Abstract

The Neotropical planthopper genus *Trigava* O'Brien, 1999 (Hemiptera, Fulgoromorpha, Dictyopharidae, Nersiini) is revised. Four species are included: *T. brachycephala* (Melichar, 1912) (the type species, from Peru), *T. obrieni* Song, Malenovský & Deckert, **sp. nov.** (from Brazil), *T. peruensis* Song, O'Brien & Bartlett, **sp. nov.** (from Peru), and *T. recurva* (Melichar, 1912) (from Bolivia and Peru). Lectotypes are designated for *Igava brachycephala* Melichar, 1912 and *Igava recurva* Melichar, 1912. All species are described, including habitus photographs and detailed illustrations of the male genitalia. Male and female genitalia are described for this genus for the first time. A key for identification of the species of *Trigava* and a distribution map are provided.

Key words: Auchenorrhyncha, Dictyopharinae, Fulgoroidea, identification key, *Igava*, Lappidini, morphology, planthopper, South America, taxonomy

Introduction

The genus *Trigava* O'Brien, 1999 was originally established as a segregate out of the genus *Igava* Melichar, 1912. Melichar (1912) erected *Igava* based on *Dictyophara callipepla* Gerstaecker, 1895 from Peru (the type species) and described two additional species, *Igava brachycephala* Melichar, 1912 (from Peru) and *I. recurva* Melichar, 1912 (from Peru and Bolivia). However, O'Brien (1999) disagreed with this arrangement and established a new genus *Trigava* O'Brien, 1999 for the latter two species based on Melichar's descriptions and illustrations for *I. brachycephala*. She suggested that *Trigava* may be distinguished from *Igava* by the green dorsal marginal carina of the pronotum (not continued on the tegula, absent in *Igava*), the frons of equal width basally and apically, and the shape of the head. Emeljanov (2011) placed *Trigava* in the tribe Nersiini Emeljanov, 1983 and *Igava* in the tribe Lappidini Emeljanov, 1983, respectively.

This classification was supported by a morphological phylogenetic analysis by Song et al. (2018).

Based on examination of types and additional specimens, *Trigava* is here revised. We redescribe the genus and Melichar's (1912) species and add two new species, *T. obrieni* Song, Malenovský & Deckert, sp. nov. (from Brazil) and *T. peruensis* Song, O'Brien & Bartlett, sp. nov. (from Peru). We provide an identification key and photographic illustrations for each species, showing also the structures of the male and female genitalia for the first time, described and illustrated in detail.

Material and methods

The specimens studied in the course of this work are deposited in the following institutions, which are subsequently referred to their acronyms: **LBOB**, personal collection of Lois B. O'Brien (now deposited at the University of Arizona, Tucson, Arizona, USA); **MFNB**, Museum für Naturkunde, Berlin, Germany; **MMBC**, Moravské zemské muzeum (Moravian Museum), Brno, Czech Republic; and **MTD**, Museum für Tierkunde, Dresden, Germany.

The post-abdominal segments of the specimens used for dissections were cleared in 10% KOH at room temperature for c. 6–12 hours, rinsed and examined in distilled H₂O and then transferred to 10% glycerol and enclosed in microvials pinned with the specimens. Observations were conducted under a stereomicroscope, measurements and photography under Leica M205 C stereomicroscopes equipped with a Canon EOS 7D digital camera or a Keyence VHX-5000 digital microscope with VH-Z20T and VH-ZST objectives. Some final images were compiled from multiple photographs using CombineZM 1.0.0 image stacking software and improved with the Adobe Photoshop CS5 software.

The morphological terminology and measurements used in this study follow Song et al. (2016, 2018) for most characters, Bourgoin (1993) for the female genitalia, and Bourgoin et al. (2015) for the tegmen. Species characteristics shared with the generic description are not repeated except for clarity.

Taxonomy

Family Dictyopharidae Spinola, 1839

Tribe Nersiini Emeljanov, 1983

Genus *Trigava* O'Brien, 1999

Trigava O'Brien, 1999: 60. Type species: *Igava brachycephala* Melichar, 1912; by original designation.

Diagnosis. The genus may be distinguished by the following combination of characters: cephalic process conical, strongly curved upward, and gradually narrowing apicad; vertex with posterior plane elevated above pronotum, wider (e.g., at posterior margin) than transverse diameter of eyes in dorsal view, lateral carinae abruptly constricted and curved upward in front of eyes, converging anteriad, apical margin broadly angulately convex to nearly straight; frons flat, lateral, intermediate and median carinae weakly ridged, lateral carinae nearly parallel in most of their length, gradually converging apicad in front of eyes;

pronotum with intermediate carinae ridged and nearly reaching posterior margin, upper lateral carina greenly thickened (not continued on the tegula), posterior margin angularly concave, not notched; mesonotum with lateral carinae incurved anteriad, reaching and connecting median carina; tegulae lacking carina; tegmina macropterous, veins setose on ventral surface, nodal line present, ScP+R+MP long, MP₁₊₂, MP₃₊₄ and CuA₁ forked near nodal line (near midlength), the longest folding line between MP₃ and MP₄; fore femora without spines, hind tibiae with eight apical teeth; endosomal processes sclerotised apically; phallobase with pairs of large and stout spines.

Description. General colour of body pale green to stramineous green, marked with green, ochraceous and black on head and thorax (Figs 1, 2).

Head. Head (Figs 3A–C, 4A–C, 6A–C, 7A–C) in front of eyes produced into a short cephalic process. Cephalic process conical, strongly curved upward, and gradually narrowing toward apex. Vertex (Figs 3A, 4A, 6A, 7A) with posterior plane elevated above pronotum, wider than transverse diameter of eyes in dorsal view (Figs 3A, 4A, 6A, 7A); lateral carinae keeled, gradually converging (with a lateral inflection anterior to eyes), abruptly constricted and curved upward in front of eyes, and then converging anteriad, in lateral view (Figs 3B, 4B, 6B, 7B), the process bent upward at approximately 60–90° (sometimes more than 90°) in front of eyes; median carina indistinct, somewhat depressed medially, or weakly ridged posteriorly; apical margin broadly angularly convex to nearly straight, not acuminate at apex, posterior margin ridged and broadly and angularly concave, concavity projecting distinctly beyond middle of eyes. Frons (Figs 3C, 4C, 6C, 7C) flat, elongate and relatively broad; lateral carinae weakly ridged, slightly expanded outward below antennae, nearly parallel in most of their length, gradually converging apicad in front of eyes; intermediate carinae weakly keeled, nearly reaching frontoclypeal suture; median carina complete but obscure. Frontoclypeal suture arched. Postclypeus and anteclypeus (Figs 3C, 4C, 6C, 7C) cuneate, slightly convex medially; lateral and median carinae keeled. Rostrum long, second segment slightly longer than third segment, surpassing middle coxae, third segment reaching middle of hind femora. Compound eyes large and rounded, callus postocularis forming a triangular process protruded posteriad. Antenna with very small scape; pedicel subglobose, with more than 50 sensory plaque organs distributed over entire surface; flagellum long, setuliform.

Thorax. Pronotum (Figs 3A, 4A, 6A, 7A) distinctly shorter than mesonotum medially, narrow anteriorly, broad posteriorly; anterior margin arcuately convex medially, lateral marginal areas convex and sloping with two long longitudinal carinae on each side between eyes and tegulae, upper lateral carina greenly thickened (not continued on the tegula); in dorsal view (Figs 3A, 4A, 6A, 7A), lower lateral carinae expanded just behind eyes; posterior margin angularly concave, not notched; median carina distinct, with a deep lateral pit at side; intermediate carinae keeled and nearly complete. Mesonotum (Figs 3A, 4A, 6A, 7A) distinctly tricarinate, lateral carinae incurved anteriad, reaching median carina. Tegulae lacking carina.

Tegmina (Figs 2G, H) membranous, hyaline, and macropterous, extending far beyond the tip of abdomen; veins setose on ventral surface; transverse veinlets *r-m*, *imp* and *mp-cu* connecting some short segments of veins RP, MP and CuA to form nodal line; ScP+R+MP long, much longer than basal cell; ScP+R forked in distal 3/5; MP bifurcating MP₁₊₂ and MP₃₊₄ (forming cell C3) near midlength,

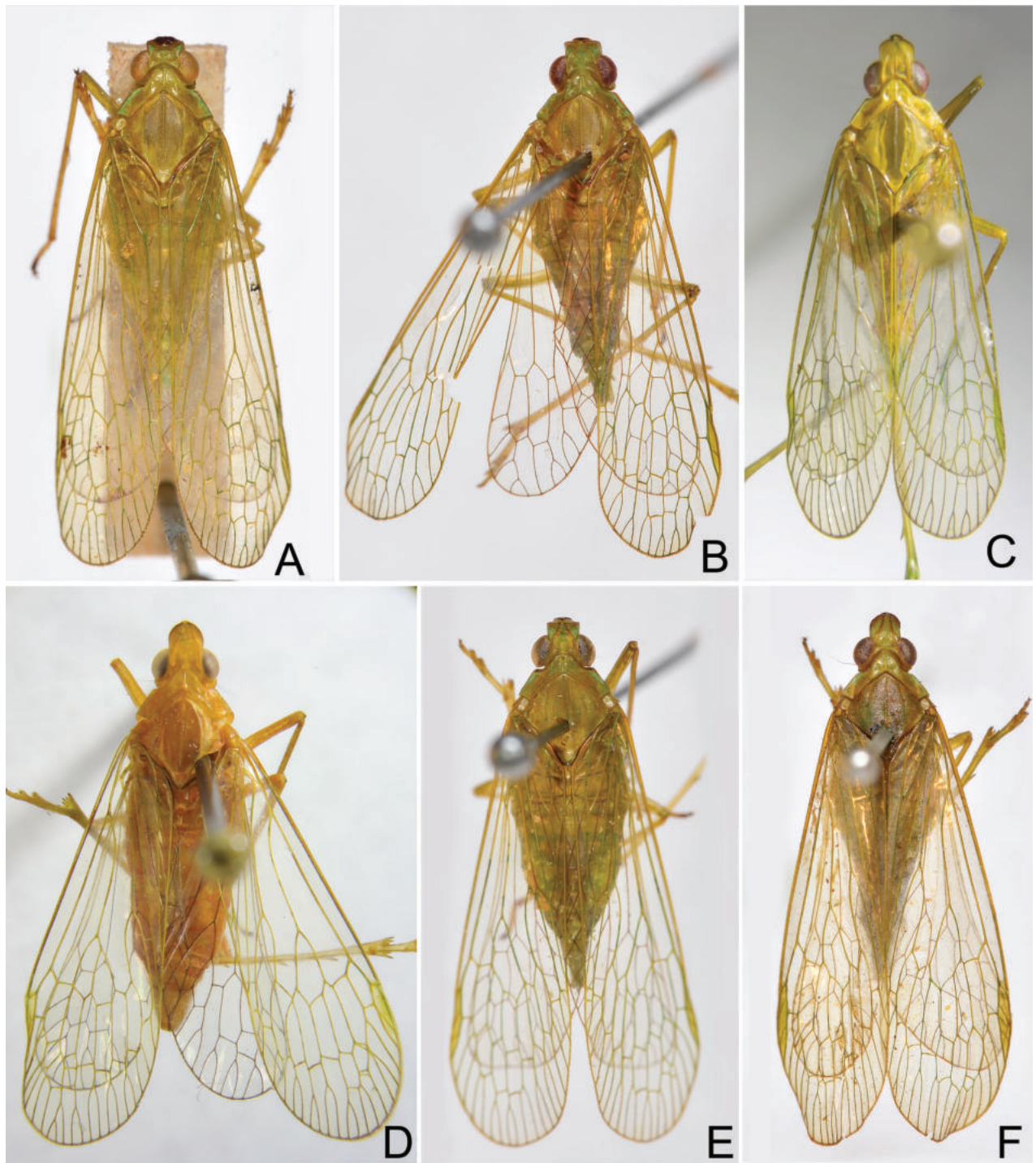


Figure 1. Habitus of *Trigava* species, dorsal view **A** *T. brachycephala* (Melichar), lectotype, male **B** *T. brachycephala* (Melichar), male **C** *T. obrieni* sp. nov., holotype, male **D** *T. obrieni* sp. nov., paratype, female **E** *T. peruensis* sp. nov., holotype, male **F** *T. recurva* (Melichar), lectotype, male.

MP₁₊₂ and MP₃₊₄ forked near level of bifurcation of ScP+R, near nodal line, MP₁, MP₂, MP₃ and MP₄ each forked at apex; CuA forked before bifurcation of MP (forming C5 cell), CuA₁ bifurcating CuA_{1a} and CuA_{1b} before *mp-cu*, near nodal line; *mp-cu* connecting MP₃₊₄ and CuA_{1a} (forming C4 cell); Pcu and A1 fused in proximal third of clavus, composite vein reaching wing margin before claval apex (not reaching CuP); numbers of apical cells of RP, MP and CuA 3, 7, 3–4,

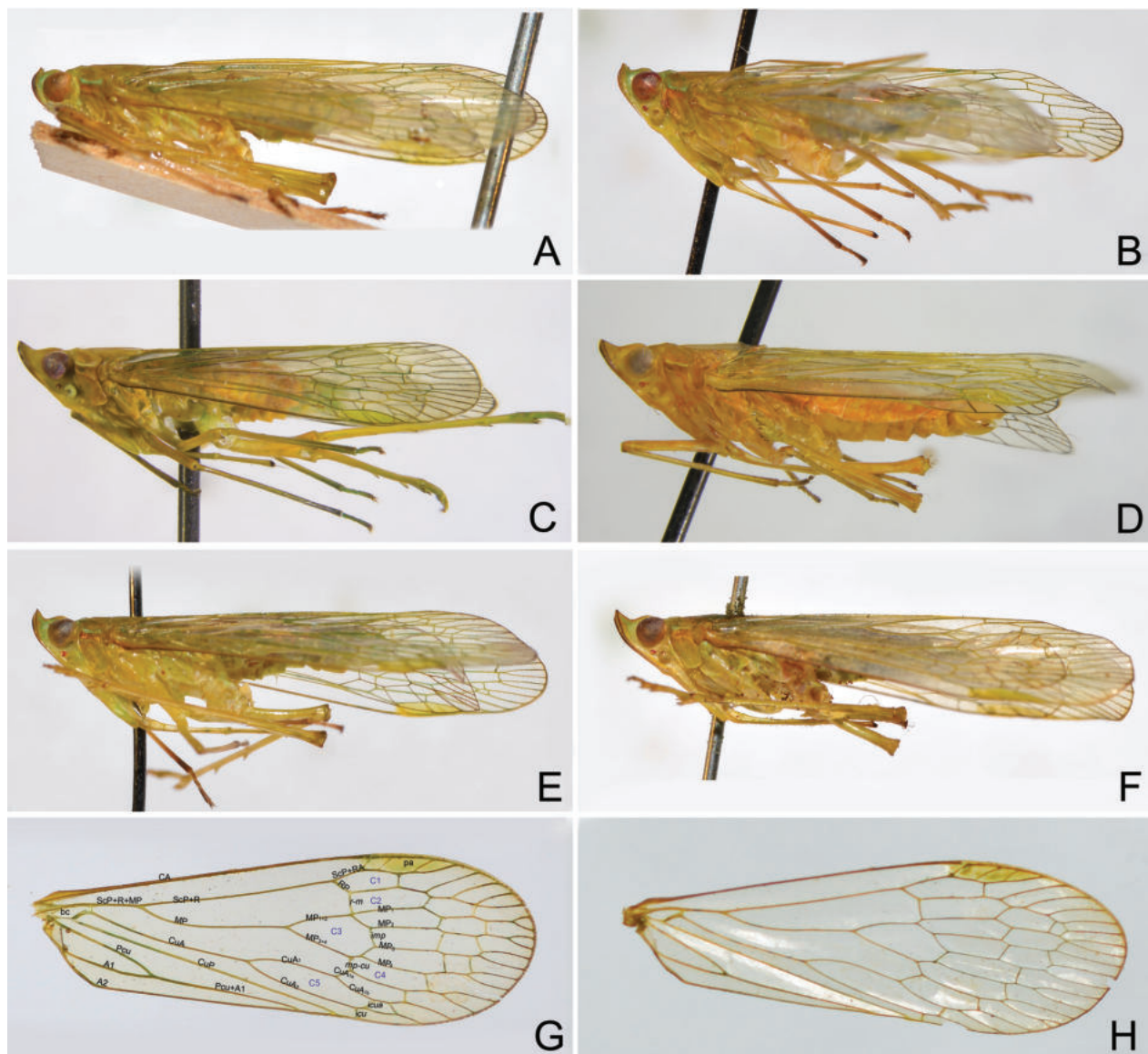


Figure 2. Habitus of *Trigava* species, lateral view **A** *T. brachycephala* (Melichar), lectotype, male **B** *T. brachycephala* (Melichar), male **C** *T. obrieni* sp. nov., holotype, male **D** *T. obrieni* sp. nov., paratype, female **E** *T. peruensis* sp. nov., holotype, male **F** *T. recurva* (Melichar), lectotype, male **G** right tegmen of *T. brachycephala* **H** right tegmen of *T. recurva*.

respectively; pterostigmal area elongate, with three cells; folding lines present, the longest one between MP_3 and MP_4 .

Hindwings with ScP+R+MP short, about a half of basal cell; ScP+RA and RP forked near apical one third; MP bifurcating MP_{1+2} and MP_{3+4} little posterior to ScP+RA and CuA; CuA bifurcating CuA_1 and CuA_2 much anterior to ScP+RA and MP, CuA_1 four-branched distally, and CuA_2 not branched; transverse veinlets *r-m* and *mp-cu* slightly posterior to bifurcation of MP.

Legs long; fore femora elongate, not flattened and dilated, without spines; fore and middle tarsomeres I and II with more than two acutellae; hind tibiae distinctly elongate, nearly twice as long as hind femora, with four lateral spines and eight apical teeth; hind tarsomeres I and II with about 7–9 and 8–9 apical teeth, respectively.

Male genitalia. Pygofer, in lateral view (Figs 3E, 4E, 6E, 7E), irregularly quadrate to pentagonal, distinctly wider ventrally than dorsally, dorsal margin slightly

excavated to accommodate segment X, dorsoposterior margins angular. Gonostyles (Figs 3F, 4F, 6F, 7F) symmetrical, in lateral view (Figs 3G, 4G, 6G, 7G) broad, base narrow, expanded distally, broadest in middle, and then tapering posteriad, apex rounded; dorsal margin with a claw-like, apically sclerotised process (dorsal process), directed dorsad, outer dorsal edge with a hook-like process near middle, directed ventrad. Aedeagus (Figs 3H–J, 4H–J, 6H–J, 7H–J) with a pair of endosomal processes extended from phallosome and curved dorso-anteriad or laterad; these processes mostly membranous, sclerotised apically, tapering posteriad to form large and stout spines; phallobase sclerotised basally and membranous and inflated apically, with paired lobes with large and stout spines. Segment X long oval, in lateral view (Figs 3E, 4E, 6E, 7E), ventral margin gradually widening from base to apex; in dorsal view (Figs 3D, 4D, 6D, 7D), with apex excavated to accommodate anal style; anal style elongate and large, beyond apical ventral margin of segment X.

Female genitalia. Gonocoxae VIII (Fig. 5D) with a membranous and flattened endogonocoxal processes (Gxp), bearing tiny setae on apex. Gonapophyses VIII (Fig. 5D) with anterior connective lamina large and sclerotized, with seven teeth of varying sizes and shapes. Gonapophyses IX (Fig. 5E, F) with posterior connective lamina triangular, symmetrical, weakly bifurcated at apex, fused with the intergonocoxal plate at base. Gonoplares (Fig. 5G, H) with two lobes homologous, first lobe (lateral lobe) axe-shaped, sclerotized, large and elongate, apical margin filmy and truncate, with cluster of long setae on apex (no sensory appendage, viz. *Igava* spp.); second lobe (posterior lobe) large, broad basally and tapering posteriad, the edge membranous containing long sclerotized plate. Segment X (Fig. 5A) trapeziform, large and broad in dorsal view, apex deeply excavated to accommodate anal style; anal style small.

Diversity and distribution. *Trigava* is revised here to contain four species including two new species. The species of the genus are distributed in the north-west of South America and were recorded from Peru, Bolivia and Brazil, as far as known (Fig. 8).

Remarks. In addition to the diagnostic characters listed by O'Brien (1999), *Trigava* may be separated from *Igava* Melichar by characters diagnostic at the tribal level, such as on the tegmen and the female genitalia (Song et al. 2018). For example, the second postnodal line of the tegmen and the apical sensory appendage of gonoplares I are absent in *Trigava*, but they are present in *Igava*.

In the tribe Nersiini, *Trigava* is externally similar to the genus *Nersia* Stål, 1862, but can be distinguished from the latter by the head strongly curved upward (slightly curved upward in *Nersia*); the median carina of vertex absent (present in *Nersia*), and the tegulae lacking carina (present in *Nersia*). See also the Discussion.

Key to the species of *Trigava*

- 1 Gonostyles with dorsal process short, hook-like process situated sub-medially, curved basad (Figs 3G, 4G); ventral lobes of aedeagus without spines (Figs 3J, 4J) **2**
- Gonostyles with dorsal process elongate, hook-like process situated more basally and curved apicad (Figs 6G, 7G); ventral lobes of aedeagus with long spines (Figs 6J, 7J)..... **3**

- 2 Head with cephalic process very short, extremely curved upward 90° (even more than 90°) in front of eyes (Fig. 3B); ventral lobes of aedeagus with a minute tooth at base (Fig. 3J) ***T. brachycephala* (Melichar)**
- Head with cephalic process relatively longer, curved upward about 60° in front of eyes (Fig. 4B); ventral lobes of aedeagus without tooth at base (Fig. 4J) ***T. obrieni* Song, Malenovský & Deckert, sp. nov.**
- 3 Head with cephalic process short, extremely curved upward about 90° in front of eyes (Fig. 6B); ventral lobes of aedeagus weakly trilobed, apex produced in a long triangular lobe (Fig. 6J) ***T. peruensis* Song, O'Brien & Bartlett, sp. nov.**
- Head with cephalic process relatively longer, curved upward about 60° in front of eyes (Fig. 7B); ventral lobes of aedeagus nearly cross-shaped, base protruded anteriorly, and apex produced in a large thumb-like lobe (Fig. 7J) ***T. recurva* (Melichar, 1912)**

***Trigava brachycephala* (Melichar, 1912)**

Figs 1A, B, 2A, B, G, 3A–J

Igava brachycephala Melichar, 1912: 49, pl. II, figs 9, 11.

Igava brachycephala Melichar: Metcalf (1946): 39.

Trigava brachycephala (Melichar): O'Brien (1999): 60.

Type locality. Peru, Department of Cuzco, Quispicanchi Province, Marcapata.

Emended description. Measurements (in mm; 3♂, 1♀). Body length from apex of head to tip of tegmina: ♂ 10.8–11.1, ♀ 11.7; head length (includes: apex of cephalic process to constricted and curved part + from curved part to base of eyes): ♂ ♀ (0.2–0.3)+(0.6–0.7); head width including eyes: ♂ 1.4–1.5, ♀ 1.6; tegmen length: ♂ 9.0–9.3, ♀ 9.6.

Coloration. Head stramineous green, apical spot between intermediate carinae of frons black, intermediate carinae of frons reddish brown, lateral areas of head green. Pronotum and mesonotum stramineous green, upper lateral carinae of pronotum green. Tegmina and hindwings membrane hyaline, veins green to greenish yellow, pterostigmal area more or less greenish ochraceous. Legs yellowish brown, base, apex and apical spines of tibiae fuscous. Abdomen dorsally and ventrally greenish ochraceous.

Structure. Head with cephalic process very short, in lateral view (Fig. 3B), strongly curved upward about 90° (or more than 90° in lectotype, Fig. 2A) in front of eyes. Vertex (Fig. 3A) broad, with ratio of length at midline to width between eyes (0.9–1.0):1. Frons (Fig. 3C) flat, relatively broad, with ratio of length at midline to maximum width 2.0:1, intermediate and median carinae obscure.

Male genitalia. Pygofer in lateral view (Fig. 3E) with ratio of ventral to dorsal width about 2.5:1; posterior margin produced angulately near middle. Gonostyles (Fig. 3F) large and broad, dorsal process short, acute apically, more or less incurved and directed dorsoanteriorly; hook-like process situated submedially, distinctly elevated above dorsal process, curved basad (Fig. 3G). Aedeagus (Fig. 3H–J) elongate, endosomal processes curved dorsoanteriorly; phallobase sclerotized and pigmented at lateral sides, membranous and slightly inflated dorsally and ventrally: dorsal lobes V-shaped at apex, directed posteriorly; a pair

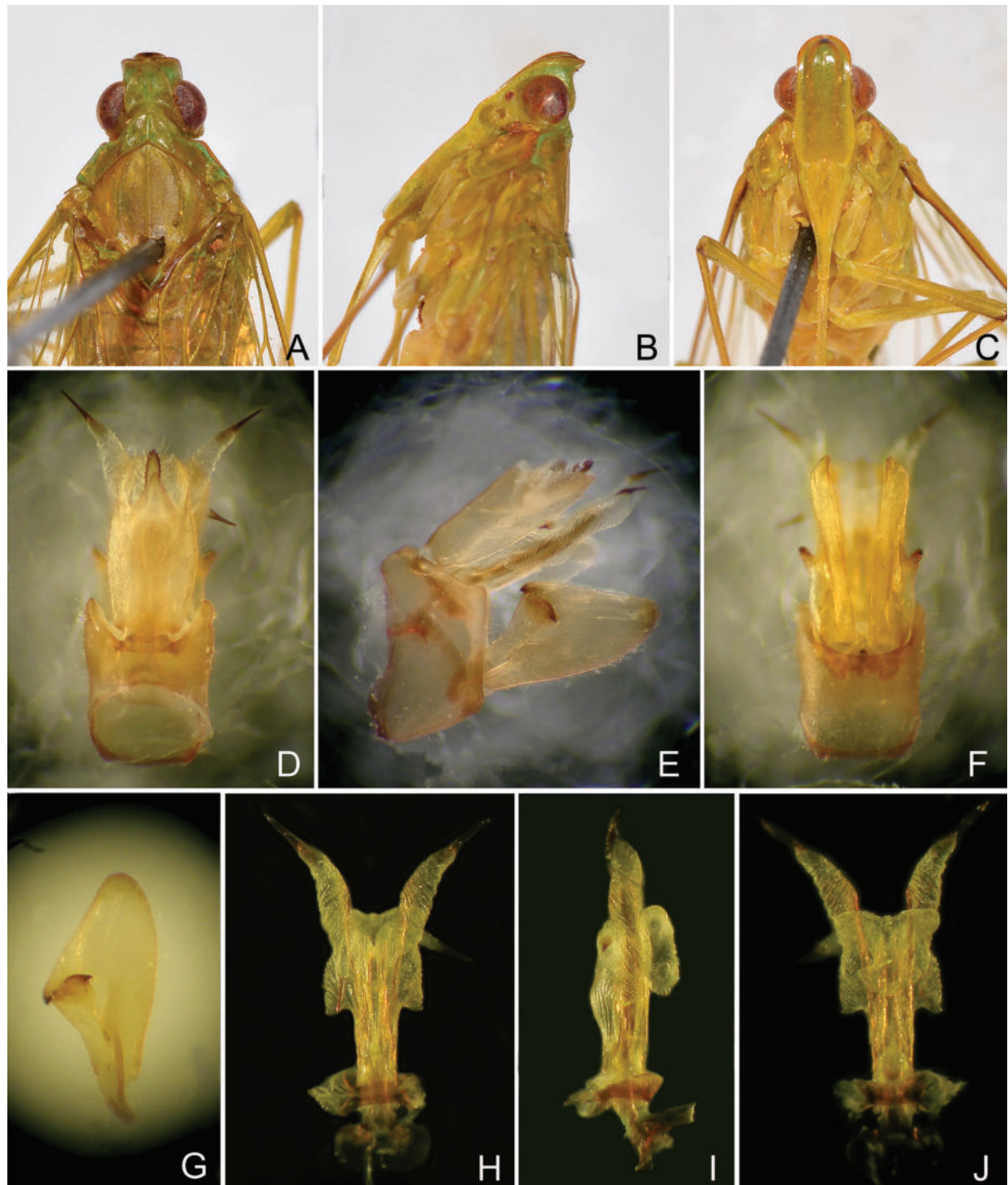


Figure 3. *Trigava brachycephala* (Melichar), male **A** head and thorax, dorsal view **B** same, lateral view **C** same, ventral view **D** pygofer and segment X, dorsal view **E** pygofer, gonostyles, aedeagus and segment X, right lateral view **F** pygofer and gonostyles, ventral view **G** left gonostyle, lateral view **H** aedeagus, dorsal view **I** aedeagus, lateral view **J** aedeagus, ventral view.

of lateral lobes large and elongate, base conical, directed anterolaterad, mostly tapering apicad, apex with a large long spine, directed posteriad; ventral lobes small, butterfly-shaped, base expanded laterad, with a minute tooth, apex produced in a pair of short and stout lobes, without spine, directed laterad. Segment X (Fig. 3D, E), in dorsal view, lateral margins more or less convex near middle, with ratio of length to width near middle about 2.0:1.

Female genitalia. As in generic description.

Type material examined. Lectotype (here designated), ♂, (1) “Peru, Marcapata”; (2) “*Enh. brachycephala* [Melichar’s handwriting], det. Melichar”; (3) “Typus” [dark red label]; (4) “Collectio Dr. L. Melichar, Moravské museum Brno”; (5) “Syntypus, *Igava brachycephala* sp.n. Melichar, 1912, ♂ [P. Lauterer’s handwriting], P. Lauterer det. 1991”; (7) “Syn- typus” [red label]; (7) “Invent. č. 4941/Ent., Mor. muzeum, Brno”; (8) “*Trigava brachycephala* [Zhi-Shun Song’s handwriting] det. Z.S. Song 2014”; (9) “Lectotypus ♂, *Igava brachycephala* Melichar, 1912, designated by Z.S. Song & I. Malenovský, 2023” [newly added red label] (MMBC; dry-mounted, glued on a rectangular card label, abdomen detached, macerated, preserved in glycerol and enclosed in a glass microvial placed on the same pin as the specimen). **Paralectotype**, 1♂, (1) “Peru S, Marcapata, Garlepp c.”; (2) “Coll. A. Jacobi, 1912 – 3” [green label]; (3) “*brachycephala*” [handwriting]; (4) “*Igava Mel.*” [handwriting]; (5) “Paralectotypus ♂, *Igava brachycephala* Melichar, 1912, labelled by I. Malenovský, 2023” [newly added red label] (MTD).

Other material examined. PERU: 1♂, “Peru, S.V. Garlepp”; “*Igava brachycephala* Mel. [H. Synave’s handwriting], H. Synave det., 1969” (MFNB); 1♂, 1♀, “Peru” (MTD).

Distribution. Southeastern Peru.

Remarks. Melichar (1912) described *Igava brachycephala* Melichar based on material from “Peru, Marcapata (Garlepp) (Mus. Budapest, Dresden)”. He did not state the number of the specimens he used for the description nor did he designate a holotype. One of his syntypes has been preserved in Melichar’s personal collection in MMBC and we used this male specimen for the redescription of the species. According to Article 74 of ICZN (1999), we designate the specimen in MMBC as the lectotype for *I. brachycephala* to stabilize the nomenclature. Another conspecific male with collecting data fully matching the original description has been located by us in MTD and was labelled by us as a paralectotype.

***Trigava obrieni* Song, Malenovský & Deckert, sp. nov.**

<https://zoobank.org/87633FF5-777E-4A66-9F5E-536B76E82C08>

Figs 1C, D, 2C, D, 4A–J, 5A–H

Type locality. Brazil, Rondônia State, 62 km SW Ariquemes, Fazenda, Rancho Grande.

Type material. Holotype ♂, **BRAZIL:** Rondônia, 62 km, SW Ariquemes, Fzda, Rancho Grande, 19-XI-1994, C.W. O’Brien & L.B. O’Brien leg. (LBOB; dry-mounted, pinned). **Paratypes: BRAZIL:** 1♂, 1♀, same data as holotype but 18-XI-1994 (LBOB); 1♂, same data as holotype but 4–16-XI-1997, J.E. Eger leg. (LBOB).

Diagnosis. *Trigava obrieni* sp. nov. is similar to *T. brachycephala* in most characters, but can be separated from the latter by the longer head curved upward about 60° in front of eyes (in *T. brachycephala*, the cephalic process is distinctly shorter and curved upward more than 90° in front of eyes) and the ventral lobes of the aedeagus without a tooth at the base (with a minute tooth at base in *T. brachycephala*). This new species also may be differentiated from *T. recurva* (Melichar) by the gonostyles with the dorsal process short and the hook-like process situated submedially and curved basad (dorsal process distinctly elongate, hook-like process situated more basally and curved apicad in *T. recurva*), and the ventral lobes of the aedeagus without long spines (with long spines in *T. recurva*).

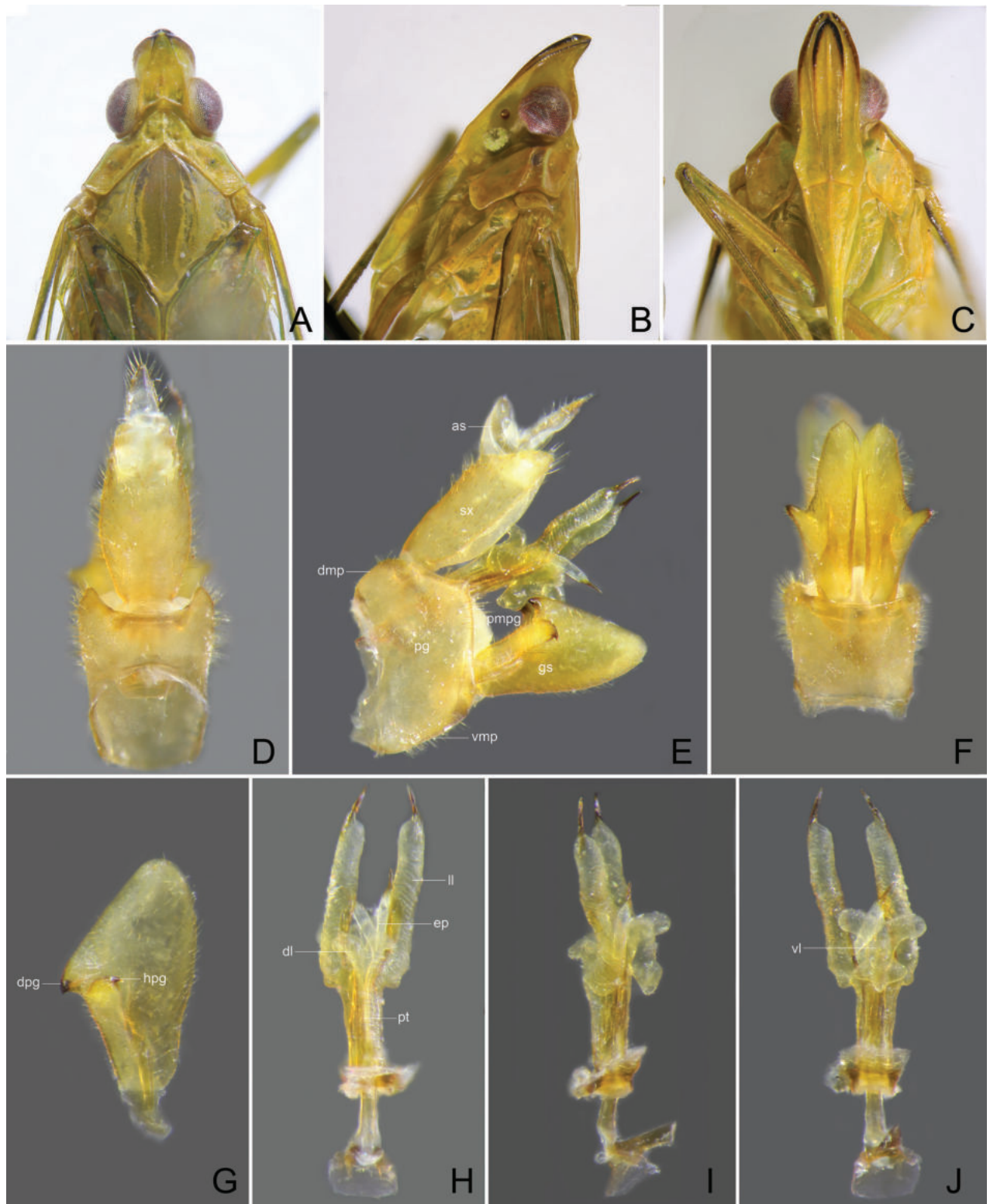


Figure 4. *Trigava obrieni* sp. nov., holotype, male **A** head and thorax, dorsal view **B** same, lateral view **C** same, ventral view **D** pygofer and segment X, dorsal view **E** pygofer, gonostyles, aedeagus and segment X, right lateral view **F** pygofer and gonostyles, ventral view **G** left gonostyle, lateral view **H** aedeagus, dorsal view **I** aedeagus, lateral view **J** aedeagus, ventral view. Abbreviations: as, anal style; dl, dorsal lobes of phallosome; dmp, dorsal margin of pygofer; dpg, dorsal process of gonostyle; ep, endosomal processes; gs, gonostyle; hpg, hook-like process of gonostyle; ll, lateral lobes of phallosome; pg, pygofer; pt, phallosome; sx, segment X; vl, ventral lobes of phallosome; vmp, ventral margin of pygofer.

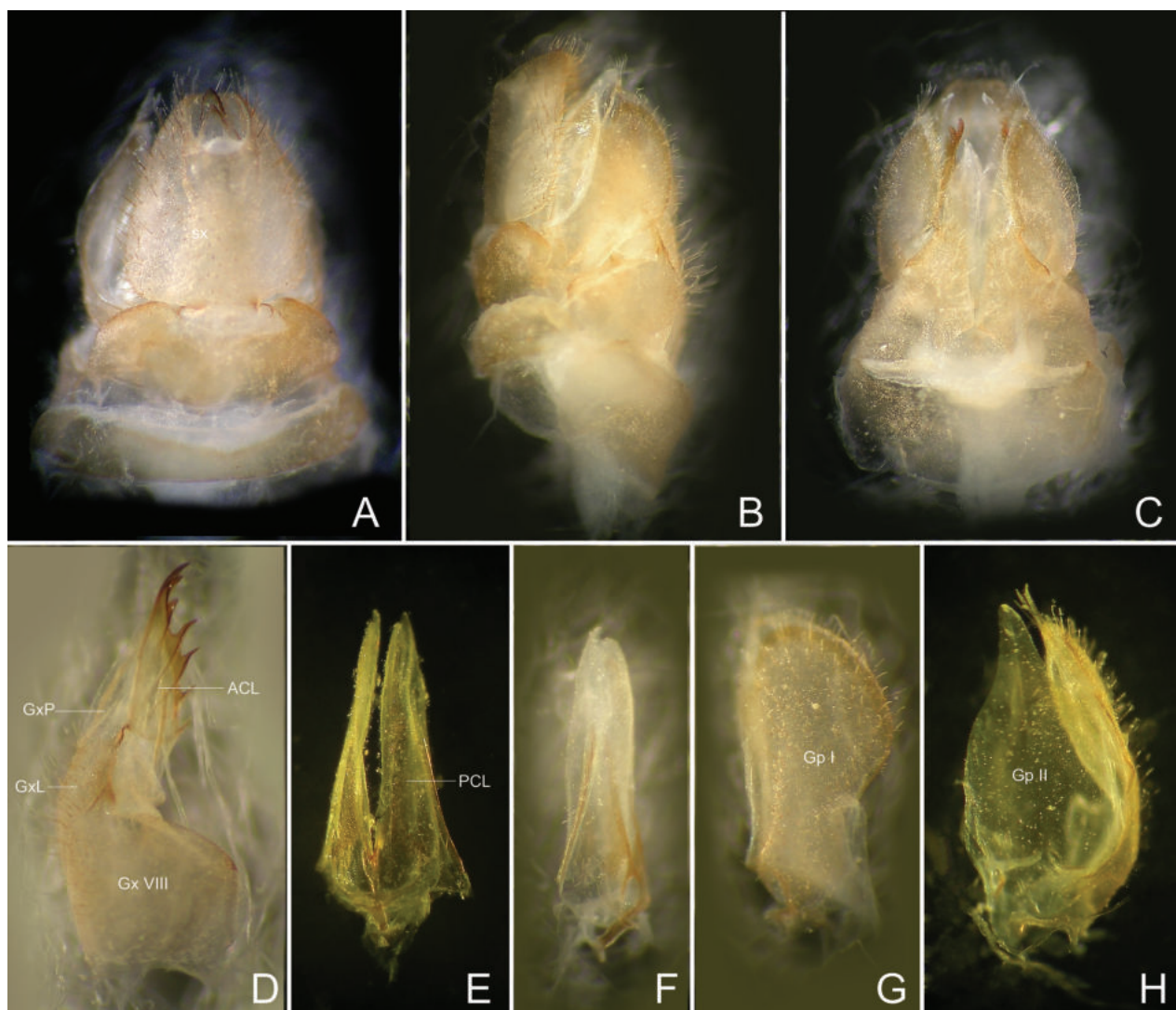


Figure 5. *Trigava obrieni* sp. nov., paratype, female **A** terminalia, dorsal view **B** same, lateral view **C** same, ventral view **D** gonapophysis VIII, lateral view **E** gonapophysis IX, ventral view **F** gonapophysis IX, lateral view **G** gonoplac, lateral view **H** gonoplac, dorsal view. Abbreviations: ACL, anterior connective lamina of gonapophysis VIII; Gp I, first lobe (lateral lobe) of gonoplac; Gp II, second lobe (posterior lobe) of gonoplac; GxL, endogonocoxal lobe; GxP, endogonocoxal process; Gx VIII, gonocoxae VIII; PCL, posterior connective lamina; sx, segment X.

Description. Measurements (in mm; 3♂, 1♀). Body length from apex of head to tip of tegmina: ♂ 10.8–11.2, ♀ 12.5; head length (includes: apex of cephalic process to constricted and curved part + from curved part to base of eyes): ♂♀ (0.4–0.5)+(1.0–1.1); head width including eyes: ♂ 1.4–1.5, ♀ 1.6; tegmen length: ♂ 8.5–8.9, ♀ 9.8.

Coloration. Head stramineous green, lateral and intermediate carinae of frons in front of eyes black to blackish brown, lateral areas in front of eyes green. Pronotum and mesonotum stramineous green, upper lateral carinae of pronotum green. Tegmina and hindwings with membrane hyaline, costal margin black to dark brown, veins green to greenish yellow, pterostigmal area more or less greenish ochraceous. Legs yellowish brown, base, apex and apical spines of tibiae fuscous. Abdomen dorsally and ventrally greenish ochraceous.

Structure. Head with cephalic process relatively long, in lateral view (Fig. 4B), curved upward about 60° in front of eyes. Vertex (Fig. 4A) broad, with ratio of

length at midline to width between eyes (1.5–1.6):1. Frons (Fig. 4C) flat, relatively broad, with ratio of length at midline to maximum width 2.4:1.

Male genitalia. Pygofer in lateral view (Fig. 4E) with ratio of ventral to dorsal width about 1.7:1; posterior margin produced into a small, apically obtuse process near middle. Gonostyles (Fig. 4F) large and broad, dorsal process short, acute apically, more or less incurved and directed dorsoanteriorly; hook-like process placed submedially, horizontal with dorsal process, curved basad (Fig. 4G). Aedeagus (Fig. 4H–J) slender and elongate, endosomal processes curved dorsoanteriorly; phallobase sclerotized and pigmented at lateral sides, membranous and slightly inflated dorsally and ventrally: dorsal lobes V-shaped at apex, curved and directed posterolaterad; a pair of lateral lobes large and elongate, thumb-like, apex with a long spine, directed posteriorly; ventral lobe small, butterfly-shaped, base expanded laterad, apex produced in a pair of thumb-like moderate lobes, without spine, directed laterad. Segment X (Fig. 4D, E), in dorsal view, with lateral margins more or less convex near middle, with ratio of length to width near middle about 2.0:1.

Female genitalia. As in generic description (Fig. 5A–H).

Etymology. The new species is named after the late Dr Charlie W. O'Brien, former professor at Florida Agricultural and Mechanical University, USA, one of the world's top experts in weevils, collector of the type specimens and husband of Dr Lois B. O'Brien, in recognition of their kindest help and support to the first author when he visited USA in 2017. The species name is to be treated as a noun in genitive case.

Distribution. Northwestern Brazil.

***Trigava peruensis* Song, O'Brien & Bartlett, sp. nov.**

<https://zoobank.org/F2AA6095-E279-4772-A1B8-CE3F0B2774F3>

Figs 1E, 2E, 6A–J

Type locality. Peru, Department of Cuzco, Cosñipata Valley.

Type material. *Holotype* ♂, **PERU**: "Peru, Dep Cuzco, Cosnipata-Ebene, 1000 m, XI-XII-[19]00, S.V. Garlepp leg." (MFNB; dry-mounted, pinned).

Diagnosis. *Trigava peruensis* sp. nov. is externally similar to *T. brachycephala*, but can be separated from the latter by the gonostyles with the dorsal process elongate and the hook-like process placed more basally and curved apicad (dorsal process short and hook-like process placed submedially and curved basad in *T. brachycephala*), and the ventral lobes of the aedeagus with long spines (without long spines in *T. brachycephala*). It can be distinguished from *T. recurva* by the shorter cephalic process curved upward about 90° in front of the eyes (the longer head curved upward about 60° in front of eyes in *T. recurva*) and the ventral lobes of the aedeagus weakly trilobed (nearly cross-shaped in *T. recurva*).

Description. Measurements (in mm; 1♂). Body length from apex of head to tip of tegmina: 11.7; head length (includes: apex of cephalic process to constricted and curved part + from curved part to base of eyes): 0.3+1.1; head width including eyes: 1.6; tegmen length: 9.7.

Coloration. Head stramineous green, lateral carinae of vertex and frons reddish brown, intermediate carinae of frons in front of eyes black to reddish brown, lateral areas in front of eyes green. Pronotum and mesonotum stramineous green,

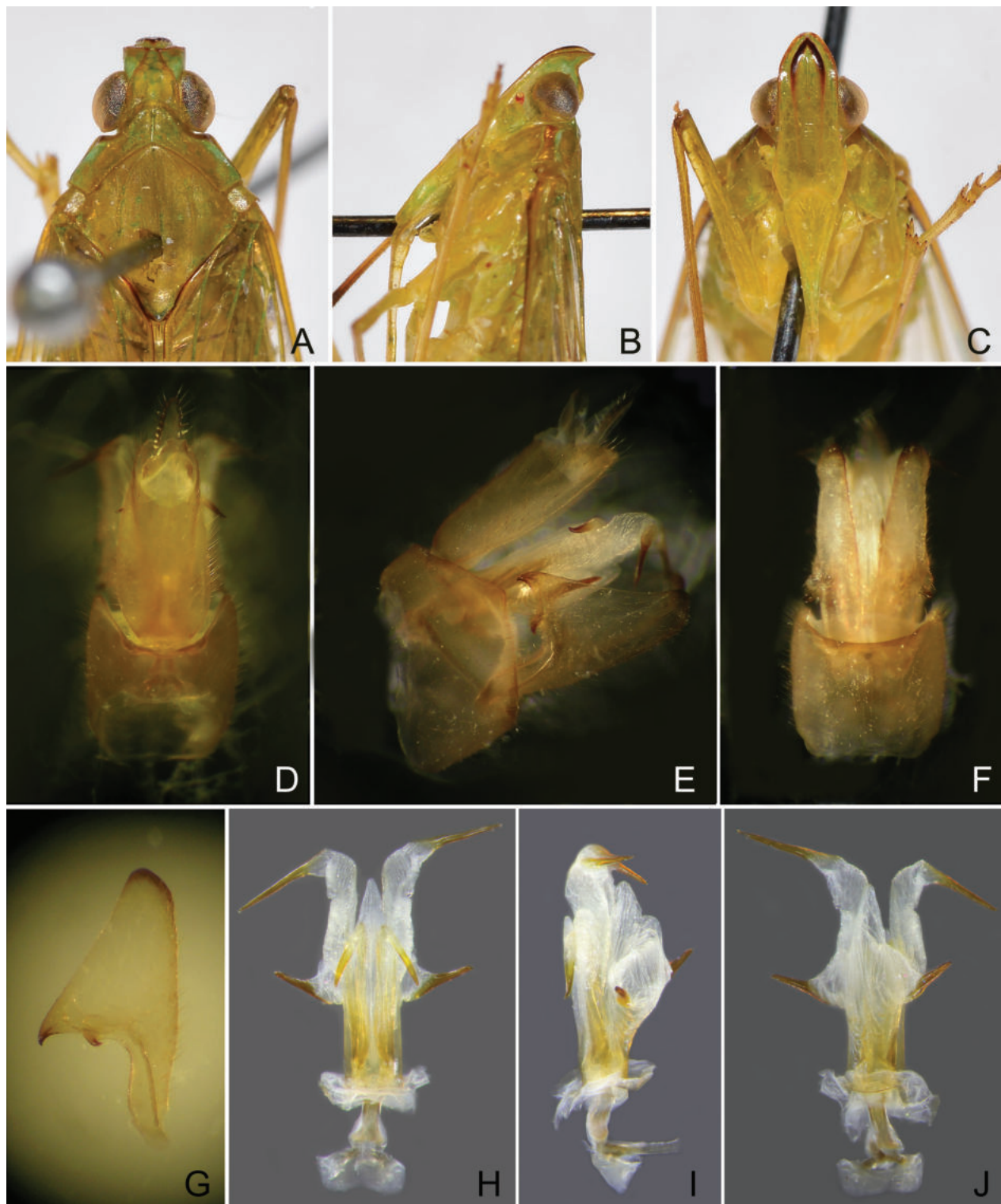


Figure 6. *Trigava peruensis* sp. nov., holotype, male **A** head and thorax, dorsal view **B** same, lateral view **C** same, ventral view **D** pygofer and segment X, dorsal view **E** pygofer, gonostyles, aedeagus and segment X, right lateral view **F** pygofer and gonostyles, ventral view **G** left gonostyle, lateral view **H** aedeagus, dorsal view **I** aedeagus, lateral view **J** aedeagus, ventral view.

upper lateral carinae of pronotum green. Tegmina and hindwings with membrane hyaline, costal margin dark brown, veins green to greenish yellow, pterostigmal area greenish ochraceous. Legs yellowish brown, base, apex and apical spines of tibiae fuscous. Abdomen dorsally and ventrally greenish ochraceous.

Structure. Head with cephalic process short, in lateral view (Fig. 6B), curved upward nearly 90° in front of eyes. Vertex (Fig. 6A) broad, with ratio of length at midline to width between eyes (1.1–1.2):1. Frons (Fig. 6C) flat, relatively broad, with ratio of length at midline to maximum width 2.2:1, intermediate and median carinae obscure.

Male genitalia. Pygofer in lateral view (Fig. 6E) with ratio of ventral to dorsal width about 2.0:1; posterior margin produced angulately near middle. Gonostyles (Fig. 6F) large and broad, dorsal process elongate, triangular, acute apically, more or less incurved and directed dorsoanteriorly; hook-like process placed sub-basally, below dorsal process, curved apicad (Fig. 6G). Aedeagus (Fig. 6H–J) large and stout, endosomal processes curved dorsoanteriorly; phallobase sclerotized and pigmented at lateral sides, membranous and slightly inflated dorsally and ventrally: dorsal lobes small, V-shaped at apex, directed posteriorly; a pair of lateral lobes large and elongate, thumb-like, tapering apicad, apex with a large long spine, directed posterolaterad; ventral lobes large, weakly trilobed, base protruded laterad, with a large long spine, apex produced in a long triangular lobe, without spine, directed posteriorly. Segment X (Fig. 6D, E), in dorsal view, with lateral margins more or less convex near middle, with ratio of length to width near middle about 2.1:1.

Female. Unknown.

Etymology. The new species is named for its occurrence in Peru. The specific epithet 'peruensis' is to be treated as a Latinized adjective in nominative singular.

Distribution. Southeastern Peru.

Trigava recurva (Melichar, 1912)

Figs 1F, 2F, H, 7A–J

Igava recurva Melichar, 1912: 49, pl. II, figs 8, 10.

Igava recurva Melichar: Metcalf (1946): 39.

Trigava recurva (Melichar): O'Brien (1999): 60.

Type locality. Bolivia, La Paz Department, Mapiri.

Emended description. Measurements (in mm; 1♂, 1♀). Body length from apex of head to tip of tegmina: ♂ 13.8, ♀ 14.1; head length (includes: apex of cephalic process to constricted and curved part + from curved part to base of eyes): ♂♀ 0.6+(0.9–1.0); head width including eyes: ♂ 1.7, ♀ 1.6; tegmen length: ♂ 11.4, ♀ 11.7.

Coloration. Head stramineous green, lateral carinae of vertex reddish brown, lateral and intermediate carinae of frons in front of eyes black to reddish brown, lateral areas in front of eyes green. Pronotum and mesonotum stramineous green, upper lateral carinae of pronotum green. Tegmina and hindwings with membrane hyaline, costal margin black to dark brown, veins green to greenish yellow, pterostigmal area more or less greenish ochraceous. Legs yellowish brown, base, apex and apical spines of tibiae fuscous. Abdomen dorsally and ventrally greenish ochraceous.

Structure. Head with cephalic process relatively long, in lateral view (Fig. 7B), curved upward about 60° in front of eyes. Vertex (Fig. 7A) broad, with ratio of length at midline to width between eyes (1.6–1.7):1. Frons (Fig. 7C) flat, relatively broad, with ratio of length at midline to maximum width 2.6:1.

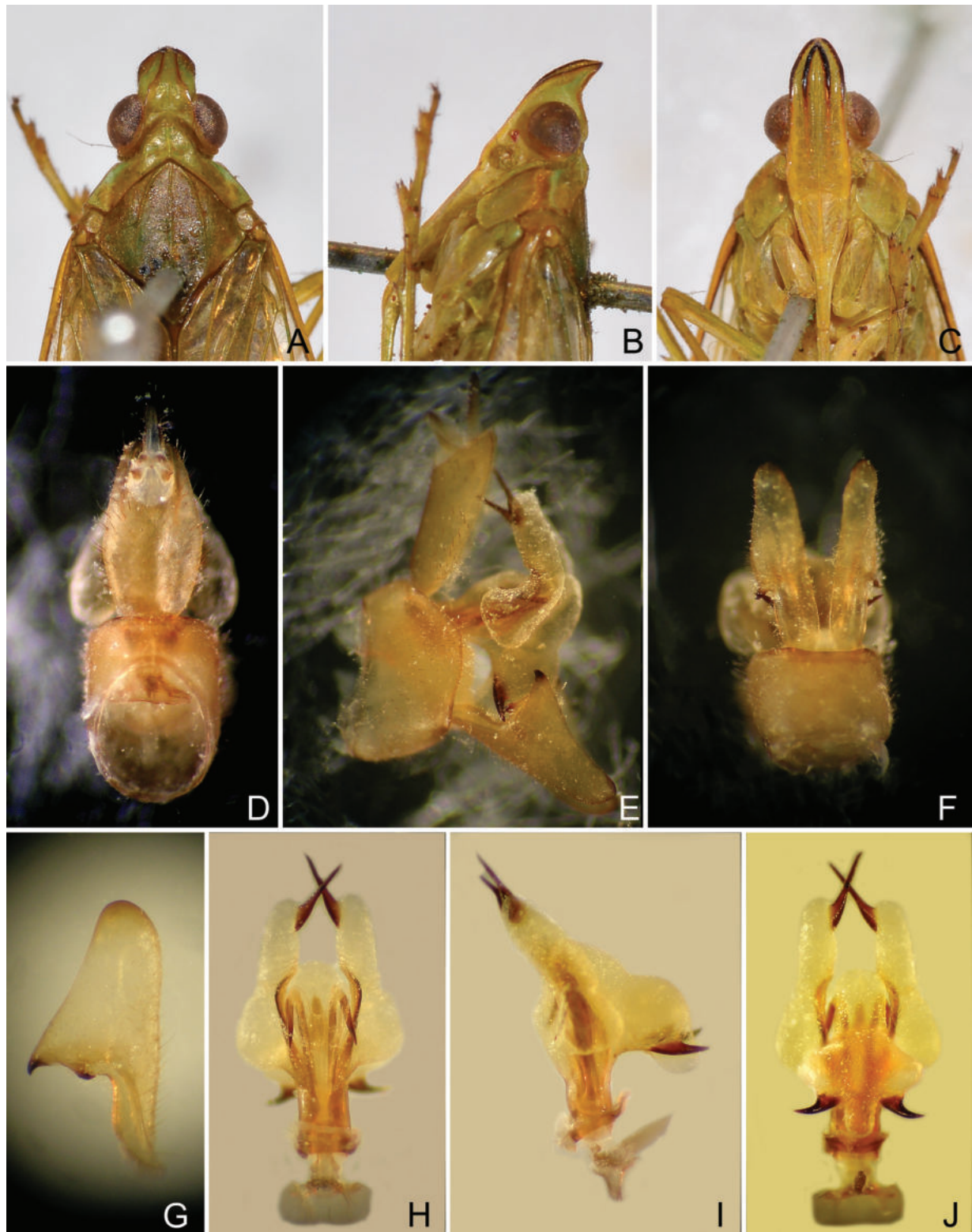


Figure 7. *Trigava recurva* (Melichar), lectotype, male **A** head and thorax, dorsal view **B** same, lateral view **C** same, ventral view **D** pygofer, and segment X, dorsal view **E** pygofer, gonostyles, aedeagus and segment X, right lateral view **F** pygofer and gonostyles, ventral view **G** left gonostyle, lateral view **H** aedeagus, dorsal view **I** aedeagus, lateral view **J** aedeagus, ventral view.

Male genitalia. Pygofer in lateral view (Fig. 7E) with ratio of ventral to dorsal width about 2.1:1; posterior margin broadly angular near middle. Gonostyles (Fig. 7F) large and broad, dorsal process elongate, triangular, acute apically, more

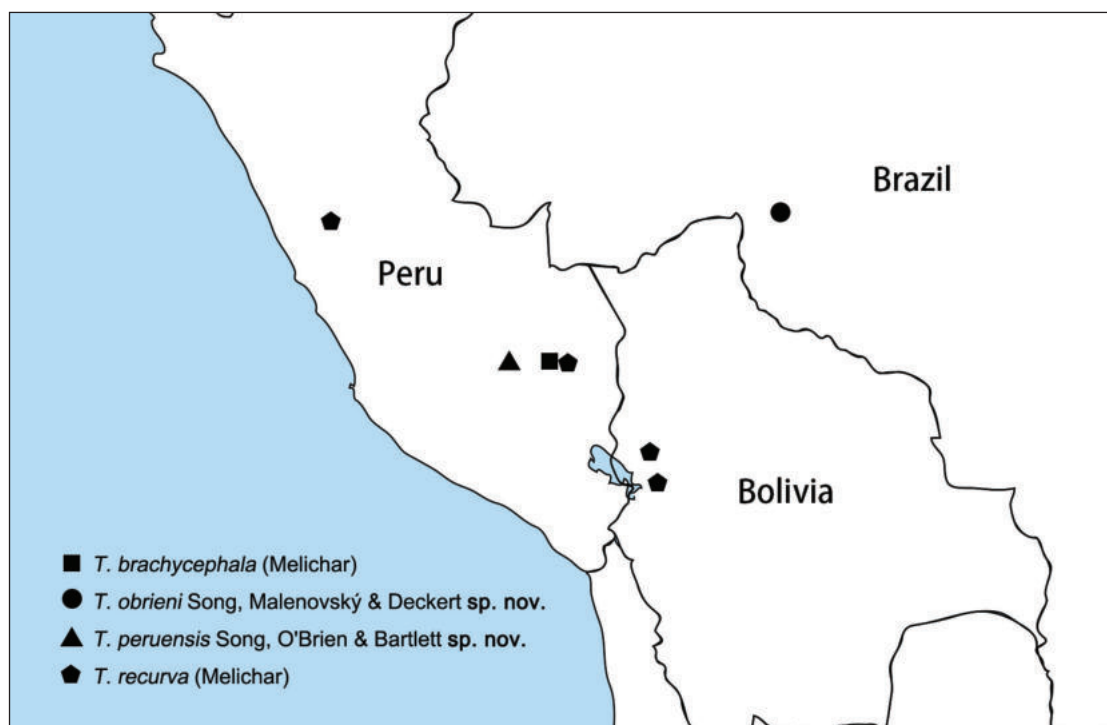


Figure 8. Geographical distribution of *Trigava* species.

or less incurved and directed dorsoanteriorly; hook-like process situated sub-basally, slightly below dorsal process, curved apicad (Fig. 7G). Aedeagus (Fig. 7H–J) large and stout, endosomal processes curved dorsoanteriorly; phallobase sclerotized and pigmented at lateral sides, membranous and slightly inflated dorsally and ventrally: dorsal lobes small, U-shaped at apex, directed posteriorly; a pair of lateral lobes large and elongate, base rounded and expanded laterad, remaining thumb-like, subapex with a large long spine, directed posteriorly; ventral lobes large, nearly cross-shaped in ventral view (Fig. 7J), base protruded anteriorly, middle expanded laterad, with a large and stout spine, apex produced in a large thumb-like lobe, without spine, directed posteriorly. Segment X (Fig. 7D, E), in dorsal view, lateral margins more or less convex near middle, with ratio of length to width near middle about 1.8:1.

Female genitalia. As in generic description.

Type material examined. **Lectotype** (here designated), ♂, (1) “Bolivia, Mapi-ri”; (2) “*recurva* [Melichar’s handwriting], det. Melichar”; (3) “Typus” [dark red label]; (4) “Collectio Dr. L. Melichar, Moravské museum Brno”; (5) “Syntypus, *Igava recurva* sp.n. Melichar, 1912, ♂ [P. Lauterer’s handwriting], P. Lauterer det 1991”; (6) “Syn- typus” [red label]; (7) “Invent. č. 4942/Ent., Mor. muzeum, Brno”; (8) “*Trigava recurva* (Melichar) [Zhi-Shun Song’s handwriting] det. Z.S. Song 2014”; (9) “Lectotypus ♂, *Igava recurva* Melichar, 1912, desig. by Z. S. Song & I. Malenovský, 2023” [newly added red label] (MMBC). **Paralectotype**, 1♀, (1) “Bolivia N, Yungas, Garlepp c.”; (2) “Coll. A. Jacobi, 1912 – 3” [green label]; (3) “*Enhydria recurva* M” [handwriting]; (4) “Paralectotypus ♀, *Igava recurva* Melichar, 1912, labelled by I. Malenovský, 2023” [newly added red label] (MTD).

Distribution. Northwestern Bolivia, southern Peru (Melichar 1912).

Remarks. *Igava recurva* Melichar was described based on an unspecified number of specimens from “Peru, Pachitea, Marcapata; Bolivien, Mapi-ri, Yungas (Garlepp) (Mus. Budapest und Dresden)” (Melichar 1912). One male syn- type from Bolivia, Mapi-ri preserved in Melichar’s personal collection in MMBC is

here used for the redescription of the species and designated as the lectotype according to Article 74 of ICZN (1999) to stabilize the nomenclature. Another conspecific female from Bolivia with collecting data matching the original description has been located by us in MTD and was labelled as a paralectotype. Specimens from Peru have not been examined by us.

Discussion

Nersiini Emeljanov, 1983 is the second largest tribe in Dictyopharidae, comprising 26 genera from the New World, mostly distributed in the Neotropical region with a few species in the Nearctic region (Emeljanov 1983, 2011; Bartlett et al. 2014; Bartlett 2023; Bourgoin 2023). Nersiini displays the greatest disparity within Dictyopharidae, such as the massive size, carinate tegulae, relatively rich venation, piercing-cutting ovipositor, and bifurcated endosomal processes (Song et al. 2018). As in many other groups of Auchenorrhyncha, the New World dictyopharid fauna currently remains inadequately studied and most genera within Nersiini lack standard revisionary studies.

According to Song et al. (2018), Nersiini is polyphyletic. The genera *Dictyopharoides* s.s. Fowler, 1900, *Paramisia* Melichar, 1912, *Pharodictyon* Fennah, 1958, *Sicoris* Stål, 1862, and *Xenochasma* Emeljanov, 2011 should be excluded from Nersiini based on their morphology. Nersiini s.s. includes three clades, the *Digitocrista*⁺ clade, the *Nersia*⁺ clade and the *Trigava*⁺ clade; the last one comprises six genera: *Trigava*, *Paralappida* Melichar, 1912, *Crocodictya* Emeljanov, 2008, *Mitrops* Fennah, 1944, *Rhynchomitra* Fennah, 1944 and a new undescribed genus represented by *Dictyopharoides inficita* Melichar, 1912 (Song et al. 2018).

In the *Trigava*⁺ clade, *Trigava* is closely related to *Paralappida*, represented by two species from Brazil, but can be easily distinguished from the latter by the following characters: the head strongly curved upward (slightly curved upward in *Paralappida*); the intermediate carinae of the frons approaching to the frontoclypeal suture (to middle of eyes in *Paralappida*); the posterior margin of the pronotum not notched (with a deep narrow notch in *Paralappida*); and the tegulae lacking a carina (present in *Paralappida*).

The four species of *Trigava* are very similar in external morphology and can be divided into two distinct lineages based on the differences in the male genitalia. Within the *brachycephala* lineage including *T. brachycephala* and *T. obrieni* sp. nov., the gonostyles have a shorter dorsal process and the hook-like process situated submedially and curved basad, and the ventral lobes of the aedeagus lack long spines; while in the *recurva* lineage including *T. recurva* and *T. peruen-sis* sp. nov., the gonostyles have an elongate dorsal process and the hook-like process situated more basally and curved apicad, and the ventral lobes of the aedeagus possess a pair of long spines.

Acknowledgements

We are grateful to Christian Schmidt (Museum für Tierkunde, Dresden, Germany) for the loan of material and to Thierry Bourgoin (Muséum National d'Histoire Naturelle, Paris, France) and Vladimir M. Gnezdilov (Zoological Institute of the Russian Academy of Sciences, Saint Petersburg, Russia) for their useful comments on the manuscript. We also wish to thank Dr Mike Wilson for his editorial help.

Additional information

Conflict of interest

The authors have declared that no competing interests exist.

Ethical statement

No ethical statement was reported.

Funding

This work was supported by the grants from the National Natural Science Foundation of China (no. 31970442) and Qing Lan Project of Jiangsu Province, China to ZSS and by the grant of the Moravian Museum in Brno from the Ministry of Culture of the Czech Republic as part of its long-term conceptual development program for research institutions (ref. MK000094862).


Author contributions

Conceptualization, visualization, writing – original draft: ZSS. Resources: LBO, IM, JD. Investigation, validation: ZSS, LBO, IM, CB. Writing – review and editing: ZSS, CB, IM, JD.

Author ORCIDs

Zhi-Shun Song  <https://orcid.org/0000-0002-5449-4646>

Igor Malenovský  <https://orcid.org/0000-0001-8840-2263>

Jürgen Deckert  <https://orcid.org/0000-0003-4211-4463>

Charles R. Bartlett  <https://orcid.org/0000-0001-9428-7337>

Data availability

All of the data that support the findings of this study are available in the main text.

References

- Bartlett CR (2023) Planthoppers of North America. <https://sites.udel.edu/planthoppers/> [Accessed on 10 March 2023]
- Bartlett CR, O'Brien LB, Wilson SW (2014) A review of the Planthoppers (Hemiptera, Fulgoroidea) of the United States. *Memoirs of the American Entomological Society* 50: 1–287.
- Bourgoin T (1993) Female genitalia in Hemiptera Fulgoromorpha, morphological and phylogenetic data. *Annales de la Société Entomologique de France* 29(3): 225–244. <https://doi.org/10.1080/21686351.1993.12277686> [Nouvelle Série]
- Bourgoin T (2023) FLOW (Fulgoromorpha Lists On the Web): a world knowledge base dedicated to Fulgoromorpha. Version 8. <http://hemiptera-databases.org/flow/> [Accessed on 18 January 2023]
- Bourgoin T, Wang RR, Asche M, Hoch H, Soulier-Perkins A, Stroiński A, Yap S, Szwed J (2015) From micropterism to hyperpterism: recognition strategy and standardized homology-driven terminology of the forewing venation patterns in planthoppers (Hemiptera: Fulgoromorpha). *Zoomorphology* 134(1): 63–77. <https://doi.org/10.1007/s00435-014-0243-6>
- Emeljanov AF (1983) Dictyopharidae from the Cretaceous deposits on the Taymyr Peninsula (Insecta, Homoptera). *Paleontologicheskij jurnal* [Палеонтологический журнал] 3: 79–85.

- Emeljanov AF (2011) Improved tribal delimitation of the subfamily Dictyopharinae and description of new genera and new species (Homoptera, Fulgoroidea, Dictyopharidae). *Entomological Review* 91(9): 1122–1145. <https://doi.org/10.1134/S0013873811090053>
- ICZN [International Commission on Zoological Nomenclature] (1999) International Code of Zoological Nomenclature. 4th Edn. The International Trust for Zoological Nomenclature c/o the Natural History Museum, London, 271 pp. <https://doi.org/10.5962/bhl.title.50608>
- Melichar L (1912) Monographie der Dictyophorinen (Homoptera). *Abhandlungen der K. K. Zoologisch-Botanischen Gesellschaft in Wien* 7(1): 1–221.
- Metcalf ZP (1946) General catalogue of the Hemiptera, Fasci. IV. Fulgoroidea, Part 8 Dictyopharidae. Smith College, Northampton, USA, 246 pp. <https://doi.org/10.1093/aesa/40.3.544>
- O'Brien LB (1999) New species of *Toropa* and *Igava* and a new genus, *Trigava* gen. n. (Hemiptera: Auchenorrhyncha: Fulgoromorpha: Dictyopharidae). *Reichenbachia* 33(1): 55–60.
- Song ZS, Webb MD, Liang AP (2016) Phylogenetic analysis of the Oriental genera of Orthopagini, 1983 (Hemiptera: Fulgoromorpha: Dictyopharidae: Dictyopharinae), with a systematic revision of the genus *Centromeria* Stål, 1870. *Zoological Journal of the Linnean Society* 178(1): 33–87. <https://doi.org/10.1111/zoj.12401>
- Song ZS, Bartlett CR, O'Brien LB, Liang AP, Bourgoin T (2018) Morphological phylogeny of Dictyopharidae (Hemiptera: Fulgoromorpha). *Systematic Entomology* 43(4): 637–658. <https://doi.org/10.1111/syen.12293>

The Trichoptera of Panama XXIV. Fifteen new species and two new country records of the caddisfly genus *Neotrichia* (Trichoptera, Hydroptilidae), with a key to all known Panamanian species

Steven C. Harris^{1,2}, Brian J. Armitage^{1,3}, Tomás A. Ríos González¹

¹ Museo de Peces de Agua Dulce e Invertebrados, Universidad Autónoma de Chiriquí, David, Panama

² Department of Biology, Pennsylvania Western University–Clarion, Clarion, PA 16214, USA

³ Sistema Nacional de Investigación de Panamá (SNI), Panama, Panama

Corresponding author: Brian J. Armitage (brian.armitage@unachi.ac.pa)

Abstract

In this paper, 15 new species of microcaddisflies in the genus *Neotrichia* Morton, 1905 (Trichoptera, Hydroptilidae) from Panama are described and illustrated: *Neotrichia abrebotella* **sp. nov.**; *Neotrichia candela* **sp. nov.**; *Neotrichia codaza* **sp. nov.**; *Neotrichia embera* **sp. nov.**; *Neotrichia flennikeni* **sp. nov.**; *Neotrichia honda* **sp. nov.**; *Neotrichia landisae* **sp. nov.**; *Neotrichia lenati* **sp. nov.**; *Neotrichia mindyae* **sp. nov.**; *Neotrichia panamensis* **sp. nov.**; *Neotrichia parajarochoita* **sp. nov.**; *Neotrichia paraxicana* **sp. nov.**; *Neotrichia snixae* **sp. nov.**; *Neotrichia spangleri* **sp. nov.**; *Neotrichia veraguasensis* **sp. nov.** In addition, two new country records are presented: *Neotrichia minutisimella* (Chambers, 1873) and *Neotrichia vibrans* Ross, 1944. Finally, the male of *N. vibrans* is re-illustrated, the female is illustrated and descriptive information given, and a key is provided to the males of all current *Neotrichia* species in Panama. There are now 45 species of *Neotrichia* and a total of 525 Trichoptera species recorded from Panama.

Key words: Aquatic insects, biodiversity, freshwater, Neotropics, protected areas



Academic editor: Ana Previšić

Received: 18 August 2023

Accepted: 8 November 2023

Published: 3 January 2024

ZooBank: <https://zoobank.org/C0589D9E-2707-4952-8673-AC6A6E6D3C77>

Citation: Harris SC, Armitage BJ, Ríos González TA (2024) The Trichoptera of Panama XXIV. Fifteen new species and two new country records of the caddisfly genus *Neotrichia* (Trichoptera, Hydroptilidae), with a key to all known Panamanian species. ZooKeys 1188: 47–90. <https://doi.org/10.3897/zookeys.1188.111346>

Copyright: © Steven C. Harris et al.

This is an open access article distributed under terms of the Creative Commons Attribution License ([Attribution 4.0 International – CC BY 4.0](https://creativecommons.org/licenses/by/4.0/)).

Introduction

A concentrated effort during the last eight years (2015–2023) has almost doubled the known caddisfly fauna of Panama from 257 to 508 species distributed among 15 families and 56 genera (e.g., Armitage et al. 2015; Harris and Armitage 2019; Harris et al. 2023). Concomitant with the increase in species was the additional gain of two families and 11 genera (e.g., Armitage et al. 2016; Armitage and Harris 2018; Armitage et al. 2022). These increases were made possible by adoption of an integrated sampling scheme involving multiple methods (primarily UV light traps and Malaise traps in combination) employed monthly for extended periods (usually January through June) at each collection site. Our knowledge of the family Hydroptilidae has been a particular beneficiary of this approach, generating more new species to science and new country records than for all other caddisfly families combined. No microcaddisfly taxa have supported this increase more than the genus *Neotrichia* Morton, 1905.

Before 2015, only three species of *Neotrichia* were known from Panama. Since then, we have added 25 new species and new country records (Table 1). Collections from selected national parks and protected areas, as well as public and private landholdings, were made during 2017–2023 and yielded 15 new species and two new country records of *Neotrichia*. Combined with the 28 known taxa, there are now 45 species of *Neotrichia* found in Panama, with 42 of them added since 2014 (31 new species and 11 new country records). The incremental additions to Panama's *Neotrichia* fauna are presented in Table 1, with associated literature references provided. We also re-illustrate the male of *Neotrichia vibrans* Ross, 1944 and provide descriptive text and illustrations for the female of that species. Finally, we provide a key to males of all 45 species of *Neotrichia* known from Panama.

The Aquatic Invertebrate Research Group (**AIRG**) at the Universidad Autónoma de Chiriquí (**UNACHI**) and its Museo de Peces de Agua Dulce e Invertebrados (**MUPADI**) is currently focused on increasing our knowledge of Trichoptera (caddisflies) and Plecoptera (stoneflies) in Panama. Toward that goal, it has secured registered projects for these two orders of aquatic insects. The new taxonomic information presented in this paper are a direct result of executing these projects.

Table 1. Progression of *Neotrichia* species added to Panama's caddisfly fauna beginning in 2015*. The left column indicates the sequence numbers in The Trichoptera of Panama publication series (citations below).

Trichoptera of Panama	Year	Number of new species	Number of new country records	Species
I	2015		1	<i>Neotrichia canixa</i> (Mosely, 1937)
II	2015	2		<i>Neotrichia pamela</i> Harris & Armitage, 2015; <i>Neotrichia parabullata</i> Harris & Armitage, 2015
IV	2016		5	<i>Neotrichia esmalda</i> (Mosely, 1937); <i>Neotrichia hiaspa</i> (Mosely, 1937); <i>Neotrichia tuxtla</i> Bueno-Soria, 1999; <i>Neotrichia unamas</i> Botosaneanu (in Botosaneanu and Alkins-Koo 1993); <i>Neotrichia xicana</i> (Mosely, 1937)
V	2018	3		<i>Neotrichia anzuelo</i> Armitage & Harris, 2018; <i>Neotrichia collierorum</i> Armitage & Harris, 2018; <i>Neotrichia tatianae</i> Armitage & Harris, 2018
VI	2018	1		<i>Neotrichia atopa</i> Thomson & Armitage, 2018
X	2019	4		<i>Neotrichia carlsoni</i> Harris & Armitage, 2019; <i>Neotrichia rambala</i> Harris & Armitage, 2019; <i>Neotrichia serrata</i> Harris & Armitage, 2019; <i>Neotrichia starki</i> Harris & Armitage, 2019
	2020	4		<i>Neotrichia espinosa</i> Armitage & Harris, 2020; <i>Neotrichia michaeli</i> Armitage & Harris, 2020; <i>Neotrichia pierpointorum</i> Armitage & Harris, 2020; <i>Neotrichia yayas</i> Armitage & Harris, 2020
XVII	2021		3	<i>Neotrichia amplexor</i> Keth, 2004; <i>Neotrichia armata</i> Botosaneanu, 1993 (in Botosaneanu and Alkins-Koo 1993); <i>Neotrichia kampa</i> Oláh & Johanson, 2011
XX	2023	2		<i>Neotrichia majagua</i> Harris, Ríos & Aguirre, 2023; <i>Neotrichia solapa</i> Harris, Ríos & Aguirre, 2023
XXIV	2023	15	2	New species or new country records in this publication: <i>Neotrichia abrebotella</i> sp. nov.; <i>Neotrichia candela</i> sp. nov.; <i>Neotrichia codaza</i> sp. nov.; <i>Neotrichia embera</i> sp. nov.; <i>Neotrichia flennikenii</i> sp. nov.; <i>Neotrichia honda</i> sp. nov.; <i>Neotrichia landisae</i> sp. nov.; <i>Neotrichia lenati</i> sp. nov.; <i>Neotrichia mindyae</i> sp. nov.; <i>Neotrichia minutissimella</i> (Chambers, 1873); <i>Neotrichia panamensis</i> sp. nov.; <i>Neotrichia parajarocho</i> sp. nov.; <i>Neotrichia paraxicana</i> sp. nov.; <i>Neotrichia snixae</i> sp. nov.; <i>Neotrichia spangleri</i> sp. nov.; <i>Neotrichia veraguasensis</i> sp. nov.; <i>Neotrichia vibrans</i> Ross, 1944
Totals:		31	11	

Trichoptera of Panama publication series: I-Armitage et al. 2015; II-Harris and Armitage 2015; IV-Armitage et al. 2016; V-Armitage and Harris 2018; VI-Thomson and Armitage 2018; X-Harris and Armitage 2019; XIV-Armitage and Harris 2020; XVII-Armitage et al. 2022; XX-Harris et al. 2023; XXIV-this paper.

* Prior to 2015, three species of *Neotrichia* were known from Panama: *N. flowersi* Harris, 1990; *N. malickyi* Harris (in Harris and Tiemann 1993); and *N. tauricornis* Malicky, 1980.

Materials and methods

Protected areas or private landholdings

Some of the collection sites referenced in this paper are found on private landholdings or national protected areas. These include the following study areas. They are referred to in a number of ways throughout the text. We are constrained from unifying the naming system for these because the collection label names and administrative codes for the various locations cannot be changed. Therefore, we present the Spanish names for each study area as a header followed by any abbreviations or label names used in parentheses. In the text that follows each study area, we provide the English version of the study area name, if in common usage, as additional information.

Reserva Privada Landis

(Landis Reserve or Landis Reserva; Fig. 1A: collection location C)

Landis Reserve is a private landholding in Chiriquí Province located north of Paso Canoas, which produces plants that are used in soil stabilization efforts. The stream sampled in this study is unnamed and of first order, located near the Costa Rican border. Ultimately, it flows into the Río Chiriquí Viejo and the Pacific Ocean. The riparian corridor is primarily forested with some open areas.

Finca La Esperanza

(Fig. 1A: collection location D)

This is a large, private landholding in Chiriquí Province near San Andres bordered by the Río Cueta and the Río Gariché, both Pacific Ocean drainages. The immediate riparian corridor is forested, although this is surrounded by agricultural lands supporting a number of permanent crops such as cacao, plantains, and native tree species.

Parque Internacional La Amistad

(PILA; Fig. 1: collection locations A and B)

The Amistad International Park is a Latin American protected area shared by Panama and Costa Rica. Including a large portion of the Cordillera de Talamanca range, it encompasses approximately 401,000 ha of upland or montane tropical forest, and is an area of high diversity and endemism.

Reserva Forestal Fortuna

(Fortuna Forest Reserve; Fig. 1A: collection location F)

Part of Panama's National System of Protected Areas, the Reserva Forestal Fortuna comprises 19,000 ha of primarily cloud forests, and an additional 500 ha of buffer zones. The 1,000 ha Fortuna Reservoir is a principal component of this protected area and is part of the Pacific drainage. The Reserva is also part of the Mesoamerican Biological Corridor, which includes the adjacent, and much larger, Bosque Protector Palo Seco (Caribbean Drainage) and Parque Internacional La Amistad (Pacific and Caribbean drainage).

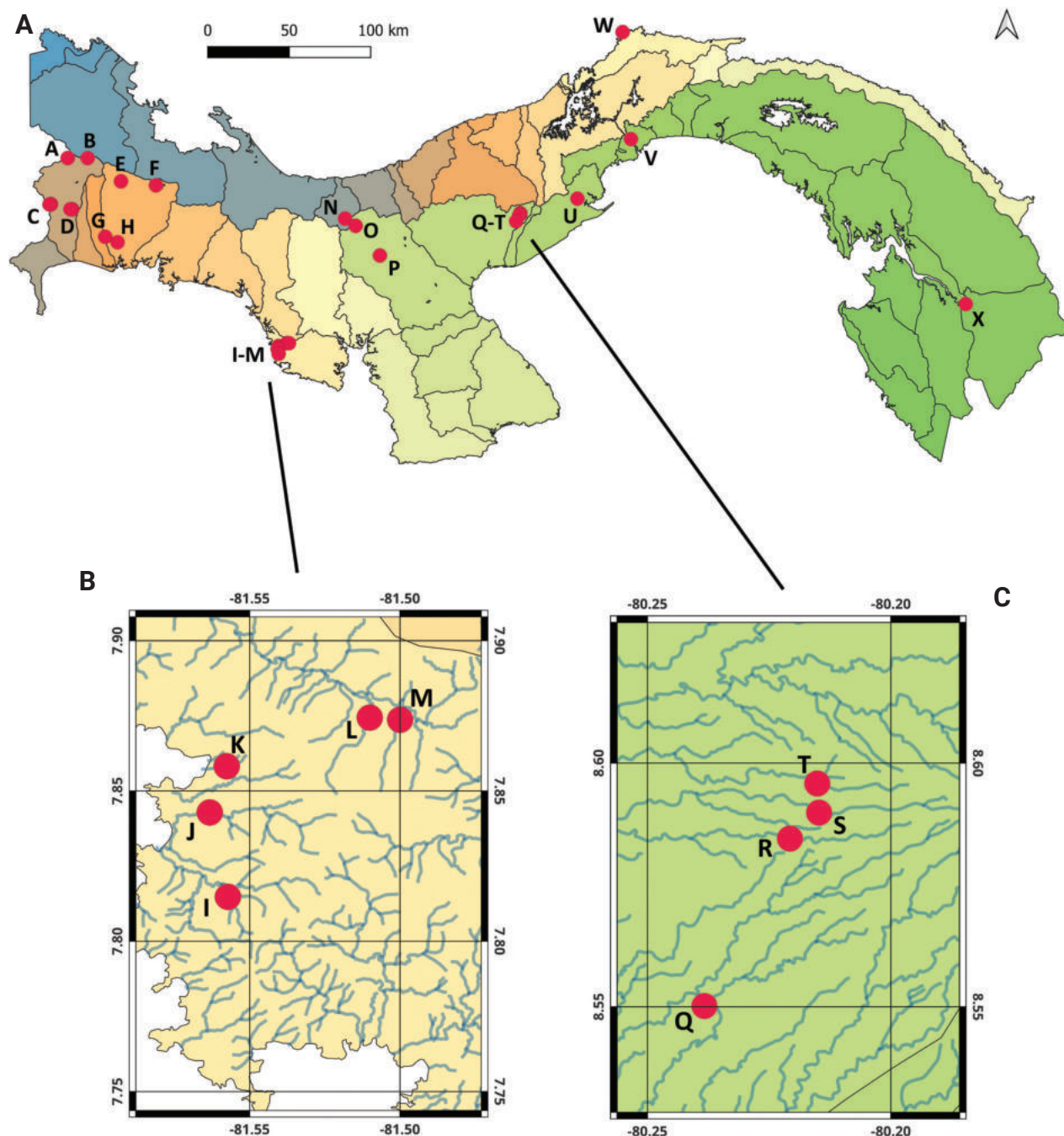


Figure 1. Maps **A** Panama, overlain by outlines of all 52 cuencas and showing all collection locations **B** collection locations (I–M) in the Pixvae area **C** collection locations (Q–T) in the Pajonal area. Key: A–Río Candela; B–Quebrada sin nombre; C–Quebrada sin nombre, locations 1 and 2; D–Quebrada sin nombre and Quebrada la Vuelta; E–Quebrada Grande; F–Quebrada Honda; G–Río Platanal; H–Quebrada San Cristobal; I–Quebrada Monita; J–Río Pixvae; K–Quebrada del Rosario; L–Quebrada La Mina; M–Quebrada El Rosario; N–Río Piedra de Moler; O–Quebrada Mulabá; P–Río Betegui; Q–Río Marica; R–Río Membrillo; S–Río Seren; T–Río Salado; U–Río Sajalices; V–Panama Canal; W–Quebrada sin nombre; X–Río Pirre. Note: Map colors are aesthetic, and do not impart any significance. Maps were generated using QGIS, v. 3.28.5-Firenze.

Parque Nacional Santa Fe

(Santa Fe NP or PNSF; Fig. 1A: collection locations N and O)

Located in the upper portion of the Santa Maria River basin in Veraguas Province, Santa Fe National Park lies near the Continental Divide and encompasses

72,636 ha. Occupying land on both the Caribbean and Pacific slopes, more than 95% of the parks area is covered with tree species which are evergreen, maintaining their leaves all year round.

Parque Nacional Altos de Campana

(Altos de Campana NP or PNAC; Fig. 1A: collection location U)

Established in 1966, Altos de Campana National Park in Panama Oeste Province is the oldest park in Panama. Covering 1,950 ha, the park lies on the Pacific slope of Panama and is covered, in part, by humid tropical and premontane forests.

Parque Nacional Darién

(Darién NP or Darién National Park; Fig. 1A: collection location X)

Darién National Park encompasses some 579,000 ha in Darién Province, adjacent to Colombia in southeastern Panama. Under formal protection since 1972, the Alto Darién Protection Forest became a national park in 1980, a World Heritage area since 1981, and, soon thereafter, a biosphere reserve by UNESCO.

All of the national parks and forest reserves indicated above are under the stewardship of the Ministerio de Ambiente de Panamá (MiAmbiente) and protected from logging and agriculture. The streams sampled under this project are 1st to 3rd order in size, are of good water quality, and are bordered by extensive, forested riparian corridors. The private landholdings above include some agricultural activities; however, all or almost all streams are associated with well-vegetated riparian corridors as they traverse the properties. Most of the streams are found in major watersheds (cuencas), including cuencas 102, 108, 115, 117, 132, 134, and 138, which are characterized in Cornejo et al. (2017). Cuenca 097 (Río Calovébora watershed; Caribbean drainage for Santa Fe National Park), Cuenca 104 (Río Escárrea; Pacific drainage), and Cuenca 116 (rivers between the Tabasará and the San Pablo; Pacific drainage), however, are not included in that book.

Methods

Collections from selected national protected areas, private landholdings, and public areas were made during 2017–2023. Both Malaise and UV light traps were used for collecting aquatic insects from streams in the national parks and protected areas of Panama. Single, overnight collections were made using UV light traps (Calor and Mariano 2012). Generally, multiple-night collections were made employing Malaise traps over four-day periods. Specimens were prepared and examined following standard methods outlined in Blahnik and Holzenthal (2004). Male genitalia were soaked in 5% KOH overnight, and washed in weakly acidified alcohol prior to examination under a dissecting scope. For illustrations, specimens were slide-mounted and viewed at 250× magnification.

Morphological terminology used for male genitalia generally follows that of Marshall (1979) and classification within the Hydroptilidae follows Thomson (2023). Paired structures are described in the singular for simplicity. Although technically, segments V through X are not part of the genitalia, traditionally descriptions of segments VII through X have been included under the genitalia

heading. We follow that practice here. If segments V and VI have distinct features, they are discussed under the male description. Total length of specimens provided in descriptions represents the length from the tip of the head to the tip of the forewing. Altitude values are given in meters above sea level (m a.s.l.). Maps were created using QGIS software, version 3.28.5-Firenze.

Holotypes listed in this publication are deposited in the University of Panama's Museo de Invertebrados (**MIUP**) or MUPADI. Paratypes and other specimens are deposited in MUPADI, the University of Minnesota Insect Collection (**UMSP**), or the first author's reference collection (**SCH**). The species listed below are in alphabetic order.

Results

Taxonomy—new species

Genus *Neotrichia* Morton, 1905

Remark. The genus *Neotrichia* (Hydroptilidae, Neotrichiinae) has a New World distribution with 211 species known from North, Central, and South America and the West Indies (Armitage et al. 2022; Gama-Neto and Passos 2023; Harris et al. 2023; Thomson 2023). In the Neotropics, there are 174 species recorded (Armitage et al. 2022; Gama-Neto and Passos 2023; Harris et al. 2023; Thomson 2023). Herein we describe and illustrate 15 new species and report two new country records for Panama.

Neotrichia abrebotella sp. nov.

<https://zoobank.org/C5D20983-BF62-4562-A8D6-C4AFF10992DB>

Fig. 2

Type locality. Panama: Chiriquí Province: Cuenca 102, Renacimiento District, Reserva Privada Landis, Location 1, Quebrada sin nombre; 8.643769°N, 82.829479°W; 755 m a.s.l.

Type material. Holotype: ♂, **PANAMA: Chiriquí Province:** Cuenca 102, Renacimiento District, Reserva Privada Landis, Location 1, Quebrada sin nombre; 8.643769°N, 82.829479°W; 755 m a.s.l.; 15–31.iii.2020; M. Landis leg.; Malaise trap; MUPADI-003-T-2023 (in alcohol). **Paratypes:** **PANAMA** • 2 ♂♂; same as holotype; except, Location 2; 8.645005°N, 82.822037°W; 575 m a.s.l.; 27.ii–6.iii.2020; M. Landis leg.; Malaise trap; MUPADI-004-T-2023 (in alcohol).

Diagnosis. *Neotrichia abrebotella* sp. nov. appears to be a member of the *N. caxima* group of Keth et al. (2015) based on the short inferior appendage with resemblance to *N. atopa* Thomson & Armitage, 2018 and *N. caxima* Mosely, 1937. It differs from *N. caxima* in the lack of sclerotized phallic processes and from *N. atopa* in the bifid appearance of the inferior appendage in lateral view and the narrow bracteole.

Description. Male. Total length 1.7–1.9 mm ($n = 3$), 18 antennal segments, wings and body brown in alcohol. **Genitalia** (Fig. 2). Abdominal segment VIII annular. Segment IX in lateral view rounded posteriorly, narrowing dorsally, anteriorly narrowing to elongate mesal apodeme; in dorsal and ventral views

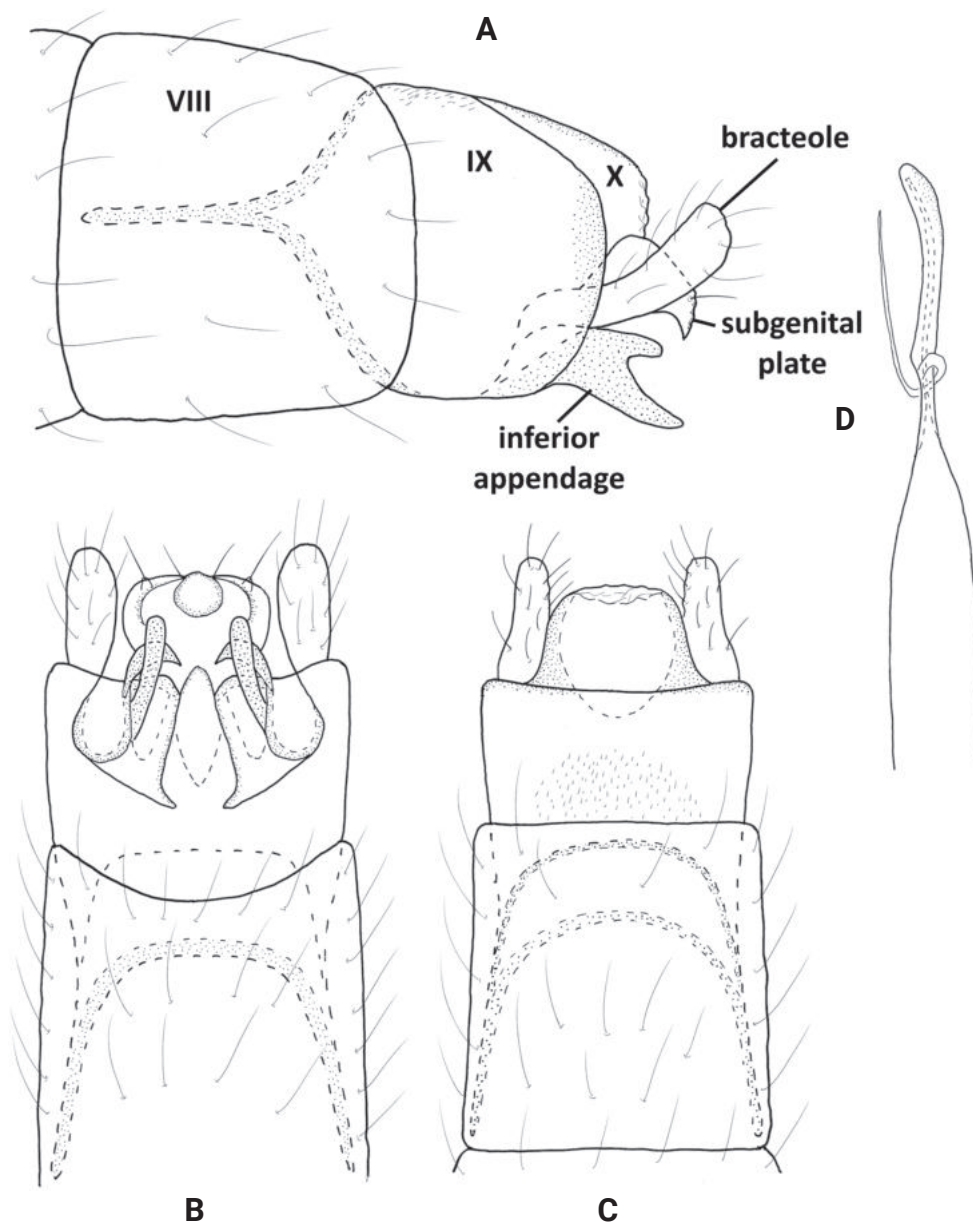


Figure 2. *Neotrichia abrebotella* sp. nov., male holotype, genitalia **A** left lateral **B** ventral **C** dorsal **D** phallus, dorsal.

quadrate, deeply incised anteriorly. Tergum X short, truncate posteriorly, tapering on lateral margins; in lateral view truncate posteriorly. Subgenital plate in lateral view wide subapically, narrowing distally to rugose, downward projecting process; in ventral view wide, truncate posteriorly with median lobe and pair of stout setae, rounded on lateral margins. Bracteole narrow basally, slightly widening distally; in dorsal and ventral views lobate. Inferior appendage short and narrow, bifid posteriorly, lower portion longer than upper; in ventral view square basally, distally bifid, dorsalmost process narrowing mesally to acute apex, ventralmost process tubular. Phallus tubular, wide basally, constricted at midlength and bearing thin paramere encircling shaft, apically thin over length.

Distribution. Panama: Chiriquí Province (Reserva Privada Landis).

Etymology. The species name *abrebotella* (bottle-opener) derives from Spanish, referring to the distinctive appearance of the inferior appendage. The name is a noun in the nominative singular standing in apposition.

***Neotrichia candela* sp. nov.**

<https://zoobank.org/D2F4AF76-536B-4F9F-8E10-3B310C115029>

Fig. 3

Type locality. Panama: Chiriquí Province: Cuenca 102, Renacimiento District, Río Candela, Finca Félix, PILA; PSPSCB-PILA-C102-2017-021; 8.90614°N, 82.72882°W; 1799 m a.s.l.

Type material. Holotype: ♂, **PANAMA: Chiriquí Province:** Cuenca 102, Renacimiento District, Río Candela, Finca Félix, PILA; PSPSCB-PILA-C102-2017-021; 8.90614°N, 82.72882°W; 1799 m a.s.l.; 1–5.ix.2017; E. Álvarez, T. Ríos, E. Pérez leg.; Malaise trap; MIUP-017-T-2023 (in alcohol).

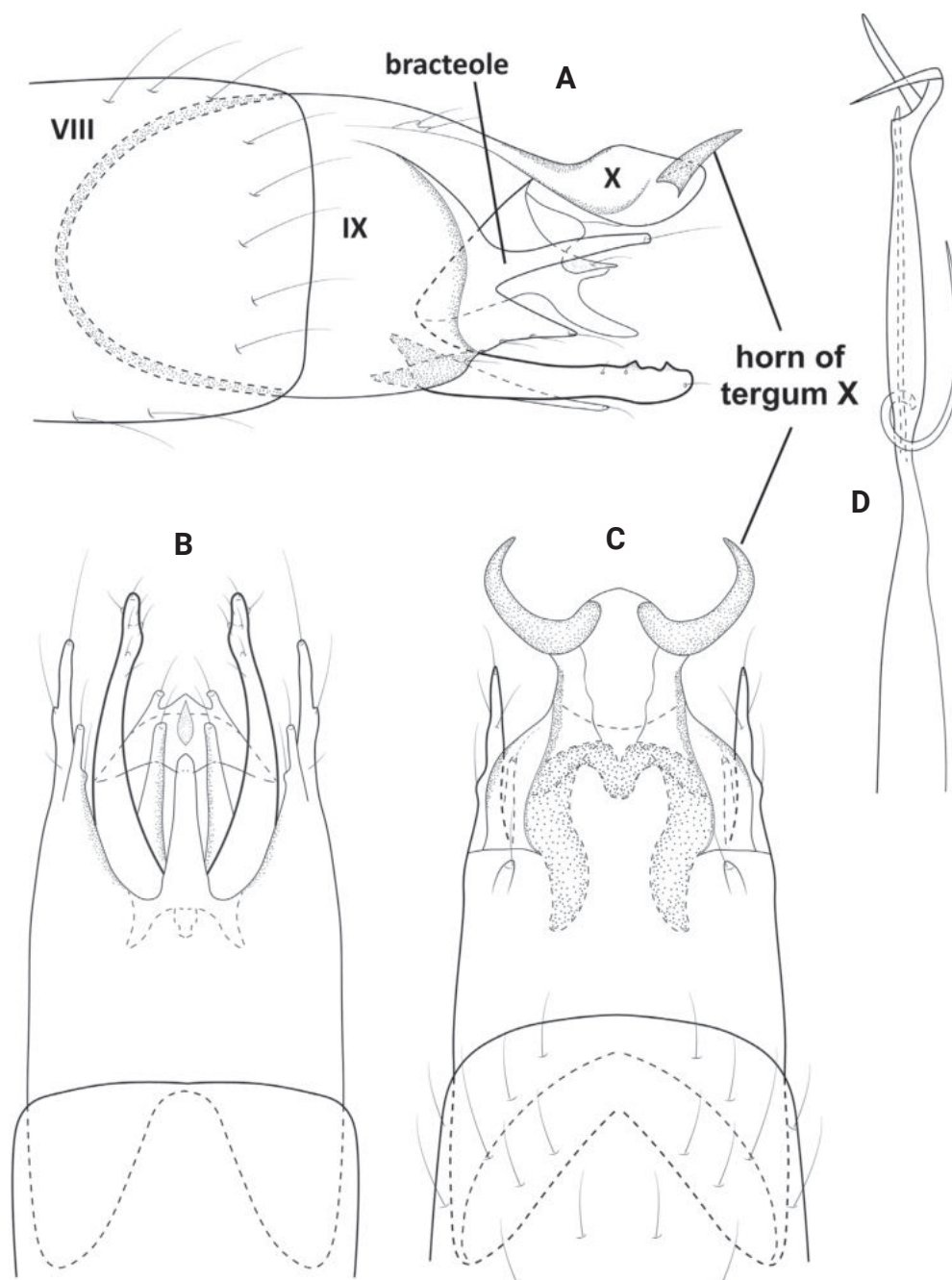


Figure 3. *Neotrichia candela* sp. nov., male holotype, genitalia **A** left lateral **B** ventral **C** dorsal **D** phallus, ventral.

Diagnosis. *Neotrichia candela* sp. nov. is a member of the *N. canixa* group of Keth et al. (2015) based on the posterior horns from tergum X, forked bracteoles, and the bifid inferior appendage. The new species appears to be similar to *N. bika* Oláh & Johanson, 2011 from French Guiana on the basis of the structure of the bracteoles and the horns of the tenth tergum. The new species is separated by the structure of the phallic apex, which has more elongate forking than that of *N. bika*, and by the lateral appearance of the inferior appendage and subgenital plate.

Description. Male. Total length 1.7 mm ($n = 1$), 18 antennal segments, wings and body brown in alcohol. **Genitalia** (Fig. 3). Abdominal segment VIII annular. Segment IX in lateral view generally ovate, rounded anteriorly and posteriorly, fused with segment X dorsally with seta-bearing lobe posterolaterally; in ventral view anterior margin deeply incised, posterior margin with thin, elongate mesal extension; in dorsal view incomplete posteriorly. Tergum X basally fused with segment IX, wide basally, tapering posteriorly forming pair of stout, symmetrical horns; in lateral view segment X elongate, dilated distally with distal horn short and tapering to acute apex. Subgenital plate in lateral view, wide basally, tapering distally to bifid apex, upper arm short, with acute apex, lower portion elongate and crescent-shaped; in ventral view triangular-shaped, apex with pair of thin lateral lobes bearing stout setae, mesally with short distal triangle and ventral sclerotized process. Bracteole in lateral view wide anteriorly, bifid posteriorly, dorsal branch twice as long as ventral branch, each bearing terminal seta; in ventral and dorsal views both branches wide basally, tapering to rounded apices. Inferior appendage rectangular in lateral view, subapically with dorsal sclerotized points, basal process elongate and thin; in ventral view bifid, outer process slightly wider basally, curving and tapering to rounded apices, inner process fused basally and narrow over length which is $\sim 1/2$ of outer process, bearing elongate seta apically. Phallus tubular, constricted at midlength and bearing thin paramere encircling shaft, apex forked with elongate processes, lower of which sharply curves laterally, ejaculatory duct protruding at base.

Distribution. Panama: Chiriquí Province (Parque Internacional La Amistad).

Etymology. This new species is named for the Río Candela in western Chiriquí Province where the species was collected. The name is a noun in the genitive case.

***Neotrichia codaza* sp. nov.**

<https://zoobank.org/F11F9E9F-D365-440D-829D-F54B295DE53E>

Fig. 4

Type locality. Panama: Panama Oeste Province: Cuenca 115, Chame District, Altos de Campana NP, Río Sajalices; PSPSCB-PNAC-C115-2018-030; 8.67625°N, 79.89748°W; 194 m a.s.l.

Type material. Holotype: ♂, PANAMA: Panama Oeste Province: Cuenca 115, Chame District, Altos de Campana NP, Río Sajalices; PSPSCB-PNAC-C115-2018-030; 8.67625°N, 79.89748°W; 194 m a.s.l.; 29.v.2018; E. Pérez, C. Nieto, M. Molinar, T. Ríos leg.; UV light trap; MIUP-018-T-2023 (in alcohol).

Other material examined. PANAMA • ♂; Coclé Province: Cuenca 134, Penonomé District, Río Salado, Pajonal Geosite; 8.59580°N, 80.21512°W; 323 m

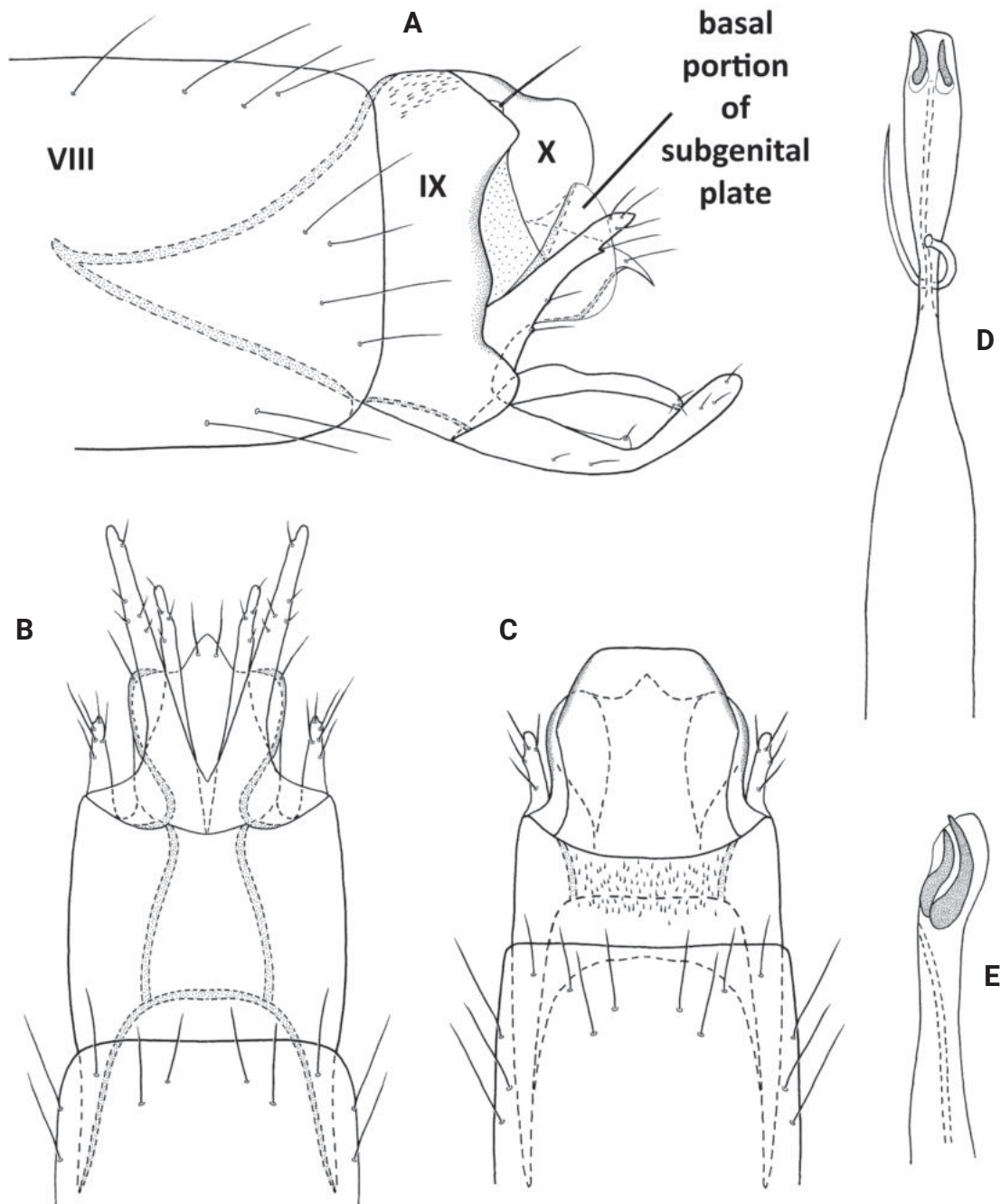


Figure 4. *Neotrichia codaza* sp. nov., male holotype, genitalia **A** left lateral **B** ventral **C** dorsal **D** phallus, dorsal **E** phallus apex, left lateral.

a.s.l.; 4.iv.2022; C. Nieto leg.; UV light trap (in alcohol) • ♂; *ibid.*, except Río Seren; 8.58983°N, 80.21476°W; 332 m a.s.l. • 2 ♂♂; *ibid.*, except Río Membrillo; 8.58450°N, 80.22074°W; 334 m a.s.l. • 17 ♂♂; *ibid.*, except, Río Marica, Pajonal Geosite, 8.55016°N, 80.23831°W; 316 m a.s.l. • 2 ♂♂; **Veraguas Province:** Cuenca 116, Quebrada del Rosario; 7.85826°N, 81.55764°W; 26 m a.s.l.; 20.i.2023; V. Rodríguez leg.; UV light trap • 3 ♂♂; *ibid.*, except Cuenca 132; Río Betegui; 8.36047°N, 80.99481°W; 144 m a.s.l.; 28.i.2023; V. Rodríguez leg.; UV light trap.

Diagnosis. *Neotrichia codaza* sp. nov. is a member of the *N. collata* group of Keth et al. (2015) based on the sclerites at the phallus apex and the projection from the subgenital plate. It is very similar to *N. parany* Oláh & Johanson, 2011

from Peru, based on the sharing of the distinctive pair of dark spines at the phallic apex. The new species is separated by the elongate, angled inferior appendage, and the lack of a mesal process from the posterior margin of segment IX.

Description. Male. Total length 1.3–1.5 mm ($n = 12$), 17 antennal segments, wings and body brown in alcohol. **Genitalia** (Fig. 4). Abdominal segment VIII annular. Segment IX in lateral view with shallow dorsal and ventral emarginations posteriorly, anteriorly tapering to acute apex; dorsally and ventrally deeply incised anteriorly, shallow emarginations posteriorly. Segment X short and lobate in lateral view; in dorsal view apically truncate, flared laterally. Subgenital plate in lateral view, wide basally, abruptly tapering apically on venter forming acute spine, basal portion developed laterad, widening distally and flaplike; in ventral view, quadrate with apicomeral extension bearing stout setae laterad, lobate laterally. Bracteole in lateral view wide basally, tapering distally to rounded apex; in ventral and dorsal views short, tapering to rounded apex. Inferior appendage wide basally with long dorsal arm, narrowing and angled dorsad at midlength and bearing stout dorsal seta, widening distally to rounded apex; in ventral view wide basally, tapering distally to rounded apex, elongate dorsal arm wide at base, tapering distally to round apex. Phallus in dorsal view wide basally and apically, bearing short paramere encircling shaft at midlength, apex with pair of short dark spines; in lateral view apical spines are close together and slightly curving dorsally.

Distribution. Panama: Panama Oeste Province (Altos de Campana National Park).

Etymology. The species name *codaza* (to elbow) derives from Spanish, referring to the bent inferior appendage in lateral view. The name is a noun in the nominative singular standing in apposition.

***Neotrichia embera* sp. nov.**

<https://zoobank.org/BB9D162B-EDD6-4CDE-A1BA-D96B38B8333D>

Fig. 5

Type locality. Panama: Darién Province: Cuenca 156, Pinogana District, Darién NP, Río Pirre, Estacion de MiAmbiente en Rancho Frio; 8.09081°N, 77.74043°W; 73 m a.s.l.

Type material. Holotype: ♂, **PANAMA: Darién Province:** Cuenca 156, Pinogana District, Darién NP, Río Pirre, Estacion de MiAmbiente en Rancho Frio; 8.09081°N, 77.74043°W; 73 m a.s.l.; 9–12.ii.2018; Malaise trap; A. Thurman leg.; MUPADI-005-T-2023 (in alcohol).

Diagnosis. This new species, with a pair of apical phallic spines, would appear to be another member of the *N. collata* group of Keth et al. (2015), with similarity to *N. anahua* (Mosely, 1937) from Mexico, and *N. kurtika* Oláh & Johanson, 2011 from French Guiana. Unlike these species, *N. embera* sp. nov. Harris, Armitage & Ríos has a posterolateral process from segment IX and bifid inferior appendages.

Description. Male. Total length 1.2 mm ($n = 1$), 17 antennal segments, wings and body brown in alcohol. **Genitalia** (Fig. 5). Abdominal segment VIII annular. Segment IX in lateral view anteriorly tapering to short upturned apodeme, posteriorly with medial lobe, distally rounded with posterolateral triangular process; ventrally with anterior and posterior margins incised mesally, posteriorly with thin

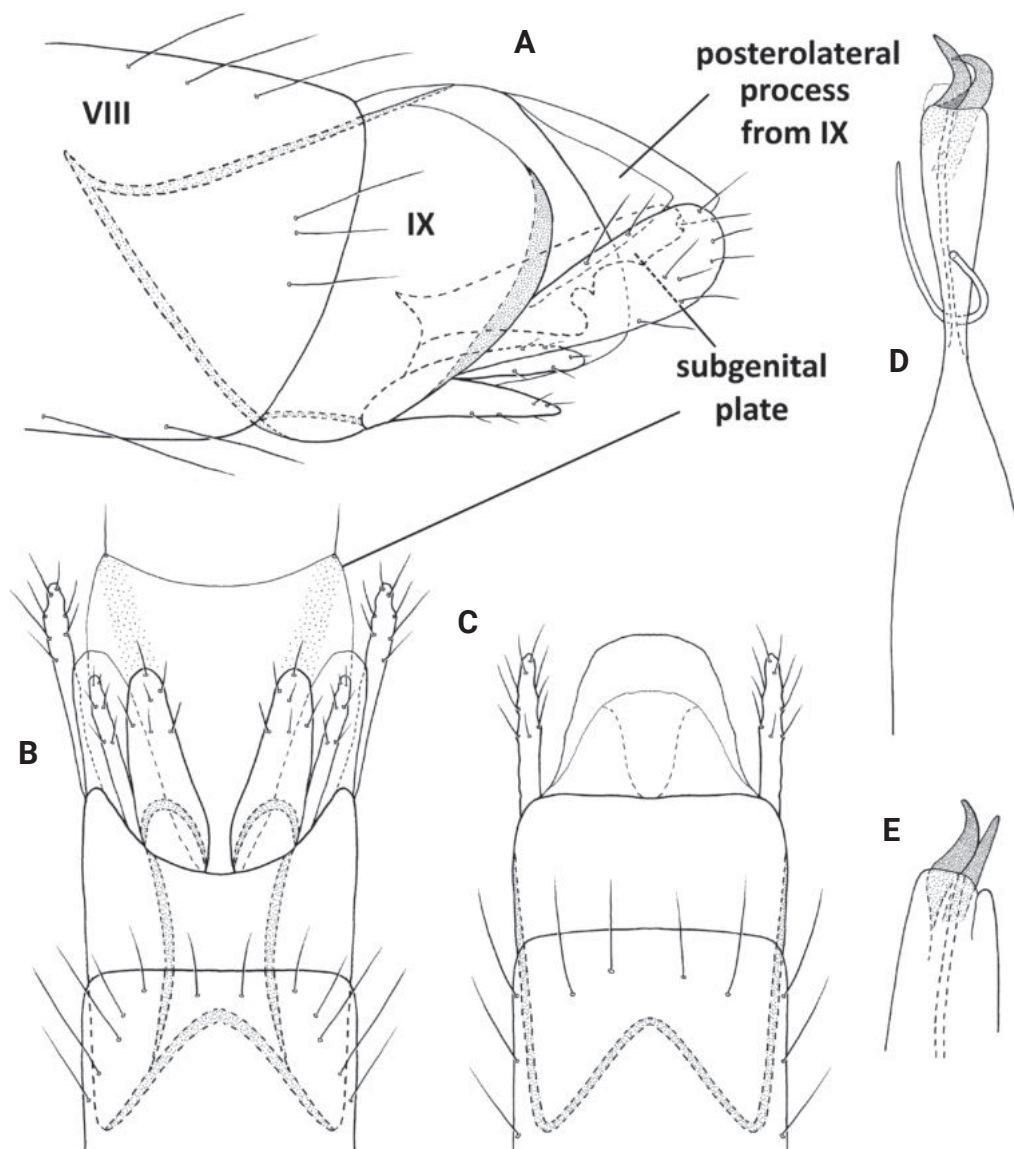


Figure 5. *Neotrichia embera* sp. nov., male holotype, genitalia **A** left lateral **B** ventral **C** dorsal **D** phallus, dorsal **E** phallus apex, left lateral.

lateral processes; dorsally truncate posteriorly. Segment X elongate, triangular in lateral view; in dorsal view tapering distally to rounded apex. Subgenital plate in lateral view narrow basally, ventral margin sinuate with lobes and points, apex with stout seta, upper margin straight; in ventral view rectangular, widening posteriorly with stout setae on distal margins, rounded laterally. Bracteole in lateral view narrow basally, widening distally to rounded apex; in ventral and dorsal views straight, narrow over length. Inferior appendage bifid, ventral arm narrowly triangular, dorsal arm ovate and same length as lower arm; in ventral view divergent and separated, lateral arms narrow over length, inner arms slightly triangular, rounded apically. Phallus in dorsal view tubular, wide basally and distally, bearing pair of stout spines apically, short paramere encircling shaft at midlength.

Distribution. Panama: Darién Province (Darién National Park).

Etymology. This species is named for the indigenous Embera people of Darién Province, where the species was collected. The name is a noun in the genitive case.

***Neotrichia flennikeni* sp. nov.**

<https://zoobank.org/90BFFF5E-7C6C-41C3-AF74-B0A58AB31547>

Fig. 6

Type locality. Panama: Chiriquí Province: Cuenca 108, David District, San Pablo Viejo, puente vía Interamericana antes de llegar a la entrada de Bagala, Río Platanal; 8.46416°N, 82.52030°W; 825 m a.s.l.

Type material. Holotype: ♂, **PANAMA: Chiriquí Province:** Cuenca 108, David District, San Pablo Viejo, puente vía Interamericana antes de llegar a la entrada de Bagala, Río Platanal; 8.46416°N, 82.52030°W; 825 m a.s.l.; 12.iv.2021; T. Ríos, Y. Aguirre leg.; UV light trap; MUPADI-006-T-2023 (in alcohol).

Diagnosis. *Neotrichia flennikeni* sp. nov. appears to be a member of the *N. vibrans* group of Keth et al. (2015) based on the posterolateral process of segment IX, and the tapered inferior appendage. The new species appears to be similar to *N. angulata* Flint, 1983 from Uruguay which also has an elongate, tapering inferior appendage and a phallus bearing a long, stout spine. The new species is distinguished by the knob-like posterolateral processes from segment IX and by the tapering, rather than angled, appearance of the inferior appendage.

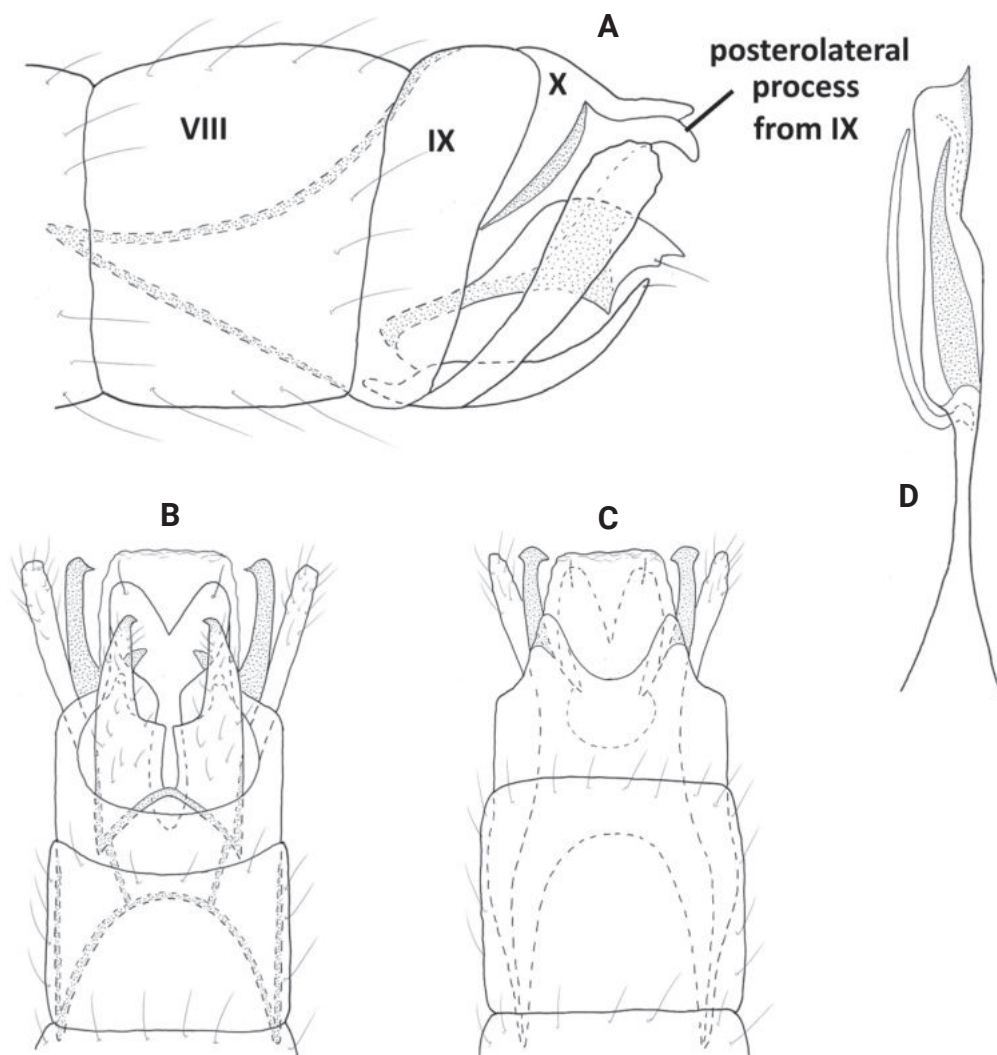


Figure 6. *Neotrichia flennikeni* sp. nov., male holotype, genitalia **A** left lateral **B** ventral **C** dorsal **D** phallus dorsal.

Description. Male. Total length 1.8 mm ($n = 1$), 18 antennal segments, wings and body brown in alcohol. **Genitalia** (Fig. 6). Abdominal segment VIII annular. Segment IX in lateral view narrow, tapering anteriorly, posteriorly with thin posterolateral process; ventrally with deep rounded posterior excision; dorsally with narrow posterior incision, posterolateral processes sclerotized and knobbed apically. Segment X narrowing posteriorly to thin shelf; in dorsal view wide basally, tapering distally to truncate apex. Subgenital plate in lateral view, narrow basally, widening distally, with acute, posteriorly projected dorsal spine, sclerotized knob posteroventrally; in ventral view narrowing basally, with pair of apical lobes each bearing stout seta. Bracteole in lateral view widening posteriorly to rounded apex; in ventral and dorsal views narrow over length. Inferior appendage in lateral view elongate and tapering, curving upward at midlength; in ventral view wide basally, sharply angled at midlength, then narrowing to acute apex which projects inward. Phallus tubular, constricted at midlength and bearing thin paramere encircling shaft, apex rectangular with elongate, stout medial spine.

Distribution. Panama: Chiriquí Province (David District).

Etymology. This species is named after Donald G. Flenniken of eastern Ohio, a teacher, naturalist, and part-time milkman who taught the second author (at age of 11) how to identify mammals from their skull bones/dentition and how to use taxonomic keys—a brief encounter that has led to a lifetime of taxonomic pursuits and pleasures. The name is a noun in the genitive case.

***Neotrichia honda* sp. nov.**

<https://zoobank.org/51E67AAC-F52B-4F24-BA70-C3DF7DBB5D35>

Fig. 7

Type locality. Panama: Chiriquí Province: Cuenca 108, Boquete District, Quebrada Honda, N Fortuna Dam, Fortuna Forest Reserve; 8.74985°N, 82.23885°W; 1132 m a.s.l.

Type material. Holotype: ♂, **PANAMA: Chiriquí Province:** Cuenca 108, Boquete District, Quebrada Honda, N Fortuna Dam, Fortuna Forest Reserve; 8.74985°N, 82.23885°W; 1132 m a.s.l.; 18.ii.2018; B. Armitage, T. Arefina-Armitage leg.; UV light trap; MUPADI-007-T-2023 (in alcohol).

Diagnosis. *Neotrichia honda* sp. nov. does not fit well in any of the species groupings established by Keth et al. (2015). The new species has forked sclerites at the apex of the phallus and has an overall resemblance to *N. gilaensis* Keth et al., 2015 from Arizona which is in the *N. collata* group, but it is also similar to *N. yavesia* Bueno-Soria, 2010 from Mexico in the *N. vibrans* group, based on the short, rectangular inferior appendages. The new species is separated by the elongate, forked sclerites of the phallus apex, the elongate anterior apodeme of segment IX, and by the sclerotized posterolateral processes from segment IX.

Description. Male. Total length 1.5 mm ($n = 1$), 18 antennal segments, wings and body brown in alcohol. **Genitalia** (Fig. 7). Abdominal segment VIII annular. Segment IX in lateral view anteriorly tapering to elongate apodeme, posteriorly rounded with posterolateral process, which is wide basally, tapering distally to an acute downward turning hook; dorsally and ventrally deeply incised anteriorly, ventrally with deep lateral incisions posteriorly, creating an elongate mesal,

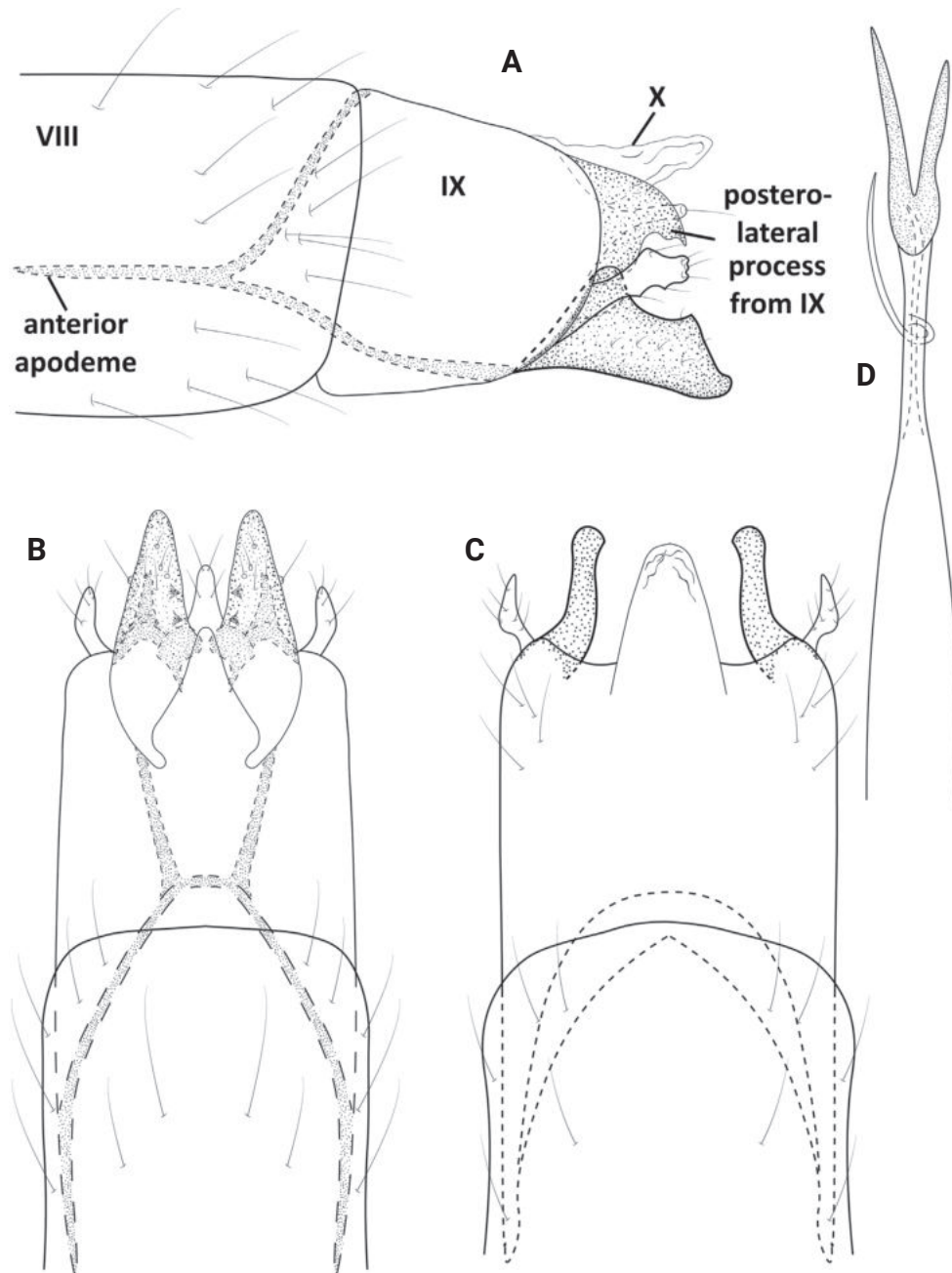


Figure 7. *Neotrichia honda* sp. nov., male holotype, genitalia **A** left lateral **B** ventral **C** dorsal **D** phallus, dorsal.

triangular lobe; dorsally with posterolateral processes narrow over length, curving slightly inward apically. Segment X elongate and thin in lateral view; in dorsal view wide basally and fused with segment IX, tapering to rounded apex. Subgenital plate in lateral view, wide basally, gradually tapering apically to rounded apex bearing elongate seta; in ventral view narrowly triangular, pair of stout setae apically. Bracteole in lateral view wide basally, then narrowing distally to truncate apex; in ventral and dorsal views narrow over length and curving mesally. Inferior appendage sclerotized and rectangular, wide basally, narrowing at midlength, then abruptly tapering to rounded apex; in ventral view triangular, rounded apically, basally with finger-like lobe. Phallus in dorsal view wide basally, bearing short paramere encircling shaft at midlength, apex divided into pair of elongate, sclerotized rods, which are nearly equal in length.

Distribution. Panama: Chiriquí Province (Fortuna Forest Reserve).

Etymology. This species is named for Quebrada Honda, a tributary of Río Chiriquí and Fortuna Reservoir in northeast Chiriquí Province, where the species was collected. The name is a noun in the genitive case.

***Neotrichia landisae* sp. nov.**

<https://zoobank.org/458EB8A1-9CD5-45DC-9A35-7F385BEC50B4>

Fig. 8

Type locality. Panama: Chiriquí Province: Cuenca 102, Renacimiento District, Reserva Privada Landis, Quebrada sin nombre, Location 2; 8.645005°N, 82.822037°W; 575 m a.s.l.

Type material. *Holotype*: ♂, PANAMA: Chiriquí Province: Cuenca 102, Renacimiento District, Reserva Privada Landis, Quebrada sin nombre, Location 2; 8.645005°N, 82.822037°W; 575 m a.s.l.; 30.iv.2020; M. Landis leg.; Malaise trap; MUPADI-008-T-2023 (in alcohol). *Paratypes*: Panama • 9 ♂♂; *ibid.*, except 30.v.2020; MUPADI-009-T-2023 (in alcohol).

Other material examined. PANAMA • 2 ♂♂; *ibid.*, except 27.ii–15.iii.2020 • 1 ♂; *ibid.*, except 15–31.iii.2020 • 2 ♂♂; *ibid.*, except Location 1, 8.643769°N, 82.829479°W; 755 m a.s.l.; 27.ii–10.iii.2020; M. Landis leg.; Malaise trap • 1 ♂; Chiriquí Province: Bugaba District, Cuenca 102, nr San Andres, Finca La Esperanza, Quebrada La Vuelta; 8.61710°N, 82.70415°W; 492 m a.s.l.; 3–20.i.2022; T. Ríos, Y. Aguirre leg.; Malaise trap • 2 ♂♂; *ibid.*, except 21.i–3.ii.2022 • 3 ♂♂; *ibid.*, except 6–20.iii.2022 • 2 ♂♂; *ibid.*, except 8–22.iv.2022 • 2 ♂♂; *ibid.*, except 8–21.v.2022 • 2 ♂♂; *ibid.*, except Quebrada sin nombre; 8.61765°N, 82.71330°W; 540 m a.s.l.; 21.i–3.ii.2022.

Diagnosis. *Neotrichia landisae* sp. nov. belongs to a cluster of similar Panamanian species with characteristic elongate posterolateral processes from abdominal segment IX, including *N. tataniae* Armitage & Harris, 2018 and *N. yayas* Armitage & Harris, 2020. The new species is separated from these species by the linear posterolateral processes from segment IX, the truncate inferior appendage, and the narrow subgenital plate in ventral view.

Description. Male. Total length 1.5–1.7 mm ($n = 15$), 18 antennal segments, wings and body brown in alcohol. **Genitalia** (Fig. 8). Abdominal segment VIII annular. Segment IX in lateral view anteriorly rounded, wide posteroventrally, narrowing dorsally, pair of elongate, thin posterolateral processes, which narrow distally; in dorsal view fused posteriorly with segment X, pair of small setaceous lobes laterally, posterolateral processes sclerotized and elongate, but dissimilar in length, anteriorly with narrow mesal incision; in ventral view with deep lateral incisions. Tergum X basally fused with segment IX, posteriorly elongate, tapering to rounded mesal lobe; in lateral view wide basally, tapering distally to acute apex. Subgenital plate in lateral view wide basally, tapering distally to narrow shelf bearing stout seta; in ventral view narrow over length, pair of setae apically. Bracteole absent or represented by thin, elongate seta-bearing process on dorsal margin of segment IX. Inferior appendage short, wide basally, widening subapically, spinose and rugose on distal margin, thin ventral process basally; in ventral view elongate and narrow, apical point turning inward, spinose

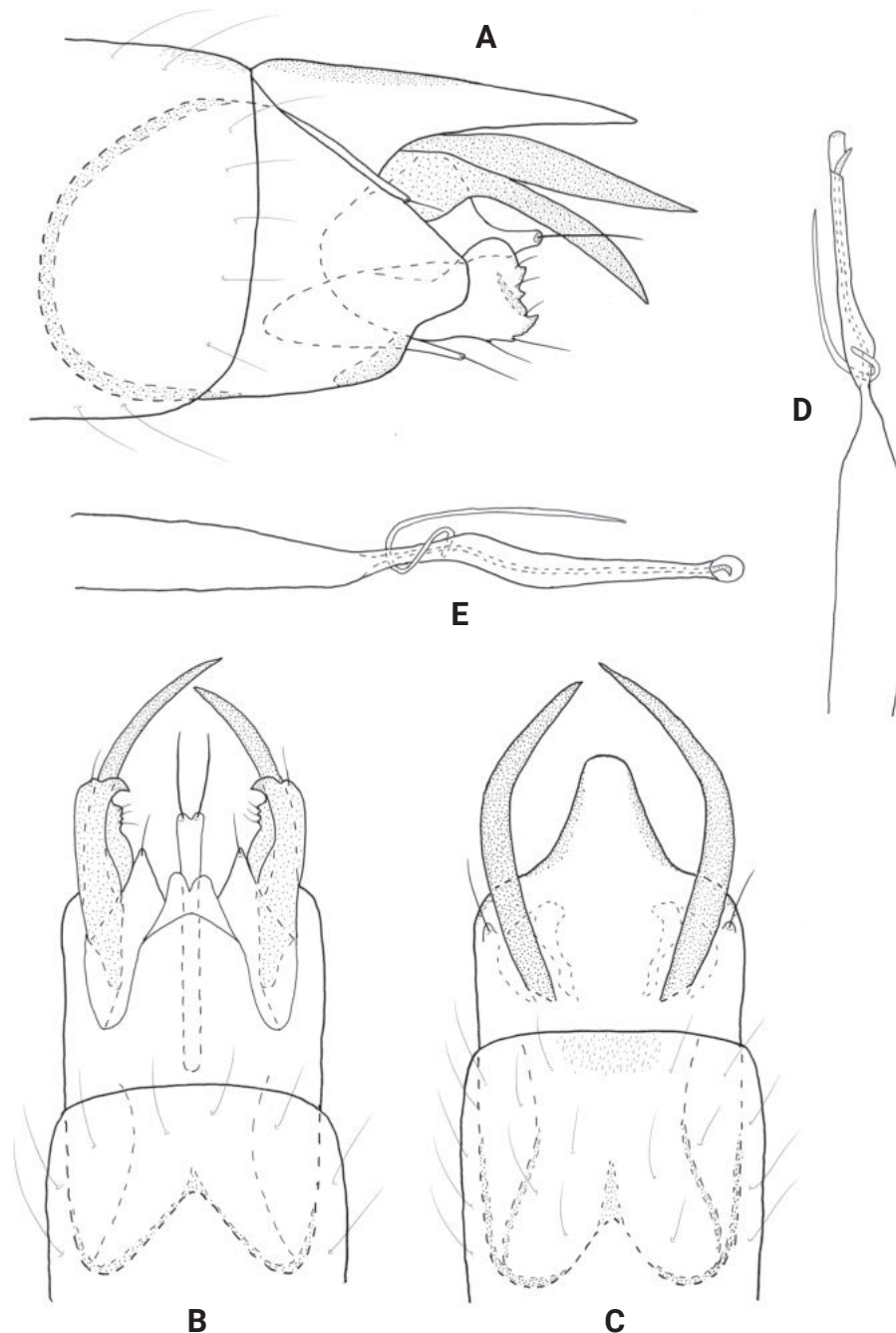


Figure 8. *Neotrichia landisae* sp. nov., male holotype, genitalia **A** left lateral **B** ventral **C** dorsal **D** phallus, dorsal **E** phallus, lateral.

subapically on mesal margin, base of inferior appendage and processes from segment IX superimposed, short triangular mesal process bearing stout seta apically. Phallus tubular, constricted at midlength and bearing thin paramere encircling shaft, apically rounded with ejaculatory duct protruding.

Distribution. Panama: Chiriquí Province (Reserva Privada Landis, Finca La Esperanza).

Etymology. This species is named for Senora Marietta Isabel Landis, owner of Reserva Privada Landis, who managed all collection events. The name is a noun in the genitive case.

***Neotrichia lenati* sp. nov.**

<https://zoobank.org/9068A45C-197D-419C-8415-CDE94274F387>

Fig. 9

Type locality. Panama: Chiriquí Province: Cuenca102, Renacimiento District, Reserva Privada Landis, Location 1, Quebrada sin nombre; 8.643769°N, 82.82979°W; 755 m a.s.l.

Type material. Holotype: ♂, **PANAMA: Chiriquí Province:** Cuenca102, Renacimiento District, Reserva Privada Landis, Location 1, Quebrada sin nombre; 8.643769°N, 82.82979°W; 755 m a.s.l.; 5–30.xii.2022; M. Landis leg.; Malaise trap; MUPADI-010-T-2023 (in alcohol).

Diagnosis. *Neotrichia lenati* sp. nov. appears to be a member of the *N. okopa* group of Keth et al. (2015) based on the tubular phallus which lacks sclerotized processes, the posterolateral process from segment IX, and the thin tapering inferior appendage. It is, perhaps, most similar to *N. connori* Keth et al., 2015 from Mexico and *N. teutonia* Flint, 1983 from Brazil, which also have tapering inferior appendages and a posterolateral process from segment IX. The new

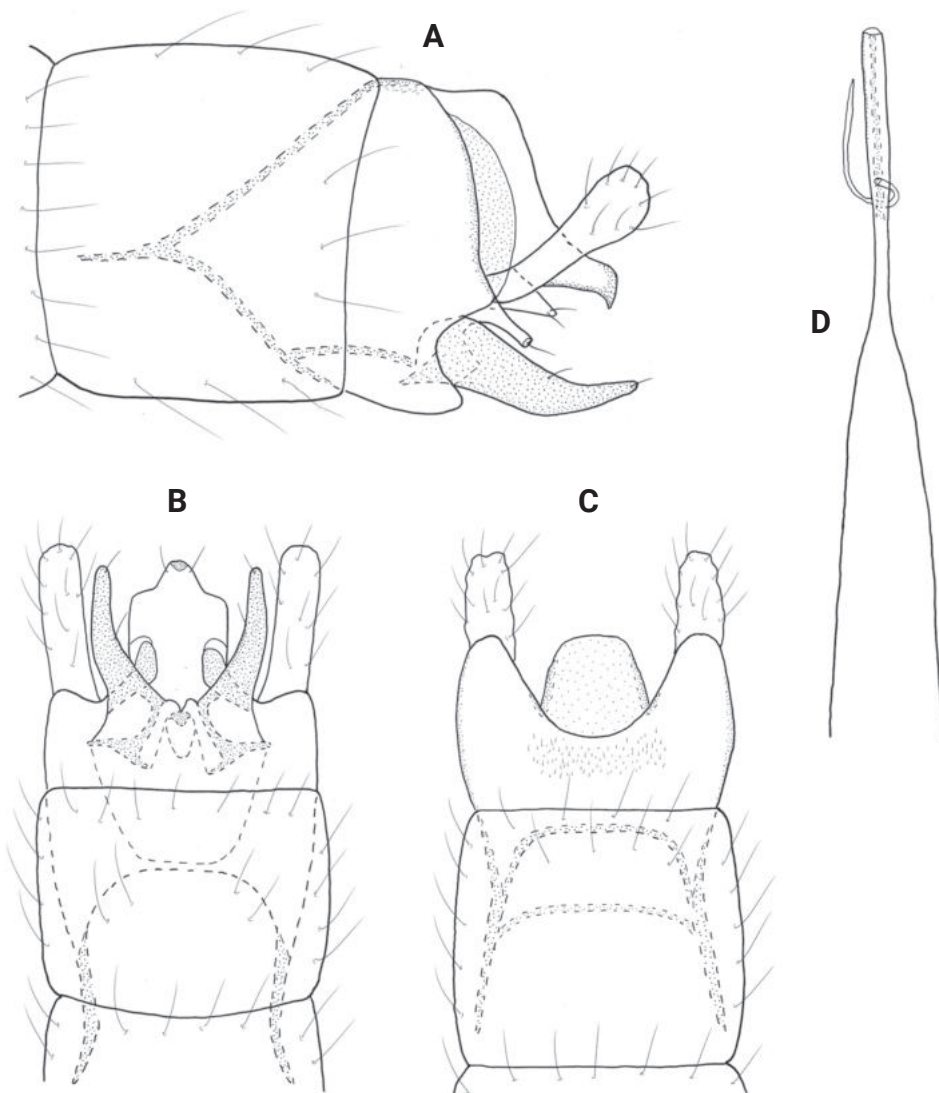


Figure 9. *Neotrichia lenati* sp. nov., male holotype, genitalia **A** left lateral **B** ventral **C** dorsal **D** phallus dorsal.

species is separated by the presence of a basal process from the inferior appendage, narrow bracteole, and the ventral location and shape of the posterolateral process from segment IX.

Description. Male. Total length 1.4 mm ($n = 1$), 18 antennal segment, wings and body brown in alcohol. **Genitalia** (Fig. 9). Abdominal segment VIII annular. Segment IX in lateral view narrow, tapering anteriorly to mesal apodeme, truncate posteriorly, with thin process posterolaterally, tapering ventrad and incised on posterior margin; in ventral view narrow, sinuate posteriorly; in dorsal view deeply incised mesally, forming rounded lateral lobes. Segment X seemingly fused with segment IX in lateral view, tapering downward to posterior projecting shelf with pointed tip; in dorsal view short, rounded distally, with truncate apex and sclerotized margins. Subgenital plate triangular in lateral view; in ventral view quadrate, lateral apices indented with stout seta, small mesal downturned lobe. Bracteole narrow in lateral view, slightly widening distally; in ventral and dorsal views narrow over length. Inferior appendage sclerotized, tapering distally and slightly curving upward at midlength, dorsobasally with thin process tipped with stout seta; in ventral view tapering distally to rounded apex, knob-like basal process on inner margin. Phallus tubular, constricted near midlength and bearing thin paramere encircling shaft, posteriorly thin and rectangular, ejaculatory duct lightly sclerotized.

Distribution. Panama: Chiriquí Province (Reserva Privada Landis).

Etymology. This species is named in memory of David R. Lenat of Raleigh, North Carolina, our friend and colleague, who was an avid researcher in taxonomy and aquatic bioassessment, and who made numerous important contributions to our knowledge of chironomids, stoneflies, caddisflies, mayflies, and many other groups of aquatic insects. The name is a noun in the genitive case.

***Neotrichia mindyae* sp. nov.**

<https://zoobank.org/7F7659D8-B935-4C3E-82CF-135B85223928>

Fig. 10

Type locality. Panama: Darién Province: Cuenca 156, Pinogana District, Darién NP, Río Pirre, Estacion de MiAmbiente en Rancho Frio; 8.09081°N, 77.74043°W; 73 m a.s.l.

Type material. Holotype: ♂, **PANAMA: Darién Province:** Cuenca 156, Pinogana District, Darién NP, Río Pirre, Estacion de MiAmbiente en Rancho Frio; 8.09081°N, 77.74043°W; 73 m a.s.l.; 9–12.ii.2018; A. Thurman leg.; Malaise trap; MUPADI-011-T-2023 (in alcohol).

Diagnosis. *Neotrichia mindyae* sp. nov. is another member of the *N. canixa* group of Keth et al. (2015) based on the posterior horns from tergum X, forked bracteoles, and the bifid inferior appendage. The new species appears to be most similar to *N. maya* Harris & Flint, 2016 from Belize on the basis of the structure of the bracteole and the horns of tergum X. The new species is separated by the structure of the phallic apex, which while forked, has the one process extremely long, similar to that of *N. maria* Bueno-Soria & Hamilton, 1986 from Mexico, and by the unequal forking of the bracteole, which are uniformly forked in *N. maria*.

Description. Male. Total length 1.5 mm ($n = 1$), 18 antennal segments, wings and body brown in alcohol. **Genitalia** (Fig. 10). Abdominal segment VIII annular.

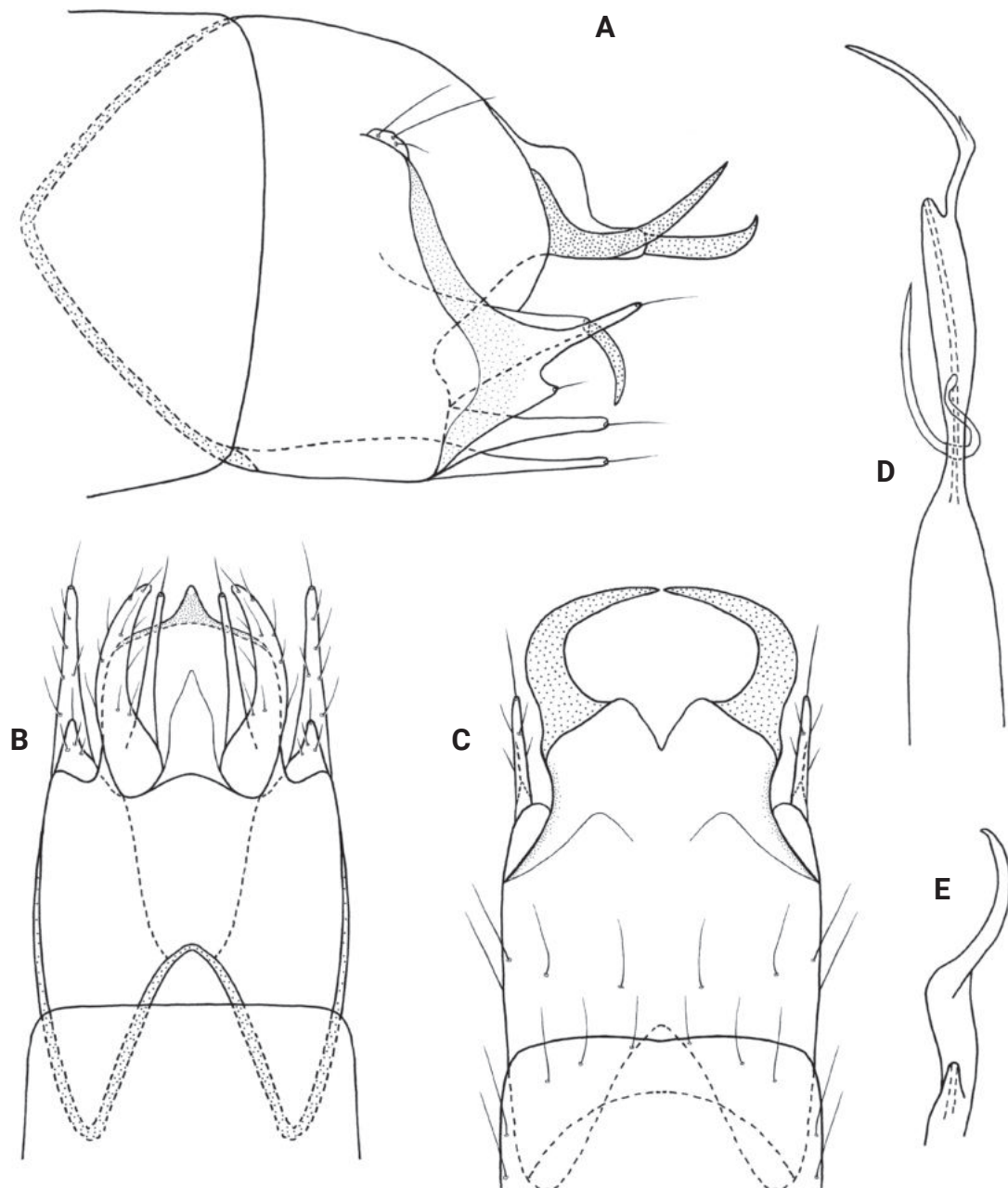


Figure 10. *Neotrichia mindyae* sp. nov., male holotype, genitalia **A** left lateral **B** ventral **C** dorsal **D** phallus, left lateral **E** phallus apex, dorsal.

Segment IX in lateral view generally ovate, rounded anteriorly and posteriorly, fused with segment X dorsally, and bearing lateral setal lobes posteriorly; in ventral view anterior margin deeply incised, posterior margin with triangular mesal extension; in dorsal view with pair of posterolateral lobes. Tergum X basally fused with segment IX, posteriorly produced into pair of thick, symmetrical horns which nearly touch mesally; in lateral view distal horns are thin and tapering to acute apices. Subgenital plate in lateral view, wide basally, tapering distally to downturned apical hook; in ventral view wide basally, rounded laterally to apicommesal extension. Bracteole in lateral view wide anteriorly, bifid posteriorly, dorsal branch elongate with apical seta, ventral branch greatly reduced with apical seta; in ventral and dorsal views both branches wide basally, tapering to

rounded apices. Inferior appendage bifid laterally, each thin arm wide basally and tapering distally to rounded apices bearing long seta; in ventral view bifid, outer process wide basally, curving and tapering to acute apices, inner process fused basally and narrow over length which is equal to outer process bearing elongate seta apically. Phallus tubular, wide basally, constricted at midlength and bearing thin paramere encircling shaft, apex with elongate lateral spike, smaller spike near base, ejaculatory duct not protruding.

Distribution. Panama: Darién Province (Darién National Park).

Etymology. This species is named for the sister of the first author, Melinda “Mindy” Harris Haupt, who used to help her brother collect bugs when they were both much younger. The name is a noun in the genitive case.

***Neotrichia panamensis* sp. nov.**

<https://zoobank.org/11AF342D-DBD6-46E8-B186-C7F90A9A4E48>

Fig. 11

Type locality. Panama: Colon Province: Cuenca 117, Portobelo District, Quebrada sin nombre, nr Jose Pobre property–Tesoro Verde; 9.60069°N, 79.61658°W; 55 m a.s.l.

Type material. Holotype: ♂, **PANAMA: Colon Province:** Cuenca 117, Portobelo District, Quebrada sin nombre, nr Jose Pobre property–Tesoro Verde; 9.60069°N, 79.61658°W; 55 m a.s.l.; 19.xii.2018; D. Garrido leg.; UV light trap; MUPADI-012-T-2023 (in alcohol). **Paratypes:** **PANAMA** • 2 ♂♂; same as holotype; MUPADI-013-T-2023 (in alcohol).

Other material examined. PANAMA • 16 ♂♂; **Veraguas Province:** Cuenca 116, Las Palmas District, Quebrada La Mina; 7.87443°N, 81.51004°W; 63 m a.s.l.; 3.ii.2023; V. Rodríguez leg.; UV light trap • 7 ♂♂; *ibid.*, except Río Indio; 7.87372°N, 81.49994°W; 57 m a.s.l.; 3.ii.2023 • 1 ♂; *ibid.*, except Río Pixvae; 7.84287°N, 81.56329°W; 17 m a.s.l.; 23.i.2023 • 4 ♂♂; *ibid.*, except Soná District, Quebrada Monita; 7.81480°N, 81.55724°W; 26 m a.s.l.; 21.i.2023.

Diagnosis. *Neotrichia panamensis* sp. nov. is another member of the *N. canixa* group of Keth et al. (2015) based on the posterior horns from tergum X, forked bracteole, and the bifid inferior appendage. The new species appears to be similar to *N. alsa* Oláh & Johanson, 2011 from Peru on the basis of the bracteoles and phallic apex, but the short inferior appendages are more like those of *N. tauricornis* Malicky, 1980 which occurs throughout the Caribbean islands, Panama, and Colombia, but the subgenital plate and bracteoles are much different in the new species compared to that of *N. tauricornis*.

Description. Male. Total length 1.5–1.7 mm ($n = 14$), 18 antennal segments, wings and body brown in alcohol. **Genitalia** (Fig. 11). Abdominal segment VIII annular. Segment IX in lateral view ovate, rounded anteriorly and sinuate posteriorly, fused with segment X dorsally, bearing a setae-bearing lobe dorsally; in ventral view anterior margin deeply incised, posterior margin sinuate, triangular mesal extension. Tergum X basally fused with segment IX, rectangular basally, pair of thin, symmetrical horns distally; in lateral view segment X is lobate, with distal horn saber-like. Subgenital plate in lateral view, wide basally, truncate distally with ventral hook tapering to acute apex; in ventral view wide basally, slightly curving to rounded apex, with mesal process flanked by stout setae. Bracteole in lateral

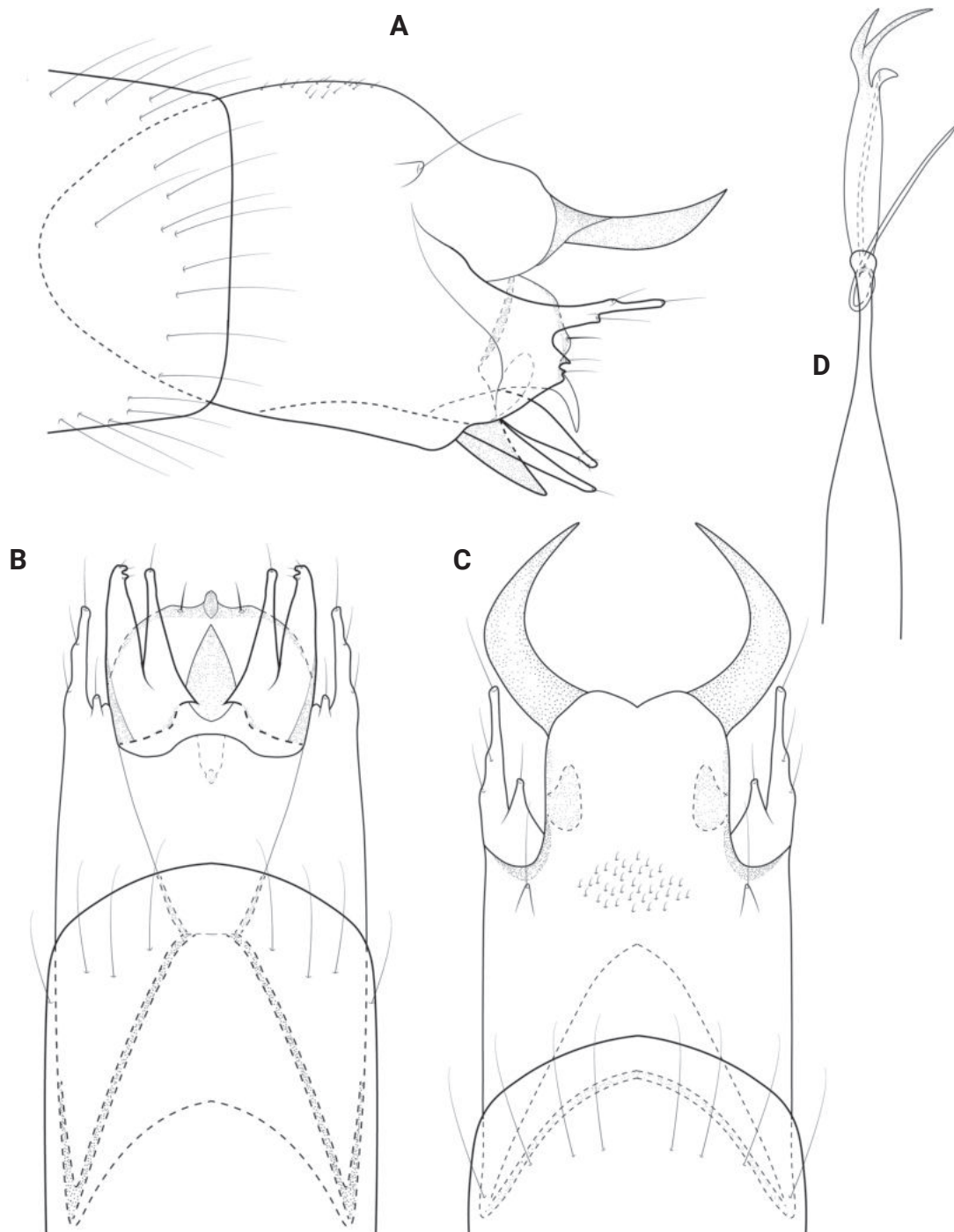


Figure 11. *Neotrichia panamensis* sp. nov., male holotype, genitalia **A** left lateral **B** ventral **C** dorsal **D** phallus, dorsal.

view wide anteriorly, slightly bifid posteriorly, dorsal branch elongate and tipped with seta, ventral branch vestigial, represented by pair of sharp points; in ventral and dorsal views lower branch represented by short knob, tapering distally. Inferior appendage short and bifid, wide basally tapering distally, basal process triangular; in ventral view bifid, outer process subrectangular, apex with mesal points, inner process same length as outer, fused and wide at base, tapering distally bearing elongate seta apically. Phallus tubular, constricted at midlength and bearing thin paramere encircling shaft, apex divided into three processes, lower process small, distally processes elongate, ejaculatory duct not protruding at base.

Distribution. Panama: Colon Province (Portobelo District); Veraguas Province (Las Palmas District).

Etymology. This species is named for the Republic of Panama where the species was collected. The name is a noun in the genitive case.

***Neotrichia parajarocho* sp. nov.**

<https://zoobank.org/5015E444-2B3B-45EF-A0AF-0506BCA35FA9>

Fig. 12

Type locality. Panama: Chiriquí Province: Cuenca 102, Bugaba District, afluyente Río Chiriquí Viejo, PILA; PSPSCB-PILA-C102-2017-022; 8.90124°N, 82.61817°W; 2354 m a.s.l.

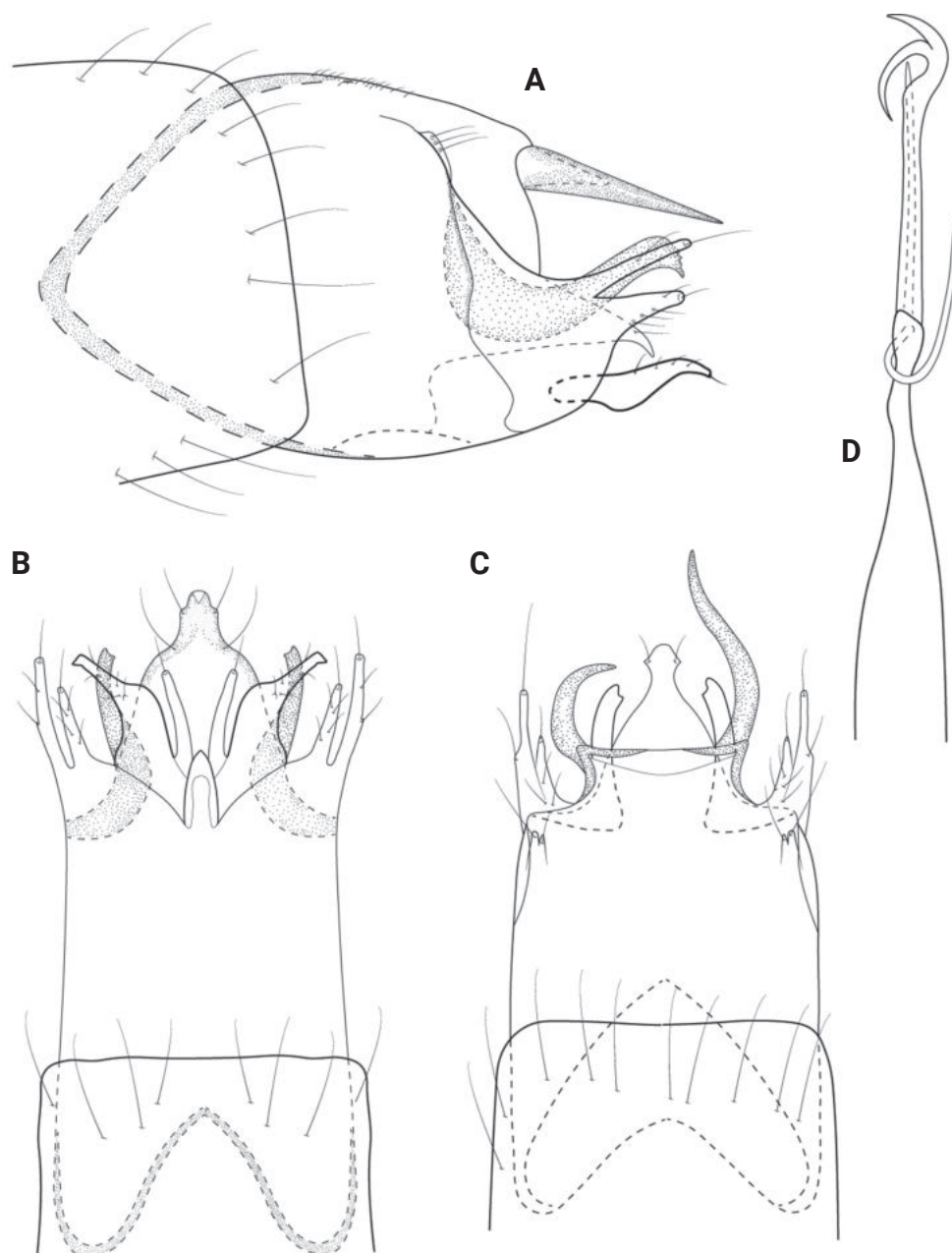


Figure 12. *Neotrichia parajarocho* sp. nov., male holotype, genitalia **A** left lateral **B** ventral **C** dorsal **D** phallus, ventral.

Type material. Holotype: ♂, **PANAMA: Chiriquí Province:** Cuenca 102, Bugaba District, afluyente Río Chiriquí Viejo, PILA; PSPSCB-PILA-C102-2017-022; 8.90124°N, 82.61817°W; 2354 m a.s.l.; 17–21.vi.2017; E. Álvarez, E. Pérez, T. Ríos leg.; Malaise trap; MIUP-019-T-2023 (in alcohol).

Diagnosis. *Neotrichia parajarochoita* sp. nov. is another member of the *N. canixa* group of Keth et al. (2015) based on the posterior horns from tergum X, forked bracteole, and the forked apex of the phallus. In many respects, the new species appears to be similar to *N. jarochoita* Bueno-Soria, 1999 and *N. palitla* Harris & Flint, 2016, both of which occur in Mexico, on the basis of the asymmetrical horns of tergum X and the structure of the bracteole. Unlike these two species, *N. parajarochoita* has a sclerotized posterolateral process from segment IX and the inferior appendages are divergent in ventral view.

Description. Male. Total length 1.4 mm ($n = 1$), 18 antennal segments, wings and body brown in alcohol. **Genitalia** (Fig. 12). Abdominal segment VIII annular. Segment IX in lateral view ovate, rounded anteriorly and sinuate posteriorly, setae-bearing lobe dorsally and fused with segment X, with upturned posterolateral process mesally, narrowing distally to serrate apex; in ventral view anterior margin emarginate, posterior margin incised mesally, with an oval mesal extension, and posterolateral processes laterad, narrow over length and curving. Tergum X basally fused with segment IX, quadrate, posterior horns asymmetrical, left horn twice as long as right; in lateral view segment X is truncated, distal horn elongate and tapering to acute apex. Subgenital plate in lateral view, wide basally, tapering distally to acute apex, which is slightly downturned; in ventral view roundly triangular, abruptly narrowed distally forming rectangular mesal extension flanked by pair of setae. Bracteole in lateral view wide anteriorly, bifid posteriorly, thin dorsal branch slightly longer than triangular ventral branch, each tipped with seta; in ventral and dorsal views wide basally, tapering distally. Inferior appendage short in lateral view, widening at midlength, then tapering to rounded apex; in ventral view bifid, outer process wide basally, narrowing distally and strongly diverging, rectangular apically with lateral spike, inner process shorter and narrower than outer process. Phallus tubular, constricted at midlength and bearing thin paramere encircling shaft, apex forked, lower fork strongly curving, ejaculatory duct protruding subapically.

Distribution. Panama: Chiriquí Province (Parque Internacional La Amistad).

Etymology. This species is named for its resemblance to *Neotrichia jarochoita*. The name is an adjective used as a substantive in the genitive case.

***Neotrichia paraxicana* sp. nov.**

<https://zoobank.org/B577FA98-7BCD-4901-AE56-655F8843BE52>

Fig. 13

Type locality. Panama: Veraguas Province: Cuenca 132, Santa Fe District, Santa Fe NP, Quebrada Mulabá, Santa Fe NP, PSPSCB-PNSF-C132-2017-009; 8.52560°N, 81.12956°W; 623 m a.s.l.

Type material. Holotype: ♂, **PANAMA: Veraguas Province:** Cuenca 132, Santa Fe District, Santa Fe NP, Quebrada Mulabá, Santa Fe NP, PSPSCB-PNSF-C132-2017-009; 8.52560°N, 81.12956°W; 623 m a.s.l.; 20.iv.2017; A. Cornejo, T. Ríos, C. Nieto leg.; UV light trap; MIUP-020-T-2023 (in alcohol).

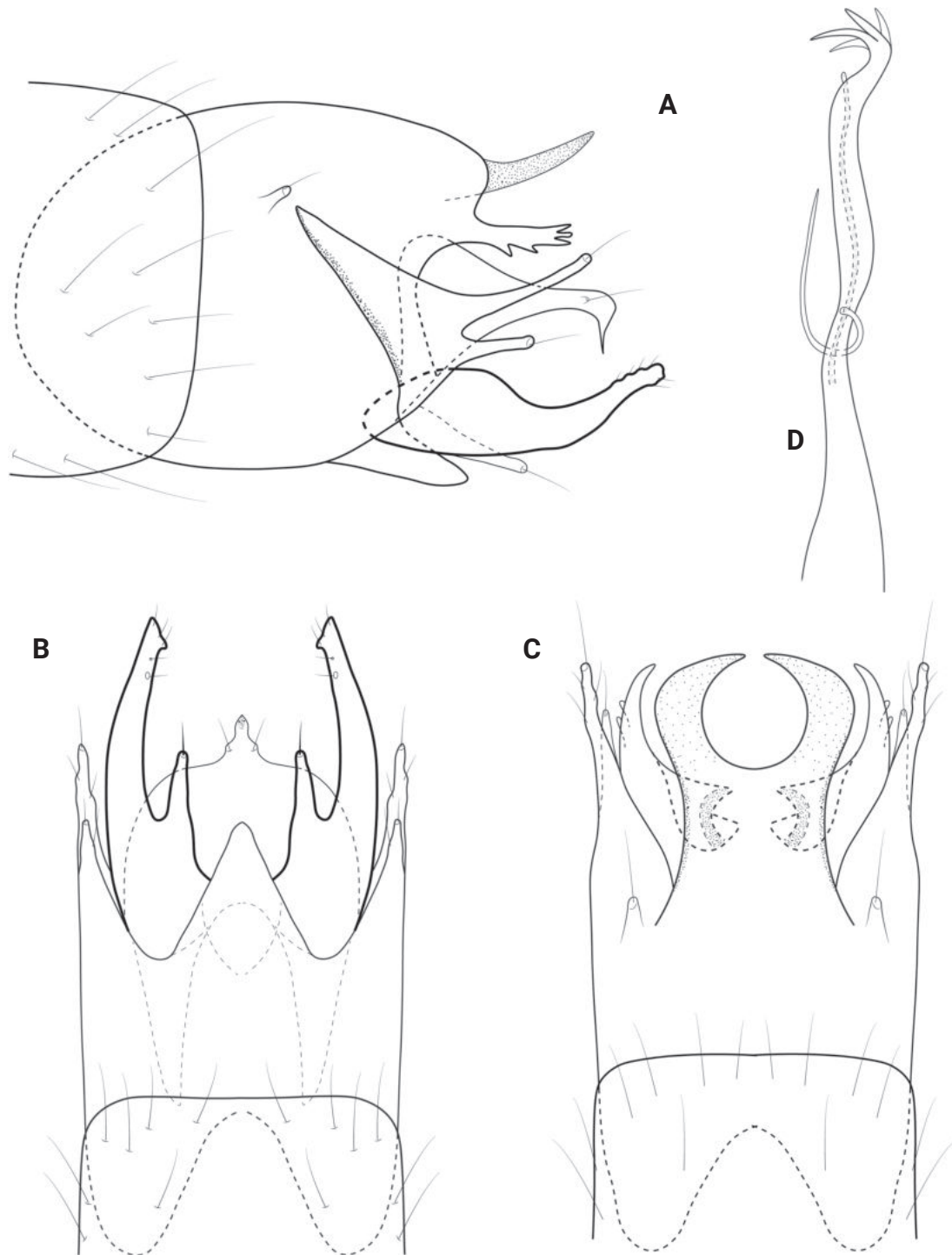


Figure 13. *Neotrichia paraxicana* sp. nov., male holotype, genitalia **A** left lateral **B** ventral **C** dorsal **D** phallus, left lateral.

Other material examined. **PANAMA** • ♂; **Veraguas Province:** Cuenca 097, Santa Fe District, Santa Fe NP, Río Piedra de Moler; PSPSCB-PNSF-C097-2017-012; 8.56553°N, 81.18817°W; 340 m a.s.l.; 20.iv.2017; A. Cornejo, T. Ríos, E. Álvarez, C. Nieto leg.; UV light trap • ♂; **Panama Province:** Panama Canal, date and locality of collection illegible on label; D. Denning leg.

Diagnosis. *Neotrichia paraxicana* sp. nov. is another member of the *N. canixa* group of Keth et al. (2015) based on the posterior horns from tergum X, forked bracteole, bifid inferior appendage, and the forked phallic apex. The new

species is most similar to *N. xicana* (Mosely, 1937), reported from Mexico and Panama (Holzenthal and Calor 2017), based on both having a posterolateral process from segment IX, which is lobate apically. However, in the new species this process is very short, and the phallic apex is multi-forked.

Description. Male. Total length 1.6–1.8 mm ($n = 3$), 18 antennal segments, wings and body brown in alcohol. **Genitalia** (Fig. 13). Abdominal segment VIII annular. Segment IX in lateral view generally ovate, rounded anteriorly, setae-bearing lobe dorsally, posteriorly fused with segment X dorsally, incised posteroventrally, short posterolateral process with multiple small lobes apically; in ventral view posterior margin deeply incised laterally, anteriorly margin broadly incised; in dorsal view posterolateral process from IX visible as a curving, tapering process with subapical lobes laterally. Tergum X basally fused with segment IX, posteriorly produced into pair of thick, symmetrical horns; in lateral view distal horn is thin and tapering to acute apex. Subgenital plate in lateral view, wide basally, tapering apically to rounded apex, with acute downward pointing spike; in ventral view wide basally, rounded laterally to apicomesal extension bearing stout setae laterad. Bracteole in lateral view wide anteriorly, bifid posteriorly, dorsal branch $\sim 2\times$ as long as ventral branch; in ventral and dorsal views both branches wide basally, tapering to rounded apices. Inferior appendage wide basally with narrow basal process ventrally, abruptly narrowing at midlength and curving upward to thin, truncated apex; in ventral view bifid, outer process elongate, wide basally and tapering to acute apices with inner spike, inner process fused basally and narrow over length, shorter than outer process. Phallus tubular, constricted at midlength and bearing thin paramere encircling shaft, apex divided into four spine-like processes, ejaculatory duct protruding subapically.

Distribution. Panama: Veraguas Province (Santa Fe National Park).

Etymology. This species is named for its overall resemblance to *Neotrichia xicana*. The name is an adjective used as a substantive in the genitive case.

***Neotrichia snixae* sp. nov.**

<https://zoobank.org/073C61D3-B348-430C-B442-3792E6BBCFFE>

Fig. 14

Type locality. Panama: Chiriquí Province: Cuenca 102, Renacimiento District, Reserva Privada Landis, Quebrada sin nombre, Location 1; 8.64379°N, 82.82949°W; 755 m a.s.l.

Type material. Holotype: ♂, **PANAMA: Chiriquí Province:** Cuenca 102, Renacimiento District, Reserva Privada Landis, Quebrada sin nombre, Location 1; 8.64379°N, 82.82949°W; 755 m a.s.l.; 15–31.iii.2020; M. Landis leg.; Malaise trap; MUPADI-014-T-2023 (in alcohol).

Other material examined. PANAMA • ♂; **Chiriquí Province:** Cuenca 108, Boquete District, Quebrada Jaramillo Abajo; 8.745827°N, 82.418083°W; 1054 m a.s.l.; 6.ii.2019; K. Castillo leg.; UV light trap.

Diagnosis. *Neotrichia snixae* sp. nov. is a member of the *N. canixa* group of Keth et al. (2015) based on the posterior horns from tergum X and the forked bracteole. The horns are asymmetrical, which is similar to that seen in *N. malickyi* Harris & Tiemann, 1993 from Panama and *N. jarochoita* Bueno-Soria,

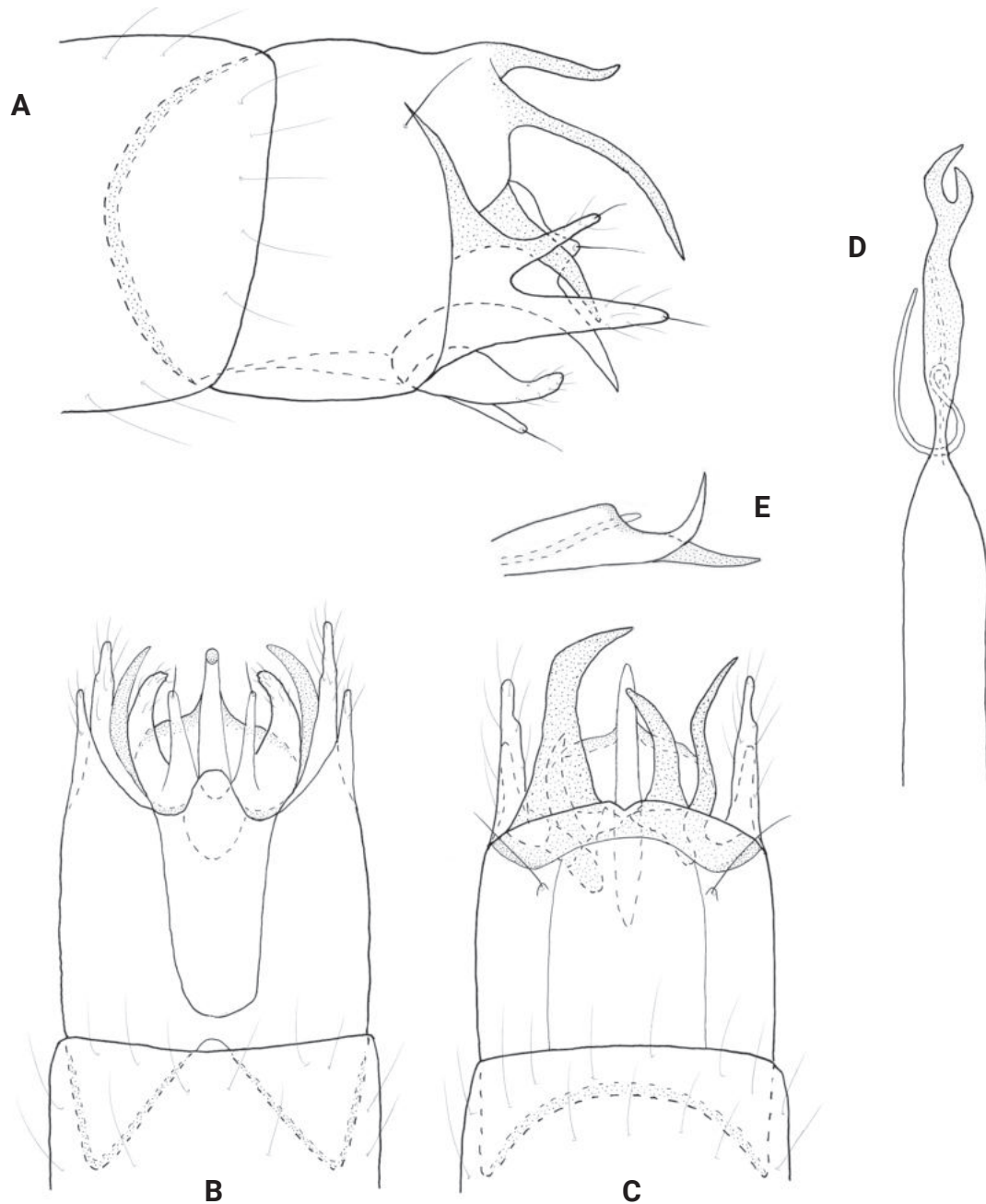


Figure 14. *Neotrichia snixae* sp. nov., male holotype, genitalia **A**, left lateral **B** ventral **C** dorsal **D** phallus, dorsal **E** phallus apex, lateral.

1999 from Mexico, both of which have the right horn longer than that of the left. The new species differs in the presence of a sclerotized posterolateral process from segment IX, which is also seen in *N. juani* Harris & Tiemann, 1993 from Texas and *N. unamas* Botosaneanu (in Botosaneanu and Alkins-Koo 1993), which occurs in Panama, and in the shape of the end of the phallus.

Description. Male. Total length 1.9 mm ($n = 2$), 18 antennal segments, wings and body brown in alcohol. **Genitalia** (Fig. 14). Abdominal segment VIII annular. Segment IX in lateral view anteriorly rounded, incomplete posteriorly, fused with X dorsally, mesally with sclerotized posterolateral process which narrows distally; in dorsal view fused posteriorly with X, pair of setaceous lobes laterally, anteriorly with rounded incision, lateral processes dissimilar in length and

shape; in ventral view with deep mesal incision. Tergum X basally fused with segment IX, quadrate, posterior horns asymmetrical, right horn longer than left and thicker, curving inward distally; in lateral view ventral horn twice as long as dorsal horn. Subgenital plate in lateral view wide basally, tapering distally to divided apex, dorsally with stout seta, ventrally with elongate downturned process which is apically acute; in dorsal and ventral views wide basally, elongate posteromesally, rounded laterally. Bracteole in lateral view bifid posteriorly, ventral branch longer than dorsal, each tipped with stout seta; in dorsal and ventral views branches unequal in length, wide basally tapering distally. Inferior appendage wide basally, gradually tapering distally to rounded slightly upturned apex, narrow ventral process basally; in ventral view wide basally, curving on inner margin to rounded apex, mesal process tapering distally and bearing stout seta. Phallus tubular, constricted at midlength and bearing thin paramere encircling shaft, apically sclerotized with narrow apical incision forming unequal branches, similar in appearance to a can-opener; in lateral view apex divided into pair of elongate, thin processes.

Distribution. Panama: Chiriquí Province (Reserva Privada Landis; Boquete District).

Etymology. Named for Dr. Shannon Nix, friend and colleague of the first author in recognition of her outstanding teaching while at Clarion University and her many scientific contributions to ecology and mycology. The name is a noun in the genitive case.

***Neotrichia spangleri* sp. nov.**

<https://zoobank.org/F5ABEE1A-A42C-4192-9A98-1615AD3B938D>

Fig. 15

Type locality. Panama: Chiriquí Province: Cuenca 108, Boquete District, Bajo Boquete, Quebrada Cheche, Hotel Fundadores; 8.77195°N, 82.43308°W; 1200 m a.s.l.

Type material. *Holotype*: ♂, PANAMA: Chiriquí Province: Cuenca 108, Boquete District, Bajo Boquete, Quebrada Cheche, Hotel Fundadores; 8.77195°N, 82.43308°W; 1200 m a.s.l.; 29.v.1983; P. Spangler, R. Faitoule, W. Steiner leg.; MUPADI-015-T-2023 (in alcohol). *Paratype*. PANAMA • ♂; same as holotype; MUPADI-016-T-2023 (in alcohol).

Other material examined. PANAMA • 2 ♂♂; Chiriquí Province: Cuenca 104, Bugaba District, La Concepción, Río Guigala, Puente antigua vías del Ferrocarril; 8.51845°N, 82.64280°W; 209 m a.s.l.; 12.iii.2021; T. Ríos, Y. Aguirre leg.; UV light trap • 2 ♂♂; *ibid.*, except Cuenca 108, Boquerón District, Río Chirigagua, Puente antes de llegar al Hotel Los Delfines; 8.48139°N, 82.54788°W; 128 m a.s.l.; 12.iv.2021; T. Ríos, Y. Aguirre leg.; UV light trap • 4 ♂♂; *ibid.*, except David District, San Pablo Viejo, puente vía Interamericana antes de llegar a la entrada de Bagala, Río Platana; 8.46416°N, 82.52030°W; 84 m a.s.l.; 12.ii.2021; T. Ríos, Y. Aguirre leg.; UV light trap • ♂; *ibid.*, except 12.iii.2021 • 2 ♂♂; *ibid.*, except 12.iv.2021 • 11 ♂♂; *ibid.*, except 6.x.2021 • 4 ♂♂; *ibid.*, except 6.xi.2021 • 2 ♂♂; **Darién Province**; Cuenca 156, Chepigana District, PND, Río Tuira, Boca de Cupe; 8.01732°N, 77.72417°W; 150 m a.s.l.; 18.ii.1985; leg. not given; UV light trap (NMNH).

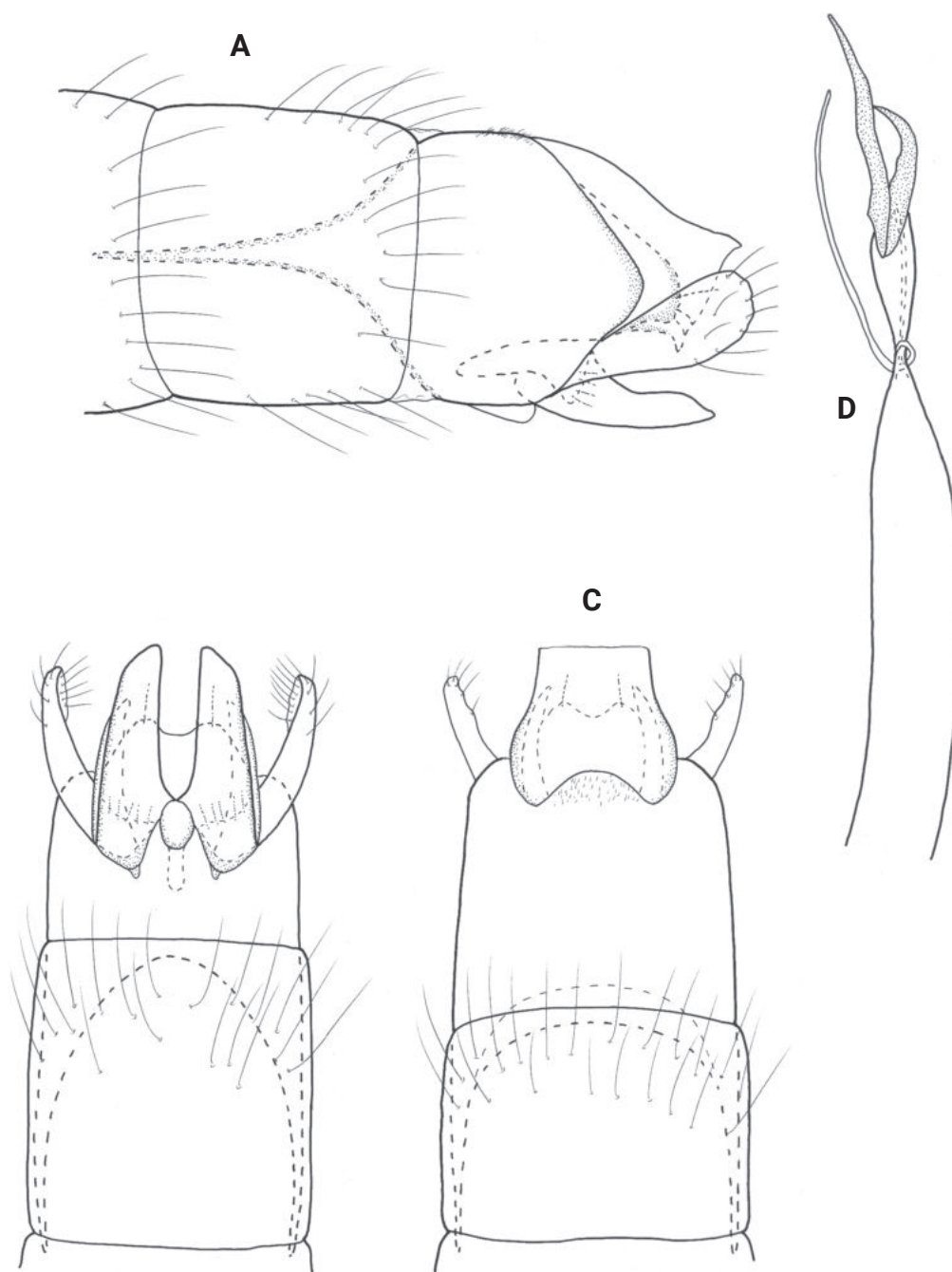


Figure 15. *Neotrichia spangleri* sp. nov., male holotype, genitalia **A** left lateral **B** ventral **C** dorsal **D** phallus, dorsal.

Diagnosis. The pair of spines at the phallic apex and the posterolateral process from segment IX places this species in the *N. collata* group of Keth et al. (2015) with similarity to *N. hiaspa* (Mosely, 1937) and *N. carlsoni* Harris & Armitage, 2019, both of which occur in Panama. The new species is separated by the shorter and wider inferior appendage, the rounded posterolateral process from segment IX, which is thin and acute in the other species, and the structure of the subgenital plate.

Description. Male. Total length 1.3–1.5 mm ($n = 10$), 18 antennal segments, wings and body brown in alcohol. **Genitalia** (Fig. 15). Abdominal segment VIII annular. Segment IX in lateral view anteriorly tapering to an elongate apodeme, posteriorly widening mesally, which gives rise to a rounded posterolateral

process; ventrally deeply incised anteriorly, posteriorly with lateral incisions forming mesal ovate structure; posterolateral processes thin, tapering to acute apices; dorsally with posterior shallowly incised laterally, setose mesally. Segment X in lateral view tapering to acute distal point; in dorsal view wide basally, rounded laterally to truncate apex. Subgenital plate in lateral view narrow, apex downturned and acute; in dorsal and ventral view wide basally, apex with mesal emargination, flanked by pair of setae. Bracteole in lateral view narrow basally, widening distally to rounded apex; in ventral and dorsal views nearly parallel-sided, curving on outer margin. Inferior appendage short, wide basally, tapering distally to broadly pointed apex; in ventral view rectangular, apex tapered to rounded point. Phallus in dorsal view tubular, bearing short paramere encircling shaft at midlength, apex with pair of elongate sclerotized rods fused basally, one rod ~ 1/2 length of other and curved.

Distribution. Panama: Chiriquí Province (Boquerón, Boquete, and Bugaba districts); Darién Province (Chepigana District).

Etymology. The species name honors the memory of Dr Paul Spangler of the National Museum of Natural History, who collected some of the specimens. The name is a noun in the genitive case.

***Neotrichia veraguasensis* sp. nov.**

<https://zoobank.org/215B4D9D-9270-49E4-8481-3F273FC34106>

Fig. 16

Type locality. Panama: Veraguas Province: Cuenca 132, Santa Fe District, Santa Fe NP, Quebrada Mulabá; PSPSCB-PNSF-C132-2017-009; 8.52560°N, 81.12956°W; 623 m a.s.l.

Type material. Holotype: ♂, PANAMA: Veraguas Province: Cuenca 132, Santa Fe District, Santa Fe NP, Quebrada Mulabá; PSPSCB-PNSF-C132-2017-009; 8.52560°N, 81.12956°W; 623 m a.s.l.; 20.iv.2017; A. Cornejo, T. Ríos, E. Álvarez, C. Nieto leg.; UV light trap; MIUP-021-T-2023 (in alcohol).

Other material examined. PANAMA • ♂; *ibid.*, except Río Piedra de Moler; PSPSCB-PNSF-C097-2017-012; 8.56553°N, 81.18817°W; 340 m a.s.l.; 20.iv.2017; MIUP (in alcohol).

Diagnosis. This new species, which lacks spines at the phallic apex, is placed in the *N. okopa* group of Keth et al. (2015), with closest similarity to *N. abbreviata* Flint, 1983 from Uruguay and *N. okopa* Ross, 1939 from throughout North America. The new species is separated by the triangular inferior appendage in lateral view, and the lack of a posterolateral process from segment IX.

Description. Male. Total length 1.6 mm ($n = 2$), 18 antennal segments, wings and body brown in alcohol. **Genitalia** (Fig. 16). Abdominal segment VIII annular. Segment IX in lateral view anteriorly tapering to short apodeme, posteriorly rounded, short truncate lobe posteroventrally; ventrally divided into two posterior bands; dorsally with anterior margin incised, posterior shallowly emarginate. Segment X triangular in lateral view; in dorsal view fused basally with segment IX, posteriorly sinuate on lateral margin and tapering to rounded apex. Subgenital plate in lateral view narrow basally, ventral margin with large sclerotized lobe at midlength, upper margin straight distally, abruptly tapered posteriorly to rounded apex bearing stout seta; in ventral view wide and rounded laterally

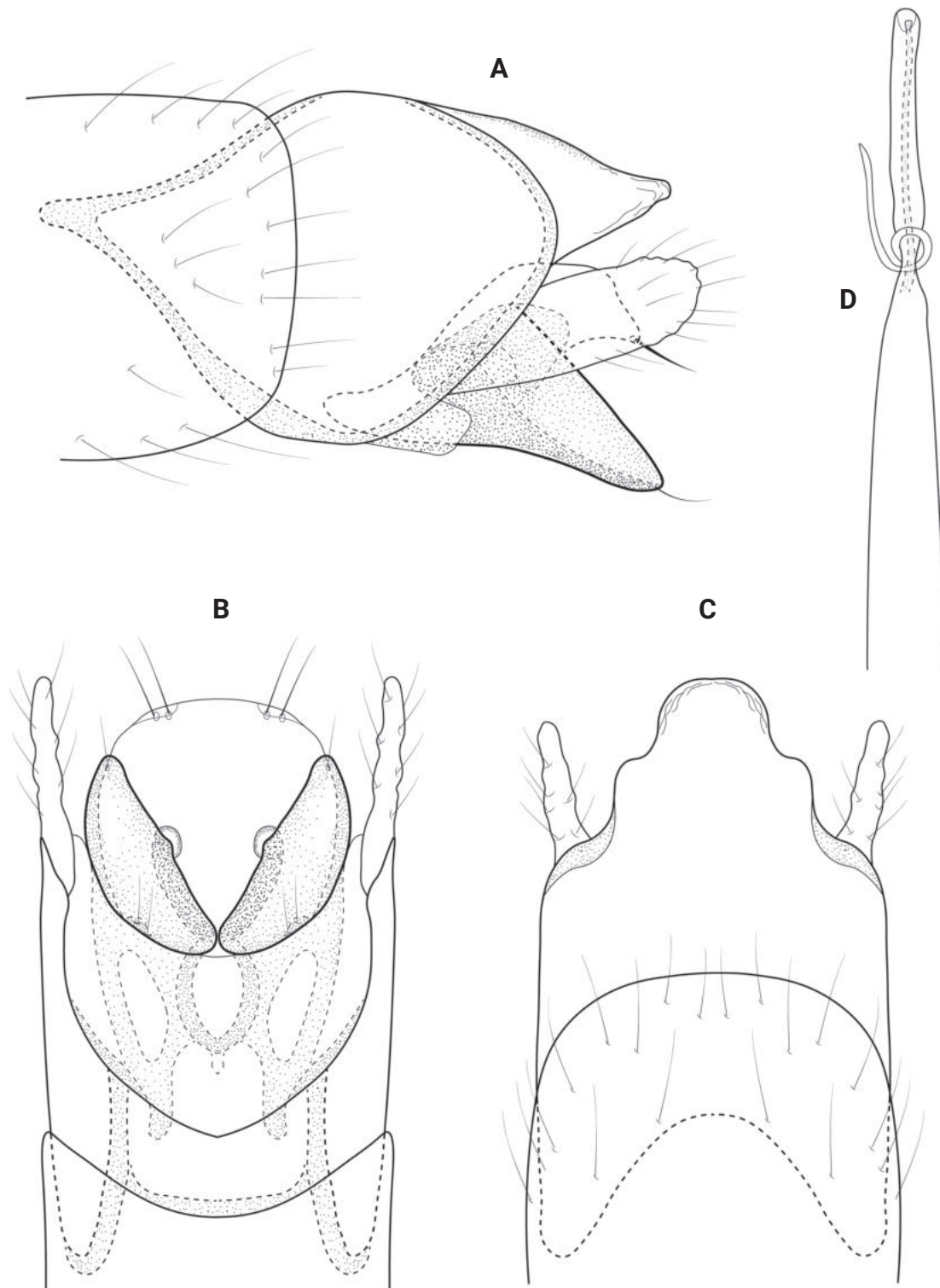


Figure 16. *Neotrichia veraguasensis* sp. nov., male holotype, genitalia **A** left lateral **B** ventral **C** dorsal **D** phallus, ventral.

to truncate apex, with setae laterally. Bracteole in lateral view parallel-sided to rounded apex; in ventral and dorsal views straight, narrow over length. Inferior appendage triangular and sclerotized; in ventral view divergent, lateral margin curving, inner margin straight, round lobe at midlength, basally with elaborate thin sclerites. Phallus in dorsal view tubular, bearing short paramere encircling shaft at midlength, apex rectangular with ejaculatory duct protruding mesally.

Distribution. Panama: Veraguas Province (Santa Fe National Park).

Etymology. This species is named for Veraguas Province where the male holotype was collected. The name is a noun in the genitive case.

New country records

Neotrichia minutisimella (Chambers, 1873)

Material examined. PANAMA • ♂; **Veraguas Province:** Cuenca 097, PNSF, afluente sin nombre de Río Calovebora; PSPSCD-PNSF-CO97-2017-011; 8.55343°N, 81.17675°W; 395 m a.s.l.; 20.iv.2017; A. Cornejo, T. Ríos, E. Álvarez, C. Nieto leg.; UV light trap.

Note. This is a new country record for Panama and a significant extension of its southern range (formerly Texas, U.S.A.).

Distribution. Canada: Manitoba; Panama: Veraguas Province (Santa Fe National Park); U.S.A.: Alabama, Arkansas, Florida, Georgia, Illinois, Indiana, Kansas, Kentucky, Louisiana, Minnesota, Mississippi, Missouri, North Carolina, Oklahoma, South Carolina, Texas.

Neotrichia vibrans Ross, 1944

Figs 17, 18

Material examined. PANAMA • 27 ♂♂, 25 ♀♀; **Chiriquí Province:** Cuenca 108, David, UNACHI–Jardin Botanico, El Cabrero, nr Quebrada San Cristobal; 8.434060°N, 82.451930°W; 45 m a.s.l.; 19.iv–3.v.2021; Y. Aguirre, T. Ríos leg.; Malaise trap • 22 ♂♂, 23 ♀♀; *ibid.*, except 5–19.iv.2021 • ♂; **Panama Oeste Province:** Cuenca 115, Chame District, Altos de Campana NP, Río Sajalices; PSPSCB-PNAC-C115-2018-030; 8.67625°N, 79.89748°W; 194 m a.s.l.; 27–31.v.2018; E. Pérez, C. Nieto, M. Molinar, T. Ríos leg.; Malaise trap.

Female (Fig. 18). The female of *N. vibrans* is slightly larger than the males, with total length from 2.0 to 2.5 mm compared to 1.8 to 2.0 mm, both having 18 antennal segments and the wings and body are brown in alcohol. Abdominal sternite VIII has a heavily sclerotized square plate (Fig. 18A), with a thin ridge on the posterior margin that narrows to an acute posteromesal point, which projects downward in lateral view, anteriorly the plate margin is rounded with a thin sinuate internal structure. The bursa copulatrix lies under the sclerotized plate of segment VIII and details are difficult to discern, but it is generally rectangular in shape, the genital chamber narrowing posteriorly to an acute point, genital chamber broadly incised anteriorly producing a pair of “feet” with heavily sclerotized inner margins, these “feet” extend posteriorly forming a mesal sclerite (Fig. 18B).

Note. This is a new country record for Panama. In addition, it is a significant southern extension of the species range, which formerly was northern Mexico. The male of this species is here re-illustrated (Fig. 17) because the figures in Keth et al. (2015) do not clearly depict the lateral view of this species. The posterolateral processes from abdominal segments IX and X are difficult to see in those drawings and the bracteole is obscured by the process from IX. As well, the figure for *N. vibrans* in Ross (1944) lacks a lateral view and the phallus is shown as the apex having a pair of lobes bearing stout spines. These lobes and

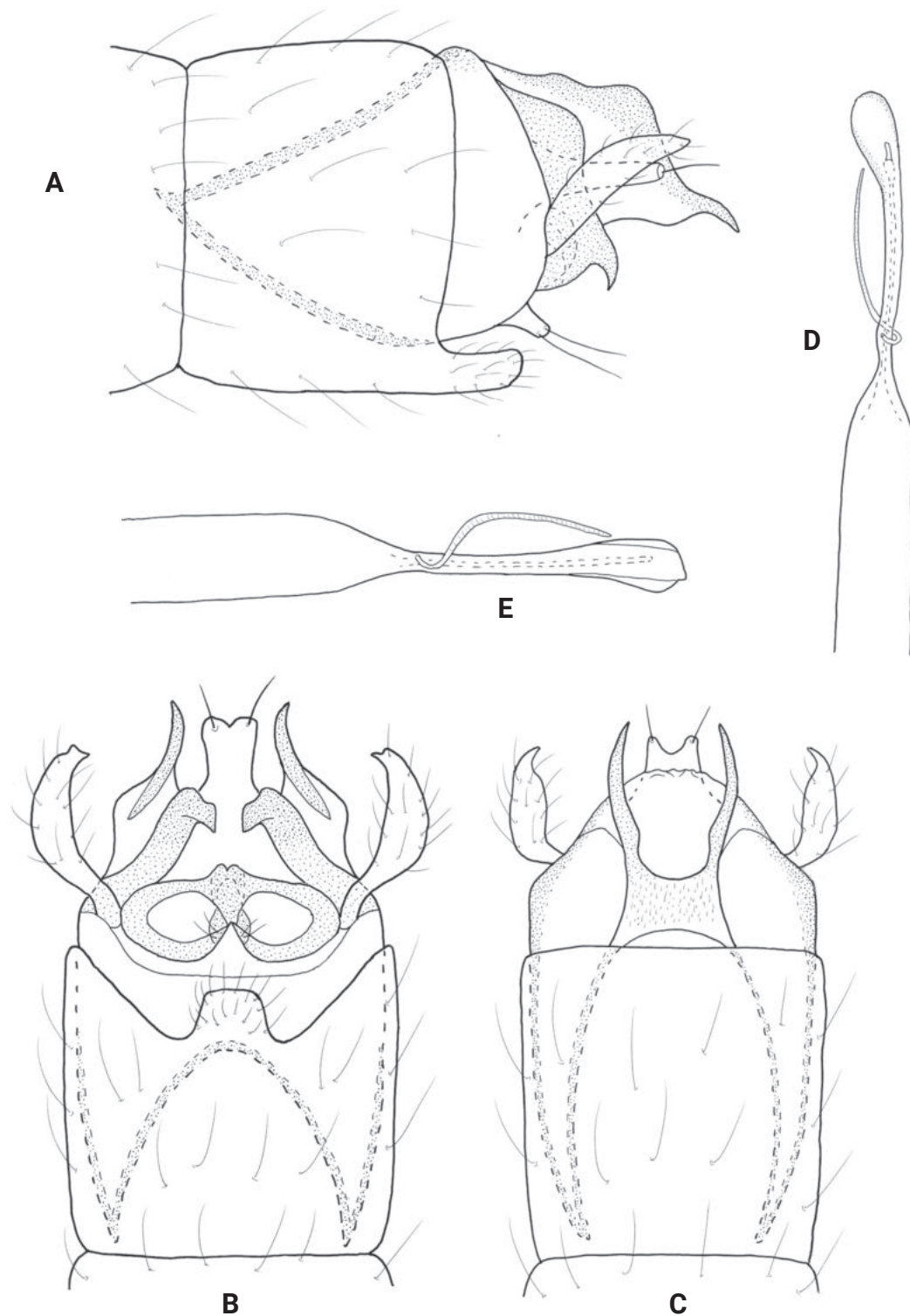


Figure 17. *Neotrichia vibrans* Ross, male genitalia **A** left lateral **B** ventral **C** dorsal **D** phallus, dorsal **E** phallus, lateral.

spines, which are also used as characters in the diagnostic key in Ross (1944), belong to the apex of the subgenital plate, with the phallus lacking apical spines.

Females of other species from the *N. vibrans* group of Keth et al. (2015) also have a sclerotized plate on the sternum of segment VIII, including *Neotrichia* ♀ sp. B (in Botosaneanu and Alkins-Koo 1993), which was tentatively identified as *N. armata* Botosaneanu, 1993, *N. iridescens* Flint, 1964, and *N. soleaferrea*

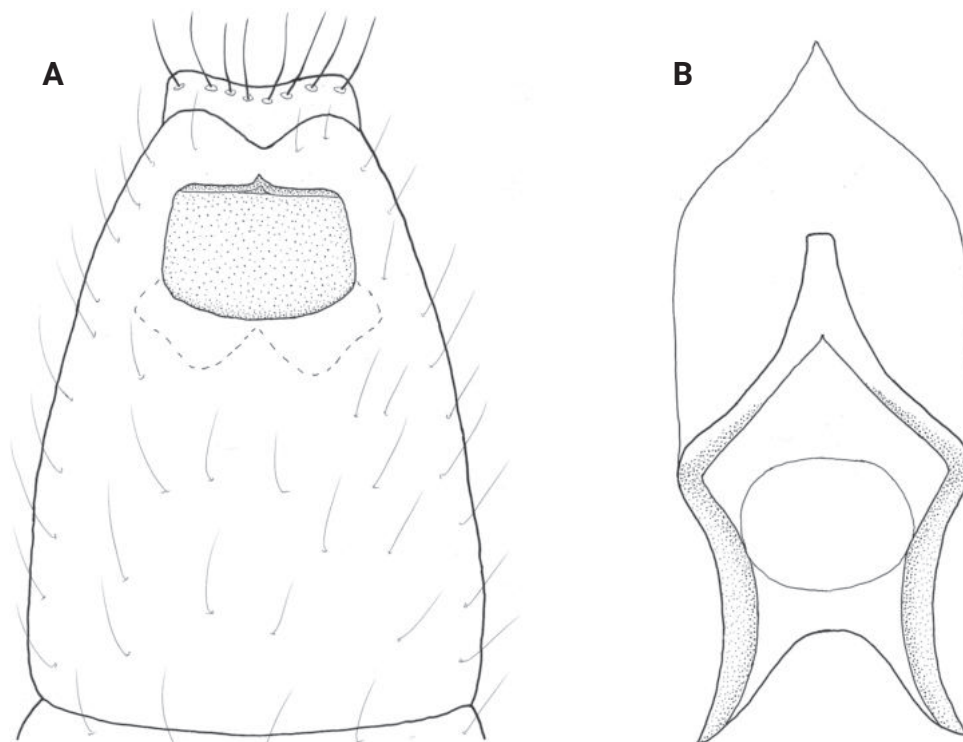


Figure 18. *Neotrichia vibrans* Ross, female genitalia **A** ventral **B** bursa copulatrix, ventral.

Botosaneanu (in Botosaneanu and Hyslop 1998). However, other members of this group have the females unidentified, or in the case of *N. heleios* Flint, 1968 the sternum of sternite VIII lacks a sclerotized plate. Also, with the exception of *N. soleaferrea*, the structure of the bursa copulatrix appears to be much different than that seen in *N. vibrans*.

The ventral plate on sternite VIII is not a characteristic unique to the *N. vibrans* group. Females in other groups have a distinctive sclerotized plate, e.g., *N. margaritena* Botosaneanu (in Botosaneanu and Vilorio 2002) of the *N. biuncifera* group (Marshall 1979). Also, females for several members of the *N. caxima* group, including *N. nesiotis* Flint & Sykora, 1993, *N. mentonensis* Frazer & Harris, 1991, *N. rasmusseni* Harris & Keth, 2002, and *N. armitagei* Harris, 1991 share this trait. In addition, many members of the *N. caxima* group also have females with the structure of the bursa copulatrix very similar to that seen in the female of *N. vibrans* (Harris and Rasmussen 2010).

Considering the above variation and overlap of characters, more associations are needed to facilitate a detailed comparison and delineation of *Neotrichia* females before we can adequately diagnose any females definitively. The descriptive text for *N. vibrans* above is a contribution toward that future comparison. Finally, we were fortunate in being able to associate the female of *N. vibrans* with the male because individuals of both sexes were found, in quantity, together in the absence of any other congeners in a non-natural botanical garden site. Most natural stream sites we have sampled in Panama have 2–7 species present in the same sample, making associations more difficult.

Distribution. Mexico: Chihuahua; Panama: Chiriquí Province (David District); U.S.A.: Alabama, Arkansas, Florida, Georgia, Illinois, Kansas, Kentucky, Maine, Minnesota, Mississippi, Missouri, New Hampshire, New York, Ohio, Oklahoma, South Carolina, Tennessee, Texas, Virginia, West Virginia, Wisconsin.

Key to the males of *Neotrichia* in Panama

Species of *Neotrichia* are difficult to identify given their tiny size, which varies from 1 to 3 mm, and the complex genitalia, on which identifications are dependent. The small size often necessitates that specimens are mounted on slides and observed at high magnification. Drawings are likewise prepared from these slide-mounted specimens. Two broad characters are often useful in making species determinations: small terminal horns located on the apex of tergum X and the presence of a posterolateral process from segment IX, which is often sclerotized. When the terminal horns are present, characters of the bracteoles, inferior appendages and phallus become important. When a posterolateral process from segment IX is present, then the appearance of these processes and their location and point of origin, the bracteoles, phallus, and inferior appendages all provide useful characters. For example, the posterolateral process can be mesal as in *N. honda* and *N. parajaroquita*, dorsal as in *N. landisae* and *N. paraxicana*, and ventral as in *N. lenati*. In some instances, what appears to be a process from segment IX is actually a part of the subgenital plate, or another structure. For simplicity and ease of using this key, we have termed what appears to be a posterior extension of segment IX as a posterolateral process.

- 1 Inferior appendages fused mesally into a plate, which is evident in ventral view (Fig. 17B; Keth et al. 2015: fig. 85C) **2**
 - Inferior appendages separate, not fused mesally as seen in ventral view (Figs 2B, 4B, 13B, 15B) **3**
- 2 Inferior appendages fused into an elongate rectangular plate (Keth et al. 2015: fig. 85C); abdominal segment VIII without a ventromesal process (Keth et al. 2015: fig. 85A) ***N. minutissimella* (Chambers, 1873)**
 - Inferior appendages fused into an ovate plate (Fig. 17B); abdominal segment VIII with a prominent ventromesal process (Fig. 17A, B) ***N. vibrans* Ross, 1944**
- 3 Horns from posterior tergum X, which vary in shape and size (Figs 10C, 12C, 14C), and may be symmetrical (Figs 3C, 13C) or asymmetrical (Figs 12C, 14C); phallus sharply narrowing apically, often bifid and recurving (Figs 3D, 11D, 12D, 13D); bracteoles typically bifid (Figs 3A, 10A, 12A, 14A) **4**
 - Horns absent from posterior tergum X (Figs 2C, 4C, 5C, 6C), although in some species the posterolateral projection from segment IX may appear to be horn-like (Fig. 8A; Armitage and Harris 2018: fig. 7A, B; Harris and Armitage 2019: fig. 16A); phallus apex various, but typically not bifid and recurved (Figs 2D, 4D, 6D, 9D, 15D), bracteoles various, but not typically bifid (Figs 2A, 4A, 5A, 7A, 15A, 16A) **20**
- 4 Horns from posterior tergum X asymmetrical (Figs 12C, 14C) **5**
 - Horns from posterior tergum X symmetrical (Figs 3C, 10C, 11C) **7**
- 5 Left-side horn of posterior tergum X longer than right-side horn (Fig. 12C); posterolateral process from segment IX present (Fig. 12A) ***N. parajaroquita* sp. nov.**
 - Right-side horn of posterior tergum X longer than left-side horn (Fig. 14C, Harris and Tiemann 1993: fig. 2C); posterolateral process from segment IX present (Fig. 14A) or absent (Harris and Tiemann 1993: fig. 2A) **6**

- 6 Posterolateral process from segment IX present; ventral branch of bracteole longer than dorsal branch (Fig. 14A) ***N. snixae* sp. nov.**
- Posterolateral process from segment IX absent (Harris and Tiemann 1993: fig. 2A); dorsal branch of bracteole longer than ventral branch (Harris and Tiemann 1993: fig. 2A) ***N. malickyi* Harris, 1993 (in Harris and Tiemann 1993)**
- 7 Linear posterior process from segment IX present (Fig. 13A) **8**
- Linear posterior process from segment IX absent (Armitage and Harris 2018: figs 5A, 6A) **12**
- 8 Linear posterior process from segment IX short, not extending beyond horns in lateral view (Fig. 13A) ***N. paraxicana* sp. nov.**
- Linear posterior process from segment IX elongate, extending beyond horns in lateral view (Harris and Armitage 2019: fig. 15A; Keth et al. 2015: fig. 22A) **9**
- 9 Linear posterior process from segment IX serrate (Harris and Armitage 2019: fig. 15A), or lobate or cleft distally (Keth et al. 2015: fig. 22A) **10**
- Linear posterior process from segment IX not serrate, or lobate or cleft distally (Fig. 11A, Keth et al. 2015: fig. 21A) **11**
- 10 Linear posterior process from segment IX in lateral view serrate on dorsal margin (Harris and Armitage 2015: fig. 14A); subgenital plate in lateral view gradually tapering distally (Harris and Armitage 2015: fig. 15A); inferior appendage in ventral view with outer process curving inward at apex, inner process elongate (Harris and Armitage 2015: fig. 15B) ***N. serrata* Harris & Armitage, 2019**
- Linear posterior process from segment IX not serrate on distal margin, cleft or lobate distally (Keth et al. 2015: fig. 22A); subgenital plate in lateral view abruptly curving ventrad apically (Keth et al. 2015: fig. 22A); inferior appendage in ventral view with outer process straight, inner process short (Keth et al. 2015: fig. 22B) ***N. xicana* (Mosely, 1937)**
- 11 Linear posterior process from segment IX widening distally and setose on margin (Keth et al. 2015: fig. 11A); subgenital plate in lateral view narrowing distally (Keth et al. 2015: fig. 11A); small rounded median process between inferior appendages in ventral view (Keth et al. 2015: fig. 11C) ***N. canixa* (Mosely, 1937)**
- Linear posterior process from segment IX saber-like, narrowing distally and without setose margin (Keth et al. 2015: fig. 21A); subgenital plate in lateral view widening distally and truncate (Keth et al. 2015: fig. 21A); large triangular process between inferior appendages in ventral view (Keth et al. 2015: fig. 22C) ***N. unamas* Botosaneanu, 1993 (in Botosaneanu and Alkins-Koo 1993)**
- 12 Dorsal branch of bracteole shorter than ventral branch (Keth et al. 2015: fig. 20A); subgenital plate trifid distally in lateral view, ventral-most branch elongate (Keth et al. 2015: fig. 20A) ***N. tauricornis* Malicky, 1980**
- Dorsal branch of bracteole longer than ventral branch, which may be vestigial (Figs 3A, 10A, 13A); subgenital plate various, but not trifid distally (Figs 10A, 13A) **13**
- 13 Bracteole with ventral branch $\geq \frac{1}{2}$ as long as dorsal branch (Fig. 3A, Armitage and Harris 2018: fig. 6A) **14**
- Bracteole with ventral branch $< \frac{1}{2}$ as long as dorsal branch and in some cases vestigial (Figs 10A, 11A) **17**

- 14 Inferior appendage in lateral view with dorsal hump at midlength (Armitage and Harris 2018: fig. 6A); horns of tergum X elongate and deeply divided to base (Armitage and Harris 2018: fig. 6B) ***N. collierorum* Armitage & Harris, 2018**
- Inferior appendage in lateral view parallel-sided (Armitage and Harris 2018: figs 3A, 5A); horns of tergum X shorter and not deeply divided to base (Armitage and Harris 2018: figs 3C, 5B) **15**
- 15 Phallus apex undivided, narrowing to elongate slender process (Armitage and Harris 2018: fig. 5D); ventral branch of bracteole short (Armitage and Harris 2018: fig. 5A) ***N. anzuelo* Armitage & Harris, 2018**
- Phallus apex divided (Harris et al. 2023: figs 3D, 4D); ventral branch of bracteole elongate (Harris et al. 2023: figs 3A, 4A) **16**
- 16 Inferior appendage in lateral view saber-shaped (Harris et al. 2023: fig. 4A), ventrally narrower at base than at midlength (Harris et al. 2023: fig. 4B); phallus apex with serrations on upper branch (Harris et al. 2023: fig. 4D); subgenital plate in lateral view narrowing distally and projecting ventrad (Harris et al. 2023: fig. 4A) ***N. majagua* Harris, Ríos & Aguirre, 2023**
- Inferior appendage in lateral view cigar-shaped (Fig. 3A), ventrally wider at base than at midlength (Fig. 3B); phallus apex without serrations on upper branch (Fig. 3D); subgenital plate in lateral view can-opener shape (Fig. 3A) ***N. candela* sp. nov.**
- 17 Phallus apex with single elongate process with small notch near base (Fig. 10D, Armitage and Harris 2020: fig. 10D, E) **18**
- Phallus apex clearly divided into two processes (Fig. 11D, Harris and Armitage 2015: fig. 4D) **19**
- 18 Posterior horns from tergum X strongly curving inward (Fig. 10C); phallus apex in dorsal view with elongate thin process (Fig. 10D); median process between inferior processes in ventral view large and pointed distally (Fig. 10B) ***N. mindyae* sp. nov.**
- Posterior horns from tergum X not strongly curving inward (Armitage and Harris 2020: fig. 10B); phallus apex in dorsal view with short curving process (Armitage and Harris 2020: fig. 10E); median process between inferior appendages in ventral view short and rounded distally (Armitage and Harris 2020: fig. 10C) ***N. michaeli* Armitage & Harris, 2020**
- 19 Dorsal branch of inferior appendage in lateral view curving and widening apically (Harris and Armitage 2015: fig. 4A); inferior appendages in ventral view with outer processes longer than inner processes and curving, median process short and truncate (Harris and Armitage 2015: fig. 4C) ***N. pamela* Harris & Armitage, 2015**
- Dorsal branch of inferior appendage in lateral view not curving and widening sub-basally (Fig. 11A); inferior appendages in ventral view with outer process equal in length to inner processes and straight, median process elongate and triangular (Fig. 11B) ***N. panamensis* sp. nov.**
- 20 Posterolateral process from segment IX, which takes different forms, from elongate (Fig. 8A–C; Harris and Armitage 2019: fig. 16A–C) to short (Figs 5A, 15A) or lobate (Figs 6A, 9A), usually this process can be seen in both lateral and dorsal view, and is typically sclerotized (Figs 7A–C, 8A–C) **21**
- Posterolateral process from segment IX absent (Fig. 16A–C; Harris 1990: fig. 8A; Thomson and Armitage 2018: fig. 8A) **36**

- 21 Posterolateral process from segment IX elongate, exceeding length of inferior appendage and bracteole, heavily sclerotized and narrowing distally to an acute point (Fig. 8A; Harris and Armitage 2019: fig. 16A; Armitage and Harris 2018: fig. 7A) **22**
- Posterolateral process from segment IX shorter, typically not exceeding length of inferior appendage and bracteole (Fig. 15A), although it may be spinose (Harris and Armitage 2019: fig. 12A); if longer than bracteole and inferior appendage then not spinose (Fig. 6A; Harris et al. 2023: fig. 6A) **26**
- 22 Inferior appendage in lateral view wide basally, greatly tapering distally to uniform width (fig. 13A in Harris and Armitage 2019); phallus apex divided into elongate spines (Harris and Armitage 2019: fig. 13D, E) ***N. hiaspa* (Mosely, 1937)**
- Inferior appendage various but not wide basally and tapering distally (Fig. 8A; Armitage and Harris 2018: fig. 7A); phallus apex various, but not divided into elongate spines (Fig. 8D) **23**
- 23 Elongate, thin ventroposterior process from segment XI; subgenital plate in lateral view with elongate ventral process (Armitage and Harris 2020: fig. 12A) ***N. yayas* Armitage & Harris, 2020**
- Elongate, thin, ventroposterior process from segment IX absent (Fig. 8A); subgenital plate in lateral view various, but without elongate ventral process (Fig. 8A) **24**
- 24 Posterolateral processes from segment IX nearly symmetrical in dorsal view (Fig. 8B; Harris and Armitage 2019: fig. 15C); inferior appendage in lateral view not deeply incised dorsally at midlength (Fig. 8A; Harris and Armitage 2019: fig. 16A) **25**
- Posterolateral processes from segment IX asymmetrical in dorsal view (Armitage and Harris 2018: fig. 7B); inferior appendage in lateral view deeply incised dorsally at midlength (Armitage and Harris 2018: fig. 7A) ***N. tatianae* Armitage & Harris, 2018**
- 25 Posterolateral process from segment IX sinuate in lateral and dorsal view (Harris and Armitage 2019: fig. 16A–C); inferior appendage in lateral view elongate, tapering distally (Harris and Armitage 2019: fig. 16A); bracteole prominent (Harris and Armitage 2019: fig. 16A) ***N. starki* Harris & Armitage, 2019**
- Posterolateral process from segment IX linear in lateral and dorsal views (Fig. 8A–C); inferior appendage in lateral view short and truncate distally (Fig. 8A); bracteole not prominent (Fig. 8A) ***N. landisae* sp. nov.**
- 26 Posterolateral process from segment IX spinose, heavily sclerotized and tapering distally (Fig. 7A; Armitage and Harris 2020: fig. 9A; Armitage and Harris 2020: fig. 11A) **27**
- Posterolateral process from segment IX various, but not spinose of heavily sclerotized (Figs 4A, 6A, 9A, 15A) **32**
- 27 Phallus apex divided into pair of elongate spines (Fig. 7D; Armitage and Harris 2020: fig. 9D, E) **28**
- Phallus apex not divided into pair of elongate spines (Armitage and Harris 2020: fig. 11D; Keth et al. 2015: fig. 55B) **29**
- 28 Segment IX in lateral view with elongate mesal process (Armitage and Harris 2020: fig. 11A); inferior appendage bifid in lateral and ventral views

(Armitage and Harris 2020: fig. 11A, B)	
..... <i>N. pierpointorum</i> Armitage & Harris, 2020	
– Segment IX in lateral view without elongate mesal process (Keth et al. 2015: fig. 55A); inferior appendage rectangular, but not bifid in lateral and ventral views (Keth et al. 2015: fig. 55A–C).....	<i>N. esmalda</i> (Mosely, 1937)
29 Inferior appendage in lateral and ventral views elongate and thin, not heavily sclerotized (Harris and Armitage 2019: fig. 12A, B; Armitage and Harris 2020: fig. 9A, B).....	30
– Inferior appendage in lateral and ventral views short and triangular, heavily sclerotized Fig. 7A, B).....	<i>N. honda</i> sp. nov.
30 Two posterolateral sclerotized processes from segment IX (Armitage and Harris 2020: fig. 9A–C); apical phallic spines equal in length (Armitage and Harris 2020: fig. 9D, E).....	<i>N. espinosa</i> Armitage & Harris, 2020
– Single posterolateral process from segment IX (Harris and Armitage 2019: fig. 12A–C); apical phallic spines unequal in length (Harris and Armitage 2019: fig. 12D, E).....	<i>N. carlsoni</i> Harris & Armitage, 2019
31 Phallus with pair of sclerotized spines (Figs 4D, E, 5D, E, 15D)	32
– Phallus with single sclerotized spine (Fig. 6D; Harris et al. 2023: fig. 15D, E) or lacking sclerotized spines (Fig. 9D)	34
32 Phallic apical spines terminal (Figs 5D, E, 15D); inferior appendage shorter than bracteole and linear (Figs 6A, 15A).....	33
– Phallic apical spines subterminal (Fig. 4D, E); inferior appendage longer than bracteole and angled dorsad at midlength (Fig. 4A)	<i>N. codaza</i> sp. nov.
33 Phallic apical spines short and nearly equal in length (Fig. 5D, E); inferior appendage bifid in lateral and ventral views (Fig. 5A, B)	<i>N. embera</i> sp. nov.
– Phallic apical spines elongate and subequal in length (Fig. 15D); inferior appendage not bifid in lateral and ventral views (Fig. 15A, B).....	<i>N. spangleri</i> sp. nov.
34 Phallus with sclerotized spine (Fig. 6D; Harris et al. 2023: 5D, E); posterolateral process from segment IX elongate, extending beyond bracteole and dorsal in position (Fig. 6A; Harris et al. 2023: fig. 5A).....	35
– Phallus without sclerotized spine (Fig. 9D); posterolateral process from segment IX short, not extending beyond bracteole and ventral in position (Fig. 9A).....	<i>N. lenati</i> sp. nov.
35 Posterolateral process from segment IX widening distally and serrate (fig. 5A, B in Harris et al. 2023); phallic spine originating apically (Harris et al. 2023: fig. 5D, E).....	<i>N. solapa</i> Harris, Ríos & Aguirre, 2023
– Posterolateral process from segment IX not widening distally or serrate (Fig. 6A, B); phallic spine originating at midlength (Fig. 6D)	<i>N. flennikeni</i> sp. nov.
36 Inferior appendages in lateral view with serrate dorsal process just past midlength (Harris and Armitage 2015: fig. 5A).....	<i>N. parabullata</i> Harris & Armitage, 2015
– Inferior appendages various but never with a serrate dorsal process just past midlength (Figs 2A, 16A; Harris 1990: fig. 8A)	37
37 Inferior appendages short in lateral view, not extending much beyond subgenital plate or bracteoles (Fig. 2A; Thomson and Armitage 2018: fig. 6A; Keth et al. 2015: fig. 42A).....	38
– Inferior appendages elongate in lateral view, typically extending well beyond the subgenital plate and bracteoles (Fig. 16A; Harris 1990: fig. 8A).....	41

- 38 Bracteole in lateral view large and nearly circular in shape (Thomson and Armitage 2018: fig. 6A) ***N. atopa* Thomson & Armitage, 2018**
- Bracteole in lateral view thin over length, not nearly circular (Fig. 2A; Keth et al. 2015: fig. 42A)..... **39**
- 39 Inferior appendage in ventral view terminating in elongate spines (Keth et al. 2015: fig. 76C) or short spines (Keth et al. 2015: fig. 42C)..... **40**
- Inferior appendage in ventral view not terminating in elongate or short spines (Fig. 2B)..... ***N. abrebotella* sp. nov.**
- 40 Inferior appendage in ventral view terminating in elongate spines (fig. 76C in Keth et al. 2015); phallus with elongate lateral rod apically (Keth et al. 2015: fig. 76B) ***N. armata* Botosaneanu, 1993 (in Botosaneanu and Alkins-Koo 1993)**
- Inferior appendages in ventral view terminating in short spines (Keth et al. 2015: fig. 42C); phallus without elongate lateral rod apically (Keth et al. 2015: fig. 42B)..... ***N. amplector* Keth, 2004**
- 41 Phallus terminating in a spine (Harris and Armitage 2019: fig. 14D) or spines (Harris 1990: fig. 8D; Keth et al. 2015: fig. 53B) **42**
- Phallus not terminating in a spine or spines (Fig. 16D; Keth et al. 2015: fig. 53B)..... **44**
- 42 Phallus terminating in a single spine (Harris and Armitage 2019: fig. 14D); subgenital plate in lateral view with complex terminal rod projecting ventrad beyond inferior appendage and subterminal rod serrate at tip (Harris and Armitage 2019: fig. 14A)..... ***N. rambala* Harris & Armitage, 2019**
- Phallus terminating in a pair of rods which can be fine (Harris 1990: fig. 8D), or stout (Keth et al. 2015: fig. 53B); subgenital plate various but not complex (Harris 1990: fig. 8A; Keth et al. 2015: fig. 53A) **43**
- 43 Rods at apex of phallus stout and elongate (Keth et al. 2015: fig. 53B); inferior appendages not bifid laterally, but triangular in ventral view (Keth et al. 2015: fig. 53A–C)..... ***N. tuxtla* Bueno-Soria, 1999**
- Rods at apex of phallus thin and short (Harris 1990: fig. 8D); inferior appendages bifid laterally and elongate ventrally (Harris 1990: fig. 8A, B) ***N. flowersi* Harris, 1990**
- 44 Inferior appendages short and triangular in lateral view (Fig. 16A) and ventral view (Fig. 16B)..... ***N. veraguasensis* sp. nov.**
- Inferior appendages elongate and rectangular in lateral and ventral views (Oláh and Johanson 2011: figs 144, 146).... ***N. kampa* Oláh & Johanson, 2011**

Discussion

With the publication of this paper, there are now 226 species of *Neotrichia* which occur in North, Central, and South America and the West Indies (Armitage et al. 2022; Gama-Neto and Passos 2023; Harris et al. 2023; Thomson 2023). Of these, 31 species are known from Mexico and 50 species from Central America, with Panama's 45 species comprising the majority of the latter. We suspect that many of Panama's 33 endemic species of *Neotrichia* would lose that status once the Trichoptera fauna in the other Central American countries becomes better known. Other than Belize, with five endemic (and total) species, no other Central American country hosts any endemics. Three species are recorded from Nicaragua, one from Costa Rica, and none are recorded from El Salvador, Guatemala, and Honduras (Thomson 2023). Given the close relationship between the

faunas of Costa Rica and Panama, we expect that they share many species. In South America, Brazil is the dominant country for this genus with 48 recorded species (Gama-Neto and Passos 2023; Santos 2023), and has the majority of the endemic species. It shares only two species with Panama (*N. tauricornis* Malicky, 1980; *N. parabullata* Harris & Armitage, 2015), so that the faunas of these two countries, though currently similar in size, are more or less distinct.

Given the rapid increase in *Neotrichia* species we have found in Panama during the last eight years (42 species, with ~ 75% of them new to science), we are no longer surprised, but still delighted, at what is revealed in our samples. With most of Panama as yet unexplored, the possibility of 75, or even 100, species of this genus in Panama is not beyond the imagination. Whereas we are just now beginning to see second and third locations for some of the *Neotrichia* we have previously described, “new” species remain the central theme of our results.

It is well known that keys to species, while useful, are usually out of date as soon as they are written. However, we developed the key presented above out of self-defense to help manage the current list, to provide a framework for new keys in the future, and, most of all, to assist us in identifying and verifying new species as they appear. In Keth et al. (2015) an attempt was made to “further organize” primarily Nearctic species into species groups. However, some of the new *Neotrichia* species we are finding in Panama raise some doubts about the validity of those groupings. Increasing knowledge of the sampling universe vis-à-vis *Neotrichia* has not necessarily brought clarification in this regard, as might be expected. Other types of analyses, including molecular, need to be brought to bear to supplement what we think we know about this most interesting genus.

Acknowledgements

Whereas the majority of the new species herein described derived from field activities of AIRG at MUPADI, six of the new species and specimen records included herein were acquired through the Sustainable Production System and Biodiversity Conservation Project (PSPSCB), conducted in a variety of Panamanian national parks and protected areas. We acknowledge the Panamanian Ministry of Environment, which managed this project with funding from the World Bank, and who provided collecting permits and other support. We thank Yusseff P. Aguirre, Eric Álvarez, Milexi Molinar, Carols Nieto, Edgar Pérez, and Aydeé Cornejo who collectively were involved in all or some of the national park collections. We also appreciate the organizational and logistical support by the Gorgas Institute and COZEM concerning this project. Collections from the Pajonal area of Panama (Fig. 1A, C) are part of a UNESCO-sponsored GeoPark Project managed by the Universidad Tecnológica de Panamá. We thank Carlos Nieto, Project Biologist, for all matters concerning the acquisition of the samples for that Project. We appreciate the artistic efforts of Leah Keth and Tatiana I. Arefina-Armitage in drawing the illustrations, and the latter’s expertise in editing the manuscript. We thank Kayla Castillo Sanchez (Boquete), Diego Garrido (Portobelo), and Viterbo Rodríguez (Santiago) for their assistance in collecting specimens. The sustained collection efforts and hospitality of Senora Marietta Isabel Landis and her staff of Reserva Privada Landis are recognized with thanks. We also appreciate Larry Wilkinson and Cathy Doig for first introducing us to Senora Landis. We express our gratitude to Patricia Kieswetter and John Jones for permitting us

to collect on their Finca La Esperanza. We also thank Ed DeWalt of the Illinois Natural History Survey for suggesting that we include drawings of the *Neotrichia vibrans* female in this publication. We are indebted to Albert Thurman for collecting in Darién Province and his logistical support. The continued, generous support of our research group by Deborah Eisberg is sincerely appreciated. Finally, we thank the reviewers and editor, for evaluating and improving this manuscript. The work involved in generating the results found in this report and the production of the manuscript itself was made possible thanks to support to the second author (BJA) by the Sistema Nacional de Investigación (SNI) of the Secretaría Nacional de Ciencia, Tecnología e Innovación (SENACYT), Panama.

Additional information

Conflict of interest

The authors have declared that no competing interests exist.

Ethical statement

No ethical statement was reported.

Funding

We acknowledge the Panamanian Ministry of Environment, which managed the Sustainable Production System and Biodiversity Conservation Project with funding from the World Bank.

Author contributions

Conceptualization: BJA. Investigation: TARG, SCH. Data curation: BJA, TARG. Formal analysis: SCH. Writing – original draft: BJA, SCH. Writing–Review and editing: BJA, SCH, TARG. Funding acquisition: BJA.

Author ORCIDs

Steven C. Harris  <https://orcid.org/0000-0002-6432-7462>

Brian J. Armitage  <https://orcid.org/0000-0003-3182-1533>

Tomás A. Ríos González  <https://orcid.org/0000-0003-0590-6488>

Data availability

All of the data that support the findings of this study are available in the main text.

References

- Armitage BJ, Harris SC (2018) The Trichoptera of Panama. V. Descriptions of new species, new country records, and a synonymy. *Insecta Mundi* 0604: 1–11.
- Armitage BJ, Harris SC (2020) The Trichoptera of Panama XIV. New species of micro-caddisflies (Trichoptera: Hydroptilidae) from Omar Torrijos Herrera National Park. *Insecta Mundi* 0750: 1–19.
- Armitage BJ, Harris SC, Holzenthal RW (2015) The Trichoptera of Panama. I. New records for caddisflies (Insecta: Trichoptera) from the Republic of Panama. *Insecta Mundi* 0435: 1–10.
- Armitage BJ, Harris SC, Blahnik RJ, Thomson RE (2016) The Trichoptera of Panama IV. New records for caddisflies (Insecta: Trichoptera) from the Republic of Panama. *Insecta Mundi* 0511: 1–13.

- Armitage BJ, Harris SC, Ríos TA, Aguirre YP, Arefina-Armitage TI (2022) The Trichoptera of Panama. XVII. One new genus record and twelve first species records of microcaddisflies (Trichoptera, Hydroptilidae) from the Republic of Panama. *Check List* 18(1): 233–239. <https://doi.org/10.15560/18.1.233>
- Blahnik RJ, Holzenthal RW (2004) Collection and curation of Trichoptera, with an emphasis on pinned material. *Nectopsyche—Neotropical Trichoptera Newsletter* 1: 8–20.
- Botosaneanu L, Alkins-Koo M (1993) The caddis flies (Insecta: Trichoptera) of Trinidad and Tobago, West Indies. *Bulletin de l'Institut Royal des Sciences Naturelles de Belgique. Entomologie* 63: 5–45.
- Botosaneanu L, Hyslop EJ (1998) A systematic and biogeographic study of the caddisfly fauna of Jamaica (Insecta: Trichoptera). *Bulletin de l'Institut Royal des Sciences Naturelles de Belgique. Entomologie* 68: 5–28.
- Botosaneanu L, Vilorio AL (2002) The caddisflies (Insecta, Trichoptera) of Isla de Margarita (Venezuela) - with description of two new species. *Mitteilungen aus dem Museum für Naturkunde in Berlin Deutsche Entomologische Zeitschrift* 49: 105–111. <https://doi.org/10.1002/mmnd.20020490108>
- Bueno-Soria J (1999) Studies in aquatic insects XV: new species of *Neotrichia* and first record of *Oxyethira hilosa* (Trichoptera: Hydroptilidae) from Mexico. *Entomological News* 110: 113–117.
- Bueno-Soria J (2010) Some new Trichoptera (Glossosomatidae, Hydroptilidae, Hydropsychidae and Polycentropodidae) from Mexico. *Proceedings of the Entomological Society of Washington* 112(1): 22–31. <https://doi.org/10.4289/0013-8797-112.1.22>
- Bueno-Soria J, Hamilton SW (1986) Estudios en insectos acuáticos VI: cinco especies nuevas de trichópteros de México: (Trichoptera: Polycentropodidae; Hydroptilidae; Hydropsychidae). *Anales del Instituto de Biología, Universidad Nacional Autónoma de México, Serie Zoología* 57: 299–310.
- Calor AR, Mariano R (2012) UV light pan traps for collecting aquatic insects. *Entomobrasilia* 5(2): 164–166. <https://doi.org/10.12741/ebrazilis.v5i2.187>
- Chambers VT (1873) Micro-Lepidoptera. *Canadian Entomologist* 5(6): 110–115, 124–128. <https://doi.org/10.4039/Ent5110-6>
- Cornejo A, López-López E, Ruiz-Picos RA, Sedeño-Díaz JE, Armitage BJ, Arefina TI, Nieto C, Tuñón A, Molinar M, Ábrego T, Pérez E, Tuñón AR, Magué J, Rodríguez A, Pineda J, Cubilla J, Avila Quintero IM (2017) Diagnóstico de la condición ambiental de los afluentes superficiales de Panamá. Ministerio de Ambiente, 326 pp.
- Flint Jr OS (1964) The caddisflies (Trichoptera) of Puerto Rico. University of Puerto Rico, Agricultural Experiment Station, Technical Paper 40: 1–80.
- Flint Jr OS (1983) Studies of Neotropical caddisflies, XXXIII: New species from austral South America (Trichoptera). *Smithsonian Contributions to Zoology* 377(377): 1–100. <https://doi.org/10.5479/si.00810282.377>
- Flint Jr OS, Sykora JL (1993) New species and records of caddisflies (Insecta: Trichoptera) from the Lesser Antilles, with special reference to Grenada. *Annals of the Carnegie Museum* 62(1): 47–62. <https://doi.org/10.5962/p.215118>
- Frazer KS, Harris SC (1991) New caddisflies (Trichoptera) from the Little River Drainage in northeastern Alabama. *Bulletin of the American Museum of Natural History* 11: 5–9.
- Gama-Neto JL, Passos MAB (2023) *Neotrichia anamariae* sp. nov.: The first record of *Neotrichia* Morton 1905 (Trichoptera: Hydroptilidae) from Maranhão State, Northeast Brazil. *Zootaxa* 5325(2): 283–288. <https://doi.org/10.11646/zootaxa.5325.2.9>
- Harris SC (1990) New species of *Neotrichia* (Trichoptera: Hydroptilidae) from Central and South America. *Journal of the New York Entomological Society* 98: 246–260.

- Harris SC (1991) New caddisflies (Trichoptera) from Alabama and Florida. *Bulletin of the American Museum of Natural History* 11: 11–16.
- Harris SC, Armitage BJ (2015) The Trichoptera of Panama. II. Ten new species of microcaddisflies (Trichoptera: Hydroptilidae). *Insecta Mundi* 0437: 1–17.
- Harris SC, Armitage BJ (2019) The Trichoptera of Panama. X. The Quebrada Rambala drainage, with description of 19 new species of microcaddisflies (Trichoptera: Hydroptilidae). *Insecta Mundi* 0707: 1–54.
- Harris SC, Flint Jr OS (2016) New species of microcaddisflies (Trichoptera: Hydroptilidae) from the western United States, Canada, Mexico and Belize. *Insecta Mundi* 0499: 1–22.
- Harris SC, Keth AC (2002) Two new microcaddisflies (Trichoptera: Hydroptilidae) from Alabama and Florida. *Entomological News* 113: 73–79.
- Harris SC, Rasmussen AK (2010) The *Neotrichia caxima* Group (Trichoptera: Hydroptilidae) in the southeastern United States. *Zootaxa* 2608(1): 25–44. <https://doi.org/10.11646/zootaxa.2608.1.2>
- Harris SC, Tiemann SG (1993) New species on *Neotrichia* from Texas and Panama, with a preliminary review of the *N. canixa* Group (Trichoptera: Hydroptilidae). *Proceedings of the Entomological Society of Washington* 95: 286–292.
- Harris SC, Ríos Gonzalez TA, Aguirre YP (2023) Trichoptera of Panama. XX. Six new microcaddisflies (Trichoptera: Hydroptilidae) and two new country records from Panama. *Aquatic Insects* 44(4): 250–272. <https://doi.org/10.1080/01650424.2023.2205397>
- Holzenthal RW, Calor AR (2017) Catalog of the Neotropical Trichoptera (Caddisflies). *ZooKeys* 654: 1–566. <https://doi.org/10.3897/zookeys.654.9516>
- Keth AC (2004) Five new species of *Neotrichia* (Trichoptera: Hydroptilidae: Neotrichiini) from southern Mexico and northern Belize. *Entomological News* 114(2003): 164–178.
- Keth AC, Harris SC, Armitage BJ (2015) The genus *Neotrichia* Morton (Trichoptera: Hydroptilidae) in North America, Mexico, and the Caribbean Islands. The Caddis Press, Columbus, Ohio, 147 pp.
- Malicky H (1980) Vier neue Köcherfliegen von den Insel Guadeloupe (Kleine Antillen, Mittelamerika) (Trichoptera). *Entomofauna* 1: 219–225. [Zeitschrift für Entomologie]
- Marshall JE (1979) A review of the genera of the Hydroptilidae (Trichoptera). *Bulletin of the British Museum (Natural History). Historical Series* 39: 135–234. [Natural History]
- Morton KJ (1905) North American Hydroptilidae. *Bulletin - New York State Museum* 86: 63–75.
- Mosely ME (1937) Mexican Hydroptilidae (Trichoptera). *Transactions of the Royal Entomological Society of London* 86(10): 151–189. <https://doi.org/10.1111/j.1365-2311.1937.tb00242.x>
- Oláh J, Johanson KA (2011) New Neotropical Hydroptilidae (Trichoptera). *Annales Historico-Naturales Musei Nationalis Hungarici* 103: 117–255.
- Ross HH (1939) Three new species of Nearctic Trichoptera. *Annals of the Entomological Society of America* 32(3): 628–631. <https://doi.org/10.1093/aesa/32.3.628>
- Ross HH (1944) The caddisflies or Trichoptera of Illinois. *Bulletin - Illinois Natural History Survey* 23(1–5): 1–326. <https://doi.org/10.21900/j.inhs.v23.199>
- Santos APM (2023) Hydroptilidae in Catálogo Taxonômico da Fauna do Brasil. PNUD. <http://fauna.jbrj.gov.br/fauna/faunadobrasil/10466> [Accessed 16 April 2023]
- Thomson RE (2023) Catalog of the Hydroptilidae (Insecta, Trichoptera). *ZooKeys* 1140: 1–499. <https://doi.org/10.3897/zookeys.1140.85712>
- Thomson RE, Armitage BJ (2018) The Trichoptera of Panama. VI. Seven new species of microcaddisflies (Insecta: Trichoptera: Hydroptilidae) from Mount Totumas Cloud Forest and Biological Reserve. *Insecta Mundi* 0613: 1–15.

DNA barcoding and morphology revealed the existence of seven new species of squat lobsters in the family Munididae (Decapoda, Galatheoidea) in the southwestern Pacific

Enrique Macpherson¹, Paula C. Rodríguez-Flores², Annie Machordom³

¹ Centre d'Estudis Avançats de Blanes (CEAB-CSIC), C. acc. Cala Sant Francesc 14, 17300 Blanes, Girona, Spain

² Department of Organismic and Evolutionary Biology, Museum of Comparative Zoology, Harvard University, 26 Oxford St., Cambridge MA 02138, USA

³ Museo Nacional de Ciencias Naturales (MNCN-CSIC), José Gutiérrez Abascal, 2, 28006 Madrid, Spain

Corresponding author: Enrique Macpherson (macpherson@ceab.csic.es)

Abstract

Specimens of squat lobsters belonging to the family Munididae Ah Yong et al., 2010, representing the genera *Garymunida* Macpherson & Baba, 2022, *Trapezionida* Macpherson & Baba, 2022 and *Typhlonida* Macpherson & Baba, 2022, were collected during several cruises around New Caledonia and Papua New Guinea, Southwest Pacific. The integrative study of these specimens revealed the presence of one new species in *Garymunida*, five in *Trapezionida* and one in *Typhlonida*. We describe and illustrate these new species, providing some new data on the taxonomy of several rare or scarcely studied species of *Trapezionida*. Molecular data from different markers (mitochondrial and nuclear) was also included, based on data availability, to support the taxonomic status of different species. Finally, a key to species for each genus is also provided.

Key words: Crustacea, integrative taxonomy, molecular characters, morphology, Pacific Ocean



Academic editor: Ingo S. Wehrtmann

Received: 31 October 2023

Accepted: 5 December 2023

Published: 3 January 2024

ZooBank: <https://zoobank.org/506BB8BF-F05B-4FCC-9560-7E4CCD13CBCC>

Citation: Macpherson E, Rodríguez-Flores PC, Machordom A (2024) DNA barcoding and morphology revealed the existence of seven new species of squat lobsters in the family Munididae (Decapoda, Galatheoidea) in the southwestern Pacific. ZooKeys 1188: 91–123. <https://doi.org/10.3897/zookeys.1188.114984>

Copyright: © Enrique Macpherson et al.
This is an open access article distributed under terms of the CC0 Public Domain Dedication.

Introduction

The genera *Garymunida*, *Trapezionida*, and *Typhlonida* were described by Macpherson & Baba, in Machordom et al. (2022) in the recent revision of the family Munididae (Machordom et al. 2022). In this revision, the evolutionary history and systematics of the family are reconstructed using an integrative approach combining morphological and molecular analyses. After the analyses of more than 290 munidid species, these authors found some potentially new species, most of them morphologically related to well-known species, but genetically distinct. In the present study, our main objective is to describe these undescribed taxa using the material studied in the revision (Machordom et al. 2022), as well as additional specimens collected in recent expeditions carried out by the Muséum national d'Histoire naturelle of Paris, in the framework of the Tropical Deep-Sea Benthos program in Papua-New Guinea (expeditions Bio-papua, Papua-niugini, Kavieng, Madeep), New Caledonia (Exbodi, Kanacono) and Chesterfield Islands (Ebisco, Kanadeep).

Garymunida Macpherson & Baba, in Machordom et al. 2022 is the sister genus of *Agononida* Baba & de Saint Laurent, 1996 and the species can be distinguished by the size of the distomesial process on the antennal article 1. At present, *Garymunida* includes 20 species, most of them distributed in the Indian and Pacific oceans, and two species present in the western Atlantic Ocean: *G. longipes* (A. Milne Edwards, 1880) and *G. schroederi* (Chace, 1939). *Trapezionida* Macpherson & Baba, in Machordom et al. 2022 is the most speciose genus in the family Munididae, containing more than 155 species, all from the Indian and Pacific Oceans. *Trapezionida* is the sister genus of *Gonionida* Macpherson & Baba, in Machordom et al. 2022, and they can be recognised by the shape of the thoracic sternite IV and the length of the P4 merus. The genus *Typhlonida* Macpherson & Baba, in Machordom et al. 2022 includes up to 25 species, all of them usually deep-water dwellers, occurring from the continental slope to the abyssal plain in the Atlantic, Indian, and Pacific oceans. The most distinctive character of most species in this genus is the small size of the cornea as well as the reduced size of some spines in the antennular and antennal peduncles (Machordom et al. 2022).

The existence of several new species of the family Munididae in New Caledonian and Papua-New Guinean waters suggests that, despite the enormous sampling effort in the area (Richer de Forges et al. 2013), the diversity of this group of decapods requires further study (De Grave et al. 2023). Recent studies in the Indian (e.g., Patel et al. 2022; Tiwari et al. 2022, 2023; Periasamy et al. 2023) and Pacific (e.g., Komai et al. 2023; Rodríguez-Flores et al. 2023) oceans confirm the numerous gaps that still exist in the taxonomy of squat lobsters. Therefore, in the present study, we describe and illustrate one new species of *Garymunida*, five of *Trapezionida*, and one of *Typhlonida*. We have also included new records and some remarks of a rare (*T. brachytes* (Macpherson, 1994)) and a complex of species (related to *T. leptitis* (Macpherson, 1994)) of *Trapezionida*. The dichotomous keys to species of the three genera have been included in order to facilitate future studies (see Suppl. material 1).

Materials and methods

Sampling and identification

The material (including the holotype of the new species) is located in the Muséum national d'Histoire naturelle, Paris (**MNHN**). The terminology and measurements follow Baba et al. (2009, 2011). The size of the specimens is indicated by the postorbital carapace length (CL), measured along the midline from the base of the rostrum to the posterior margin of the carapace. The rostrum was measured from its base (situated at the level of the orbit) to the distal tip. Measurements of appendages were taken in dorsal (pereopod 1), lateral (antennule, pereopods 2–4) and ventral (antenna) midlines. Abbreviations used are: **Mxp3**, maxilliped 3; **P1–P4**, pereopods 1–4; **M** = male; **F** = female; **ovig.** = ovigerous.

Molecular data

The sequences of the different genes for each new species and comparative material were obtained from Machordom et al. (2022). The molecular data

used for this study are deposited on GenBank (www.ncbi.nlm.nih.gov/genbank/) under the following accession numbers: *Garymunida namora* sp. nov. (cytochrome oxidase subunit one COI: OP215605, 16S rRNA: OP195946), *Trapezionida brachytes* (COI: OP215696, 16S: OP196034), *T. brevitars* sp. nov. (COI: OP215698, 16S: OP196036), *T. diluta* sp. nov. (COI: OP215699, 16S: OP196037), *T. leptitis* (16S: OP196069), *T. macilenta* sp. nov. (COI: OP215694, 16S: OP196032), *T. microtes* sp. nov. (COI: OP215712, 16S: OP196081), *T. pulex* sp. nov. (COI: OP215702 to 04, 16S: OP196040 to 42), *Typhlonida eluminata* sp. nov. (COI: OP215758, 16S: OP196095, 18S rRNA -18S: OP196339).

Genetic distances between species were estimated using uncorrected divergences (p) calculated using PAUP version 4.0 (build 167) (Swofford 2004; see also Machordom et al. 2022).

Systematic account

Superfamily Galatheaidea Samouelle, 1819

Family Munididae Ah Yong, Baba, Macpherson & Poore, 2010

Genus *Garymunida* Macpherson & Baba, 2022 in Machordom et al. 2022

***Garymunida namora* sp. nov.**

<https://zoobank.org/4EA2A39A-F9A5-4DAC-AA42-C337942B452B>

Figs 1, 2

Garymunida sp. 2: Machordom et al. 2022: table 2, fig. 3.

Material. Holotype: NEW CALEDONIA. Spanbios Stn CP5155, 5 July 2021, 20°05.9'S, 163°42.6'E, 573–575 m: male, 13.9 mm (MNHN-IU-2021-9330).

Paratype: PAPUA NEW GUINEA. Biopapua Stn CP3682, 27 September 2010, 04°37.820'S, 149°27.940'E, 515–812 m: 1 female, 16.0 mm (MNHN-IU-2011-3173).

Description. Carapace: Approximately as long as wide, dorsally moderately convex. Transverse ridges usually microscopically granular, mostly interrupted, with dense, very short setae, and a few scattered long non-iridescent setae. Some granular scales on hepatic and anterior branchial regions. Main transverse striae on posterior part of carapace interrupted in cardiac region. Two strong epigastric, two protogastric behind epigastric and two parahepatic spines on gastric regions. One row of four or five strong branchiocardiac spines. Posterior margin with two median spines. Upper orbital margins slightly oblique; lower orbital margins visible dorsally, laterally with minute spine, mesially with low rounded process. Lateral margins moderately convex. Anterolateral spine strong, located at carapace anterolateral angle, reaching level of sinus between rostrum and supraocular spines. Second marginal spine before cervical groove well developed. Branchial margins feebly convex, with 4 spines. Rostrum spiniform, half as long as remaining carapace, slightly sinuous and nearly horizontal in lateral view. Supraocular spines exceeding midlength of rostrum and reaching or overreaching end of cornea, divergent, directed slightly upwards. Pterygostomian region unarmed ending anteriorly in rounded tip.

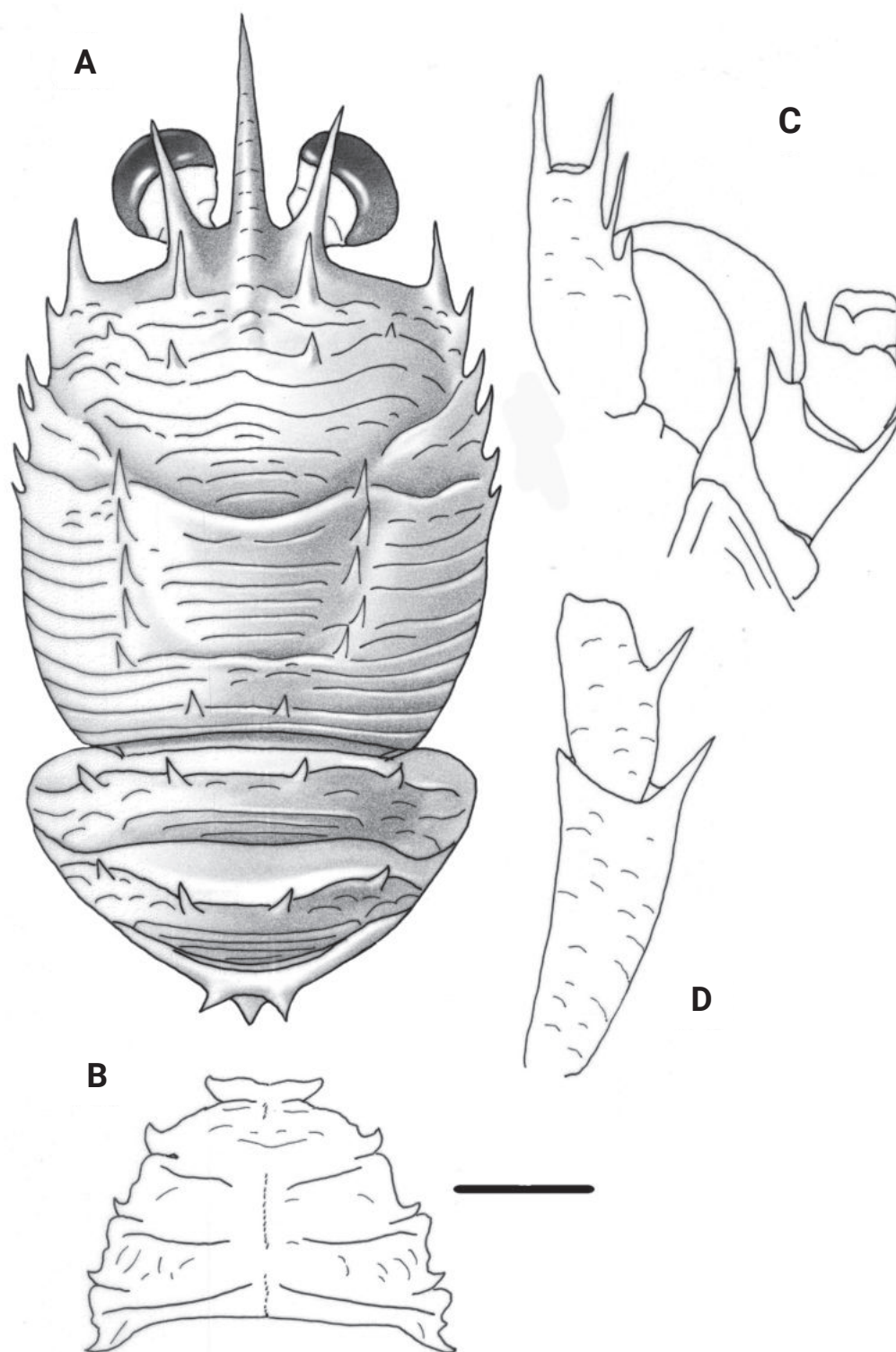


Figure 1. *Garymunida namora* sp. nov., male holotype, 13.9 mm (MNHN-IU-2021-9330), New Caledonia **A** carapace and pleon, dorsal view **B** sternal plastron **C** cephalic region, showing antennular and antennal peduncles, ventral view **D** right Mxp3 ischium and merus, lateral view. Scale bars: 2.0 mm (**A**, **B**); 1.0 mm (**C**, **D**).

Thoracic sternum: 0.6× as wide as long. Sternite III with median shallow notch. Sternite IV with anterior part as wide than sternite III, with some short striae. Sternites IV–VI with a few striae on lateral sides. Sternite III ~ 5× as wide as long; sternite IV nearly 2.5× as wide as long, and 2× as wide as sternite III.

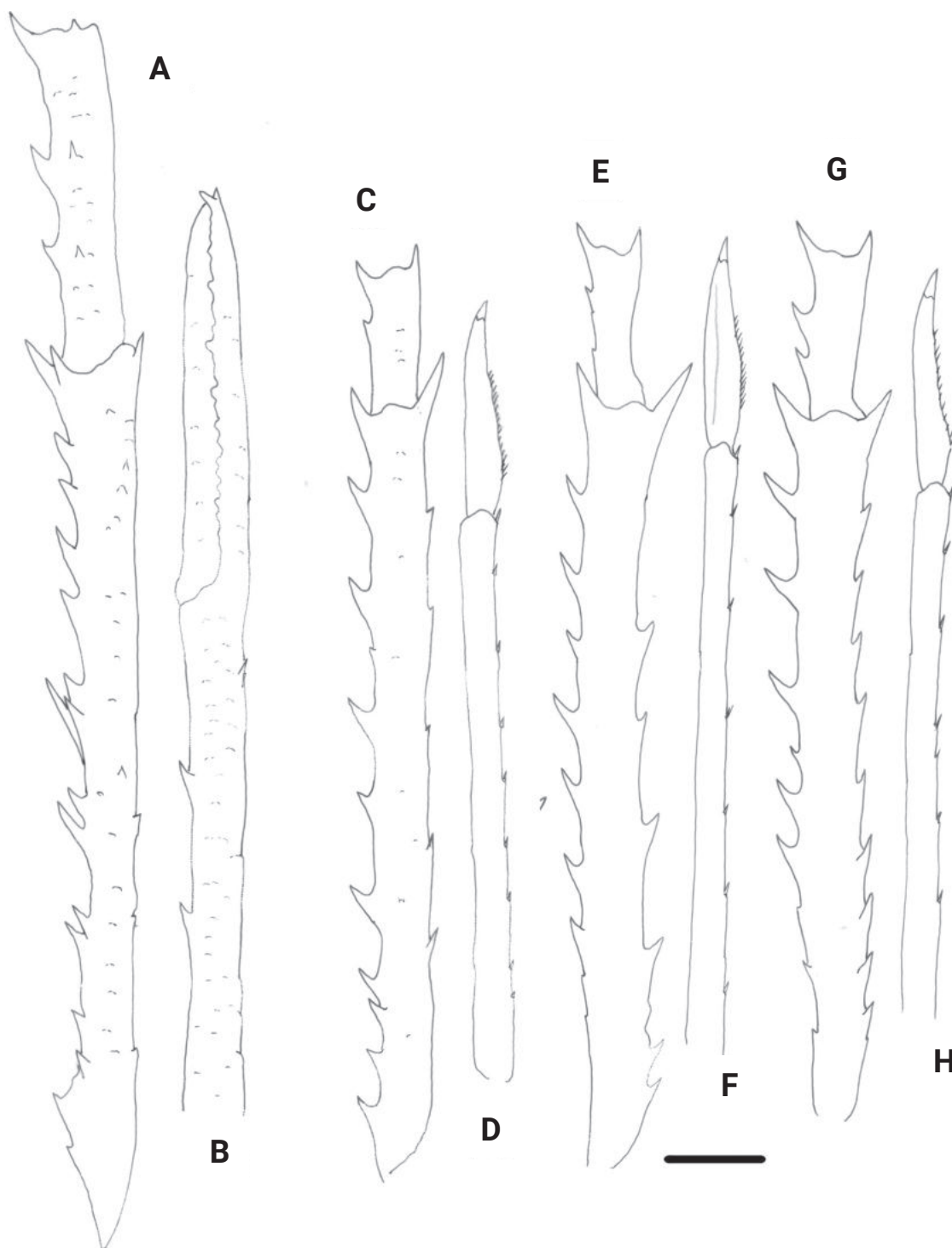


Figure 2. *Garymunida namora* sp. nov., male holotype, 13.9 mm (MNHN-IU-2021-9330), New Caledonia **A** right P1, merus and carpus, dorsal view **B** right P1, palm and fingers, dorsal view **C** right P2, merus and carpus, lateral view **D** right P2, propodus and dactylus, lateral view **E** right P3, merus and carpus, lateral view **F** right P3, propodus and dactylus, lateral view **G** right P4, merus and carpus, lateral view **H** right P4, propodus and dactylus, lateral view. Scale bar: 10.0 mm.

Pleon: Tergites II and III each with four spines on anterior margin; tergite IV with two median spines on anterior ridge and median spine on posterior ridge.

Eye: Large, cornea dilated, maximum corneal diameter ~ 0.4 distance between bases of anterolateral spines.

Antennule: Article 1 (distal spines excluded), $\sim 1/4$ carapace length, slightly overreaching cornea, with two distal spines, mesial spine longer than lateral spine; two spines on lateral margin, proximal one small, located at midlength of segment, distal one long, not overreaching distolateral spine.

Antenna: Article 1 with one short process on mesial margin, reaching end of article 2; article 2 with two distal spines, mesial spine shorter than lateral spine, reaching midlength of article 3; article 3 with distomesial spine; article 4 unarmed.

Mxp3: Ischium $\sim 2\times$ length of merus measured along dorsal margin, distoventrally bearing strong spine. Merus with one strong median spine on flexor margin; extensor margin unarmed.

P1: $3.0\times$ carapace length, with scattered long plumose setae. Merus with row of mesial spines; a few small, scattered spines on dorsal side. Carpus $5\times$ as long as broad; with spines along mesial margin and a few minute spines on dorsal side. Palm $7.5\times$ as long as broad, with a few small dorsal spines; one or two spines along mesial and lateral margins. Fingers $0.8\times$ palm length.

P2–P4: Long and slender, with numerous long non-plumose and non-iridescent setae along extensor margin of articles. P2 $3.0\times$ carapace length. Meri slightly shorter posteriorly (P2 merus as long as P3 merus; P3 merus 0.9 length of P4 merus); P2 merus $1.5\times$ carapace length, $13.0\text{--}13.5\times$ as long as broad, $1.4\times$ longer than P2 propodus; P3 merus $12.5\times$ as long as broad; P4 merus $11.5\times$ as long as broad. Extensor and flexor margins of P2–P4 meri with row of $9\text{--}11$ and $6\text{--}10$ spines, respectively, proximally diminishing spines; lateral sides unarmed, more squamate in P4. P2–P4 carpi with $2\text{--}4$ spines on extensor margin; lateral surface with several granules sub-parallel to extensor margin; flexor margin with distal spine. Propodi $14.5\text{--}17.0\times$ as long as broad; extensor margin unarmed; flexor margin with $7\text{--}9$ slender movable spines, distal end without fixed spine. Dactyli slender, length 0.4 that of propodi; flexor margin with $13\text{--}17$ movable spinules, proximal and distal fourth unarmed, without a spinule at the base of the unguis; P2 dactylus $8.2\times$ as long as wide.

Genetic data. COI, 16S.

Etymology. "*Namora*" is a mythological woman participating in the creation of New Guinea. Used as noun in apposition.

Remarks. The closest species to the new species is *G. procera* (Ahyong & Poore, 2004), from New Caledonia, Queensland, New South Wales and New Zealand, *G. imitata* (Macpherson, 2006), from French Polynesia, and *G. soelae* (Baba, 1986), from Kyushu-Palau Ridge, Taiwan, Indonesia, SW Australia, and Fiji. These species have the pleomere IV tergite armed with median spine on posterior transverse ridge, the article 1 of the antennal peduncle with moderate-sized process, not reaching article 4, and a pair of protogastric spines behind median pair of epigastric spines. However, the new species differ easily from the other three species in the following characters:

- The cardiac region is unarmed in the new species, whereas there are some median spines in the other three species.
- The posterior ridge of the carapace has two median spines in *G. namora*, whereas there are six spines in the other three species.
- The divergences between *G. namora* and the morphologically or phylogenetically closest species are $\sim 14\%$ for COI (respect to *G. imitata*,

G. procera or *G. longipes*). These values drop to 6.1–8.6% when 16S is analysed and comparisons are made respect to *G. simillima*, *G. imitata*, *G. laurentae*, *G. procera*, or *G. longipes*.

Distribution. Papua-New Guinea and New Caledonia, between 515 and 812 m.

Genus *Trapezionida* Macpherson & Baba, 2022 in Machordom et al. 2022

***Trapezionida brachytes* (Macpherson, 1994)**

Fig. 3

Munida brachytes Macpherson 1994: 450, fig. 8. — Baba 2005: 260. — Baba et al. 2008: 89.

Trapezionida aff. *apheles*: Machordom et al. 2022: table 2, suppl. figs S1–S6.

Material. Holotype: NEW CALEDONIA, Smib 5 Stn 86, 13 September 1989, 22°19.8'S, 168°42.8'E, 320 m: male, 3.7 mm (MNHN Ga 2580).

NEW CALEDONIA, Chesterfield Islands. Ebisco Stn CP2495, 6 October 2005, 24°44.11'S, 159°42.9'E, 217–350 m: 1 male, 4.4 mm (MNHN-IU-2016-5803). — Stn DW2526, 9 October 2005, 22°47.492'S, 159°22.890'E, 340–355 m: 1 male, 4.4 mm (MNHN-IU-2013-19882). Kanadeep 1 Stn DW5006, 19 September 2017, 22°07'S, 159°19'E, 340–550 m: 1 ovigerous female, 4.5 mm, 1 female, 4.4 mm (MNHN-IU-2017-2519). — Stn DW5011, 19 September 2017, 22°13'S, 159°03'E, 320–350 m: 1 male, 5.2 mm (MNHN-IU-2014-13918), 1 female, 3.7 mm (MNHN-IU-2017-2926).

Diagnosis. (modified from Macpherson 1994) Carapace slightly longer than broad, with a few secondary striae between main transverse ridges. Gastric region with three or four pairs of epigastric spines. Parahepatic, branchial dorsal and postcervical spines absent. Frontal margins transverse. Lateral margins slightly convex. First lateral spine slightly mesial to anterolateral angle, short, clearly not reaching level of sinus between rostrum and supraocular spines. Branchial margins with five minute spines, posterior spines sometimes obsolescent. Rostrum spiniform. Supraocular spines short, not reaching midlength of rostrum and clearly not reaching end of cornea. Surface of thoracic sternum smooth; sternite IV trapezoidal, anterior margin contiguous to sternite III along $\frac{3}{4}$ of its length. Pleomere tergites unarmed, tergites II and III each with one transverse ridge on tergite behind anterior ridge. Cornea much wider than peduncle. Antennular article 1 with two well-developed distal spines, distomesial spine as long as or shorter than distolateral. Antennal article 1 with short distomesial spine nearly reaching midlength of article 2; article 2 with distomesial and distolateral spines reaching or nearly reaching end of article 3. Extensor margin of Mxp3 merus unarmed. P1 palm with well-developed spines along lateral and mesial margins continuing along fixed and movable fingers, respectively. Extensor margins of P2–P4 meri unarmed, one distal spine only; flexor margins with some well-developed spines followed proximally by several eminences; P2–P4 dactyli slender, as long as or slightly shorter than propodi; with movable spinules along nearly entire flexor margin, with ultimate spinule near unguis (sometimes lost, as in holotype); P2 dactylus 5.5–6.3× as long as wide; P4 merus > $\frac{1}{2}$ length of P2 merus.

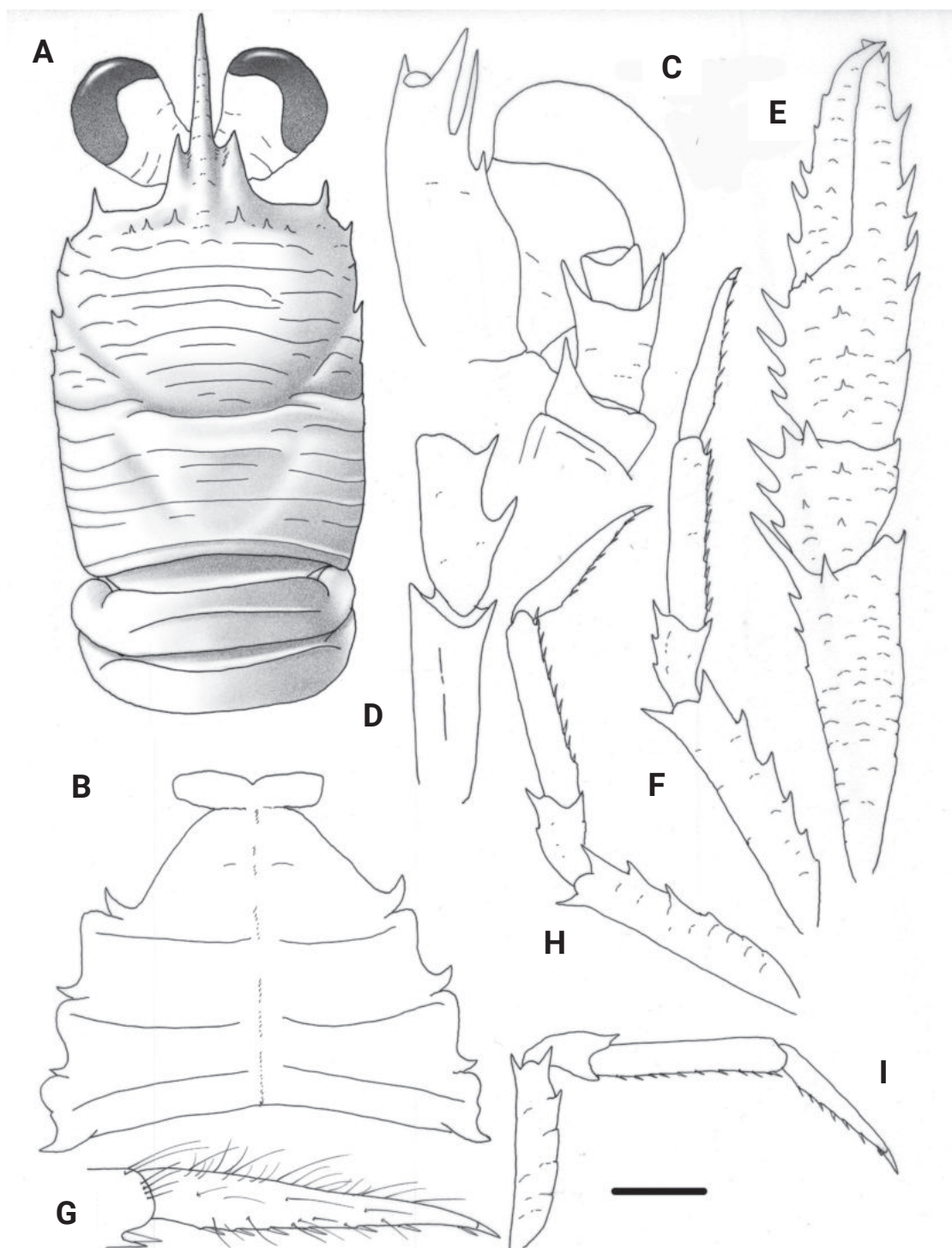


Figure 3. *Trapezionida brachytes* (Macpherson, 1994), female, 3.7 mm (MNHN-IU-2017-2926), New Caledonia **A** carapace and pleon, dorsal view **B** sternal plastron **C** cephalic region, showing antennular and antennal peduncles, ventral view **D** right Mxp3 ischium and merus, lateral view **E** right P1, dorsal view **F** right P2, lateral view **G** dactylus of right P2, lateral view **H** right P3, lateral view **I** right P4, lateral view. Scale bars: 1.0 mm (**A**, **E**, **F**, **H**, **I**); 0.5 mm (**B**, **C**, **D**, **G**).

Genetic data. COI, 16S.

Remarks. *Trapezionida brachytes* was only known by one male collected in New Caledonia. The new material collected in New Caledonia and Chesterfield Islands agree quite well with the holotype, although the distomesial spine of the

antennular article 1 is shorter than the distolateral spine (subequal in the holotype). Furthermore, the distalmost movable spinule along the flexor margin of the P2–P4 dactyli can be lost (although the insertion point is always present). Therefore, these characters should be considered with caution because these spines/spinules can be broken or regenerating in some specimens.

Morphologically and genetically the closest species of *T. brachytes* is *T. stia* (Macpherson, 1994), also known from New Caledonia and Chesterfield islands.

Trapezionida stia and *T. brachytes* can be distinguished by the following characters:

- Pleomeres III and IV tergites have an additional ridge behind the anterior ridge in *T. stia*, whereas these additional ridges are absent in the new species.
- P2–P4 dactyli are shorter and stouter in *T. stia* than in *T. brachytes*. The dactyli are $\sim 2/3$ the propodi length in *T. stia*, whereas they are as long as or slightly shorter than propodi in *T. brachytes*. The P2 dactylus is 6.1–6.3 \times as long as wide in the new species, instead of 4 \times in *T. stia*. Finally, the terminal 1/3 of the flexor margin of the dactyli are unarmed in *T. stia*, whereas there are spines along the entire margin in *T. brachytes*.
- Genetically *T. brachytes* is different from *T. stia* (5.96% 16S) and (10.6% COI).

Distribution. New Caledonia and Chesterfield Islands, between 310 and 550 m.

Trapezionida brevitass sp. nov.

<https://zoobank.org/BB8E911E-4EC6-438C-8D86-81D6DD43BCE2>

Fig. 4

Trapezionida aff. *forncis*: Machordom et al. 2022: table 2, suppl. figs S1–S6.

Material. Holotype: NEW CALEDONIA. Smib 8 Stn DW163, 28 January 1993, 24°49.12'S, 168°08.93'E, 310–460 m: male, 4.1 mm (MNHN-IU-2017-1336).

Paratype: NEW CALEDONIA. Norfolk 2 Stn DW2024, 21 October 2003, 23°27.92'S, 167°50.90'E, 370–371 m: 1 male, 4.6 mm (MNHN-IU-2014-13973).

Description. Carapace: Slightly longer than broad, moderately convex, with a few secondary striae and scales between main transverse ridges. Dorsal ridges with dense short plumose setae and a few scattered long iridescent setae. Gastric region with four pairs of epigastric spines, longest pair behind supraocular spines, one pair between largest pair of spines. One parahepatic, two branchial dorsal and one postcervical spine on each side. Frontal margins oblique. Lateral margins slightly convex. First lateral spine at anterolateral angle, moderately long, clearly not reaching level of sinus between rostrum and supraocular spines; one–two small spines in front of anterior branch of cervical groove; end of anterior branch of cervical groove without tuft of iridescent setae. Branchial margins slightly convex, with four spines. Rostrum spiniform, $\sim 0.6\times$ length of remaining carapace, slightly upwards directed, dorsally slightly carinated. Supraocular spines reaching midlength of rostrum and not reaching end of cornea, slightly divergent, directed slightly upwards. Pterygostomian region unarmed, ending in blunt angle.

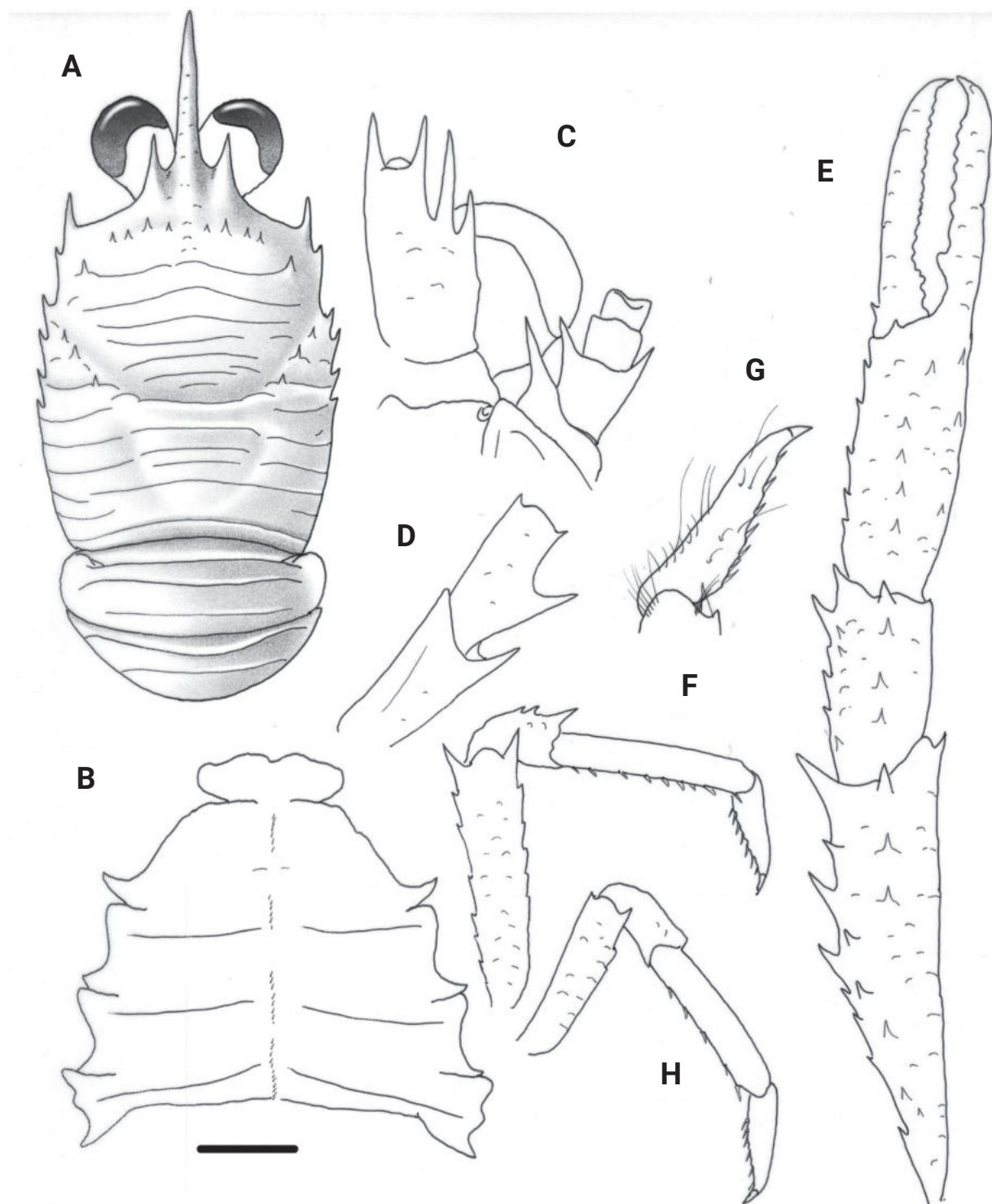


Figure 4. *Trapezionida brevitars* sp. nov., male holotype, 4.1 mm (MNHN-IU-2017-1336), New Caledonia **A** carapace and pleon, dorsal view **B** sternal plastron **C** cephalic region, showing antennular and antennal peduncles, ventral view **D** right Mxp3 ischium and merus, lateral view **E** right P1, dorsal view **F** right P2, lateral view **G** dactylus of right P2, lateral view **H** right P4, lateral view. Scale bars: 1.0 mm (**A**, **E**, **F**, **H**); 0.5 mm (**B**, **C**, **D**, **G**).

Thoracic sternum: 0.8× as long as broad. Surface of thoracic sternites IV–VI smooth. Sternite IV trapezoidal, anterior margin contiguous to sternite III along $\frac{3}{4}$ of its length. Sternite III 3.5× as wide as long; sternite IV 2.5× as wide as long, and 2.3× as wide as sternite III.

Pleon: Anterior ridge of pleomere tergites unarmed; tergites II and III each with one uninterrupted transverse ridge on tergite behind anterior ridge, absent on tergites IV and V; some iridescent setae on each side of anterior ridges of tergites; posteromedian margin of tergite VI straight.

Eye: Ocular peduncle as long as broad. Cornea dilated, maximum corneal diameter 0.4 distance between bases of anterolateral spines.

Antennule: Article 1 (distal spines excluded) ~ 0.3× carapace length, 2× as long as wide (excluding spines), slightly exceeding end of cornea, with two distal spines, distomesial subequal or slightly longer than distolateral; two spines on lateral margin, proximal one short, located at midlength of segment, distal one long, nearly reaching end of distolateral spine.

Antenna: Article 1 with distomesial spine slightly exceeding distal margin of article 2. Article 2 with subequal distomesial and distolateral spines, nearly reaching end of article 3. Article 3 unarmed.

Mxp3: Ischium with strong distal spine on flexor margin. Merus shorter than ischium; flexor margin with 2 spines, proximal stronger than distal; extensor margin with small distal spine. Carpus unarmed.

P1: 3.5–3.7× carapace length, with minute scales, short plumose setae on each scale, and some scattered long spines. Merus 1.3× length of carapace, 2.2× as long as carpus, with some dorsal and mesial spines, distomesial spine strong, not reaching first quarter of carpus. Carpus 0.8 length of palm, 2.3× as long as broad, with some spines along mesial and dorsal sides. Palm 1.8–2.3× as long as broad, with some small dorsal spines; row of spines along mesial and lateral margins. Fingers as long as palm; movable with small proximal spine at base, otherwise unarmed, with minute distal spine on fixed finger.

P2–P4: Moderately long and slender, covered with setose scales, with some long plumose setae and some long iridescent setae along extensor margin of articles. P2 2.0× carapace length. Meri shorter posteriorly (P3 merus 0.9× length of P2 merus, P4 merus 0.8× length of P3 merus); P2 merus 0.8× length of carapace, 4.2× as long as broad, 1.4× as long as P2 propodus; P3 merus 4.5× as long as broad, 1.3× length of P3 propodus; P4 merus 3.5× as long as broad, 1.1× length of P4 propodus. Extensor margins of P2–P3 meri with row of seven–eight proximally diminishing spines, one small distal spine on P4; flexor margins distally with one–two spines followed proximally by several eminences; lateral sides unarmed. Carpi with three spines on extensor margin of P2–P3, one minute distal spine on P4; lateral surface with several granules sub-parallel to extensor margin on P2–P4; flexor margin with distal spine. Propodi 4.5–5.5× as long as broad; extensor margin unarmed; flexor margin with four–ten slender movable spines on P2–P4, distal end with one minute fixed spine. Dactyli slender, length 0.6 that of propodi; flexor margin with six–seven movable spinules, without spinule at base of unguis, distal third unarmed; P2 dactylus 4.0× as long as wide. P4 merocarpal articulation reaching anterior end of cervical groove; P4 merus > ½ length of P2 merus.

Genetic data. COI, 16S.

Etymology. From the Latin, *brevitas*, shortness, in reference to the small size of the species.

Remarks. *Trapezionida brevitata* belongs to the group of species having four spines on the branchial lateral margins of the carapace, frontal margins oblique, thoracic sternites without granules or carinae, anterior ridge of the

pleomeres II and III tergites unarmed, article 1 of antennule with subequal distal spines or distomesial spine slightly longer than distolateral, extensor margin of Mxp3 merus with small distal spine and flexor margin of P2–P4 dactyli with spinules along entire margin. The new species is closely related to *T. fornacis* (Macpherson, 2006) and *T. descensa* (Macpherson, 2006), both from French Polynesia. However, the three species differ from each other in some characters.

The differences between *T. brevitass* and *T. fornacis* are as follows:

- The dorsal carapace surface has two branchial dorsal spines in *T. brevitass*, and only one in *T. fornacis*.
- The pleomeres II and III tergites each with one uninterrupted transverse ridge on tergite behind anterior ridge in the new species, these ridges are interrupted or scale-like in *T. fornacis*.
- The distal spines of the antennular article 1 are subequal or slightly different in the new species, whereas the distomesial spine is clearly longer than the distolateral in *T. fornacis*.
- The distomesial spine of the antennal article 1 is very long, reaching the end of the antennal peduncle in *T. fornacis*, whereas this spine only slightly exceeds the antennal article 2.
- The dorsal surface of P1 palm is unarmed in *T. fornacis*, whereas it has numerous spines in *T. brevitass*.

Genetically both species are different. *T. brevitass* showed high divergence values with *T. fornacis* (15.9% COI).

The differences between *T. brevitass* and *T. descensa* are as follows:

- The dorsal carapace surface has two branchial dorsal spines in *T. brevitass*, and only one in *T. descensa*.
- P2–P4 are more slender in *T. descensa* (P2 merus and dactylus, 6 and 5× as long as wide, respectively) than in *T. brevitass* (P2 merus and dactylus, 4 and 4× as long as wide, respectively).
- Genetically both species are different. *T. brevitass* showed divergence values with *T. descensa* of ~ 4.3% for COI).

Distribution. New Caledonia, at 310–460 m.

***Trapezionida diluta* sp. nov.**

<https://zoobank.org/DF07441C-1C86-49E7-9BEB-BDDF8141E36A>

Fig. 5

Trapezionida aff. *gordoe*: Machordom et al. 2022: table 2, suppl. figs S1–S6.

Material. Holotype: NEW CALEDONIA. Lifou 2000 Stn DW1462, 9 November 2000, 20°47.1'S, 167°03.2'E, 70–120 m: male, 4.3 mm (MNHN-IU-2016-9652).

Paratypes: NEW CALEDONIA. Lifou 2000 Stn DW1462, 9 November 2000, 20°47.1'S, 167°03.2'E, 70–120 m: 3 males, 3.5–4.6 mm, 1 ovigerous female, 3.9 mm (MNHN-IU-2014-13974).

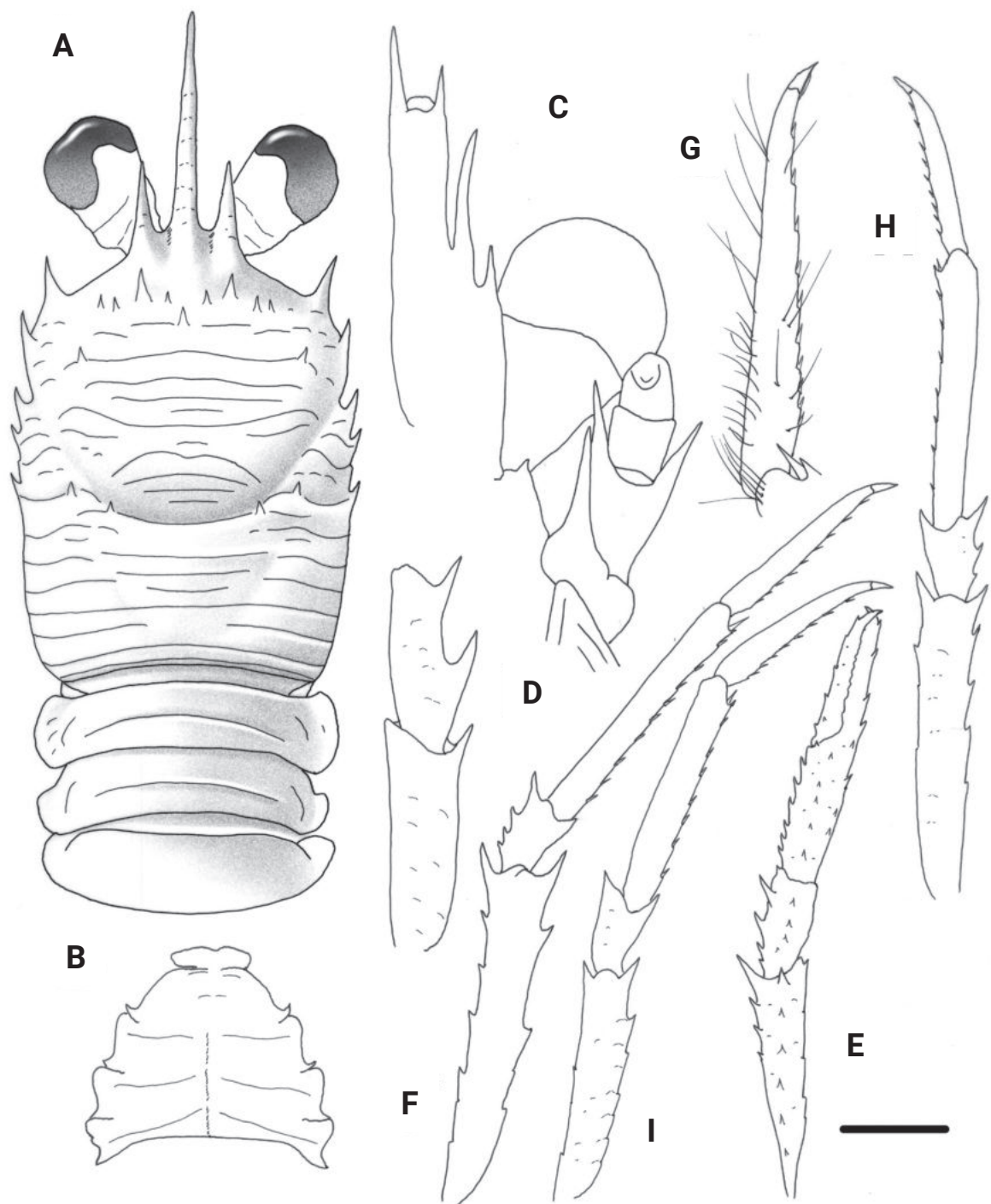


Figure 5. *Trapezionida diluta* sp. nov., male holotype, 4.3 mm (MNHN-IU-2016-9652), New Caledonia **A** carapace and pleon, dorsal view **B** sternal plastron **C** cephalic region, showing antennular and antennal peduncles, ventral view **D** right Mxp3 ischium and merus, lateral view **E** right P1, dorsal view **F** right P2, lateral view **G** dactylus of right P2, lateral view **H** left P3, lateral view **I** right P4, lateral view. Scale bars: 1.0 mm (**A**, **B**, **F**, **H**, **I**); 0.5 mm (**C**, **D**, **G**); 2.0 mm (**E**).

Description. Carapace: 1.2× as long as broad, moderately convex, with a few secondary striae between main transverse ridges. Ridges with short non-iridescent setae and few scattered long iridescent setae. Intestinal region without scales. Gastric region with four or five pairs of epigastric spines, longest pair behind supraocular spines, one pair between longest pair; one median

protogastric spine. One parahepatic, one anterior branchial, and one postcervical spine on each side. Frontal margins oblique. Lateral margins slightly convex and convergent posteriorly. First lateral spine at anterolateral angle, long, not reaching level of sinus between rostrum and supraocular spines; second spine well developed, in front of anterior branch of cervical groove, $< \frac{1}{2}$ length of first spine. Branchial margins straight, with three or four spines. Rostrum spiniform horizontal, $\sim 0.4\text{--}0.6\times$ length of remaining carapace, not dorsally carinated. Supraocular spines reaching midlength of rostrum and not reaching end of cornea, subparallel, slightly upwards directed. Pterygostomian flap unarmed, ending in round tip.

Thoracic sternum: $0.8\times$ as long as wide. Surface of thoracic sternites IV–VI smooth, only a few short scales on sternite IV. Sternite III $3.5\times$ as wide as long. Sternite IV trapezoidal, anterior margin contiguous to sternite III along $\frac{3}{4}$ of its length; $2.5\times$ as wide as long, and $2.0\times$ as wide as sternite III.

Pleon: Ridges of pleomeres unarmed; tergites II and III each with uninterrupted transverse ridge on tergite behind anterior ridge: tergites IV and V with anterior ridge only; posteromedian margin of tergite VI straight.

Eye: Ocular peduncle longer than broad. Cornea dilated; maximum diameter $0.4\times$ distance between bases of anterolateral spines.

Antennule: Article 1 (distal spines excluded) very long, $\sim 0.5\times$ carapace length, $3.5\times$ as long as wide (excluding spines), clearly overreaching end of cornea, with two distal spines, mesial spine longer than lateral; two spines on lateral margin, proximal one short, located at midlength of segment, distal one long, not reaching end of distal spines.

Antenna: Article 1 with distomesial spine barely exceeding article 2. Article 2 with distomesial spine, exceeding article 3; distolateral spine as long as or slightly larger than distomesial, exceeding article 3. Articles 3 and 4 unarmed.

Mxp3: Ischium with well-developed spine on flexor distal margin. Merus shorter than ischium; flexor margin with two spines, median slightly stronger than distal spine; extensor margin unarmed. Carpus unarmed.

P1: $2.3\text{--}3.0\times$ carapace length, with scattered long plumose setae, and some long iridescent setae; some short setae on spines and scales. Merus $1.0\text{--}1.1$ length of carapace, $2.0\text{--}2.2\times$ as long as carpus, with some dorsal and mesial spines; distal spines strong, distomesial spine barely reaching proximal fourth of carpus. Carpus $0.8\text{--}1.0$ length of palm, $2.3\text{--}2.5\times$ as long as broad; with spines along mesial and dorsal sides. Palm $2.3\text{--}2.8\times$ as long as broad, with row of small dorsal spines; one row of spines along mesial and lateral margins, continuing along movable and lateral fingers, respectively. Length of fingers $1.1\text{--}1.3\times$ that of palm.

P2–P4: Long and slender, with some short setae and some scattered iridescent setae along extensor margins of all articles. P2 $2.1\text{--}2.2\times$ carapace length. Meri shorter posteriorly (P3 merus $0.8\text{--}0.9\times$ length of P2 merus, P4 merus $0.8\text{--}0.9\times$ length of P3 merus); P2 merus $0.7\text{--}0.8\times$ carapace length, $5.8\text{--}6.5\times$ as long as broad, $1.2\text{--}1.3\times$ as long as P2 propodus; P3 merus $6.0\text{--}6.2\times$ as long as broad, $1.2\text{--}1.2\times$ as long as P3 propodus; P4 merus $4.5\text{--}4.7\times$ as long as broad, as long as P4 propodus. Extensor margins of meri with row of 5–7 proximally diminishing spines on P2–P3, one or two spines on P4; flexor margins with three or four spines followed proximally by several eminences; lateral sides unarmed. Carpi with three or four spines on extensor margin of P2–P3, one distal

on P4; lateral surface with several granules sub-parallel to extensor margin on P2–4; flexor margin with well-developed distal spine. Propodi 6.5–7.6× as long as broad; extensor margin unarmed; flexor margin with eight–ten slender movable spines on P2–P4, one fixed distal spine. Dactyli slender, length 0.7–0.8× that of propodi; flexor margin with 10–11 movable spinules along entire border, with ultimate spinule at base of unguis, penultimate spine equidistant between antepenultimate and ultimate spines; P2 dactylus 7.4–7.5× as long as wide. P4 merocarpal articulation exceeding anterior end of cervical groove; P4 merus > ½ length of P2 merus.

Genetic data. COI, 16S.

Etymology. From the Latin, *dilutus*, thin, in reference to the shape of the antennular peduncle.

Remarks. *Trapezionida diluta* belongs to the group of species having the anterior ridge of the pleomere II tergite unarmed, the thoracic sternites smooth and the antennular article 1 very slender, exceeding eye, and with the distomesial spine longer than the distolateral spine. The new species is close to *T. macilenta* sp. nov., from Papua-New Guinea (see below under the Remarks of this species).

Distribution. New Caledonia, 70–120 m.

Trapezionida leptitis (Macpherson, 1994)

Munida leptitis Macpherson 1994: 487, fig. 27. — Baba 2005: 267 (in part). — Macpherson 2006: 318 (in part). — Baba et al. 2008: 104 (in part). — Baba et al. 2009: 171, figs 151–152. — Macpherson 2013: 301 (in part).

Trapezionida leptitis: Machordom et al. 2022: table 2, suppl. figs S1–S6.

Material. Holotype: NEW CALEDONIA, Loyalty Islands, Musorstom 6 Stn DW431, 18 February 1989, 20°22.25'S, 166°10'E, 21 m: female, 3.4 mm (MNHN-IU-2014-10854 (= MNHN Ga2810)). **Paratype:** NEW CALEDONIA, Loyalty Islands, Musorstom 6 Stn DW392, 13 February 1989, 20°47.32'S, 167°04.60'E, 340 m: 1 ovigerous female, 4.4 mm (MNHN-IU-2017-8971). FRENCH POLYNESIA, Tarasoc Stn DW3413, 13 October 2009, 16°34'S, 151°46'W, 385–486 m: 2 males, 4.5–6.0 mm, 4 ovigerous females, 4.0–5.2 mm, 1 female, broken (MNHN-IU-2010-5816), 1 ovigerous female, 5.3 mm (MNHN-IU-2016-520). — Lifou 2000 Stn 1650, 15/18 November 2000, 20°54.15'S, 167°01.7'E, 120–250 m: 2 female, 2.5–3.4 mm (MNHN-IU-2016-519). — Stn 1442, 13–14 November 2000, 20°46.4'S, 167°02'E, 47 m: 1 ovigerous female, 4.2 mm (MNHN-IU-2014-13820).

Colour in life (from Baba et al. 2009). Ground colour of body and appendages orange. P1 with numerous red spots, mesial borders of articles darker than lateral margins; proximal half of fingers whitish, distal half reddish, tips white. P2–P4 scattered with red spots; dactyli whitish.

Genetic data. COI, 16S.

Remarks. This species has been cited in numerous localities from the West and Central Pacific. However, as it was mentioned in previous papers (see above) some slight morphological differences among specimens from different areas were observed, suggesting the existence of a complex of species. Therefore, after the morphological and molecular revision of the material from

the different areas, we have confirmed the existence of two species (see below in the Remarks of *T. pulex* sp. nov.).

Distribution. The species has been collected in New Caledonia, French Polynesia and Taiwan. The depth range of the specimens examined is 21–486 m.

***Trapezionida macilenta* sp. nov.**

<https://zoobank.org/6366F93A-8096-43F6-8FFD-31F15DC11275>

Figs 6, 9A

Trapezionida aff. *acola*: Machordom et al. 2022: table 2, suppl. figs S1–S6.

Material. Holotype: Papua-New Guinea. Papua Niugini Stn PT05, 3 December 2012, 05°12.4'S, 145°49.3'E, 80 m: male, 5.7 mm (MNHN-IU-2013-1094).

Description. Carapace: 1.2× as long as broad, feebly convex, with a few secondary striae and scales between main transverse ridges. Ridges with very short plumose setae and a few scattered long iridescent setae. Intestinal region without scales. Gastric region with five pairs of epigastric spines, longest pair behind supraocular spines, one pair between longest pair; one median protogastric spine. One parahepatic, one anterior branchial, and one postcervical spine on each side. Frontal margins oblique. Lateral margins slightly convex and convergent posteriorly. First lateral spine at anterolateral angle, well-developed, not reaching level of sinus between rostrum and supraocular spines; two or three small spines in front of anterior branch of cervical groove. Branchial margins slightly convex, with five spines. Rostrum spiniform, ~0.8× length of remaining carapace, slightly upwards directed, not dorsally carinated. Supraocular spines reaching midlength of rostrum and not reaching end of cornea, subparallel, slightly upwards directed. Pterygostomial region unarmed, ending in round tip.

Thoracic sternum: 0.7× as long as broad. Surface of thoracic sternites IV–VI smooth, only a few short scales on sternite IV. Sternite III 3.7× as wide as long. Sternite IV trapezoidal, anterior margin contiguous to sternite III along $\frac{3}{4}$ of its length; 2.5× as wide as long, and 2.0× as wide as sternite III.

Pleon: Ridges of pleomeres unarmed; somites II and III each with three uninterrupted transverse ridges on tergite behind anterior ridge; pleomeres IV and V with anterior ridge only; posteromedian margin of pleomere VI straight.

Eye: Ocular peduncle longer than broad. Cornea moderately dilated, maximum corneal diameter 0.3 distance between bases of anterolateral spines.

Antennule: Article 1 (distal spines excluded) very long, ~0.5× carapace length, 3.0× as long as wide (excluding spines), clearly overreaching end of cornea, with two distal spines, mesial spine longer than lateral; two spines on lateral margin, proximal one short, located at midlength of segment, distal one long, not reaching end of distal spines.

Antenna: Article 1 with distomesial spine not exceeding article 2. Article 2 with distomesial spine, exceeding article 3, distolateral spine shorter than distomesial, slightly exceeding article 3. Articles 3 and 4 unarmed.

Mxp3: Ischium with well-developed spine on flexor distal margin. Merus slightly shorter than ischium; flexor margin with two spines, median slightly stronger than distal spine; extensor margin with minute distal spine. Carpus unarmed.

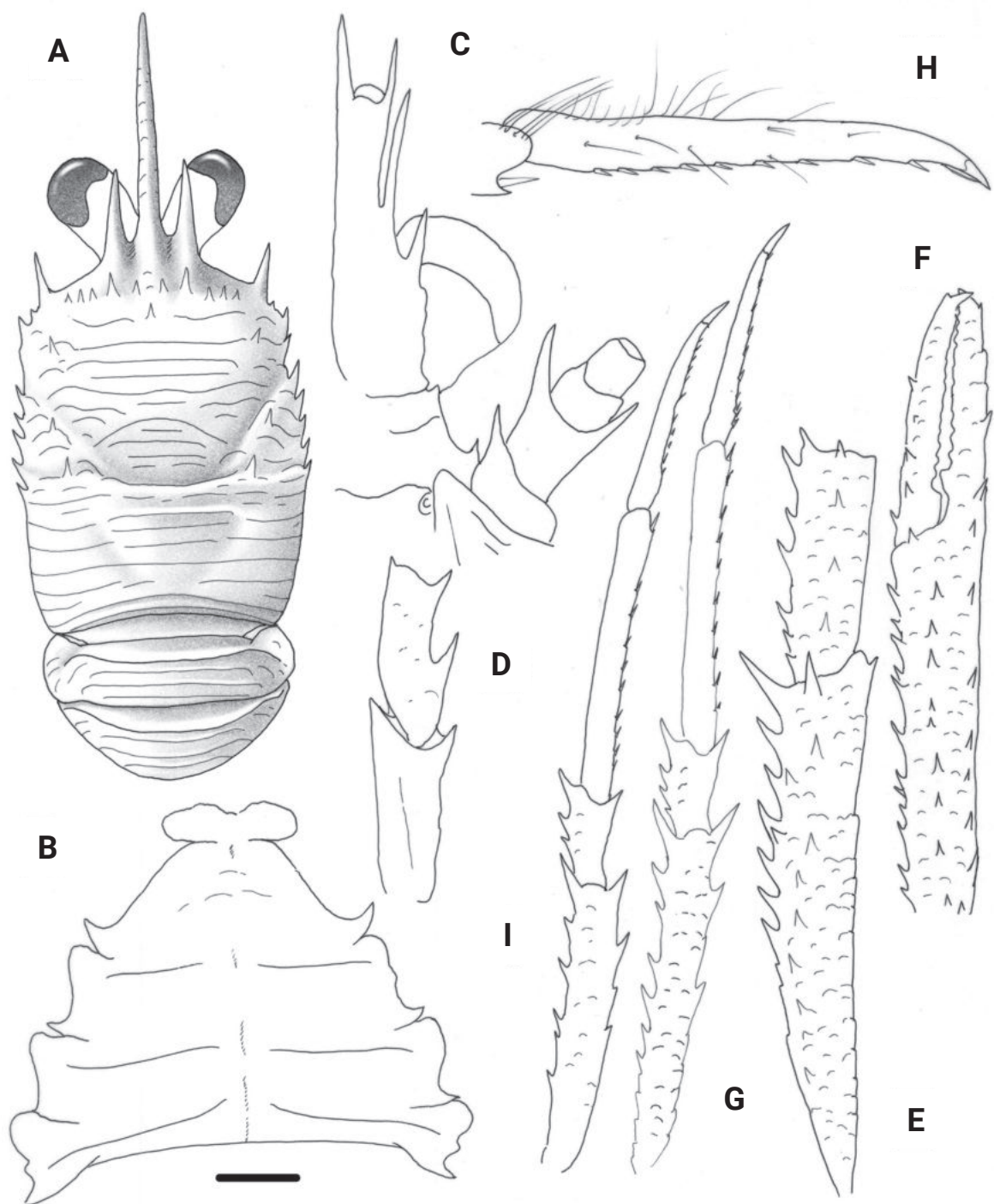


Figure 6. *Trapezionida macilenta* sp. nov., male holotype, 5.7 mm (MNHN-IU-2013-1094), Papua-New Guinea **A** carapace and pleon, dorsal view **B** sternal plastron **C** cephalic region, showing antennular and antennal peduncles, ventral view **D** right Mxp3 ischium and merus, lateral view **E** right P1, merus and carpus, dorsal view **F** right P1, palm and fingers, dorsal view **G** right P2, lateral view **H** dactylus of right P2, lateral view **I** right P3, lateral view. Scale bars: 1.0 mm (**A**, **E**, **F**, **G**, **I**); 0.5 mm (**B**, **C**, **D**, **H**).

P1: 4× carapace length, with scattered long plumose setae, and some long iridescent setae; some short setae on spines and scales. Merus 1.5 length of carapace, 2.2× as long as carpus, with some dorsal and mesial spines; distal

spines strong, distomesial spine barely reaching proximal fourth of carpus. Carpus 0.6× length of palm, 3.2× as long as broad, with spines along mesial and dorsal sides. Palm 4.4× as long as broad, with row of dorsal spines; one row of spines along mesial and lateral margins, continuing along movable and lateral fingers, respectively. Fingers 0.7× length of palm.

P2–P3 (P4 lost): Long and slender, with some short setae and some scattered iridescent setae along extensor margins of all articles. P2 2.8 carapace length. Meri shorter posteriorly (P3 merus 0.9× length of P2 merus); P2 merus as long as carapace, 7.2× as long as broad, 1.2× as long as P2 propodus; P3 merus 6.2× as long as broad, 1.1× as long as P3 propodus. Extensor margins of meri with row of six–eight proximally diminishing spines on P2–P3; flexor margins with three or four spines followed proximally by several eminences; lateral sides unarmed. Carpi with three or four spines on extensor margin; lateral surface with several granules sub-parallel to extensor margin; flexor margin with well-developed distal spine. Propodi 9.0–9.5× as long as broad; extensor margin unarmed; flexor margin with nine or ten slender movable spines, one fixed distal spine. Dactyli slender, length 0.8× that of propodi; flexor margin with ten movable spinules along entire border, with ultimate spinule at base of unguis; P2 dactylus 8.0× as long as wide.

Colour in life. Ground colour of the carapace, pleon and appendages orange with large reddish patches. P1–P4 with reddish and whitish transverse bands. Distal P1 palm reddish (Fig. 9A).

Genetic data. COI, 16S.

Etymology. From the Latin, *macilentus*, thin, in reference to the long and slender antennular peduncle.

Remarks. *Trapezionida macilenta* belongs to the group of species having one median protogastric spine, anterior ridge of the pleomere II tergite unarmed, thoracic sternites smooth and the antennular article 1 very slender, with the distomesial spine longer than the distolateral spine.

The new species is closely related to *T. diluta* sp. nov. from New Caledonia (see above). However, both species are easily distinguished by several characters:

- The branchial lateral margin of the carapace has four spines in *T. diluta* and five in *T. macilenta*. The pleomeres II and III tergites each with two or three uninterrupted transverse ridges behind the anterior ridge *T. macilenta*, whereas there is only one transverse ridge in *T. diluta*.
- The extensor margin of the Mxp3 merus has one minute distal spine in *T. macilenta*, absent in *T. diluta*.
- Genetically both species are different. *T. macilenta* showed high divergence values compared with *T. diluta* (6.42% COI, 4.6% 16S).

Distribution. Papua-New Guinea, 80 m depth.

***Trapezionida microtes* sp. nov.**

<https://zoobank.org/AB42F369-2D53-4AB1-89FD-EEA3C6083348>

Fig. 7

Trapezionida pumila: Machordom et al. 2022: table 2, suppl. figs S1–S6 (non *T. pumilla* Macpherson, 2004).

Material. Holotype: VANUATU. Santo Stn AT9, 17 September 2006, 15°41.5'S, 167°01.3'E, 481 m: ovigerous female, 3.4 mm (MNHN-IU-2017-1337). **Paratypes:** PHILIPPINES. Musorstom 2 Stn DG32, 24 November 1980, 13°40'N, 120°54'E, 192–220 m: 1 male, 2.0 mm, 2 ovigerous females, 2.3–2.4 mm, 1 female, 2.1 mm (MNHN-IU-2014-13975). New Caledonia. Halipro 2 Stn BT94, 24 November 1996, 23°33'S, 167°42'E, 448–880 m: 1 male, 3.0 mm (MNHN-IU-2014-13978). – Lithist Stn DW1, 10 August 1999, 23°37.4'S, 167°42.07'E, 440 m: 1 ovigerous female, 3.3 mm (MNHN-IU-2014-13979).

Description. Carapace: Slightly longer than broad, with a few scales between main transverse ridges in epigastric and anterior branchial areas. Ridges with very short setae. Gastric region with five pairs of epigastric spines, longest pair behind supraocular spines, one pair between longest pair. One parahepatic spine on each side. Frontal margins transverse. Lateral margins subparallel and convergent posteriorly. First lateral spine at anterolateral angle, well-developed, not reaching level of sinus between rostrum and supraocular spines. Branchial margin with four small spines. Rostrum slightly triangular, ~ 0.5× length of remaining carapace, slightly upwards directed, dorsally carinated. Supraocular spines short, not reaching midlength of rostrum and clearly not reaching end of cornea, subparallel. Pterygostomian region unarmed, ending in a round tip.

Thoracic sternum: 0.8× as long as wide. Surface of thoracic sternites IV–VI smooth, only a few short scales on sternite IV. Sternite III 3.5× as wide as long. Sternite IV trapezoidal, anterior margin contiguous to sternite III along $\frac{3}{4}$ of its length; 2.5× as wide as long, and 2.3× as wide as sternite III.

Pleon: Ridges of pleomeres unarmed; tergites II and III each with one or two uninterrupted transverse ridges on tergite behind anterior ridge: tergites IV and V with anterior ridge only; posteromedian margin of tergite VI straight.

Eye: Ocular peduncle longer than broad, cornea dilated, maximum corneal diameter 0.3 distance between bases of anterolateral spines.

Antennule: Article 1 (distal spines excluded) ~ 0.3× carapace length, 2.0× as long as wide (excluding spines), not overreaching end of cornea, with two distal spines, mesial spine shorter than lateral; two spines on lateral margin, proximal one short, located at midlength of segment, distal one long, not reaching end of distolateral spines.

Antenna: Article 1 with short distomesial spine not exceeding end of article 2. Article 2 with distomesial and distolateral subequal spines, not reaching end of article 3. Article 3 with distomesial spine.

Mxp3: Ischium with well-developed spine on flexor distal margin. Merus slightly shorter than ischium; flexor margin with two spines, median slightly stronger than distal spine; extensor margin with minute distal spine. Carpus unarmed.

P1: 2.5× carapace length, with scattered long setae and some short setae on spines and scales. Merus 0.9× carapace length, 2.0× as long as carpus, with some dorsal and mesial spines; distal spines strong, distomesial spine barely reaching proximal fourth of carpus. Carpus as long as palm, 2.0× as long as broad, with spines along mesial and dorsal sides. Palm 2.0× as long as broad, with row of minute dorsal spines; one row of spines along mesial and lateral margins. Fingers unarmed, 1.3× length of palm.

P2–P4: Long and slender, with some short setae and some scattered iridescent setae along extensor margins of all articles. P2 2.2× carapace length. Meri

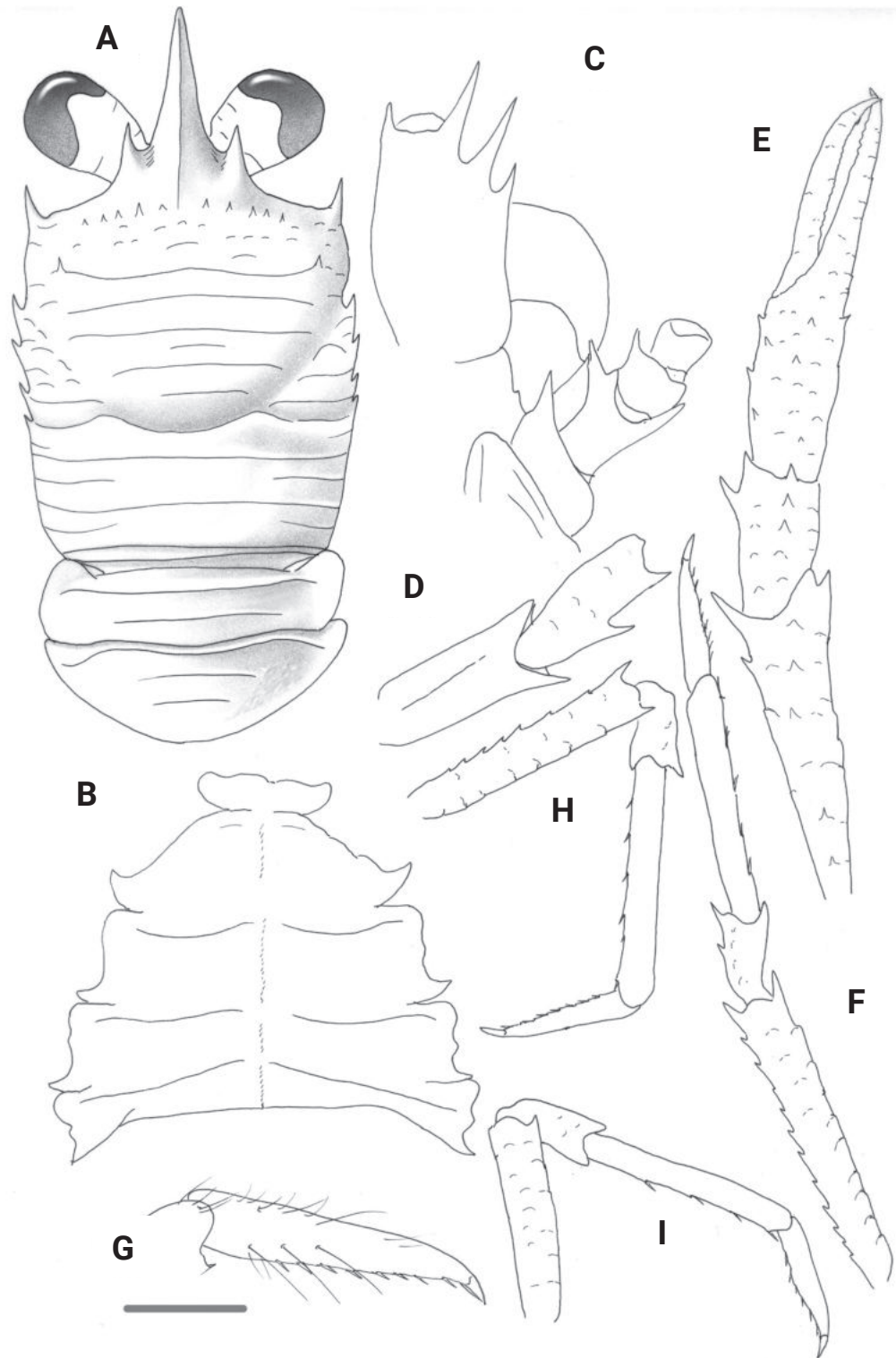


Figure 7. *Trapezionida microtes* sp. nov., ovigerous female holotype, 3.4 mm (MNHN-IU-2017-1337), Vanuatu **A** carapace and pleon, dorsal view **B** sternal plastron **C** cephalic region, showing antennular and antennal peduncles, ventral view **D** right Mxp3 ischium and merus, lateral view **E** right P1, dorsal view **F** right P2, lateral view **G** dactylus of right P2, lateral view **H** right P3, lateral view **I** right P4, lateral view. Scale bars: 1.0 mm (**A**, **E**, **F**, **H**, **I**); 0.5 mm (**B**, **C**, **D**, **G**).

shorter posteriorly (P3 merus 0.9× length of P2 merus, P4 merus 0.7× length of P3 merus); P2 merus 0.9× carapace length, 6.0× as long as broad, 1.4× as long as P2 propodus; P3 merus 5.5× as long as broad, 1.2× as long as P3 propodus.

Extensor margins of meri with row of 10–12 proximally diminishing spines on P2–P3, only distal spine on P4; flexor margins with three or four spines followed proximally by several eminences on P2–P3, only distal spine on P4; lateral sides unarmed. Carpi with one or two spines on extensor margin; lateral surface with several granules sub-parallel to extensor margin; flexor margin with well-developed distal spine. Propodi 6.0 (P2), 5.5 (P3), 4.2 (P4) × as long as broad; extensor margin unarmed; flexor margin with four or five slender movable spines, one fixed minute distal spine. Dactyli slender, length 0.6–0.7 that of propodi; flexor margin with eight or nine movable spinules along entire border, with ultimate spinule at base of unguis; P2 dactylus 5.0× as long as wide. P4 merocarpal articulation reaching anterior end of cervical groove; P4 merus > ½ length of P2 merus.

Genetic data. COI, 16S.

Etymology. From the Greek, *mikros*, small, in reference to the small size of the species.

Remarks. *Trapezionida microtes* belongs to the group of species having four spines on the branchial lateral margins of the carapace, rostrum narrowly triangular (not spiniform), short supraocular spines, thoracic sternites smooth, moderately large eyes, pleomere II tergite unarmed, and the distomesial spine of the antennular article 1 smaller than the distolateral spine.

The new species is closely related to *T. alonsoi* (Macpherson, 1994) from New Caledonia area and *T. pumilla* (Macpherson, 2004) from Tonga. However, *T. microtes* is easily distinguished from these species by several characters:

- The branchial lateral margin has four spines in the new species, whereas it is armed with five spines (rarely three or four) in *T. alonsoi* and *T. pumilla*.
- The extensor margin of the Mxp3 merus has a distal spine in *T. alonsoi* and *T. pumilla*, whereas it is unarmed in the new species.
- The P2–P4 dactyli are clearly more slender in *T. microtes* than in *T. alonsoi*: 5.0× vs. 2.5× as long as wide.
- Genetically *T. microtes* showed high divergence values with *T. alonsoi* (6.43% COI, 3.77% 16S). No genetic data is available for *T. pumilla*.

The new species is also close to *T. trigonocornus* from Japan (Komai 2012). However, the dorsal surface of the carapace has branchial dorsal and postcervical spines in *T. trigonocornus*, whereas these spines are absent in the new species. No genetic data is available for *T. trigonocornus*.

Distribution. Vanuatu, New Caledonia, at 192–880 m.

***Trapezionida pulex* sp. nov.**

<https://zoobank.org/FF992C41-5EC1-4109-9206-EB62CB87243B>

Figs 8, 9B

Munida leptitis: Macpherson 1996: 394, fig. 14. — Macpherson 1997: 607. — Macpherson 2000: 419. — Macpherson 2004: 263. — Baba 2005: 267 (in part). — Macpherson 2006: 318 (in part). — Baba et al. 2008: 104 (in part). — Macpherson 2013: 301 (in part). — Macpherson et al. 2020: 59. (non *M. leptitis* Macpherson, 1994).

Trapezionida aff. *leptitis*1: Machordom et al. 2022: table 2, suppl. figs S1–S6.

Material. Holotype: NEW CALEDONIA, Exbodi Stn DW3902, 19°53'S, 165°49'E, 410 m, 22 September 2011: male, 5.4 mm (MNHN-IU-2016-5809). **Paratypes:** INDONESIA, Kei Islands, Karubar Stn DW02, 22 October 1991, 05°47'S, 132°13'E, 209–240 m: 3 males, 4.8–5.3 mm, 2 females, 3.6–4.3 mm, 1 juv. 2.4 mm (MNHN-IU-2014-14752, MNHN-IU-2016-516). PAPUA-NEW GUINEA, Biopapua Stn CP3759, 14 October 2010, 03°59.690'S, 153°37.070'E, 287–352 m: 1 ovigerous female, 5.3 mm (MNHN-IU-2011-3829). — Papua Niugini Stn CP4016, 12 December 2012, 05°40'S, 148°14'E, 280–285 m: 1 female, 3.2 mm (MNHN-IU-2016-5816). — Madeep Stn DW4310, 3 May 2014, 09°50'S, 151°31'E, 390–500 m: 1 male, 4.2 mm (MNHN-IU-2016-5804). — Stn DW4311, 3 May 2014, 09°50'S, 151°32'E, 270–486 m: 1 male, 5.7 mm, 1 ovigerous female, 5.2 mm (MNHN-IU-2015-828). — Kavieng 2014 Stn DW4485, 5 September 2014, 02°26'S, 149°54'E, 240–242 m: 1 male, 3.4 mm (MNHN-IU-2014-9905). Solomon Islands, Salomon 1 Stn CP1831, 05 October 2001, 10°12.1'S, 161°19.2'E, 135–325 m: 1 ovigerous female, 6.0 mm; (MNHN-IU-2016-2997), 3 males, 3.4–5.5 mm, 1 ovigerous female, 3.7 mm, 1 female, 5.0 mm (MNHN-IU-2014-14750). Vanuatu, Musorstom 8 Stn CP983, 23 September 1994, 19°22'S, 169°28'E, 475–480 m: 1 male, 3.5 mm (MNHN-IU-2016-515). New Caledonia, Chesterfield Islands, Ebisco Stn CP2620, 20 October 2005, 20°05.864'S, 160°22.318'E, 270–532 m: 1 female, 5.8 mm (MNHN-IU-2014-14714). — Kanadeep 1 Stn DW5007, 22°12'S, 159°02'E, 19 September 2017, 290–750 m: 1 male, 5.6 mm (MNHN-IU-2013-19924). New Caledonia, Terrasse Stn DW3083, 24 October 2008, 22°27'S, 167°25'E, 470–570 m: 1 male, 5.2 mm (MNHN-IU-2011-4956). — Exbodi Stn CP3927, 26 September 2011, 18°36'S, 164°20'E, 381 m: 1 ovigerous female, 4.7 mm (MNHN-IU-2016-5815). — Stn DW3928, 26 September 2011, 18°38'S, 164°20'E, 362–402 m: 2 males, 4.5–5.2 mm (MNHN-IU-2016-5811). — Stn DW3930, 26 September 2011, 18°37'S, 164°26'E, 448–464 m: 2 males, 5.3–6.0 mm (MNHN-IU-2011-6466). — Stn DW3937, 27 September 2011, 18°37'S, 164°26'E, 446–604 m: 1 male, 7.8 mm (MNHN-IU-2013-1793), 2 males, 4.2–6.0 mm, 2 ovigerous females, 5.2–6.0 mm, 1 female, 3.8 mm (MNHN-IU-2011-7263). — Stn CP3841, 10 September 2011, 22°23'S, 167°24'E, 477–503 m: 2 ovigerous females, 4.8–5.3 mm (MNHN-IU-2016-5819). — Stn DW3847, 13 September 2011, 22°04'S, 168°41'E, 414–435 m: 1 ovigerous female, 4.4 mm (MNHN-IU-2013-1882). — Stn CP3848, 13 September 2011, 22°03'S, 168°42'E, 430–440 m: 3 males, 4.2–5.1 mm, 4 ovigerous females, 4.4–4.7 mm (MNHN-IU-2014-18231). — Stn CP3849, 13 September 2011, 22°03'S, 168°41'E, 360–560 m: 1 male, 6.0 mm (MNHN-IU-2016-5812). — Kanacono Stn DW4764, 27 August 2016, 23°20'S, 168°15'E, 350–356 m: 1 male, 7.0 mm (MNHN-IU-2017-8561). Wallis and Futuna Islands, Musorstom 7 Stn DW605, 13°21.3'S, 176°08.4'W, 335–340 m, 26 June 1992: 1 ovigerous female, 4.5 mm (MNHN-IU-2016-517), 7 males, 3.1–6.1 mm, 3 ovigerous females, 4.4–5.3 mm, 2 females, 3.6–4.0 mm (MNHN-IU-2014-14735). Tonga, Bordau 2 CP1545, 5 June 2000, 21°17'S, 175°17'W, 444–447 m: 3 males, 4.1–6.2 mm, 1 ovigerous female, 6.0 mm (MNHN-IU-2014-14739). — Stn CP1643, 21°04.54'S, 175°22.50'W, 487 m, 22 June 2000: 2 males, 5.7–6.8 mm (MNHN-IU-2014-14748), 1 female, 4.6 mm (MNHN-IU-2016-518).

Description. Carapace: Slightly longer than broad, feebly convex, with some secondary striae and scales between main transverse ridges. Dorsal ridges with dense short setae, and numerous scattered, long, non-iridescent setae. Gastric region with four or five pairs of epigastric spines, longest pair behind

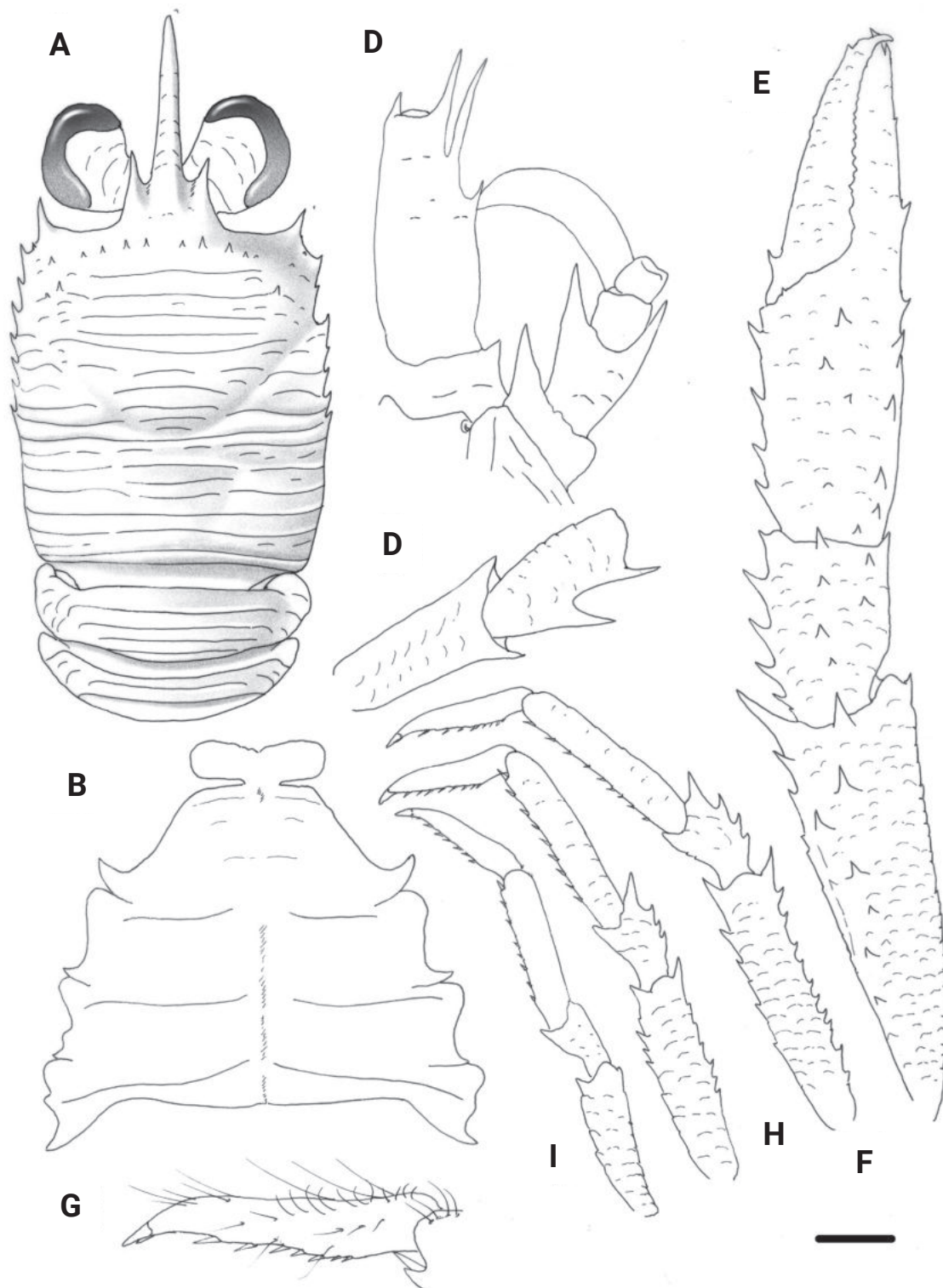


Figure 8. *Trapezionida pulex* sp. nov., male holotype, 5.4 mm (MNHN-IU-2016-5809), New Caledonia **A** carapace and pleon, dorsal view **B** sternal plastron **C** cephalic region, showing antennular and antennal peduncles, ventral view **D** right Mxp3 ischium and merus, lateral view **E** right P1, dorsal view **F** left P2, lateral view **G** dactylus of left P2, lateral view **H** left P3, lateral view **I** left P4, lateral view. Scale bars: 1.0 mm (**A, E, F, H, I**); 0.5 mm (**B, C, D, G**).

supraocular spines, with intermediate pair of minute spines between large epigastric pair. One or two small hepatic and one parahepatic spine on each side, branchial dorsal and postcervical spines absent. Frontal margins transverse.

Lateral margins slightly convex. First lateral spine on anterolateral angle, short, clearly not reaching level of sinus between rostrum and supraocular spines; two small spines in front of anterior branch of cervical groove; end of anterior branch of cervical groove with tuft of iridescent setae. Branchial margins straight, with five small spines, decreasing in size posteriorly. Rostrum spiniform, $\sim 0.6\text{--}0.7\times$ length of remaining carapace, laterally carinate, slightly upwards directed. Supraocular spines short, not reaching midlength of rostrum and clearly not reaching end of cornea, subparallel, directed slightly upwards. Grooves between rostrum and supraocular spines moderately shallow. Pterygostomian region unarmed, ending in round tip.

Thoracic sternum: Approximately $0.7\times$ as long as wide. Maximum width of sternum at sternite VII. Surface of thoracic IV–VI sternites smooth, with a few short striae in sternite IV. Sternite IV trapezoidal; anterior margin wide and subparallel to sternite III along its entire length. Sternite III $\sim 2.5\text{--}3.0\times$ as wide as long, sternite IV $2.5\times$ as wide as long, $2.5\times$ as wide as sternite III.

Pleon: Tergites II and III each unarmed along anterior ridge, with three uninterrupted transverse ridges on tergite behind anterior ridge, tergites IV and V each with two uninterrupted transverse ridges; ridges with some short setae and a few iridescent setae.

Eye: Cornea dilated, much wider than peduncle. Maximum corneal diameter 0.4 distance between bases of anterolateral spines.

Antennule: Article 1 more than $2.0\times$ as long as wide, with two well-developed distal spines, distomesial spine clearly shorter than distolateral; two lateral spines, distal much longer than proximal and nearly exceeding distolateral spine.

Antenna: Article 1 with short distomesial spine nearly reaching end of article 2. Article 2 with distomesial and distolateral spines exceeding end of article 3. Article 3 unarmed.

Mxp3: Ischium with strong distal spine on flexor margin. Merus shorter than ischium; flexor margin with two spines, proximal stronger than distal; extensor margin unarmed or with minute spine. Carpus unarmed.

P1: $2.5\text{--}2.7$ (females), $3.0\text{--}3.2$ (males) \times carapace length, squamate, covered with numerous long plumose and iridescent setae along mesial margin of articles. Merus $1.0\text{--}1.2$ length of carapace, $2.1\text{--}2.2\times$ as long as carpus, with some dorsal and mesial spines; distal spines strong, distomesial spine nearly reaching proximal third of carpus. Carpus $0.9\text{--}1.0$ length of palm, $1.4\text{--}1.6\times$ as long as broad, with strong spines along mesial margin, some small spines on dorsal side. Palm $1.3\text{--}1.7\times$ as long as broad, with some small dorsal spines; well-developed spines along lateral and mesial margins. Fingers $1.2\text{--}1.4\times$ as long as palm; fixed finger with spines along lateral margin; movable finger with basal and distal spines.

P2–P4: Moderately long and slender, with numerous iridescent setae along extensor margin of articles. P2 $1.9\text{--}2.0\times$ carapace length. Meri shorter posteriorly (P3 merus $0.8\text{--}0.9$ length of P2 merus, P4 merus $0.7\text{--}0.8$ length of P3 merus); P2 merus $0.7\text{--}0.8$ length of carapace, $4.8\text{--}4.9\times$ as long as broad, $1.3\text{--}1.4\times$ as long as P2 propodus; P3 merus $4.8\text{--}4.2\times$ as long as broad, $1.2\text{--}1.3\times$ as long as P3 propodus; P4 merus $3.5\text{--}3.7\times$ as long as broad, $1.1\text{--}1.2\times$ length of P4 propodus. Extensor margins of P2–P4 meri with row of spines, decreasing in size proximally; flexor margins with some well-developed spines followed proximally by several eminences; lateral sides unarmed. Carpi with three or four spines on extensor margin of

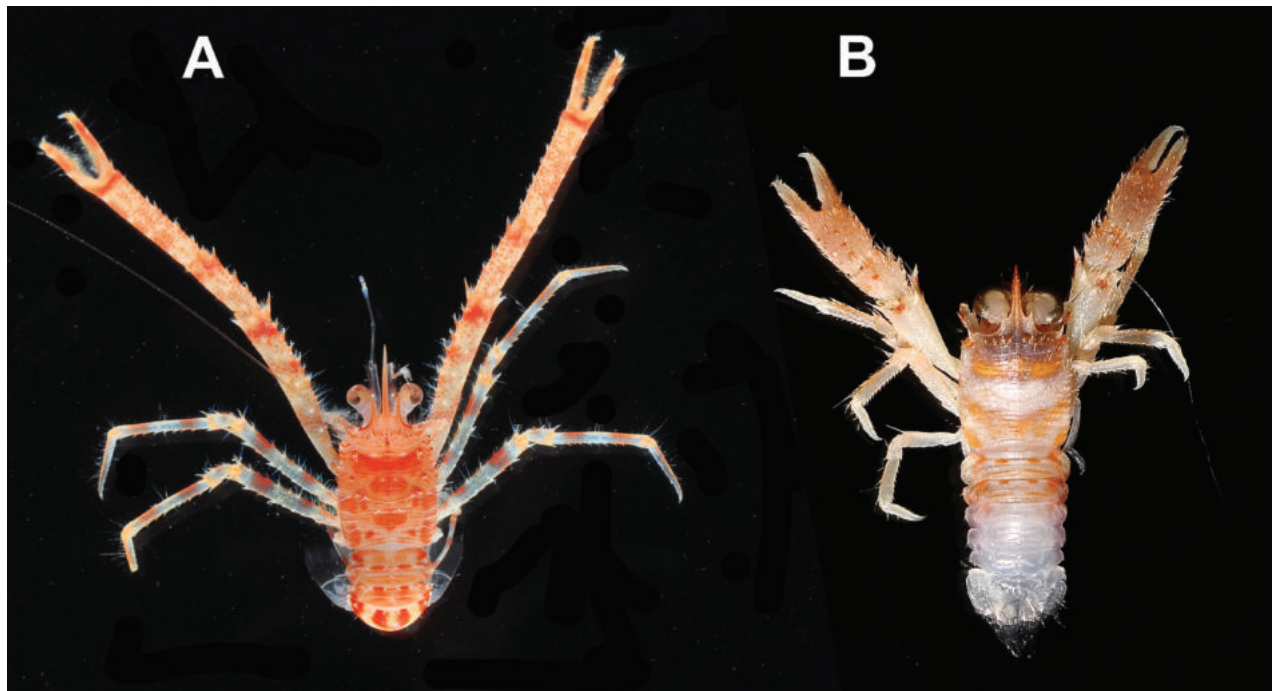


Figure 9. Colour in life **A** *Trapezionida macilenta* sp. nov., male holotype, 5.7 mm (MNHN-IU-2013-1094), Papua-New Guinea **B** *Trapezionida pulex* sp. nov., ovigerous female paratype, 4.4 mm (MNHN-IU-2013-1882), New Caledonia.

P2–P3, unarmed on P4; lateral surface with several granules sub-parallel to extensor margin on P2–P4; flexor margin with distal spine. Propodi 4.0–4.7× as long as broad; extensor margin unarmed; flexor margin with nine or ten slender movable spines on P2–P4, distal end with one fixed spine. Dactyli slender, slightly shorter than propodi; flexor margin with 7–9 movable spinules, with ultimate spinule at base of unguis, penultimate spine much closer to antepenultimate than to ultimate spine; P2 dactylus 3.7–4.5× as long as wide. P4 merocarpal articulation not reaching anterior end of cervical groove; P4 merus ~ ½ length of P2 merus.

Colour in life. Ground colour of carapace and pleomere tergites pale orange. Rostrum orange, supraocular spines whitish. Transverse whitish stripes on median and posterior parts of carapace. Median and lateral parts of pleomere tergites with orange spots. P1–P4 pale orange without transverse stripes; P1 with a few dorso-median red spots; distal portion of fingers whitish. P2–P4 dactyli whitish (Fig. 9B).

Genetic data. COI, 16S.

Etymology. From the Latin, *pulex*, flea, in reference to the small size of the species.

Remarks. The new species is morphologically very close to *T. leptitis* (Macpherson, 1994) (see above), which was described from specimens collected in New Caledonia, and it was found later off Wallis and Futuna area, Taiwan, Indonesia, Papua-New Guinea, Vanuatu, Fiji, Tonga, and French Polynesia (see Macpherson et al. 2020 and references cited therein). Nevertheless, some slight morphological differences among specimens suggest the existence of a complex of cryptic species with overlapping distribution ranges. The molecular analysis of specimens from the different localities has demonstrated the existence of two species, *T. leptitis* and *T. pulex*. Both species are genetically distinct, although only separated morphologically by slight differences.

Both species can be differentiated by the following aspects:

- The thoracic sternite III is more slender in *T. leptitis* than in *T. pulex* (3.5–4.5× as wide as long in *T. leptitis* and 2.5–3.0× in *T. pulex*).
- The P2–P4 are more slender in *T. pulex* than in *T. leptitis*. The propodi are 5.3–5.7× as long as broad and the dactyli 5.0× as long as broad in *T. pulex*. These values are 4.0–4.6 and 3.7–4.5×, respectively, in *T. leptitis*.
- The colour patterns of both species are different. For instance, the dorsal surface of the P1 has numerous red spots in *T. leptitis*, whereas these spots are very few in *T. pulex*.
- Genetically the new species is different from *T. leptitis*: 7.44% 16S and 13.54% COI.

Distribution. The species is found in Indonesia, Vanuatu, Loyalty Islands, New Caledonia, Wallis and Futuna Islands, Fiji, Tonga, and French Polynesia. The depth range of these specimens is 135–750 m.

Genus *Typhlonida* Macpherson & Baba, 2022 in Machordom et al. 2022

Typhlonida eluminata sp. nov.

<https://zoobank.org/DC2ED9D2-2F9E-4C5D-B3CA-C24513DA6109>

Fig. 10

Typhlonida sp.: Machordom et al. 2022: fig. 3H, table 2.

Material. Holotype: NEW CALEDONIA, Exbodi Stn DW3941, 19°04'S, 164°03'E, 980–1090 m, 28 September 2011: female, 6.6 mm (MNHN-IU-2011-6787).

Description. Carapace: Slightly longer than broad, feebly convex, with a few secondary striae between main transverse ridges and some scales on gastric and anterior branchial areas. Dorsal ridges with dense short plumose setae, and a few scattered long setae. Gastric region with two pairs of epigastric spines, longest pair behind supraocular spines. Parahepatic, branchial dorsal and postcervical spines absent. Frontal margins slightly oblique. Lateral margins slightly convex. First lateral spine at anterolateral angle, well-developed, reaching level of sinus between rostrum and supraocular spines; one small spine in front of anterior branch of cervical groove. Branchial margins slightly convex, with five spines, decreasing in size posteriorly. Rostrum spiniform, ~ 0.5× length of remaining carapace, horizontal. Supraocular spines reaching midlength of rostrum and exceeding end of cornea, subparallel, directed slightly upwards. Pterygostomian region ending in round tip.

Thoracic sternum: Approximately 0.7× as long as wide. Surface of thoracic IV–VI sternites smooth, with a few short striae in sternite IV. Sternite III ~ 4× as wide as long. Sternite IV triangular, anterior margin clearly narrower than preceding sternite, anterolateral margins slightly convex; 2.0× as wide as long, 2.3× as wide as sternite III.

Pleon: Pleomere II tergite with three–four pairs of spines along anterior ridge, with one uninterrupted transverse ridge on tergite behind anterior ridge; tergites III and IV each with additional ridge behind anterior ridge; ridges with some short setae and a few iridescent setae.

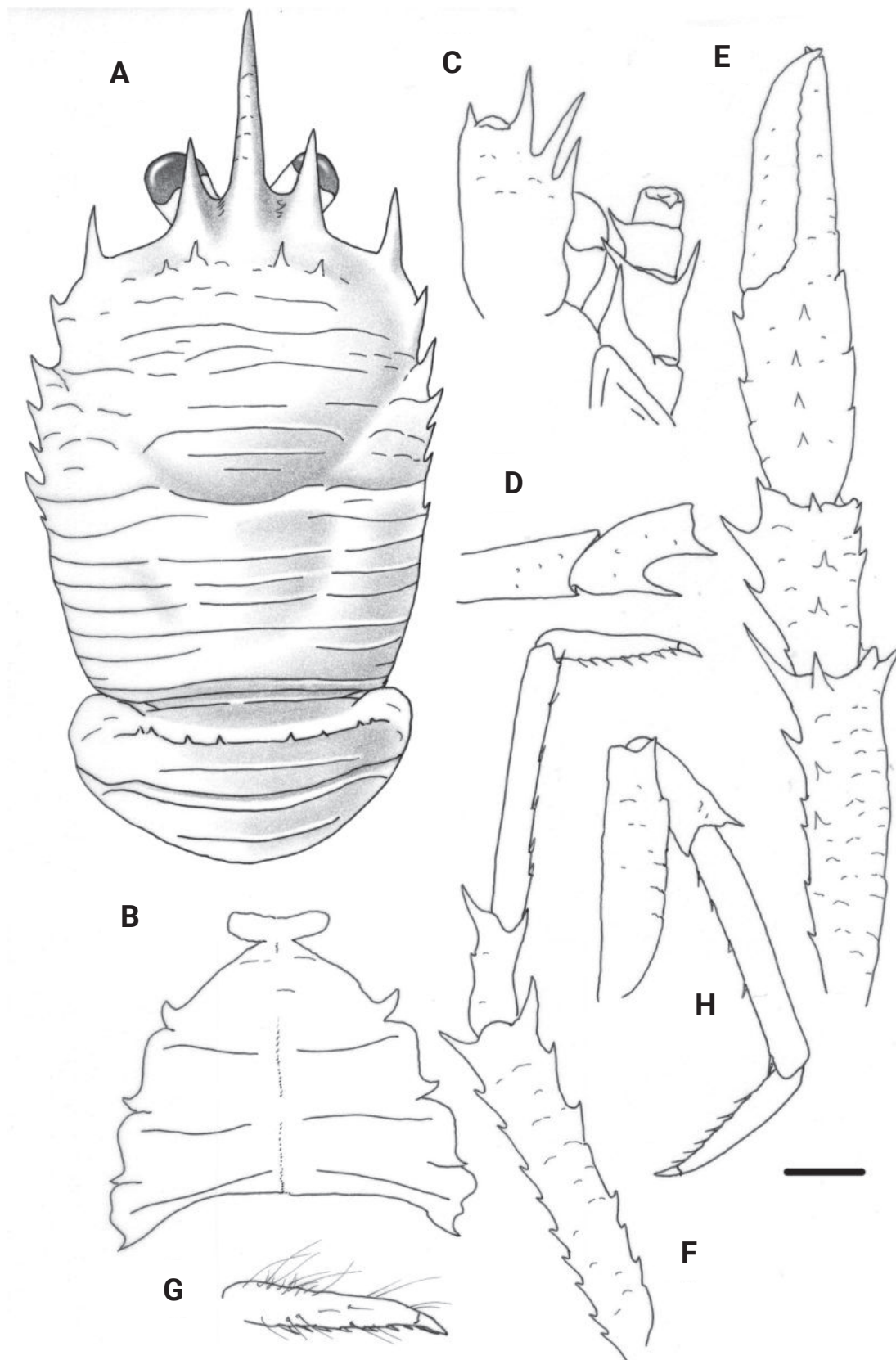


Figure 10. *Typhlonida eluminata* sp. nov., female holotype, 6.6 mm (MNHN-IU-2011-6787), New Caledonia **A** carapace and pleon, dorsal view **B** sternal plastron **C** cephalic region, showing antennular and antennal peduncles, ventral view **D** right Mxp3 ischium and merus, lateral view **E** right P1, dorsal view **F** right P2, lateral view **G** dactylus of right P2, lateral view **H** right P4, lateral view. Scale bars: 1.0 mm (**A**, **E**, **F**, **H**); 0.6 mm (**B**, **C**, **D**, **G**).

Eye: Cornea not dilated, as wide as peduncle. Maximum corneal diameter $< 0.3\times$ distance between bases of anterolateral spines.

Antennule: Article 1 (basal) $0.7\times$ as wide as long, with two well-developed distal spines, distomesial spine shorter than distolateral; two lateral spines, distal much longer than proximal and not reaching distolateral spine.

Antenna: Article 1 with short distomesial spine reaching end of article 2. Article 2 with subequal distomesial and distolateral spines not reaching end of article 3; article 3 with well-developed distomesial spine.

Mxp3: Ischium with strong distal spine on flexor margin. Merus shorter than ischium; flexor margin with two well-developed spines, proximal stronger than distal; extensor margin unarmed. Carpus unarmed.

P1: $2.2\times$ carapace length, with dense long setae along mesial and dorsal margins of articles, more numerous in paratypes than in holotype. Merus $0.9\times$ length of carapace, $2.1\times$ as long as carpus, with some dorsal and mesial spines; distal spines strong, distomesial spine nearly reaching proximal $1/3$ of carpus. Carpus $0.9\times$ length of palm, $2.0\times$ as long as broad, with strong spines along mesial margin, some small spines on dorsal side. Palm $2.0\times$ as long as broad, with row of small dorsal spines; well-developed spines along lateral and mesial margins. Fingers $1.2\times$ as long as palm; movable finger unarmed, fixed finger with distal spine.

P2–P4: Moderately long and slender, with some plumose setae and scattered longer setae along extensor margin of articles. P2 $2.0\times$ carapace length. Meri successively shorter posteriorly (P3 merus $0.9\times$ length of P2 merus, P4 merus $0.7\times$ length of P3 merus); P2 merus $0.8\times$ length of carapace, $5.2\times$ as long as broad, $1.5\times$ as long as P2 propodus; P3 merus $5.0\times$ as long as broad, $1.3\times$ as long as P3 propodus; P4 merus $4.0\times$ as long as broad, $1.2\times$ length of P4 propodus. Extensor margins of P2–P4 meri with row of spines, decreasing in size proximally; flexor margins with well-developed distal spine followed proximally by several spines or eminences; lateral sides unarmed. Carpi with distal spine on extensor margin of P2–P4; lateral surface with several granules sub-parallel to extensor margin on P2–P4; flexor margin with distal spine. Propodi 7.5 (P2) to 6.0 (P4) \times as long as broad; extensor margin unarmed; flexor margin with five or six slender movable spines on P2–P4, distal end with one fixed spine. Dactyli slender, 0.6 – $0.7\times$ as long as propodi; flexor margin with seven–eight movable spinules, with ultimate spinule at base of unguis, penultimate spine equidistant between antepenultimate and ultimate spines; P2 dactylus $4.5\times$ as long as wide.

Genetic data. COI, 16S, 18S.

Etymology. From the Latin, *eluminatus*, blinded, in reference to the small eyes.

Remarks. *Typhlonida eluminata* belongs to the group of species having five minute spines on the branchial lateral margins of the carapace, short supraocular spines, eyes small, cornea as wide as peduncle, maximum corneal diameter $< 0.3\times$ distance between bases of anterolateral spines, the anterior ridge of the pleomere II tergite with spines and the distomesial spine of the antennal article 1 well-developed, exceeding midlength of article 2. The new species is closely related to *T. typhle* (Macpherson, 1994), from New Caledonia and *T. galalala* (McCallum et al., 2021) from NW Australia.

The new species can be distinguished from *T. typhle* by the presence of a distomesial spine on the antennal article 3 in the new species, which is absent in *T. typhle*. Furthermore, the anterolateral spine of the carapace clearly not reaching the level of the sinus between the rostrum and the supraocular spines in *T. typhle*, whereas this spine is reaching this sinus in the new species. Finally, the flexor margin of the Mxp3 merus has two well-developed spines in the new species, whereas there is only one median spine in *T. typhle*.

The differences between *T. typhle* and *T. galalala* are the following:

- The anterolateral spine of the carapace is as long as the supraocular spine in the new species, whereas it is smaller in *T. galalala*.
- The P2 merus is longer than the carapace in *T. galalala*, whereas it is shorter in the new species.
- The dorsal surface of the P1 palm is unarmed in *T. galalala*, whereas there are some small spines in the new species.
- Genetically the new species is different from *T. typhle* and *T. galalala*: *T. eluminata* diverges respect to *T. typhle* 3.97% for 16S and 11.42% for COI, and the values are ~ 11.61% for COI and 3.86% for 16S compared to *T. galalala*.

The new species is also close to *T. lanciaria* (Cabezas et al., 2011), from Taiwan, but this species has the cornea clearly wider than the peduncle. Furthermore, both species are genetically quite different (3.01% for 16S) and 13.4% (COI).

Distribution. New Caledonia, between 980 and 1090 m.

Acknowledgements

We thank our colleagues who made specimens available for study: P. Bouchet, L. Corbari, B. Richer de Forges, A. Crosnier, S. Samadi, and P. Martin-Lefèvre of MNHN, Paris. We are also indebted to all the chief scientists, captains, and crew of the research vessels of different cruises that provided the specimens used in this study. Thanks to K. Schnabel and T. Komai for their valuable comments to the manuscript.

The material used in this study originates from numerous shore-based expeditions and deep-sea cruises conducted, respectively, by MNHN and Pro-Natura International as part of the Our Planet Reviewed programme and by MNHN and Institut de Recherche pour le Développement as part of the Tropical Deep-sea Benthos programme. The specimens from recent expeditions in Papua New Guinea and New Caledonia were collected on board the R.V. Alis during the following deep-sea cruises: Biopapua (<https://doi.org/10.17600/10100040>), Papua Niugini (<https://doi.org/10.17600/1800084>), Madeep (<https://doi.org/10.17600/14004000>) and Kavieng 2014 (<https://doi.org/10.17600/14004400>), Ebisco (<https://doi.org/10.17600/5100080>), Tarasoc (<https://doi.org/10.17600/9100040>), Norfolk 2 (<https://doi.org/10.17600/3100030>), Exbodi (<https://doi.org/10.17600/11100080>), Terrasse (<https://doi.org/10.17600/8100100>), Kanakono (<https://doi.org/10.17600/16003900>), Kanadeep (<https://doi.org/10.17600/17003800>)

and Spanbios (<https://doi.org/10.17600/18000701>). These cruises were operated by Muséum National d'Histoire Naturelle (MNHN) and Institut de Recherche pour le Développement (IRD) as part of the research program “Tropical Deep Sea Benthos”.

All expeditions operated under the regulations then in force in the countries in question and satisfy the conditions set by the Nagoya Protocol for access to genetic resources (MoU APA-NC-25 between New-Caledonia and MNHN, MoU MNHN-Province Sud APA_NCPS_2016_012 & MNHN-Nouvelle-Calédonie APA-NC01 MoU Nouvelle-Calédonie APA-NC07). The Papua New Guinea expeditions were operated under a permit delivered by the Papua New Guinea Department of Environment and Conservation. Funders and sponsors include the Total Foundation, Prince Albert II of Monaco Foundation, Stavros Niarchos Foundation, Richard Lounsbery Foundation, and the French Ministry of Foreign Affairs.

Additional information

Conflict of interest

The authors have declared that no competing interests exist.

Ethical statement

No ethical statement was reported.

Funding

Molecular data were obtained thanks to the partial support of a Spanish Ministry of Science and Innovation projects (REF. CTM2013-48163-C2-1-R and CTM 2014-57949-R). PCRF was supported by a Biodiversity postdoctoral Fellowship program from the MCZ.

Author contributions

All authors have contributed equally.

Author ORCIDs

Enrique Macpherson  <https://orcid.org/0000-0003-4849-4532>

Paula C. Rodríguez-Flores  <https://orcid.org/0000-0003-1555-9598>

Annie Machordom  <https://orcid.org/0000-0003-0341-0809>

Data availability

All of the data that support the findings of this study are available in the main text or Supplementary Information.

References

- Ahyong ST, Poore GCB (2004) Deep-water Galatheidæ (Crustacea: Decapoda: Anomura) from southern and eastern Australia. *Zootaxa* 472(1): 3–76. <https://doi.org/10.11646/zootaxa.472.1.1>
- Ahyong ST, Baba K, Macpherson E, Poore GCB (2010) A new classification of the Galatheoidea (Crustacea: Decapoda: Anomura). *Zootaxa* 2676(1): 57–68. <https://doi.org/10.11646/zootaxa.2676.1.4>

- Baba K (1986) Two new anomuran Crustacea (Decapoda: Anomura) from north-west Australia. The Beagle, Occasional Papers of the Northern Territory Museum of Arts and Sciences 3: 1–5. <https://doi.org/10.5962/p.260869>
- Baba K (2005) Deep-sea chirostylid and galatheid crustaceans (Decapoda: Anomura) from the Indo-West Pacific, with a list of species. Galathea Reports 20: 1–317.
- Baba K, de Saint Laurent M (1996) Crustacea Decapoda: Revision of the genus *Bathymunida* Balss, 1914, and description of six new related genera (Galatheidae). In: Crosnier A (Ed.) Résultats des Campagnes MUSORSTOM, volume 15. Mémoires du Muséum National d'Histoire Naturelle, Paris 168: 433–502.
- Baba K, Macpherson E, Poore GCB, Ah Yong ST, Bermudez A, Cabezas P, Lin C-W, Nizinski M, Rodrigues C, Schnabel K (2008) Catalogue of squat lobsters of the world (Crustacea: Decapoda: Anomura – families Chirostylidae, Galatheidae and Kiwaidae). Zootaxa 1905(1): 1–220. <https://doi.org/10.11646/zootaxa.1905.1.1>
- Baba K, Macpherson E, Lin CW, Chan T-Y (2009) Crustacean Fauna of Taiwan: squat lobsters (Chirostylidae and Galatheidae). Taipei: National Science Council, Taiwan, R.O.C, ix + 312 pp.
- Baba K, Ah Yong ST, Macpherson E (2011) Chapter 1. Morphology of the marine squat lobsters. In: Poore GCB, Ah Yong ST, Taylor J (Eds) The biology of squat lobsters. CSIRO Publishing, Melbourne and CRC Press, Boca Raton, 1–37.
- Cabezas P, Lin CW, Chan TY (2011) Two new species of the deep-sea squat lobster genus *Munida* Leach, 1820 (Crustacea: Decapoda: Munididae) from Taiwan: morphological and molecular evidence. Zootaxa 3036(1): 26–38. <https://doi.org/10.11646/zootaxa.3036.1.2>
- Chace FA (1939) Reports on the scientific results of the first Atlantis Expedition to the West Indies, etc. Preliminary descriptions of one new genus and seventeen new species of decapod and stomatopod Crustacea. Memorias de la Sociedad Cubana de Historia Natural 13: 31–54.
- De Grave S, Decock W, Dekeyser S, Davie PJF, Fransen CJM, Boyko CB, Poore GCB, Macpherson E, Ah Yong ST, Crandall KA, de Mazancourt V, Osawa M, Chan TY, Ng PKL, Lemaitre R, van der Meij SET, Santos S (2023) Benchmarking global biodiversity of decapod crustaceans (Crustacea: Decapoda). Journal of Crustacean Biology 43(3): 1–9. <https://doi.org/10.1093/jcabi/ruad042>
- Komai T (2012) Squat Lobsters of the Genus *Munida* Leach, 1820 (Crustacea: Decapoda: Anomura: Munididae) from the Sagami Sea and Izu Islands, Central Japan, with descriptions of 10 new species. Natural History Research 12: 1–69.
- Komai T, Tsuchida S, Fujiwara Y (2023) Squat lobsters of the superfamily Chirostyloidea (Decapoda: Anomura) from seamounts on the Nishi-Shichito and Mariana ridges, North-West Pacific off Japan, with descriptions of two new species. Zootaxa 5293(1): 45–73. <https://doi.org/10.11646/zootaxa.5293.1.2>
- Machordom A, Ah Yong ST, Andreakis N, Baba K, Buckley D, García-Giménez R, McCallum A, Rodríguez-Flores PC, Macpherson E (2022) Deconstructing the squat lobster genus *Munida* to reconstruct the evolutionary history and taxonomy of the family Munididae (Crustacea, Anomura, Galatheoidea). Invertebrate Systematics 36: 926–970. <https://doi.org/10.1071/IS22013>
- Macpherson E (1994) Crustacea Decapoda: Studies on the genus *Munida* Leach, 1820 (Galatheidae) in New Caledonia and adjacent waters with descriptions of 56 new species. In: Crosnier A (Ed.) Résultats des Campagnes MUSORSTOM, volume 12. Mémoires du Muséum National d'Histoire Naturelle, Paris 161, 421–569.

- Macpherson E (1996) Crustacea Decapoda: species of the genera *Munida* Leach, 1820 and *Paramunida* Baba, 1988 (Galatheidae) from the seas around the Wallis and Futuna Islands. In: Crosnier A (Ed.) Résultats des Campagnes MUSORSTOM, volume 15. Mémoires du Muséum National d'Histoire Naturelle, Paris 168, 387–421.
- Macpherson E (1997) Crustacea Decapoda: species of the genera *Agononida* Baba & de Saint Laurent, 1996 and *Munida* Leach, 1820 (Galatheidae) from the KARUBAR cruise. In: Crosnier A, Bouchet P (Eds) Résultats des Campagnes MUSORSTOM, volume 16. Mémoires du Muséum National d'Histoire Naturelle, Paris 172, 597–612.
- Macpherson E (2000) Crustacea Decapoda: Species of the genera *Agononida* Baba & de Saint Laurent, 1996 and *Munida* Leach, 1820 (Galatheidae) collected during the MUSORSTOM 8 cruise in Vanuatu. In: Crosnier A (Ed.) Résultats des Campagnes MUSORSTOM, Volume 20. Mémoires du Muséum National d'Histoire Naturelle, Paris 180, 407–426.
- Macpherson E (2004) Species of the genus *Munida* Leach, 1820 and related genera from Fiji and Tonga (Crustacea: Decapoda: Galatheidae). In: Marshall BA, Richer de Forges B (Eds) Tropical Deep-Sea Benthos, Volume 23. Mémoires du Muséum National d'Histoire Naturelle, Paris 191, 231–292.
- Macpherson E (2006) New species and new occurrence of Galatheoidea (Crustacea, Decapoda) from New Caledonia. *Zoosystema* 28: 669–681.
- Macpherson E (2013) New species and new occurrences of squat lobsters (Crustacea, Decapoda, Munididae, Eumunididae) from French Polynesia. In: Ahyong ST, Chan TY, Corbari L, Ng PKL (Eds) Tropical Deep-Sea Benthos 27. Mémoires du Muséum national d'Histoire naturelle, Paris 204, 287–309.
- Macpherson E, Rodríguez-Flores PC, Machordom A (2020) Squat lobsters of the families Munididae and Munidopsidae from Papua New Guinea. In: Ahyong ST, Chan TY, Corbari L (Eds) Tropical Deep-Sea Benthos 31, Papua New Guinea. Mémoires du Muséum national d'Histoire naturelle, Paris 213, 11–120.
- McCallum AW, Ahyong ST, Andreakis N (2021) New species of squat lobsters of the genus *Munida* from Australia. *Memoirs of the Museum of Victoria* 80: 113–152. <https://doi.org/10.24199/j.mmv.2021.80.06>
- Milne Edwards A (1880) Reports on the results of dredging under the supervision of Alexander Agassiz, in the Gulf of Mexico and in the Caribbean Sea, etc. VIII. Études préliminaires sur les Crustacés. *Bulletin of the Museum of Comparative Zoology at Harvard College* 8: 1–168. [pls 1, 2]
- Patel K, Padate V, Osawa M, Tiwari S, Vachhrajani K, Trivedi J (2022) An annotated checklist of anomuran species (Crustacea: Decapoda) of India. *Zootaxa* 5157(1): 1–100. <https://doi.org/10.11646/zootaxa.5157.1.1>
- Periasamy R, Kurian PJ, Ingole B (2023) Two new deep-water species of squat lobsters (Crustacea: Anomura: Galatheoidea) from the Central and Southwest Indian Ridge. *Zootaxa* 5231(2): 165–178. <https://doi.org/10.11646/zootaxa.5231.2.3>
- Richer de Forges B, Chan TY, Corbari L, Lemaitre R, Macpherson E, Ahyong ST, Ng PKL (2013) The MUSORSTOM-TDSB deep-sea benthos exploration program (1976–2012): An overview of crustacean discoveries and new perspectives on deep-sea zoology and biogeography. Ahyong ST, Chan TY., Corbari L, Ng PKL (Eds) Tropical Deep-Sea Benthos 27. Mémoires du Muséum national d'Histoire naturelle, Paris 204: 13–66.
- Rodríguez-Flores PC, Seid CA, Rouse GW, Giribet G (2023) Cosmopolitan abyssal lineages? A systematic study of East Pacific deep-sea squat lobsters (Decapoda: Galatheoidea: Munidopsidae). *Invertebrate Systematics* 37(1): 14–60. <https://doi.org/10.1071/IS22030>

- Samouelle G (1819) The entomologists' useful compendium; or an introduction to the knowledge of British Insects, comprising the best means of obtaining and preserving them, and a description of the apparatus generally used; together with the genera of Linné, and modern methods of arranging the Classes Crustacea, Myriapoda, spiders, mites and insects, from their affinities and structure, according to the views of Dr. Leach. Also an explanation of the terms used in entomology; a calendar of the times of appearance and usual situations of near 3,000 species of British Insects; with instructions for collecting and fitting up objects for the microscope. Thomas Boys, London, 496 pp. [412 pls] <https://doi.org/10.5962/bhl.title.120094>
- Swofford DL (2004) PAUP 4.0 for Macintosh: Phylogenetic Analysis Using Parsimony (Software and User's Book for Macintosh).
- Tiwari S, Padate VP, Cubelio SS, Osawa M (2022) Two new species of the genus *Galathea* Fabricius, 1793 (Crustacea: Decapoda: Anomura: Galatheididae) from the Andaman Sea, India. *Zootaxa* 5219(2): 175–184. <https://doi.org/10.11646/zootaxa.5219.2.6>
- Tiwari S, Padate VP, Cubelio SS (2023) Chirostyloid and galatheoid squat lobsters (Decapoda: Anomura) from Andaman and Nicobar Islands, India, with three new species. *Journal of Natural History* 57(9–12): 520–556. <https://doi.org/10.1080/00222933.2023.2192429>

Supplementary material 1

Dichotomous keys to species of the three genera - *Garymunida*, *Trapezionida* and *Typhlonida*

Authors: Enrique Macpherson, Paula C. Rodríguez-Flores, Annie Machordom

Data type: docx

Explanation note: Key to species of the genus *Garymunida* Macpherson & Baba, in Machordom et al. 2022. Key to species of the genus *Trapezionida* Macpherson & Baba, in Machordom et al. 2022. Key to species of the genus *Typhlonida* Macpherson & Baba, in Machordom et al. 2022.

Copyright notice: This dataset is made available under the Open Database License (<http://opendatacommons.org/licenses/odbl/1.0/>). The Open Database License (ODbL) is a license agreement intended to allow users to freely share, modify, and use this Dataset while maintaining this same freedom for others, provided that the original source and author(s) are credited.

Link: <https://doi.org/10.3897/zookeys.1188.114984.suppl1>

Reclassification of Cybistrinae Sharp, 1880 in the Neotropical Region (Coleoptera, Adephaga, Dytiscidae), with description of new taxa

Kelly B. Miller¹, Mariano C. Michat², Nelson Ferreira Jr³

¹ Department of Biology and Museum of Southwestern Biology, University of New Mexico, Albuquerque, NM 87131-0001, USA

² Instituto de Biodiversidad y Biología Experimental y Aplicada, CONICET-Universidad de Buenos Aires, Buenos Aires, Argentina

³ Laboratório de Entomologia, Departamento de Zoologia, Instituto de Biologia, Universidade Federal do Rio de Janeiro, Rio de Janeiro, RJ, Brasil

Corresponding author: Kelly B. Miller (kbmiller@unm.edu)

Abstract

The classification of the Neotropical Cybistrinae Sharp, 1880 (Coleoptera: Adephaga: Dytiscidae) is extensively revised based on a phylogenetic analysis of morphological features of the group. A new genus, *Nilssondytes* **gen. nov.** is described for a unique new species, *Nilssondytes diversus* **sp. nov.** from Venezuela. The New World genus, *Megadytes* Sharp, 1882, with several subgenera, was found to not be monophyletic. The type species of *Megadytes*, *Dytiscus latus* Fabricius, 1801 and the species *Cybister parvus* Trémouilles, 1984 were found to be monophyletic together, and phylogenetically more closely related to *Cybister* Curtis, 1827 than to other species assigned to *Megadytes* sensu stricto, which were found to also be monophyletic. The name *Megadytes* is here restricted to include only *Megadytes latus* and *Megadytes parvus*. These two species assigned to this newly restricted genus concept are reviewed and diagnosed. A new genus, *Metaxydytes* **gen. nov.**, is erected to include all the other species currently assigned to *Megadytes* sensu stricto. The current subgenus names assigned to *Megadytes*, *Bifurcitus* Brinck, 1945, *Paramegadytes* Trémouilles & Bachmann, 1980, and *Trifurcitus* Brinck, 1945, are elevated to genus rank since they are variously paraphyletic. The two species assigned to *Cybister* (*Neocybister*) Miller, Bergsten & Whiting, 2007, *Cybister* (*Neocybister*) *festae* Griffini, 1895, and *Cybister* (*Neocybister*) *puncticollis* (Brullé, 1837) re reviewed and diagnosed with the former redescribed and its type specimens considered for the first time since its description. Another evidently new species and possible new genus, *Megadytes* species, IR57 (Ribera et al. 2008), from Peru, is also characterized, but not formally treated because of lack of important data for the single, partial specimen. Diagnostic features are illustrated for the entire group.

Resumen

La clasificación de Cybistrinae Sharp, 1880 neotropicales (Coleoptera: Adephaga: Dytiscidae) se revisa ampliamente con base en un análisis filogenético de características morfológicas del grupo. Un nuevo género, *Nilssondytes* **gen. nov.** se describe para la única nueva especie *Nilssondytes diversus* **sp. nov.** de Venezuela. Se encontró que el género, *Megadytes* Sharp, 1882, del Nuevo Mundo y con varios subgéneros, no es monofilético. Se encontró que la especie tipo de *Megadytes*, *Dytiscus latus* Fabricius, 1801 y la especie *Cybister parvus* Trémouilles, 1984 forman un grupo monofilético y filogenéticamente más estrechamente relacionado con *Cybister* Curtis, 1827 que con otras



Academic editor: Michael Ivie

Received: 25 July 2023

Accepted: 3 November 2023

Published: 8 January 2024

ZooBank: <https://zoobank.org/997ADB92-AFA7-4979-82A2-B81C00EF3AEA>

Citation: Miller KB, Michat MC, Ferreira Jr N (2024) Reclassification of Cybistrinae Sharp, 1880 in the Neotropical Region (Coleoptera, Adephaga, Dytiscidae), with description of new taxa. ZooKeys 1188: 125–168. <https://doi.org/10.3897/zookeys.1188.110081>

Copyright: © Kelly B. Miller et al.

This is an open access article distributed under terms of the Creative Commons Attribution License ([Attribution 4.0 International – CC BY 4.0](https://creativecommons.org/licenses/by/4.0/)).

especies asignadas a *Megadytes* sensu stricto, que se encontró que también forman un grupo monofilético. El nombre *Megadytes* se restringe aquí para incluir solo a *Megadytes latus* y *Megadytes parvus*. Se revisan y diagnostican estas dos especies asignadas a este nuevo concepto restringido del género. Un nuevo nombre, *Metaxydytes* **gen. nov.**, se erige para incluir a todas las demás especies actualmente asignadas a *Megadytes* sensu stricto. Los nombres subgenéricos actuales asignados a *Megadytes*, *Bifurcitus* Brinck, 1945, *Paramegadytes* Trémouilles y Bachmann, 1980 y *Trifurcitus* Brinck, 1945, se elevan al rango de género, **nuevo estado**, ya que son parafiléticos de diversas formas. Se revisan y diagnostican las dos especies asignadas a *Cybister* (*Neocybister*) Miller, Bergsten y Whiting, 2007, *Cybister* (*Neocybister*) *festae* Griffini, 1895 y *Cybister* (*Neocybister*) *puncticollis*, redescubriendo la primera y considerando sus especímenes tipo por primera vez desde su descripción. Otra especie evidentemente nueva y posible nuevo género, *Megadytes*, IR57 (Ribera et al. 2008), de Perú, también se caracteriza, pero no se trata formalmente debido a la falta de datos importantes para el único espécimen parcial. Las características diagnósticas se ilustran para todo el grupo.

Key words: Diving beetle, phylogeny, South America, taxonomy, water beetle

Introduction

Cybistrinae Sharp, 1880 prior to this paper included seven genera, some with subgenera, from throughout much of the world, but especially in lower latitudes. The classification of the group was phylogenetically revised most recently by Miller et al. (2007). Until now, the New World has included two genera, *Megadytes* Sharp and *Cybister* Curtis. *Megadytes* has included 21 species in four subgenera (Miller and Bergsten 2016; Nilsson and Hájek 2023) mainly from the Neotropical region but also from the southeastern Nearctic. The New World *Cybister* until recently has included three species in *C. (Cybister)* from North and Central America (Miller 2013), two species of *C. (Neocybister)* Miller, Bergsten & Whiting from South America and one species, *Cybister parvus* Trémouilles, from South America, which has remained unplaced with respect to subgenus (Trémouilles and Bachmann 1980; Trémouilles 1984; Miller and Bergsten 2016; Nilsson and Hájek 2023). Remarkably, an overlooked new species of very large-bodied *Cybister* was recently added to *Cybister (Cybister)* from Mexico, *Cybister (Cybister) poblanus* Arce-Pérez, Novelo-Gutiérrez & Fery, 2021 supporting the idea that, among water beetles, the larger-bodied groups of species tend to be more overlooked taxonomically (Miller 2013).

Cybistrines in the Neotropical region occur especially in sunny lentic situations with extensive emergent vegetation, although they may be found in many aquatic habitats. Some species can be abundant at certain sites, but many are only rarely collected and are uncommon in collections. Neotropical cybistrines include the largest diving beetles in the world (Hendrich et al. 2019).

Upon the discovery of new taxa and reevaluation of certain described species with some unique character combinations, it became clear that the situation with Cybistrinae in South America is more complicated than the current classification reflects. The goal of this paper is to revise the Neotropical Cybistrinae genus groups and some of the species groups. The largest group of Neotropical species, historically placed in *Megadytes*, is not reviewed here and remains in need of revision with only analysis of the southern species having

been made by Trémouilles and Bachmann (1980). The previous paper revising the classification of Cybistrinae of the world by Miller et al. (2007) should be consulted for additional illustrations, details and discussion about the group, and the project presented here supplements that paper specifically.

Material and methods

Methods for specimen preparation and examination largely follow Miller et al. (2007) and Miller and Bergsten (2016).

Specimens were examined or are referenced from the following collections:

DZRJ	Coleção Entomológica Prof. José Alfredo Pinheiro Dutra, Departamento de Zoologia, Universidade Federal do Rio de Janeiro, Rio de Janeiro, Brazil (N. Ferreira Jr);
KBMC	Kelly B. Miller Collection, University of New Mexico, Albuquerque, NM, USA (K. B. Miller);
MIZA	Museo del Instituto de Zoología Agrícola Francisco Fernández Yépez, Universidad Central de Venezuela, Maracay, Venezuela (L. Joly);
MLP	Museo de La Plata, La Plata, Argentina (P. M. Dellapé);
MNHN	Museum National d'Histoire Naturelle, Paris, France (A. Mantilleri);
MRSN	Museo Regionale di Scienze Naturali di Torino (Museum of Turin) (F. Giachino);
MSBA	Museum of Southwestern Biology, Division of Arthropods, University of New Mexico, Albuquerque, NM, USA (K. B. Miller);
MZLU	Museum of Zoology, University of Lund, Lund, Sweden (J. Ekström);
MZSP	Museu de Zoologia, Universidade de São Paulo, São Paulo, Brazil (S. A. Casari);
SEMC	Snow Entomological Collection, University of Kansas, Lawrence, KS, USA (A. E. Z. Short);
USNM	United States National Museum, Department of Entomology, Washington, DC, USA (L. Chamorro).

Measurements are based on the range of available specimens and/or published values. Measurements were taken either using a standard steel ruler (longer measurements) or an ocular scale on a Zeiss Discovery V8 dissecting microscope at 50× magnification (shorter measurements). Emphasis was placed on measuring the largest and smallest specimens to describe the range of size in a species. Measurements include: (1) total length (TL); (2) greatest width across elytra (GW); (3) greatest pronotal width (PW); (4) greatest width of the head (HW); (5) distance between the eyes (EW); (6) narrowest width of metaventral wing (MV, Fig. 6); and (7) width across lateral portion of metacoxa (MC, Fig. 6). The ratios TL/GW, HW/EW, and MC/MV were also calculated to provide an indication of overall shape, eye size, and relative sizes of morphological features. Published measurements were included for some species if they are outside the range of observed specimens.

Male and female genitalia were dissected using methods similar to Miller (2001), Miller and Bergsten (2014, 2016), and Miller et al. (2007, 2009). Line drawings were created by sketching the structure in pencil using a drawing tube attached to a Zeiss Discovery V8 microscope then scanning and digitizing the sketch, inking, and editing using Adobe Illustrator.

Distribution data are based on examined specimens and published accounts for better-known species. Species historically placed in *Megadytes* have not been revised, and there may be confusion regarding their species identities in publications, so only type localities are referenced for these unrevised groups.

Fresh material suitable for DNA sequence acquisition and analysis was unavailable for many of the new and reinterpreted taxa treated here. Therefore, phylogenetic analysis is based on morphological characters historically used for these groups and a subset of taxa representative of the evident phylogenetic diversity and morphological combinations exhibited by Cybistrinae taxa (e.g., Miller et al. 2007). A few characters are newly analyzed. See below and the Appendix 1 for character discussions.

Numerous characters relevant to Cybistrinae phylogeny are reviewed by Miller et al. (2007) for adults and by Ferreira Jr (2000) and Michat (2006, 2017) for larva and those papers should be consulted for information regarding the morphology analyzed in this paper (see Appendix 1). However, some clarification is required for certain characters important for the classification and reclassification of taxa included here and for Cybistrinae in general. There are also some new characters included in this analysis. These are discussed below and in the Appendix 1. Character coding is included in Suppl. material 1.

One of these problematic characters is the nature of the metatarsal claws (Character (hereafter Char. 25). In certain Australian and Afrotropical Cybistrinae genera (*Austrodytes* Watts, *Onychohydrus* Schaum & White, *Regimbartina* Chatanay, *Spencerhydrus* Sharp & *Sternhydrus* Brinck), the metatarsal claws are unequal in length with the anterior claw shorter than the posterior. But in those species historically placed in *Megadytes* and *Cybister* the claws are characterized by a wider variety of configurations (Figs 15–18, 21–24, 26–29). Some genus groups (e.g., *M. (Bifurcitus)* Brinck and *M. (Trifurcitus)* Brinck) have males and females each with equal-length metatarsal claws. Others are sexually dimorphic with either males or both males and females with the posterior claw reduced and shorter than the anterior claw or absent altogether (see Table 1). Because of the complexity of this variation, the claw features are problematic for coding. A single character is analyzed for this with multiple additive states (Char. 25, Figs 15–29).

Another complicated set of characters includes the male genitalia. The medial margin of male abdominal sternite IX (Char. 31) is either linear (with each medial margin together parallel, Figs 53, 56, 57) or with the medial margins each distinctly emarginate (Figs 51, 52, 54, 55). Emarginate medial margins are characteristic of *Cybister* (Miller et al. 2007) and species here placed in a redefined *Megadytes* (see below). All other Cybistrinae have linear medial margins. Other male genitalic features include the shape of the apex of the male ventral sclerite (Char. 34, see Miller 2001 for discussion of this structure). In South American *Cybister* the apex is distinctly bifid (Figs 31, 34) and in certain species previously in *Megadytes* (see below) it is apicolaterally lobate and finely setose (Figs 42, 43, 45, 47). In other groups it is variable at the species level.

The female reproductive tract (RT) in Cybistrinae is distinctive and requires explanation. In cybistrines there is a single genital opening with an extremely long, heavily muscular vagina (Miller 2001). The spermatheca is elongate and tubular and attached to an enlarged sac-like region at the base of the common oviduct at the end of the vagina (Figs 58, 59, 61–66). There are a pair

Table 1. Numbers and relative lengths of metatarsal claws in males and females of genera of Cybistrinae.

	Male	Female
<i>Austrodytes</i>	2 claws, anterior < posterior	2 claws, anterior < posterior
<i>Spencerhydrus</i>	2 claws, anterior < posterior	2 claws, anterior < posterior
<i>Sternhydrus</i>	2 claws, anterior < posterior	2 claws, anterior < posterior
<i>Onychohydrus</i>	2 claws, anterior < posterior	2 claws, anterior < posterior
<i>Regimbartina</i>	2 claws, anterior < posterior	2 claws, anterior < posterior
<i>Nilssondytes</i>	2 claws, anterior > posterior	2 claws, anterior > posterior
<i>Bifurcitus</i>	2 claws, anterior = posterior	2 claws, anterior = posterior
<i>Trifurcitus</i>	2 claws, anterior = posterior	2 claws, anterior = posterior
<i>Metaxydytes</i>	2 claws, anterior = posterior	2 claws, anterior > posterior
<i>Paramegadytes</i>	2 claws, anterior = posterior	2 claws, anterior > posterior
<i>Megadytes</i>	2 claws, anterior > posterior	2 claws, anterior > posterior
<i>Cybister</i>	1 claw	Some species with 1 claw, some species with 2 claws, anterior > posterior, few species dimorphic, either 1 claw or 2 claws, if 2, anterior > posterior

of structures (possibly gland reservoirs, although sperm have been found in these regions Miller 2001) on the sides of this sac-like region (Char. 36, Figs 58, 59, 61–66). The basic structure is relatively conserved across Cybistrinae with mainly differences in relative lengths of various structures. The gonocoxae are together fused and knifelike for endophytic oviposition (Char. 39, Figs 58–66). The vagina terminates ventrally between the fused gonocoxae with two elongate sclerotized rami (Figs 58–66; Miller 2001). There is some species level variation in the relative sizes and shapes of these structures and whether the rami are smooth (Figs 58–63, 66) or corrugated (Char. 42; Figs 64, 65). The gonocoxosternite exhibits variation in relative size and shape as well (Figs 58–66). The medial margin is distinctly emarginate in Neotropical *Cybister* females (Figs 58, 59) and has a distinctive series of spinous setae in most species previously placed in *Megadytes* (*Megadytes*) and *Megadytes* (*Paramegadytes*) Trémouilles & Bachmann (Figs 60, 62, 63). Several characters are coded to capture this variation (see Appendix 1).

A particularly problematic set of characters is the subdivisions of antennomeres and maxillary and labial palpomeres in larvae (Chars 45–53). Species of Dytiscinae and Cybistrinae in particular, but other groups as well, have subdivided antennomeres and maxillary and labial palpomeres in various instars giving these structures the appearance of a greater number of segments. Technically they are not additional segments, but are instead subdivisions called articles by Michat et al. (2017). However, homologizing and coding these subdivisions is problematic. For one thing, it can be somewhat challenging determining which of the basic antennomeres and palpomeres are the ones that are subdivided. In addition, it seems likely that these subdivisions may be correlated both within a single larval instar, but also between larval instars and between antennae and palps. That is, it appears that specimens with at least one subdivided antennomere or palpomere have others subdivided, or if subdivided in the antennae, they are also subdivided in the palps making them potentially non-independent. In addition, in some cases, subdivided antennomeres appear to be retained

between instars, but not in others (they tend to accumulate between instars). For this analysis, these characters are coded separately, as they are by Michat et al. (2017). An effort was made to maximize information gained by coding these characters but also avoiding overweighting of them. Other phylogenetic characters are discussed more thoroughly in the Appendix 1 and cited references.

The matrix was developed and trees were examined and analyzed using WinClada (Nixon 2002). Characters were analyzed in a parsimony framework using NONA (Goloboff 1995) and the commands “h 10000,” “mu* 400,” and “h/100.” Trees accumulated during this process were further swapped using the command “max*.” Resultant trees were examined under various optimizations and consensus trees were calculated using WinClada (Nixon 2002).

Results

Cybistrinae Sharp, 1880

Cybistrini Sharp, 1880, as group of ‘*Dytisci complicati*’.

Type genus. *Cybister* Curtis, 1827.

Diagnosis and classification. These are large to very large Dytiscidae (length 13.0–47.0 mm). The subfamily is demonstrably monophyletic and is characterized by the following synapomorphies (among others): in adults (Miller et al. 2007; Miller and Bergsten 2014, 2016), (1) the apicoventral elytral setal patch small, composed of a field of short, coarse setae; (2) a large cluster of apically bifid setae present on the posteroapical surface of the metatibia (Fig. 1); (3) the anteroapical metatibial spur acuminate and broader than the posteroapical spur (Figs 1–3); and (4) the oblongum cell sub-triangular (Fig. 7); in larvae (Ferreira Jr 2000; Michat et al. 2017), (5) the anterior margin of the frontoclypeus trilobed (Figs 67–71), (6) antennomeres II and III each subdivided into three articles (in three instars), (7) the premaxillary lobes well developed and projected anteriorly, (8) maxillary palpomere III subdivided into three articles in instars II and III, (9) labial palpomeres I and II each subdivided into two articles in all three instars, (10) a dense row of short spiniform setae in the third basal of the ventral margin of the protarsus (although also characteristic of a number of other diving beetle taxa), (11) protarsus with a ventral row of spines (spinulae, not setae), and meso- and metatarsus each with a row of setae (other dytiscids have spinulae on all tarsi), (12) tergal sclerites reduced to small rectangular plates in abdominal segments I to VI, (13) a subapically located anus, and (14) strongly reduced urogomphi. Male cybistrines have the synapomorphy of protarsomeres I–III broadly laterally expanded into a “palette” that is broader than its medial dimension with a large field of adhesive setae ventrally. Most cybistrines are dark greenish to black, often with a lateral yellow margin along the pronotum and/or the elytron, depending on the species, genus or subgenus. These features with several additional synapomorphies in the female genitalia, larvae, other morphological systems, and DNA sequence data make this group among the most characteristic in Dytiscidae (Nilsson 1988; Ferreira Jr 2000; Miller 2000, 2001; Miller et al. 2007; Miller and Bergsten 2014, 2016; Michat et al. 2017).

Cybistrinae prior to this study included seven genera, several with single or few species and *Megadytes* and *Cybister*, each of which are species rich and

include multiple subgenera. The most recent phylogenetic classification of the group was developed by Miller et al. (2007).

The subfamily Cybistrinae has long been associated with Dytiscinae as a tribe of that subfamily and sister to the rest of the clade (e.g., Miller 2000, 2001), but was somewhat reluctantly elevated to subfamily rank by Miller and Bergsten (2014) after they found cybistrines not resolved together with dytiscines. The two clades share an exceptional number of adult and larval features in common, however, and new data and additional taxon sampling may change an understanding of their relationships. Morphological characters supporting monophyly of Dytiscinae and cybistrines are numerous, adults have: (1) the anterior margins of the eyes rounded, not emarginate; (2) the median lobe of the male aedeagus bilaterally symmetrical with a distinct, elongate ventral sclerite; (3) females with a single genital opening in the female reproductive tract for both reception of sperm and oviposition (secondarily within Adephaga); and (4) the female gonocoxae fused together along their dorsal margins, evidently plesiomorphically to facilitate endophytic oviposition although apomorphically this is lost (Miller and Bergsten 2014, 2016). Also, larvae have (among other less clear features): (1) abdominal segments VII–VIII with distinct lateral fringes of natatory setae (present also on abdominal segment VIII in instars II and III of Coptotominae), and (2) the larval antennomeres and maxillary and labial palpomeres subdivided into articles (Ferreira Jr 2000; Michat et al. 2017). Although generally regarded as characteristic of Dytiscinae + Cybistrinae, the subdivision of larval antennomeres and palpomeres in the included taxa is quite variable and likely involves multiple independent characters requiring further investigation to determine homologies within this general condition (see discussion above and character coding scheme below). Subdivision of antennae and palps also occurs (probably homoplasiously) in other diving beetle taxa in different ways.

Immature semaphoronts. Cybistrinae larvae are very characteristic within Dytiscidae (see diagnostic features above). They are often prominent and abundant large predators in systems where they occur. Knowledge of larvae in the group is increasing, but lags behind knowledge of adults, and even lags well behind knowledge of larvae of other diving beetle groups, despite their conspicuousness, although they have been investigated within the context of the phylogeny and taxonomy of Dytiscinae and Cybistrinae (Larson et al. 2000; Alarie et al. 2011; Michat et al. 2017). Table 2 details the state of descriptive knowledge of the morphology of the three instars of each genus group and a key is presented to the known taxa (see below). The pupa of *Megadytes* (*Paramegadytes*) *glaucus* Brullé was described by Crespo (1982). Eggs are unknown for Cybistrinae in general.

Distribution. Cybistrinae are found throughout the world, mainly at low latitudes. Most members of the group are tropical, although some occur north to southern Canada and northern Europe and south through temperate South America and Australia and throughout southern Africa.

Phylogeny. Parsimony analysis of the matrix resulted in seven equally parsimonious cladograms (length 102, CI = 68, RI = 93) one of which is shown in Fig. 75 with characters and states optimized on branches. Disagreement among trees is primarily within *Cybister*, but also in relative placement of *Nils-sondytes* and *Paramegadytes*. In some solutions, *Paramegadytes* is resolved as

Table 2. Descriptive knowledge of each larval instar for Cybistrinae. Known instars indicated with "X".

	Instar			Citations
	I	II	III	
<i>Austrodytes</i>				
<i>Bifurcitus</i>			X	Ferreira Jr (1993, 2000); Michat (2006)
<i>Cybister</i> (<i>Cybister</i>)	X	X	X	Fiori (1949); Watts (1964); Alarie et al. (2011)
<i>Cybister</i> (<i>Megadytoides</i>)				
<i>Cybister</i> (<i>Melanectes</i>)				
<i>Cybister</i> (<i>Neocybister</i>)				
<i>Megadytes</i>			X	Ferreira Jr et al. (2006)
<i>Metaxydytes</i>	X	X	X	Ferreira Jr (1995); Michat (2010)
<i>Nilssondytes</i>				
<i>Onychohydus</i>	X	X	X	Watts (1963, 1964); Alarie et al. (2011)
<i>Paramegadytes</i>	X	X	X	Crespo (1982); Michat (2006)
<i>Regimbartina</i>				
<i>Spencerhydus</i>	X	X	X	Michat et al. (2019)
<i>Sternhydus</i>	X	X	X	Watts (1964); Michat et al. (2015)
<i>Trifurcitus</i>			X	Ferreira Jr (1995); Michat (2006, 2010)

sister to a clade of species previously in *Megadytes* (in a new genus described below), and in other solutions is sister to the clade *Megadytes* + *Cybister*. Similarly, *Nilssondytes* is either resolved as sister to a large clade containing a new genus (previously in *Megadytes*), *Paramegadytes*, *Megadytes*, and *Cybister* or is sister to *Megadytes* + *Cybister*. This conflict resulted in a consensus cladogram (Fig. 76) with *Nilssondytes* and *Paramegadytes* in unresolved positions with respect to a new genus (previously in *Megadytes*) and *Megadytes* + *Cybister*.

Cybistrinae and Dytiscinae have historically been regarded as individually monophyletic and together monophyletic (with cybistrines as a tribe within Dytiscinae) based on a large number of adult and larval morphological characters (e.g., Miller 2001, and see above). The most extensive phylogenetic analysis of the family to date by Miller and Bergsten (2014), however, resulted in Cybistrinae and Dytiscinae not together monophyletic, with each of the groups individually monophyletic as historically constituted. In the analysis presented here which is admittedly more limited only to morphological features and fewer taxa, Cybistrinae and Dytiscinae are each monophyletic, and they are together monophyletic (Figs 75, 76).

Taxonomic implications of phylogenetic analyses. An analysis of Cybistrinae and reclassification was presented by Miller et al. (2007) (as Cybistrini in Dytiscinae). Based on that work, Cybistrinae include certain genera characterized by apomorphic features, but also genera characterized by plesiomorphies that do not include any Neotropical species. These are primarily Australian in distribution including *Spencerhydus* Sharp, 1882, *Austrodytes* Watts, 1978, *Onychohydus* Schaum & White, 1847, and *Sternhydus* Brinck, 1945, but also the one Afrotropical species in the genus *Regimbartina* Chatanay, 1911 (Miller et al. 2007). The remaining two genera, *Megadytes* Sharp, 1882 (as historically defined), and its several subgenera, and *Cybister* Curtis, 1827 (also with several

subgenera) were found to be together monophyletic based especially (unambiguously) on the presence of an oblique groove across the posterior surface of the metatrochanter (Fig. 8), as well as DNA sequence data, with strong support (Miller et al. 2007). These genera occur in the Neotropical region. *Megadytes* (as then defined) was found to be monophyletic as was *Cybister* (Miller et al. 2007). All South American species of Cybistrinae are evidently part of this clade since they have an oblique, ventral metatrochanteric groove (Miller et al. 2007, and see below).

The analysis presented here is somewhat limited as regards taxon sampling overall, but it expands the Cybistrinae taxa available with morphological data and results largely support previous analyses including; 1) monophyly of Cybistrinae, 2) monophyly of the Australian genera (*Regimbartina* not included here) 2) monophyly of *Cybister* (except *Cybister parvus*), and 3) monophyly of taxa previously included in *Megadytes* together with *Cybister* (Figs 75, 76; Miller et al. 2007; Miller and Bergsten 2014). However, the addition of newly discovered taxa and poorly known historical taxa with unique new combinations of morphological features resulted in some new phylogenetic relationships. Specifically, *Megadytes*, as historically constituted, is not monophyletic (Figs 75, 76). Previously recognized subgenera of *Megadytes* (several elevated to genus rank, see below) and some of those species historically in *Megadytes* (*Megadytes*) (here placed in a new genus, see below) are not monophyletic (Figs 75, 76). An undescribed species from northern South America is ambiguously resolved near these two groups based on a unique combination of features requiring a new genus (Figs 75, 76, see below). In addition, two species (previously *Megadytes latus* Fabricius and *Cybister parvus*) with an intermediate character combination between *Megadytes* and *Cybister* are resolved in a monophyletic group between these other two groups requiring generic reclassification, as well (see below).

Reclassification of Neotropical Cybistrinae

***Bifurcitus* Brinck, 1945, stat. nov.**

Figs 1, 2, 64, 67

Bifurcitus Brinck, 1945: 8.

Type species. *Cybister giganteus* Laporte, 1835: 99 by original designation (= *Dytiscus lherminieri* Guérin-Méneville, 1829).

Diagnosis. Within Cybistrinae *Bifurcitus* have (1) the lateral margins of the pronotum and elytra margined with yellow, (2) males and females each with two equal-length metatarsal claws, and (3) the posterior metatibial spur bifid (Figs 1, 2). These are the largest of all diving beetles with adult specimens 36–47 mm in total length (Hendrich et al. 2019). Third instar larvae have (1) the median lobe of the frontoclypeus truncate apically with a tuft of setae (Fig. 67), (2) the median and lateral lobes of the frontoclypeus separated by a wide emargination (Fig. 67), (3) the lateral lobes of the frontoclypeus apically simple (Fig. 67), (4) the lateral lobes of the frontoclypeus obtusely angulate (Fig. 67), and (5) the cephalic capsule relatively short (head length / head width < 1.20).

Phylogenetic relationships. *Bifurcitus* is sister group to the similar *Trifurcitus* (Figs 75, 76; Miller et al. 2007). Both have males and females with equal-length metatarsal claws and the anterior metatibial spur either bifid or trifid (although these two conditions may not be homologous) (Figs 1–3).

Discussion. Although previous evidence suggested that the several subgenera of “*Megadytes*” are monophyletic, monophyly of this group is not supported here based in part on the discovery of undescribed cybistrine species with unique combinations of character states (Figs 75, 76). Given the situation, it seems appropriate to recognize these subgenera at the genus rank including *Bifurcitus*.

There are three currently valid species in *Bifurcitus* which were differentiated and characterized recently by Hendrich et al. (2019).

***Cybister* Curtis, 1827**

Figs 5, 7, 9, 10, 15–18, 30–35, 51, 52, 58, 59, 66, 72

Type species. *Dytiscus lateralis* Fabricius, 1798.

Diagnosis. Within Cybistrinae *Cybister* is characterized by the following: (1) a series of setae present along the posteroventral apical margin of the mesotarsomeres of males and pro- and mesotarsomeres of females (Fig. 5); (2) males with a single metatarsal claw, females with one or two, and if two, then the posterior claw small (some species with females dimorphic, some with a small posterior claw, others with only a single claw) (Figs 15–18); and (3) the medial margin of the lobes of the male abdominal sternite IX emarginate (Figs 51, 52). Larvae of *Cybister* (*Neocybister*) are unknown.

Distribution. *Cybister* are found in all major biogeographic regions but are most diverse in the Afrotropical and Oriental regions, mainly in low latitudes. The group is not diverse in the Neotropical region where it is largely replaced in numbers of species and individuals by species previously in *Megadytes* (*Megadytes*) (most of these in a newly described genus, see below).

Phylogenetic relationships of Neotropical *Cybister*. *Cybister* is the sister group to *Megadytes* as newly constituted (Figs 54, 76, see below). The Neotropical species of *Cybister* are in the subgenus *Cybister* (*Neocybister*) Miller, Bergsten & Whiting, 2007, which is restricted to the New World (Miller et al. 2007). This subgenus was resolved as sister group to all other *Cybister* in the analysis by Miller et al. (2007). It is resolved nested within *Cybister* here based on morphological data (Figs 75, 76), although previously examined molecular data (Miller et al. 2007) are not analyzed here. More investigation is needed. The two South American species are different from other *Cybister* in having (1) females always with a second, rudimentary posterior claw (Figs 15–18), (2) the medial margin of the gonocoxa distinctly emarginate (Figs 58, 59), and (3) the apex of the ventral sclerite of the male median lobe distinctly bifid (Figs 31, 34).

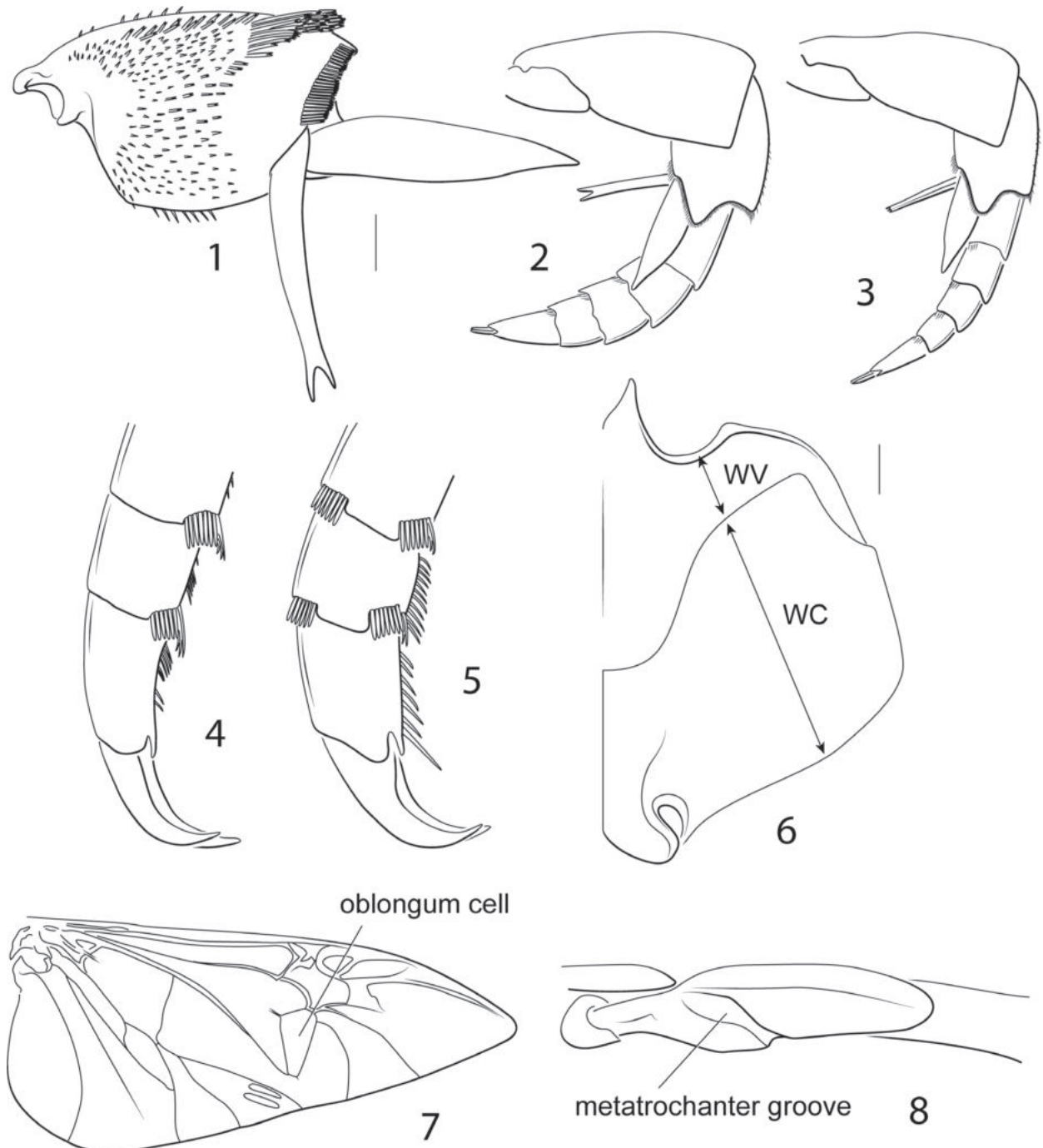
Key to *Cybister* species of the Neotropical region

South of Mexico and Caribbean islands including Cuba and the Bahamas.

- 1 Size larger (TL = 26.6–27.6 mm); male median lobe in ventral aspect apically broadly expanded, apex very broad, subtruncate with medial, small point

or projection, median lobe broadly expanded medially and apically making lateral margins distinctly sinuate (Fig. 34) ***Cybister puncticollis* (Brullé)**

- Size smaller (TL = 20.3–21.7 mm); male median lobe in ventral aspect apically very slightly expanded, apex truncate without medial small point or projection, median lobe slightly expanded laterally in basal half, but margins not characteristically sinuate (Fig. 31) ***Cybister festae* (Griffini)**



Figures 1–8. Cybistrinae morphological features **1** *Bifurcitus lherminieri*, right metatibia, posterior surface **2** *Bifurcitus lherminieri*, left metaleg, anterior surface **3** *Trifurcitus robustus*, left metaleg, anterior surface **4** *Metaxydytes fraternus*, left mesotarsomeres III–V, posterior surfaces **5** *Cybister tripunctatus*, left mesotarsomeres III–V, posterior surfaces **6** *Megadytes latus*, left half of metaventrite and left metacoxa (WV = metaventrite wing width, WC = metacoxal width) **7** *Cybister tripunctatus*, right metathoracic wing **8** *Trifurcitus robustus*, right metatrochanter, ventral surface. Scale bars: 1.0 mm.

***Cybister (Neocybister) festae* Griffini, 1895**

Figs 9, 15, 16, 30–32, 51, 58, 72

Cybister festae Griffini, 1895: 1.

Cybister (Meganectes) festae: Brinck 1945: 18.

Cybister (Neocybister) festae: Miller et al. 2007: 54; Nilsson and Hájek 2023: 84.

Type locality. Panama, Darién, Matusagrati Lake (Laguna della Pita).

Type specimens. The syntype specimens are in Museo Regionale di Scienze Naturali di Torino (Museum of Turin, MRSN) (Fig. 72). Images of the specimens were examined (Fig. 72, courtesy of F. Giachino, MRSN). Two specimens are included in the type series, a male and a female (Fig. 72; Griffini 1895). Neither are dissected. The male specimen is here designated as the lectotype to stabilize the nomenclature of the species (see Material examined below; Fig. 72). Although the male is not dissected and the genitalia were not examined, the specimens agree well with the others examined for this study in size, shape, coloration, distribution, and other features.

Diagnosis. This species differs from the other Neotropical *Cybister* species, *C. puncticollis*, in smaller size (TL = 20.3–21.7 mm in *C. festae* vs. 26.6–27.6 mm in *C. puncticollis*) and the shape of the male genitalia. The male median lobe in *C. puncticollis* is apically broadly expanded (Fig. 34) whereas in *C. festae* the median lobe is apically less strongly expanded with lateral margins that are somewhat more parallel-sided (Fig. 31). The specimens examined match the description of *C. festae*, but it is possible that the species illustrated and described here is not the same as *C. festae* since the lectotype (in MRSN) was not dissected.

Description. Measurements. TL = 20.3–21.7 mm, GW = 11.7–13. mm, PW = 8.8–9.2 mm, HW = 5.1–5.5 mm, EW = 2.9–3.0 mm, TL/GW = 1.7–1.8, HW/EW = 1.7–1.8, WC/WV = 4.3–4.4. Body shape oval, widest slightly posterior of middle; lateral margins broadly curved, continuously curved between pronotum and elytron. Depressed and somewhat flattened in lateral aspect.

Coloration. Head dark green-black, clypeus and labrum pale yellow. Pronotum dark green-black, with broad lateral yellow marginal band, medial margin of band distinctly delimited, band separated from posterolateral margin by narrow green strip (Fig. 9). Elytron dark green-black with broad lateral yellow marginal band, medial margin of band distinctly delimited, lateral margin of band slightly remote from lateral elytral margin for medial portion of length, extending laterally to margin of elytron anteriorly and posteriorly, apex of yellow band diffusing into coloration of elytron (Fig. 9). Ventral surfaces mostly black except antennae and palpi orange, pro- and mesothoracic legs with basal segments (trochanter and femur) pale orange and apical segments (tibia and tarsus) testaceous, metathoracic legs with mix of testaceous and orange, propleuron and elytral epipleuron pale orange to testaceous, and with small orange maculae laterally on abdominal ventrites IV–VI.

Sculpture and structure. Head broad, anteriorly produced, eyes prominent; dorsal surface evenly covered with exceptionally fine micropunctures but appearing smooth and shiny. Pronotum with lateral margins evenly and shallowly curved; surface of pronotum similar to surface of head in micropunctuation; pronotum dorsally evenly curved. Elytron with margins very broadly curved, more

strongly curved posteriorly; surface similar to surface of head in micropunctuation and surface appearance. Prosternal process anteriorly rounded, surface nearly flat throughout and moderately broad, apex broadly elongate and sharply pointed. Metaventral wing narrow ($WC/WV = 4.3\text{--}4.4$); surface smooth, with extremely fine microsculpture, shiny. Lateral portion of metacoxa large, broad, surface smooth and shiny, with extremely fine microsculpture; metacoxal lines short and strongly curved, well-incised, extending anteriorly less than half distance across metacoxa. Abdominal ventrites smooth, unsculptured.

Male genitalia. Male median lobe in lateral aspect slender throughout length, apically slender, straight, and apically pointed, dorsal sclerite slender, evenly curved basally, apically straight, and slender, (Fig. 30); in ventral aspect broad basally, laterally somewhat constricted medially, apically broadly truncate (Fig. 31). Lateral lobe slender broad basally, apically strongly narrowed and slender, with long dorsal series of setae (Fig. 32).

Female genitalia (Fig. 58). Gonocoxosternite moderately broad, basal portion broadly ovate; gonocoxae together knifelike, evenly convergent to apex; rami smooth, short; vagina elongate; spermatheca elongate, $\sim 2/3$ length of vagina.

Sexual dimorphism. Males have a broad protarsal palette with ventral adhesive setae with apical structures in the form of elongate flattened spatulate surfaces; males also have mesotarsomeres with posteroventral fields of setae which are absent in females. Females lack natatory setae along the ventral margins of the metatarsomeres, but these are present in males. Males have a single metatarsal claw (the anterior, Fig. 15), whereas females have a second posterior claw that is $\sim 2/3$ length of the anterior, curved, and apically sharp (Fig. 16).

Variation. Two specimens were examined, a male and a female. The female has the extent and intensity of greenish-rufous coloration somewhat greater than the male and is larger, but otherwise the two specimens are similar.

Distribution. This species is known from the type locality in the Darién in Panama (Griffini 1895; Brinck 1945) and Venezuela, Apure State (new country record).

Material examined. The lectotype (here designated) in MRSN is labeled, "Laguna d. Pita (Darien) [handwritten]/ *Cybister festae* ♂ Griffini tipo./ *Cybister festae* (tipo) Griffini Darien [green label, black line border, horizontal black lines]." Other than the type specimens (not directly examined), two specimens were examined from Apure State, between La Ye and Bruzual, Venezuela from a roadside lake (7.6443333 -69.3000667) (SEMC, accession numbers: SEMC0846768, SEMC0846766).

***Cybister (Neocybister) puncticollis* (Brullé, 1837)**

Figs 10, 17, 18, 33–35, 52, 59

Dyticus puncticollis Brullé, 1837: 46.

Cybister puncticollis: Aubé 1838: 52.

Trogus puncticollis: Gemminger and Harold 1868: 460.

Megadytes puncticollis: Sharp 1882: 709; van den Branden 1885: 29; Regimbart 1889: 267; 1904: 225; Chatanay 1910: 434; Bruch 1915: 479; Zimmermann 1919: 235; 1920: 256; Wilke 1921: 24; Bruch 1927: 543; Blackwelder 1944: 80; Brinck 1945: 8; Mouchamps 1957: 283; Trémouilles and Bachmann 1980: 105.

Cybister (Meganectes) kemneri Brinck, 1945: 18; Trémouilles and Bachmann 1980: 105.

Cybister (Meganectes) puncticollis: Trémouilles and Bachmann 1980: 105.

Cybister (Neocybister) puncticollis: Miller et al. 2007: 54; Nilsson and Hájek 2023: 84.

Type locality. *Cybister puncticollis*: Bolivia, San Miguel. *Cybister kemneri*: Brazil, La Plata, Amazonas, Rio Autaz.

Type specimen. *Cybister puncticollis*, in MNHN (not examined). *Cybister kemneri*, in MZLU (not examined).

Diagnosis. This species is larger (Fig. 10) than the other Neotropical species in the genus, *C. festae* (Fig. 9) and the male genitalia are distinctly different (Figs 33–35). See above under that species for details about this and additional diagnostic differences between these two species of *Cybister*.

Description. Measurements. TL = 26.6–27.6 mm, GW = 15.0–15.9 mm, PW = 10.8–11.6 mm, HW = 6.5–6.8 mm, EW = 3.7–3.8 mm, TL/GW = 1.7–1.8, HW/EW = 1.7–1.8, WC/WV = 2.9–3.2. Body shape oval, widest slightly posterad of middle; lateral margins broadly curved, continuously curved between pronotum and elytron. Depressed and somewhat flattened in lateral aspect.

Coloration. Head dark green, clypeus and labrum pale yellow. Pronotum dark green, with broad lateral yellow marginal band (Fig. 10), medial margin of band distinctly delimited, band separated from posterolateral margin by narrow green strip (Fig. 10). Elytron dark green with broad lateral yellow marginal band, medial margin of band distinctly delimited, lateral margin of band slightly remote from lateral elytral margin for medial portion of length, extending laterally to margin of elytron anteriorly and posteriorly, apex of yellow band diffusing into coloration of elytron, less distinct (Fig. 10). Ventral surfaces mostly black except antennae and palpi orange, pro- and mesothoracic legs mostly orange, tarsi dark orange, metathoracic legs testaceous, anterodorsal surface of tibia orange, propleuron and elytral epipleuron pale orange to testaceous, and with small orange maculae laterally on abdominal ventrites IV–VI.

Sculpture and structure. Head broad, anteriorly produced, eyes prominent; dorsal surface evenly covered with exceptionally fine micropunctures but smooth and shiny. Pronotum with lateral margins evenly and shallowly curved; surface of pronotum similar to surface of head in micropunctuation; pronotum dorsally evenly curved. Elytron with margins very broadly curved, more strongly curved posteriorly; surface similar to surface of head in micropunctuation and surface appearance. Prosternal process anteriorly distinctly emarginate medially, remaining surface nearly flat throughout and moderately broad, apex broadly elongate and sharply pointed. Metaventral wing narrow (WC/WV = 2.9–3.2); surface smooth, with extremely fine microsculpture, shiny. Lateral portion of metacoxa large, broad, surface smooth and shiny, with extremely fine microsculpture; metacoxal lines short and curved, extending anteriorly less than half distance across metacoxa. Abdominal ventrites smooth, relatively unsculptured.

Male genitalia. Male median lobe in lateral aspect moderately slender throughout, evenly curved, apically abruptly expanded with a narrowly rounded apex, ventral sclerite slender and evenly curved basally, apically straight and apically pointed (Fig. 33); in dorsal aspect median lobe moderately broad

basally, lateral margins broadly sinuate, apex broadly expanded, with apex broadly sub-truncate, medially broadly pointed (Fig. 34). Lateral lobe moderately broad throughout length, evenly curved, apex narrowly rounded, with long series of setae along dorsal margin (Fig. 35).

Female genitalia. Vagina extremely elongate, slender; with enlarged area at base of common oviduct and spermatheca, with enlarged lateral sacs on this enlarged area; spermatheca extremely slender and elongate (Fig. 59); gonocoxae together slender and apically pointed (Fig. 59); gonocoxosternite broad, anterolateral lobe broad, medial margin distinctly, narrowly emarginate, basomedially with field of setae (Fig. 59).

Sexual dimorphism. Males have a broad protarsal palette with ventral adhesive setae with apical structures in the form of elongate flattened spatulate surfaces; males also have mesotarsomeres with posteroventral fields of setae which are absent in females. Females lack natatory setae along the ventral margins of the metatarsomeres, but these are present in males. Males have a single metatarsal claw (the anterior claw, Fig. 17), whereas females have a second, posterior claw that is $\sim 1/2$ the length of the anterior, is abruptly curved apically and sharply pointed (Fig. 18).

Variation. Specimens vary somewhat in size and coloration, with some specimens more greenish and others darker, less greenish.

Distribution. This species is known from Argentina, Bolivia, Brazil, French Guyana, and Peru. There is also a previously unpublished record from Paraguay.

Material examined. Specimens were examined from Argentina, Bolivia, Peru, and Paraguay.

***Megadytes* Sharp, 1882**

Figs 6, 12, 13, 21–24, 39–47, 54, 55, 60, 68

Megadytes Sharp, 1882: 701.

Type species. *Megadytes latus* Fabricius, 1801: 260.

Classification. The concept of the genus presented here differs significantly from previous ones (e.g., Trémouilles and Bachmann 1980; Miller et al. 2007; Miller and Bergsten 2016). The type species of *Megadytes* is *M. latus* Fabricius, 1801, a species which differs in important phylogenetic characters from most other species historically assigned to *Megadytes*. Here the species *M. latus* is placed together with *Megadytes parvus* comb. nov. in *Megadytes*, whereas the other species historically in *Megadytes* are placed in other genera based on the phylogenetic hypothesis developed here (Figs 75, 76). Given the character distribution in this group and the diagnosis of the type species, *M. latus*, this new classification is unavoidably disruptive of the historical concept of the genus (which included all species here placed in the genera *Bifurcitus* stat. nov., *Paramegadytes* new status, and *Trifurcitus* new status, see below) and a new genus described below. The unusual characteristics of *M. parvus* were recognized by Trémouilles (1984) who placed the species in *Cybister* (*Meganectes*) Brinck, 1945.

Diagnosis. Within Cybistrinae *Megadytes* are similar to *Cybister* (Figs 51, 52) in having the medial margin of the lobes of the male abdominal sternum IX

emarginate (Figs 54, 55), but differ from *Cybister* (Fig. 5) in lacking a series of setae along the posterodorsal apical angle of the mesotarsomeres of males and pro- and mesotarsomeres of females (as in Fig. 4). This places them in an intermediate phylogenetic position between other Cybistrinae and *Cybister* (Figs 75, 76, see below). Males and females both have two metatarsal claws with the posterior claw strongly reduced (Figs 21–24). Third instar larvae (based on *M. latus*) have (1) the median lobe of the frontoclypeus truncate apically with a tuft of setae, (2) the median and lateral lobes of the frontoclypeus separated by a wide emargination (Fig. 68), (3) the lateral lobes of the frontoclypeus apically simple (Fig. 68), (4) the lateral lobes of the frontoclypeus acutely angulate (Fig. 68), and (5) the cephalic capsule relatively long (head length / head width > 1.25).

Distribution. *Megadytes* are found in the Neotropical region. *Megadytes parvus* is known only from the type locality in Bahia State, Brazil, and *M. latus* is known from Brazil, Uruguay, Argentina, French Guiana, and Venezuela.

Phylogenetic relationships. *Megadytes* is sister to *Cybister* (Figs 75, 76) based on both genera with distinctly emarginate medial margins of abdominal sternite IX in males (Figs 51–55). However, *Megadytes* lack a series of setae at the apicodorsal angle of the posterior surface of mesotarsomeres I–IV (and of protarsomeres I–IV of females). This feature is remarkably consistent across the numerous *Cybister* species in the world (Miller et al. 2007).

Key to *Megadytes* species

- 1 Size larger (TL = 19.5–23.2 mm), and relatively broader (TL/GW = 1.7–1.8) (Fig. 13); male median lobe in lateral aspect moderately slender, evenly curved throughout along dorsal and ventral margins (Fig. 44) ***Megadytes latus* (Fabricius)**
- Size smaller (TL = 13.0–14.6 mm), and relatively narrower (TL/GW = 1.9–2.1) (Fig. 12); male median lobe in lateral aspect broad, subapically with ventral margin (ventral sclerite) abruptly and strongly curved dorsad (Fig. 39) ***Megadytes parvus* (Trémouilles)**

***Megadytes latus* (Fabricius, 1801)**

Figs 6, 13, 21, 22, 44–47, 54, 60, 68

Dytiscus latus Fabricius, 1801: 260.

Trogus latus: Gemminger and Harold 1868:459.

Megadytes latus: Sharp 1882: 706; van den Branden 1885: 110; Chatanay 1910: 435; Bruch 1915: 478; Zimmermann 1919: 235; 1920: 256; Bruch 1927: 543; Guignot 1946: 118; Mouchamps 1957: 282; Trémouilles and Bachmann 1980: 108.

Cybister (*Megadytes*) *latus*: Wilke 1921: 248.

Megadytes lata: Blackwelder 1944: 80.

Megadytes (*Megadytes*) *latus*: Brinck 1945: 7.

Type locality. South America.

Type specimens. Syntypes in Zoological Museum der Universität Kiel, Germany, not examined.

Diagnosis. This species differs from *M. parvus* in its larger size (TL = 19.5–23.2 mm in *M. latus*, Fig. 13 vs. TL = 13.0–14.6 mm in *M. parvus*, Fig. 12), broader shape (TL/GW = 1.7–1.8 in *M. latus*, Fig. 13, vs. TL/GW = 1.9–2.1 in *M. parvus*, Fig. 12) as well as features of the male genitalia. In *M. latus* the male median lobe is relatively simple and evenly curved in lateral aspect with the apex narrowly rounded to somewhat pointed (Fig. 44). In *M. parvus* the median lobe is very broad in lateral aspect with the dorsal sclerite strongly expanded ventrally and curved with the apex strongly recurved (Fig. 39). The lateral lobe in *M. latus* is very slender apically (Fig. 44), but in *M. parvus* it is relatively broad throughout (Fig. 41).

Description. Measurements. TL = 19.5–23.2 mm, GW = 11.4–13.4 mm, PW = 8.7–10.3 mm, HW = 5.3–6.2 mm, EW = 3.1–4.0 mm, TL/GW = 1.7–1.8, HW/EW = 1.6–1.7, WC/WV = 2.7–3.4. Body shape large and broadly oval, widest slightly posteriad of middle; lateral margins broadly curved, continuously curved between pronotum and elytron. Depressed and somewhat flattened in lateral aspect.

Coloration. Head dark green to dark brown, anteriorly somewhat green-rufous, clypeus pale rufous, labrum pale yellow. Pronotum dark green to dark brown, laterally broadly dark green-rufous. Elytron dark green with broad lateral green-rufous margins in some specimens. Ventral surfaces black, legs dark rufous.

Sculpture and structure. Head broad, anteriorly produced, eyes prominent; dorsal surface evenly covered with exceptionally fine microsculpture and dispersed micropunctures. Pronotum with lateral margins evenly and shallowly curved; surface of pronotum similar to surface of head in microsculpture and micropunctuation; pronotum somewhat swollen anteriorly. Elytron with margins very broadly curved, more strongly curved posteriorly; surface similar to surface of head in microsculpture, but with extensive, very fine micropunctuation over entire surface. Prosternal process anteriorly rounded, surface flat and moderately broad, apex broadly elongate and sharply pointed. Metaventral wing moderately broad, ~ 1/3 width of lateral portion of metacoxa; surface smooth, without sculpturing. Lateral portion of metacoxa large, broad, surface smooth, without sculpturing; metacoxal lines short and fine, extending anteriorly less than half distance across metacoxa. Abdominal ventrites smooth, unsculptured.

Male genitalia. Male median lobe in lateral aspect moderately slender throughout, evenly curved, apically narrowed, apex narrowly pointed (Fig. 44); in dorsal aspect moderately narrow, apically narrowed to narrowly rounded apex, ventral sclerite slender throughout length, apically abruptly expanded, apex rounded (Fig. 45). Lateral lobe slender throughout length, apically very slender, with long series of setae along dorsal margin (Fig. 46).

Female genitalia. The only female examined has the internal genitalia missing. Externally, the female gonocoxosternite is broad with the medial margin linear; the gonocoxae are together fused and knifelike, broad anteriorly, abruptly constricted subapically and apically linear to narrowly rounded apex (Fig. 60); rami short; other internal structures (vagina, spermatheca, etc.) not observed.

Sexual dimorphism. Males have a broad protarsal palette with ventral adhesive setae with apical structures in the form of elongate flattened structures; males also have mesotarsomeres with posteroventral fields of setae. Females lack natatory setae along the ventral margins of the metatarsomeres, but these are present in males. Males and females each have two metatarsal claws with

the posterior shorter, but females have the posterior claw slightly longer than in the male (Figs 21, 22).

Variation. Specimens exhibit variation in size (TL = 19.5–23.2 mm) but are consistent in shape (TL/GW = 1.7–1.8), and male genitalic shape and other features are relatively consistent across the range of the species. There is some variation in coloration with most specimens dark green-black, but a single specimen from the Gran Sabana, Venezuela (MIZA) is dorsally strikingly green. This specimen is also smaller than most (TL = 19.5 mm) and may represent a distinctive regional population or separate species.

Distribution. This species is known from Argentina, Brazil, French Guiana, Uruguay (Sharp 1882; Blackwelder 1944; Mouchamps 1957; Trémouilles and Bachmann 1980; Trémouilles 1989b), and Venezuela (MIZA, new country record).

Material examined. Few specimens of this species exist in collections. Two specimens from Argentina, one from Bolivia (new country record), one from Brazil (KBMC), and a specimen from the Gran Sabana, Venezuela (MIZA) were examined for this study.

***Megadytes parvus* (Trémouilles, 1984), comb. nov.**

Figs 12, 23, 24, 39–43, 55

Cybister parvus Trémouilles, 1984: 187.

Type locality. Brazil, Bahia State, Santa Rita.

Type specimens. Holotype and nine paratypes in Museu de Zoologia, Universidade de São Paulo, Brazil and two paratypes, one male and one female, in Museo de La Plata, La Plata, Argentina.

Diagnosis. This species differs from the other species in the genus, *M. latus*, in smaller size (TL = 13.0–14.6 mm), narrower shape (TL/GW = 1.9–2.1) (Fig. 12) and features of the male genitalia (Figs 39–43). See above under *M. latus* for details about these differences between the two species.

Description. Measurements. TL = 13.0–14.6 mm, GW = 6.2–7.7 mm, PW = 5.4–5.9 mm, HW = 3.3–3.4 mm, EW = 2.0–2.1 mm, TL/GW = 1.9–2.1, HW/EW = 1.6–1.7, WC/WV = 4.1–4.8. Body shape elongate oval, widest slightly posterior of middle; lateral margins broadly curved, continuously curved between pronotum and elytron (Fig. 12). Depressed and somewhat flattened in lateral aspect.

Coloration. Head dark green to green-rufous throughout. Pronotum dark green with broad lateral green-rufous margins. Elytron dark green with broad lateral green-rufous margins. Ventral surfaces dark rufous.

Sculpture and structure. Head broad, anteriorly produced, eyes prominent; dorsal surface evenly covered with extremely fine microsculpture and micropunctures. Pronotum with lateral margins evenly and broadly curved; surface similar to surface of head in microsculpture and micropunctuation; pronotum somewhat swollen anteriorly. Elytron with margins very broadly curved; surface similar to surface of head in microsculpture, but with extensive, very fine micropunctuation. Prosternal process anteriorly rounded, surface flat and broad, apex elongate and sharply pointed. Metaventral wing moderately broad, ~ 1/3 width of lateral portion of metacoxa; surface smooth, without sculpturing. Lateral portion of metacoxa large, broad, surface smooth, without sculpturing; metacoxal

lines short, extending anteriorly less than half distance across metacoxa. Abdominal ventrites smooth, unsculptured.

Male genitalia. Male median lobe in lateral aspect broad throughout, subapically somewhat expanded, apically narrowed, apex with multiple small processes (Fig. 39); in dorsal aspect moderately narrow, evenly narrowed apically, apex narrowly lobed, ventral sclerite apically broadly lobed, extending to near apex (Fig. 40). Lateral lobe broad throughout length, evenly curved, apex rounded, with long series of setae along ventral margin (Fig. 41).

Female genitalia. The single female specimen available for examination lacks female genitalia which apparently have been dissected and lost.

Sexual dimorphism. Males have a broad protarsal palette with ventral adhesive setae with apical structures in the form of elongate flattened structures; males also have mesotarsomeres with posteroventral fields of setae. Females lack natory setae along the ventral margins of the metatarsomeres, but these are present in males. Males and females each have unequal length metatarsal claws with the posterior shorter, but in males the posterior claw is relatively longer than in females, and distinctly, but only somewhat, shorter than the anterior (~ 4/5 of length).

Variation. Two paratype specimens were examined, a male and a female. The female has the extent and intensity of greenish-rufous coloration somewhat greater than the male, but otherwise the two specimens are similar.

Distribution. This species is known only from Santa Rita, Bahia State, Brazil. Indication by Trémouilles (1984) of the locality “Santa Rita” to Goyas State, Brazil is erroneous. In Brazil, there are several locations called Santa Rita, but in all labels of the type materials indicate “Santa Rita BA” in clear reference to Bahia State, Brazil (BA = abbreviation of Bahia) and not to Goiás State (= GO). “Goyaz” is an old spelling of Goiás State.

Habitat. Nothing is known of the habitat of this species.

Material examined. Twelve specimens in MZSP – holotype male and nine paratypes, six males and three females, each specimen labeled, “Santa Rita BA – Brasil IV.1958 E. Dente col. [label with black line border]/ *Cybister* (*Cybister*) *parvus* E. Tremouilles [handwritten] 1990 det. E. R. Tremouilles [label with black line border]/ *Cybister* (*Meganectes*) *parvus*. 1984 Tremouilles [red label, black line border, handwritten]”. Holotype, one paratype female and the other paratypes respectively labeled, “Holotypus [red label, black line border], Holotypus [red label, black line border], Paratypes [label with black line border]”; two paratypes in MLP – one male and one female, each specimen labeled, “Santa Rita BA – Brasil IV.1958 E. Dente col. [label with black line border]/ *Cybister* (*Cybister*) *parvus* E. Tremouilles [handwritten] 1990 det. E. R. Tremouilles [label with black line border]/ PARATYPUS/ MUSEO DE LA PLATA PARATIPO *Cybister* (*Meganectes*) *parvus*. 1984 Tremouilles [red label, black line border, handwritten].”

***Metaxydytes* gen. nov.**

<https://zoobank.org/99CCA782-DD1A-4DE2-8D5D-F71909BE0E8F>

Figs 4, 28, 29, 57, 62, 69

Megadytes sensu auctorum.

Type species. *Megadytes fraternus* Sharp, 1882: 708, by current designation.

Diagnosis. These species have males with equal-length metatarsal claws and females with two claws of unequal length with the posterior claw distinctly reduced (Figs 28, 29). The medial margins of male sternite IX are linear, not emarginate (Fig. 57). This group and *Paramegadytes* are similar in having females with the medial margins of the gonocoxosternite with a series of spinous setae (Fig. 62). From *Paramegadytes* these species differ in being smaller (≤ 24 mm in *Metaxydytes*, compared with ≥ 27 mm in *Paramegadytes*) and having the metasternal wings relatively narrow ($WC/WV = 2.5\text{--}2.6$ in *Metaxydytes*, compared with $WC/WV = 1.8\text{--}1.9$ in *Paramegadytes*). Third instar larvae have; (1) the median lobe of the frontoclypeus truncate apically with a tuft of setae (Fig. 69), (2) the median and lateral lobes of the frontoclypeus separated by a narrow emargination (Fig. 69), and (3) the lateral lobes of the frontoclypeus apically simple and acutely angulate (Fig. 69).

Etymology. *Metaxydytes* is from the Greek *metaxy*, meaning “between,” and *dytes*, meaning “diver,” the root word for many genera of Dytiscidae including in this subfamily. The genus is named to signify its intermediate phylogenetic placement among other genera of Cybistrinae.

Phylogenetic relationships. This genus may be sister group to *Paramegadytes* based especially on the presence of distinctive stiff, spinous setae along the medial margins of the female gonocoxosternite (Miller et al. 2007), although in the analyses presented here the group is ambiguously resolved near *Nilssondytes*, *Paramegadytes* and *Megadytes* + *Cybister* (Figs 75, 76).

Discussion. These species were previously placed in *Megadytes*. The type species of *Megadytes* s. str. is *M. latus* which belongs to a different genus from all other known species previously placed in *Megadytes* (Figs 75, 76) requiring this new name for those species now in *Metaxydytes*. The species of *Metaxydytes* have never been completely revised, although Trémouilles (1989a, b) and Trémouilles and Bachmann (1980) addressed the species in southern South America. The genus is in need of a comprehensive revision.

***Nilssondytes* gen. nov.**

<https://zoobank.org/DF8AFDB0-B369-4936-B231-84B942B58258>

Figs 11, 19, 20, 36–38, 53, 61, 73

Type species. *Nilssondytes diversus* sp. nov., by current designation.

Diagnosis. From other Cybistrinae this genus differs in having: (1) the metatibial spurs apically simple, (2) metacoxal lines clearly present, (3) the pronotum and elytron with broad, distinct lateral yellow bands along margins (Fig. 11), (4) males and females each with two metatarsal claws, the posterior much reduced in both sexes (Figs 19, 20), (5) the prosternum and prosternal process relatively shallowly but distinctly sulcate, (6) the medial margins of the male sternite IX straight, not emarginate (Fig. 53), (7) no cluster or line of setae at the apicodorsal angle of the posterior surface of the mesotarsomeres, and (8) the ventral surface of the metatrochanter with an oblique, transverse groove. The single species in this genus (described below) is somewhat similar in size, shape and coloration to *Metaxydytes laevigatus* (Olivier) and may be present among series of that species in collections. *Nilssondytes* differ from *M. laevigatus* in several features (see above) including

the presence of yellow lateral elytral margins (Fig. 11) which are absent in *M. laevigatus*. Larvae are unknown.

Etymology. This genus is named *Nilssondytes* from the Latin *dytes* meaning “diver,” and *Nilsson*, after the great diving beetle worker and excellent friend, Anders Nilsson, in honor of his inestimable contribution to the science of diving beetle biology.

Phylogenetic relationships. The single species of *Nilssondytes* is part of the clade that includes species with an oblique metatrochanteric groove, but it has an unresolved position with respect to other genera (Figs 75, 76). The presence of a reduced posterior metatarsal claw in both males and females (Figs 19, 20) with the straight medial margins of the male abdominal sternite IX (Fig. 53) is a unique combination of features within Cybistrinae. Unique among this larger clade is also the sulcate prosternum and prosternal process which is somewhat similar to the Australian genera *Spencerhydrus* and *Sternhydrus*.

***Nilssondytes diversus* sp. nov.**

<https://zoobank.org/3F2BEED6-5AA7-4394-9309-788F3ACFACD1>

Figs 11, 19, 20, 36–38, 53, 61, 73, 74

Type locality. Venezuela, Amazonas State, roadside pond ca. 7 km S Samaria-po 5°10.900'N, 67°46.078'W, 95 m elev.

Diagnosis. This is the only species in the genus and is characterized by its diagnostic combination (see above). Typically, species-level features include the shape of the male median lobe which is unique. In ventral aspect the apex is abruptly constricted with the apex narrowly truncate with laterally pointed processes (Fig. 37). In lateral aspect, the median lobe is moderately evenly curved on the dorsal margin, lobe apically abruptly narrowed with the apex elongate and slender, apically narrowly rounded (Fig. 36).

Description. Measurements. TL = 16.7–19.4 mm, GW = 9.6–10.7 mm, PW = 7.0–8.1 mm, HW = 4.2–4.7 mm, EW = 2.7–2.9 mm, TL/GW = 1.7–1.8, HW/EW = 1.6–1.7, WC/WV = 3.1–3.2. Body shape suboval, slightly expanded posteriorly, widest at ~ 3/5 of length; lateral margins evenly, continuously curved between pronotum and elytron. Depressed and somewhat flattened in lateral aspect (Figs 11, 73).

Coloration (Figs 11, 73). Head dark green, anterior clypeal margin yellow, more so laterally, testaceous near eyes. Pronotum dark green with broad lateral yellow margin, posteriorly interrupted and green in one of the four examined specimens, in other specimen yellow extending to posterior angle. Elytron dark green with broad lateral yellow band, separated narrowly from lateral margin, slightly expanded near apex. Ventral surfaces largely black, testaceous on head, basal leg segments and elytral epipleuron.

Sculpture and structure. Head broad, frontoclypeal lines elongate, straight, strongly oblique; anterior clypeal margin broadly, shallowly, and evenly concave; dorsal surface evenly covered with fine microsculpture and micropunctures. Pronotum with lateral margins evenly and broadly curved; surface similar to surface of head in microsculpture and micropunctuation. Elytral lateral margin evenly and slightly curved for most of length, apically broadly curved; surface of elytron similar to surface of head in microsculpture and micropunctuation.

Prosternal process apically rounded, ventral surface distinctly sulcate, apex robust, acutely pointed. Metaventral wing broad, slightly less than 1/3 width of lateral portion of metacoxa ($WC/WV = 3.1-3.2$); surface smooth, without sculpturing. Lateral portion of metacoxa large, broad, surface smooth, without sculpturing; metacoxal lines short, extending less than half distance across metacoxa. Abdominal ventrites smooth, unsculptured.

Male genitalia. Male median lobe in lateral aspect shallowly curved, apically abruptly narrowed, apex narrowed, slightly curved, apically narrowly rounded, broad medially (Fig. 36). In dorsal aspect broad throughout most of length, apically abruptly narrowed, apex laterally produced, submedially with broad, elongate lobes on each side, ventral sclerite short, apically sharp, acuminate, extending to 3/5 length of median lobe, apex sharply pointed (Fig. 37). Lateral lobe broad in basal half, apically distinctly narrowed, apex narrowly rounded, with series of elongate setae along more than apical half of dorsal margin of lateral lobe (Fig. 38).

Female genitalia. With a single genital opening, vagina elongate, slender, with enlarged, bulbous region at base of common oviduct; spermatheca short, curved, at apex of enlarged region, with soft tissue region on each side of enlarged region (Fig. 61); gonocoxae together broad, apically broadly pointed (Fig. 61); gonocoxosternite broad, with elongate anterolateral lobe, with medial margin sublinear, without conspicuous setae (Fig. 61).

Sexual dimorphism. Males have a characteristic broad protarsal palette with ventral adhesive setae. Males also have mesotarsomeres with clumps of posteroventral setae. Females lack pro- and mesotarsal expansions or adhesive setae. Both males and females have two metatarsal claws with the posterior shorter than the anterior, but females have the posterior somewhat more curved than in males (Figs 19, 20). Females have distinctive microsculpture on the surface of the elytron anteriorly in the form of a field of short striae which is absent in males.

Variation. Five specimens were examined. One specimen has the lateral pronotal yellow band extending to the posterior margin of the pronotum, the others have a narrow dark green separation from the posterior margin.

Distribution. This species is known from few localities in Venezuela along the northwestern margins of the Guiana Shield craton (Fig. 74).

Natural history. The only natural history information available from labels is "roadside pond," "river margin," and "rock outcropping."

Etymology. The species is named from the Latin *diversus*, meaning "different," in recognition of the different lengths of the metatarsal claws in both males and females (Figs 19, 20).

Material examined. **Holotype**, male labeled, "VENEZUELA: Amazonas State 5°10.900'N, 67°46.078'W, 95 m ca. 7 km S. Samariapo 15.i.2009; leg. Short, Miller, García, Camacho, Joly VZ09-0115-02X: roadside pond/ SM0846115 KUNHM-ENT [barcode label]/ HOLOTYPE: *Nilssonodytes diversus* Miller, Michat and Ferreira-Jr., 2023 [red label with double black line border]." **Paratypes**, 1 male labeled, "Suapure VENEZ. Caura River 4.20.1900 [handwritten] E.A. Klagges.", 1 female labeled "VENEZUELA: Bolivar State 7°41'23.6"N, 64°1'56.0"W, 134 m ca. 14 km E Rio Aro; 5.viii.2008 leg. A. Short & M. García AS-08-073; rock outcropping/ SM0829328 KUNMH-ENT [barcode label]," 1 female labeled "VENEZUELA: Guárico State 8°6.226'N, 66°26.228'W, 52 m UCV San Nicolasito Field Station: Rio Aguaro; 10.i.2009 leg. Short, Miller, Joly, García, Camacho;

VZ09-0110-01A/ SEMC0852602 KUNHM-ENT," 1 male labeled "VENEZUELA: Bolivar State 6.58694°N; 67.02912°W Rio Caripito 12.i.2009; leg. Short Miller VZ09-0112-02A: river margin/ SM0844405 KUNHM-ENT [barcode label]." All paratypes with, "...PARATYPE *Nilssondytes diversus* Miller, Michat and Ferreira-Jr., 2023 [blue label with black line border]."

***Paramegadytes* Trémouilles & Bachmann, 1980, stat. nov.**

Figs 26, 27, 56, 63, 70

Paramegadytes Trémouilles & Bachmann, 1980: 101.

Type species. *Dyticus glaucus* Brullé, 1837: 46 by original designation.

Diagnosis. Like *Metaxydytes* these species have both metatibial spurs apically simple, the medial margins of male abdominal sternite IX straight, and both males and females with two metatarsal claws, males with equal-length claws and females with the posterior claw reduced (Figs 26, 27). Females also share the characteristic of the medial margins of the gonocoxosternite with a series of spinous setae (Fig. 63). The lateral pronotal margin has a diffuse, but distinctive lateral pale band. From *Metaxydytes* these specimens are larger with the metaventrite wings relatively broader (see above under *Metaxydytes* for details of diagnostic comparisons). Third instar larvae have (1) the median lobe of the frontoclypeus truncate apically with a tuft of setae (Fig. 70), (2) the median and lateral lobes of the frontoclypeus separated by a wide emargination (Fig. 70), and (3) the lateral lobes of the frontoclypeus bilobed (Fig. 70).

Phylogenetics. This may be the sister genus to *Metaxydytes* (Figs 75, 76; Miller et al. 2007) although here it is in an unresolved position relative to *Nilssondytes*, *Metaxydytes* and *Megadytes* + *Cybister* (Figs 75, 76). See under *Metaxydytes* for further discussion.

Discussion. There are currently two valid species in this genus, *P. australis* (Germain) and *P. glaucus* (Brullé). Trémouilles and Bachmann (1980) characterized and differentiated them.

***Trifurcitus* Brinck, 1945, stat. nov.**

Figs 3, 8, 65, 71

Trifurcitus Brinck, 1945: 8.

Type species. *Cybister fallax* Aubé, 1838b: 54, by original designation.

Diagnosis. These are former *Megadytes* species with the anterior metatibial spur apically trifid (Fig. 3). Specimens are very large for diving beetle species (TL = 27–36 mm). They are somewhat similar to *Bifurcitus* specimens. See under that genus for diagnostic comparisons. Larvae are distinctive in having the median lobe of the frontoclypeus sharp apically without an apical tuft of setae.

Phylogenetic relationships. *Trifurcitus* is sister group to *Bifurcitus* (Figs 75, 76). Both males and females have equal-length metatarsal claws and the anterior metatibial spur is either bifid (Figs 1, 2) or trifid (Fig. 3), although these two conditions may possibly not be homologous.

Discussion. See above under *Bifurcitus* for more discussion of these two taxa. Six species are currently recognized. Although they have not been revised thoroughly, most of the species were described or illustrated by Trémouilles (1989a) and Trémouilles and Bachmann (1980).

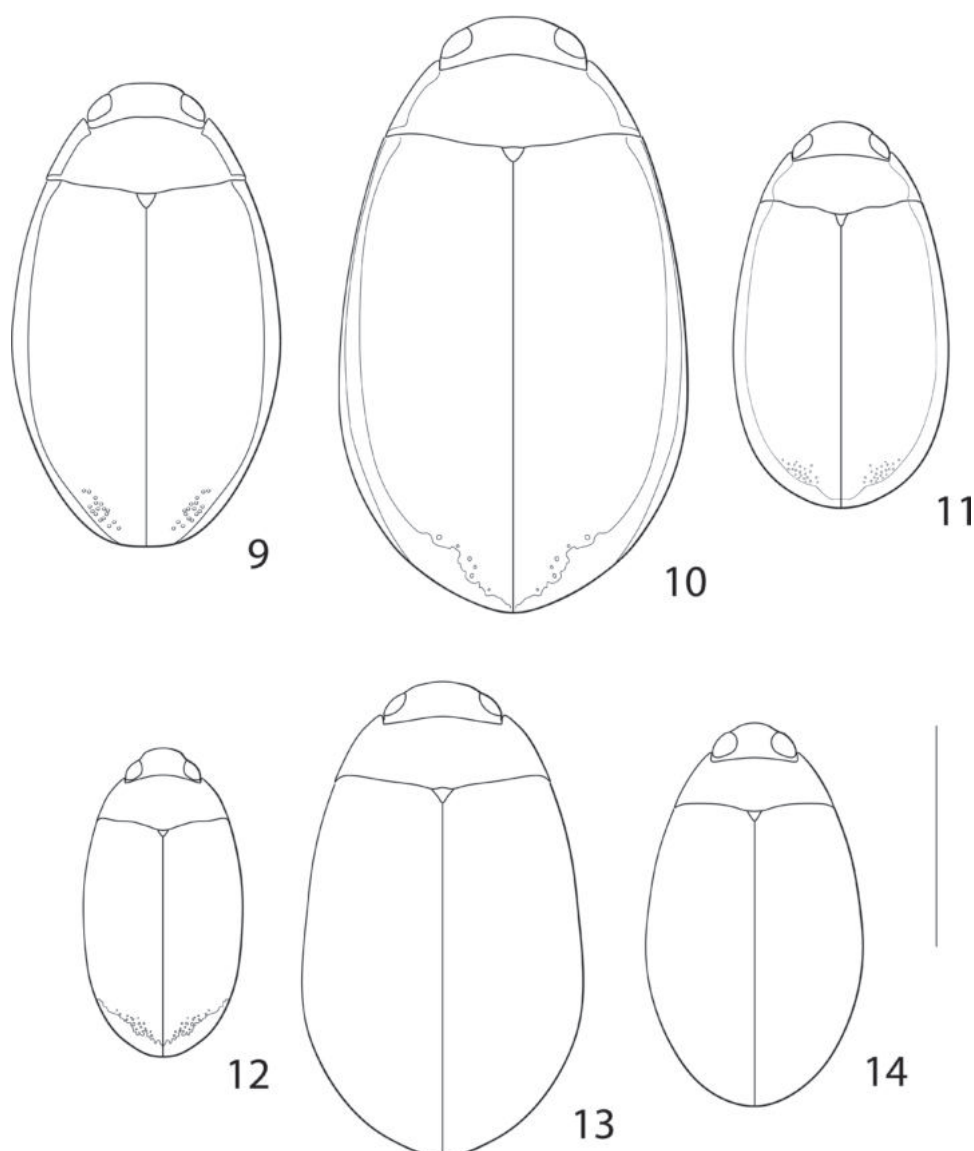
Other species

“*Megadytes* species” Ribera et al. 2008

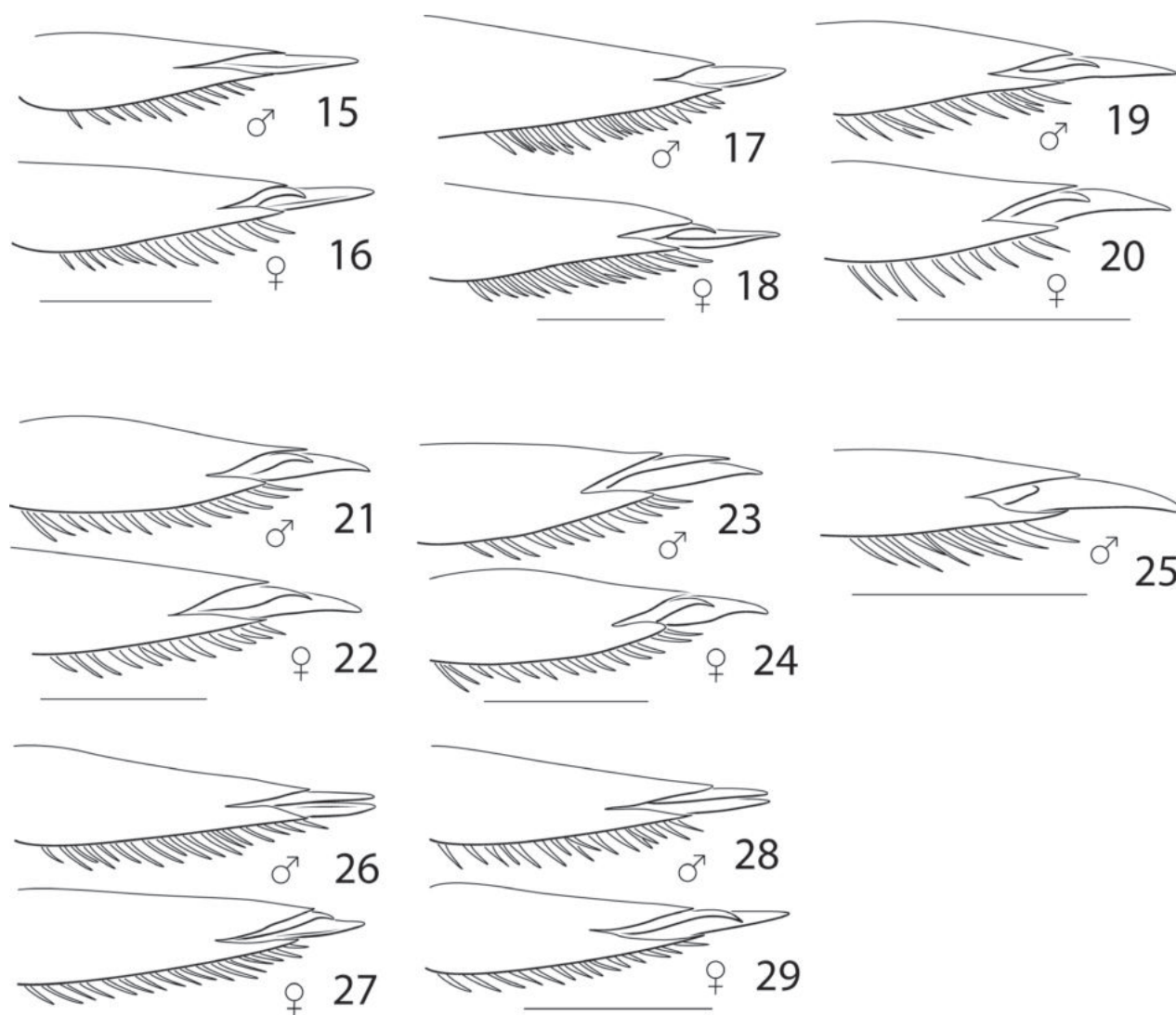
Figs 14, 25, 48–50

Megadytes species IR57: Ribera et al. 2008: 25.

Discussion. This single male specimen of a cybistrine from Peru presents some problems. It appears to be an undescribed species based on the male genitalia (Figs 48–50). The specimen was DNA sequenced and analyzed for

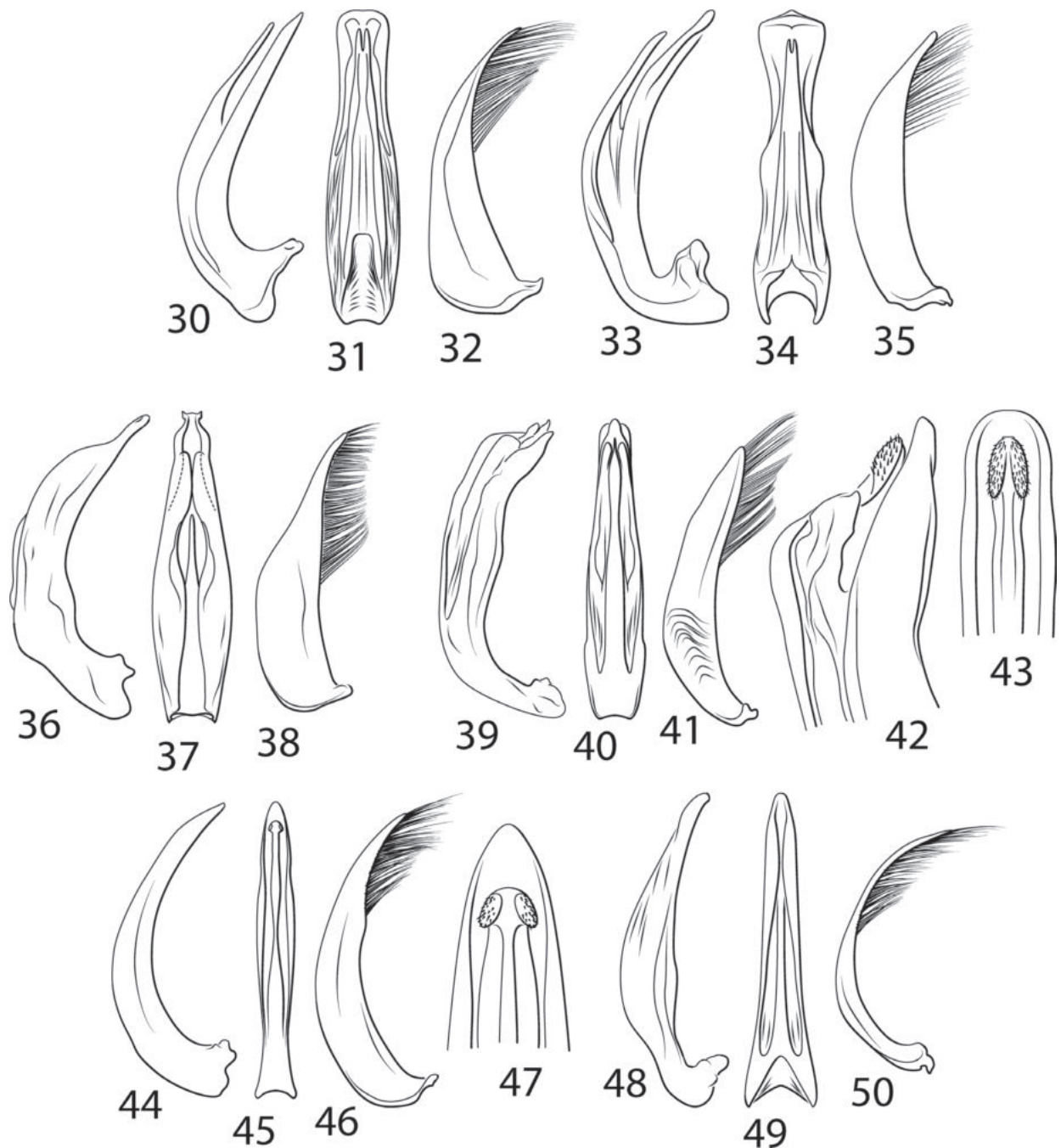


Figures 9–14. Neotropical Cybistrinae species, habitus **9** *Cybister festae* **10** *Cybister puncticollis* **11** *Nilssondytes diversus* **12** *Megadytes parvus* **13** *Megadytes latus* **14** species “IR57” (Ribera et al. 2008). Scale bar: 10.0 mm.



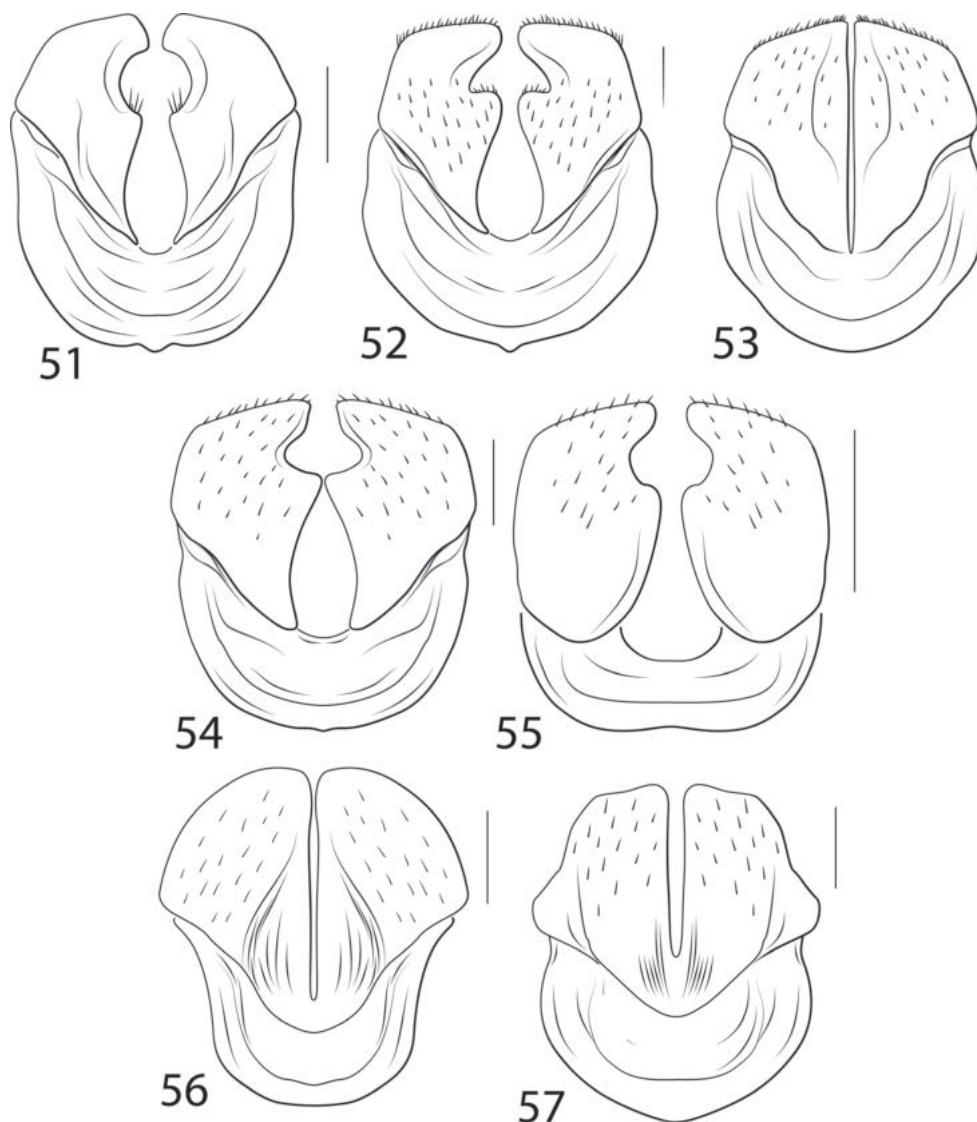
Figures 15–29. Neotropical Cybistrinae species, metatarsal claws and tarsomere VI of males and females **15, 16** *Cybister festae* **17, 18** *Cybister puncticollis* **19, 20** *Nilssondytes diversus* **21, 22** *Megadytes latus* **23, 24** *Megadytes parvus* **25** species “IR57” (Ribera et al. 2008) **26, 27** *Paramegadytes glaucus* **28, 29** *Metaxydytes fraternus*. Scale bars: 1.0 mm.

a project by Ribera et al. (2008) where it was found to be in a group with species then assigned to *Megadytes* (including species of *M. (Bifurcitus)*, *M. (Paramegadytes)* and *M. (Megadytes)*). The male specimen currently includes a single metathoracic leg (the other is absent). On it, there are two unequal length metatarsal claws with the posterior short, much shorter than the anterior (Fig. 25), which places it outside the historical diagnosis of *Megadytes* which includes males with equal-length metatarsal claws (although see above). However, the specimen is missing important morphological structures for further interpreting its placement within Cybistrinae including the mesothoracic legs (which are important for examining the posterodorsal series of setae on the mesotarsomeres) and components of the genital capsule (which are important for examining the emargination of the medial margins of abdominal sternite IX). Because of this, the specimen cannot be placed within a known genus. Nor is it reasonable to place it in a new genus or expand the definition of an existing genus to include it given the lack of information about its features. Hopefully, additional specimens



Figures 30–50. Neotropical Cybistrinae species, male genitalia **30–32** *Cybister festae*: **30** median lobe, right lateral aspect **31** median lobe, ventral aspect **32** right lateral lobe, right lateral aspect **33–35** *Cybister puncticollis*: **33** median lobe, right lateral aspect **34** median lobe, ventral aspect **35** right lateral lobe, right lateral aspect **36–38** *Nilssondytes diversus*: **36** median lobe, right lateral aspect **37** median lobe, ventral aspect **38** right lateral lobe, right lateral aspect **39–43** *Megadytes parvus*: **39** median lobe, right lateral aspect **40** median lobe, ventral aspect **41** right lateral lobe, right lateral aspect **42** apex of median lobe, right lateral aspect **43** apex of median lobe, ventral aspect **44–47** *Megadytes latus*: **44** median lobe, right lateral aspect **45** median lobe, ventral aspect **46** right lateral lobe, right lateral aspect **47** apex of median lobe, ventral aspect **48–50** species “IR57” (Ribera et al. 2008): **48** median lobe, right lateral aspect **49** median lobe, ventral aspect **50** right lateral lobe, right lateral aspect.

will be found to allow this species to be described and placed. The species is described here to the extent possible to allow for future identification and investigation.



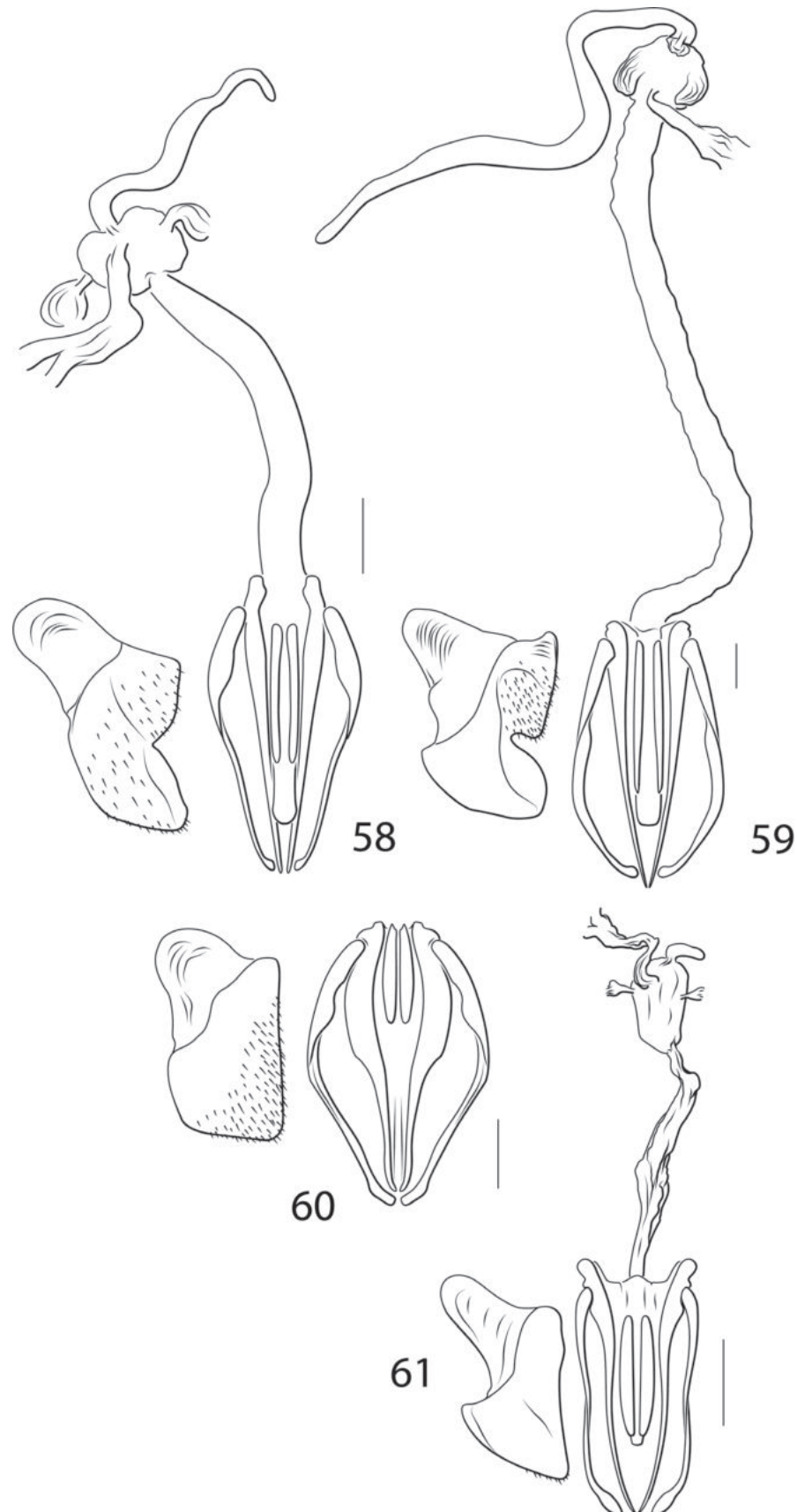
Figures 51–57. Neotropical Cybistrinae species, male sternite IX, ventral aspect **51** *Cybister festae* **52** *Cybister puncticollis* **53** *Nilssondytes diversus* **54** *Megadytes latus* **55** *Megadytes parvus* **56** *Paramegadytes glaucus* **57** *Metaxydytes fraternus*. Scale bars: 1.0 mm.

Collection locality. Peru, Atalapa, Rio Carbon at Rio Madre de Dios, in river, Apr 1999 (Ribera et al. 2008).

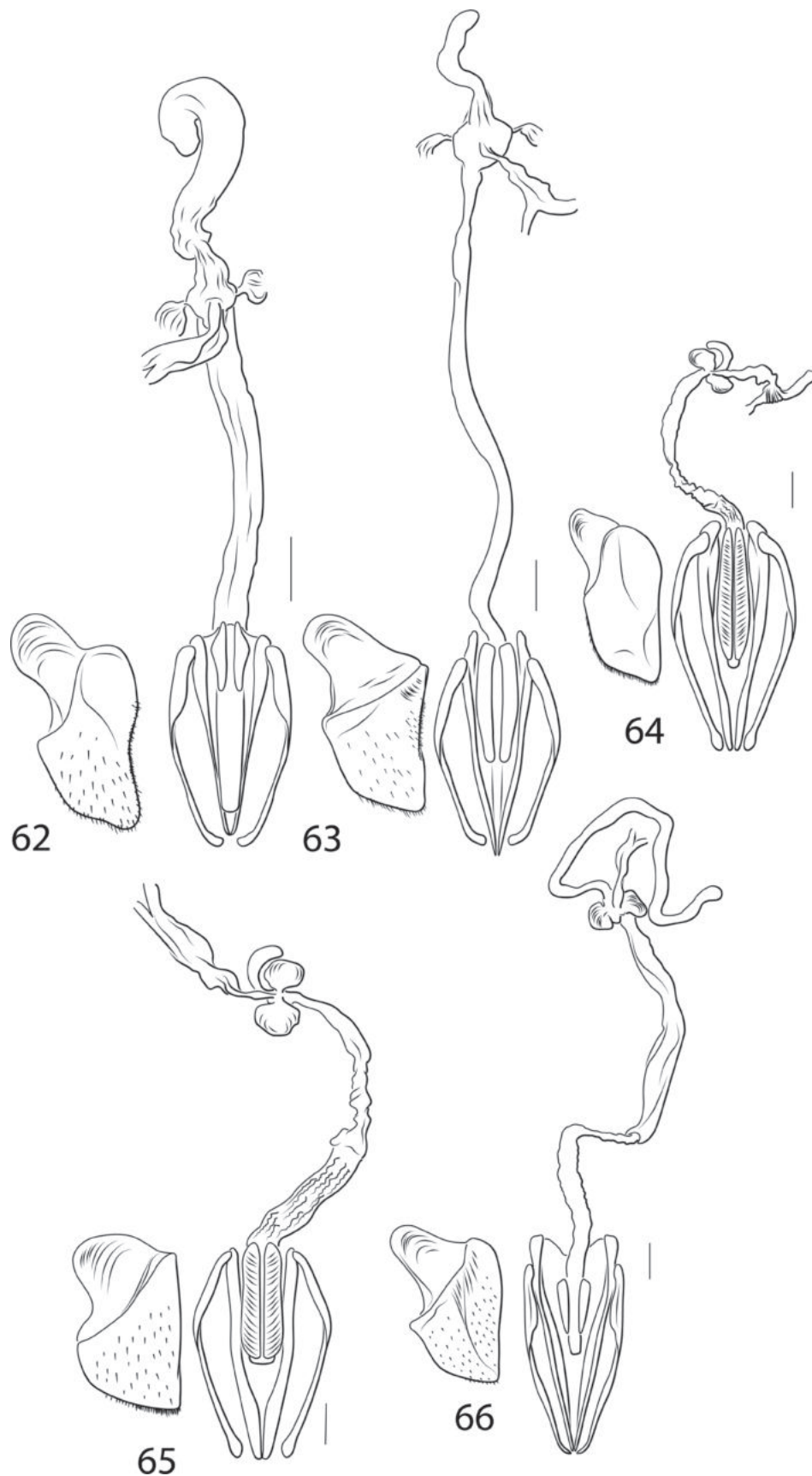
Description. Measurements. TL = 17.5 mm, GW = 10.4 mm, PW = 12.8 mm, HW = 4.8 mm, EW = 2.4 mm, TL/GW = 1.7, HW/EW = 2.0, WC/WV = 4.2. Body shape (Fig. 14) broad, expanded posteriorly, widest at ~ 3/5 of length; lateral margins evenly, continuously curved between pronotum and elytron. Depressed and somewhat flattened in lateral aspect.

Coloration. All dorsal surfaces dark reddish brown, without yellow margins on pronotum or elytron. Ventral surfaces entirely dark reddish brown, somewhat more reddish on ventral surfaces of prothorax and pro- and mesothoracic legs.

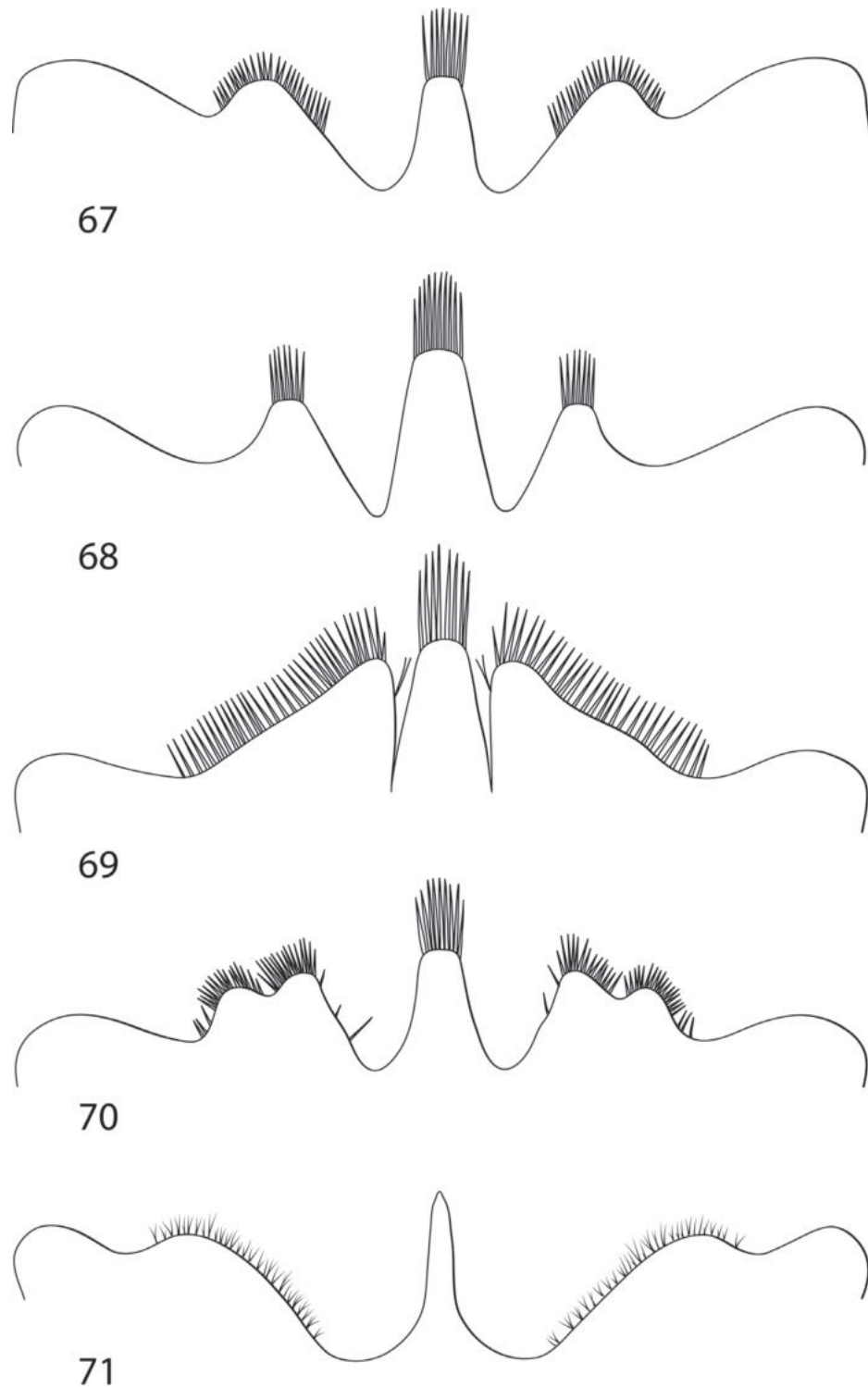
Sculpture and structure. Head broad; anterior clypeal margin broadly, shallowly and evenly concave; eyes large (HW/EW = 2.0). Dorsal surface shiny and evenly covered with fine micropunctures on head and pronotum, very few sparse micropunctures on elytron. Pronotum with lateral margins evenly and broadly curved. Elytral lateral margin evenly and slightly curved for most of length, apical-



Figures 58–61. Neotropical Cybistrinae species, female genitalia including left gonocoxosternite, ventral aspect, except Fig. 60 without internal genitalia **58** *Cybister festae* **59** *Cybister puncticollis* **60** *Megadytes latus* **61** *Nilssondytes diversus*. Scale bars: 1.0 mm.



Figures 62–66. Neotropical Cybistrinae species, female genitalia including left gonocoxosternite, ventral aspect **62** *Metaxydytes fraternus* **63** *Paramegadytes glaucus* **64** *Bifurcitus lherminieri* **65** *Trifurcitus robustus* **66** *Cybister fimbriolatus*. Scale bars: 1.0 mm.



Figures 67–71. Third instar larva, anterior clypeal margin **67** *Bifurcitus magnus* **68** *Megadytes latus* **69** *Metaxydytes carcharias* **70** *Paramegadytes glaucus* **71** *Trifurcitus fallax*.

ly broadly curved. Prosternal process apically broadly, shallowly concave, ventral surface flat throughout, apex robust, acutely pointed. Metaventral wing narrow, ~ 1/4 width of lateral portion of metacoxa ($WC/WV = 4.2$); surface smooth, with extremely fine punctation. Lateral portion of metacoxa large, broad, surface smooth, with dispersed, very fine micropunctures; metacoxal lines short, extending only ~ 1/3 distance across metacoxa. Abdominal ventrites smooth, unsculptured.



Figure 72. *Cybister* (*Neocybister*) *festae*, lectotype male (left) and paralectotype female (right). Photograph courtesy of F. Giachino, MRSN.



Figure 73. *Nilssondytes diversus*, holotype specimen. Scale bar: 5.0 mm.

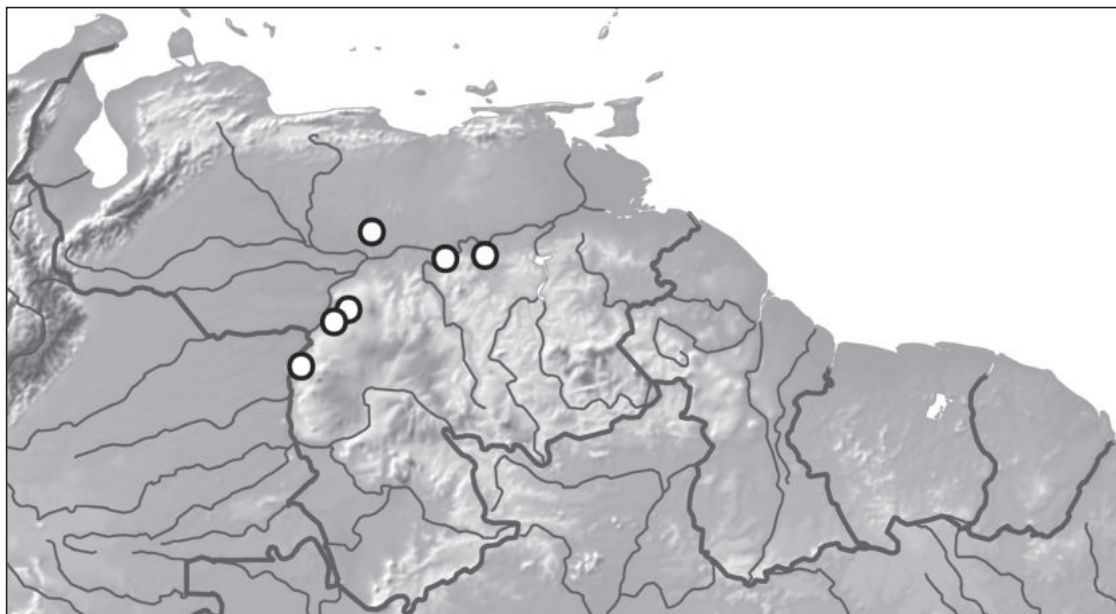


Figure 74. Distribution of *Nilssondytes diversus* in northern South America.

Male genitalia. Male median lobe in lateral aspect slender, broader submedially and gradually narrowed apically to slightly curved apex, apex bluntly rounded (Fig. 48). In dorsal aspect slender, evenly and gradually narrowed to narrowly rounded apex; dorsal sclerite very slender and elongate (Fig. 49). Lateral lobe extremely slender throughout, broadly curved with long series of long setae along dorsal margin (Fig. 50).

Female genitalia. Females are not known.

Sexual dimorphism. Only a single male was examined. However, this male has a characteristic broad protarsal palette with ventral adhesive setae. Males also have mesotarsomeres with clumps of posteroventral setae. Other typical sexually dimorphic features cannot be compared.

Variation. Only a single specimen was examined.

Material examined. A single male specimen examined labeled, "271297 PERU ZUNGARO COHA 16u:TO [handwritten, somewhat illegible]."

Key to genus groups of Adult Cybistrinae of the world

Adapted from Miller et al. (2007) and Miller and Bergsten (2016) and including revised classification of some groups, see below.

- 1 Posterior metatibial spur bi- or trifurcate (e.g., Figs 1, 2); Neotropical.....**2**
- Posterior metatibial spur simple (e.g., Fig. 3); Neotropical and other regions.....**3**
- 2 Posterior metatibial spur bifurcate (Figs 1, 2) ...***Bifurcitus* Brinck, stat. nov.**
- Posterior metatibial spur trifurcate..... ***Trifurcitus* Brinck, stat. nov.**
- 3 Prosternal process longitudinally conspicuously sulcate; Australian and Neotropical**4**
- Prosternal process without longitudinal sulcus although lateral margins may be variously bordered and anterior portion may be shallowly sulcate or excavated; distribution various**6**

- 4 Metacoxal lines absent **Sternhydrus** Brinck
- Metacoxal lines present **5**
- 5 Prosternal process longitudinally narrowly and deeply sulcate throughout length; male and female each with metatarsal claws unequal in length, anterior claw shorter than posterior claw **Spencerhydrus** Sharp
- Prosternal process longitudinally broadly sulcate, mainly in anterior half; male and female each with metatarsal claws unequal in length, posterior claw rudimentary and short (Figs 19, 20) **Nilssondytes** gen. nov.
- 6 Metacoxal lines absent; Australian **Onychohydrus** Schaum
- Metacoxal lines present; distribution various **7**
- 7 Male with a single metatarsal claw, female either with one claw or with an additional, small posterior rudimentary claw (Figs 15–18); with postero-ventral series of setae near apical margin of mesotarsomeres of males and pro- and mesotarsomeres of females (Fig. 5) *Cybister* Curtis) **8**
- Male and female with two metatarsal claws, in some cases with posterior claw rudimentary and small (Figs 21–29); without posteroventral series of setae on pro- and mesotarsomeres (Fig. 4) **11**
- 8 Elytron without distinct yellow lateral margins; female always with a second, rudimentary posterior metatarsal claw **9**
- Elytron with distinct yellow lateral margins; female with either a single metatarsal claw or with a second rudimentary posterior claw **10**
- 9 Pronotum with distinct yellow lateral margins
..... **Cybister (Megadytoides)** Brinck
- Pronotum without distinct yellow lateral margins
..... **Cybister (Melanectes)** Brinck
- 10 Female with a single metatarsal claw or, in few species, dimorphic with some specimens with a second, rudimentary posterior claw; apex of dorsal sclerite of male median lobe various, but not bifid; medial margin of female gonocoxosternite straight or slightly concave; distribution North and Central America, Africa, Eurasia and Australia, absent from most of Neotropical Region except Mexico and certain Caribbean islands
..... **Cybister (Cybister)** Curtis
- Female always with two metatarsal claws, posterior claw short and curved (Figs 15–18); apex of dorsal sclerite of male median lobe bifid (Figs 31, 34); medial margin of female gonocoxosternite distinctly emarginate (Figs 58, 59); species from Panama to southern South America
..... **Cybister (Neocybister)** Miller, Bergsten & Whiting
- 11 Dorsal surface light green with sparsely distributed, small black dots, laterally without distinct pale margins; central Afrotropical
..... **Regimbartina** Chatanay
- Dorsal surface dark green to green-black without black dots, laterally with or without distinct pale margins; Australian, Nearctic or Neotropical **12**
- 12 Prosternal process with distinct lateral carinae; male and female metatarsal claws similar, anterior claw shorter than posterior; dorsal surface dark green with distinct lateral pale margins; Australian
..... **Austrodytes** Watts
- Prosternal process without distinct lateral carinae; male and female claws various, male with either equal-length metatarsal claws or with posterior claw reduced, shorter than anterior, female with two claws, posterior re-

- duced, shorter than anterior (Figs 21–29); dorsal surface dark green to brown or black with or without lateral pale margins; Neotropical or southern Nearctic **13**
- 13 Male and female both with two metatarsal claws, anterior claw shorter than posterior (Figs 21–24); male with medial margins of sternite IX emarginate (Figs 54, 55)..... **Megadytes Sharp**
- Male with two metatarsal claws that are subequal in length, female with two metatarsal claws, with posterior claw shorter, rudimentary (Figs 26–29); male with medial margins of sternite IX straight (Figs 56, 57) **14**
- 14 Size large, TL ≥ 27 mm; metasternal wings relatively broad (WC/WV = 1.8–1.9) **Paramegadytes Trémouilles & Bachmann, stat. nov.**
- Size smaller, TL ≤ 24 mm; metasternal wings relatively narrow (WC/WV = 2.5–2.6)..... **Metaxydytes, gen. nov.**

Key to Instar III larvae of Neotropical Cybistrinae

Nilssondytes and *Cybister* (*Neocybister*) not included (larvae unknown)

- 1 Median lobe of frontoclypeus apically sharp, without apical tuft of setae (Fig. 71)..... **Trifurcitus Brinck, stat. nov.**
- Median lobe of frontoclypeus apically truncate, with apical tuft of setae (Figs 67–70) **2**
- 2 Median and lateral lobes of frontoclypeus separated by a narrow emargination (Fig. 69) **Metaxydytes, gen. nov.**
- Median and lateral lobes of frontoclypeus separated by a wide emargination (Figs 67, 68, 70)..... **3**
- 3 Lateral lobes of frontoclypeus bilobed (Fig. 70) **Paramegadytes Trémouilles & Bachmann, stat. nov.**
- Lateral lobes of frontoclypeus with a single lobe (Figs 67, 68)..... **4**
- 4 Lateral lobes of frontoclypeus acute (Fig. 68); cephalic capsule relatively long (ratio head length / head width > 1.25)..... **Megadytes Sharp**
- Lateral lobes of frontoclypeus obtuse (Fig. 67); cephalic capsule relatively short (ratio head length / head width < 1.20).... **Bifurcitus Brinck, stat. nov.**

List of Neotropical genera and species of Cybistrinae

***Bifurcitus* Brinck, 1945, stat. nov.**

Bifurcitus ducalis (Sharp, 1882: 713); Brazil.

Bifurcitus lherminieri (Guérin-Méneville, 1829: pl. 8); type locality not given, Guadeloupe by indication.

= *Cybister giganteus* Laporte, 1835: 99; Brazil.

= *Trogus olivieri* Crotch, 1872: 205, by indication to *Dytiscus costalis* Fabricius sensu Olivier 1795: 9; French Guiana (Cayenne), Suriname.

Bifurcitus magnus (Trémouilles & Bachmann, 1980: 118); Argentina, Santa Fe.

***Cybister* Curtis, 1927**

***Cybister* (*Neocybister*) Miller, Bergsten, & Whiting, 2007**

Cybister festae Griffini, 1895: 1; Panama, Darién, Matusagrati Lake (Laguna della Pita).

Cybister puncticollis (Brullé, 1837: 46) (*Dytiscus*); Bolivia, San Miguel.
= *Cybister kemneri* Brinck, 1945: 18; Brazil, La Plata, Amazonas, Rio Autaz.

Megadytes Sharp, 1882

Megadytes latus (Fabricius, 1801: 260) (*Dytiscus*); South America.
Megadytes parvus Trémouilles, 1984: 187; Brazil, Bahia State, Santa Rita, comb. nov.

Metaxydytes, new genus

Metaxydytes carcharias (Griffini, 1895: 5) (*Megadytes*); Paraguay, Apa River, Asunción, comb. nov.
Metaxydytes ecuadorius (Zimmermann, 1919: 236) (*Megadytes*); Ecuador, Esmeraldas, comb. nov.
Metaxydytes flohri (Sharp, 1882: 709) (*Megadytes*); Mexico, comb. nov.
Metaxydytes fraternus (Sharp, 1882: 708) (*Megadytes*); Panama, comb. nov.
Metaxydytes guayanensis (Wilke, 1920: 249) (*Cybister*); Guyana, comb. nov.
Metaxydytes guignoti (Mouchamps, 1957: 284) (*Megadytes*); Costa Rica, Bebedero, comb. nov.
Metaxydytes laevigatus (Olivier, 1791: 308) (*Dytiscus*); French Guiana (Cayenne), comb. nov.
Metaxydytes marginithorax (Perty, 1830: 15) (*Dytiscus*); Brazil, comb. nov.
Metaxydytes steinheili (Wehncke, 1876: 359) (*Trogus*); Colombia, Medellín, comb. nov.

Nilssondytes, gen. nov.

Nilssondytes diversus, sp. nov.; Venezuela, Amazonas State.

Paramegadytes Trémouilles & Bachmann, 1980, stat. nov.

Paramegadytes australis (Germain, 1854: 326) (*Cybister*); Chile, Santiago.
= *Megadytes expositus* Sharp, 1882: 705; Chile.
Paramegadytes glaucus (Brullé, 1837: pl. 4) (*Dytiscus*); Argentina, Buenos Aires; Uruguay, Maldonado, Montevideo.
= *Cybister aeneus* Ormancey, 1843: 332; Brazil.
= *Cybister biungulatus* Babington, 1842: 3; Uruguay, Rio de la Plata, Maldonado.

Trifurcitus Brinck, 1945, stat. nov.

Trifurcitus aubei (Wilke, 1920: 245) (*Cybister*), by indication to *Dytiscus costalis* Fabricius sensu Aubé 1838: 50; French Guiana.
ssp. *meridionalis* Mouchamps, 1957: 286; Brazil, Amazonas.
Trifurcitus fallax (Aubé, 1838: 54) (*Cybister*); French Guiana (Cayenne).
Trifurcitus gravidus (Sharp, 1882: 712) (*Megadytes*); Brazil, Santa Cruz.
Trifurcitus obesus (Sharp, 1882: 710) (*Megadytes*); Panama.
Trifurcitus perplexus (Sharp, 1882: 711) (*Megadytes*); South America.
Trifurcitus robustus (Aubé, 1838: 49) (*Cybister*); Brazil.

Neotropical Cybistrinae incertae sedis with respect to genus

?? *costalis* (Fabricius, 1775: 230) (*Dytiscus*); Suriname.
?? *obovatus* (Kirby, 1826: 694) (*Dytiscus*); Brazil.
“*Megadytes* species, IR57”, (undescribed species, unknown genus, Ribera et al. 2008).

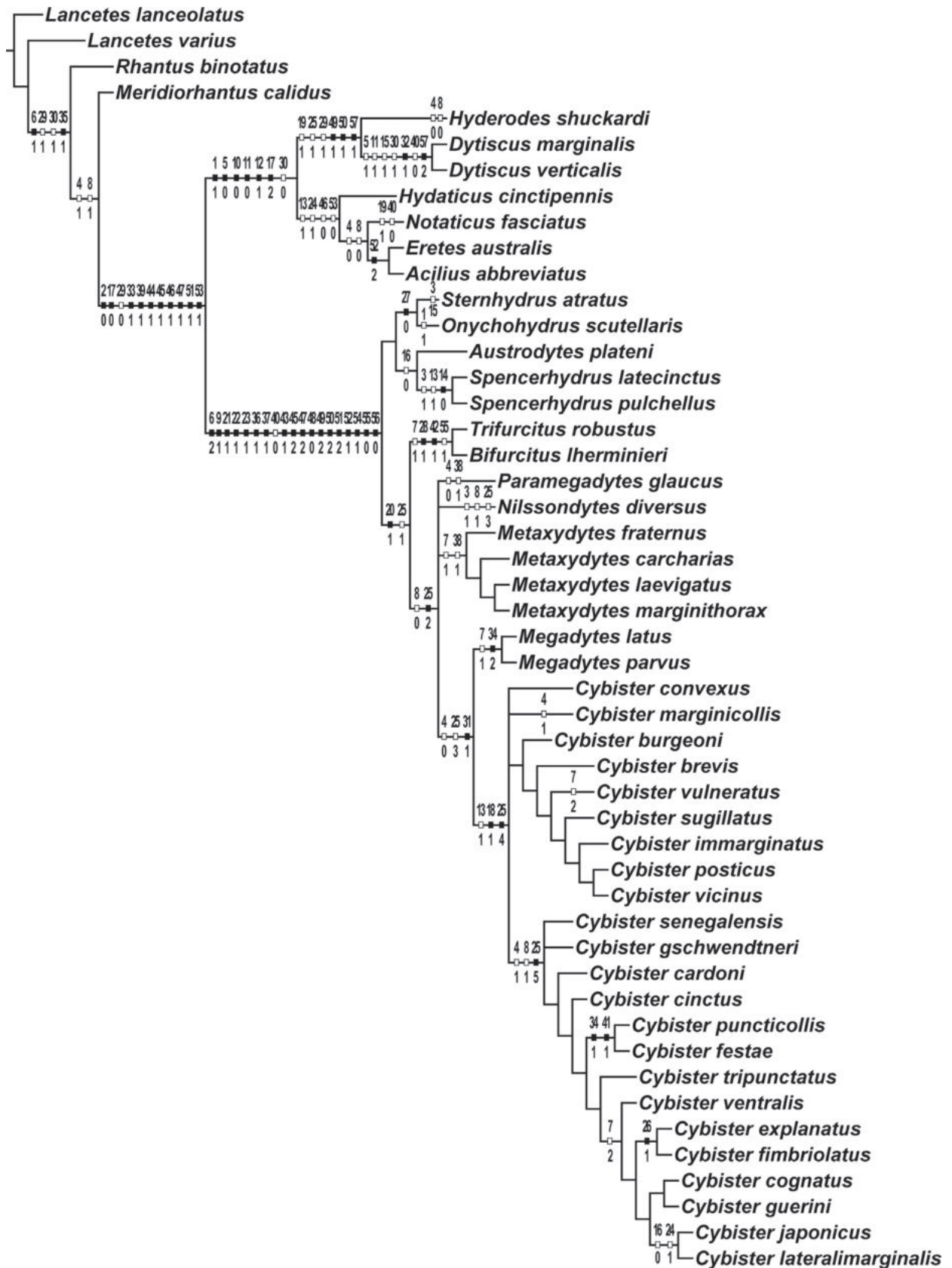


Figure 75. One of seven cladograms derived from parsimony analysis of 57 morphological characters from Cybistrinae and other Dytiscidae (len = 105, CI = 68, RI = 92) with characters mapped using 'fast' optimization in WinClada. Black hash marks indicate unambiguous changes, white hash marks indicate homoplasious changes or reversals. Numbers above hash marks are character numbers, those below hash marks are derived state numbers.

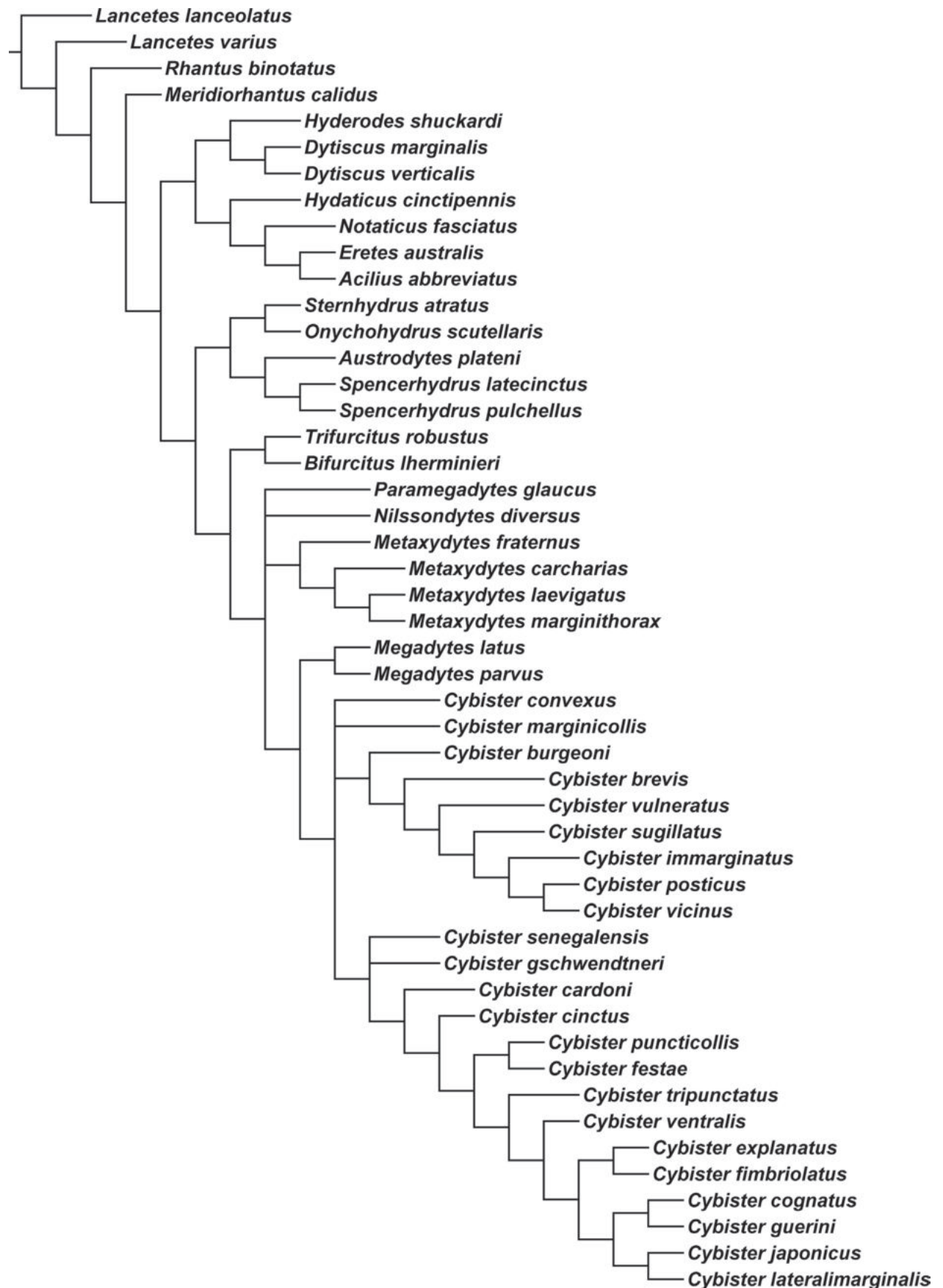


Figure 76. Consensus cladogram of seven equally parsimonious cladograms from parsimony analysis of 57 morphological characters from Cybistrinae and other Dytiscidae morphology.

Acknowledgements

KBM thanks A.E.Z. Short for collaboration in Venezuela.

Additional information

Conflict of interest

The authors have declared that no competing interests exist.

Ethical statement

No ethical statement was reported.

Funding

Portions of this project were funded by NSF grants #DEB-1353426, #DEB-0845984, and #DEB-0816904 (KBM and A.E.Z. Short, PIs).

Author contributions

All authors have contributed equally.

Author ORCIDs

Kelly B. Miller  <https://orcid.org/0009-0004-1093-4066>

Mariano C. Michat  <https://orcid.org/0000-0002-1962-7976>

Nelson Ferreira Jr  <https://orcid.org/0000-0002-5932-7695>

Data availability

All of the data that support the findings of this study are available in the main text or Supplementary Information.

References

- Alarie Y, Michat MC, Miller KB (2011) Notation of primary setae and pores on larvae of Dytiscinae (Coleoptera: Dytiscidae), with phylogenetic considerations. *Zootaxa* 3087(1): 1–55. <https://doi.org/10.11646/zootaxa.3087.1.1>
- Arce-Pérez R, Novelo-Gutiérrez R, Fery H (2021) *Cybister* (s. str.) *poblanus* sp. n. from Mexico and notes on other species of Cybistrinae (Coleoptera: Dytiscidae). *Zootaxa* 5061(2): 323–339. <https://doi.org/10.11646/zootaxa.5061.2.5>
- Bertrand HPI (1928) Larves et nymphes des Dytiscidae, Hygrobiides et Haliplides. *Encyclopedia Entomologica* 10, [vi +] 366 pp.
- Blackwelder RE (1944) Checklist of the Coleopterous insects of Mexico, Central America, the West Indies, and South America. *Bulletin – United States National Museum* 185: 1–188. <https://doi.org/10.5479/si.03629236.185.i>
- Blunck H (1917) Die Entwicklung des *Dytiscus marginalis* L. vom Ei bis zur Imago: 2. Tl.: die Metamorphose (der Habitus der Larve). *Zeitschrift für Wissenschaftliche Zoologie* 117: 1–129.
- Brinck P (1945) Nomenklatorische und systematische Studien über Dytisciden, III. Die Klassifikation der Cybisterinen. *Kungliga Fysiografiska Sällskapets Handlingar* 56: 1–20.
- Burmeister E-G (1976) Der ovipositor der Hydradephaga (Coleoptera) und seine phylogenetische Bedeutung unter besonderer Berücksichtigung der Dytiscidae. *Zoomorphologie* 85(3): 165–257. <https://doi.org/10.1007/BF00993515>

- Crespo FA (1982) *Megadytes* (*Paramegadytes*) *glaucus* (Brulle) descripcion del tercer estadio larval y de la pupa (Dytiscidae, Coleoptera). *Physis* 41: 7–13. [B Aires]
- Ferreira Jr N (1993) Descricao da larva de *Megadytes giganteus* (Castelnau, 1834) com notas biologicas (Coleoptera: Dytiscidae). *Revista Brasileira de Entomologia* 37: 57–60.
- Ferreira Jr N (1995) Description of the larvae of *Megadytes fallax* (Aubé) and *M. marginithorax* (Perty) (Coleoptera: Dytiscidae). *Coleopterists Bulletin* 49: 313–318.
- Ferreira Jr N (2000) Morfologia externa da larva de *Megadytes giganteus* (Laporte, 1834) (Coleoptera, Dytiscidae) e evidências sobre a condição monofilética da tribo Cybistrini. *Revista Brasileira de Entomologia* 44: 57–69.
- Ferreira Jr N, Nicolini LB, Nessimian JL (2006) Description of the third instar larva of *Megadytes latus* (Fabricius) (Coleoptera, Dytiscidae), with an identification key for described larvae of the genus. *Revista Brasileira de Zoologia* 23(3): 792–795. <https://doi.org/10.1590/S0101-81752006000300025>
- Fiori G (1949) Contributi alla conoscenza morfologica ed etologica dei coleotteri III. Le larve dell'*Acilius sulcatus* L. e del *Cybister lateralimarginalis* De Geer (Dytiscidae). *Bollettino dell'Istituto di Entomologia dell'Università di Bologna* 17: 234–264.
- Goloboff P (1995) NONA. 2.0 edn. Published by the author, Tucumán, Argentina.
- Griffini A (1895) Nuova specie di Dytiscide raccolta nel Darien dal Dr. E. Festa. *Bollettino dei Musei di Zoologia ed Anatomia Comparata della Reale Università di Torino* 10: 1–4.
- Hendrich L, Manuel M, Balke M (2019) The return of the Duke—locality data for *Megadytes ducalis* Sharp, 1882, the world's largest diving beetle, with notes on related species (Coleoptera: Dytiscidae). *Zootaxa* 4586(3): 517–535. <https://doi.org/10.11646/zootaxa.4586.3.8>
- Larson DJ, Alarie Y, Roughley RE (2000) Predaceous diving beetles (Coleoptera: Dytiscidae) of the Nearctic Region, with emphasis on the fauna of Canada and Alaska. National Research Council of Canada Research Press, Ottawa, Ontario, Canada, 982 pp.
- Michat MC (2006) Descriptions of larvae of *Megadytes* (Coleoptera: Dytiscidae: Dytiscinae): the hypothesis of monophyletic origin revisited. *European Journal of Entomology* 103(4): 831–842. <https://doi.org/10.14411/eje.2006.114>
- Michat MC (2010) Descriptions of larvae of *Megadytes* (Coleoptera: Dytiscidae: Dytiscinae): The subgenera *Trifurcitus* and *Megadytes* s. str., ground plan of chaetotaxy of the genus and phylogenetic analysis. *European Journal of Entomology* 107(3): 377–392. <https://doi.org/10.14411/eje.2010.047>
- Michat MC, Alarie Y, Watts CH (2015) Phylogenetic placement of the genus *Sternhydrus* (Coleoptera: Dytiscidae: Cybistrini) based on larval morphology, with description of *S. atratus*. *Annals of the Entomological Society of America* 108(5): 881–892. <https://doi.org/10.1093/aesa/sav067>
- Michat MC, Alarie Y, Miller KB (2017) Higher-level phylogeny of diving beetles (Coleoptera: Dytiscidae) based on larval characters. *Systematic Entomology* 42(4): 734–767. <https://doi.org/10.1111/syen.12243>
- Michat MC, Alarie Y, Watts CHS (2019) Dealing with a hairy beast-larval morphology and chaetotaxy of the Australian endemic diving beetle genus *Spencerhydrus* (Coleoptera, Dytiscidae, Cybistrini). *ZooKeys* 884: 53–67. <https://doi.org/10.3897/zookeys.884.38391>
- Miller KB (2000) Cladistic analysis of the tribes of Dytiscinae and the phylogenetic position of the genus *Notaticus* Zimmermann (Coleoptera; Dytiscidae). *Insect Systematics & Evolution* 31(2): 165–177. <https://doi.org/10.1163/187631200X00363>

- Miller KB (2001) On the phylogeny of the Dytiscidae (Coleoptera) with emphasis on the morphology of the female reproductive tract. *Insect Systematics & Evolution* 32(1): 45–92. <https://doi.org/10.1163/187631201X00029>
- Miller KB (2003) The phylogeny of diving beetles (Coleoptera: Dytiscidae) and the evolution of sexual conflict. *Biological Journal of the Linnean Society* 79(3): 359–388. <https://doi.org/10.1046/j.1095-8312.2003.00195.x>
- Miller KB (2013) Review of the genus *Cybister* Curtis, 1827 (Coleoptera: Dytiscidae: Dytiscinae: Cybistrini) in North America. *Coleopterists Bulletin* 67(4): 401–410. <https://doi.org/10.1649/0010-065X-67.4.401>
- Miller KB, Bergsten J (2014) The phylogeny and classification of diving beetles (Coleoptera: Dytiscidae). In: Yee DA (Ed.) *Ecology, Systematics, and Natural History of Predaceous Diving Beetles (Coleoptera: Dytiscidae)*. Springer, New York, 49–172. https://doi.org/10.1007/978-94-017-9109-0_3
- Miller KB, Bergsten J (2016) *Diving Beetles of the World*. Johns-Hopkins University Press, Baltimore, 336 pp.
- Miller KB, Bergsten J, Whiting MF (2007) Phylogeny and classification of diving beetles in the tribe Cybistrini (Coleoptera, Dytiscidae, Dytiscinae). *Zoologica Scripta* 36(1): 41–59. <https://doi.org/10.1111/j.1463-6409.2006.00254.x>
- Miller KB, Bergsten J, Whiting MF (2009) Phylogeny and classification of the tribe Hydaticini (Coleoptera: Dytiscidae): partition choice for Bayesian analysis with multiple nuclear and mitochondrial protein-coding genes. *Zoologica Scripta* 38(6): 591–615. <https://doi.org/10.1111/j.1463-6409.2009.00393.x>
- Mouchamps R (1957) Contribution a la connaissance des Cybisterini (Col Dytiscidae) du Musee d'Histoire Naturelle de Vienne (9e note). *Annalen des Naturhistorischen Museums in Wien* 61: 278–287.
- Nilsson AN (1988) A review of primary setae and pores on legs of larval Dytiscidae (Coleoptera). *Canadian Journal of Zoology* 66(10): 2283–2294. <https://doi.org/10.1139/z88-339>
- Nilsson AN, Hájek J (2023) A World Catalogue of the Family Dytiscidae, or the Diving Beetles (Coleoptera, Adephaga). 1.1.2023: 1–319.
- Nixon KC (2002) *WinClada*. 1.00.08 edn. Published by the author, Ithaca.
- Ribera I, Vogler AP, Balke M (2008) Phylogeny and diversification of diving beetles (Coleoptera: Dytiscidae). *Cladistics* 24(4): 563–590. <https://doi.org/10.1111/j.1096-0031.2007.00192.x>
- Sharp D (1882) On aquatic carnivorous Coleoptera or Dytiscidae. *Scientific Transactions of the Royal Dublin Society* 2: 179–1003. <https://doi.org/10.5962/bhl.title.9530>
- Trémouilles ER (1984) Notas sobre Coleoptera acuáticos Neotropicales. I. *Cybister* (*Meganectes*) *parvus* sp. nov. del Brasil (Coleoptera, Dytiscidae). *Revista de la Sociedad Entomológica Argentina* 43: 187–190.
- Trémouilles ER (1989a) Notas sobre Coleoptera acuáticos Neotropicales. II. Nuevos aportes al conocimiento del genero *Megadytes* Sharp (Coleoptera, Dytiscidae). Sobre ejemplares del British Museum (Natural History). *Revista de la Sociedad Entomológica Argentina* 45: 153–157.
- Trémouilles ER (1989b) Notas sobre Coleoptera acuáticos neotropicales. III. Datos ampliatorios sobre distrucion geografica de especies de *Megadytes* Sharp (Coleoptera, Dytiscidae). *Revista de la Sociedad Entomológica Argentina* 45: 159–161.
- Trémouilles ER, Bachmann AO (1980) La tribu Cybisterini en la Argentina (Coleoptera, Dytiscidae). *Revista de la Sociedad Entomológica Argentina* 39: 101–125.

Watts CHS (1963) The larvae of Australian Dytiscidae. Transactions of the Royal Entomological Society of South Australia 87: 23–40.

Watts CHS (1964) The larvae of Australian *Cybister* spp. Curt., *Homeodytes* spp. Reg. and *Hyderodes shuckardi* Hope (Coleoptera: Dytiscidae). Transactions of the Royal Society of South Australia 88: 145–156.

Appendix 1

Morphological characters used in phylogenetic analysis. Citations are provided for previous use of the characters in phylogenetic analyses. These should be consulted for more detailed descriptions and review of these characters.

Adult

Head

1. Setae on mandible; (0) discontinuous line, (1) continuous line (Char. 1, Miller 2000).
2. Eyes; (0) anteriorly emarginate, (1) anteriorly rounded (Char. 2, Miller 2000).

Thorax

3. Prosternal process; (0) not sulcate, (1) sulcate (Char. 48, Miller 2001).
4. Lateral marginal yellow band on pronotum; (0) absent (Figs 12–14), (1) present (Figs 9–11) (Char. 4, Miller et al. 2007).
5. Apicoventral setal patch on elytron; (0) absent, (1) present (Char. 8, Miller 2000).
6. Apicoventral setal patch on elytron; (0) line of stiff setae only along apical margin, (1) large field of fine setae, (2) large field of stiff setae (Char. 9, Miller 2000). Coded as “?” for taxa without an apicoventral setal patch (Char. 5).
7. Sexual sculpture on female elytron; (0) without short striae, (1) with short, longitudinal striae on elytra (2) with extensive anastomosing lines (Char. 7, Miller 2003).
8. Lateral marginal yellow band on elytron; (0) absent (Figs 12–14), (1) present (Figs 9–11) (Char. 9, Miller et al. 2007).
9. Oblongum cell on metathoracic wing; (0) oval shaped, (1) subtriangular (Fig. 7) (Char. 10, Miller et al. 2007).

Legs

10. Male anterior protibial spur; (0) absent, (1) present (Char. 11, Miller 2000).
11. Male posterior protibial spur; (0) absent, (1) present (Char. 12, Miller 2000).
12. Ventral protarsal adhesive setae on male; (0) apically with elongate, thin, flattened structures, (1) apically rounded, sucker-shaped (Char. 13, Miller 2000).
13. Posteroapical marginal setae on mesotibia; (0) absent medially, (1) present across entire margin (Char. 15, Miller 2000).
14. Posterodorsal series of setae on mesotibia; (0) apically simple, (1) apically bifid (Char. 17, Miller 2000).
15. Posteroventral series of setae on mesotibia; (0) apically simple, (1) apically bifid (Char. 18, Miller 2000).
16. Ventral adhesive setae on male mesotarsomeres; (0) absent, (1) present (Char. 22, Miller 2000).

17. Ventral adhesive setae on male mesotarsomeres; (0) dense field of apically simple setae, (1) apically with elongate, thin, flattened structures, (2) setae apically sucker-shaped (Char. 23, Miller 2000). Coded as “?” for taxa without ventral adhesive setae on male mesotarsomeres (Char. 15).
18. Line of setae at posterodorsal apical angle on mesotarsomeres I–IV (and protarsomeres I–IV of female); (0) absent, (1) present. Note that this series of setae was erroneously described as being “posteroventral” in position by Miller et al. (2007). All cybistrines have posteroventral series of setae, but only members of *Cybister* have a posterodorsal series of setae. This error was pointed out and corrected by Arce-Pérez et al. (2021).
19. Metacoxal processes: (0) not concave laterally; (1) concave laterally (Char. 6, Miller 2000).
20. Oblique groove across posterior surface of metatrochanter; (0) absent, (1) present (Char. 24, Miller 2000).
21. Natatory setae on dorsal margin of metafemur; (0) absent, (1) present (Char. 27, Miller 2000).
22. Anterior metatibial spur; (0) similar to posterior spur, unmodified, (1) apically acuminate, much broader than posterior spur (Figs 1–3) (Char. 31, Miller 2000).
23. Posterodorsal series of setae on metatibia; (0) a linear series, (1) a cluster (Fig. 1) (Char. 29, Miller 2000).
24. Natatory setae on ventral margin of metatarsomeres; (0) absent on females, present on males, (1) present in both sexes (Char. 36, Miller 2000).
25. Metatarsal claws; (0) male and female each with two claws, anterior shorter than posterior, (1) male and female with two claws, each the same length, (2) male and female with two claws, male with each the same length, female with posterior shorter than anterior (Figs 26–29), (3) male and female each with two claws, posterior shorter than anterior (Figs 19–25), (4) male with a single claw, female with two claws, posterior shorter than anterior (Figs 15–18), (5) male and female each with a single claw (Char. 35, Miller 2000).
26. Male stridulatory device using metacoxa and metatrochanter: (0) absent; (1) present (Char. 26, Miller et al. 2007).
27. Metacoxal lines; (0) absent, (1) present (Char. 27, Miller et al. 2007).
28. Anterior metatibial spur; (0) simple, (1) bifid or trifid (Figs 1–3). It seems likely that a spur that is apically branched is homologous whether it is bifid or trifid.

Abdomen

29. Transverse carinae on dorsolateral surface of abdominal ventrite II; (0) absent, (1) present (Char. 59, Miller 2001).

Male genitalia

30. Series of long setae on dorsal margin of lateral lobe; (0) absent, (1) present (Figs 32, 35, 38, 41, 46, 50) (Char. 38, Miller 2000).
31. Medial margin of male abdominal ventrite IX; (0) linear (Figs 53, 56, 57), (1) emarginate (Figs 51, 52, 54, 55).
32. Setae on dorsal margin of median lobe; (0) absent, (1) present (Char. 54, Miller 2003).

33. Male median lobe; (0) asymmetrical, (1) symmetrical (Figs 31, 34, 37, 40, 43, 45, 47, 49) (Char. 62, Miller 2001).
34. Apex of ventral sclerite; (0) various, (1) bifid (Figs 31, 34), (2) expanded and bilobate, spiny (Figs 42, 43, 45, 47).

Female genitalia

35. Female genital configuration; (0) Hydroporinae-type; (1) Dytiscinae-type (Char. 1, Miller 2001).
36. Accessory glands (or possibly other structures) on either side of base of common oviduct; (0) absent, (1) present (Figs 58, 59, 61–66) (Char. 32, Miller 2001).
37. Very large muscles surrounding vagina; (0) absent, (1) present (Char. 33, Miller 2001).
38. Series of short, stiff setae along medial margin of gonocoxosternite; (0) absent, (1) present (Figs 60, 62, 63) (Char. 14, Miller 2001).
39. Gonocoxae; (0) not fused, (1) fused along medial margin (Figs 58–66) (Char. 41, Burmeister 1976; Miller 2000).
40. Apicolateral setal pencil on gonocoxa; (0) absent, (1) present (Char. 44, Miller 2000).
41. Medial margin of gonocoxa; (0) not emarginate (Figs 60–66), (1) emarginate (Figs 58, 59).
42. Rami at apex of vagina; (0) smooth (Figs 58–63, 66), (1) laterally corrugated (Figs 64, 65).

Larva

Head

43. Anterior margin of clypeus; (0) evenly curved, (1) strongly excavated (Figs 67–71) (Char. 70, Miller 2003).
44. Rudimentary visual organ; (0) absent, (1) present. In larvae of Dytiscinae, anteromedially of the anterior row of stemmata there is a clear and rounded spot in the cuticle (Ferreira Jr 2000) called a “rudimentary visual organ” by Blunck (1917) and an “ocular spot” by Bertrand (1928).
45. Subdivision of the cephalic appendages (antenna, maxillary and labial palpi) into articles; (0) not subdivided, (1) subdivision of at least one segment into two articles, beginning with the second instar, (2) subdivision of at least one segment into three articles, beginning with the first instar (non-additive).
46. Antennomere I; (0) not subdivided, (1) subdivided into two articles.
47. Antennomeres II and III, subdivision; (0) not subdivided, (1) basal segment subdivided resulting in two unequal articles, beginning in the second instar, (2) basal segment subdivided into three articles, subequal in length, beginning with the first instar (non-additive).
48. Galea; (0) absent, (1) present.
49. Maxillary palpomere I (not including palpifer); (0) not subdivided, (1) basal segment subdivided, resulting in two unequal articles, beginning with the second instar, (2) basal segment subdivided into two subequal articles beginning with the first instar (non-additive).
50. Maxillary palpomere II; (0) not subdivided, (1) basal segment subdivided, resulting in two unequal articles beginning with the second instar, (2)

basal segment subdivided into two subequal articles beginning with first instar (non-additive).

- 51. Maxillary palpomeres III; (0) not subdivided, (1) basal segment subdivided, resulting in two unequal articles, (2) basal segment subdivided into two subequal articles (non-additive).
- 52. Apicomedial margin of labial prementum; (0) unmodified, (1) with single rounded projection, (2) with single, elongate, spinous projection.
- 53. Labial palpomeres; (0) not secondarily subdivided, (1) secondarily subdivided.

Abdomen

- 54. Abdominal tergites I–VI; (0) large, covering dorsum of each segment (1) reduced to a small plate located anteriorly on dorsum of segment.
- 55. Venter of abdominal segment VII; (0) not sclerotized, (1) sclerotized.
- 56. Urogomphi; (0) reduced, (1) well developed.
- 57. Urogomphi; (0) without fringe of setae, (1) with fringe of setae along lateral margins only; (2) with fringe of setae along lateral and medial margins.

Supplementary material 1

Character coding for phylogenetic analysis







Authors: Kelly B. Miller, Mariano C. Michat, Nelson Ferreira Jr

Data type: docx

Copyright notice: This dataset is made available under the Open Database License (<http://opendatacommons.org/licenses/odbl/1.0/>). The Open Database License (ODbL) is a license agreement intended to allow users to freely share, modify, and use this Dataset while maintaining this same freedom for others, provided that the original source and author(s) are credited.

Link: <https://doi.org/10.3897/zookeys.1188.110081.suppl1>

Biogeographic factors contributing to the diversification of Euphoniinae (Aves, Passeriformes, Fringillidae): a phylogenetic and ancestral areas analysis

Melisa Vázquez-López^{1,2}, Sandra M. Ramírez-Barrera¹, Alondra K. Terrones-Ramírez¹,
Sahid M. Robles-Bello¹, Adrián Nieto-Montes de Oca¹, Kristen Ruegg³, Blanca E. Hernández-Baños¹

¹ Museo de Zoología, Departamento de Biología Evolutiva, Facultad de Ciencias, Universidad Nacional Autónoma de México, Ciudad de México, Mexico

² Posgrado en Ciencias Biológicas, Universidad Nacional Autónoma de México, Ciudad de México, Mexico

³ Colorado State University, Fort Collins, Colorado, USA

Corresponding author: Blanca E. Hernández-Baños (behb@ciencias.unam.mx)



Academic editor: Grace P. Servat

Received: 26 May 2023

Accepted: 6 November 2023

Published: 8 January 2024

ZooBank: <https://zoobank.org/C143F759-A293-4508-BD25-F5A7ED250D23>

Citation: Vázquez-López M, Ramírez-Barrera SM, Terrones-Ramírez AK, Robles-Bello SM, Nieto-Montes de Oca A, Ruegg K, Hernández-Baños BE (2024) Biogeographic factors contributing to the diversification of Euphoniinae (Aves, Passeriformes, Fringillidae): a phylogenetic and ancestral areas analysis. ZooKeys 1188: 169–195. <https://doi.org/10.3897/zookeys.1188.107047>

Copyright: © Melisa Vázquez-López et al.
This is an open access article distributed under terms of the Creative Commons Attribution License ([Attribution 4.0 International – CC BY 4.0](https://creativecommons.org/licenses/by/4.0/)).

Abstract

Factors such as the Andean uplift, Isthmus of Panama, and climate changes have influenced bird diversity in the Neotropical region. Studying bird species that are widespread in Neotropical highlands and lowlands can help us understand the impact of these factors on taxa diversification. Our main objectives were to determine the biogeographic factors that contributed to the diversification of Euphoniinae and re-evaluate their phylogenetic relationships. The nextRAD and mitochondrial data were utilized to construct phylogenies. The ancestral distribution range was then estimated using a time-calibrated phylogeny, current species ranges, and neotropical regionalization. The phylogenies revealed two main Euphoniinae clades, *Chlorophonia* and *Euphonia*, similar to previous findings. Furthermore, each genus has distinctive subclades corresponding to morphology and geography. The biogeographic results suggest that the Andean uplift and the establishment of the western Amazon drove the vicariance of *Chlorophonia* and *Euphonia* during the Miocene. The *Chlorophonia* lineage originated in the Andes mountains and spread to Central America and the Mesoamerican highlands after the formation of the Isthmus of Panama. Meanwhile, the ancestral area of *Euphonia* was the Amazonas, from which it spread to trans-Andean areas during the Pliocene and Pleistocene due to the separation of the west lowlands from Amazonas due to the Northern Andean uplift. *Chlorophonia* and *Euphonia* species migrated to the Atlantic Forest during the Pleistocene through corridors from the East Andean Humid Forest and Amazonas. These two genera had Caribbean invasions with distinct geographic origins and ages. Finally, we suggested taxonomic changes in the genus *Euphonia* based on the study's phylogenetic, morphological, and biogeographic findings.

Key words: Atlantic Forest, Caribbean, diversification, Euphoniinae, Isthmus of Panama, Neotropical, trans-cis Andean areas

Introduction

The Neotropical region is known for its significant diversity, which results from a combination of events including the Andean uplift, the formation of the Isthmus of Panama, changes in the Amazon basin and riverine landscape,

and variations in vegetation biomes due to climatic oscillations and geologic events (Mittermeier et al. 2005; Hoorn et al. 2010; Smith and Klicka 2010; Ribas et al. 2012; Fox et al. 2015; Capurucho et al. 2018; Carneiro et al. 2018; Thode et al. 2019; Méndez-Camacho et al. 2021). Studies on biogeography and phylogeny have helped to identify the key drivers of biodiversity in the region. For instance, research on the phylogenetic relationships of widespread Neotropical avian lineages has revealed that biogeographic patterns may have resulted from multiple historical events at different periods (Smith et al. 2014), which have impacted highland and lowland species differently.

The Andean uplift had a significant impact on the diversification of both highland and lowland avifauna. One example of how the Andes Mountain range has impacted avifauna diversification is through the gradual uplift chain. This process resulted in speciation as species dispersed from lowlands to different altitudes (Ribas et al. 2007). Additionally, vicariant speciation occurred along the separated mountain blocks and changes in highland biomes due the climatic shifts (Gutiérrez-Zuluaga et al. 2021). Another way in which the Andean uplift influenced the avifauna is through the Miocene-Pliocene Northern uplift pulses. These pulses transformed the landscape of the northwestern Amazonas areas, creating a humid forest where there was once a wetland. This event was responsible for many Amazonas bird lineages originating in Western Amazonas (Carneiro et al. 2018). The Andean chain also separated avian lineages of the Pacific lowland forest from those of western Amazonas during the Pliocene. The impact of the Andean uplift on these biomes has also been observed in younger avian lineages (Reyes et al. 2023). In the lowlands, the Dry Diagonal also created a divide between the East Areas of the Amazonas, resulting in the formation of the Atlantic Forest, a biome with various endemic bird species. Biogeographic and phylogenetic research indicates that the diversification in this region may have been impacted by historical cycles of moist forest corridors in different parts of the Dry Diagonal that connected the Amazonas and the East Andean Forests with the Atlantic Forest (Capurucho et al. 2018; Trujillo-Arias et al. 2018). The Isthmus of Panama also played a role in the diversity of bird species in both the highlands and lowlands, facilitating the exchange of taxa in northward and southward directions across the Isthmus (Antonelli et al. 2010; Smith and Klicka 2010).

Phylogenetic and biogeographic studies on Neotropical birds that are widespread in highland and lowland tropical forests can provide insight into the drivers of biodiversity in lineages that inhabit the main Neotropical biomes. An interesting model taxon is the subfamily Euphoniinae, which belongs to the cosmopolitan family Fringillidae and is an extensive Neotropical endemic lineage (Zuccon et al. 2012). The subfamily consists of two genera, *Chlorophonia* (Bonaparte, 1851) and *Euphonia* (Desmarest, 1806), according to the current classification by the American Ornithological Society (Chesser et al. 2021). The first phylogenetic and biogeographic revision for this group was published just three years ago (Imfeld et al. 2020), which was significant for understanding Euphoniinae diversity in three different contexts: phylogenetic relationships, taxonomic implications, and biogeographic history. The study confirmed the paraphyly of the genus *Euphonia*, with the blue-headed Euphonias being the sister group of the *Chlorophonia* (Imfeld et al. 2020), based on this they formally resurrected the genus *Cyanophonia* (Bonaparte, 1851). However, the paraphyly was resolved by included these species into *Chlorophonia* genus (Chesser et al. 2021). This work also revealed that the genus

Euphonia represents the most speciose and oldest group in the subfamily (Imfeld et al. 2020), with five clades that partially agree with the previous morphological grouping (Isler and Isler 1999). Biogeographic analysis indicated that the ancestor of Euphoniinae arrived in South America from the Eastern Hemisphere via a transoceanic route (13.8–7.1 Mya), and then diversified in South America (Imfeld et al. 2020). The biogeographic patterns for the two Euphoniinae genera are different. The blue-headed *Chlorophonia* were widespread throughout North and South America until 1.8 Mya, and species diversification in this group could be the result of vicariant speciation drivers by Pleistocene climate cycles that isolated highland Neotropical forests (Imfeld et al. 2020). Meanwhile, in *Euphonia* and the rest of *Chlorophonia*, the older lineages evolved in South America, and the adaptations to the tropical environment implied northward migrations until the Isthmus of Panama was entirely formed, after which the tropical forest expanded to North America (Imfeld et al. 2020). According to the authors, these migrations to new areas resulted in new lineage diversification in both genera and added evidence that the Isthmus of Panama could have been completely closed during the Pliocene (Imfeld et al. 2020). The study also identified two independent Caribbean migrations from South America by island-hopping and over-water dispersal (Imfeld et al. 2020).

Despite this remarkable knowledge on Euphoniinae diversification, there are still unanswered questions. While it is suggested that the Euphoniinae lineage reached South America via a transoceanic route, doubt has been cast on this explanation by biogeographic evidence that indicates that deep lineages of Fringillidae could have originated in North America at an earlier stage (Oliveros et al. 2019), and the deepest nodes of other Fringillidae subfamilies have Palearctic distributions (Zuccon et al. 2012; Tietze et al. 2013). There is more than one example of Neotropical lineages that arrived from North America. Moreover, the arrival of Nearctic lineages to southern areas seems to be explained by the hypothesis of winter expansion ranges during the Miocene in Nearctic birds, which supports the northern origin of some Neotropical birds and posterior niche conservatism in the Neotropics (Kondo et al. 2008; Rolland et al. 2014; Winger et al. 2014; Zink and Gardner 2017). Furthermore, the factors that promoted the diversification of Euphoniinae in South America are still unclear because the study by Imfeld et al. (2020) did not represent the subregions in the Neotropics. This study aims to reconstruct the biogeographic history of Euphoniinae using a calibrated phylogeny and ancestral areas reconstruction based on current species ranges, South American Neotropical biomes, and Neotropical regionalization. Our main goal is to identify the biogeographic factors that led to the diversification of Euphoniinae, and our secondary objective is to reevaluate the phylogenetic relationships of Euphoniinae, using multiple samples of individual species and some allopatric subspecies to explore some intraspecific lineages for future research on the diversity of Euphoniinae. We also discuss the taxonomic implications of our findings.

Materials and methods

Sampling

We obtained 94 samples from the following collections: Louisiana State University Museum of Natural Science (**LSU**), The Field Museum of Natural History (**FMNH**), The Academy of Natural Sciences Philadelphia (**ANSP**), The Natural

History Museum at the University of Kansas (**KU**), The Museo Alfonso L. Herrera Facultad de Ciencias (**MZFC**), The American Museum of Natural History (**AMNH**), and The Consejo Superior de Investigaciones Científicas (**CSIC**) (Suppl. material 1: table S1). This dataset included 23 tissue samples from the eight species of the genus *Chlorophonia* and 65 samples from 22 of 25 species of the genus *Euphonia*. Tissue samples were not available only for three species of Euphoniinae (*E. chalybea*, *E. trinitatis*, and *E. concinna*). We could not obtain DNA from toe pad samples, so they are not included in our analysis. We included samples from allopatric morphotypes of three subspecies: *Chlorophonia cyanea cyanea*, *C. musica sclateri*, and *C. musica musica*. Also, we included representatives of the subspecies of three polytypic species: *E. chlorotica*, *E. violacea*, and *E. xanthogaster*. We included three representatives of the Carduelinae subfamily as outgroups: two samples of *Coccotharustes abeillei* and one of *Haemorrhous mexicanus*. Samples deposited at the MZFC collection were obtained under a field collection permit provided by the Instituto Nacional de Ecología, SEMARNAT, Mexico (FAUT-0169). To estimate divergence times, we incorporated three samples of the Fringillinae subfamily: *F. coelebs*, *F. montifringilla*, and one sample of *Rhodinocichla rosea* representing the sister group to Fringillidae, the New World nine-primaried Oscines (See Divergence time estimation below).

Laboratory processing and preparation for nextRAD sequencing

We extracted total genomic DNA from the tissue samples using the DNeasy tissues kit (Qiagen, Valencia, CA, USA) or the phenol: chloroform protocol (Hillis et al. 1996). The quality of DNA extractions was verified using gel electrophoresis. The DNA concentration was determined with a Qubit 3 fluorometer (ThermoFisher). The RAD sequence data was obtained using the nextRAD protocol (Russello et al. 2015) by the company SNPsaurus (<http://snpsaurus.com/>) (See Suppl. material 1: text S1 for details). The nextRAD libraries were sequenced on a single lane of an Illumina HiSeq 4000 with a single-end 150 bp protocol (University of Oregon). Raw sequence reads are available at GenBank SRA (BioProject accession PRJNA875486, see Suppl. material 1: table S1, the raw data are in the figshare repository: <https://doi.org/10.6084/m9.figshare.20744656>).

Quality filtering and de novo alignment

We used IPYRAD 0.9.50 (Eaton and Overcast 2020) to filter the raw reads and perform de novo alignment of the nextRAD data. To filter reads by quality, we only retained reads with a Phred Q score of 43, and adapters were strictly filtered. We retained reads with more than 100 base pairs. We avoided variations due to sequencing errors by setting to 12 the minimum statistical depth and minimum depth for majority-rule base calling parameters. We set the maximum number of unique alleles to two and the maximum proportion of shared polymorphic sites per locus to 0.5. To minimize paralogues in the alignment we optimized the cluster threshold (CT) with five metrics. The first three of these metrics were proposed by McCartney-Melstad et al. (2019): (1) the correlation of pairwise divergence with pairwise missingness, (2) the mean bootstrap values in a maximum likelihood tree-building framework, and (3) the cumulative variance of the first three PCs. The fourth was the total number of loci and SNPs recovered

(proposed by Mastretta-Yanes et al. 2015), and the fifth was the heterozygosity, proposed by Ilut et al. (2014). The rest of the parameters were set to their default values. The minimum number of samples with data for a locus to be included in the alignments was set to 43 (~ 50%). We performed the phylogenetic and time calibrated analysis using this final nextRAD sequence alignment.

Laboratory processing and alignment for the ND2 marker

We amplified the mitochondrial marker ND2 (NADH Dehydrogenase Subunit 2; Sorrenson 1999) via PCR in 12.5 mL reactions at a temperature of 54 °C. The sequencing was done by the Laboratorio de Secuenciación Genómica de la Biodiversidad y de la Salud, Instituto de Biología, UNAM. Sequence alignment was done with the algorithm MUSCLE (Edgar 2004) in the CIPRES Science Gateway (Miller et al. 2010). We included 68 sequences obtained from our tissue samples, for eight species of the genus *Chlorophonia* and 22 species of the genus *Euphonia* (GenBank accession numbers OP056102–OP056169, also see Suppl. material 1: table S1). Sequences were obtained from GenBank (Suppl. material 1: table S2) for *Chlorophonia occipitalis*, *E. affinis*, *E. godmani*, and *E. chlorotica*, including two samples from Imfeld et al. 2020 for *E. affinis* and *E. jamaica*. We also added outgroup species (one individual of *Haemorhous mexicanus*, one of *Coccothraustes coccothraustes*, and one of *Fringilla coelebs*) obtained from GenBank (Suppl. material 1: table S2).

Phylogenetic analyses

For the alignment of the nextRAD sequences, we calculated the partitions and evolutionary models using PARTITIONFINDER 2 (Lanfear et al. 2016) under the following configuration: branch lengths linked, rcluster search algorithm (Lanfear et al. 2012), and Bayesian Information Criterion (BIC) for model selection. Then, a Maximum Likelihood (ML) tree was generated using RAXML v. 8.0.0 (Stamatakis 2014) in the CIPRES Science Gateway (Miller et al. 2010), using the partitions obtained above under a GTRGAMMA nucleotide substitution model with 1000 bootstrap replicates, using simple bootstrap analysis. For the mitochondrial ND2 marker, we obtained the evolutionary model for each codon position with PARTITIONFINDER 2 (Lanfear et al. 2012). Then, we generated a ML phylogeny with RAXML v. 8.0.0 (Stamatakis 2014), using the partitions obtained above under a GTRGAMMA nucleotide substitution model with 1000 bootstrap replicates.

Time calibration tree

Divergence times were estimated for nextRAD sequences matrix with BEAST 2.6.3 (Bouckaert et al. 2019) implemented in the CIPRES Science Gateway (Miller et al. 2010). We assigned the partition schemes and evolutionary models obtained with PARTITIONFINDER 2 (Lanfear et al. 2012) (See section Phylogenetic analyses). We used secondary dating with a normal distribution and a calibration point based on the divergence between Fringillidae and the New World nine-primaried Oscines (17.1104 Mya; 95% HPD 14.7743–19.6278) calculated by Oliveros et al. (2019). For the molecular clock model, we selected the normal relaxed molecular clock following the recommendations of Drummond et al. (2006) and Li and Drummond (2012). We ran 50,000,000 generations, sampling every 1,000 genera-

tions, then we corroborated the effective sample size ($ESS > 200$) with TRACER v. 1.7.1 (Rambaut et al. 2018). Finally, we discarded the first 2,000 trees as burn-in and produced the maximum clade credibility tree with the highest 95% probability densities in TREE ANNOTATOR v. 1.8.0 (Rambaut and Drummond 2013). The tree was visualized with FIGTREE v. 1.4.1 (Rambaut and Drummond 2014).

Biogeographic range estimation

We estimated the biogeographic history of Euphoniinae species with BioGeoBears (Biogeography with Bayesian and likelihood Evolutionary Analysis in R Scripts) (Matzke 2013). This package implements a likelihood version of Dispersal Vicariance Analysis (DIVA; Ronquist 1997), Dispersal-Extinction Cladogenesis (DEC) from the LAGRANGE program (Ree and Smith 2008), and BayArea and Bayesian Binary Model (BBM) (RASP; Yu et al. 2015). We did not include the +j due to controversy over these models (see Ree and Smith 2008; Ree and Sanmartín 2018; Matzke 2022).

We used the nextRAD matrix data to obtain a calibrated tree (see section above for specifications) and we collapsed the sampling tree to a specie tree as is suggested in the WikiSite of BioGeoBears (http://phylo.wikidot.com/biogeobears-mistakes-to-avoid#no_specimen_trees). Because we were unable to sample all subspecies across the subfamily, we performed the BioGeoBears analysis at the species level. We defined seven areas based on the current species distributions of Euphoniinae, the principal biomes of South America (Nores 2020) and the Biogeographical regionalization of the Neotropical region by Morone (2014), using as reference the shapefiles by Löwenberg (2014): Caribbean; Mexican Transition Zone + Mesoamerica + Central America; Andes; Pacific W of Andes; Amazonas (the Amazon rainforest); Dry diagonal; and Paraná-Atlantic Forest. We allowed the occupation of up to three areas based on the ranges of the extant species. Finally, we compared the six different models for statistical fit via comparison of the Akaike weight (w_i) values. BioGeoBears (Matzke 2013) was used to obtain the range expansion (d), and range contraction (e).

Results

Quality filtering and de novo alignment

The percentage of reads that passed the quality filters was 97.66–98.95%, and the number of retained reads per sample ranged from 1,016,414 to 6,242,114. The optimal CT value was 0.87 (see the Suppl. material 1: Text S1 for details) Consensus sequence heterozygosis ranged from 0.00312 to 0.01760. The alignment used for phylogenetic inference recovered 2,570 loci and a total of 369,000 bp, the mean locus length was 141. The percentage of missing data for the sequence matrix was 37.43%, and the sample coverage ranged from 2165 loci to 311 loci (Suppl. material 1: tables S3, S4).

Phylogenetic analyses

For the nextRAD alignment, a total of 29 partitions were identified (See Suppl. material 1: table S5). The nextRAD ML phylogeny showed strong support for

two main clades, A and B, which had two and three strongly supported subclades, respectively (A1, A2 and B1, B2, B3; bootstrap values for all five clades = 100) (Fig. 1). These clades were also recovered in the ND2 ML phylogeny with lower support (Fig. 2). Clade A1 contained the green *Chlorophonia* species: *C. callophrys*, *C. cyanea*, *C. flavirostris*, *C. occipitalis*, and *C. pyrrhophrys*. Clade A2 contained the Blue-headed Euphonias: *C. elegantissima*, *C. cyanocephala*, and *C. musica*. Clade B1 contained the blue-black throated Euphonias: *E. affinis*, *E. chlorotica*, *E. finschi*, *E. godmani*, *E. saturata*, *E. luteicapilla*, *E. plumbea*, *E. saturata*, and *E. jamaica*. The sample of *E. affinis* from the study of Imfeld et al. (2020) was in the *E. luteicapilla* clade. The B2 clade contained nine species that we refer as the rufous Euphonias since they have characteristic patches of rufous color on their bellies, crest and/or undertail-coverts: *E. anneae*, *E. cayennensis*, *E. fulvicrisa*, *E. imitans*, *E. gouldi*, *E. mesochrysa*, *E. pectoralis*, *E. rufiventris*, and *E. xanthogaster*. The B3 clade contained the yellow-throated Euphonias: *E. chrysopasta*, *E. hirundinacea*, *E. lanirostris*, *E. minuta*, and *E. violacea*).

The nextRAD phylogeny and ND2 phylogeny presented some differences in the clade B2 (Figs 1, 2). In the ND2, tree *E. gouldi* was closer to *E. imitans* (bootstrap value = 52), while in the nextRAD tree *E. gouldi* was the sister species of *E. fulvicrisa*. Interestingly, in the nextRAD phylogeny *E. rufiventris* was paraphyletic with respect to *E. pectoralis*, whereas *E. cayennensis* was strongly supported as monophyletic (bootstrap value = 100). However, in the ND2 phylogeny, *E. rufiventris* was closer to *E. cayennensis* (bootstrap value = 78), and *E. pectoralis* was the sister group (bootstrap value = 100). *E. chrysopasta* also showed disagreement in its phylogenetic relationships between the nextRAD and ND2 trees: in the nextRAD tree it was placed in clade B3 with the yellow throated-euphonias (bootstrap value = 100), while in the ND2 tree it was placed in the rufous Euphonias group (bootstrap value = 87) (Fig. 2).

Our sampling included allopatric subspecies with unique morphotypes for *C. musica* and *C. cyanea*. We found a split between *C. musica musica* from the Dominican Republic and *C. musica sclateri* from Puerto Rico. A split also was recovered between the *C. cyanea cyanea* populations from Paraguay and the rest of the *C. cyanea* samples. We included in the genus *Euphonia* intraspecific samples for *E. chlorotica*, *E. xanthogaster* and *E. violacea* species. For the species *E. chlorotica*, we included six samples, which represented four subspecies—*E. c. serrirrostris* from Paraguay, *E. chlorotica amazonica* from Brazil, *Euphonia chlorotica amazonica* from Brasil and *E. c. taczanowskii* from Bolivia and Peru (Hilty 2020b)—which formed a monophyletic group without phylogenetic structure within the group. For *Euphonia xanthogaster*, the sample from Panama, *E. xanthogaster chocoensis*, was the sister taxon of the rest of the *E. xanthogaster* samples, and the samples from Cochabamba Bolivia formed a clade and represented the subspecies *E. x. ruficeps*. In *E. violacea*, our phylogeny recovered two clades, one for *E. v. rodwayi* from Trinidad and Tobago and *E. violacea violacea* from Guyana, and another from East Brazil, which corresponded to *E. violacea aurantiicollis*.

Calibrated tree

The Euphoniinae crown age was 7.58 Mya ago (95% HPD= 5.52–9.76) (Fig. 3). The *Chlorophonia* node split 5.52 Mya (95% HPD = 3.87–7.39), with the blue-headed *Chlorophonia* originating 1.8 Mya (95% HPD = 1.21–2.52)

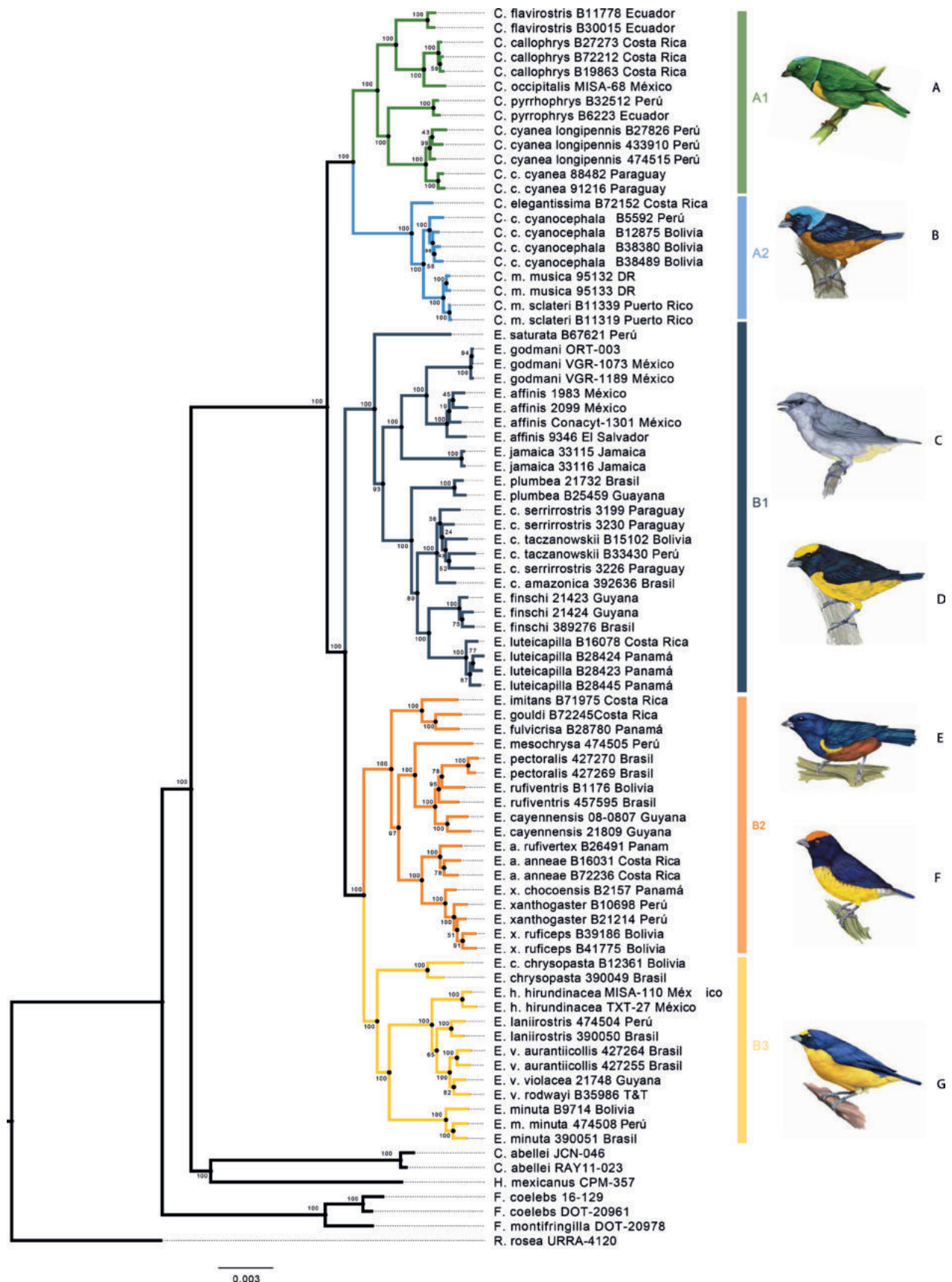


Figure 1. Maximum likelihood phylogeny with nextRAD data for Euphoniinae. A1, A2: genus *Chlorophonia*, B1, B2, and B3 genus *Euphonia*. From top to bottom, the illustrations depict **A** *C. occipitalis* **B** *C. elegantissima* **C** *E. jamaica* **D** *E. luteicapilla* **E** *E. pectoralis* **F** *E. anaeae* **G** *E. hirundinacea*. The illustrations were created by Germán García Lugo.

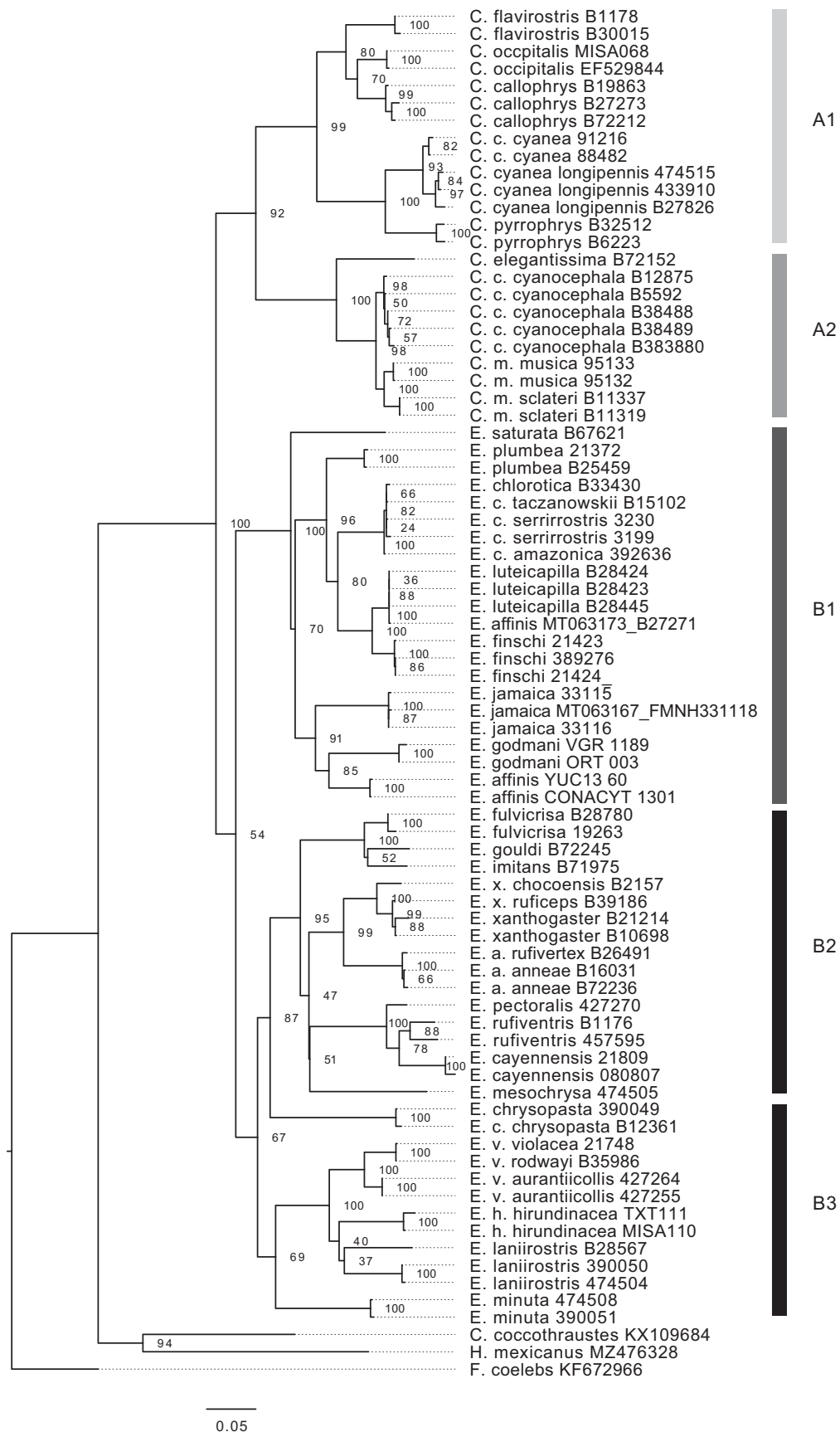


Figure 2. Maximum likelihood phylogeny based on ND2 data for Euphoniinae. A1 and A2: genus *Chlorophonia*, B1, B2, and B3 genus *Euphonia*.

and the green *Chlorophonia* node emerging 3.77 Mya (95% HPD = 2.63–5.10) (Fig. 3). The *Euphonia* crown age was estimated at 6.65 Mya ago (95% HPD = 5.28–9.13). Within *Euphonia*, the clade B1 node originated 5.05 Mya (95% HPD = 4.06–7.12), and clade B2–B3 5.66 Mya (95% HPD = 4.58–7.77), B2 node 4.20 Mya (95% HPD = 2.96, 5.53), B3 4.15 Mya (95% HPD = 2.99, 5.50) (Fig. 3).

Biogeographic range estimation

Our BioGeoBEARS results suggested that Fig. 4 was the best supported biogeographic model for our data, with an Akaike weight (ω_i) of 0.0004 (Table 1) (See Suppl. material 1: figs S1–S3). The range expansion d value was 0.041, and the value of range extinction was of $1.0e-12$. According to our results, the Euphoniinae ancestor established in northern South America, Andes, and Amazonas 7.58 Mya ago. Then, the Euphoniinae ancestral populations split into two main clades, *Euphonia* in the lowlands of Amazonas and *Chlorophonia* in the Andes. The blue-headed *Chlorophonia* ancestor was widespread in Mesoamerica, Caribbean, and South America, and the green *Chlorophonia* ancestor remained in the Andes. Within the blue headed *Chlorophonia*, *C. elegantissima* split in Mesoamerica. In contrast, the ancestor of *C. cyanocephala* and *C. musica* split in the Andes and the Caribbean. Currently, *C. cyanocephala* occupies two regions—the Andes and the Paraná-Atlantic Forest (by *C. cyanocephala cyanocephala*). *Chlorophonia musica* split in the Caribbean. Then, within the green *Chlorophonia*, *C. cyanea cyanea* invaded the Paraná-Atlantic Forest, and *Chlorophonia pyrrhophrys* stayed in the Andes. Finally, the ancestor of *Chlorophonia flavirostris*, *C. occipitalis*, and

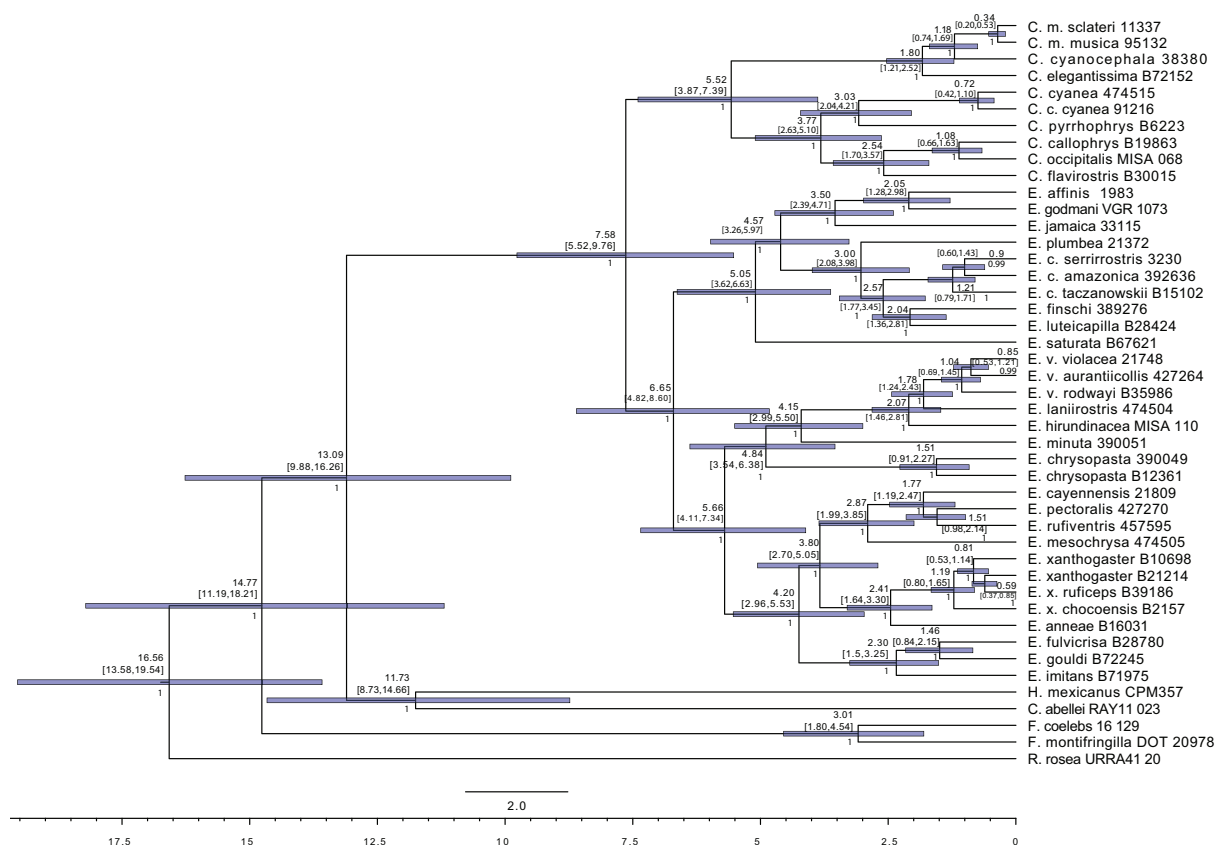


Figure 3. Time Calibrated Tree based on nextRAD data for Euphoniinae.

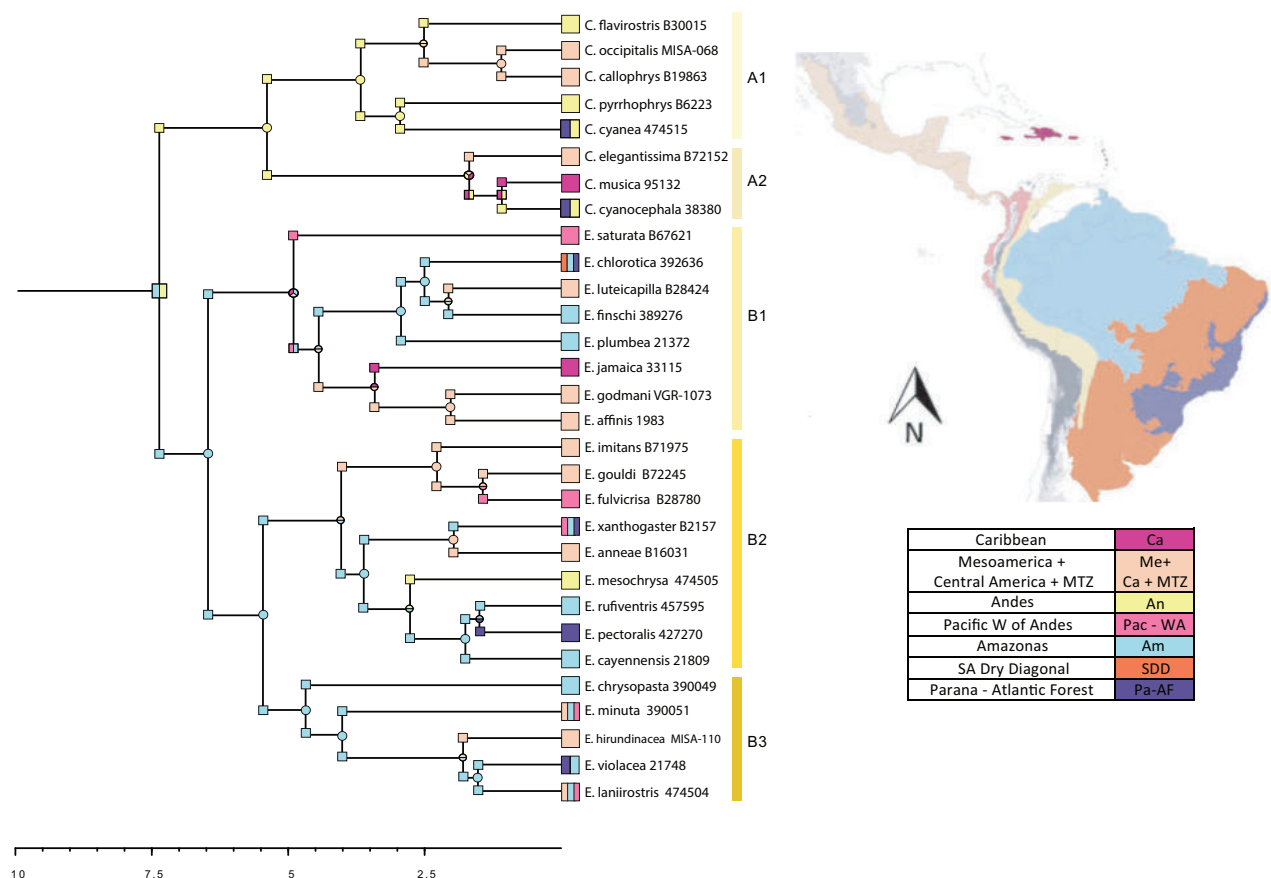


Figure 4. Biogeographical ancestral area reconstruction from BioGeoBEARS. Time Calibrated Tree with hypothetical ancestral areas and present areas and Biogeographical areas used in this study. The areas were mapped using ArcGIS (ArcMAP 10.2.2; Esri, Redlands, CA, USA) and the Biogeographic Regionalization on the Neotropical region shapefiles (Löwenberg 2014; Morrone 2014) see the text for more information.

C. callophrys moved northward and colonized Mesoamerica by range expansion. The first split event of *Euphonia* occurred in the biogeographic area of Amazonas, following by the split of the three main clades of *Euphonia* with different ancestral area: 1. Amazonas, Pacific W Andes, and Mesoamerica for *Euphonia* B1, 2. Amazonas and Mesoamerica for B2, and 3. Amazonas for B3. In the three main clades, posterior speciation events involved range expansion to trans-Andes areas such as Mesoamerica (by *E. imitans*, *E. gouldi*, *E. fulvicrisa*, *E. anaeae*, *E. minuta*, *E. hirundinacea*, *E. luteicapilla*, *E. affinis*, and *E. godmani*), and the Pacific (by *E. fulvicrisa*, *E. saturata*, and *E. xanthogaster*). There were also dispersals into other South American areas: Paraná-Atlantic Forest (by *E. xanthogaster*, *E. pectoralis*, *E. violacea*, and *E. chlorotica*) and the Andes area (by *E. mesochrysa*).

Discussion

This study aimed to identify the biogeographic patterns of Euphoniinae in the Neotropical Region and enhance our understanding of their phylogenetic relationships. The analysis revealed that the Euphoniinae ancestor likely migrated to the Neotropics from North America and arrived to South America via the Isthmus of Panama. In the Neotropics, the establishment of the Western Amazonas and the Northern Andean Miocene pulse likely led to vicariance events

between *Chlorophonia* and *Euphonia* ancestor. The ancestral range of *Chlorophonia* was in the Andes, whereas that of *Euphonia* was in the Amazonas. Speciation occurred in situ in the Andes for the green *Chlorophonia*, and the blue-headed *Chlorophonia* were widespread in the Neotropical highlands and the Caribbean. In *Euphonia*, some lineages diversified in trans-Andean areas by range expansion, while others reached South America's eastern zones, including the eastern Amazonas, Dry Diagonal, and Atlantic Coast. The findings are mostly consistent with the phylogeny reported by Imfeld et al. (2020) and other morphologically based groupings (Sibley and Monroe 1990; Isler and Isler 1999). Based on the results, in the discussion we propose genus-level taxonomic rearrangements.

Phylogenetic relationships

Our analysis of the phylogenetic relationships between Euphoniinae has identified two main groups, known as *Chlorophonia* and *Euphonia*, according to the current classification by the American Ornithological Society (Chesser et al. 2021). Within *Chlorophonia*, we have identified two distinct subgroups: *Chlorophonia* sensu stricto and the blue-headed *Chlorophonia*, subgroups A1 and A2 respectively, as shown in Figs 1, 2. These findings have been strongly supported by high bootstraps in both the nextRAD and ND2 phylogenies, which are consistent with the work of Imfeld et al. (2020). The relationships among the eight *Chlorophonia* species are also consistent with the findings of Imfeld et al. Our nextRAD phylogeny has confirmed that *Chlorophonia occipitalis* and *C. callophrys* are sister species, as previously shown in the mitochondrial phylogeny of Imfeld et al. (2020). Although some authors previously considered these to be a single species (Isler and Isler 1999), they are now recognized as separate species due to differences in their physical characteristics and geographic distributions.

The genus *Euphonia* is separated into three main groups (B1, B2, and B3) in both the nextRAD (Fig. 1) and the ND2 (Fig. 2) phylogenies. We will now present the significant findings for each of these groups in *Euphonia*. The *Euphonia* B1 group consists of the species from group 2 suggested by Isler and Isler (1999) plus *E. jamaica*, which was not associated with any species in Isler and Isler (1999). The coloration patterns support the evolutionary relationships between the members of this group, with the basal coloration pattern being the blue-black throat and yellow belly found in *E. saturata* and its two sister groups. One of these groups is the clade of *E. affinis* + *E. godmani*, whose sister group is *E. jamaica* (Figs 1, 2). Our calibrated phylogeny and ancestral reconstruction (Figs 3, 4) suggest that the ancestral lineage of these three species established in Mesoamerica and Central America from South America 2.39–4.71 Mya, likely due to the closure of the Panama Isthmus and the establishment of tropical forest in this area (Smith and Klicka 2010). Later, *E. affinis* and *E. godmani* split due to the formation of dry forest vegetation in the west Mesoamerica lowlands (Vázquez-López et al. 2020). The ancestral population of *E. jamaica* could have reached the island from Mesoamerica (see Fig. 4), and its unique color pattern is likely the result of environmental adaptations to the island, as suggested by Pregill and Olson (1981; cited in Isler and Isler 1999). In another group, we find *E. luteicapilla* as the sister taxon of *E. finschi*, and these two taxa formed a group with *E. chlorotica* and *E. plumbea*. Our phylogeny is consistent with

the geographic distribution of this group, as these species are distributed from Panama to South America with allopatric distributions. The predominant color pattern is blue-black throat and yellow belly, though *E. plumbea* is an exception. The species *E. trinitatis* and *E. concinna* were not included in the present study but were placed in this group by Imfeld et al. (2020), which did not include *E. godmani*. In this work, *E. affinis* + *E. godmani* are the sister group of *E. jamaica*, rather than *E. luteicapilla*, as previously reported by Imfeld et al. (2020). Indeed, in the ND2 phylogeny, the *E. affinis* sample of Imfeld et al. (2020) (MT063173) is embedded in the *E. luteicapilla* group, suggesting that the *E. affinis* sample of Imfeld et al. (2020) may have been misidentified. Future phylogenetic research that samples these species with more than one specimen could provide new information about this group's evolutionary relationships and diversification.

The phylogenetic relationships in the B2 and B3 clades are similar in those in the Imfeld et al. (2020) phylogeny, as well as the species groups of Sibley and Monroe (1990) and Isler and Isler (1999). Although these clades are sisters, they have differences in their color patterns, indicating species radiation. The *Euphonia imitans*, *E. gouldi*, and *E. fulvicrisa* species are in one clade, while *E. anneae* and *E. xanthogaster* are in another, consistent with the phylogeny of Imfeld et al. (2020) and previous species groups. The phylogenetic relationships coincide with coloration and geographic distribution, as these species are allopatric. Another clade contains *E. mesochrysa*, *E. pectoralis*, *E. rufiventris*, and *E. cayennensis*, with high support for the nextRAD phylogeny. The phylogenetic relationships of *E. pectoralis*, *E. rufiventris*, and *E. cayennensis* are less clear due to discordance between nuclear and mitochondrial data. Despite the uncertain relationships, the phylogenetic patterns could result from the history of the distribution of their habitat. These species inhabit humid forests with allopatric distributions in the Amazonas and the Atlantic Forest. However, evidence suggests that these biomes may have been in contact in the past, through corridors across the Dry Diagonal or the Northern Areas of the Atlantic East Coast (Prates et al. 2016; Trujillo-Arias et al. 2018). Further research is needed to resolve these species' phylogenetic relationships and biogeographic patterns. The B3 clade includes five species, with *E. violacea*, *E. laniirostris*, and *E. hirundinacea* forming a group due to their similar coloration (Isler and Isler 1999). Meanwhile, *E. minuta* and *E. chrysopasta* form their own group in Isler and Isler (1999). The ND2 phylogeny shows different relationships, with *E. chrysopasta* as the external branch of the B2 clade in the mitochondrial tree and as the external branch of the clade B3 in the nextRAD phylogeny. The relationship between *E. hirundinacea* and *E. laniirostris* may be inaccurate due to the lack of *E. chalybea* in the phylogeny, which is the external branch of these three species in the Imfeld et al. (2020) phylogeny. Further research is needed to resolve these species' phylogenetic relationships and biogeographic patterns.

Our research discovered distinct lineages in both *C. cyanea* and *C. musica* allopatric morphotype samples, which were strongly supported in the nextRAD phylogeny. The *C. cyanea cyanea* in the Atlantic Forest exhibited a different coloration pattern compared to other subspecies (Hilty and Bonan 2020), and the calibrated phylogeny backed the split for the *C. cyanea cyanea* clade 0.72 Mya ago. This may have been due to movement from the East Andes to the Atlantic Forest, crossing the corridor in the dry areas of the Cerrado and Chaco (Trujillo-Arias et al. 2017). *Chlorophonia musica* has two distinct clades in

our phylogenies, one from Puerto Rico and one from the Dominican Republic. *Chlorophonia musica* has three subspecies with allopatric distribution and differences in coloration, leading to these subspecies being considered separate species on multiple occasions (Greeney 2021). The phylogenies show intra-specific lineages for *E. xanthogaster* and *E. violacea* (Figs 1, 2). More extensive sampling is required to evaluate species boundaries in *E. xanthogaster* due to geographic variation and large genetic distance between samples and remarkable geographic variation (Hilty 2020a; Imfeld et al. 2020). Samples of *E. violacea rodwayi* and *E. violacea violacea* formed a monophyletic group, while *E. violacea aurantiicollis* formed its own clade; this subspecies is larger and isolated in the Atlantic Forest. These findings emphasize the importance of future studies with extensive sampling to better understand species limits and diversification in Euphoniinae (Vázquez-López et al. 2020).

Neotropical biogeographic patterns in Euphoniinae

Our analysis using BioGeoBEARS indicated that the biogeographic model DIVA-LIKE is the most suitable (see Table 1). The models suggest that range expansion and vicariance were the primary mechanisms behind the diversification of Euphoniinae in the Neotropical Region (see Table 1). Euphoniinae was present in South America ~ 7.58 million years ago (5.52–9.76 Mya) (Fig. 4). This suggests that the Euphoniinae lineage could have reached South America from North America across the first emergences of the Isthmus of Panama (Morgan 2008; Verzi and Montalvo 2008; Bacon et al. 2015; Montes et al. 2015). It is possible that the Euphoniinae ancestor colonized the Neotropics from North America (Oliveros et al. 2019) due to the expansion of their winter ranges during the Miocene climate changes, followed by range contraction in the northern areas. There is substantial evidence of this pattern in Neotropical decedents of temperate avian lineages (Kondo et al. 2008; Rolland et al. 2014; Winger et al. 2014; Zink and Gardner 2017). After diversifying in South America, Euphoniinae could not recolonize temperate zones due to niche conservatism (Winger et al. 2019). Our results suggest that the two main lineages of Euphoniinae occupied the Andes and Amazonas during the late Miocene (Fig. 4), with *Chlorophonia* (5.52 Mya) in the Andes and *Euphonia* (6.65 Mya) in the Amazonas (Figs 3, 4). This pattern could result from the Central and North Andes uplift pulses and the establishment of the Western Amazonas (Antonelli et al. 2010; Hoorn et al. 2010; Carneiro et al. 2018). The *Chlorophonia* genus has an ancestor that was primarily found in the Andes mountains, and only a few subspecies (*C. cyanea*, *C. musica*, and *C. cyanocephala*) have dispersed to lowlands. Similar patterns have been observed in other Andean bird species (Sedano et al. 2010; Beckman and Witt 2015). The biogeographic results suggest that the majority

Table 1. BioGeoBEARS analysis models, parameters, and scores. Models. Values of Log-Likelihood (LnL), Numbers of Parameters (P), Range expansion (d), Range Contraction (e), Akaike Information Criterion (AIC), and Akaike weight (ω_i).

Model	LnL	P	d	e	AIC	ω_i
DEC	-98.32	2	0.039	0.032	200.6	2.9e-06
DIVALLIKE	-93.32	2	0.041	1.0e-12	190.6	0.0004
BAYAREALIKE	-103.2	2	0.043	0.26	210.5	2.1e-08

of speciation events for the A1 clade occurred in the Andes, with some range expansion events to the Central American Forests and one event of dispersion to Eastern South America. Meanwhile, the ancestor of the A2 clade dispersed in Mesoamerica, the Andes and the Caribbean ~ 1.8 million years ago, before *C. elegantissima* split in Mesoamerica and after *C. musica* split in the Caribbean (Fig. 3); similar patterns were found by Imfeld et al. (2020). In contrast, the biogeographic results for the genus *Euphonia* suggests that the ancestor of the main clades of *Euphonia* originated in the Amazonas region, likely in the western area; this pattern has been previously observed in other bird taxa (Carneiro et al. 2018; Silva et al. 2019). Allopatric distributions are common among sister species in *Euphonia*, this could be resulted from range expansion and some dispersal events to new areas followed by vicariance, as the biogeographic results indicate. The three main clades of *Euphonia* have different ancestral areas, and there were two independent trans-Andean migration events: Pacific W Andes and Mesoamerica for *Euphonia* B1 and Mesoamerica for *Euphonia* B2. Meanwhile, B3 remained in the Amazonas. Further discussion on the areas and timing of Euphoniinae diversification in the Neotropics can be found below.

Trans-Andean diversification and the role of the Isthmus of Panama

According to the biogeographic analysis, multiple invasions to trans-Andean areas occurred with different origins and ages in both *Euphonia* and *Chlorophonia*. During the Pliocene, the *Euphonia* B1 and B2 lineages moved from the Amazonas to trans-Andean areas, while another three lineages split after reaching the trans-Andean areas during the Pleistocene: *E. luteicapilla*; *E. anneae* – *E. xanthogaster*; and the ancestor of *E. hirundinacea*, *E. lanirostris*, and *E. violacea*. The Pliocene splits from the Amazon could be explained by the isolation of the lowland forests west of the Amazon basin by the final Northern uplift (8–4 Mya) (Gregory-Wodzicki 2000; Pérez-Consuegra et al. 2021), while the younger trans-Andean lineages could be explained by dispersal events after the northern Andean uplift. Additionally, the analysis suggests that *E. mesochrysa* split in the Andes, after the range expansion of its ancestor. For *Chlorophonia*, diversification in the trans-Andean areas involved range expansion to Central America from the Andes. The A2 clade was in northern areas, and *C. elegantissima* split in Mesoamerica. This pattern agrees with the previous report for Euphoniinae (Imfeld et al. 2020) and with the sinking finches (Beckman and Witt 2015). Overall, the trans-Andean species established in Mesoamerica and Central America during the Pliocene and Pleistocene, which could be the effect of the entirely closed of the Isthmus of Panama and Neotropical habitats outside of South America, before 3.5 Mya ago (Smith and Klicka 2010; Bacon et al. 2015; Imfeld et al. 2020).

Diversification in the Cis Andean areas

The distribution patterns of Euphoniinae in the East side of South America contrast between *Chlorophonia* and *Euphonia* since the analyses suggest that *Chlorophonia* reached east areas from the Andes and *Euphonia* reached east areas from the Amazonas (Fig. 4). The Atlantic Forest is separated from the East South Andean Forest by the dry diagonal of South America. However, many related avian lineages inhabit both biomes, which suggests a past connection. Additionally,

paleoclimatic studies suggest that the East South Andean Forest and Atlantic Forest were connected during the Quaternary by cyclical corridors of humid forest in the currently dry areas of the Cerrado and Chaco (Trujillo-Arias et al. 2017). This evidence, along with our phylogenetic analysis, suggest that *C. cyanea* could have reached the Atlantic Forest by the Cerrado and Chaco corridors ~ 0.7233 Mya (Fig. 3), consistent with other endemic lineages of the Atlantic Forest (Trujillo-Arias et al. 2017, 2018; Cabanne et al. 2019). In *Euphonia*, older taxa are found in the western area of the Amazonas and younger taxa in the areas east of the Amazon basin (Fig. 4): *E. plumbea*, *E. finschi*, and *E. chlorotica*. This pattern could be the result of a combination of factors such as Andean uplift, Pleistocene climate, and changes in the river (Hoorn et al. 2010; Carneiro et al. 2018; Silva et al. 2019). However, a detailed description of the Amazonian diversification of these taxa is outside the scope of this work. The Amazonas is isolated from the Atlantic Humid Forest by the Dry Diagonal, and some *Euphonia* species have allopatric populations in the Atlantic Forest. *Euphonia chlorotica* is an exception, as it migrated from the Amazon River to the Dry Diagonal and the Atlantic Forest ~ 2.57 Mya, probably during the Plio-Pleistocene expansion of the Dry Diagonal (Coscáron and Morrone 1998; Luebert et al. 2011; Luebert 2021). Meanwhile, the related species, *E. rufiventris*, *E. cayennensis*, and *E. pectoralis*, have separate distributions in the Western-Central Amazonas, East Amazonas, and Atlantic Forest, respectively. According to the calibrated tree and the biogeographic analysis, it is likely that *E. pectoralis* arrived in the Atlantic Forest from either the Southeast Amazonas or Northeastern Brazil, the corridors proposed between the Amazonas and Atlantic Forest (Prates et al. 2016; Trujillo-Arias et al. 2018). Similar phylogenetic patterns were found for *E. violacea aurantiicollis*, an Atlantic Forest subspecies. Other *Euphonia* species also inhabit the Atlantic Forest area, such as *E. xanthogaster xanthogaster*, *E. chalybea*, and *E. chlorotica amazonica*, but were not included in the biogeographic analysis. Further research on phylogeography will help us better understand the biogeographic pattern for each *Chlorophonia* and *Euphonia* species in the East Atlantic Coast area.

Caribbean invasions

In Euphoniinae, two species are distributed in the Caribbean: *E. jamaica* and *C. musica*. The biogeographic analysis conducted has revealed that they migrated to the Caribbean from continental North American and South American regions at different times. The findings suggest that the ancestor of *C. cyanocephala* – *C. musica* was in South America and the Caribbean during the Pleistocene period, which occurred ~ 1.18 million years ago, possibly traveling in a northward direction from the Andes as was described by Imfeld et al. (2020). Meanwhile, the *E. jamaica* lineage arrived in the Caribbean earlier, ~ 3.5 million years ago, after migrating from the Mesoamerica-MTZ-CA area, possibly over water. The Parsimony Biogeographic Patterns of the Caribbean Basin have revealed that the Greater Antilles and Yucatan-Central American countries are sister areas, nested from north to south (Vázquez-Miranda et al. 2007).

Taxonomic revisions

Imfeld et al. 2020 proposed the resurrection of *Cyanophonia* (Bonaparte, 1851) as the genus of blue-headed *Euphonia* and they assigned *Cyanophonia musica*

as the type species for the genus (Gmelin 1789). Type locality: Santo Domingo, Dominican Republic). However, in the Sixty-second Supplement to the American Ornithological Society's Checklist of North American Birds (Chesser et al. 2021), the three blue-headed *Euphonia* were merged into the genus *Chlorophonia*. We believe that the blue-headed *Euphonia* taxonomy needs to be reconsidered, and we also recommended the resurrection of *Cyanophonia* (Bonaparte, 1851) to denote the three species of blue-headed *Chlorophonia*. Furthermore, three lines of evidence suggest an independent evolutionary history of these three species from the rest of *Chlorophonia*:

1. The differences in the color pattern (Fig. 1) — the blue head patches are a shared character between the *Chlorophonia sensu stricto* and blue-headed *Chlorophonia*. However, *Chlorophonia sensu stricto* has a predominantly green coloration, while blue-headed *Chlorophonia* have a rufous belly and glossy dark blue back and throat.
2. The phylogenetic distinction — all the phylogenies so far show a well-supported split into two clades.
3. The biogeographic patterns also show differences between these groups — both share an ancestral population in the Andes, but in *Chlorophonia sensu stricto* cladogenesis continued in the Andes and from there reached other South American Areas and Mesoamerica; meanwhile, the blue-headed *Chlorophonia* lineages were widespread in North and South America. Imfeld et al. (2020) also reported these differences in the biogeographic patterns.

We also propose that the *Euphonia* taxonomy be reviewed, since this is a larger group than *Chlorophonia* – *Cyanophonia*, with three phylogenetic groups that also display morphological particularities.

1. The first group include the groups proposed by Isler and Isler (1999), 1 *Euphonia jamaica* and 2 – *E. saturata*, *E. chlorotica*, *E. luteicapilla*, *E. finschi*, *E. plumbea*, *E. godmani*, *E. affinis*, *E. trinitatis*, and *E. concinna*. These species inhabit lowlands habitats and display the classic *Euphonia* pattern of dark blue throat with yellow belly (Fig. 1). Even *E. plumbea* displays similar patterns but with paler coloration. *Euphonia jamaica* has a classic finch bill and does not have the pattern of a black throat; however, we assign it to this group because of its phylogenetic position.
2. The second group include the Isler and Isler (1999) group 3: *E. violacea*, *E. lanirostris*, *E. hirundinacea*, *E. chalybea*; group 6 *E. minuta*; and *E. chrysopasta* from group 7. These species display a pattern of yellow throat, yellow crest, and black back that can have purple, blue or green gloss. In this group *E. chrysopasta* and *E. minuta* do not show yellow throat plumage, however, the females display a similar pattern to *E. hirundinacea* and *E. chalybea*.
3. The third group has nine species of three of the groups Isler and Isler (1999); group 5: *E. fulvicrissa*, *E. imitans*, *E. gouldi*, *E. mesochrysa*; group 7: *E. anneae*, *E. xanthogaster*; and group 8: *E. rufiventris*, *E. pectoralis*, and *E. cayennensis*. The character that defines this group is the rufous color patches, which can be on the belly, the crest and/or the undertail-coverts, in adult males and females.

The genus *Euphonia* was established by Desmarest (1806) with a female specimen of *Euphonia olivacea*, which is listed as a synonym of *Euphonia minuta* in the ‘Histoire naturelle des Tangaras, des Manakins et des Todiers’ by name (date), but without a clear description for the genus:

The bird for which we give a figure named Euphone olive is entirely in a different case. It does not have very bright colors, and its small size makes us suspect that it is a female or a young individual, but we do not know to what species to refer it because its plumage presents no clue which could serve to establish a connection. It was recently sent to the Jardin des Plantes among many birds from Cayenne.

Bonaparte (1851) suggested the genus *Pyrrhuphonia* for finch-billed *Euphonia*, the type species of which is *Euphonia jamaica* (Linnaeus, C 1766) (type locality: Jamaica). Cabanis (1861) suggest the genus *Phonasca* for *Euphonia* similar to *E. chlorotica* and *E. violacea*, and he listed the following species as *Phonasca*: *E. chlorotica*, *E. xanthogaster*, *E. fulvicrissa*, *E. trinitatis*, *E. luteicapilla*, *E. affinis*, *E. minuta*, *E. chalybea*, *E. hirundinacea*, *E. lanirostris*, and *E. violacea*. In that work, he described *E. saturata* and *E. luteicapilla*. Many *Euphonia* species were described under the genus *Tanagra* (Linnaeus 1764 or 1766); however, this genus is unavailable because it has been suppressed and placed on the Official Indices of Rejected and Invalid Names in Zoology (ICZN Opinion 852, Bull. Zool. Nom., 25: 74–75, 27 September 1968), since it was described twice for very different species. Also, this genus was widely used to name species that now are in different families (e.g., Thraupidae: *Anisoganthus notabilis*, Passerilidae: *Chlorospingus flavopectus*, Cardinalidae: *Piranga ludoviciana*, Fringillidae: *Euphonia affinis*).

Consequently, we propose that the blue-black throated group remain as *Euphonia* (Desmarest, 1806), since it is the core group of the “true” *Euphonia* clade, with ten species, and these species display the characteristic pattern coloration of euphonias. The oldest *Euphonia* species in this group were described by Linnaeus (1766)—*E. jamaica* and *E. chlorotica*—of these two only *Euphonia chlorotica* has the classic euphonia pattern coloration. The yellow-throated group could be named *Phonasca* (Cabanis, 1861), which was previously nominated for five of the six species of this group by Cabanis (1861). We designate the Violaceous Euphonia, *Phonasca violacea* as the type species, since it is the first species described in 1758 by Linnaeus. Finally, we propose a new genus for the rufous clade: *Rufiphonia* gen. nov. based on their rufous patches, and we designate the Rufous-bellied *Euphonia* *Rufiphonia rufiventris* (Vieillot, 1819) as the type species. We propose a new genus because there is no available name for a third group in *Euphonia*.

***Rufiphonia* Vázquez-López & Hernández-Baños, gen. nov.**

<https://zoobank.org/D112E1E4-502C-438F-BF66-2C081D6D5745>

Type species. *Rufiphonia rufiventris* (Vieillot, 1819). Type locality: Perú.

Included species. *Rufiphonia fulvicrissa* (Sclater, 1857), type locality: Santa Martha, New Granada; *R. imitans* (Hellmayr, 1936), type locality: El Pozo, Rio Terraba, Costa Rica; *R. gouldi* (Sclater, 1857), type locality: Guatemala; *R. me-*

sochrysa (Salvadori, 1873) type locality: No locality given, Bogotá, Colombia; *R. anneae* (Cassin, 1865), type locality: Santa Rosa, Costa Rica, *R. xanthogaster* (Sundevall, 1834), type locality: Río de Janeiro, Brazil; *R. pectoralis* (Latham, 1801), and *R. cayennensis* (Gmelin, 1789), type locality: Guyana.

Morphological description. Most males of this genus display the classic *Euphonia* pattern of dark blue throat and back with yellow belly, with four exceptions. *R. gouldi* and *R. mesochrysa* have olive upper parts with grey-blue glosses. The males of *R. cayennensis* and *R. pectoralis* have predominantly dark and glossy metallic-blue plumage. Also, the males could have a forehead in yellow or rufous, a rufous belly, and undertail coverts in rufous. The females are primarily olive with contrasting rufous patches on the forehead, belly, or undertail coverts.

Diagnosis. The new genus can be distinguished from all other *Euphonia* species by the rufous color patches, which can be on the belly, the crest, and/or the undertail-coverts, in both male and female adults.

Conclusions

1. The nextRAD and ND2 phylogenies obtained in this study are generally consistent with the UCE and mitochondrial phylogenies of Imfeld et al. (2020).
2. Minor clades contained morphologically similar species with allopatric distribution ranges.
3. The biogeographic results suggest that the Andean uplift and the establishment of the western Amazonas drove the vicariance of *Chlorophonia* and *Euphonia* during the Miocene, with the Andes and the Amazonas as each ancestral area, respectively. The green *Chlorophonia* has an ancestor that was primarily found in the Andes mountains; after the establishment of the Isthmus of Panama, the *Chlorophonia* lineage reached the Central American and Mesoamerican highlands from the Andes. In contrast, *Euphonia* suggests that the ancestor of the main clades of *Euphonia* could have originated in the western Amazonas. The genus *Euphonia* reached trans-Andean areas from the Amazonas during the Pliocene and Pleistocene as a consequence of the vicariance of the west lowlands and the Amazonas. *Chlorophonia* and *Euphonia* species reached the Atlantic Forest biome during the Pleistocene, probably through the corridors that connected the East Andean Humid Forest and the Amazonas. *Chlorophonia* and *Euphonia* each had a Caribbean invasion with different geographic origins and ages.
4. We recommend recognizing the genus *Cyanophonia* for the species *Chlorophonia musica*, *Chlorophonia cyanocephala*, and *Chlorophonia elegantissima* since they represent a differentiated lineage in phylogeny, in their coloration patterns, and in their biogeographic history. Lastly, we propose a revision of the taxonomy of the genus *Euphonia* because there are three differentiated lineages at the phylogenetic, biogeographic, and morphological levels.

Acknowledgments

We thank the following institutions and people for providing samples: Museo de Zoología Alfonso L. Herrera (UNAM), Museum of Natural Science (Louisiana State University), The Natural History Museum (UK), The Academy of Natural

Sciences (ANSP), Field Museum of Natural History (FMNH), Consejo Superior de Investigaciones Científicas (CSIC). Donna Dittman (LSU), M. Robbins (UK), Nate Rice (ANSP), Paul Sweet (AMNH), and John Bates (FMNH). We thank Alejandro Gordillo Martínez, Isabel Vargas Fernández, and Raul Ivan Martínez Becerril for technical help. We thank the Laboratorio de Cómputo de Alto Rendimiento de la Facultad de Ciencias (UNAM) for providing facilities to perform the research reported in this paper, and to Miguel Angel Perez Leon for technical support in the informatics process. We thank Germán García Lugo for making the illustrations of Euphoniinae species (see his work at Instagram profile: @germangarcialugo). We thank Lynna Kiere for reviewing the English. This paper forms part of the requirements for obtaining a Doctoral degree of Alma Melisa Vázquez López at the Posgrado en Ciencias Biológicas, Universidad Nacional Autónoma de México (UNAM).

Additional information

Conflict of interest

The authors have declared that no competing interests exist.

Ethical statement

No ethical statement was reported.





Funding

This research was supported by PAPIIT/DGAPA, Universidad Nacional Autónoma de México (UNAM), through a grant to Blanca E. Hernández-Baños (IN204017 and IN214523). Alma Melisa Vázquez López was supported by a scholarship from CONA-CyT and PAPIIT-DGAPA (IN220620).

Author contributions

M. Vázquez-López designed the research and performed the research, worked in the laboratory, analyzed data, and wrote the paper. S.M. Ramírez-Barrera analyzed the data and reviewed the paper. A.K. Terrones-Ramírez analyzed the data and reviewed the paper. S.M. Robles-Bello worked in the laboratory and analyzed the data. A. Nieto-Montes de Oca reviewed the analyses and the results and the final version of the paper. K. Ruegg reviewed the analyses and the results and the final version of the paper. B.E. Hernández-Baños designed the research, reviewed the results and wrote the paper.

Author ORCIDs

Melisa Vázquez-López  <https://orcid.org/0000-0002-1365-1860>
Sandra M. Ramírez-Barrera  <https://orcid.org/0009-0005-3999-1934>
Alondra K. Terrones-Ramírez  <https://orcid.org/0000-0002-1486-0023>
Sahid M. Robles-Bello  <https://orcid.org/0000-0003-1126-0150>
Adrián Nieto-Montes de Oca  <https://orcid.org/0000-0002-8150-8361>
Kristen Ruegg  <https://orcid.org/0000-0001-5579-941X>
Blanca E. Hernández-Baños  <https://orcid.org/0000-0002-6222-4187>

Data availability

All of the data that support the findings of this study are available in the main text or Supplementary Information.

References

- Antonelli A, Quijada-Mascareña A, Crawford AJ, Bates J, Velazco PM, Wüster W (2010). Molecular studies and phylogeography of Amazonian tetrapods and their relation to geological and climatic models. In: Hoorn C, Wesselingh FP (Eds) Amazonia: Landscape and Species Evolution: A look into the past. Blackwell Publishing, UK, 386–404. <https://doi.org/10.1002/9781444306408>
- Bacon CD, Silvestro D, Jaramillo C, Smith BT, Chakrabarty P, Antonelli A (2015) Biological evidence supports an early and complex emergence of the Isthmus of Panama. *Proceedings of the National Academy of Sciences of the United States of America* 112(19): 6110–6115. <https://doi.org/10.1073/pnas.1423853112>
- Beckman EJ, Witt CC (2015) Phylogeny and biogeography of the New World siskins and goldfinches: Rapid, recent diversification in the Central. *Molecular Phylogenetics and Evolution* 87: 28–45. <https://doi.org/10.1016/j.ympev.2015.03.005>
- Bonaparte CL (1851) Note sur les Tangaras, leurs affinités, et descriptions d'espèces nouvelles. *Revue et Magasin de Zoologie Pure et Appliquée* 2: 129–138.
- Bouckaert R, Vaughan TG, Barido-Sottani J, Duchêne S, Fourment M, Gavryushkina A, Heled J, Jones G, Kühnert D, De Maio N, Matschiner M, Mendes FK, Müller NF, Ogilvie HA, du Plessis L, Popinga A, Rambaut A, Rasmussen D, Siveroni I, Suchard MA, Wu C-H, Xie D, Zhang C, Stadler T, Drummond AJ (2019) BEAST 2.5: An advanced software platform for Bayesian evolutionary analysis. *PLOS Computational Biology* 15(4): e1006650. <https://doi.org/10.1371/journal.pcbi.1006650>
- Cabanis JL (1861) Uebersicht der im Berliner Museum befindlichen Vögel von Costa Rica. *Journal für Ornithologie* 8(1860): 321–336. <https://doi.org/10.1007/BF02002664>
- Cabanne GS, Campagna L, Trujillo-Arias N, Naoki K, Gómez I, Miyaki CY, Santos FR, Dantas GPM, Aleixo A, Claramunt S, Rocha A, Caparroz R, Lovette IJ, Tubaro PL (2019) Phylogeographic variation within the Buff-browed Foliage-gleaner (Aves: Furnariidae: *Syndactyla rufosuperciliata*) supports an Andean-Atlantic forests connection via the Cerrado. *Molecular Phylogenetics and Evolution* 133: 198–213. <https://doi.org/10.1016/j.ympev.2019.01.011>
- Capurrocho JMG, Ashley MV, Ribas CC, Bates JM (2018) Connecting Amazonian, Cerrado, and Atlantic Forest histories: Paraphyly, old divergences, and modern population dynamics in tyrant-manakins (Neopelma/Tyrannetes, Aves: Pipridae). *Molecular Phylogenetics and Evolution* 127: 696–705. <https://doi.org/10.1016/j.ympev.2018.06.015>
- Carneiro L, Bravo GA, Aristizábal N, Cuervo AM, Aleixo A (2018) Molecular systematics and biogeography of lowland antpittas (Aves, Grallariidae): The role of vicariance and dispersal in the diversification of a widespread Neotropical lineage. *Molecular Phylogenetics and Evolution* 120: 375–389. <https://doi.org/10.1016/j.ympev.2017.11.019>
- Chesser RT, Billerman SM, Burns KJ, Cicero C, Dunn JL, Hernández-Baños BE, Kratter AW, Lovette IJ, Mason NM, Rasmussen PC, Remsen Jr JV, Stotz DF, Winker K (2021) Sixty-second Supplement to the American Ornithological Society's Check-list of North American Birds. *The Auk* 138(3): 1–37. <https://doi.org/10.1093/ornithology/ukab037>
- Coscaron MDC, Morrone JJ (1998) Cladistics and biogeography of the assassin bug genus *Rasahus* Amyot & Serville (Heteroptera: Reduviidae: Peiratinae). *Zoologische Mededelingen* 72: 73–87.
- Desmarest AG (1806) Histoire naturelle des tangaras, des manakins et des todiers (in French). Garnery, Paris, 35 pp. <https://doi.org/10.5962/bhl.title.119558>

- Drummond AJ, Ho SYW, Phillips MJ, Rambaut A (2006) Relaxed phylogenetics and dating with confidence. *PLOS Biology* 4(5): 700–710. <https://doi.org/10.1371/journal.pbio.0040088>
- Eaton DA, Overcast I (2020) ipyrad: Interactive assembly and analysis of RADseq datasets. *Bioinformatics* 36(8): 2592–2594. <https://doi.org/10.1093/bioinformatics/btz966>
- Edgar RC (2004) MUSCLE: Multiple sequence alignment with high accuracy and high throughput. *Nucleic Acids Research* 32(5): 1792–1797. <https://doi.org/10.1093/nar/gkh340>
- Fox M, Bodin T, Shuster DL (2015) Abrupt changes in the rate of Andean Plateau uplift from reversible jump Markov Chain Monte Carlo inversion of river profiles. *Geomorphology* 238: 1–14. <https://doi.org/10.1016/j.geomorph.2015.02.022>
- Gmelin JF (1789) Caroli a Linné Systema Naturae per Regna Tria Naturae, Secundum Classes, Ordines, Genera, Species, cum Characteribus, Differentiis, Synonymis, Locis. Tomus I, Pars 2. Editio decima tertia, aucta, reformata [pp. 501–1032]. Impensis Georg Emanuel Beer. Pipra musica, Lipsiae, Leipzig, 1004 pp.
- Greeney HF (2021) Antillean Euphonia (*Chlorophonia musica*), version 2.1. In: Keeney BK, Gerbracht J (Eds) Birds of the World. Cornell Lab of Ornithology, Ithaca. <https://doi.org/10.2173/bow.anteup1.02.1> [Accessed on 09.09.2023]
- Gregory-Wodzicki KM (2000) Uplift history of the Central and Northern Andes: A review. *GSA Bulletin* 112 (7): 1091–1105. [https://doi.org/10.1130/0016-7606\(2000\)112<1091:UHOTCA>2.0.CO;2](https://doi.org/10.1130/0016-7606(2000)112<1091:UHOTCA>2.0.CO;2)
- Gutiérrez-Zuluaga AM, González-Quevedo C, Oswald JA, Terrill RS, Pérez-Emán JL, Parra JL (2021) Genetic data and niche differences suggest that disjunct populations of *Diglossa brunneiventris* are not sister lineages. *The Auk* 138(3): 1–14. <https://doi.org/10.1093/ornithology/ukab015>
- Hellmayr CE (1936) Field Museum of Natural History Publication, Zoological Series. Ser., 13 pt9, 63 pp.
- Hillis DM, Mable BK, Larson A, Davis S, Zimmer EA (1996) Nucleic acids. IV. Sequencing and cloning. In Hillis DM, Moritz C, Mable BK (Eds) Molecular Systematics, Sinauer Associates, Sunderland, Massachusetts, 321–381.
- Hilty S (2020a) Orange-bellied Euphonia (*Euphonia xanthogaster*), version 1.0. In: del Hoyo J, Elliott A, Sargatal J, Christie DA, de Juana E (Eds) Birds of the World. Cornell Lab of Ornithology, Ithaca. <https://doi.org/10.2173/bow.orbeup1.01> [Accessed on 09.09.2023]
- Hilty S (2020b) Purple-throated Euphonia (*Euphonia chlorotica*), version 1.0. In: del Hoyo J, Elliott A, Sargatal J, Christie DA, de Juana E (Eds) Birds of the World. Cornell Lab of Ornithology, Ithaca. <https://doi.org/10.2173/bow.puteup1.01> [Accessed on 09.09.2023]
- Hilty S, Bonan A (2020) Blue-naped Chlorophonia (*Chlorophonia cyanea*), version 1.0. In: del Hoyo J, Elliott A, Sargatal J, Christie DA, de Juana E (Eds) Birds of the World. Cornell Lab of Ornithology, Ithaca. <https://doi.org/10.2173/bow.blnc1.01> [Accessed on 09.09.2023]
- Hoorn C, Wesselingh FP, Steege H, Bermudez MA, Mora A, Sevink J, Sanmartín I, Sanchez-Meseguer A, Anderson CL, Figueiredo JP, Jaramillo C, Riff D, Negri FR, Hooghiemstra H, Lundberg J, Stadler T, Särkinen T, Antonelli A (2010) Amazonia Through Time: Andean Uplift, Climate Change, Landscape Evolution, and Biodiversity. *Science* 330(6006): 927–931. <https://doi.org/10.1126/science.1194585>
- Ilut DC, Nydam ML, Hare MP (2014) Defining loci in restriction-based reduced representation genomic data from non-model species: Sources of bias and diagnostics for

- optimal clustering. *BioMed Research International* 2014: 675158. [9 pp] <https://doi.org/10.1155/2014/675158>
- Imfeld TS, Barker FK, Brumfield RT (2020) Mitochondrial genomes and thousands of ultraconserved elements resolve the taxonomy and historical biogeography of the *Euphonia* and *Chlorophonia* finches (Passeriformes: Fringillidae). *The Auk* 137(3): 1–25. <https://doi.org/10.1093/auk/ukaa016>
- Isler ML, Isler PR (1999) *The Tanagers: Natural History, Distribution, and Identification* (2nd ed). Smithsonian Institution Press, Washington, DC, USA, 406 pp.
- Kondo B, Peters JL, Rosensteel BB, Omland E (2008) Coalescent analyses of multiple loci support a new route to speciation in birds. *Evolution; International Journal of Organic Evolution* 62(5): 1182–1191. <https://doi.org/10.1111/j.1558-5646.2008.00345.x>
- Lanfear R, Calcott B, Ho SYW, Guindon S (2012) PartitionFinder: Combined Selection of Partitioning Schemes and Substitution Models for Phylogenetics Analyses. *Molecular Biology and Evolution* 29(6): 1695–1701. <https://doi.org/10.1093/molbev/mss020>
- Lanfear R, Frandsen PB, Wright AM, Senfeld T, Calcott B (2016) PartitionFinder 2: New methods for selecting partitioned models of evolution for molecular and morphological phylogenetic analyses. *Molecular Biology and Evolution* 34(3): 772–773. <https://doi.org/10.1093/molbev/msw260>
- Li WLS, Drummond AJ (2012) Model Averaging and Bayes Factor Calculation of Relaxed Molecular Clocks in Bayesian Phylogenetics. *Molecular Biology and Evolution* 29(2): 751–761. <https://doi.org/10.1093/molbev/msr232>
- Linnaeus C (1758) *Systema naturae per regna tria naturae: secundum classes, ordines, genera, species, cum characteribus, differentiis, synonymis, locis*. Laurentii Salvii 1758–1759 1(1) 881: e182. <https://doi.org/10.5962/bhl.title.542>
- Linnaeus C (1764) *Museum S:ae R:ae M:tis Adolphi Friderici regis Svecorum, Gothorum, Vandalorumque ... Laur. Salvius, Holmiae* (Vol. 2) prodromus: 1–110. [1]
- Linnaeus C (1766) *Systema naturae, per regna tria naturae: secundum classes, ordines, genera, species cum characteribus, differentiis, synonymis, locis*. Vindobonae, Vienna, Typis Ioannis Thomae 1767–1770 1(1): e533. <https://doi.org/10.5962/bhl.title.156772>
- Löwenberg P (2014) Neotropical region: A shapefile of Morrone's biogeographical regionalization. *Zootaxa* 3802(2): 1–26. <https://doi.org/10.11646/zootaxa.3802.2.12>
- Luebert F (2021) The two South American dry diagonals. *Frontiers of Biogeography* 13(4): e51267. <https://doi.org/10.21425/F5FBG51267>
- Luebert F, Hilger HH, Weigend M (2011) Diversification in the Andes: Age and origins of South American *Heliotropium* lineages (Heliotropiaceae, Boraginales). *Molecular Phylogenetics and Evolution* 61(1): 90–102. <https://doi.org/10.1016/j.ympev.2011.06.001>
- Mastretta-Yanes A, Arrigo N, Alvarez N, Jorgensen TH, Piñero D, Emerson BC (2015) Restriction site-associated DNA sequencing, genotyping error estimation and de novo assembly optimization for population genetic inference. *Molecular Ecology Resources* 15(1): 28–41. <https://doi.org/10.1111/1755-0998.12291>
- Matzke NJ (2013) Probabilistic historical biogeography: New models for founder-event speciation, imperfect detection, and fossils allow improved accuracy and model-testing. *Frontiers of Biogeography* 5(4): 242–248. <https://doi.org/10.21425/F55419694>
- Matzke NJ (2022) Statistical comparison of DEC and DEC+J is identical to comparison of two ClaSSE submodels, and is therefore valid. *Journal of Biogeography* 49: 1805–1824. <https://doi.org/10.1111/jbi.14346>

- McCartney-Melstad E, Gidiş M, Shaffer HB (2019) An empirical pipeline for choosing the optimal clustering threshold in RADseq studies. *Molecular Ecology Resources* 19(5): 1195–1204. <https://doi.org/10.1111/1755-0998.13029>
- Méndez-Camacho K, Leon-Alvarado O, Miranda-Esquivel DR (2021) Biogeographic evidence supports the Old Amazon hypothesis for the formation of the Amazon fluvial system. *PeerJ* 9: e12533. <https://doi.org/10.7717/peerj.12533>
- Miller MA, Pfeiffer W, Schwartz T (2010) Creating the CIPRES Science Gateway for inference of large phylogenetic trees. 2010 Gateway Computing Environments Workshop, GCE 2010. <https://doi.org/10.1109/GCE.2010.5676129>
- Mittermeier RA, Gil PR, Hoffman M, Pilgrim J, Brooks T, Mittermeier CG, Lamoureux J, da Fonseca GAB (2005) Hotspots Revisited: Earth's Biologically Richest and Most Endangered Terrestrial Ecoregions. Conservation International, Washington, 392 pp.
- Montes C, Cardona A, Jaramillo C, Pardo A, Silva JC, Valencia V, Ayala C, Pérez-Angel LC, Rodríguez-Parra LA, Ramírez V, Niño H (2015) Middle Miocene closure of the Central American Seaway. *Science* 348(6231): 226–229. <https://doi.org/10.1126/science.aaa2815>
- Morgan GS (2008) Vertebrate fauna and geochronology of the Great American Biotic Interchange in Northamerica. *Neogene Mammals: Bulletin* 44: 1–93.
- Morrone JJ (2014) Biogeographical regionalization of the Neotropical region. *Zootaxa* 3782(1): 001–110. <https://doi.org/10.11646/zootaxa.3782.1.1>
- Nores M (2020) Avian Diversity in Humid Tropical and Subtropical South American Forests, with a Discussion About Their Related Climatic and Geological Underpinnings. In: Rull V, Carnaval A (Eds) *Neotropical Diversification: Patterns and Processes. Fascinating Life Sciences*. Springer Cham, 145–188. https://doi.org/10.1007/978-3-030-31167-4_8
- Oliveros CH, Field DJ, Ksepka DT, Keith Barker F, Aleixo A, Andersen MJ, Alström P, Benz BW, Braun EL, Braun MJ, Bravo GA, Brumfield RT, Chesser T, Claramunt S, Cracraft J, Cuervo AM, Derryberry EP, Glenn TC, Harvey MG, Faircloth BC (2019) Earth history and the passerine superradiation. *Proceedings of the National Academy of Sciences of the United States of America* 116(16): 7916–7925. <https://doi.org/10.1073/pnas.1813206116>
- Pérez-Consuegra N, Ott RF, Gregory DH, Galve JP, Pérez-Peña V, Mora A (2021) Neogene variations in slab geometry drive topographic change and drainage reorganization in the Northern Andes of Colombia. *Global and Planetary Change* 206: e103641. <https://doi.org/10.1016/j.gloplacha.2021.103641>
- Prates I, Rivera D, Rodrigues MT, Carnaval AC (2016) A mid-Pleistocene rainforest corridor enabled synchronous invasions of the Atlantic Forest by Amazonian anole lizards. *Molecular Ecology* 25(20): 5174–5186. <https://doi.org/10.1111/mec.13821>
- Pregill GK, Olson SL (1981) Zoogeography of West Indian Vertebrates in Relation to Pleistocene Climatic Cycles. *Annual Review of Ecology and Systematics* 12(1): 75–98. <https://doi.org/10.1146/annurev.es.12.110181.000451>
- Rambaut A, Drummond AJ (2013) TreeAnnotator version 1.8.0. <https://beast.community/treeannotator> [Accessed on 01.09.2022]
- Rambaut A, Drummond AJ (2014) FigTree version 1.4.1. <https://beast.community/treeannotator> [Accessed on 01.09.2022]
- Rambaut A, Drummond AJ, Xie D, Baele G, Suchard MA (2018) Posterior Summarization in Bayesian Phylogenetics Using Tracer 1.7. *Systematic Biology* 67(5): 901–904. <https://doi.org/10.1093/sysbio/syy032>
- Ree RH, Smith SA (2008) Maximum Likelihood Inference of Geographic Range Evolution by Dispersal, Local Extinction, and Cladogenesis. *Systematic Biology* 57(1): 4–14. <https://doi.org/10.1080/10635150701883881>

- Reyes P, Bates JM, Naka LN, Miller MJ, Caballero I, González-Quevedo C, Parra JL, Rivera-Gutiérrez HF, Bonaccorso E, Tello JG (2023) Phylogenetic relationships and biogeography of the ancient genus *Onychorhynchus* (Aves: Onychorhynchidae) suggest cryptic Amazonian diversity. *Journal of Avian Biology* 03159(11–12): e03159. <https://doi.org/10.1111/jav.03159>
- Ribas CC, Moyle RG, Miyaki CY, Cracraft J (2007) The assembly of montane biotas: linking Andean tectonics and climatic oscillations to independent regimes of diversification in *Pionus* parrots. *Proceedings of the Royal Society B, Biological Sciences* 274(1624): 2399–2408. <https://doi.org/10.1098/rspb.2007.0613>
- Ribas CC, Aleixo A, Nogueira ACR, Miyaki CY, Cracraft J (2012) A palaeobiogeographic model for biotic diversification within Amazonia over the past three million years. *Proceedings of the Royal Society B, Biological Sciences* 279(1729): 681–689. <https://doi.org/10.1098/rspb.2011.1120>
- Ree RH, Sanmartín I (2018) Conceptual and statistical problems with the DEC+J model of founder-events speciation and its comparison with DEC via model selection. *Journal of Biogeography* 45(4): 741–749. <https://doi.org/10.1111/jbi.13173>
- Rolland J, Jiguet F, Jønsson KA, Condamine FL, Morlon H (2014) Settling down of seasonal migrants promotes bird diversification. *Proceedings of the Royal Society B, Biological Sciences* 281: e20140473. <https://doi.org/10.1098/rspb.2014.0473>
- Ronquist F (1997) Dispersal-Vicariance analysis: A new approach to the quantification of historical biogeography. *Systematic Biology* 46(1): 195–203. <https://doi.org/10.1093/sysbio/46.1.195>
- Russello MA, Waterhouse MD, Etter PD, Johnson EA (2015) From promise to practice: Pairing non-invasive sampling with genomics in conservation. *PeerJ* 3: e1106. <https://doi.org/10.7717/peerj.1106>
- Sedano RE, Kevin JB, Riddle B (2010) Are the Northern Andes a species pump for Neotropical birds? Phylogenetics and biogeography of a clade of Neotropical tanagers (Aves: Thraupini) *Journal of Biogeography* 37(2): 325–343. <https://doi.org/10.1111/j.1365-2699.2009.02200.x>
- Sibley CG, Monroe BL (1990) *Distribution and Taxonomy of Birds of the World*. Yale University, Connecticut, 1111 pp.
- Silva SM, Peterson AT, Carneiro L, Burlamaqui TCT, Ribas CC, Sousa-Neves T, Miranda LS, Fernandes AM, d'Horta FM, Araújo-Silva LE, Batista R, Bandeira CHMM, Dantas SM, Ferreira M, Martins DM, Oliveira J, Rocha TC, Sardelli CH, Thom G, Rêgo PS, Santos MP, Sequeira F, Vallinoto M, Aleixo A (2019) A dynamic continental moisture gradient drove Amazonian bird diversification. *Sciences Advanced* 3; 5(7): eaat5752. <https://doi.org/10.1126/sciadv.aat5752>
- Smith BT, Klicka J (2010) The profound influence of the Late Pliocene Panamanian uplift on the exchange, diversification, and distribution of New World birds. *Ecography* 33(2): 333–342. <https://doi.org/10.1111/j.1600-0587.2009.06335.x>
- Smith BT, McCormack JE, Cuervo AM, Hickerson MJ, Aleixo A, Cadena CD, Pérez-Emán J, Burney CW, Xie X, Harvey MG, Faircloth BC, Glenn TC, Derryberry EP, Prejean S, Fields S, Brumfield RT (2014) The drivers of tropical speciation. *Nature* 515(7527): 406–409. <https://doi.org/10.1038/nature13687>
- Sorenson MD (1999) Avian mtDNA primers. <http://people.bu.edu/MSOREN/Bird.mt.Primers.pdf>
- Stamatakis A (2014) RAXML Version 8: A tool for Phylogenetic Analysis and Post-Analysis of Large Phylogenies. *Bioinformatics* 30(9): 1312–1313. <https://doi.org/10.1093/bioinformatics/btu033>

- Thode VA, Sanmartín I, Lohmann L (2019) Contrasting patterns of diversification between Amazonian and Atlantic Forest clades of Neotropical lianas (Amphilophium, Bignoniaceae) inferred from plastid genomic data. *Molecular Phylogenetics and Evolution* 133: 92–103. <https://doi.org/10.1016/j.ympev.2018.12.021>
- Tietze DT, Päckert M, Martens J, Lehmann H, Sun YH (2013) Complete phylogeny and historical biogeography of true rosefinches (Aves: Carpodacus). *Zoological Journal of the Linnean Society* 169(1): 215–234. <https://doi.org/10.1111/zoj.12057>
- Trujillo-Arias N, Dantas GPM, Arbeláez-Cortés E, Naoki K, Gómez MI, Santos FR, Miyaki CY, Aleixo A, Tubaro PL, Cabanne GS (2017) The niche and phylogeography of a passerine reveal the history of biological diversification between the Andean and the Atlantic forests. *Molecular Phylogenetics and Evolution* 112: 107–121. <https://doi.org/10.1016/j.ympev.2017.03.025>
- Trujillo-Arias N, Calderón L, Santos FR, Miyaki CY, Aleixo A, Witt CC, Tubaro LP, Cabanne GS (2018) Forest corridors between the central Andes and the southern Atlantic Forest enabled dispersal and peripatric diversification without niche divergence in a passerine. *Molecular Phylogenetics and Evolution* 128: 221–232. <https://doi.org/10.1016/j.ympev.2018.08.005>
- Vázquez-López M, Morrone JJ, Ramírez-Barrera SM, López-López A, Robles-Bello SM, Hernández-Baños BE (2020) Multilocus, phenotypic, behavioral, and ecological niche analyses provide evidence for two species within *Euphonia affinis* (Aves, Fringillidae). *ZooKeys* 952: 129–157. <https://doi.org/10.3897/zookeys.952.51785>
- Vázquez-Miranda H, Navarro-Sigüenza AG, Morrone JJ (2007) Biogeographical patterns of the avifaunas of the Caribbean Basin Islands: A parsimony perspective. *Cladistics* 23(2): 180–200. <https://doi.org/10.1111/j.1096-0031.2006.00133.x>
- Verzi DH, Montalvo CI (2008) The oldest South American Cricetidae (Rodentia) and Mustelidae (Carnivora): Late Miocene faunal turnover in central Argentina and the Great American Biotic Interchange. *Palaeogeography, Palaeoclimatology, Palaeoecology* 267(3–4): 284–291. <https://doi.org/10.1016/j.palaeo.2008.07.003>
- Vieillot LJP (1819) Nouveau dictionnaire d'histoire naturelle, appliquée aux arts, à l'agriculture, à l'économie rurale et domestique, à la médecine, etc. Nouvelle édition 32: e426.
- Winger BM, Barker FK, Ree RH (2014) Temperate origins of long-distance seasonal migration in the New World song-birds. *Proceedings of the National Academy of Sciences of the United States of America* 111(33): 12115–12120. <https://doi.org/10.1073/pnas.1405000111>
- Winger BM, Auteri GG, Pegan TM, Weeks BC (2019) A long winter for the Red Queen: Re-thinking the evolution of seasonal migration. *Biological Reviews of the Cambridge Philosophical Society* 94(3): 737–753. <https://doi.org/10.1111/brv.12476>
- Yu Y, Harris AJ, Blair C, He X (2015) RASP (Reconstruct Ancestral State in Phylogenies): A tool for historical biogeography. *Molecular Phylogenetics and Evolution* 87: 46–49. <https://doi.org/10.1016/j.ympev.2015.03.008>
- Zink RM, Gardner AS (2017) Glaciation as a migratory switch. *Science Advances* 3(9): e1603133. <https://doi.org/10.1126/sciadv.1603133>
- Zuccon D, Prys-Jones R, Rasmussen PC, Ericson PGP (2012) The phylogenetic relationships and generic limits of finches (Fringillidae). *Molecular Phylogenetics and Evolution* 62(2): 581–596. <https://doi.org/10.1016/j.ympev.2011.10.002>

Supplementary material 1

Supplementary information

Authors: Melisa Vázquez-López, Sandra M. Ramírez-Barrera, Alondra K. Terrones-Ramírez, Sahid M. Robles-Bello, Adrián Nieto-Montes de Oca, Kristen Ruegg, Blanca E. Hernández-Baños

Data type: pdf

Explanation note: **table S1**. List of specimens studied and their provenance. **table S2**. ND2 sequences obtained from Genbank. **table S3**. Results after filtering and clustering nextRAD data from Euphoniinae samples and outgroup samples. **table S4**. Sample coverage for nextRAD data from Euphoniinae samples and outgroup samples. **table S5**. Substitution models for nucleotide data partitions selected using the BIC in PartitionFinder. **text S1**. Laboratory process and sequence preparation for nextRAD sequencing. **text S2**. Quality filtering and Denovo alignment results. **figure S1**. DEC_maxareas3_v1 B=Caribbean C=Mesoamerica D=Andes E=Pacific F=Amazonas G=Chacoan H=Paraná-Atlantic Forest. **figure S2**. DIVALIKE_maxareas3_v1 B=Caribbean C=Mesoamerica D=Andes E=Pacific F=Amazonas G=Chacoan H=Paraná-Atlantic Forest. **figure S3**. BAYAREALIKE_maxareas3_v1 B=Caribbean C=Mesoamerica D=Andes E=Pacific F=Amazonas G=Chacoan H=Paraná-Atlantic Forest.

Copyright notice: This dataset is made available under the Open Database License (<http://opendatacommons.org/licenses/odbl/1.0/>). The Open Database License (ODbL) is a license agreement intended to allow users to freely share, modify, and use this Dataset while maintaining this same freedom for others, provided that the original source and author(s) are credited.

Link: <https://doi.org/10.3897/zookeys.1188.107047.suppl1>

Seven new species and four new records of Psychomyiidae (Insecta, Trichoptera) from China

Lang Peng¹, Zhen Deng¹, Yu-hua Zhang¹, Meng Wang¹, Chang-hai Sun¹, Bei-xin Wang¹

¹ Department of Entomology, College of Plant Protection, Nanjing Agricultural University, Nanjing 210095, China

Corresponding authors: Chang-hai Sun (chsun@njau.edu.cn); Bei-xin Wang (wangbeixin@njau.edu.cn)

Abstract

Seven new species of the family Psychomyiidae Walker, 1852 are described and illustrated from China; they are *Psychomyia shuni* **sp. nov.**, *Ps. mangshanensis* **sp. nov.**, *Ps. capricornis* **sp. nov.**, *Lype sagittalis* **sp. nov.**, *Paduniella fasciaria* **sp. nov.**, *Pa. sanyaensis* **sp. nov.**, and *Tinodes aviformis* **sp. nov.** The genus *Lype* is reported for the first time from mainland China. In addition, four psychomyiids are found to be new to the Chinese caddis fauna: *Psychomyia indra* Malicky & Chantaramongkol, 1993; *Paduniella andamanensis* Malicky, 1979; *Pa. dendrobia* Malicky & Chantaramongkol, 1993; and *Tinodes gabona* Johanson & Oláh, 2008. Moreover, *Psychomyia polyacantha* Li, Qiu & Morse, 2021 is reviewed and synonymized with *Psychomyia imamah* Malicky, 2020.

Key words: Caddisflies, morphology, new geographical records, new synonym, Oriental Region



Academic editor: Ana Previšić

Received: 7 September 2023

Accepted: 8 December 2023

Published: 8 January 2024

ZooBank: <https://zoobank.org/1D4965D8-1D46-41DE-95D6-5B05BFEFD9D1>

Citation: Peng L, Deng Z, Zhang Y-h, Wang M, Sun C-h, Wang B-x (2024) Seven new species and four new records of Psychomyiidae (Insecta, Trichoptera) from China. ZooKeys 1188: 197–218. <https://doi.org/10.3897/zookeys.1188.112359>

Copyright: © Lang Peng et al.

This is an open access article distributed under terms of the Creative Commons Attribution License ([Attribution 4.0 International – CC BY 4.0](https://creativecommons.org/licenses/by/4.0/)).

Introduction

The family Psychomyiidae Walker, 1852 currently includes 648 extant species in eight genera, of which 202 species are included in the genus *Psychomyia* Latreille, 1829 (Latreille 1829–1830; Laudee et al. 2020; Malicky 2020; Peng et al. 2020; Qiu and Morse 2021; Morse 2023), 316 species in *Tinodes* Curtis, 1834 (Curtis 1834; Malicky 2020; Peng et al. 2022; Morse 2023), 79 species in *Paduniella* Ulmer, 1913 (Ulmer 1913; Malicky et al. 2019; Morse 2023), 23 species in *Eoneureclipsis* (Kimmins 1955; Malicky 2020; Suwannarat et al. 2020; Morse 2023; Peng et al. 2023), 15 species in *Lype* McLachlan, 1878 (McLachlan 1878; Morse 2023), 11 species in *Metalype* Klapálek, 1898 (Klapálek 1898; Morse 2023), and one species each in the genera *Padangpsyche* Malicky, 1993 and *Trawaspsyche* Malicky, 2004 (Malicky 1993, 2004). They are widely distributed in the world's major biogeographic regions except for the Neotropical and Antarctic regions, of which more than 400 species are in the Oriental Region.

In this study, we describe three new species of the genus *Psychomyia* (*Psychomyia shuni* sp. nov., *Ps. mangshanensis* sp. nov., and *Ps. capricornis* sp. nov.), two of *Paduniella* (*Paduniella fasciaria* sp. nov. and *Pa. sanyaensis* sp. nov.), and one each in *Lype* (*Lype sagittalis* sp. nov.) and *Tinodes* (*Tinodes aviformis* sp. nov.). The genus *Lype* is newly reported from mainland China. In addition, the present study provides four new geographical records for China

(*Psychomyia indra* Malicky & Chantaramongkol, 1993; *Paduniella andamanensis* Malicky, 1979; *Pa. dendrobia* Malicky & Chantaramongkol, 1993; *Tinodes gapbona* Johanson & Oláh, 2008) and suggests a species synonymy (*Psychomyia polyacantha* Li, Qiu & Morse, 2021 (in Qiu and Morse 2021), syn. nov. of *Psychomyia imamiah* Malicky, 2020).

Materials and methods

Sample collection

Adult specimens were captured in 100% ethanol by light traps with ultraviolet light bulbs and by Malaise trap. All specimens were stored in 95% ethanol immediately after being sorted into species. All specimens and collectors or collecting institutions are listed in Table 1; the collectors including Dr Christy Jo Geraci (CJG), Mr Wei Cao (CW), Ms Xiao Chen (CX), Dr Xin-yu Ge (GXY), Prof. John C. Morse (JCM), Mr Kun Jiang (JK), Mr Wei Han (HW), Dr You-wen Li (LYW), Ms Lang Peng (PL), Dr Hai-tian Song (SHT), Prof. Lian-fang Yang (YLF), Mr Hao-ming Zang (ZHM), Ms Jin Zhu (ZJ), Prof. Xin Zhou (ZX), Institute of Zoology, Guangdong Academy of Sciences (GDAS).

Morphological study

Male abdomens used for illustrations were cleared with 10% NaOH solution and heated to 90 °C for 10 min to remove all the non-chitinous tissues. Then the cleaned genitalia were rinsed in distilled water and mounted on a depression slide with lactic acid for examination. Genitalia structures of males were traced with the pencil using a Nikon Eclipse 80i microscope equipped with a camera lucida. Pencil drawings were scanned with an Epson Perfection (V30 SE) scanner, then placed as templates in Adobe Photoshop v. 19.0 (Adobe Inc 2018) software and inked digitally with a Wacom CTL-671 tablet to produce final illustrations. Then each abdomen was stored in a microvial together with the remainder of the specimen in 95% ethanol. All specimens are deposited in the Insect Collection, Nanjing Agricultural University, Nanjing, Jiangsu Province, P.R. China (NJAU).

Terminology

The terminology of the male genitalia for the genus *Psychomyia* mainly follows Schmid (1998), with the adoption of the term “mesal ridge” from Qiu and Morse (2021) to refer to the piece along the inner side of each superior appendage; the term “basoventral process” refers to a single or paired protruding structure at the base of the phallosome, and “basal process” refers to the paired protruding structure at the base of the superior appendages. Terminology for the genus *Lype* largely follows Schmid (1998), with the adoption of the term “subapical projection of aedeagus” from Arefina (2002) to refer to the dorsal process near the distal end of the aedeagus. Terminology for the genus *Paduniella* follows Li and Morse (1997), and that for the genus *Tinodes* follows Peng et al. (2022). To ensure coherency, “superior appendages” are used to refer to the “preanal appendages”, and “coxopodite” and “harpago” are used to refer to the first and second segments of the inferior appendages, respectively.

Table 1. Detailed information on Psychomyiidae specimens collected in China. Specific dates are for specimens collected by light trap, while a date range represents specimens collected by Malaise trap over several days.

No.	Province/ municipality	City/ county	Site	Geographic coordinates	Elevation (m)	Date	Collector(s)	Specimens
1	Fujian 福建	Long- yan 龙岩	Liangyeshan National Nature Reserve 梁野山国家级自然保护区	25°12.37'N, 117°11.03'E	750	2-vii-2021	ZJ HW	<i>Ps. capricornis</i> 2♂
2	Gansu 甘肃	Wen- xian 文县	Bifeng Gully 碧峰沟	32°44.72'N, 105°14.64'E*	650	16-vi-1998	YLF	<i>Ps. imamiah</i> 6♂
3	Guangdong 广东	Huizhou 惠州	Yuguishan Nature Reserve 玉桂山自然保护区	22°25.80'N, 113°26.39'E	290	17-ix–22-x-2020	GDAS	<i>T. gapbona</i> 2♂
4	Guangdong 广东	Zhao- qing 肇庆	Dinghushan National Nature Reserve 鼎湖山国家级自然保护区	23°09.50'N, 112°32.46'E	170	9-ix–9-x-2021	GDAS	<i>T. gapbona</i> 20♂
5	Hainan 海南	Ledong 乐东	Jianfengling National Forest Park, Rainforest Valley 尖峰岭国家森林公园, 雨林谷	18°44.72'N, 108°56.08'E	640	17-iv-2019	SHT	<i>Ps. indra</i> 1♂
6	Hainan 海南	Sanya 三亚	Tangta reservoir 汤他水库	18°24.55'N, 109°23.27'E	240	24-vii-2022	PL ZHM	<i>Pa. fasciaria</i> 26♂16♀
7	Hainan 海南	Sanya 三亚	Hongxinxi River 红新溪河	18°27.78'N, 109°27.88'E	150	22-vii-2022	PL ZHM	<i>Pa. sanyaensis</i> 3♂
8	Hainan 海南	Sanya 三亚	Fuwan reservoir 福万水库	18°16.80'N, 109°28.94'E	60	25-vii-2022	PL ZHM	<i>Pa. sanyaensis</i> 2♂ <i>T. aviformis</i> 1♂
9	Hunan 湖南	Chen- zhou 郴州	Mangshan National Forest Park 莽山国家森林公园	24°58.80'N, 112°55.65'E	730	1-ix-2020	CW	<i>Ps. mangshanensis</i> 11♂
10	Hunan 湖南	Shaoy- ang 邵阳	Shunhuangshan National Forest Park 舜皇山国家森林公园	26°23.78'N, 111°00.47'E	750	22-viii-2020	CW	<i>Ps. shuni</i> 2♂
11	Hunan 湖南	Shaoy- ang 邵阳	Yaorenping hydropower station 瑶人坪水电站	26°14.95'N, 110°30.26'E	900	24-v-2021	PL	<i>Ps. shuni</i> 1♂
12	Hunan 湖南	Shaoy- ang 邵阳	Jiuxi Bamboo Tower Villa 九溪竹楼山庄	26°24.39'N, 110°05.68'E	630	25-v-2021	PL	<i>L. sagittalis</i> 2♂
13	Hunan 湖南	Shaoy- ang 邵阳	Guanyinxing 观音形	26°24.77'N, 110°05.39'E	550	28-v-2021	PL	<i>L. sagittalis</i> 1♂
14	Sichuan 四川	Kang- ding 康定	Dadu River, Wasigou 大渡河, 瓦斯沟	30°04.53'N, 102°09.61'E	1430	29-vi-2005	ZX CJG	<i>Ps. imamiah</i> 16♂
15	Sichuan 四川	Pingwu 平武	tributary of Fujiang, 19 km E of Pingwu downtown 涪江支流, 平武县东19千米	32°24.72'N, 104°45.49'E	1090	27-vi-1990	JCM	<i>Ps. imamiah</i> 200+♂
16	Sichuan 四川	Pingwu 平武	17 km E of Ping-wu trib. of Fujianghe 涪江河支流, 平武县东17千米	32°24.48'N, 104°44.36'E*	1090	27-vi-1990	YLF LYW	<i>Ps. imamiah</i> 200+♂
17	Sichuan 四川	Yibin 宜宾	Xining River 西宁河	28°41.15'N, 103°45.97'E	370	12-v-2020	GXY CX	<i>Pa. dendrobia</i> 1♂
18	Yunnan 云南	Jing- hong 景洪	Yunjinghong Street G214 G214国道, 允景洪街道	22°01.75'N, 100°52.12'E	660	26-vii-2021	JK	<i>Pa. andamanensis</i> 1♂

* indicates the lack of original records for geographic coordinates; the data are based on location information.

Results

Taxonomy

Psychomyia shuni Peng & Sun, sp. nov.

<https://zoobank.org/1FC53A2C-FA77-40B1-A8BC-124A3B949D5E>

Fig. 1A–D

Type materials. Holotype: CHINA • 1♂; Hunan Province, Shaoyang City, Xinning County, Shunhuangshan National Forest Park; 26°23.78'N, 111°00.47'E; alt. 750 m; 22-viii-2020; light trap; W. Cao leg.; NJAU Tricho-20200822-0001.

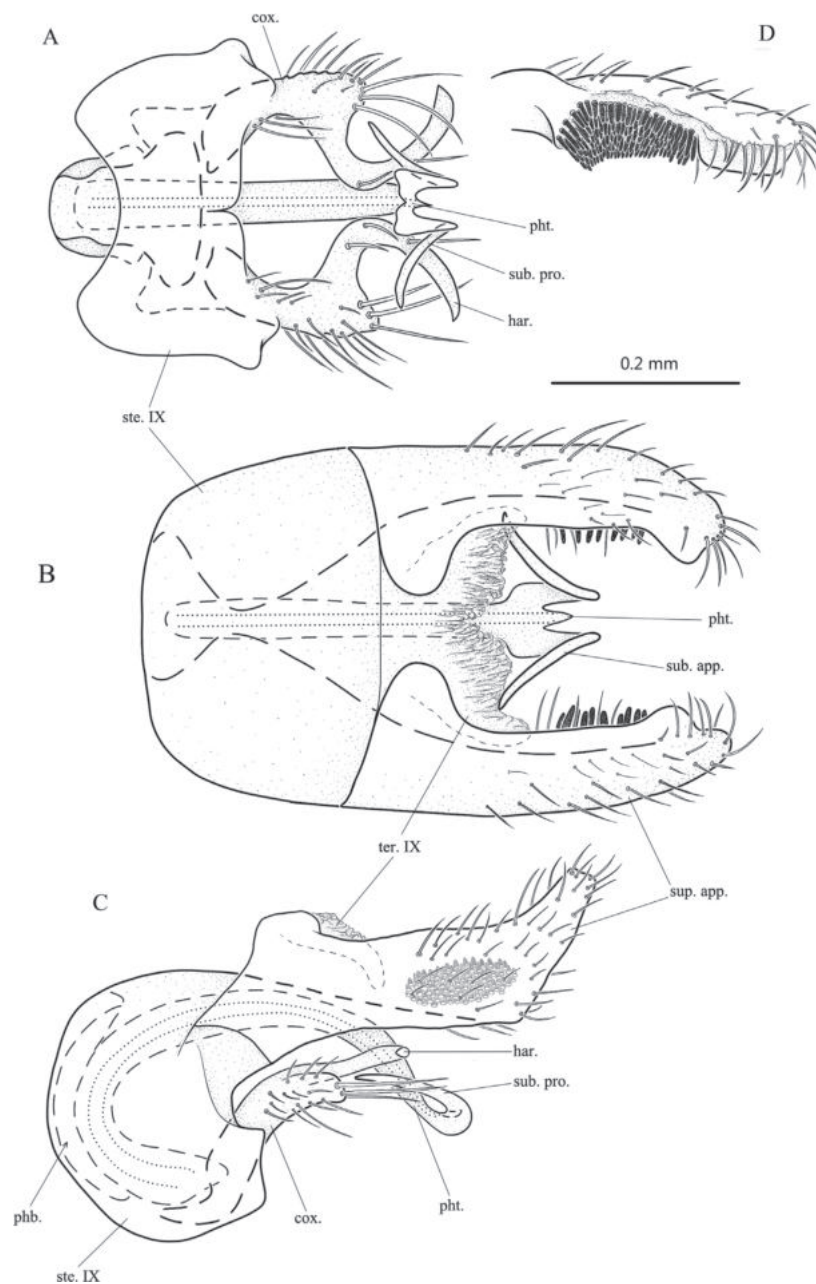


Figure 1. *Psychomyia shuni* sp. nov., male adult, holotype **A** genitalia, ventral **B** genitalia, dorsal **C** genitalia, left lateral **D** superior appendage, ventral. Abbreviations: ste. IX = sternum IX; ter. IX = tergum IX; sup. app. = superior appendage (paired); cox. = coxopodite (paired); har. = harpago (paired); phb. = phallobase; pht. = phallosome; sub. pro. = subapical process of phallic apparatus.

Paratypes: CHINA • 1♂; same data as holotype; NJAU Tricho-20200822-0002 • 1♂; Hunan Province, Shaoyang City, Chengbu County, Yaorenping hydropower station; 26°14.95'N, 110°30.26'E; alt. 900 m; 24-v-2021; light trap; L. Peng leg.; NJAU Tricho-20210524-0001.

Diagnosis. This species is unique among *Psychomyia* in that the coxopodites and the harpagones are completely fused and together form an S or Z shape in ventral view.

Description. Male. Length of each forewing 3.6–3.8 mm ($n = 3$); holotype 3.7 mm. Specimens in alcohol with compound eyes black; body brown dorsally and light yellow ventrally. Forewings with forks II–V present, hind wings with forks II, III, and V present. **Genitalia.** Sternum IX nearly trapezoidal with anterior margin concave in ventral view (Fig. 1A); rounded, semicircular in lateral view (Fig. 1C). Tergite IX produced from dorsoposterior margin of sternum IX, membranous, somewhat bowl-shaped with apical margin sinuate and partially hidden under two superior appendages in dorsal view (Fig. 1B), tongue-shaped in lateral view (Fig. 1C). Superior appendages in dorsal view wide and long, each with larger mesobasal lobe and smaller subapical lobe both directed mesad and with apex truncate (Fig. 1B), twisted and clavate, each with inner side having cluster of spines subapically in ventral view (Fig. 1D); subrectangular in lateral view, each with blunt basodorsal process, angled posterodorsad at 2/3 length to truncate apex (Fig. 1C). Phallobase slender, basally directed anterad and evenly recurved posterad in lateral view (Fig. 1C). Phallosome tubular, basally directed anterad, evenly recurved dorsad, caudad at midlength, and posteroventrad distally; apically depressed and trifurcate, acute mesally and with pair of long, subapical processes projecting caudad, then recurved dorsad and diverging anterolaterad (Fig. 1A–C). Inferior appendages in ventral view sigmoid (Fig. 1A), in lateral view strongly C-shaped (Fig. 1C); coxopodites elongate-rectangular in lateral view, heavily setose, and fused with slender harpago (Fig. 1C).

Etymology. Latin noun in genitive singular. The new species is named after Shun, a leader of tribal alliances in ancient China, who is considered an important founder of the Chinese civilization. Moreover, the holotype and one of the paratypes were collected at Mt Shun-huang, the mountain named after Shun.

Distribution. China (Hunan).

***Psychomyia mangshanensis* Peng & Sun, sp. nov.**

<https://zoobank.org/2D8150C9-717B-46BF-A82D-E3DFDB7EA29A>

Fig. 2A–C

Type materials. Holotype: CHINA • 1♂; Hunan Province, Chenzhou City, Yizhang County, Mangshan National Forest Park; 24°58.80'N, 112°55.65'E; alt. 730 m; 1-ix-2020; light trap; W. Cao leg.; NJAU Tricho-20200901-0001.

Paratypes: CHINA • 10♂; same data as holotype; NJAU Tricho-20200901-0002 to Tricho-20200901-00011.

Diagnosis. This species is similar to *Psychomyia cuspidata* Li, Qiu & Morse, 2021 from China (Qiu and Morse 2021). However, *P. mangshanensis* sp. nov. can be easily distinguished by the following characteristics: (1) each superior appendage has a small triangular protrusion in the middle of the ventral margin in lateral view, which is missing in *P. cuspidata*; (2) the basal process of each

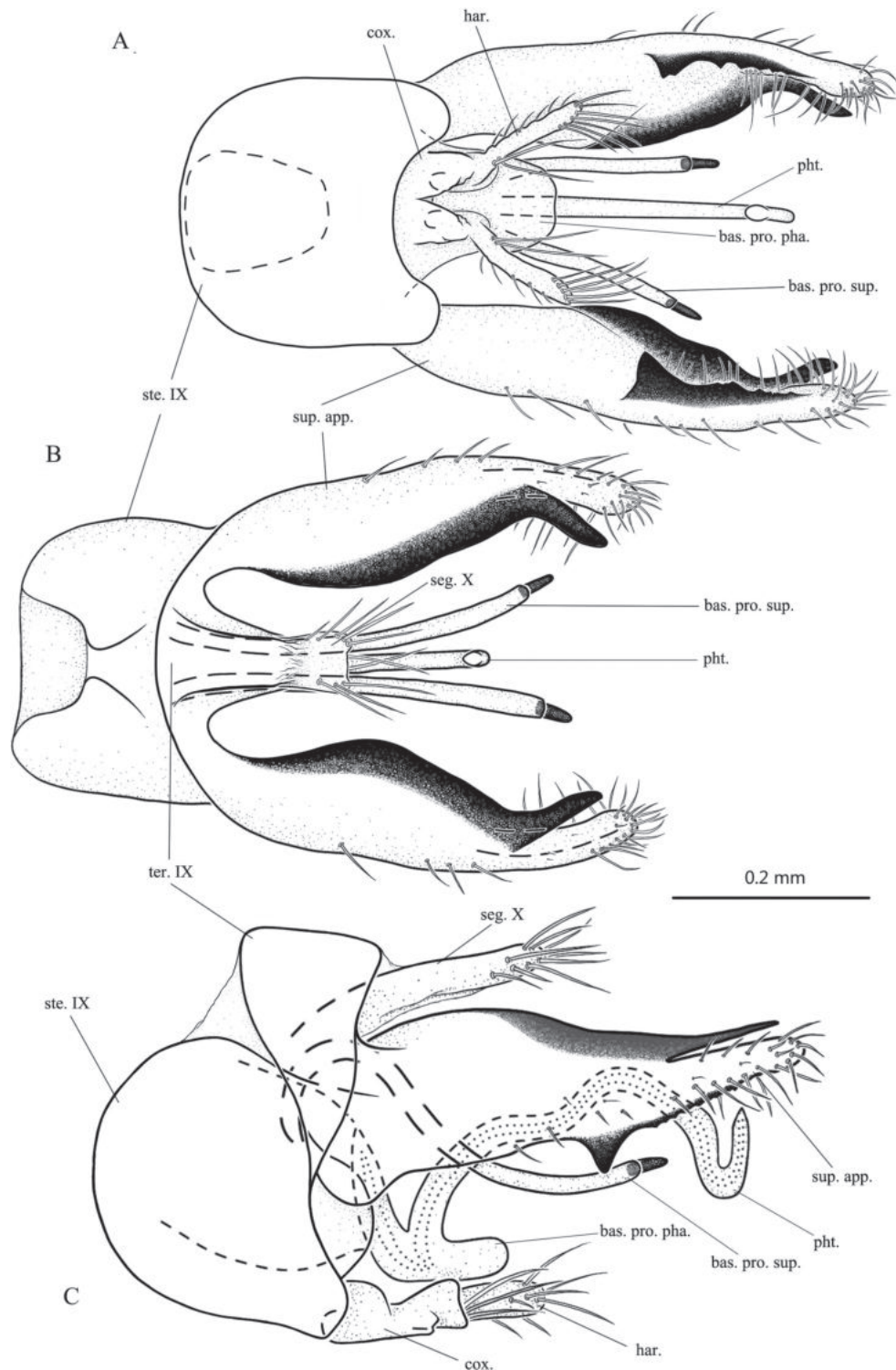


Figure 2. *Psychomyia mangshanensis* sp. nov., male adult, holotype **A** genitalia, ventral **B** genitalia, dorsal **C** genitalia, left lateral. Abbreviations: ste. IX = sternum IX; ter. IX = tergum IX; seg. X = segment X; sup. app. = superior appendage (paired); bas. pro. sup. = basal process of superior appendage (paired); cox. = coxopodite (paired); har. = harpago (paired); pht. = phallosome; bas. pro. pha. = basoventral process of phallic apparatus.

superior appendage is unbranched and with thick spine apically, whereas each superior appendage is two-branched, each branch has a thick spine apically in *P. cuspidata*; and (3) the phallosome is slightly wavy at midlength in lateral view but with an obtuse angle in *P. cuspidata*.

Description. Male. Length of each forewing 2.8–3.1 mm ($n = 10$), holotype forewing 3.0 mm. Specimens in alcohol with compound eyes black; body dark brown dorsally and light brown ventrally. Forewings each with forks II–V present, and hind wings each with forks II and V present. **Genitalia.** Sternum IX subrectangular in ventral, dorsal, and lateral views (Fig. 2A, C). Tergite IX short and triangular in dorsal and lateral views (Fig. 2B, C). Division between tergite IX and segment X indiscernible in dorsal view (Fig. 2B) but distinguished by membrane in lateral view (Fig. 2C). Segment X parallel-sided, same width as apex of tergite IX, apically truncate in dorsal view, digitate in lateral view (Fig. 2C); with several long thick apical setae in dorsal and lateral views (Fig. 2B, C). Superior appendages well developed in lateral view, each tapering from base towards apex, divided into one narrow dorsomesal branch and one broad ventrolateral branch subapically; dorsomesal branch sclerotized and bare, acute in lateral view, ventrolateral branch setose about twice as wide as upper branch in lateral view (Fig. 2C); in ventral and dorsal views (Fig. 2A, B), dorsomesal branches of superior appendages angled mesad, ventrolateral branches curved slightly mesad; paired basal processes of superior appendages tubular, and slender, each with thick spine apically; in lateral view each with base directed dorsad, then recurved posteroventrad and evenly curved caudad (Fig. 2C); in ventral and dorsal views each slightly curving outwards (Fig. 2A, B). Phallobase slender, lanceolate in lateral view (Fig. 2C). Phallosome tubular, with base produced caudad in lateral view (Fig. 2C), main portion sinuate, with apex hooked dorsad; phallosome stick-like in ventral view (Fig. 2A), basoventral process plate-shaped, three times wider than main portion of phallosome. Inferior appendages extending posterolaterad; coxopodites subtriangular, with their bases fused in ventral view (Fig. 2A); subrectangular, about 3 times as long as tall with middle of dorsal margin concave in lateral view (Fig. 2C); harpagones setose, arising from apices of coxopodites, fingerlike (Fig. 2A, C).

Etymology. Latin feminine adjective *mangshanensis*, referring to the type locality.

Distribution. China (Hunan).

***Psychomyia capricornis* Peng & Sun, sp. nov.**

<https://zoobank.org/8B56550A-37E4-45D0-832F-BC73AB818566>

Fig. 3A–D

Type materials. Holotype: CHINA • 1♂; Fujian Province, Longyan City, Wuping County, Liangyeshan National Nature Reserve; 25°12.37'N, 117°11.03'E; alt. 750 m; 2-vii-2021; light trap; J. Zhu & W. Han leg.; NJAU Tricho-20210702-0001.

Paratype: CHINA • 1♂; same data as holotype; NJAU Tricho-20210702-0002.

Diagnosis. This species is similar to *Psychomyia shuni* sp. nov. from China in having the superior appendages with dense spines mesally and in having well-developed subapical processes on the phallic apparatus. However, *P. capricornis* sp. nov. can be easily distinguished by the long, slender processes arising from the bases of the coxopodites, which are absent in *P. shuni*.

Description. Male. Length of each forewing 3.5–3.7 mm ($n = 2$), holotype forewing 3.7 mm. Specimens in alcohol with compound eyes black, body brown dorsally, light yellow ventrally. Forewings with forks II–V present, hind wings with forks II, III, and V present. **Genitalia.** Sternum IX nearly trapezoidal

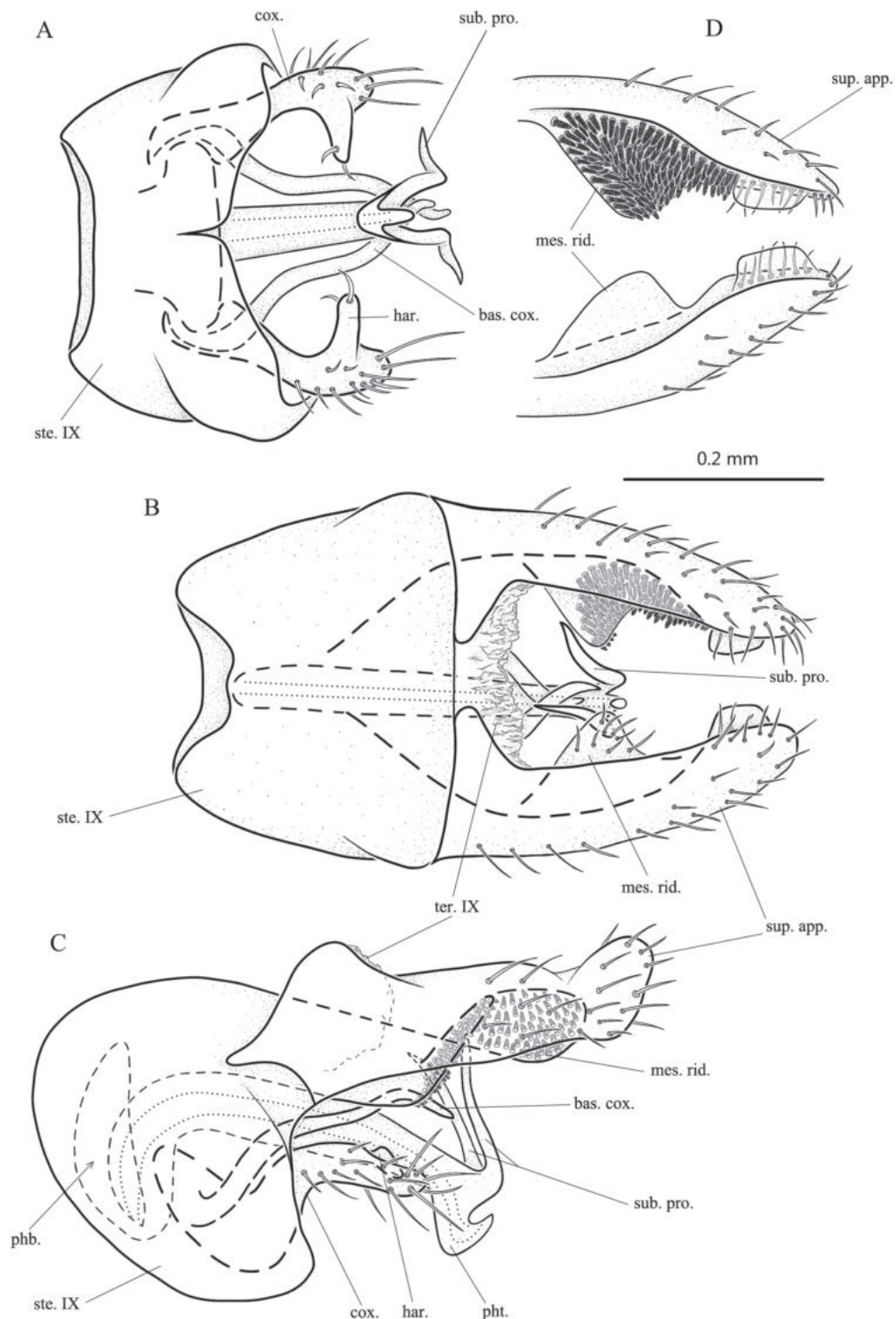


Figure 3. *Psychomyia capricornis* sp. nov., male adult, holotype **A** genitalia, ventral **B** genitalia, dorsal **C** genitalia, left lateral **D** superior appendages, ventral (mesal spines omitted on right superior appendage). Abbreviations: ste. IX = sternum IX; ter. IX = tergum IX; sup. app. = superior appendage (paired); mes. rid. = mesal ridge of a superior appendage (paired); cox. = coxopodite (paired); bas. cox. = basal process of coxopodite (paired); har. = harpago (paired); phb. = phallobase; pht. = phalotheca; sub. pro. = subapical process of phallic apparatus.

with anterior margin concave in dorsal view (Fig. 3B); rounded anteriorly, subelliptical in lateral view (Fig. 3C); with posterior margin narrowly notched mesally in ventral view (Fig. 3A). Tergite IX membranous with irregular posterior margin

in dorsal view (Fig. 3B); hemispherical in lateral view (Fig. 3C). Superior appendages elongate-triangular in dorsal view (Fig. 3B); subrectangular in lateral view (Fig. 3C), anterior margin of each produced into apodeme, distal half setose, upper margin sinuate and lower margin straight, with apex oblique and rounded; each with base produced dorsomesad (Fig. 3B, C); mesal ridge cambered and subtriangular with ventral side covered with spines (Fig. 3B, D); elliptical in lateral view (Fig. 3C); and with subapex produced into blunt process mesally in ventral and dorsal views (Fig. 3B, D). Phallobase hemispherical in lateral view (Fig. 3C). Phallosome directed dorsad basally, then curved dorsocaudad about 90°, subapically with dorsal margins produced into pair of slender and apically acute subapical processes (or “horns”), and distal end hooked dorsad (Fig. 3C); in ventral and dorsal views subapical processes curved outwards at middle (Fig. 3A). Coxopodites setose, each with subapical harpago produced inwards as triangular process in ventral view (Fig. 3A); inconspicuous in lateral view (Fig. 3C). Long, slender, bare process arising from base of each coxopodite, sinuate, apically acute in ventral and lateral views (Fig. 3A, C); extending far beyond apex of coxopodite and harpago, and with distal ends of opposing processes crossed above phallosome in ventral and dorsal views (Fig. 3A, B).

Etymology. The Latin feminine adjective *capricornis* means “goat’s horn”, referring to the shape of the pair of subapical processes on the phallic apparatus.

Distribution. China (Fujian).

***Lype sagittalis* Peng & Sun, sp. nov.**

<https://zoobank.org/5375CC60-19B5-4322-B59A-4856D5F5F6F5>

Fig. 4A–E

Type materials. *Holotype*: CHINA • 1♂; Hunan Province, Shaoyang City, Suining County, Jiuxi Bamboo Tower Villa; 26°24.39'N, 110°05.68'E; alt. 630 m; 25-v-2021; light trap; L. Peng leg.; NJAU Tricho-20210525-0001. *Paratypes*: CHINA • 1♂; same data as holotype; NJAU Tricho-20210525-0002 • 1♂; Hunan Province; Shaoyang City, Suining County, Guanyinxing; 26°24.77'N, 110°05.39'E; alt. 550 m; 28-v-2021; light trap; L. Peng leg.; NJAU Tricho-20210528-0001.

Diagnosis. This species is similar to *Lype lubaretsi* Arefina, 2005 from Russia. However, the new species can be easily distinguished by the following characteristics: (1) longitudinally, sternum IX of *L. sagittalis* sp. nov. is subtriangular in lateral view, rather than subrectangular in *L. lubaretsi*; (2) each of the coxopodites of the new species is subcircular in lateral view, but elliptical in *L. lubaretsi*; (3) the fused coxopodites in ventral view have a narrow mesal notch in the new species, rather than with a wide mesal notch in *L. lubaretsi*; (4) the aedeagus is sagittal, with its apex truncate in dorsal view and pipe-shaped in lateral view in *L. sagittalis* sp. nov., but nearly triangular with apex broad in ventral view, triangular with a sharp apex in lateral view in *L. lubaretsi*.

Description. Male. Length of each forewing 4.2–4.4 mm ($n = 3$), holotype 4.4 mm. Specimens in alcohol with compound eyes black; antennae, legs, and thorax brown; wings light brown without any distinctive markings; abdomen dark brown dorsally, pale yellow ventrally. **Genitalia:** Sternum IX subrectangular, anterior margin shallowly concave, posterior margin more deeply concave in ventral view (Fig. 4A); subtriangular in lateral view (Fig. 4C). Tergite IX covered with fine microchaetae.

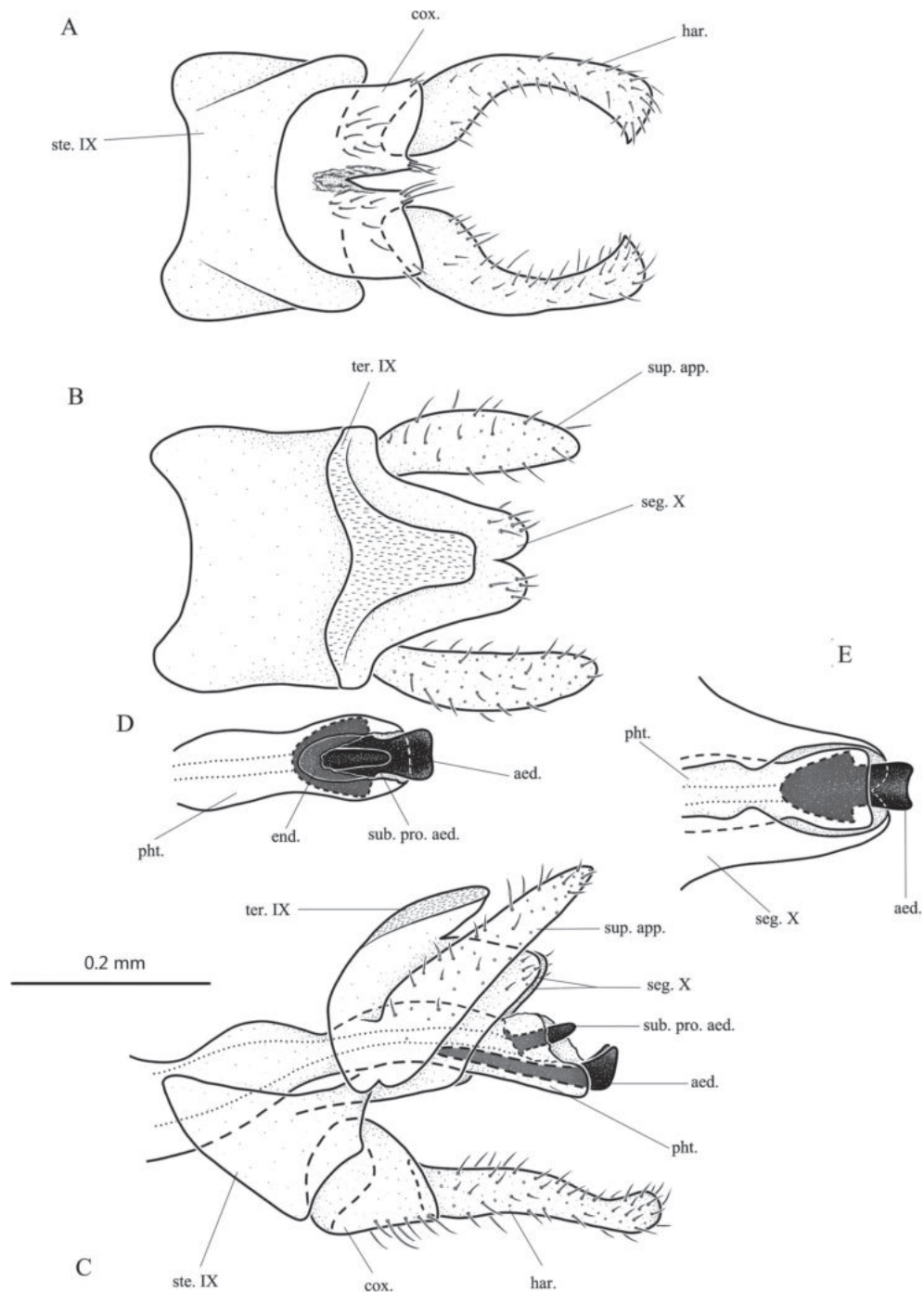


Figure 4. *Lype sagittalis* sp. nov., male adult, holotype **A** genitalia, ventral **B** genitalia, dorsal **C** genitalia, left lateral **D** phallosome apex, dorsal **E** phallosome apex and segment X, ventral. Abbreviations: ste. IX = sternum IX; ter. IX = tergum IX; seg. X = segment X; sup. app. = superior appendage (paired); cox. = coxopodite (paired); har. = harpago (paired); pht. = phallosome; aed. = aedeagus; sub. pro. aed. = subapical projection of aedeagus.

tae, subtriangular with distal end truncate in dorsal view (Fig. 4B); tongue-shaped in lateral view (Fig. 4C), broadly fused with segment X. Segment X subrectangular and almost surrounding phallic apparatus in lateral and ventral views (Fig. 4C, E); apex excised mesally in dorsal view (Fig. 4B). Superior appendages elongate-oval in dorsal view (Fig. 4B); lanceolate, tilted posterodorsad in lateral view (Fig. 4C). Coxopodites each subcircular in lateral view (Fig. 4C); bases fused with each other in ventral view and with narrow notch between them apically about half

their length, each with setose posteromesal corner produced caudad (Fig. 4A). Harpagones twice as long as coxopodites, each more-or-less parallel-sided, each with lower margin slightly concave, upper margin sinuate in lateral view (Fig. 4C); the pair divergent basally, evenly curved laterad and mesad to become somewhat forcipiform, with bases and distal ends enlarged in ventral view (Fig. 4A). Phallosome massive, constricted at middle in lateral view (Fig. 4C), with apical margin membranous. Aedeagus sclerotized, depressed, broad in dorsal and ventral views (Fig. 4D, E); pipe-shaped in lateral view (Fig. 4C). Subapical projection of aedeagus sclerotized, finger-like in lateral and dorsal views (Fig. 4C, D).

Etymology. The Latin feminine adjective *sagittalis*, meaning “arrow-shaped”, and refers to the shape of the aedeagus in dorsal and ventral views.

Distribution. China (Hunan).

***Paduniella fasciaria* Peng & Sun, sp. nov.**

<https://zoobank.org/80C19FBF-FCB6-457E-80BA-E585E4E4F6FE>

Fig. 5A–E

Type materials. *Holotype*: CHINA • 1♂; Hainan Province, Sanya City, Tianya district, Tangta reservoir; 18°24.55'N, 109°23.27'E; alt. 240 m; 24-vii-2022; light trap; L. Peng & H. Zang leg.; NJAU Tricho-20220724-0001. *Paratypes*: 25♂, 16♀; same data as holotype; NJAU Tricho-20220724-0002 to Tricho-20220724-0042.

Diagnosis. This species is similar to *Paduniella sampati* Malicky & Chantaramongkol, 1993 from Thailand in having the superior appendages furcated at their bases in dorsal view and in the shape of the phallic apparatus in the lateral view. However, *P. fasciaria* sp. nov. can be easily distinguished by the possession of a slender median process.

Description. Male. Length of each forewing 2.6–3.0 mm ($n = 10$), holotype 2.9 mm. Specimens with compound eyes black, antennae approximately of same length as forewings; body brown; head, bases of antennae, thorax covered with brown, short hair; wings mostly covered with brown, short hair; each forewing with transversal white band at middle (Fig. 5D, E). **Genitalia.** Sternum IX subrectangular with anterodorsal angle produced into subrectangular process in lateral view (Fig. 5C); and transversely elongate-rectangular with anterior margin having deep U-shaped incision in ventral view (Fig. 5A). Tergum IX membranous, with base fused with superior appendages, somewhat clavate in lateral view (Fig. 5C), directed posterodorsad; transversely subrectangular in dorsal view, with anterior margin slightly convex and posterior margin undulated (Fig. 5B). Superior appendages large, forming a parallelogram shape in lateral view (Fig. 5C); in dorsal view (Fig. 5B) each with basal portion furcate, basolateral lobe slightly longer than inner one, tapering distally with apex curved mesad and crossing apex of opposing superior appendage, setose subapically. Sclerotized strips slightly clavate in lateral view (Fig. 5C) and somewhat V-shaped in dorsal view (Fig. 5B). Median process mostly slender with sharp apex, insertion between sclerotized strips broad in dorsal view (Fig. 5B). Inferior appendages each with basal half broad, then abruptly narrowed at mid length and tapered towards apex in lateral view (Fig. 5C); basal half broad, then abruptly narrowed, with apex slightly enlarged and curved mesad in ventral view (Fig. 5A), mesal branch lamellar, setose, arising from middle part of inner surface (Fig. 5B, C). Phallobase well developed, basally clavate in lateral

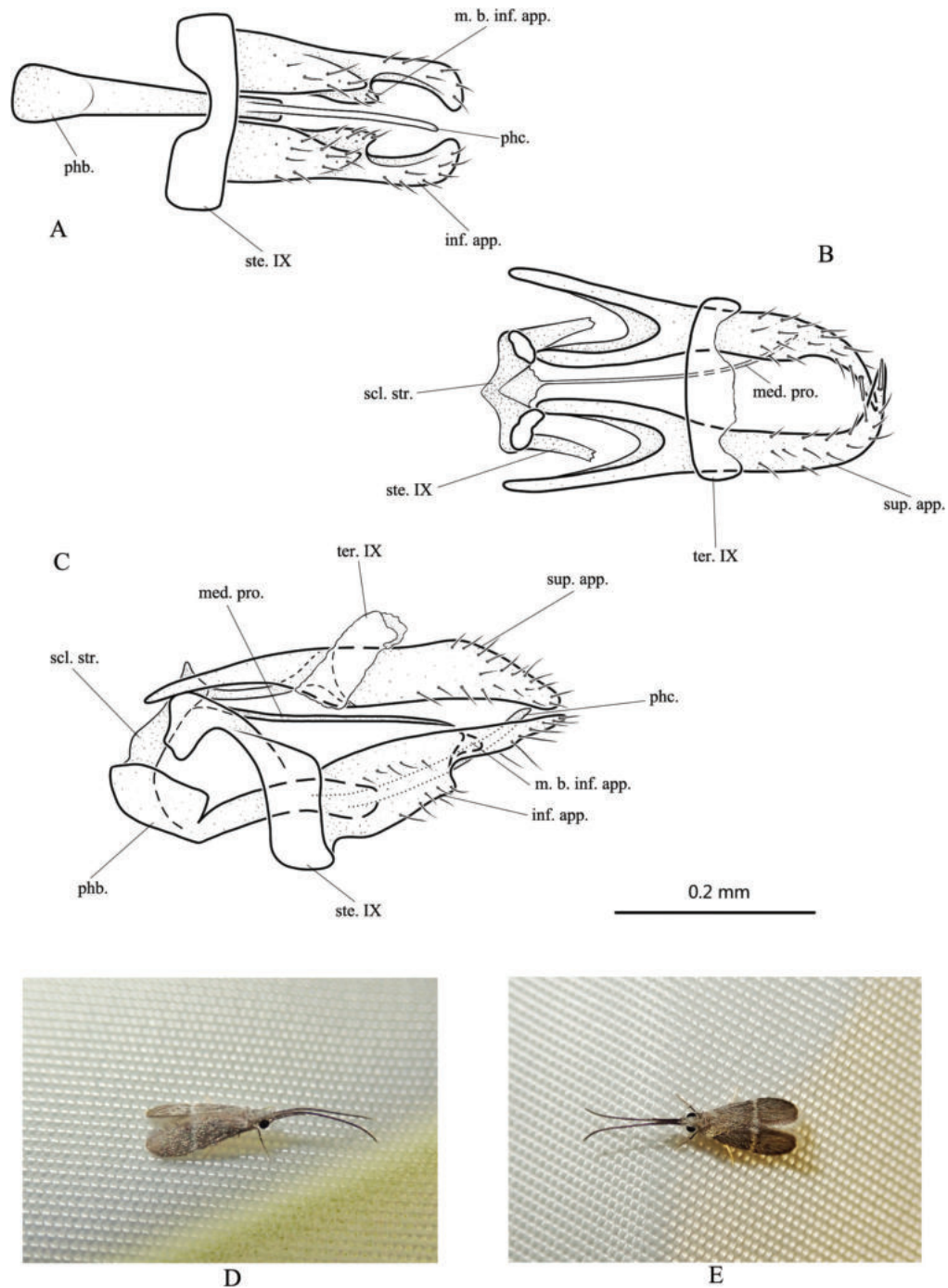


Figure 5. *Paduniella fasciaria* sp. nov., male adult, holotype (**A–C**) and paratypes (**D, E**) **A** genitalia, ventral **B** genitalia, dorsal **C** genitalia, left lateral **D** male adult habitus, right lateral **E** male adult habitus, dorsal. Abbreviations: ste. IX = sternum IX; ter. IX = tergum IX; sup. app. = superior appendage (paired); med. pro. = median process; inf. app. = inferior appendage (paired); m. b. inf. app. = mesal branch of inferior appendage (paired); scl. str. = sclerotized strip; phb. = phallobase; phc. = phallicata. The scale bar refers to **A–C**.

view (Fig. 5C); with upper margin having deep incision in ventral and lateral views (Fig. 5A, C), tapering from base to apex, phallicata tubular, curved slightly upwards in lateral view (Fig. 5C); about same length as phallobase (Fig. 5A, C).

Etymology. The Latin feminine adjective *fasciaria*, meaning “banded,” refers to the band of white hairs across each wing in dorsal view.

Distribution. China (Hainan).

***Paduniella sanyaensis* Peng & Sun, sp. nov.**

<https://zoobank.org/291BCBF2-64D5-4144-9B56-1533FE24E023>

Fig. 6A–C

Type materials. Holotype: CHINA • 1♂; Hainan Province, Sanya City, Tianya district, Hongxin village, Hongxinxi River; 18°27.78'N, 109°27.88'E; alt. 150 m; 22-vii-2022; light trap; L. Peng & H. Zang leg.; NJAU Tricho-20220722-0001.

Paratypes: CHINA • 2♂; same data as holotype; NJAU Tricho-20220722-0002 to Tricho-20220722-0003 • 2♂; Hainan Province, Sanya City, Tianya district, Fuwan reservoir; 18°16.80'N, 109°28.94'E; alt. 60 m; 25-vii-2022; light trap; L. Peng & H. Zang leg.; NJAU Tricho-20220725-0001 to Tricho-20220725-0002.

Diagnosis. This species is similar to *Paduniella nama* Johanson & Oláh, 2010 from Vietnam. However, *P. sanyaensis* sp. nov. can be easily distinguished by the following characteristics: (1) the tergum IX is similar in width to the sclerotized strips in lateral view, whereas in *P. nama* tergum IX significantly wider than sclerotized strips; (2) the superior appendages are elongate-triangular in lateral view, but subrectangular in *P. nama*; and (3) the phallobase is enlarged, nearly triangular in lateral view, a feature missing in *P. nama*.

Description. Male. Length of each forewing 2.1–2.3 mm ($n = 5$), holotype 2.3 mm. Specimens in alcohol uniformly pale yellow-brown, antennae annulate with brown. **Genitalia.** Sternum IX in lateral view with lower portion subrectangular and upper portion produced anterodorsad on each side into slender lobe

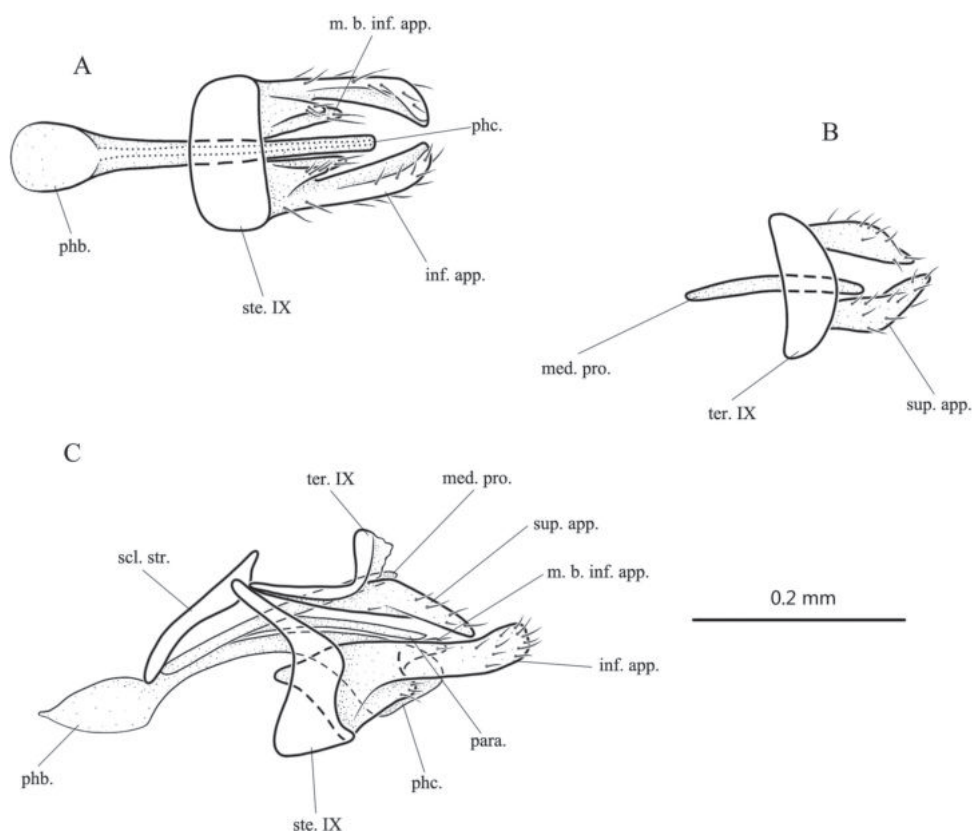


Figure 6. *Paduniella sanyaensis* sp. nov., male adult, holotype **A** genitalia, ventral **B** genitalia, dorsal **C** genitalia, left lateral. Abbreviations: ste. IX = sternum IX; ter. IX = tergum IX; sup. app. = superior appendage (paired); med. pro. = median process; inf. app. = inferior appendage (paired); m. b. inf. app. = mesal branch of inferior appendage (paired); para. = paramere; scl. str. = sclerotized strip; phb. = phallobase; phc. = phallicata.

(Fig. 6C); in ventral view transversely subrectangular (Fig. 6A). Sclerotized portion of tergum IX L-shaped, upturned distally, distal end membranous in lateral view (Fig. 6C); somewhat crescentic in dorsal view (Fig. 6B). Superior appendages elongate-triangular in lateral view (Fig. 6C); lightly twisted and triangular in dorsal view (Fig. 6B). Sclerotized strips slightly clavate in lateral view (Fig. 6C). Median process slender, tubular, arising from anterior bases of sclerotized strips above phallobase (Fig. 6B, C). Inferior appendages each with basal 1/4 broad, then narrower, with upper and lower margins parallel to each other and slightly sinuous, apex truncate in lateral view (Fig. 6C); curved mesad with apex slightly enlarged in ventral view (Fig. 6A); mesal branch of each inferior appendage arising from middle part of inner surface, elongate-triangular in ventral view (Fig. 6A). Phallobase well developed, subtriangular, about half as long as phallicata in lateral view (Fig. 6C); subcircular in ventral view (Fig. 6A); phallicata curved posteroventrad, compressed, with apex enlarged in lateral view (Fig. 6C); slender in ventral view (Fig. 6A); paramere slender, shorter than phallicata in lateral view (Fig. 6C).

Etymology. Latin feminine adjective *sanyaensis*, the name referring to the location of the type locality in Sanya City.

Distribution. China (Hainan).

***Tinodes aviformis* Peng & Sun, sp. nov.**

<https://zoobank.org/6B523126-44D5-4152-BC2B-3C8971A42BCD>

Fig. 7A–E

Type materials. Holotype: CHINA • 1♂; Hainan Province, Sanya City, Tianya district, Fuwan reservoir; 18°16.80'N, 109°28.94'E; alt. 60 m; 25-vii-2022; light trap; L. Peng & H. Zang leg.; NJAU Tricho-20220725-0003.

Diagnosis. This species is similar to *Tinodes igok* Kimmins, 1955 from Malaysia in the composition and morphology of the male genitalia, but it can be distinguished by: (1) two unpaired inner branches of the phallic sheath processes, of which one is short and straight and the other one curved, whereas both branches are curved in *T. igok*; (2) the mesal digitate process of each coxopodite is shorter than the harpago, curved, and with a sharp apex in ventral view, but is undulated and almost the same length as the harpago in *T. igok*; and (3) the phallic guide is divided into two branches with the dorsal one extending backward beyond the coxopodites in lateral view, rather than having only one uncinate branch that is not longer than the coxopodites in *T. igok*.

Description. Male. Length of each forewing 3.1 mm ($n = 1$). Specimen in alcohol with compound eyes black, antennae yellowish white; thorax and legs brown, wings light brown without any distinctive markings; abdomen dark brown dorsally, pale yellow ventrally. **Genitalia.** Sternum IX transversely subrectangular in ventral view (Fig. 7A); subtriangular in lateral view (Fig. 7C). Tergum IX covered with microchaetae, with anterior margin slightly sinuate and middle of posterior margin produced posterad in dorsal view (Fig. 7B); broader and subapically angled slightly caudad in lateral view (Fig. 7C). Segment X membranous, closely fused with tergum IX, its posterior margin nearly truncate in dorsal view (Fig. 7B); subrhomboid in lateral view (Fig. 7C). Superior appendages each with distal half setose, clavate, and with apex rounded in lateral view (Fig. 7C); parallel-sided in dorsal view (Fig. 7B). Phallic sheath process consisting of paired lateral

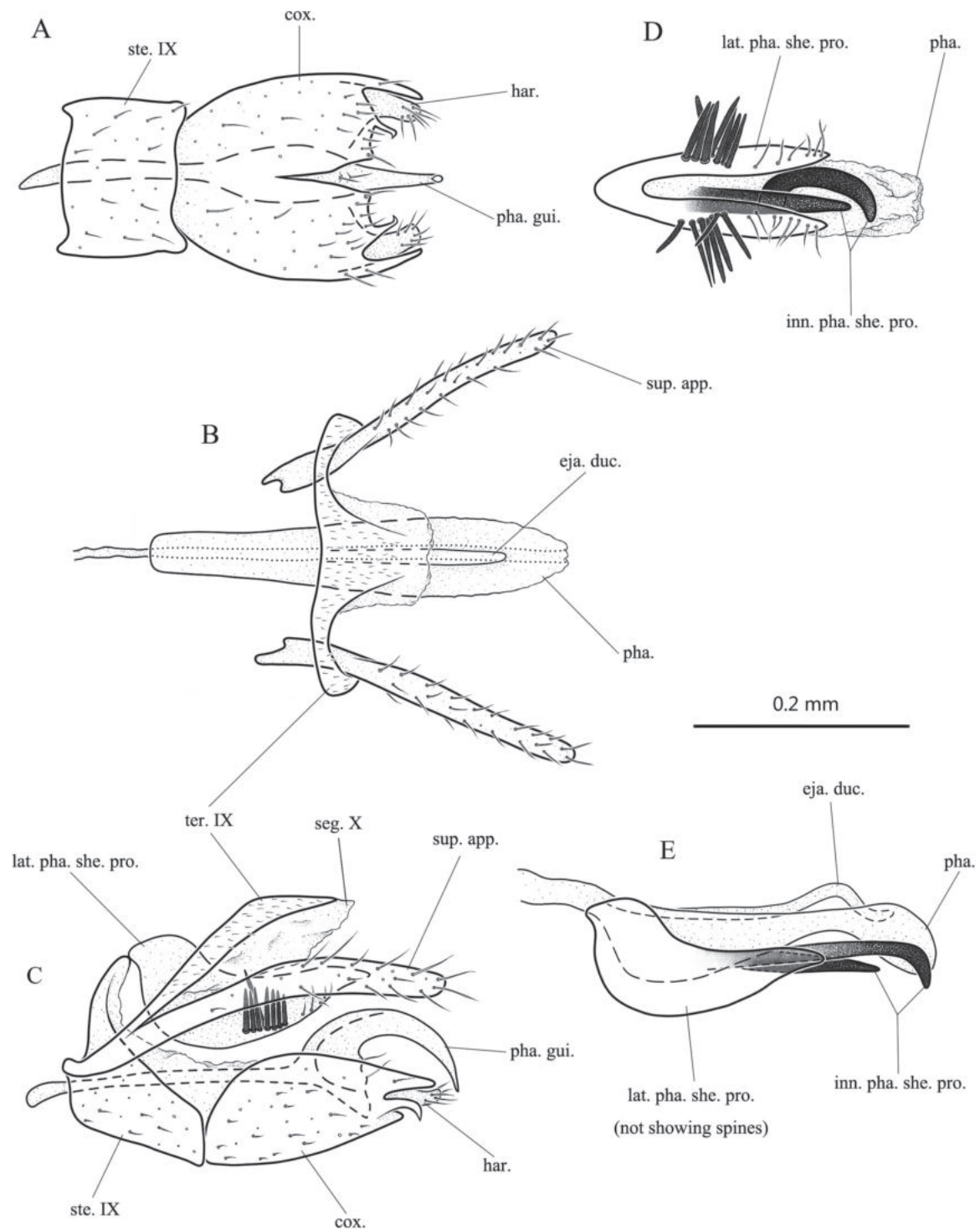


Figure 7. *Tinodes aviformis* sp. nov., male adult, holotype **A** genitalia, ventral **B** genitalia, dorsal **C** genitalia, left lateral **D** phallic complex, ventral **E** phallic complex, left lateral. Abbreviations: ste. IX = sternum IX; ter. IX = tergum IX; seg. X = segment X; sup. app. = superior appendage (paired); cox. = coxopodite (paired); har. = harpago (paired); pha. = phallus; pha. gui. = phallic guide; inn. pha. she. pro. = inner phallic sheath process; lat. pha. she. pro. = lateral phallic sheath process (paired); eja. duc. = ejaculatory duct.

branches and unpaired inner branches; paired lateral branches compressed and spoon-like, semicircular, and resembling nesting bird in lateral view (Fig. 7C, E), each with several strong spines at middle near ventral edge and distal half setose; fused basally, resembling pair of clam shells in ventral view (Fig. 7D); two

unpaired inner branches strongly sclerotized (Fig. 7D, E); one of them straight, one curved; phallus slightly extending beyond tip of phallic sheath process, with distal end membranous in ventral view (Fig. 7D), base and apex swollen in lateral view (Fig. 7E); ejaculatory duct slender, with subapex S-shaped in lateral view (Fig. 7C). Phallic guide with subapex wider and then divided into two branches in lateral view (Fig. 7C), dorsal branch slender, curved downwards distally and gradually narrowed to sharp apex; ventral branch short. Coxopodites elliptical in lateral view (Fig. 7C); fused with each other basally in ventral view (Fig. 7A), each with posterodorsal angle digitate and posterior margin having tiny submesal digitate process; harpago setose, small, and simple (Fig. 7A, C).

Etymology. The Latin masculine adjective *aviformis*, meaning “bird-shaped,” and refers to the shape of the pair of lobes of the lateral phallic sheath process in lateral view.

Distribution. China (Hainan).

***Psychomyia indra* Malicky & Chantaramongkol, 1993**

Psychomyia indra Malicky & Chantaramongkol, 1993: 1162 (type locality: Thailand, Tramot; ♂).

Material examined. CHINA – Hainan Province • 1 ♂; Ledong County, Jianfeng Town, Jianfengling National Forest Park, Rainforest Valley; 18°44.72'N, 108°56.08'E; alt. 640 m; 17-iv-2019; light trap; H. Song leg.; NJAU Tricho-20190417-0001.

Distribution. China (Hainan [new record]); Thailand.

***Paduniella andamanensis* Malicky, 1979**

Paduniella andamanensis Malicky, 1979: 98 (type locality: India, Süd-Andaman, Nayachul-Fluß bei Mongelutonge, Lichtfang [India, South Andaman, Naya-chul River, near Manglutan, light trap]; ♂).

Material examined. CHINA – Hainan Province • 1 ♂, Yunnan Province, Xishuangbanna Dai Autonomous Prefecture, Jinghong City, Yunjinghong Street G214; 22°01.75'N, 100°52.12'E; alt. 660 m; 26-vii-2021; light trap; K. Jiang leg.; NJAU Tricho-20210726-0001.

Distribution. China (Yunnan [new record]); India (Andaman Islands).

***Paduniella dendrobia* Malicky & Chantaramongkol, 1993**

Paduniella dendrobia Malicky & Chantaramongkol, 1993: 1159 (type locality: Thailand, Doi Inthanon; ♂).

Material examined. CHINA – Sichuan Province • 1 ♂; Yibin City, Pingshan County, Xining River; 28°41.15'N, 103°45.97'E; alt. 370 m; 12-v-2020; X.Y. Ge & X. Chen leg.; NJAU Tricho-20200512-0001.

Distribution. China (Sichuan [new record]); Thailand.

***Tinodes gapbona* Johanson & Oláh, 2008**

Tinodes gapbona Johanson & Oláh, 2008: 7 (type locality: Vietnam, Hoabinh towards Dabac; ♂).

Materials examined. CHINA – Guangdong Province • 2♂; Huizhou City, Yuguishan Nature Reserve; 22°25.80'N, 113°26.39'E; alt. 290 m; 17-ix–22-x-2020; Malaise trap; Institute of Zoology, Guangdong Academy of Sciences leg.; NJAU Tricho-20201022-0001 to Tricho-20201022-0002 • 20♂; Zhaoqing City, Dinghushan National Nature Reserve; 23°09.50'N, 112°32.46'E; alt. 170 m; 9-ix–9-x-2021; Malaise trap; Institute of Zoology, Guangdong Academy of Sciences leg.; NJAU Tricho-20201009-0001 to Tricho-20201009-0020.

Distribution. China (Guangdong [new records]); Vietnam.

***Psychomyia imamah* Malicky, 2020**

Psychomyia polyacantha Li, Qiu & Morse, 2021 (in Qiu and Morse 2021) syn. nov. (type locality: China, Sichuan Province, Pingwu County, tributary of Fu-Jiang, 19 km E of Pingwu downtown, 32°24.72'N, 104°45.49'E, alt. 1090 m; ♂).

Materials examined. CHINA – Sichuan Province • 200+♂; Pingwu County, tributary of Fujiang, 19 km E of Pingwu downtown; 32°24.72'N, 104°45.49'E; alt. 1090 m; 27-vi-1990; J.C. Morse leg.; NJAU Tricho-19900627-0001 to Tricho-19900627-0200 • 200+♂; Pingwu downtown; 17 km E of Pingwu trib. of Fujianghe; 32°24.48'N, 104°44.36'E; alt. 1090 m; 27-vi-1990; L. Yang & Y. Li leg.; NJAU Tricho-19900627-0201 to Tricho-19900627-0400 • 16♂, Kangding County, Guzazhen Town, Dadu River, Wasigou, at suspension foot-bridge, across the river from G318 at 2819.9 km stone marker 30°04.53'N, 102°09.61'E, alt. 1430 m, 29-vi-2005, Coll. X. Zhou, CJ Geraci leg.; NJAU Tricho-20050629-0001 to Tricho-20050629-0016 – Gansu Province • 6♂; Wenxian County, Bikou Town, Bifeng Gully; 32°44.72'N, 105°14.64'E; alt. 650 m; 16-vi-1998; L. Yang leg.; NJAU Tricho-19980616-0001 to Tricho-19980616-0006.

Distribution. China (Sichuan, Gansu).

Remarks. The specimens that we examined included topotypes that were collected at the same time as the type specimen of this species (Qiu and Morse 2021). We found that the harpagones each had four apical processes, which is rare in *Psychomyia*, occurring only in *P. polyacantha* and *P. imamah*. By comparing these specimens and published descriptions and figures of the male genitalia of these two species, we believe that the morphological characteristics of the two species overlap. The type locality of *P. polyacantha* is in the basin of the Fujiang River, and the Fujiang River flows into the Jialing River, and the paratypes of *P. polyacantha* and the holotype of *P. imamah* are from the basin of the Dadu River, which merges into the Minjiang River. Both the Jialing and Minjiang rivers are tributaries of the Yangtze, and their upstream habitats are similar and geographically adjacent. In summary, we identify *P. polyacantha* as a synonym of *P. imamah*.

Discussion

The Psychomyiidae is a moderately sized family of caddisflies (Holzenthal et al. 2007). However, the number of species has increased rapidly in recent years as new species are discovered and named; in 2008 there were about 400 species (de Moor and Ivanov 2008), in 2019 there were about 600 species (Morse et al. 2019), and now there are more than 650 species (including this study). Though the members of this family are widespread over nearly all the world (Holzenthal et al. 2007), the family's species diversity is uneven across zoogeographical regions. Psychomyiids are found mostly in the Oriental and Palaearctic regions, with the combined total number of species in those two regions constituting more than 90% of the world's species for this family. Of the two regions, the Oriental Region is the only one with all eight psychomyiid genera present, and it has about 65% of the world's recorded species, significantly higher than the number of Palaearctic species, which constitute about 25% of the species among six genera (*Psychomyia*, *Tinodes*, *Paduniella*, *Metalype*, *Eoneureclipsis*, and *Lype*). Additionally, the Afrotropical region has three genera (*Tinodes*, *Paduniella*, and *Lype*) and 6.9% of the world's species, the Nearctic region has four genera (*Psychomyia*, *Tinodes*, *Paduniella*, and *Lype*) and 2.8% of the world's species, and the Australian region has only one genus (*Tinodes*) and 1.5% of the world's species. China covers parts of the Oriental and Palaearctic regions and has more than 111 species in six genera (including those in this study), constituting about 17% of psychomyiid species, of which six genera (*Psychomyia*, *Tinodes*, *Paduniella*, *Metalype*, *Eoneureclipsis*, and *Lype*) and 100 species are recorded in China's Oriental region, and four genera (*Psychomyia*, *Tinodes*, *Paduniella*, and *Metalype*) and 18 species are recorded in its Palaearctic region.

Most of the species in our study were collected from low latitudes, with a few from mid-latitudes (Table 1). Collection sites are near the source of streams or near a reservoir. Headwater streams had high forest cover and were small and cool, which is consistent with most psychomyiid larvae living in cool running water (Fig. 8A–D). While *Tinodes aviformis* sp. nov. was collected near a reservoir, similar to the habitats of some *Tinodes*, which have been reported to live in isolated stream pools in western North America and in lake littorals in Europe (Flint 1964; Wiggins 1996).

The male genitalia of the family vary among psychomyiid genera. In some genera, such as *Paduniella* and *Lype*, the structures of the male genitalia are simple enough to use common terms for describing them; however, in other genera, for example, in the genus *Tinodes*, extra structures are present in the genitalia, resulting in the different understanding on their homology, and accordingly, the terminology for the structures has varied among authors. The situation hinders phylogenetic study of the family based on morphology. We sincerely hope that, with phylogenetic studies using DNA sequences, the homology of these extra structures will become more generally understood and consensus for these terms will one day be reached, making interpretation of the evolution of the morphology and functional traits of these interesting and ecologically important animals more reliable.

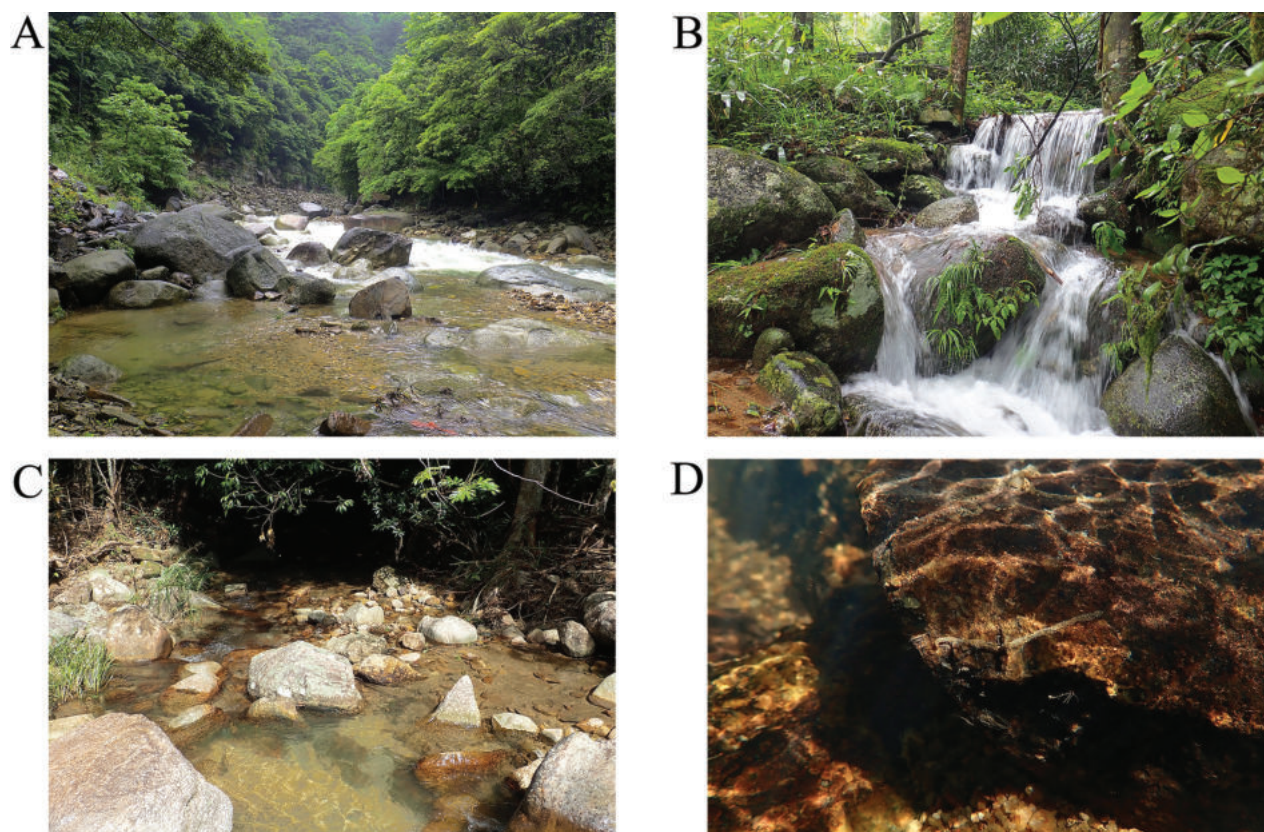


Figure 8. Photographs of habitat **A** a slow-flowing stream in the upper reaches of Yaorenping Hydropower Station, in Hunan Province **B** a rapids flowing stream in the upper reaches of Yaorenping Hydropower Station, in Hunan Province **C** a temporary pond in Jianfengling National Forest Park, Rainforest alley, in Hainan Province **D** the retreat of Psychomyiidae larvae and substratum composition of Hongxinxi River, in Hainan Province.

Acknowledgements

This research was supported by the National Natural Science Foundation of China (no. 41771052 and no. 32200364). We sincerely thank the Institute of Zoology, Guangdong Academy of Sciences and Prof. Hongying Sun from Nanjing Normal University for providing us with precious opportunities to visit the Nanling region and Hainan Province for collections. We are very thankful to Dr Haitian Song from the Fujian Academy of Forestry for selflessly donating caddisfly specimens. We also thank Prof. John Morse from Clemson University, USA, Dr Christy Jo Geraci, and Prof. Xin Zhou for contributions to the Trichoptera fauna of China, and we give special thanks to the friends of the first author, Dr Xinyu Ge, Mr Haoming Zang, Mr Kun Jiang, Mr Wei Cao, and Ms Zhu Jing for their great support during the field study, and for selflessly donating caddisfly specimens. We cordially thank reviewers Prof. John Morse and Prof. Hiroyuki Nishimoto for their valuable comments and recommendations on the manuscript.

Additional information

Conflict of interest

The authors have declared that no competing interests exist.

Ethical statement

No ethical statement was reported.

Funding

No funding was reported.

Author contributions

Conceptualization: all authors. Data curation: LP, ZD, YZ. Formal analysis: LP, ZD, YZ; Funding acquisition: MW, BW. Investigation: LP, ZD, YZ, CS. Methodology: LP, ZD, YZ, CS. Project administration: MW, CS, BW; Resources, LP, ZD, MW, BW; Software, LP, ZD, YZ. Supervision: CS, BW. Validation: LP, CS. Visualization: LP. Writing – original draft: LP. Writing – review and editing: MW, CS.

Author ORCIDs

Lang Peng  <https://orcid.org/0000-0002-5644-8248>

Zhen Deng  <https://orcid.org/0009-0004-4611-908X>

Yu-hua Zhang  <https://orcid.org/0009-0001-8259-4038>

Meng Wang  <https://orcid.org/0000-0001-5903-3171>

Chang-hai Sun  <https://orcid.org/0000-0003-4061-1028>

Bei-xin Wang  <https://orcid.org/0000-0002-5253-8799>

Data availability

All of the data that support the findings of this study are available in the main text.

References

- Adobe Inc (2018) Adobe Photoshop (Version: CC 2018 19.0). <https://www.adobe.com/products/photoshop.html>
- Arefina TI (2002) Two new species of caddisflies (Insecta: Trichoptera) from the Russian Far East. *Far Eastern Entomologist = Dal'nevostochnyi Entomolog* 112: 1–7.
- Arefina TI (2005) Two new species and new records of caddisflies (Insecta: Trichoptera) from the Far East of Russia. *Zootaxa* 1088(1): 45–53. <https://doi.org/10.11646/zootaxa.1088.1.6>
- Curtis J (1834) Description of some hitherto nondescript British species of mayflies of anglers. *The London and Edinburgh Philosophical Magazine and Journal of Science* 3(4): 120–125. [212–218.] <https://doi.org/10.1080/14786443408648276>
- de Moor FC, Ivanov VD (2008) Global diversity of caddisflies (Trichoptera: Insecta) in freshwater. In: Balian EV, Lévêque C, Segers H, Martens K (Eds) *Freshwater Animal Diversity Assessment* 198: 393–407. https://doi.org/10.1007/978-1-4020-8259-7_41
- Flint Jr OS (1964) Notes on some Nearctic Psychomyiidae with special reference to their larvae (Trichoptera). *Proceedings of the United States National Museum* 115(3491): 467–481. <https://doi.org/10.5479/si.00963801.115-3491.467>
- Holzenthal RW, Blahnik RJ, Prather AL, Kjer KM (2007) Order Trichoptera Kirby, 1813 (Insecta), caddisflies. *Zootaxa* 1668(1): 639–698. <https://doi.org/10.11646/zootaxa.1668.1.29>
- Johanson KA, Oláh J (2008) Description of seven new *Tinodes* species from Asia (Trichoptera: Psychomyiidae). *Zootaxa* 1854(1): 1–15. <https://doi.org/10.11646/zootaxa.1854.1.1>

- Johanson KA, Oláh J (2010) Description of six new species of Oriental *Paduniella* (Insecta: Trichoptera: Psychomyiidae). *Zootaxa* 2548(1): 43–56. <https://doi.org/10.11646/zootaxa.2548.1.3>
- Kimmins DE (1955) Results of the Oxford University Expedition to Sarawak, 1932. Order Trichoptera. *Sarawak Museum Journal* 6: 374–442.
- Klapálek F (1898) Zpráva o Neuropterách a Pseudoneuropterách sbíraných v Bosně a Hercegovin. *Vestník České Akademie Císare Frantiska Josefa pro vědy, slovesnost a umení v Praze Rozpravy* 7: 126–134.
- Latreille PA (1829–1830) Les crustacés, les arachnides et les insectes: distribués en familles naturelles. In: Cuvier G (Ed.) *Le Règne Animal Distribué D'après son Organization, pour Servir de Base à l'Histoire Naturelle des Animaux et D'introduction à l'Anatomie Compare*, Nouvelle Édition, rev. et aug. Chez Déterville, Paris, 584 pp. [+ pls 1–5; pp. i–xxiv, 1–556.] <https://doi.org/10.5962/bhl.title.11575>
- Laudee P, Kong C, Malicky H (2020) New species of caddisflies (Trichoptera: Psychomyiidae, Hydropsychidae, Leptoceridae) from Mekong tributaries, Cambodia. *Zootaxa* 4853(1): 133–138. <https://doi.org/10.11646/zootaxa.4853.1.9>
- Li YJ, Morse JC (1997) The *Paduniella* (Trichoptera: Psychomyiidae) of China, with a phylogeny of the world species. *Insecta Mundi* 11: 281–299.
- Malicky H (1979) Neue Köcherfliegen (Trichoptera) von den Andamansen-Inseln. *Zeitschrift der Arbeitsgemeinschaft Österreichischer Entomologen* 30: 97–109.
- Malicky H (1993) Neue asiatische Köcherfliegen (Trichoptera: Philopotamidae, Polycentropodidae, Psychomyiidae, Ecnomidae, Hydropsychidae, Leptoceridae). *Linzer Biologische Beiträge* 25: 1099–1136.
- Malicky H (2004) Neue Köcherfliegen aus Europa und Asien. *Braueria* 31: 36–42.
- Malicky H (2020) Beiträge zur Kenntnis chinesischer Köcherfliegen (Insecta, Trichoptera). *Linzer Biologische Beiträge* 52: 417–455.
- Malicky H, Chantaramongkol P (1993) Neue Trichopteren aus Thailand. Teil 2: Rhyacophilidae, Philopotamidae, Polycentropodidae, Ecnomidae, Psychomyiidae, Xiphocentronidae, Helicopsychidae, Odontoceridae (Arbeiten über thailändische Köcherfliegen Nr.12) (Fortsetzung). *Linzer Biologische Beiträge* 25: 1137–1187.
- Malicky H, Melnitsky SI, Ivanov VD (2019) Fauna of caddisflies (Insecta: Trichoptera) of the Phuket Island, Thailand. *Russian Entomological Journal* 28(4): 425–432. <https://doi.org/10.15298/rusentj.28.4.11>
- McLachlan R (1878) A Monographic Revision and Synopsis of the Trichoptera of the European Fauna, Part 7. Van Voorst, London, 349–428. [pls 38–44.]
- Morse JC (2023) Trichoptera World Checklist. <https://trichopt.app.clemson.edu/welcome.php> [Accessed 01 May 2023]
- Morse JC, Frandsen PB, Graf W, Thomas JA (2019) Diversity and ecosystem services of Trichoptera. *Insects* 10(5): e125. <https://doi.org/10.3390/insects10050125>
- Peng L, Wang BX, Sun CH (2020) Four new species of *Psychomyia* (Trichoptera: Psychomyiidae) from China, with re-descriptions of two species. *Zootaxa* 4860(2): 227–242. <https://doi.org/10.11646/zootaxa.4860.2.5>
- Peng L, Ge XY, Sun CH, Wang BX (2022) Five new species of *Tinodes* (Trichoptera: Psychomyiidae) from China. *Zootaxa* 5196(2): 280–290. <https://doi.org/10.11646/zootaxa.5196.2.8>
- Peng L, Zang H, Sun C, Wang L, Wang B (2023) Four new species of the genus *Eoneureclipsis* (Trichoptera: Psychomyiidae) from China inferred from morphology and DNA barcodes. *Insects* 14(2): e158. <https://doi.org/10.3390/insects14020158>

- Qiu S, Morse JC (2021) New species of the genus *Psychomyia* Latreille (Trichoptera: Psychomyiidae) from China, with a phylogeny of oriental species. *Transactions of the American Entomological Society* 147(2): 503–594. <https://doi.org/10.3157/061.147.0204>
- Schmid F (1998) Genera of the Trichoptera of Canada and Adjoining or Adjacent United States. *The Insects and Arachnids of Canada Part 7*. NRC, Ottawa, 319 pp.
- Suwannarat N, Malicky H, Laudee P (2020) Four new species of caddisflies (Trichoptera: Polycentropodidae, Psychomyiidae, Hydropsychidae, Odontoceridae) from Khao Nan and Tai Rom Yen National Parks, southern Thailand. *Zootaxa* 4801(3): 577–583. <https://doi.org/10.11646/zootaxa.4801.3.10>
- Ulmer G (1913) Über einige von Edw. Jacobson auf Java Gesammelte Trichopteren, zweiter Beitrag. *Notes from the Leyden Museum* 35: 78–101.
- Walker F (1852) *Catalogue of the Specimens of Neuropterous Insects in the Collection of the British Museum, Part I: Phryganides–Perlides*. British Museum, London, 192 pp.
- Wiggins GB (1996) *Larvae of the North American Caddisfly Genera (Trichoptera)* (2nd edn.). University of Toronto Press, Toronto, 472 pp. <https://doi.org/10.3138/9781442623606>

Replacement names for two species of *Orthacanthus* Agassiz, 1843 (Chondrichthyes, Xenacanthiformes), and discussion of *Giebelodus* Whitley, 1940, replacement name for *Chilodus* Giebel, 1848 (Chondrichthyes, Xenacanthiformes), preoccupied by *Chilodus* Müller & Troschel, 1844 (Actinopterygii, Characiformes)

Loren E. Babcock¹ 

¹ School of Earth Sciences, Orton Geological Museum, The Ohio State University, Columbus, OH, 43210, USA
Corresponding author: Loren E. Babcock (babcock.5@osu.edu)



Academic editor: Bruno Melo
Received: 24 June 2023
Accepted: 4 December 2023
Published: 8 January 2024

ZooBank: <https://zoobank.org/B6BBB2F0-B9FF-4E76-B354-3D7CF36310C9>

Citation: Babcock LE (2024)
Replacement names for two species of *Orthacanthus* Agassiz, 1843 (Chondrichthyes, Xenacanthiformes), and discussion of *Giebelodus* Whitley, 1940, replacement name for *Chilodus* Giebel, 1848 (Chondrichthyes, Xenacanthiformes), preoccupied by *Chilodus* Müller & Troschel, 1844 (Actinopterygii, Characiformes). ZooKeys 1188: 219–226. <https://doi.org/10.3897/zookeys.1188.108571>

Copyright: © Loren E. Babcock.
This is an open access article distributed under terms of the Creative Commons Attribution License ([Attribution 4.0 International – CC BY 4.0](https://creativecommons.org/licenses/by/4.0/)).

Abstract

Three species assigned to the same nominal genus of Paleozoic xenacanthiform shark have been combined with the name *Orthacanthus gracilis* (Chondrichthyes, Xenacanthiformes, Orthacanthidae). *Orthacanthus gracilis* (Giebel, 1848), which was originally combined as *Chilodus gracilis* Giebel, 1848, is the senior synonym; it has priority over both *Orthacanthus gracilis* (Newberry, 1857), which was originally combined as *Diploodus gracilis* Newberry, 1857, and *Orthacanthus gracilis* Newberry, 1875a. Proposed species-group replacement names are *Orthacanthus lintonensis* **nom. nov.** for *O. gracilis* (Newberry, 1857) and *Orthacanthus adamas* **nom. nov.** for *O. gracilis* Newberry, 1875a. *Chilodus gracilis* Giebel, 1848 is designated as the type species of *Chilodus* Giebel, 1848; this species becomes the type species for *Giebelodus* Whitley, 1940, which is a replacement name for *Chilodus* Giebel, 1848 (preoccupied by *Chilodus* Müller & Troschel, 1844, Actinopterygii). *Giebelodus* Whitley, 1940 is a junior subjective synonym of *Orthacanthus* Agassiz, 1843.

Key words: Carboniferous, Chilodontidae, headstander, junior homonym, Orthacanthidae, shark

Introduction

Three species of xenacanthiform sharks described from Carboniferous strata have been assigned to the same nominal genus and combined with the name *Orthacanthus gracilis* (Chondrichthyes, Xenacanthiformes, Orthacanthidae), either originally or subsequently. The basionym of the senior synonym, in its original combination, *Chilodus gracilis* Giebel, 1848, is homonymous with the name of an extant species of characiform fish, *Chilodus gracilis* Isbrücker & Nijssen, 1988 (Actinopterygii, Characiformes, Chilodontidae). *Chilodus* is a genus-group name that was proposed for two different nominal genera. One is a genus of characiform fish (Müller and Troschel 1844: 85–86) and the other is a genus of extinct xenacanthiform shark (Giebel 1848: 352).

The purpose of this paper is to clarify, detangle, and stabilize the nomenclature of these genus-group and species-group names.

Nomenclatural history

Species-group names of fossil xenacanthiform sharks that have been combined as *Orthacanthus gracilis* are as follows:

1. *Chilodus gracilis* Giebel, 1848 (Fig. 1A), reassigned to *Orthacanthus* Agassiz, 1843 by Boy and Martens (1991) and Hampe (1994, 2003). According to Articles 23.3.5, 52, 57, and 60.3 of the International Code of Zoological Nomenclature (International Commission on Zoological Nomenclature 2000), this species has priority over two species named by Newberry (1857, 1875a) (see below) that have the name *Orthacanthus gracilis* originally or after recombination.
2. *Diplodus gracilis* Newberry, 1857 (Fig. 1B), reassigned to *Orthacanthus* by Hampe (1994, 2003). It is a junior secondary homonym of *Orthacanthus gracilis* (Giebel, 1848) when both species are treated as valid species of *Orthacanthus* Agassiz, 1843 (Hampe 1994: 56–63). To remove the homonymy, the name *Orthacanthus lintonensis* nom. nov. is proposed as a new replacement name for *Diplodus gracilis* (Newberry, 1857).
3. *Orthacanthus gracilis* Newberry, 1875a (Fig. 1C). This species is a junior secondary homonym of *Chilodus gracilis* Giebel, 1848 when *C. gracilis* Giebel, 1848 is placed in *Orthacanthus* Agassiz, 1843 (Hampe 1988, 1994, 2003; Boy and Martens 1991: figs 1, 8). To remove the homonymy, the name *Orthacanthus adamas* nom. nov. is proposed as a new replacement name for *Orthacanthus gracilis* Newberry, 1875a.

Proposals of *Chilodus* as a genus-group name are as follows:

1. *Chilodus* Müller & Troschel, 1844 was erected for an extant characiform fish with *Chilodus punctatus* Müller & Troschel, 1844 (Actinopterygii, Characiformes, Chilodontidae) as the type species, by monotypy.
2. *Chilodus* Giebel, 1848 was erected for an extinct Paleozoic xenacanthiform shark (Chondrichthyes, Xenacanthiformes, Orthacanthidae), embracing two species, *Chilodus tuberosus* Giebel, 1848 (Fig. 1D) and *Chilodus gracilis* Giebel, 1848 (Fig. 1A).

The type species of *Chilodus* Giebel, 1848, designated here for nomenclatural stability, is *Chilodus gracilis* Giebel, 1848. It is the best-known species and the only one that Giebel (1848) included in *Chilodus* that is represented by a known, existing type specimen (Hampe 1994; Fig. 1A). Designation of this species as the type species follows Recommendation 69A of the Code (International Subcommission on Zoological Nomenclature 2000). The other species originally included in *Chilodus* Giebel, 1848, *C. tuberosus* Giebel, 1848, was synonymized by Giebel (1849) with *Lamna carbonaria* Germar, 1844 (Fig. 1E); but see Romanovski (1857), who retained the combination *C. tuberosus* Giebel, 1848. Here, *L. carbonaria*, including *C. tuberosus* as a junior subjective synonym, is recombined as *Orthacanthus carbonarius* (Germar, 1844).

Whitley (1940: 243) proposed the name *Giebelodus* as a replacement name for *Chilodus* Giebel, 1848 because the genus-group name is preoccupied by *Chilodus* Müller & Troschel, 1844. Following Article 67.8 of the Code (International Commission on Zoological Nomenclature 2000), *C. gracilis* Giebel, 1848 automatically becomes the type species of *Giebelodus* Whitley, 1940.

Chilodus gracilis Giebel, 1848 is here assigned to *Orthacanthus*, and *Giebelodus* Whitley, 1940 is thus a junior subjective synonym of *Orthacanthus* Agassiz, 1843.

Uses of the combination *Chilodus gracilis* are as follows:

1. *Chilodus gracilis* Giebel, 1848 (Chondrichthyes, Xenacanthiformes, Orthacanthidae), a fossil shark described from the Carboniferous of Germany.
2. *Chilodus gracilis* Isbrücker & Nijssen, 1988 (Actinopterygii, Characiformes, Chilodontidae), an extant freshwater characiform fish also known as the graceful headstander, described from Trovão, Rio Aaupés, Amazonas, Brazil.

Chilodus gracilis Isbrücker & Nijssen, 1988 is not a junior homonym of *C. gracilis* Giebel, 1848 because, according to the exception in Art. 57.8 of the Code, and the related example, homonymy between identical species-group names in combination with homonymous generic names having the same spelling but established for different nominal genera is to be disregarded (International Commission on Zoological Nomenclature 2000).

Systematics

Class Chondrichthyes Huxley, 1880

Subclass Elasmobranchii Bonaparte, 1838

Superorder Euselachii Hay, 1902

Order Xenacanthiformes Berg, 1955

Family Orthacanthidae Heyler & Poplin, 1990 (see van der Laan 2018)

Genus *Orthacanthus* Agassiz, 1843

***Orthacanthus gracilis* (Giebel, 1848)**

Fig. 1A

Chilodus gracilis Giebel, 1848: 352–353.

Chilodus gracilis: Giebel 1849: 70, pl. XXIX, fig. 2.

Pleuracanthus sp.: Gocht 1955: pl. VIII, fig. 5.

Orthacanthus-Typ UG: Schneider 1985: 91–92, fig. 2.

Orthacanthus carbonarius (Germar, 1844): Schneider 1988: pl. 1, fig. 4.

Orthacanthus gracilis (Giebel, 1848): Boy and Martens 1991: figs 1, 8.

Orthacanthus gracilis: Hampe 1994: 56–63, figs 1–5.

Orthacanthus gracilis: Hampe 2003: 209–210.

Holotype. Tooth; Geiseltalmuseum Halle, GTM 1095, previously illustrated by Giebel (1849: pl. XXIX, fig. 2) and Hampe (1994: Fig. 1a–c).

Type locality. Slate of the Wettin-Schichten (Carboniferous) from Wettin, north of Halle, Saale area, Saxony-Anhalt, Germany.

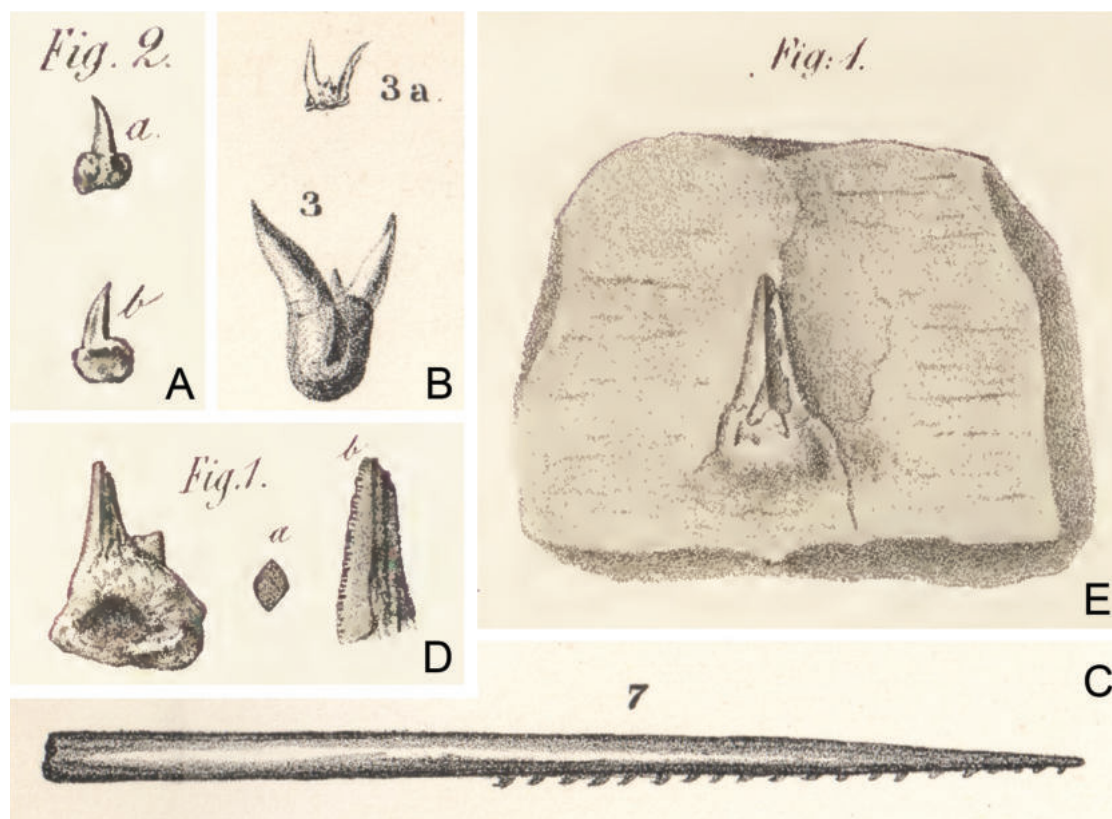


Figure 1. Original 19th century figures of Carboniferous-age xenacanthiform shark fossils from Saxony-Anhalt, Germany, and Ohio, USA **A** *Orthacanthus gracilis* (Giebel, 1848), tooth, holotype (Geiseltalmuseum Halle, GTM 1095), two views; reproduced from Giebel (1849: pl. XXIX, fig. 2a, b), 7.7 mm long. Wettin-Schichten, Wettin/Saalegebiet, Saxony-Anhalt, Germany **B** *Orthacanthus lintonensis* nom. nov., replacement name for *Diplodus gracilis* Newberry, 1857a, two teeth, syntypes (repository unknown); reproduced from Newberry (1875a: pl. LVIII, figs. 3, 3a), ca 5 and 13 mm long. Upper Freeport Coal, Allegheny Group, Diamond Coal Mine, Linton, Ohio, USA **C** *Orthacanthus adamas* nom. nov., replacement name for *Orthacanthus gracilis* Newberry, 1875a, dorsal spine, illustration is a composite based on syntypes (Orton Geological Museum, OSU 4467A, 4467B); reproduced from Newberry (1875a, pl. LIX, fig. 7), ca 71 mm long. Upper Freeport Coal, Allegheny Group, Diamond Coal Mine, Linton, Ohio, USA **D** *Orthacanthus carbonarius* (Germar, 1844), two teeth, syntypes (repository unknown) of *Chilodus tuberosus* Giebel, 1848; reproduction of Giebel (1849: pl. XXIX, figs. 1, 1a, 1b as), length unknown. Wettin-Löbejun, Saxony-Anhalt, Germany **E** *Orthacanthus carbonarius* (Germar, 1844), tooth, syntype (repository unknown) of *Lamna carbonaria* Germar, 1844; reproduced from Germar (1844: pl. 1, fig. 1), ca 20 mm long. Presumably from Saxony-Anhalt, Germany.

Remarks. The basionym *Chilodus gracilis* Giebel, 1848 is designated herein as the type species of *Chilodus* Giebel, 1848. Whitley (1940: 243) proposed *Giebelodus* as a replacement name for *Chilodus* Giebel, 1848 (preoccupied by *Chilodus* Müller & Troschel, 1844), and *C. gracilis* Giebel, 1848 is thus the type species of *Giebelodus*. Following Boy and Martens (1991) and Hampe (1994, 2003), *Giebelodus gracilis* (Giebel, 1848), which is known only from teeth, is referred to the genus *Orthacanthus* Agassiz, 1843.

***Orthacanthus lintonensis* nom. nov.**

Fig. 1B

Diplodus gracilis Newberry, 1857: 99.

Diplodus gracilis: Newberry 1873: 334–336.

Diplodus gracilis: Newberry 1874: 330–331.

Diplodus gracilis: Newberry 1875a: 45, pl. LVIII, figs 3, 3a.
Diplodus gracilis: Newberry 1875b: 45, pl. LVIII, figs 3, 3a.
Xenacanthus gracilis (Newberry, 1857): Olson 1946: 290–291.
Xenacanthus compressus (Newberry, 1857): Hotton 1952: 496, 499.
Orthacanthus compressus (Newberry, 1857): Hook and Baird 1986: table 2.
Orthacanthus gracilis (Newberry, 1857): Hampe 1988: 292.
Orthacanthus compressus: Hook and Baird 1988: table 1.
Orthacanthus gracilis: Hampe 1994: 63.
Orthacanthus compressus: Johnson 1999: 243–245.
Orthacanthus gracilis: Hampe 2003: 209–210.

Syntypes. Teeth, repository unknown, previously illustrated by Newberry (1875a: 45, pl. LVIII, figs 3, 3a; 1875b: 45, pl. LVIII, figs 3, 3a).

Type locality. Upper Freeport Coal (Carboniferous), from the Diamond Coal Mine, Linton, Jefferson County, Ohio, USA.

Etymology. The species refers to Linton, Ohio, the type locality.

Remarks. The new species-group name *Orthacanthus lintonensis* nom. nov. replaces *Diplodus gracilis* Newberry, 1857, which after recombination as *Orthacanthus gracilis* (Newberry, 1857) is a junior secondary homonym of *Orthacanthus gracilis* (Giebel, 1848).

Detailed study of xenacanthiform materials from the Linton Lagerstätte is needed, and the type specimens need to be re-examined. Much of the systematic work on fish taxa described from Linton after 1900 has involved non-type specimens. Indeed, most published illustrations of Linton fish types are line-art drawings (e.g. Newberry 1873, 1874, 1875a, 1875b; herein, Fig. 1B, C), often with generous “restoration,” few of the types, even the ones whose repositories are known, have been photographically illustrated. Pending restudy of the type specimens of xenacanthiform sharks from the Linton Lagerstätte, *O. lintonensis* nom. nov. is proposed here as an available name that can compete in priority with other names, not as a junior synonym of any other species (compare Hotton 1952; Hook and Baird 1986; Johnson 1999).

***Orthacanthus adamas* nom. nov.**

Fig. 1C

Orthacanthus gracilis Newberry, 1875a: 56–57, pl. LIX, fig. 7.
Orthacanthus gracilis: Newberry 1875b: 56–57, pl. LIX, fig. 7.
Orthacanthus gracilis: Cope 1881: 163.
Pleuracanthus (*Orthacanthus*) *gracilis*: Case 1900: 701, pl. I, fig. 4.
Orthacanthus gracilis: Morningstar 1924: 53.
Xenacanthus gracilis (Newberry, 1875a): Olson 1946: 287.
Xenacanthus gracilis: Hook and Baird 1986: 179, table 2.
Xenacanthus gracilis: Hook and Baird 1988: table 1.
Orthacanthus gracilis: Hampe 2004: 209.

Syntypes. Two dorsal spines, Orton Geological Museum, The Ohio State University, Columbus, Ohio, USA (OSU) 4467A, 4467B, previously illustrated as a composite by Newberry (1875a: pl. LIX, fig. 7; 1875b: pl. LIX, fig. 7).

Type locality. Upper Freeport Coal (Carboniferous), from the Diamond Coal Mine, Linton, Jefferson County, Ohio, USA.

Etymology. *Adamas* (Latin, diamond), in allusion to the Diamond Coal Mine, where the species was first collected.

Remarks. The new species-group name *Orthacanthus adamas* nom. nov. replaces *Orthacanthus gracilis* Newberry, 1875a, which is a junior homonym of *Orthacanthus gracilis* (Giebel, 1848). Newberry (1875a: pl. LIX, fig. 7; 1875b: pl. LIX, fig. 7) illustrated this species with a composite figure based on syntypic dorsal spines. This species should not be confused with the other xenacanthiform species from Linton bearing the species epithet *gracilis*, based on teeth, and also referred to *Orthacanthus*, as discussed above. Replacement names for both taxa will reduce potential confusion. Cope (1881) and Case (1900) extended the stratigraphic range of this species into the Permian.

Acknowledgements

I am indebted to the reviewers, R. van der Laan, B. Sidlauskas, M. Kottelat, and an anonymous reviewer, plus the academic editor B.F. Melo, for insightful and helpful reviews and comments that have substantially improved this manuscript.

Additional information

Conflict of interest

The author has declared that no competing interests exist.

Ethical statement

No ethical statement was reported.

Funding

No funding was reported.

Author contributions

Writing – original draft: LEB.

Author ORCID

Loren E. Babcock  <https://orcid.org/0000-0002-9324-9176>

Data availability

All of the data that support the findings of this study are available in the main text.







References

- Agassiz L (1843) Recherche sur les Poissons fossiles. Vol. 3. Contenant l'Histoire de l'Ordre des Placoides. Petitpierre, Neuchâtel: 157–390.
- Berg LS (1955) Classification of Fishes, both Recent and Fossil (2nd ed., revised by Pavolvsky EN). Travaux de l'Institut Zoologique de l'Académie des Sciences de l'URSS 20, 286 pp.
- Bonaparte CL (1838) Selachorum tabula analytica. Nuovi Annali delle Scienze Naturali 1(2): 195–214.

- Boy JA, Martens T (1991) Zur Problematik chronostratigraphischer Korrelationen im mitteleuropäischen Rotliegend (?oberstes Karbon – Perm). *Newsletters on Stratigraphy* 25(3): 163–192. <https://doi.org/10.1127/nos/25/1991/163>
- Case EC (1900) The vertebrates from the Permian bone bed of Vermilion County, Illinois. *The Journal of Geology* 8(8): 698–729. <https://doi.org/10.1086/620866>
- Cope ED (1881) Catalogue of the Vertebrata of the Permian formation of the United States. *American Naturalist* 15(2): 162–164.
- Germar EF (1844) Fischüberreste [Piscium reliquiae] In Germar EF Die Versteinerungen des Steinkohlengebirges von Wettin und Löbejün im Saalkreise. Heft [Fasciculus] 1: 1–3. [Petrificata Stratorum Lithanthracum Wettini et Lobejuni in Circulo Salae.] [C.A. Schwetschke und Sohn, Halle.] <https://doi.org/10.5962/bhl.title.169070>
- Giebel CG (1848) Die Fische der Vorwelt, mit steter Berücksichtigung der lebenden Fische. In Giebel CG Fauna der Vorwelt mit steter Berücksichtigung der lebenden Thiere. Erster Band: Wirbelthiere. Dritte Abtheilung: Fische, Brockhaus, Leipzig, 467 pp. <https://doi.org/10.5962/bhl.title.24938>
- Giebel CG (1849) Fischüberreste [Piscium reliquiae]. In: Germar EF (Ed.) Die Versteinerungen des Steinkohlengebirges von Wettin und Löbejün im Saalkreise [Petrificata Stratorum Lithanthracum Wettini et Lobejuni in Circulo Salae.] Heft [Fasciculus] 6: 69–79. C.A. Schwetschke und Sohn, Halle.
- Gocht H (1955) Acanthodierstacheln und andere Fischreste im Unteren Rotliegenden bei Manebach. *Hallesches Jahrbuch für mitteldeutsche Erdgeschichte* 2: 110–111.
- Hampe O (1988) Über die Bezeichnung des *Orthacanthus* (Chondrichthyes: Xenacanthida; Oberkarbon-Unterperm). *Paläontologische Zeitschrift* 62(3/4): 285–296. <https://doi.org/10.1007/BF02989499>
- Hampe O (1994) Neue Erkenntnisse zur permokarbonischen Xenacanthiden-Fauna (Chondrichthyes: Elasmobranchii) und deren Verbreitung im südwestdeutschen Saar-Nahe-Becken. *Neues Jahrbuch für Geologie und Paläontologie. Abhandlungen* 192(1): 53–87.
- Hampe O (2003) Revision of the Xenacanthida (Chondrichthyes: Elasmobranchii) from the Carboniferous of the British Isles. *Transactions of the Royal Society of Edinburgh. Earth Sciences* 93(3): 191–237. <https://doi.org/10.1017/S0263593300000419>
- Hay OP (1902) Bibliography and catalogue of the fossil Vertebrata of North America. *Bulletin of the United States Geological Survey* 179: 1–868. <https://doi.org/10.5962/bhl.title.20094>
- Heyler D, Poplin C (1990) Systematics and relationships among the Xenacanthiformes (Pisces, Chondrichthyes) in the light of Carboniferous and Permian material. *Acta Musei Reginaehradecensis Series A, Scientiae Naturales* 22 [for 1989]: 69–78.
- Hook RW, Baird D (1986) The Diamond Coal Mine of Linton, Ohio, and its Pennsylvanian-age vertebrates. *Journal of Vertebrate Paleontology* 6(2): 174–190. <https://doi.org/10.1080/02724634.1986.10011609>
- Hotton N III (1952) Jaws and teeth of American xenacanth sharks. *Journal of Paleontology* 26(3): 489–500.
- Huxley TH (1880) On the application of the laws of evolution to the arrangement of the Vertebrata, and more particularly of the Mammalia. *Proceedings of the Zoological Society of London* 43: 649–662.
- International Commission on Zoological Nomenclature (2000) International Code of Zoological Nomenclature (4th ed.; Ride WDL et al., Eds). <https://www.iczn.org/the-code/the-international-code-of-zoological-nomenclature/>

- Isbrücker IJH, Nijssen H (1988) Review of the South American characiform fish genus *Chilodus*, with description of a new species, *C. gracilis* (Pisces, Characiformes, Chilodontidae). *Beaufortia* 38(3): 47–56.
- Johnson GD (1999) Denticions of late Palaeozoic *Orthacanthus* species and a new species of? *Xenacanthus* (Chondrichthyes: Xenacanthiformes) from North America. *Acta Geologica Polonica* 49(3): 215–266.
- Morningstar H (1924) Catalogue of type fossils in the Geological Museum of The Ohio State University. *The Ohio Journal of Science* 24: 31–64.
- Müller J, Troschel FH (1844) Beschreibung neuer Asteriden. *Archiv für Naturgeschichte* 10(1): 81–99. <https://doi.org/10.5962/bhl.part.10809>
- Newberry JS (1857) Descriptions of several new genera and species of fossil fishes from the Carboniferous strata of Ohio. *Proceedings of the Academy of Natural Sciences*. Vol. 8 [for 1856]: 96–100.
- Newberry JS (1873) Descriptions of fossil fishes. Report of the Geological Survey of Ohio. Volume I. Geology and Palaeontology. Part II. Palaeontology, 247–355.
- Newberry JS (1874) Beschreibung der fossilen Fische. Bericht über die Geologische Aufnahme von Ohio. I. Band. Geologie und Paläontologie. II. Theil. Paläontologie: 247–350.
- Newberry JS (1875a) Descriptions of fossil fishes. Report of the Geological Survey of Ohio. Volume II. Geology and Palaeontology. Part II. Palaeontology, 1–64.
- Newberry JS (1875b) Beschreibung fossiler Fische. Bericht über die Geologische Aufnahme von Ohio. II. Band. Geologie und Paläontologie. II. Theil. Paläontologie: 1–64.
- Olson EC (1946) Fresh- and brackish-water vertebrate-bearing deposits of the Pennsylvanian of Illinois. *The Journal of Geology* 54(5): 281–305. <https://doi.org/10.1086/625364>
- Romanovski G (1857) Ueber die Verschiedenheit der beiden Arten: *Chilodus tuberosus* Gieb. und *Dicrenodus okensis* Rom. *Bulletin de la Société impériale des Naturalistes de Moscou* 30(2): 290–295.
- Schneider J (1985) Elasmobranchier-Zahntypen (Pisces, Chondrichthyes) und ihre stratigraphische Verbreitung im Karbon und Perm der Saale-Senke (DDR). *Freiberger Forschungshefte C* 400: 90–100.
- Schneider J (1988) Grundlagen der Morphogenie, Taxonomie und Biostratigraphie isolierter Xenacanthodier-Zähne (Elasmobranchii). *Freiberger Forschungshefte C* 419: 71–80.
- van der Laan R (2018) Family-group names of fossil fishes. *European Journal of Taxonomy* 466: 1–167. <https://doi.org/10.5852/ejt.2018.466>
- Whitley G (1940) The Nomenclator Zoologicus and some new fish names. *The Australian Naturalist* 10(7): 241–243.

New morphological and biological contributions to adults and immature forms of *Pissonotus paraguayensis* (Fulgoromorpha, Delphacidae) in wetlands of Argentina

Ana M. Marino de Remes Lenicov^{1,2}, Ana C. Faltlhauser^{2,3,4}, Alvaro Foieri^{1,5}, Nicolas A. Salinas^{2,3,4}, M. Cristina Hernández³, Alejandro J. Sosa^{2,3}

1 División Entomología, Facultad de Ciencias Naturales y Museo, Universidad Nacional de La Plata, La Plata, Argentina

2 Consejo Nacional de Investigaciones Científicas y Técnicas, Ciudad Autónoma de Buenos Aires, Argentina

3 Fundación para el Estudio de Especies Invasivas, Hurlingham, Buenos Aires, Argentina

4 Universidad de Buenos Aires, Facultad de Ciencias Exactas y Naturales, Departamento de Ecología, Genética y Evolución, CABA, Buenos Aires, Argentina

5 Comisión de Investigaciones Científicas, La Plata, Buenos Aires, Argentina

Corresponding authors: Ana M. Marino de Remes Lenicov (marinoremes@gmail.com); Ana C. Faltlhauser (anafaltlhauser@gmail.com)



Academic editor: Ilia Gjonov
Received: 28 September 2023
Accepted: 11 December 2023
Published: 8 January 2024

ZooBank: <https://zoobank.org/A6670243-A4CC-4B07-A73D-2DBC437BA13D>

Citation: Marino de Remes Lenicov AM, Faltlhauser AC, Foieri A, Salinas NA, Hernández MC, Sosa AJ (2024) New morphological and biological contributions to adults and immature forms of *Pissonotus paraguayensis* (Fulgoromorpha, Delphacidae) in wetlands of Argentina. ZooKeys 1188: 227–250. <https://doi.org/10.3897/zookeys.1188.113350>

Copyright:

© Ana M. Marino de Remes Lenicov et al.
This is an open access article distributed under terms of the Creative Commons Attribution License ([Attribution 4.0 International – CC BY 4.0](https://creativecommons.org/licenses/by/4.0/)).

Abstract

In the search for insects as biological control agents for the water primrose, the delphacid *Pissonotus paraguayensis* (Delphacidae) was found on *Ludwigia grandiflora* subsp. *hexapetala* (Onagraceae) in a wetland of Central East Argentina. The morphology of the unknown females (brachypterous and macropterous) and immature stages are described and illustrated. Adults and nymphs were collected in wetlands of Del Plata River Basin, from Buenos Aires to the northeastern part of Argentina. A rearing methodology was developed to perform biological studies. Both winged forms and structural features of the female genitalia are described for the first time at the genus level. Eggs and immature stages are described and keyed; fifth nymphal instars may be easily recognised by the yellowish colouration, blackish on dorsal of head, thorax and abdomen with conspicuous yellowish pits, ventrally only darkened on base of frons extended to lower level of eyes and dorsal surface of antennomeres I and II, and legs with distinctive black marks at femoro-tibial joint and apex. The geographical distribution is updated, expanding its range into Argentina, making Buenos Aires the southernmost limit of the genus in America. Biological information of the species is also reported here: life cycle, fecundity, oviposition behaviour, and host plant. Field observations showed that *P. paraguayensis* breeds, feeds, and causes damage to *L. g.* subsp. *hexapetala*. This delphacid presents a certain degree of specificity to the *Ludwigia* species in the *Jussiaea* section in host specificity tests. More studies are required to test this species as a potential biological control agent.

Key words: Biology, female wing polymorphism, host range, immature stages key, *Ludwigia*, morphology, new record distribution, planthopper

Introduction

The water primrose, *Ludwigia g.* subsp. *hexapetala* (Hook. & Arn.) G.L. Nesom & Kartesz, Michx. (Onagraceae) is a native South American plant (Wagner et al. 2007) that has been introduced in many countries around the world, invading both

aquatic and riparian ecosystems, and is considered among the most aggressive weeds in the world (Thouvenot et al. 2013). In the search for insects as biological control agents for water primrose, a delphacid *Pissonotus paraguayensis* Bartlett, 2000 was found on this plant in a wetland of Central East Argentina. This delphacid species has a detailed description of the brachypter male but little is known about the female form and nothing about its immature stages and biology.

Pissonotus Van Duzee, 1897 is a genus widespread in North America, from southern Canada, with a few species in the Caribbean and Neotropics (Bartlett and Deitz 2000). Since the description of the first eight North American species by Van Duzee, several authors have studied this genus, describing new species or relocating them within *Pissonotus* from other genera (Spooners 1912; Crawford 1914; Metcalf 1923; Muir and Giffard 1924; Oman 1947). The first revision of the genus was carried out by Morgan and Beamer (1949) and more recently Bartlett and Deitz (2000) presented an integrative contribution about aspects of its taxonomy, phylogenetic relationships, distribution and host plant associations with descriptions and keys for all 43 recognised species. This revision shows that colour and the morphological features provided mostly by male genitalia, particularly the shape of the paired median processes of the pygofer, are distinctive among the species. Although wing polymorphism is frequent in delphacid populations, brachypterism in both sexes prevails in more than half of the species of the genus, and the macropters are more erratically found (Bartlett and Deitz 2000). The wing dimorphism, as a life history strategy in *Pissonotus*, was investigated by Denno et al. (1991) and Denno and Roderick (1990), who used this feature to test hypotheses concerning the effects of persistence and architectural complexity of habitat on the occurrence and dispersion of populations.

Further studies are needed on immature stages of the genus, their morphology, and behaviour. Of North American species, only *P. delicatus* Van Duzee is known from immature stages (Wilson and Tsai 1991). Knowledge of immature morphology also adds new characters for identification, taxonomic diagnosis, and phylogenetic analysis as proposed by Yang and Fang (1993), Chen and Yang (1995), and Emeljanov (1996, 2002). This information can help estimate their richness, diversity and particularly, their association with invasive host plants.

Bartlett and Deitz (2000) reported aspects of the geographical distribution pattern and some information about host plants of *Pissonotus* spp. In same contribution, mentioned that 91% of the total species occur in North America while 6% (3 species) are restricted to South American environments, two of them, *P. boliviensis* Bartlett and *P. neotropicus* (Muir) are recorded from Argentina.

Plant associations are relatively rare, and only 20 of 43 species have their hosts recorded, although they have been confirmed in few species. Those records suggest that *Pissonotus* feeds primarily on dicots, especially Asteraceae with some few exceptions on other aquatic host plants outside of this family. For example, *P. boliviensis*, distributed in Central South America, was reported in Bolivia on Pontederiaceae: *Pontederia rotundifolia* L. and *Pontederia* sp. as hosts; and *P. piceus* (Van Duzee), widely distributed in Central and Eastern United States of America (USA), Central America, Northern South America, and the Caribbean were recorded in the USA on Onagraceae: *Ludwigia peploides* (H.B.K.) Raven (as *Jussiaea diffusa* Forskal) (Morgan and Beamer 1949), *L. grandiflora* (Michx.) Greuter & Burdet and *L. uruguayensis* (Camb.) Hara (now *L. g.* subsp. *grandiflora*

(Michx.) Greuter & Burdet and *L. g.* subsp. *hexapetala*). Additionally, this last species has several other hosts, including species in the Poaceae and non-Poaceae families (Wilson et al. 1994; Bartlett and Deitz 2000). Particularly in Argentina, eight species of Delphacidae have been the subjects of research, specifically investigating their level of association with macrophytes (Sosa et al. 2004, 2007; Mariani et al. 2013; Remes Lenicov and Cabrera Walsh 2013). Among these species, information regarding their life cycles has been gathered for three of them (Sosa et al. 2005; Mariani et al. 2007; Marino de Remes Lenicov et al. 2017).

During an ongoing search for native South American herbivores as potential biological control agents against *L. g.* subsp. *hexapetala*, three unidentified delphacids were collected (Hernández and Cabrera Walsh 2014). Those specimens were examined and are reported here as *P. paraguayensis*.

Herein this study presents new morphological features of the female and immature stages of *P. paraguayensis* contributing to the complete description of the species including a standard COI barcode sequence and a key to the instars. It also documents new distribution records, rearing methodology and biological information based on field and laboratory observations. Since this delphacid could be considered a biological control candidate, the host range is estimated.

Materials and methods

Insect collection

Between 2009 and 2011, specimens of delphacids (adults and nymphs) were collected by Hernández and Cabrera Walsh (2014) feeding on *L. g.* subsp. *hexapetala*. Samples were identified as *P. paraguayensis*, collection field trips were resumed in 2019 in areas where *L. g.* subsp. *hexapetala* is most commonly distributed (from Buenos Aires to the northeastern part of Argentina). Adults and nymphs of *P. paraguayensis* were collected both, by aspirating individuals from the leaves and stems of field host plants, and laboratory colonies. Specimens were preserved in 70% EtOH for morphological studies. Live adults and immature specimens from the lower Delta were used to describe colour patterns (Table 1).

Rearing methodology

During summer months (December to March), general culture consisted of outdoor pools (1×1.5 m) with *L. g.* subsp. *hexapetala* plants brought from the field and enclosed in square meshed cages. In cooler months (May to August) or if there is no availability of greenhouse conditions, *P. paraguayensis* can also be reared in small containers inside rearing chambers at FuEDEI facilities. We were able to maintain colonies in two types of containers with different water availability and size. One to three L cylindrical plastic containers with polyester gauze or nylon covers and enough water to irrigate the plant roots (Fig. 1A). Here, 10–20 cm plants can be placed vertically but insects are harder to observe or retrieve. The second device consisted of 20×15×5 cm rectangular plastic containers with pierced plastic lids and polyester gauze. Stems were placed horizontally and inside water picks for irrigation (Fig. 1B). Excess condensation on the walls is not recommended.

Table 1. First distribution sites for *Pissonotus paraguayensis* in Argentina (geographical coordinates in Degrees, Minutes, and Seconds (DMS)).

Location	Province	GPS coordinates	Observation date	Status	Host plant
Arroyo Ceibal	Santa Fe	28°42'57.7"S, 59°26'21.7"W		Hernández et al. 2014*	<i>Ludwigia grandiflora</i> subsp. <i>hexapetala</i>
Médanos	Entre Ríos	33°25'25.4"S, 59°5'47.4"W	30-03-2022	new	<i>Ludwigia grandiflora</i> subsp. <i>hexapetala</i>
Islas del Ibicuy	Entre Ríos	33°41'50.4"S, 58°55'12.3"W	05-02-2022	new	<i>Ludwigia grandiflora</i> subsp. <i>hexapetala</i>
Brazo Largo	Entre Ríos	33°51'53.4"S, 58°52'59.4"W	05-03-2022	new	<i>Ludwigia grandiflora</i> subsp. <i>hexapetala</i>
San Pedro	Buenos Aires	34°40'46.9"S, 59°38'52.4"W	06-02-2022	new	<i>Ludwigia grandiflora</i> subsp. <i>hexapetala</i>
Otamendi	Buenos Aires	34°03'48.2"S, 58°49'19.6"W		Hernández et al. 2014*	<i>Ludwigia grandiflora</i> subsp. <i>hexapetala</i>
Luján	Buenos Aires	34°33'57.6"S, 59°4'4.8"W	11-03-2022	new	<i>Ludwigia grandiflora</i> subsp. <i>hexapetala</i>
Dique Luján	Buenos Aires	34°21'17.1"S, 58°41'13.0"W	20-07-2023	new	<i>Ludwigia grandiflora</i> subsp. <i>hexapetala</i>
Magdalena	Buenos Aires	35°3'48.9"S, 57°33'14.9"W	03-11-2021	new	<i>Ludwigia grandiflora</i> subsp. <i>hexapetala</i>
La Plata	Buenos Aires	35°0'50.2"S, 58°0'36.6"W	03-01-2023	new	<i>Ludwigia grandiflora</i> subsp. <i>hexapetala</i>

* reported as sp. 1, sp. 2, and sp. 3.

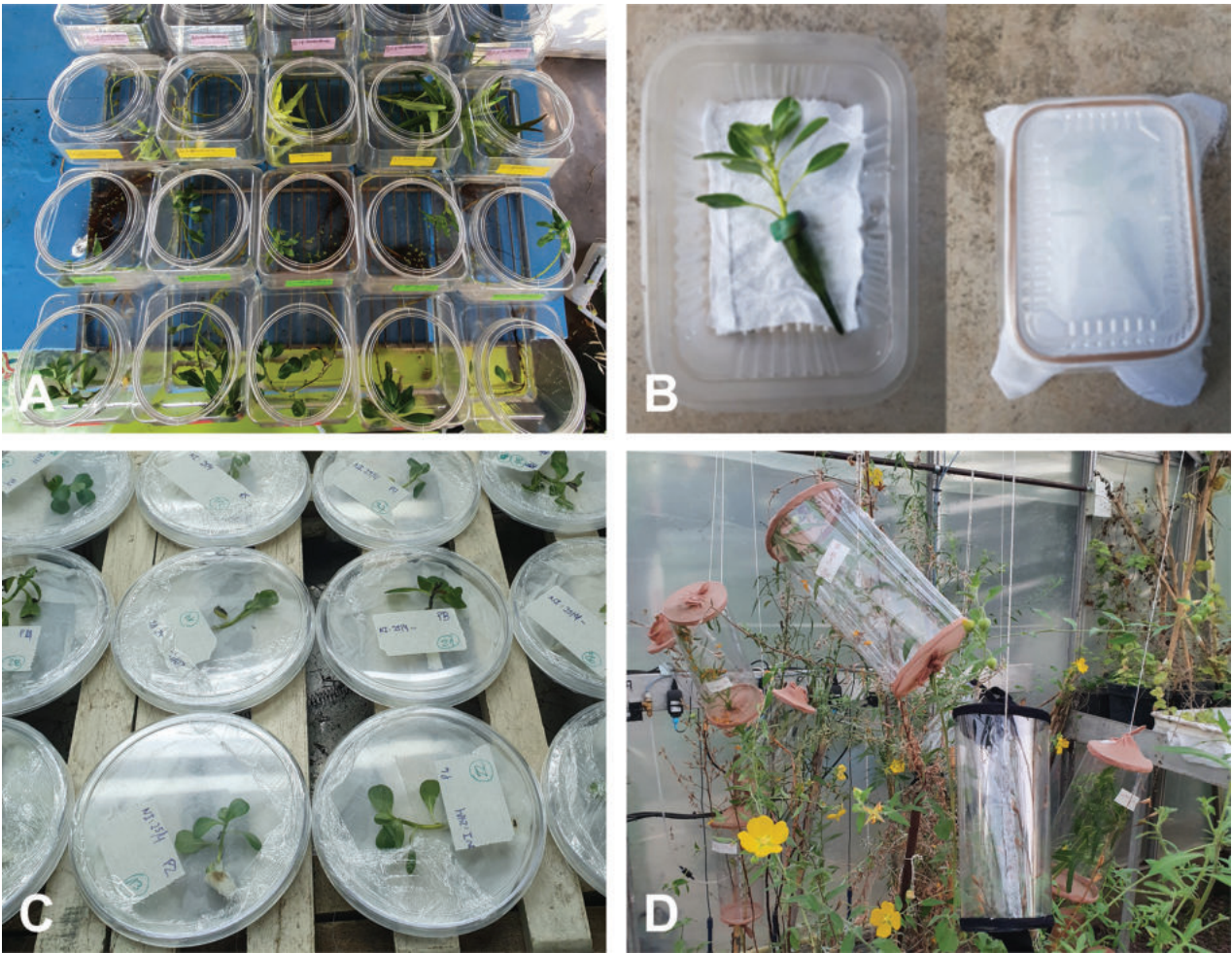


Figure 1. Different rearing and test devices for *Pissonotus paraguayensis* **A** device for aquatic plants utilised for rearing and host range tests **B** device for rearing and tests with plants in water-pics **C** small petri dishes with *L. g. susp. hexapetala* utilised in life cycle study **D** hanging plastic cylinders utilised in host range test for terrestrial plants.

Morphology

Identification of *P. paraguayensis* was based on the original description and photographs of the holotype from the Arizona State University, Lois B. O'Brien Collection (**ASU: ASULOB**). Female (brachypters and macropters) specimens, captured in the same place and host plant were structurally matched with available males, then used for dissections, images and complementary descriptions are deposited in the Museo de La Plata entomological collection (**MLP**). Immature stages: description was based on 24-hour-old nymphs from laboratory colonies. Specimens were submitted to 95% ethyl ether to preserve colour, cleared in cold 10% KOH solution and fixed in Faure liquid for microscopic examination and illustration. Eggs: obtained by dissecting oviposition scars. First instar: described in detail, focused on major differences are highlighted for older stages and also between presumptive brachypterous and macropterous forms of the fifth instar. Measurements: range and median, given in mm, taken from anaesthetised specimens. Dimensions were expressed as **L.**: total body length (from the tip of vertex to the tip of abdomen), **W.**: maximum body width (across the widest part of the mesothorax), **t.l.**: thoracic length (from the anterior margin of the pronotum to the posterior margin of the metanotum along the midline). Other measurements are relative. Morphological terminology and measurements of adults follow Bartlett and Deitz (2000), but the wing venation and female genitalia refer to Bourgoïn et al. (2015) and Asche (1985) respectively. Carination and arrangement of pits of nymphs generally follows Vilbaste (1968) updated after by Yang and Yeh (1994). External morphology was observed with a Leica EZ5 stereomicroscope and photographs were taken with an adapted RRID 18 HD digital camera and a Canon EOS 90D. Illustrations were imported into Adobe Photoshop 7.0 for labelling and plate composition.

DNA extraction and sequencing

DNA was extracted from whole bodies of adults using Qiagen DNeasy Blood & Tissue Kit. A fragment of 658 bp of the cytochrome c oxidase I (COI) gene was amplified using universal barcoding primers LC01490 and HCO2198 (Folmer et al. 1994). PCR amplification was done in a 25 µL volume using the following thermocycling protocol: 2 min at 95 °C; 5 cycles of 40 secs at 94 °C, 40 secs at 45 °C, 1 min at 72 °C; 35 cycles of 40 secs at 94 °C, 40 secs at 51 °C, 1 min at 72 °C; 5 min at 72 °C; held at 4 °C. PCR products were checked in 1% agarose gels and purified by adding 0.5 µL (10 u) Exonuclease I (Exo I) and 1 µL (1 u) Shrimp Alkaline Phosphatase (SAP). Samples were incubated at 37 °C for 15 min and reaction was stopped by heating the mixture at 85 °C for 15 min. Both strands of each fragment were sequenced using Sanger technology in Macrogen Inc. sequencing service (South Korea) with the same primers used for PCR amplification. Sequence quality check, primer trimming, and alignment were performed on CodonCode Aligner version 10.0.2. Sequences were deposited in GenBank after running a BLAST search to check for possible contaminations.

Biology

Tests were performed inside rearing chambers (25 °C, 12 hrs. light/12 hrs. dark). Mature couples ($n = 10$) were collected from the colony and placed individually in rectangular plastic containers (20×15 cm) with fine pierced lids. Inside, a 10-cm long stem of *L. g.* subsp. *hexapetala* with a water pic was exposed for 24 hrs to each couple (Fig. 1B). Only brachypterous females were used for this test since macropterous females might have different reproductive behaviour. After the exposure, the number of oviposition scars per stem were recorded and plants were stored again in the rearing chamber until nymph emergence. Development time of eggs and the number of emerged nymphs per stem after 24 hrs of exposure were recorded. Also, laboratory-reared plants were dissected to quantify the number of eggs per oviposition scars.

To follow the developmental time of the immature stages, newly emerged nymphs ($n = 50$) were randomly selected from the previously mentioned containers and placed individually in Petri dishes with 5-cm long stems and wet tissue paper (Fig. 1C). Nymphs were observed every 1–2 days and developmental time for each instar was recorded by checking for exuviae. All means are reported with \pm SD.

To estimate the host range, no-choice tests were performed in a greenhouse with controlled temperatures (26 °C day/24 °C night) and natural light conditions (summer). Because the planthopper is a sap-feeding insect, whole plants were utilised. Depending on the plant species life form, two different devices were used. If the plant was terrestrial or did not resist/withstand stems being cut to be enclosed in small containers, hanging acetate cylinders with nylon mesh on both ends were placed containing ~ 15 cm of a stem (Fig. 1D). Each cylinder was placed on independent plants. If plants were aquatic, then a single 15-cm long stem was placed inside a 3-lt plastic container with water and polyester gauze as a lid (Fig. 1A). For each plant species, between three and five repetitions were carried out, depending on plant availability. Inside each device, one male and one brachypterous female of *P. paraguayensis* were released to test survival and oviposition. For survival, the number of days elapsed from the beginning of the experiment until the death event of both males and females, were recorded. Two types of feeding controls were set up: one with the insects on the known host plant, *L. g.* subsp. *hexapetala* as a positive control, and another with insects only with wet tissue paper as a negative control with no food. The experiment was terminated at 52 days. For the test plant list, nine *Ludwigia* species were considered, six from the *Jussiaea* section, to which the main host plant belongs (*L. grandiflora* (Michx.) Greuter & Burdet subsp. *grandiflora*, *L. g.* subsp. *hexapetala*, *L. peploides* (Kunth) P. H. Raven subsp. *peploides*, *L. p.* subsp. *montevicensis* (Spreng.) P. H. Raven, *Ludwigia peploides* (Kunth) P. H. Raven subsp. *glabrescens* (O. Kuntze) P. H. Raven and *Ludwigia hookeri* (Micheli) H. Hara; two from the *Macrocarpon* section, *Ludwigia bonariensis* (Micheli) Hara and *Ludwigia neograndiflora* (Munz) Hara; and one from the *Myrtocarpus* section, *Ludwigia sericea* (Cambess.) Hara. Two other species, one closely related species from another genus of Onagraceae, *Oenothera affinis* Cambess. and one that is not closely related but commonly co-exist in the natural habitat, *Myriophyllum aquaticum* (Vell.) Verdc were also evaluated.

Data analysis

Survival data of females was analysed through Kaplan-Meier survival curves using the 'survfit' and 'ggsurvplot' functions from Survival package (ver. 3.4-0) of RStudio statistical program (ver. 2023.06.1). A non-parametric Log-rank statistical test was used to assess statistical differences in overall survival. To better understand the influence of each test plant in *P. paraguayensis* survival, the Cox regression model was employed to estimate the hazard ratio (HR) and *P* values based on χ^2 test, and 95% confidence intervals (95%-CI). HR is the rate of occurrence of an event during a given time interval, where $HR > 1$ means that exposure to the factor increases the rate of occurrence of the event, and $HR < 1$ decreases the rate. If the $HR = 1$ we say that the factor behaves as the reference (Kleinbaum and Klein 2012). Forest Plot for Cox proportional hazards model was created using the 'coxph' and 'ggforest' functions of R packages survival and survminer (0.4.9). $P < 0.05$ defined significance. All analyses were conducted with R 4.3.1 (R Core Team 2022).

Results

Morphology of *Pissonotus paraguayensis* Bartlett, 2000: 144

Adult

This species was described in detail by the author from a brachypterous male from Paraguay; the brachypterous female was briefly discussed, referring only to its body size with some observations on the variations in colour patterns among specimens from different geographic locations (Bartlett and Deitz 2000).

Male (Fig. 2). Although the brachypterous male has been fully described and illustrated by the author, we added representative images of that morph in order to facilitate its association and recognition, given the dimorphic sexual coloration of this species.

Female (Figs 3, 4). Note: As Bartlett and Deitz (2000) noted, females of *Pissonotus* have been little used in taxonomy probably due to the scarce availability of specimens reliably associated with males. Illustrations and complementary comments not included in the original description, particularly on variation in colour between or within conspecific populations and descriptions of some structural features of the female genitalia are given for the first time.

Brachypter. Body length: 2.91–3.16 (3.01, $n = 5$); tegmina length: 0.80–0.90 (0.82, $n = 4$) (Fig. 3A, B).

Colouration: In dorsal view body generally dark brown, paler on vertex and along midline of abdomen and widening above genital and anal segments. Vertex and upper frons are mostly brownish with carinae and anterior margin paler. Tegmina dark brown with a distinguishable distal transverse narrow white band, sometimes medially incomplete; veins concolourous with venation obscure becoming obsolete toward apex (not reticulate). In ventral view, head with a distinctive transverse whitish band on epistomal margin of frons, which extends laterally along the genae to the base of the pre- and mesocoxae; blackish brown area over postclypeus and basal $\frac{1}{2}$ of coxae contrasting with the yellowish colouration of anteclypeus, rostrum, thoracic sternites and legs. Apex of rostrum,

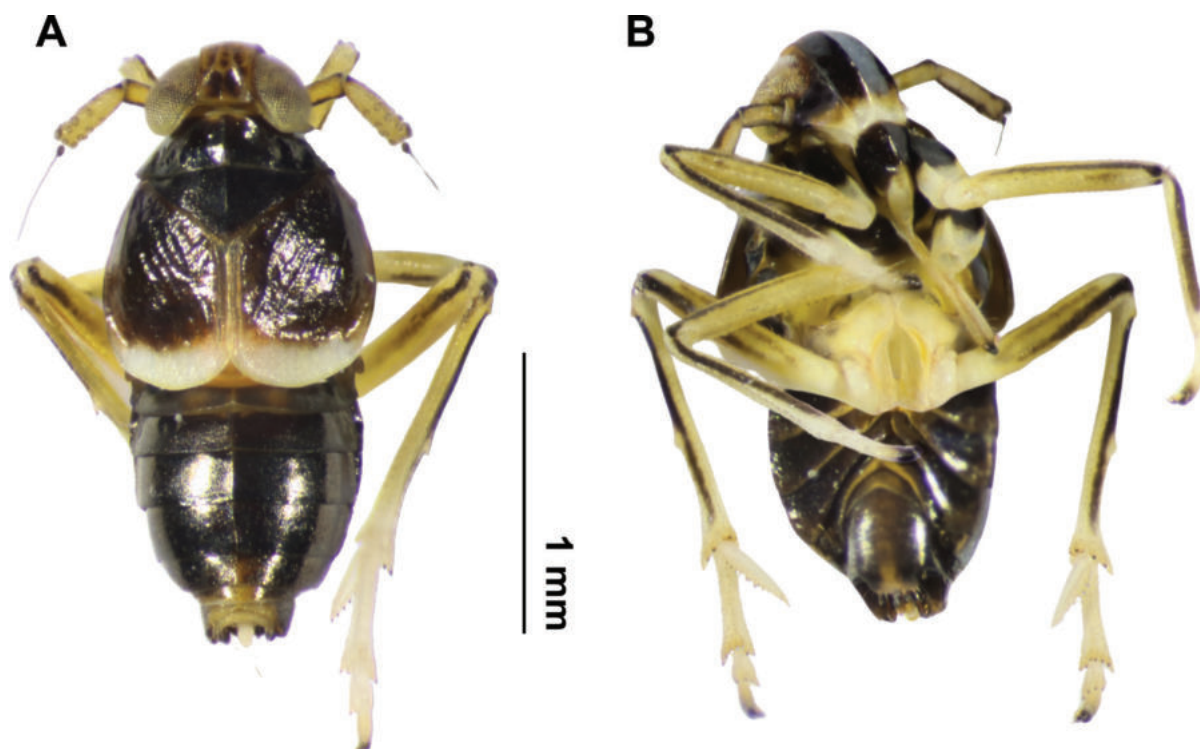


Figure 2. *Pissonotus paraguayensis*. Habitus. Brachypter male **A** dorsal view **B** ventral view.

longitudinal anterior highlights on antennomeres I and II and dorsal margins of femora and tibiae, and the apex of last tarsal segments and ungues, black. Abdomen paler along midventral line from sternum V to the caudal region.

Structure: Antennal foveae elevated, placed close to ventral margin of the compound eye. Tegmina quite longer as broad (6:1), distally rounded on leading margin and apically truncate, not exceeding tergite II. Calcar slender, moderately foliaceous; shorter than basitarsus (0.8:1), usually with a row of 13–15 black tipped teeth on ventral margin with 2–4 smaller teeth irregularly spaced external to the row (Fig. 4E).

Macropter. Total length (including wings): 3.66–3.70 (3.68, $n = 4$). Body length (excluding wings): 3.00 (3.00, $n = 4$), fore-wings length: 2.90 ($n = 4$). (Fig. 3C, D).

Colouration: Similar to brachypterous form in colour pattern of head, antennae, sternothorax, and legs. General body colouration uniformly darker; with distinctive yellowish areas: dorsally, restricted on caudal apex of mesonotum, base of tegula and anal segment, and ventrally, on the posterior margin of abdominal sternites, pregenital sternite, inner margins of gonocoxa VIII and gonapophysis VIII. Wings semi-hyaline, fore-wing veins light brown, proximal portion of remigium and clavus and some longitudinal and transverse veins, quite dark.

Structure: Similar to the brachypterous form, with mesothorax more robust. Wings fully developed, longer than abdomen, fore-wings extending $\sim 1/3$ of their length beyond the tip; hind-wings shorter. Fore-wing with a simple venation pattern, with scattered small seta-bearing tubercles irregularly distributed on the veins. Remigium veins mainly non-bifurcated, nodal cells poorly defined, sometimes absent, with four long postnodal cells distally open, CuP apically weakened; pre and post nodal cells elongated; clavus in angle, postclaval margin forming an obtuse angle (100–120°).

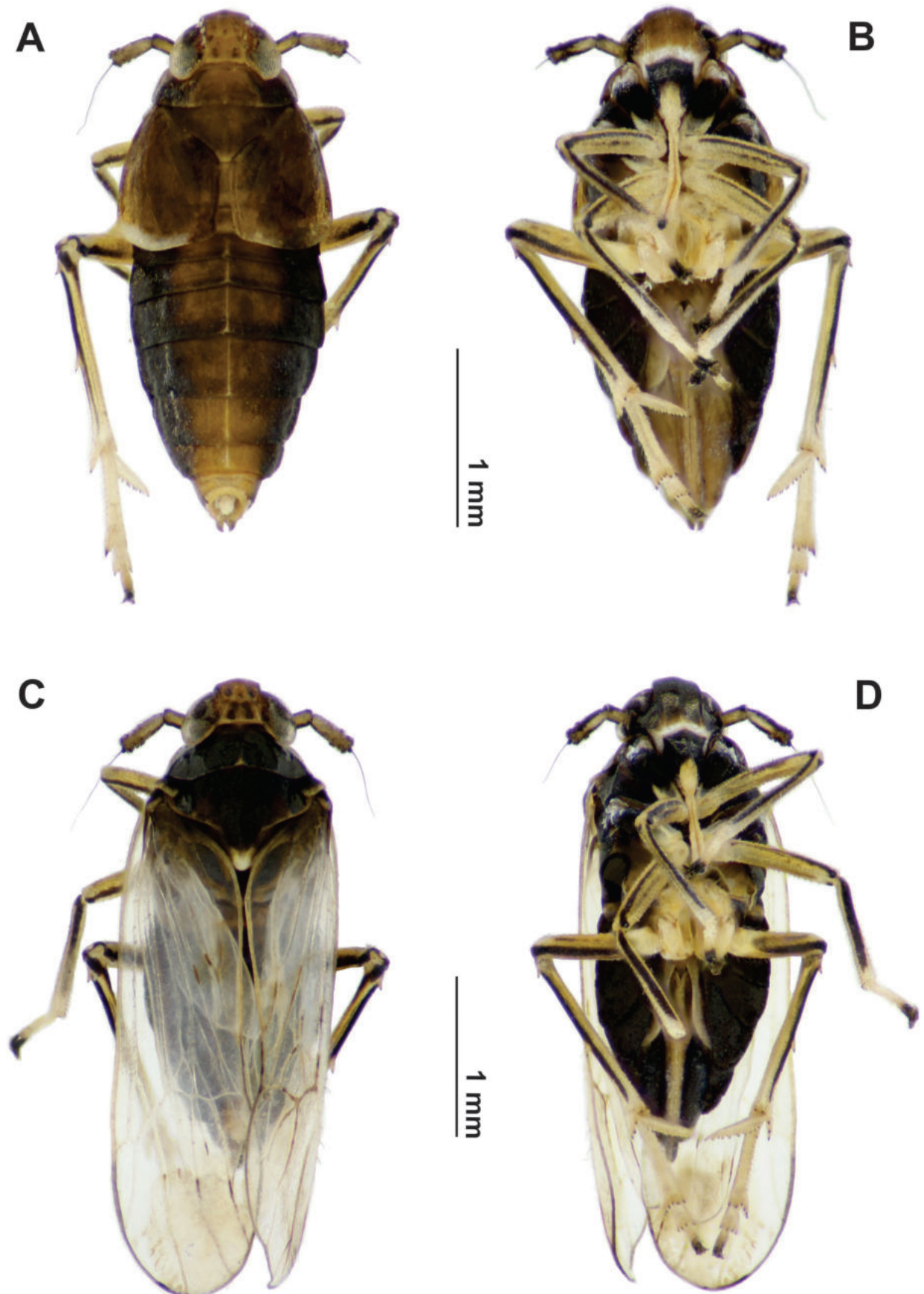


Figure 3. *Pissonotus paraguayensis*. Habitus. Brachypter female **A** dorsal view **B** ventral view. Macropter female **C** dorsal view **D** ventral view.

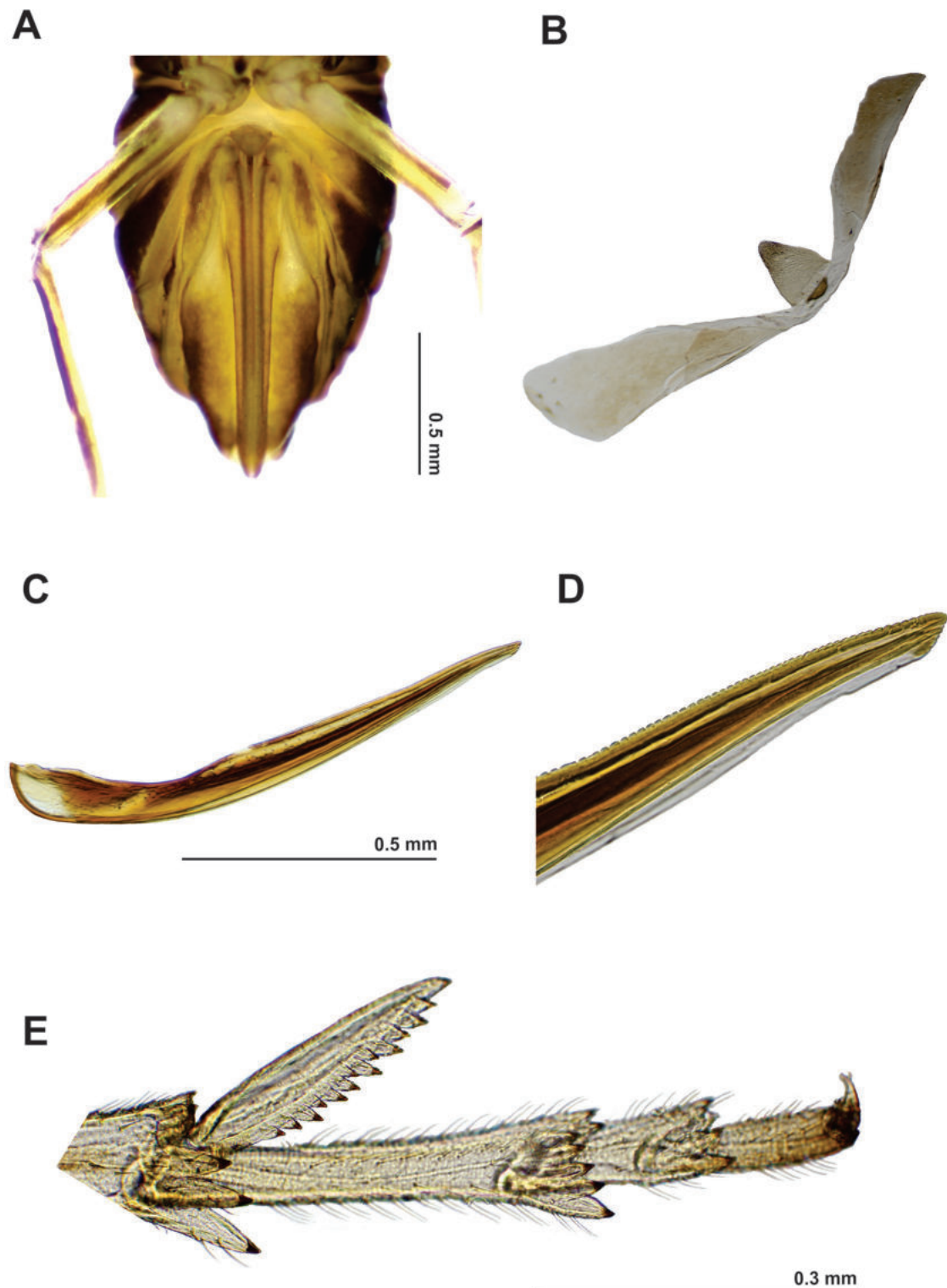


Figure 4. *Pissonotus paraguayensis* female **A** abdomen, genital region, ventral view **B** pregenital sternite **C** gonapophysis IX **D** apex of gonapophysis IX **E** apex of hind leg (post tibial spur and tarsi) of adults.

Genitalia (Fig. 4A–D): Ovipositor sclerotised and relatively long and narrow, shortly surpassing the posterior margin of anal segment. Pregenital sternite subtriangular, elongate, longer in middle line than its wide at its widest part (1.5:1), anterior margin strongly narrowed “like a neck” and lightly rounded at apex (Fig. 4A, B). Gonocoxa VIII, more or less lanceolate, regularly expanded at

base; as long as 1/3 the length of the gonapophyses VIII (Gy VIII) which is uniformly slender and elongated. Gonapophyses IX slender, slightly curved, wider at basal 1/3, distal 1/3 with minute teeth on dorsal margin (Fig. 4C, D); dorsal gonoplac (Gp) or third valvula uniformly wide. Anal style moderately short.

Host Plant. In the field, adults and nymphs were observed feeding on *Ludwigia grandiflora* subsp. *hexapetala*.

Recorded natural enemies. None.

Distribution. South Central South America: Brazil, Paraguay and apparently Bolivia (Bartlett and Deitz 2000). Argentina: Santa Fé, Entre Ríos and Buenos Aires.

Pissonotus paraguayensis was found in wetlands of central Argentina that belong to the Del Plata Basin, expanding its geographic range to central-east of Argentina and now making Buenos Aires province its southernmost limit of distribution in America (Table 1).

DNA barcode. The two sequenced specimens (1♀b, 1♂b) from Brazo Largo, Entre Ríos (33°51'53.4"S, 58°52'59.4"W) had the same 658 bp COI haplotype, which was deposited in GenBank under accession number OR523788.

Material examined. ARGENTINA: 6♀b, 1♀m, Buenos Aires, Otamendi, 34°13'04"S, 58°55'52"W, s/ L. g. subsp. *hexapetala*, 21-01-2019, Faltlhauser col.; 10♂, same place and host, 10-03-2019, Hernández col.; 15 ♂, same place and host, 07-06-2019, Hernández col.; 1 ♀m, 8-10-2008, (named 1 ♀ Delphacidae), Cabrera Walsh col.; 15♂, 3♀b, laboratory reared (FuEDEI), 7-06-2019, Hernández; 5♀m, 2♀b, 1♂b, Buenos Aires, Magdalena, 35°3'48.9"S, 57°33'14.9"W, s/ L. g. subsp. *hexapetala*, 3-11-2021, Faltlhauser col.

Remarks. Although the colour pattern is useful to recognise members of the genus, some variations were observed among brachypterous specimens of both sexes. General colouration varies from black to blackish-orange, particularly the distal transverse white band of tegmina that may be complete, medially incomplete, or exceptionally absent, and the dorsal surface of the abdomen with more diffuse colouration towards the caudal region. Nevertheless, the distinctive pattern colouration described on the head and thorax is rather uniform in both sexes and morphs. The drumming organ in males shows a dimorphic distinctive yellowish colouration. Macropterous forms show more homogeneous colouration among specimens.

Immature stages. Fig. 5.

Key to the instars of *Pissonotus paraguayensis*

- 1 Metatarsi two-segmented. General colour pale, uniform yellow on dorsal view2
- Metatarsi tri-segmented, or metatarsomere 2 partially subdivided in the middle. General colour grey to pale yellow dorsally mottled dark brown and cream4
- 2 Body uniformly yellow, antenna uniformly grey. Metatibia without lateral spines, spur < 2× length of the longest apical spines of the metatibia. Antennal pedicel without sensorial pits (Fig. 5A, B) **First instar**
- Body yellow with a dark marking on upper frons, antenna, apex of rostrum, femoro-tibial joins, dorsal pro and mesotarsite, apex of tarsites and ungues. Metatibia with lateral spines, spur > 2× the length of the longest apical spine of the metatibia. Antennal pedicel with sensorial pits3

- 3 Metatibial spur without marginal teeth. Metatarsomere 1 with a transverse apical row of 4 spines (Fig. 5C, D)..... **Second instar**
- Metatibial spur with ≥ 2 marginal teeth. Metatarsomere 1 with a transverse apical row of 5 spines (Fig. 5F) **4**
- 4 Metatibial spur with two or three marginal teeth. Wing pads weakly developed, barely projecting laterally (Fig. 5E, F) **Third instar**
- Metatibial spur with ≥ 3 marginal teeth. Wing pads developed **5**
- 5 Metatibial spur with 4 or 5 marginal teeth. Fore-wing pads laterally reaching the middle of hind-wing pad (Fig. 5G, H) **Fourth instar**
- Metatibial spur with 7–9 marginal teeth. Fore-wing pads covering lateral 2/3 of hind wing pads; hind-wing pads not reaching third tergite (Fig. 5I, J) (brachypterous form) or extending near apex of hind wing pads, overlapping third tergite (Fig. 6A, B) (macropterous form)..... **Fifth instar**

Description: Eggs. (Fig. 7A) ($n = 10$). Length: 0.86, width: 0.23.

Eggs milky white, ellipsoidal. Chorion translucent.

First Instar. (Fig. 5A, B) ($n = 5$). L:1.04 (0.93–1.07) W: 0.33 (0.29–0.36); t.l: 0.35 (0.25–0.41).

Uniform whitish body; with distinctive red eyes; uniform greyish antennal segments.

Form elongate, subcylindrical, dorsoventrally slightly flattened. Vertex subquadrate, with lateral margins often divergent in front and behind the eyes; length sub-equal to width (1.2:1); fastigium (lateral view) rounded; lateral and submedian carinae of vertex extending onto frons. Frons with lateral margin slightly convex and carinate, $\sim 2\times$ longer than wide in midline, regularly wider towards the frontoclypeal suture; lateral margins carinate and paralleled by submedian carina which is prominent at base and regularly evanescent towards apex; each laterofrons at level below the eyes $1.5\times$ wider than interfrons; with 13 sensorial pits on each side: nine pits on area between submedian and lateral carinae (six visible in ventral view, three in dorsal view); dorsally four pits between lateral carina and eyes. Antennae three-segmented; scape, short, slightly wider than long, antennal pedicel sub-cylindrical $\sim 2\text{--}2.5\times$ the length of scape, without sensory pits; base of flagellum bulbous $\sim 0.5\times$ the pedicel length. Rostrum reaching the posterior margin of metacoxae, apical segment $0.6\times$ longer than subapical.

Thoracic nota divided into three pairs of plates by longitudinal mid-dorsal line. Pronotal plates subtrapezoidal, lateral carinae divergent and slightly convex towards posterior margin. Each plate with seven pits extending from near middorsal line posterolaterally to lateral margin (two pits in line next to lateral carinae on posterior $\frac{1}{2}$ of segment and five pits extending laterally from the external side of carina along the posterior border of plate, one proximal to it and four most lateral not visible in dorsal view). Mesonotum as long as metanotum. Mesonotal plate with four pits, two median on disk, and two next to lateral margin. Pro, meso, and metatarsi with two tarsomeres; apical tarsomeres subconical, curved, with a pair of apical claws. Metatibiae without lateral spines, with apical transverse row of four stiff spines; tiny spur $< 2\times$ the length of longest apical spines of the metatibia and $\sim 1/4$ length of metatarsomere 1. Metatarsomere 1 shorter than metatarsomere 2 (0.5:1) with four apical spines.

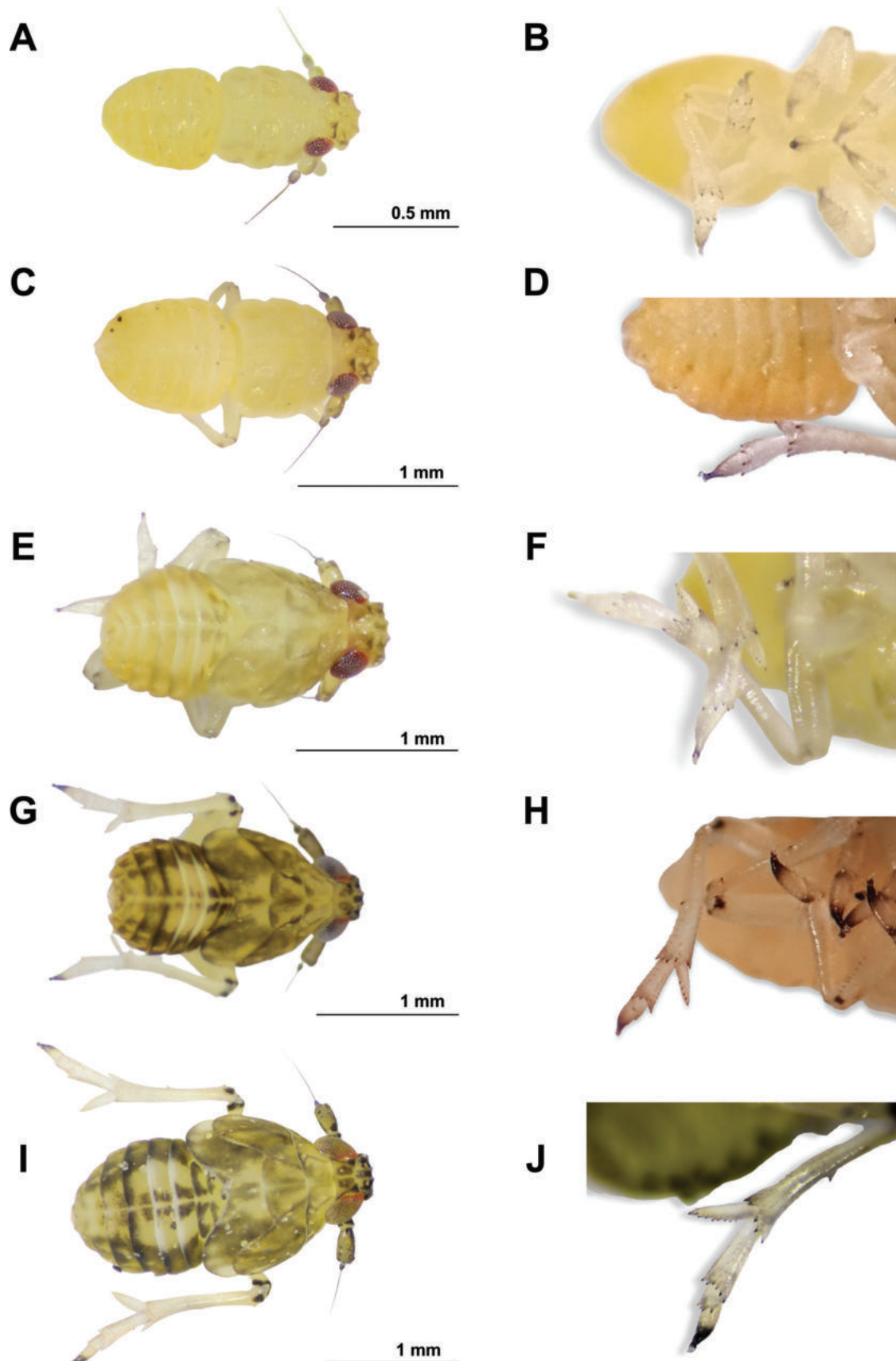


Figure 5. Immature stages in dorsal view of *Pissonotus paraguayensis* **A** first instar **C** second instar **E** third instar **G** fourth instar **I** fifth instar (presumptive brachypter form). Apical portion (from tibiae) of hind leg **B** first instar **D** second instar **F** third instar **H** fourth instar **J** fifth instar (presumptive brachypter form). Scale bars: 0.5 mm (**A**); 1mm (**C**, **E**, **G**, **I**).

Abdomen with nine apparent segments, widest across segment 5. Tergite 5 with one pit and tergites 6–8 each with three pits on either side of the midline. Segment 9 surrounds anus with three pits on each side, two subapical and one dorsal median.

Second Instar. (Fig. 5C, D) ($n = 5$). L: 1.57 (1.54–1.61); W: 0.61 (0.61–0.73); t.l.: 0.48 (0.44–0.52).

Pale yellowish body, with distinctive black markings on the head and legs: a stripe on apex of vertex and upper frons extended at lower level of the eyes, along the frontal surface of antennal segments I and II, and several marks limited to: upper border of antennal fovea, apex of rostrum, outside apices of femoro-tibial joints, base of basitarsus and apices of legs.

Antennal foveae elevated, placed under the compound eyes, close to its lower margin; antennal pedicel sub-cylindrical $\sim 3\times$ the length of scape, with three small pits: two on apical margin and the third subapical on posterior surface; flagellum whip-like distally, bulbous at base, $\sim 0.25\times$ the pedicel length. Rostrum extends almost to bases of metacoxae, apical segment $0.2\times$ shorter than subapical. Pro, meso, and metanotum subequal, pronotum slightly shorter (0.7:1); posterior margin of mesonotum straight at middle, metanotum deeply excavated. Wing-pads undeveloped. Metatibiae with two small lateral spines (one near base and one in basal $\frac{1}{2}$), and five stiff spines on the apical transversal row; spur $\sim 1/4$ length of metatarsomere 1, with two similar sized teeth, one on lateral aspect added to the apical. Metatarsomere 1 as long as metatarsomere 2, with apical transversal row of five spines.

Third instar. (Fig. 5E, F) ($n = 4$). L: 1.78 (1.62–1.81); W: 0.89 (0.85–0.93); t. l.: 0.56 (0.50–0.62).

Similar pattern colour to second instar, with darker markings.

Antennal pedicel sub-cylindrical, $\sim 3\times$ the length of scape, with four to five sensory pits; flagellum with bulbous portion ~ 0.1 the pedicel length. Rostrum overlapping the bases of metacoxae, apical segment $0.3\times$ shorter than subapical.

Mesonotal plate with the two discal pits on both sides of the lateral carinae. Fore-wing pads short, each covering $1/2$ of metanotal segment laterally, with three pits, a pair on costal area and another near middle. Metanotum plates median length as long as mesonotum, shallowly excavated on posterior margin. Metatrochanter subcylindrical, with row of ten or eleven interlocking flattened folds on posteromedial aspect. Metatibial spur $3/4$ the length of metatarsomere 1, with one apical tooth and two to three teeth on lateral margin. Metatarsomere 1 with apical transverse row of five spines; apical tarsomere with an arrange of fine sensory hairs along it.

Fourth instar. (Fig. 5G, H) ($n = 10$). L: 1.80 (1.69–1.89); W: 0.87 (0.73–1.00); t. l.: 0.55 (0.51–0.56).

Colour pattern similar to former instar. Most specimens with conspicuous brownish marking along dorsal portions of thoracic nota continuing onto wings pads and abdomen.

Antennal pedicel sub-cylindrical $\sim 2\times$ the length of scape, with approx. five or six pits on the apical $\frac{1}{2}$ (Fig. 5B). Rostrum extending to bases of metacoxae, apical segment slightly shorter than subapical.

Fore-wing pads short, each covering $\sim 1/2$ of hind wing pad, laterally with three pits, one on costal area and two next to subcostal carina. Metanotum median length sub-equal to mesonotum; hind-wing pad oval, reaching the base

of the first abdominal segment. Metatibial spur almost as long as the metatarsomere 1 in middle, with one apical tooth and three or four on lateral margin. Metatarsi with two tarsomeres: tarsomere 1 with apical transverse row of six spines, tarsomere 2 subconical, similar to apical tarsomeres of other legs, slightly shorter than length of tarsomere 1, partially subdivided in middle, with three short ventrolateral spines in middle of plantar surface.

Fifth instar. Presumptive brachypterous form (Fig. 5I, J) ($n = 10$) L: 2.27 (2.18–2.36); W: 0.99 (0.96–1.01); t. l: 0.65 (0.62–0.70). Presumptive macropterous form (Fig. 6A, B) ($n = 2$). L: 2.3; W: 1; t.l: 0.9.

Colour pattern similar to former instars but darker. Dorsally blackish mottled with light to dark brown and cream on head, thorax and abdomen, with notorious yellowish pits; ventrally, head with postclypeus also darkened at base. Obvious black mark on legs: on base of coxae, outside apices of femoro-tibial joint, longitudinal stripes on dorsal margins of femora and tibiae, basal tarsomere of pro and mesotarsi and the apex of last tarsal segments and claws.

Form elongate, sub-cylindrical, widest across mesothoracic wing pads. Head lightly protruding beyond the anterior margin of eyes, $\sim 1/4$ of the eyes length. Vertex subquadrate, length slightly longer than wide (1:07), anterior margin straight, posterior convex, basal compartments shallowly concave; lateral and submedian carinae prominent, continuing onto frons from the level of middle of the eyes to clypeal margin. Frons sub-rectangular; widest at middle, width. $\sim 0.9\times$ the length; carinate lateral margins slightly convex, these lateral carinae extending from vertex to clypeal border and paralleled by a pair of straighter submedian carinae regularly evanescent towards clypeal border. Clypeus narrowing distally, consisting of subconical basal postclypeus not carinated along

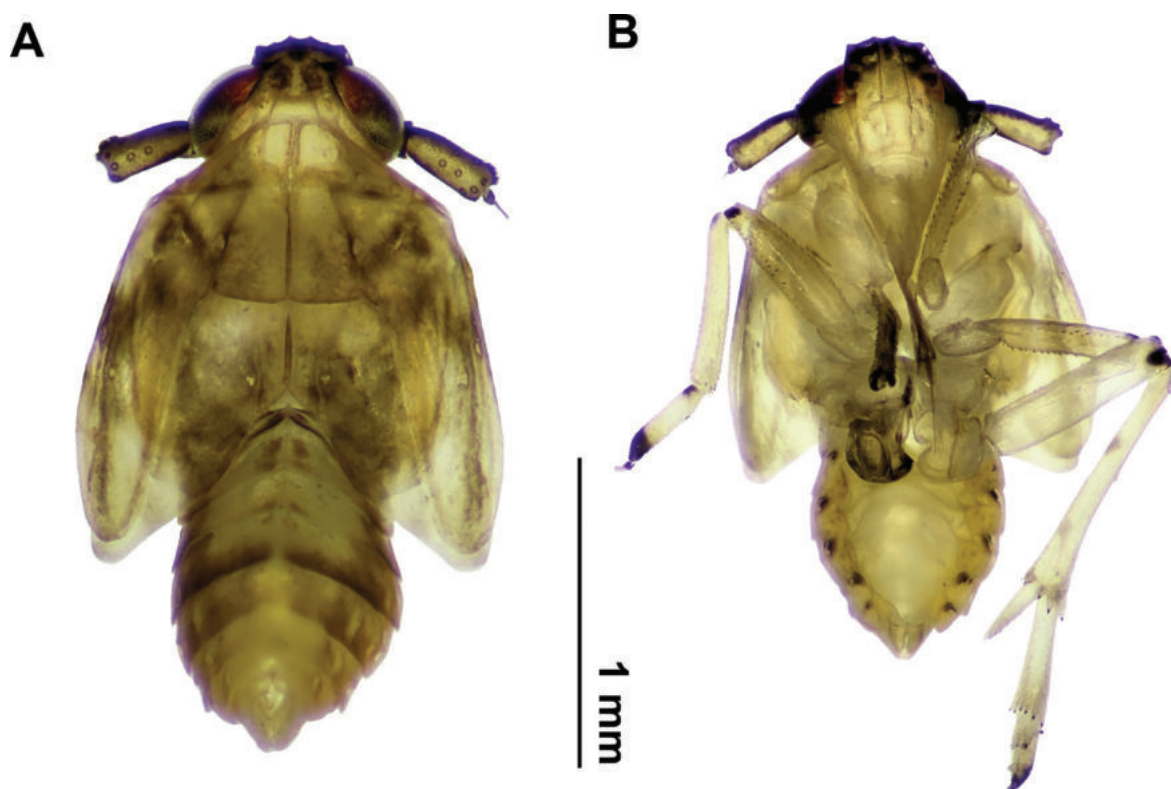


Figure 6. Fifth instar (presumptive macropterous form) *Pissonotus paraguayensis* **A** dorsal view **B** ventral view.

its length, and cylindrical distal anteclypeus. Antennae with scape cylindrical, length subequal to width; pedicel subcylindrical, $\sim 3\times$ longer than scape, with nine or ten pits on the apical $\frac{1}{2}$. Rostrum surpassing mesocoxae, apical segment slightly longer than apical (1.2:1).

Pronotal plates sub rectangular; anterior margin follows posterior margin of head, posterior border almost straight; each plate with straight short posterolaterally directed carina originating on anterior margin in median $\frac{1}{3}$ and terminating near middle of plate, carina bordered along inner margin by row of six pits extending posterolaterally to lateral border of plate (three pits in line next to lateral carinae and three near posterior margin; one lateralmost pits not visible in dorsal view). Mesonotal median length $\sim 1.5\times$ that of pronotum; each plate bearing an elongate lobate wingpad covering lateral $\frac{1}{2}$ of metanotal wingpad; with posterolaterally directed carina originating on anterior margin in median $\frac{1}{4}$ and terminating on posterior margin, with five pits: two on notum, one on each side of carina, and three laterad (two on wingpad). Metanotal median length $\sim 0.75\times$ that of mesonotum; each plate bearing an elongate lobate wingpad extending to tergite 2; with weak longitudinal carina originating on anterior margin in median terminating near posterior margin; one pit on wingpad, just lateral to carina. When developing to macropterous adults the fore-wing pads extend up to the apices of the hind pads, reaching tergite 5.

Pro- and mesocoxae elongate, posteromedially directed; metacoxae fused to sternum. Metatrochanter subcylindrical, with a row of 12–14 flattened folds on the posteromedial aspect which interlocks with those on the adjoining trochanter. Metatibiae with subtriangular, slender, moderately foliaceous spur, a little shorter than metatarsomere 1, with a row of seven-nine teeth on lateral margin and one apical tooth. Metatarsomere 1, longer than tarsomere 2 plus 3 (1:05), with apical transverse row of seven black-tipped spines on plantar surface; tarsomere 2 cylindrical, with apical transverse row of four black-tipped spines on plantar surface; tarsomere 3 sub conical, similar to apical tarsomere of other legs.

Abdomen with nine apparent segments, slightly flattened dorsoventrally, widest across segment 5. Segment 9 surrounds anus with three evident pits on each side, two subapical and one dorsal median, in both sexes.

Specimens examined. ARGENTINA: Otamendi, Buenos Aires (34°03'48.2"S, 58°49'19.59"W), 10 nymphs V, 10 nymphs IV, 10 nymphs III, 10 nymphs II and 10 nymphs I, 07-06-2019, on *L. g.* subsp. *hexapetala*, Faltlhauser col.; 2 nymphs III, 1 nymph I; 21-I-19, on *L. g.* subsp. *hexapetala*, Faltlhauser col.

Biology

Field observations

In this region, the early months of summer are not the most suitable to find this planthopper. A peak of abundance in the Buenos Aires region was observed between March and July. In the field, they were found on *Ludwigia grandiflora* subsp. *hexapetala*, normally higher up on the plant. Adults and nymphs tended to move to the underside of the leaves and stems or hop to the water surface when disturbed. Adults were more often found on glabrescent stems. The insertion of eggs on the plant stems produces a corkscrew distortion damage that can be easily observed (Fig. 7B).



Figure 7. **A** *Pissonotus paraguayensis* eggs oviposited in *Ludwigia grandiflora* subsp. *hexapetala* **B** damage observed on *L. g.* subsp. *hexapetala* produced by ovipositions **C** oviposition marks.

Life history

The female of *Pissonotus paraguayensis* inserts its eggs in the plant tissue on either side of the leaf and in the upper part of the stems further away from the water surface (Fig. 7A-C). After 24 hrs of exposure to *L. g.* subsp. *hexapetala*, brachypterous females produced an average of 18.13 ± 3.68 oviposition scars (range 13–23; $n = 10$, hereafter means are reported with \pm SD) in a 10-cm stem at 25 °C. Each oviposition scar had a mean number of 2.3 ± 0.82 eggs (range 1–3; $n = 10$) (Fig. 7C). The mean development time from oviposition to hatch was 10.6 ± 0.9 days (range 9–12; $n = 214$). Generation time (egg to adult) was 36.71 ± 1.98 days (range 33–41; $n = 21$). The development time for nymphs I, II, III, IV, and V were 6.7 ± 0.5 days (range 6–8; $n = 36$), 3.2 ± 0.7 days (range 2–6, $n = 35$), 4.6 ± 1.0 (range 3–7; $n = 31$), 4.1 ± 1.2 days (range 2–6; $n = 25$), 7.1 ± 1.6 days (range 5–11, $n = 21$) respectively. Female adults can live over 50 days ($n = 30$) in laboratory conditions.

Host range

This species of delphacid was found in the field on *L. g.* subsp. *hexapetala*. However, survival and host range revealed that *P. paraguayensis* was able to survive in other congeneric species to the known host plant. Through the Kaplan-Meier analysis, we observed that *P. paraguayensis* had better survival probability for species inside the *Jussiaea* section except for *L. g.* subsp. *grandiflora*. Log-Rank tests determined that there were significant median differences in the survival probability between plant species, both for females and males ($\chi^2 = 117$, 11 df, $p = < 2e^{-16}$; $\chi^2 = 93.3$, 11 df, $p = 4e^{-15}$, respectively (Suppl. material 1)). Cox proportional hazard analysis revealed that both males and females of *P. paraguayensis* behaved similarly (Fig. 8A, B). *P. paraguayensis* survived an average of five days without food, only water, and the same performance was observed when offered *M. aquaticum* and *O. affinis*. There were no significant differences between species inside the *Jussiaea* section, surviving the longest in *L. g.* subsp. *hexapetala* (45.8 ± 10.0 days). However, *Ludwigia g.* subsp. *grandiflora* was detrimental to survival, dying even sooner than the control. Survival in species of other *Ludwigia* sections was significantly lower (HR closer to 1) and are not considered suitable hosts.

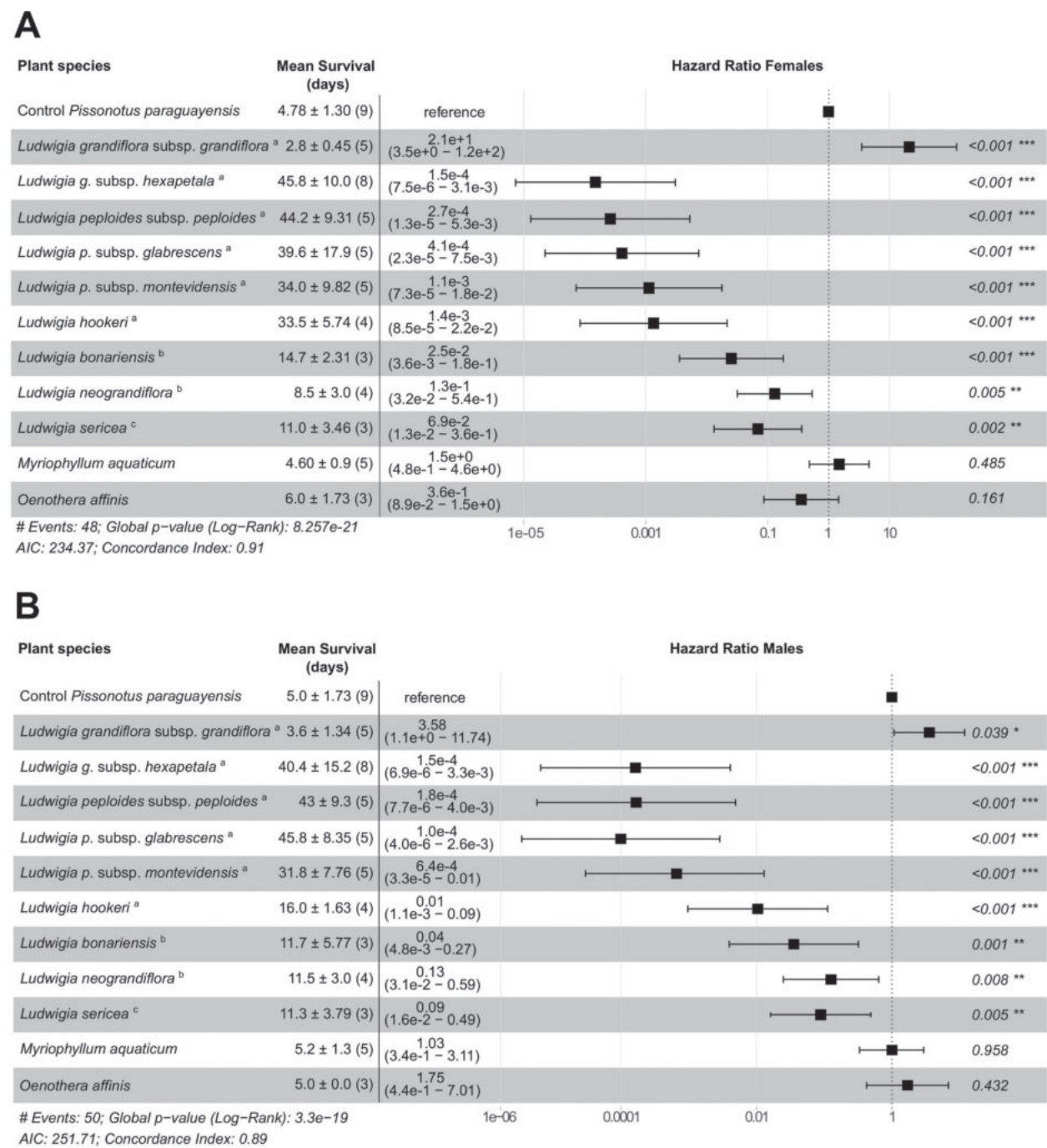


Figure 8. Forest plot of Cox proportional hazard analysis for *Pissonotus paraguayensis* **A** females and **B** males survival where hazard ratio (HR) > 1 means that exposure to the factor increases the rate of occurrence of the event (cavity lost), and HR < 1 decreases the rate. If the HR = 1 the factor does not influence survival (Kleinbaum and Klein 2012). HR are depicted by box symbols with confidence bands and parenthetical values representing 95% confidence intervals. The p values represent Wald test of significance and magnitude of significance is denoted with asterisks (*). AIC, Akaike information criterion. Small letters next to plant species indicate sectional classification of *Ludwigia*: ^a *Jussiaea*, ^b *Macrocarpon*, ^c *Myrtocarpus* based on Raven (1963) and Wagner et al. (2007).

Discussion

This study contributes to the actualisation of *Pissonotus paraguayensis* by describing adult females (brachypterous and macropterous) and immature stages for the first time. Although the female genitalia had not been described

or used in *Pissonotus* systematics, the combination of pregenital sternite and ovipositor morphology of *P. paraguayensis* is here proposed as a new complementary diagnostic trait for the delimitation of the genus and its species. However, future studies will allow us to analyse its importance. Photographs of *P. marginatus* Van Duzee female available in Bartlett (2020) show the presence of the pregenital sternite although it did not receive any mention by the author.

Macropterous females, previously unknown for the species, show the venation pattern quite simplified, which could correspond to the brachypterism pattern described by Bourgoïn et al. (2015). DNA-based taxonomic methods can help clarify species relationships within this group as well as aid in the identification of both adult and immature stages. The obtained COI sequence for *P. paraguayensis* is the first one recorded for the genus in South America and joins 14 other species for which sequences are available on GenBank and BOLD databases at the time of writing (7 Sept 2023). Of the 43 known species of the *Pissonotus* genus, only the North American *P. delicatus* had the immature stages described (Bartlett and Deitz 2000). Based on the Wilson and Tsai (1991) description, fifth instar nymphs of *P. paraguayensis* differ from the latter mainly by the pattern colouration: blackish colouration on dorsal of head, thorax and abdomen with conspicuous yellowish pits, ventrally only darkened on base of frons extended to lower level of the eyes and dorsal surface of antennomeres I and II, and legs with distinctive black marks on femoro-tibial join and apex.

Immature stages of *P. paraguayensis* can be distinguished from other three species of delphacids that inhabit and feed on aquatic macrophytes in Argentina, *Megamelus scutellaris* Berg (Sosa et al. 2005), *M. bellicus* Remes Lenicov and Sosa (Mariani et al. 2007) and *Lepidolphax pistiae* Remes Lenicov (Marino de Remes Lenicov et al. 2017), by a combination of morphological and colouration features. These main features are the yellowish colouration without defined stripes on frontoclypeal area, distinctive blackish marks on the upper front of the head, basal antennal segments, thorax, legs and abdomen; also the slender spur has eight subequal marginal fine black tipped teeth.

The previous distribution range reported for *P. paraguayensis* was Paraguay, Bolivia, and Brazil (Bartlett and Deitz 2000). This work provides an updated distribution, expanding its range for the first time into Argentina, being Buenos Aires the southernmost limit of the genus (35°3'48.9"S, 57°33'14.9"W). Moreover, the aquatic invasive plant, *L. g.* subsp. *hexapetala* is recorded as the only known host plant in natural conditions.

Little information is known on the ecology of the genus. Records from Buenos Aires province indicate that *P. paraguayensis* was more frequently observed in autumn months, specifically from March to July. This differs from the recorded patterns for the South American species *P. boliviensis* and *P. neotropicus*, which are primarily observed between January and April, as reported by Bartlett and Deitz (2000). In the field, *P. paraguayensis* can be indirectly detected by observing a corkscrew or wavy distortion of the *L. g.* subsp. *hexapetala* stems produced by the damage of the egg insertions.

Although there are no natural enemies recorded for this species, members of the Order Hymenoptera (Dryinidae and Mymaridae) and Strepsiptera have been reported as parasitoids of adults and nymphs of three North American species (adults of *P. dorsalis* (Van Duzee), third instar of *P. delicatus* and eggs of *P. quadripustulatus* (Van Duzee)) (Stiling and Moon 2005). Bartlett (2020) (and

updates) mentioned *Anagrus flaveolus* Waterhouse (Mymaridae) as an egg parasite of *Pissonotus* sp. and an undetermined Dryinidae on probably *Pissonotus concolor* Bartlett.

Summarising information on the species biology and host plants, host range tests showed that *P. paraguayensis* presents a certain degree of specificity to the *Jussiaea* section of the genus *Ludwigia* and that therefore it can survive not only in *L. g.* subsp. *hexapetala*. Even though *L. g.* subsp. *grandiflora* is closely related to the main host plant, it was the only species inside the section where *P. paraguayensis* did not survive. Stems of this species are covered by dense pubescence of soft, viscid hairs, sticky when fresh, which usually trap small insects impeding any further movements. The results obtained are similar to others observed in the search for other control agents for *L. g.* subsp. *hexapetala* (Reddy et al. 2021; DaSilva et al. 2022). The species of the section *Jussiaea* form a distinctive, closely related group, especially due to the apparent lack of genetic barriers between entities of this group (Zardini et al. 1991). Nearly all species of this section can be crossed with one another and produce vigorous F1 hybrids (Peng 1990); therefore, finding a control agent specific to one of those species has been proven to be difficult. However, *P. paraguayensis* did not survive in the other *Ludwigia* species tested outside *Jussiaea*. There are successful records of delphacids as biological control agents against invasive aquatic plants, *Prokelisia marginata* (Van Duzee) to control *Spartina alterniflora* Loisel. in Western USA (Grevstad et al. 2003) and *M. scutellaris* to control *Pontederia crassipes* (Mart.) Solms. in South Africa and USA (Tipping et al. 2014; Paterson et al. 2023). With the new morphological and biological knowledge about *P. paraguayensis*, it is now possible to move forward and perform more host specificity tests (e.g. multiple generations, ovipositions, field population dynamics) with larger test plant lists to establish if this planthopper can be proposed as a biological agent against *Ludwigia*.

In conclusion, the description of both forms of *P. paraguayensis* females and immature stages presented in this work, not only contributes to the species complete description but also provides new morphological and molecular tools to identify the species inside the genus. The collection of *P. paraguayensis* in Argentina has extended the distribution of the species and genus and enriched the country's biodiversity. A new rearing methodology was developed both to establish an indoor/outdoor colony and to perform different tests in laboratory conditions to learn more about its biology and potential as a biological control agent.

Acknowledgements

We want to thank to Dr Emmy Engasser (O'Brien Collection Specialist, Arizona State University) and Charles Bartlett (University of Delaware, Department of Entomology and Wildlife Ecology) for their suggestions and for providing us with photos of the type specimen; Dr Arnaldo Maciá (CIC: Comisión de Investigaciones Científicas de la Provincia de Buenos Aires, Argentina) for critically reading and making language edits of the manuscript. Finally, we extend our thanks to the reviewers for their valuable comments and suggestions that improved the manuscript.

Additional information

Conflict of interest

The authors have declared that no competing interests exist.

Ethical statement

No ethical statement was reported.

Funding

La Plata National University (UNLP) (Grant N° 730); Fundación para el Estudio de Especies Invasivas (FuEDEI); Consejo Nacional de Investigaciones Científicas y Técnicas (CONICET).

Author contributions

Conceptualization: AMMRL, AJS, ACF, MCH. Data curation: AMMRL, NAS, ACF. Formal analysis: AMMRL, AJS, ACF. Funding acquisition: AMMRL, AJS. Investigation: MCH, ACF, AJS, AMMRL, AF. Methodology: ACF, MCH, AMMRL. Project administration: ACF, AMMRL, AJS. Resources: AJS, AMMRL. Software: ACF, NAS, AF. Supervision: MCH, AJS, AMMRL. Validation: ACF, MCH. Visualization: ACF, AMMRL. Writing - original draft: ACCF, MCH, AJS, AMMRL. Writing - review and editing: NAS, AJS, AMMRL, MCH, AF, ACF.

Author ORCIDs

Ana M. Marino de Remes Lenicov  <https://orcid.org/0000-0001-8678-5408>

Ana C. Faltlhauser  <https://orcid.org/0000-0003-3121-3650>

Alvaro Foieri  <https://orcid.org/0000-0001-5623-3629>

Nicolas A. Salinas  <https://orcid.org/0000-0002-1055-4475>

M. Cristina Hernández  <https://orcid.org/0000-0003-4382-773X>

Alejandro J. Sosa  <https://orcid.org/0000-0002-1680-8712>

Data availability

All of the data that support the findings of this study are available in the main text or Supplementary Information.

References

- Asche M (1985) Zur phylogenie der Delphacidae Leach, 1815 (Homoptera Cicadina Fulgoromorpha). Marburger Entomologische Publikationen 2(1–2): 1–910.
- Bartlett CR (2020) [and updates] Planthoppers of North America. <https://sites.udel.edu/planthoppers/> [Accessed on 01 Mar 2023]
- Bartlett CR, Deitz LL (2000) Revision of the New World Delphacid Planthopper Genus *Pissonotus* (Hemiptera: Fulgoroidea). Thomas Say Publications in Entomology, Entomological Society of America, 234 pp. <https://doi.org/10.4182/AKAE8776>
- Bourgoin T, Wang R, Asche M, Hoch H, Soulier-Perkins A, Stroiński A, Yap S, Szewdo J (2015) From micropterism to hyperpterism: recognition strategy and standardized homology-driven terminology of the forewing venation patterns in planthoppers (Hemiptera: Fulgoromorpha). Zoomorphology 134(1): 63–77. <https://doi.org/10.1007/s00435-014-0243-6>

- Chen S, Yang CT (1995) The metatarsi of the Fulgoroidea (Homoptera: Auchenorrhyncha). Chinese Journal of Entomology 15: 257–269.
- Crawford L (1914) A contribution toward a monograph of the homopterous insects of the family Delphacidae of North and South America. Proceedings of the United States National Museum 46(2041): 557–641. <https://doi.org/10.5479/si.00963801.46-2041.557>
- DaSilva A, Reddy AM, Pratt PD, Friedman MSH, Grewell BJ, Harms NE, Faltlhauser AC, Chamorro ML (2022) Biology of immature stages and host range characteristics of *Sudauleutes bosqi* (Coleoptera: Curculionidae), a candidate biological control agent of exotic *Ludwigia* spp. in the USA. The Florida Entomologist 105(3): 243–249. <https://doi.org/10.1653/024.105.0310>
- Denno RF, Roderick GK (1990) Population Biology of Planthoppers. Annual Review of Entomology 35(1): 489–520. <https://doi.org/10.1146/annurev.en.35.010190.002421>
- Denno RF, Roderick GK, Olmstead KL, Dobel HG (1991) Density related migration in planthoppers (Homoptera: Delphacidae): the role of habitat persistence. American Naturalist 138(6): 1513–1541. <https://doi.org/10.1086/285298>
- Emeljanov AF (1996) On the question of the classification and phylogeny of the Delphacidae (Homoptera, Cicadina), with reference to larval characters. Entomological Review 75(9): 134–150. Entomologicheskoe Obozrenie 74(4): 780–794, 944–945.
- Emeljanov AF (2002) Contribution to classification and phylogeny of the family Cixiidae (Hemiptera, Fulgoromorpha). Denisia 04, Zugleich Kataloge des OÖ. Landesmuseums, Neue Folge. Biologiezentrum Linz 176: 103–112.
- Folmer O, Black M, Hoeh W, Lutz R, Vrijenhoek R (1994) DNA primers for amplification of mitochondrial cytochrome c oxidase subunit I from diverse metazoan invertebrates. Molecular Marine Biology and Biotechnology 3(5): 294–299.
- Grevstad FS, Strong DR, Garcia-Rossi D, Switzer RW, Wecker MS (2003) Biological control of *Spartina alterniflora* in Willapa Bay, Washington using the plant hopper *Prokelisia marginata*: Agent specificity and early results. Biological Control 27(1): 32–42. [https://doi.org/10.1016/S1049-9644\(02\)00181-0](https://doi.org/10.1016/S1049-9644(02)00181-0)
- Hernández MC, Cabrera Walsh G (2014) Insect Herbivores Associated with *Ludwigia* Species, Oligospermum section, in their Argentine distribution. Journal of Insect Science 14(1): 201. <https://doi.org/10.1093/jisesa/ieu063>
- Kleinbaum DG, Klein M (2012) Introduction to Survival Analysis. In: Survival Analysis. Statistics for Biology and Health. Springer, New York, 1–43. https://doi.org/10.1007/978-1-4419-6646-9_1
- Mariani R, Sosa A, Marino de Remes Lenicov AM (2007) *Megamelus bellicus* Remes Lenicov & Sosa (Hemiptera: Delphacidae) immature stages and biology. Revista de la Sociedad Entomológica Argentina 66(3–4): 189–196. [RSEA]
- Mariani R, Sosa AJ, Marino de Remes Lenicov AM (2013) A new species of *Megamelus* from Argentina and the reassignment of *Stenocranus maculipes* (Berg) (Hemiptera: Delphacidae). Revista de la Sociedad Entomológica Argentina 72(3–4): 169–178. [RSEA]
- Marino de Remes Lenicov AMM, Defea B, Rusconi J, Cabrera Walsh G (2017) Studies on the immature stages of the planthopper *Lepidelpfax pistiae* (Hemiptera: Delphacidae), a potential biocontrol agent for the aquatic weed *Pistia stratiotes* (Araceae) from Argentina (Hemiptera: Fulgoromorpha). Austral Entomology 56(4): 384–391. <https://doi.org/10.1111/aen.12248>
- Metcalf ZP (1923) A key to the Fulgoridae of Eastern North America with descriptions of new species. Journal of the Elisha Mitchell Scientific Society 38: 139–230. <https://doi.org/10.5962/bhl.part.7606>

- Morgan LW, Beamer RH (1949) A revision of three genera of Delphacine Fulgorids from America North of Mexico (Homoptera-Fulgoridac-Delphacinac). *Journal of the Kansas Entomological Society* 22(1): 212–241. <https://www.jstor.org/stable/25081893>
- Muir FAG, Giffard WM (1924) Studies in North American Delphacidae. *Bulletin of the Experimental Station of Hawaiian Sugar Planters Association. Division of Entomology. Honolulu* 15: 1–53.
- Oman PW (1947) The types of Auchenorrhynchos Homoptera in the Iowa State College collection. *Iowa State College Journal of Science* 21: 161–228.
- Paterson ID, Motitsoe SN, Coetzee JA, Hill MP (2023) Recent post-release evaluations of weed biocontrol programmes in South Africa: A summary of what has been achieved and what can be improved. *BioControl*. <https://doi.org/10.1007/s10526-023-10215-4>
- Peng CI (1990) Taiwan, and its origin. *Botanical Bulletin of Academia Sinica* 31: 343–349.
- R Core Team (2022) R: A language and environment for statistical computing. R Foundation for Statistical Computing, Vienna, Austria. <https://www.R-project.org/> [Accessed 1 August 2023]
- Raven PH (1963) Amphotropical relationships in the floras of North and South America. *The Quarterly Review of Biology* 38(2): 151–177. <https://doi.org/10.1086/403797>
- Reddy AM, Pratt PD, Grewell BJ, Harms NE, Cibils-Stewart X, Cabrera Walsh G, Faltlhauser A (2021) Biological and host range characteristics of *Lysathia flavipes* (Coleoptera: Chrysomelidae), a candidate biological control agent of invasive *Ludwigia* spp. (Onagraceae) in the USA. *Insects* 12(5): 471. <https://doi.org/10.3390/insects12050471>
- Remes Lenicov AMM, Cabrera Walsh G (2013) A new genus and species of Delphacini associated to hydrophytic plants in Argentina (Hemiptera, Fulgoromorpha, Delphacidae). *The Florida Entomologist* 96(4): 1350–1358. <https://doi.org/10.1653/024.096.0414>
- Sosa AJ, de Remes Lenicov AMM, Mariani R, Cordo H (2004) Redescription of *Megamelus scutellaris* Berg (Hemiptera: Delphacidae), a candidate for biological control of water hyacinth. *Annals of the Entomological Society of America* 97(2): 271–275. [https://doi.org/10.1603/0013-8746\(2004\)097\[0271:ROMSBH\]2.0.CO;2](https://doi.org/10.1603/0013-8746(2004)097[0271:ROMSBH]2.0.CO;2)
- Sosa AJ, de Remes Lenicov AMM, Mariani R, Cordo H (2005) Life history of *Megamelus scutellaris* Berg with description of immature stages (Hemiptera, Delphacidae). *Annals of the Entomological Society of America* 98(1): 66–72. [https://doi.org/10.1603/0013-8746\(2005\)098\[0066:LHOMSW\]2.0.CO;2](https://doi.org/10.1603/0013-8746(2005)098[0066:LHOMSW]2.0.CO;2)
- Sosa AJ, de Remes Lenicov AMM, Mariani R (2007) Species of *Megamelus* (Hemiptera-Delphacidae) associated with Pontederaceae in South America. *Annals of the Entomological Society of America* 100(6): 798–809. [https://doi.org/10.1603/0013-8746\(2007\)100\[798:SOMHDA\]2.0.CO;2](https://doi.org/10.1603/0013-8746(2007)100[798:SOMHDA]2.0.CO;2)
- Spooner CS (1912) Some new species of Delphacidae. *Canadian Entomologist* 44(8): 233–242. <https://doi.org/10.4039/Ent44233-8>
- Stiling P, Moon DC (2005) Quality or Quantity: The Direct and Indirect Effects of Host Plants on Herbivores and Their Natural Enemies. *Oecologia* 142(3): 413–420. <https://doi.org/10.1007/s00442-004-1739-4>
- Thouvenot L, Haury J, Thiebaut G (2013) A success story: Water primroses, aquatic plant pests. *Aquatic Conservation* 23(5): 790–803. <https://doi.org/10.1002/aqc.2387>
- Tipping PW, Sosa A, Pokorny EN, Foley J, Schmitz DC, Lane JS, Cole MS, Nichols G (2014) Release and establishment of *Megamelus scutellaris* (Hemiptera: Delphacidae) on water hyacinth in Florida. *The Florida Entomologist* 97(2): 804–806. <https://doi.org/10.1653/024.097.0264>
- Van Duzee EP (1897) A preliminary review of the North American Delphacidae. *Bulletin of Buffalo Society of Natural Science* 5: 225–261.

- Vilbaste J (1968) Preliminary key for the identification of the nymphs of North European Homoptera Cicadina. I. Delphacidae. *Annales Entomologici Fennici* 34: 65–74.
- Wagner WL, Hoch PC, Raven PH (2007) Revised classification of the Onagraceae. *Systematic Botany Monographs* 83: 1–240.
- Wilson SW, Tsai JH (1991) Descriptions of Nymphs of the Delphacid Planthopper *Pissonotus delicatus* (Homoptera: Fulgoroidea). *Journal of the New York Entomological Society* 99 (2): 242–247. <https://www.jstor.org/stable/25009897>
- Wilson SW, Mitter C, Denno RF, Wilson MR (1994) Evolutionary patterns of host plant use by delphacid planthoppers and their relatives. In: Denno RF, Perfect TJ (Eds) *Planthoppers: their ecology and management*. Springer US, Boston, 7–113. https://doi.org/10.1007/978-1-4615-2395-6_2
- Yang CT, Fang SJ (1993) Phylogeny of Fulgoromorpha nymphs, first results. In: Drosopoulos S, Petrakis PV, Claridge MF, de Virijer PWF (Eds) *Proceeding 8th Auchenorrhyncha Congress*; 9–13 Aug., Delphi, Greece, 25–26.
- Yang CT, Yeh WB (1994) Nymphs of Fulgoroidea (Homoptera: Auchenorrhyncha) with descriptions of two new species and notes on adults of Dictyopharidae. *Chinese Journal of Entomology, Special Publication* 8, 189 pp.
- Zardini EM, Gu H, Raven PH (1991) On the separation of two species within the *Ludwigia uruguayensis* complex (Onagraceae). *Systematic Botany* 16(2): 242–244. <https://doi.org/10.2307/2419276>

Supplementary material 1

Graphical figures of Kaplan-Meier curves of *Pissonotus paraguayensis* males and female survival probability on different test plants

Authors: Ana M. Marino de Remes Lenicov, Ana C. Faltlhauser, Alvaro Foieri, Nicolas A. Salinas, M. Cristina Hernández, Alejandro J. Sosa

Data type: docx

Explanation note: Kaplan-Meier curves of male and female *Pissonotus paraguayensis* survival probability on different test plants (colours). Non-parametric Log-rank statistical test was used to assess statistical differences in overall survival.

Copyright notice: This dataset is made available under the Open Database License (<http://opendatacommons.org/licenses/odbl/1.0/>). The Open Database License (ODbL) is a license agreement intended to allow users to freely share, modify, and use this Dataset while maintaining this same freedom for others, provided that the original source and author(s) are credited.

Link: <https://doi.org/10.3897/zookeys.1188.113350.suppl1>

Three new species of the planthopper genus *Oecleopsis* Emeljanov, 1971 from China (Hemiptera, Fulgoromorpha, Cixiidae)

Sha-Sha Lv^{1,2}, Lin Yang^{1,2}, Yu-Bo Zhang³, Yan Zhi⁴, Pei Zhang⁵, Xiang-Sheng Chen^{1,2}

¹ Institute of Entomology, Guizhou University, Guiyang, Guizhou, 550025, China

² The Provincial Special Key Laboratory for Development and Utilization of Insect Resources of Guizhou, Guizhou University, Guiyang, Guizhou, 550025, China

³ Anshun University, College Agriculture, Anshun, Guizhou, 561000, China

⁴ Laboratory Animal Center, Guizhou Medical University, Guiyang, Guizhou, 550025, China

⁵ Xingyi Normal University for Nationalities, Xingyi, Guizhou, 562400, China

Corresponding author: Xiang-Sheng Chen (chenxs3218@163.com)

Abstract

Three new species of the genus *Oecleopsis* Emeljanov, 1971 from China, *O. acerbus* Lv & Chen, **sp. nov.** and *O. panxianensis* Lv & Chen, **sp. nov.** from Guizhou Province, and *O. digitatus* Lv & Chen, **sp. nov.** from Sichuan Province, are described and illustrated. With these additions, the number of species in the genus is increased to 18. An updated identification key and checklist of all known species of *Oecleopsis* are provided as well as a map of their geographic distributions.

Key words: Distribution, Fulgoroidea, morphology, Pentastirini, taxonomy



Academic editor: Mike Wilson

Received: 11 October 2023

Accepted: 6 December 2023

Published: 10 January 2024

ZooBank: <https://zoobank.org/8FA97BD5-C39C-46EF-BC14-75CA83A4F54A>

Citation: Lv S-S, Yang L, Zhang Y-B, Zhi Y, Zhang P, Chen X-S (2024) Three new species of the planthopper genus *Oecleopsis* Emeljanov, 1971 from China (Hemiptera, Fulgoromorpha, Cixiidae). ZooKeys 1188: 251–264. <https://doi.org/10.3897/zookeys.1188.114008>

Copyright: © Sha-Sha Lv et al.

This is an open access article distributed under terms of the Creative Commons Attribution License ([Attribution 4.0 International – CC BY 4.0](https://creativecommons.org/licenses/by/4.0/)).

Introduction

Emeljanov (1971) established the planthopper genus *Oecleopsis* with the type species *Oecleopsis artemisiae* (Matsumura, 1914) and transferred *O. cucullatus* (Noualhier, 1896) from the genus *Oliarus* Stål, 1862 into the genus *Oecleopsis*. This genus belongs to the tribe Pentastirini of the subfamily Cixiinae (Hemiptera, Fulgoromorpha, Cixiidae) (Emeljanov 1971; Bourgoïn 2023). Van Stalle (1991) described *O. articara* Van Stalle, 1991, and transferred the following seven species from *Oliarus* Stål, 1862 to *Oecleopsis*: *O. petasatus* (Noualhier, 1896), *O. mori* (Matsumura, 1914), *O. sinicus* (Jacobi, 1944), *O. yoshikawai* (Ishihara, 1961), *O. bifidus* (Tsaour, Hsu & Van Stalle, 1988), *O. chiangi* (Tsaour, Hsu & Van Stalle, 1988), and *O. elevatus* (Tsaour, Hsu & Van Stalle, 1988). Guo et al. (2009) reviewed the genus and described three new species from China, *O. spinosus* Guo, Wang & Feng, 2009, *O. tiantaiensis* Guo, Wang & Feng, 2009, and *O. wuyiensis* Guo, Wang & Feng, 2009. Zhi et al. (2018) described two new species from China, *O. laminatus* Zhi & Chen, 2018 and *O. productus* Zhi & Chen, 2018. Until now, 15 species have been recorded in the genus, which are widely distributed in the Palaearctic (China, Japan, Russia, and Korea) and Oriental (China, Cambodia, Indonesia, Malaysia, and Thailand) regions (Holt et al. 2013; Bourgoïn 2023).

Herein, three new species from China, *O. acerbus* Lv & Chen sp. nov., *O. panxianensis* Lv & Chen, sp. nov. and *O. digitatus* Lv & Chen, sp. nov., are described and illustrated. Hence, the species number of *Oecleopsis* is raised to 18. All *Oecleopsis* species are recorded from China (Guo et al. 2009; Zhi et al. 2018; Luo et al. 2022; Bourgoin 2023).

Material and methods

The external morphology terminologies are as follows: male genitalia follows Bourgoin (1987), female genitalia follows Bourgoin (1993), and wing venation follows Bourgoin et al. (2015). Body measurements are from apex of vertex to tip of forewing; vertex length was measured the median length of vertex (from apical transverse carina to tip of basal emargination). All measurements are in millimeters (mm). External morphology and drawings were done under the Leica MZ 12.5 stereomicroscope. Photographs were taken with NIKON SMZ 25 and VHX-1000E digital camera. Illustrations were scanned with CanoScan LiDE 200 and imported into Adobe Photoshop 7.0 for labeling and plate composition. The dissected male and female genitalia are preserved in glycerin in small plastic tubes pinned together with the specimens. The distribution map was generated with ARCGIS 10.7.

The type specimens examined are deposited in the Institute of Entomology, Guizhou University, Guiyang, Guizhou Province, China (IEGU).

Results

Taxonomy

Class Insecta Linnaeus, 1758

Order Hemiptera Linnaeus, 1758

Infraorder Fulgoromorpha Evans, 1946

Family Cixiidae Spinola, 1839

Subfamily Cixiinae Spinola, 1839

Tribe Pentastirini Emeljanov, 1971

Oecleopsis Emeljanov, 1971

Oecleopsis Emeljanov, 1971: 621; Anufriev and Emeljanov 1988: 460; Van Stalle 1991: 20; Guo et al. 2009: 46; Zhi et al. 2018: 3.

Type species. *Oliarus artemisiae* Matsumura, 1914, original designation.

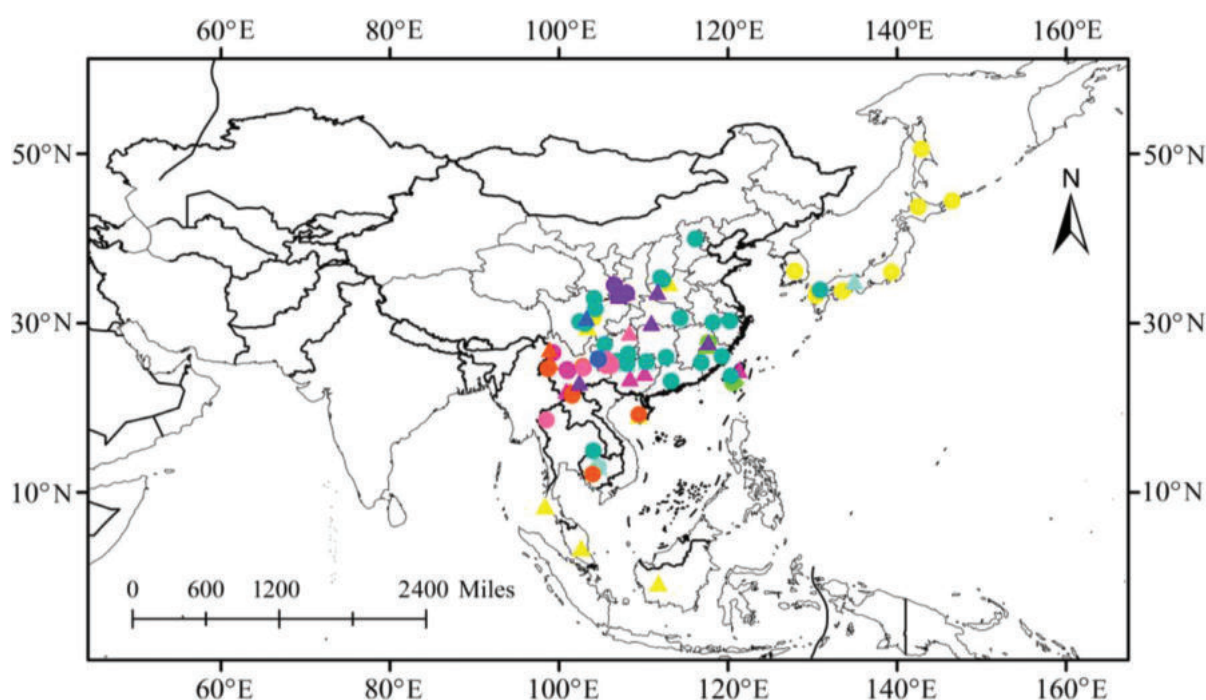
Diagnosis. For the diagnosis of *Oecleopsis* see Van Stalle (1991: 20) and Guo et al. (2009: 46).

Distribution. China, Japan, Korea, Russia, Thailand, Malaysia, Indonesia and Cambodia (Fig. 1).

Checklist and distributions of species of *Oecleopsis* Emeljanov, 1971

O. artemisiae (Matsumura, 1914); China (Sichuan Province), Japan (Chishima, Hokkaido, Honshu, Kyushu, Shikoku, Tsushima Islands), Korea, Russia (Kunashir Island).

- O. articara* Van Stalle, 1991; China (Hainan, Henan, Sichuan, Guizhou Provinces), Indonesia (Borneo State), Malaysia (Borneo, Pahang States).
O. bifidus (Tsauro, Hsu & Van Stalle, 1988); China (Fujian, Taiwan Provinces).
O. chiangi (Tsauro, Hsu & Van Stalle, 1988); China (Fujian, Taiwan Provinces).
O. cucullatus (Noualhier, 1896); China (Guangdong, Hubei Provinces), Cambodia.
O. elevatus (Tsauro, Hsu & Van Stalle, 1988); China (Guizhou, Taiwan Provinces, Guangxi Zhuang Autonomous Region), Japan (Honshu Island).
O. laminatus Zhi & Chen, 2018; China (Yunnan Province).
O. mori (Matsumura, 1914); China (Guangxi Zhuang Autonomous Region, Yunnan, Taiwan Provinces).
O. petasatus (Noualhier, 1896); China (Hainan, Sichuan, Yunnan Provinces), Cambodia.
O. productus Zhi & Chen, 2018; China (Yunnan Province).
O. sinicus (Jacobi, 1944); China (Anhui, Beijing, Fujian, Guangdong, Guizhou, Hubei, Henan, Hunan, Shanxi, Sichuan, Zhejiang, Taiwan Provinces, Guangxi Zhuang Autonomous Region), Cambodia, Japan (Kyushu Island).
O. spinosus Guo, Wang & Feng, 2009; China (Shaanxi Province).
O. tiantaiensis Guo, Wang & Feng, 2009; China (Gansu, Shaanxi Provinces).



Oecleopsis artemisiae (Matsumura, 1914) (●); *O. articara* Van Stalle, 1991 (▲); *O. bifidus* (Tsauro, Hsu & Van Stalle, 1988) (●); *O. chiangi* (Tsauro, Hsu & Van Stalle, 1988) (▲); *O. cucullatus* (Noualhier, 1896) (●); *O. elevatus* (Tsauro, Hsu & Van Stalle, 1988) (▲); *O. laminatus* Zhi & Chen (●); *O. mori* (Matsumura, 1914) (▲); *O. petasatus* (Noualhier, 1896) (●); *O. productus* Zhi & Chen (▲); *O. sinicus* (Jacobi, 1944) (●); *O. spinosus* Guo, Wang & Feng, 2009 (▲); *O. tiantaiensis* Guo, Wang & Feng, 2009 (●); *O. wuyiensis* Guo, Wang & Feng, 2009 (▲); *O. yoshikawai* (Ishihara, 1961) (●); *O. acerbus* Lv & Chen **sp. nov.** (▲); *O. panxianensis* Lv & Chen **sp. nov.** (●); *O. digitatus* Lv & Chen **sp. nov.** (▲).

Figure 1. Geographic distributions of *Oecleopsis* species.

- O. wuyiensis* Guo, Wang & Feng, 2009; China (Fujian, Henan, Hunan, Shaanxi, Yunnan Provinces).
O. yoshikawai (Ishihara, 1961); China (Guizhou, Yunnan Provinces), Thailand (Doi Inthanon National Park).
O. acerbus Lv & Chen sp. nov.; China (Guizhou Province).
O. panxianensis Lv & Chen sp. nov.; China (Guizhou Province).
O. digitatus Lv & Chen sp. nov.; China (Sichuan Province).

Key to species of *Oecleopsis* Emeljanov, 1971

- 1 Vertex at least three times as long as broad **2**
 - Vertex less than three times as long as broad **6**
- 2 Apex of endosoma circular **3**
 - Apex of endosoma not circular **4**
- 3 Left side near apex of periandrium with a short spinose process; dorsal margin of endosoma with a long spinose process and left side with a short process (Zhi et al. 2018: figs 31–34) ***O. productus***
 - Left side of periandrium without spinose process; dorsal margin of endosoma without process and left side with a long process (Van Stalle 1991: fig. 79) ***O. articara***
- 4 Aedeagus with four processes in total (Van Stalle 1991: fig. 72)
..... ***O. petasatus***
 - Aedeagus with three processes in total **5**
- 5 Apical process of endosoma bifurcated at basal part, rami long (Fig. 3K–N) ***O. panxianensis* sp. nov.**
 - Apical process of endosoma bifurcated at apical part, rami short relatively (Zhi et al. 2018: figs 17–20) ***O. laminatus***
- 6 Apical process of endosoma not bifurcated **7**
 - Apical process of endosoma bifurcated **10**
- 7 Apex of endosoma with four processes (Tsaur et al. 1988: fig. 10F, G)
..... ***O. elevatus***
 - Apex of endosoma without four processes **8**
- 8 Left side of periandrium at apex of aedeagus with a short spine (Zhi et al. 2018: fig. 46) ***O. yoshikawai***
 - Left side of periandrium at apex of aedeagus without a spine **9**
- 9 Periandrium with a moderately long spine, situated on right-dorsal margin, directed dorsocephalad (Tsaur et al. 1988: fig. 8C, D) ***O. chiangi***
 - Periandrium with a short spine, situated on right side of periandrium at apex of aedeagus, directed ventrad (Guo et al. 2009: figs 10, 11) ***O. spinosus***
- 10 Rami of bifurcation symmetrical, almost equal in length **11**
 - Rami of bifurcation asymmetrical, unequal in length **13**
- 11 Endosoma with one subapical process (Tsaur et al. 1988: fig. 9C, D)
..... ***O. bifidus***
 - Endosoma with two subapical processes **12**
- 12 Spine on right side of periandrium at apex of aedeagus very long and slender (Anufriev and Emeljanov 1988: fig. 358; Van Stalle 1991: fig. 101)
..... ***O. artemisiae***
 - Spine on right side of periandrium at apex of aedeagus very short, basal part wide (Van Stalle 1991: fig. 92) ***O. sinicus***

- 13 Left ramus of bifurcation rudimentary, only a small protuberance (Guo et al. 2009: figs 20, 21) ***O. tiantaiensis***
- Left ramus of bifurcation well developed **14**
- 14 Length of right ramus of bifurcation about three times as long as that of left ramus (Van Stalle 1991: fig. 85)..... ***O. mori***
- Length of right ramus of bifurcation less than three times as long as that of left ramus **15**
- 15 Ventral margin near base of periandrium with a spinose process (Guo et al. 2009: figs 31, 32)..... ***O. wuyiensis***
- Ventral margin near base of periandrium without a spinose process **16**
- 16 Dorsal process of endosoma suddenly narrowed at middle part, long, needle-shaped (Fennah 1956: fig. 3 G) ***O. cucullatus***
- Dorsal process of endosoma not suddenly narrowed at middle part, not long and needle-shaped..... **17**
- 17 Dorsal process of endosoma directed ventrocephalad, lateral margins straight; ventral process constricted in the middle, curved ventrocephalad on left side (Fig. 2K–N) ***O. acerbus* sp. nov.**
- Dorsal process of endosoma directed dorsocephalad, lateral margins slightly curved; ventral process smoothly tapering at end, curved ventrad on left side (Fig. 4K–N) ***O. digitatus* sp. nov.**

***Oecleopsis acerbus* Lv & Chen, sp. nov.**

<https://zoobank.org/754684CF-A1BB-4257-8655-A714390309A9>

Figs 2A–N, 5A–C

Type materials. **Holotype:** CHINA • ♂; Guizhou Province, Yanhe County, Xinjing Town; 28°53'N, 108°17'E; sweeping, 7 June 2007; Pei Zhang leg.; IEGU. **Paratypes:** 7♂♂, 3♀♀; CHINA • Guizhou Province, Yanhe County, Xinjing Town; 28°53'N, 108°17'E; sweeping, 7 June 2007; Zheng-Guang Zhang & Pei Zhang leg.; IEGU.

Diagnosis. The salient features of the new species include: vertex (Fig. 2A, C) less than three times as long as broad; spinose process near apex of periandrium on right side (Fig. 2K) short, nib-like; left side (Fig. 2L) apical process of endosoma bifurcated, rami of bifurcation asymmetrical; two subapical spines, dorsal process long and tapering to apex, lateral margins straight, ventral process constricted in the middle.

Measurements. Total length: male 7.20–7.76 mm ($n = 8$), female 7.61–8.05 mm ($n = 3$).

Description. **Coloration.** General color grayish brown (Fig. 2A, B). Vertex blackish brown. Eyes yellowish brown, ocelli yellowish. Frons yellowish to blackish brown, carinae lighter; rostrum blackish brown. Pronotum blackish brown with carinae yellowish or light brown. Mesonotum blackish brown, carinae brown. Forewings semitranslucent, light grayish brown, distal part with several small patches, stigma yellowish brown. Hindwings semitransparent. Abdomen yellowish brown.

Head and thorax. Vertex (Fig. 2A, C) narrow, 2.36 times longer than wide. Frons (Fig. 1D) with distinct median carina, longer in middle line than wide at widest portion (about 1.33:1). Clypeus (Fig. 2D) with distinct median and lateral carinae. Rostrum elongate, surpassing hind-coxae. Pronotum (Fig. 2C) wider than

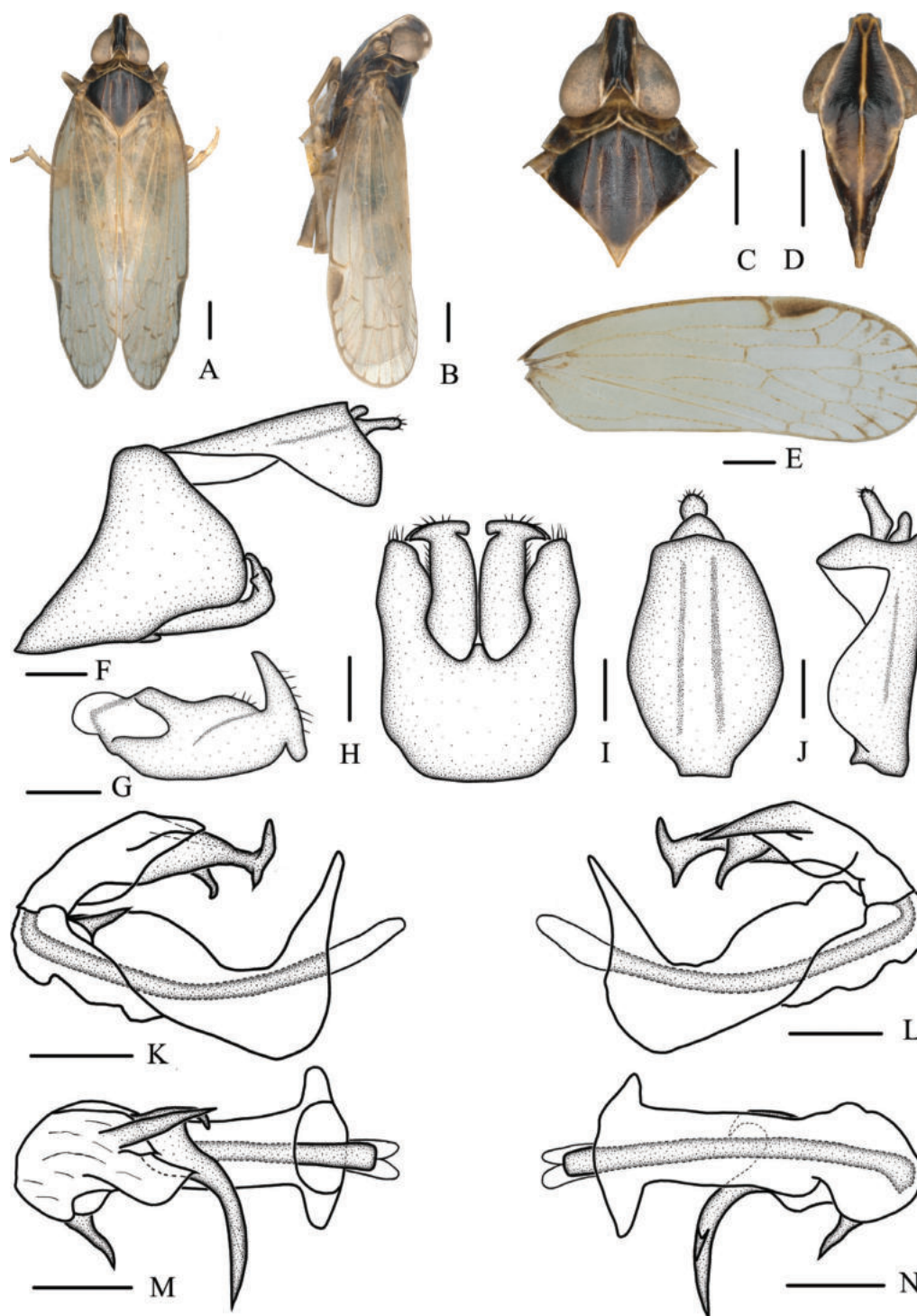


Figure 2. A–N *Oecleopsis acerbus* sp. nov., male **A** habitus, dorsal view **B** habitus, lateral view **C** head and thorax, dorsal view **D** frons, ventral view **E** forewing **F** male terminalia, lateral view **G** gonostyli, inner lateral view **H** pygofer and gonostyli, ventral view **I** anal segment, dorsal view **J** anal segment, right lateral view **K** aedeagus, right side **L** aedeagus, left side **M** aedeagus, dorsal view **N** aedeagus, ventral view. Scale bars: 0.2 mm.

maximum width of head (including eyes) (1.30:1), lateral and median carinae present. Mesonotum (Fig. 2C) about 6.41 times longer than pronotum in midline, with 5 carinae, distal part of median carina blurry. Forewings (Fig. 2E) slender, longer than maximal width (2.85:1), with 12 apical and 6 subapical cells; fork ScP+R distal to fork CuA₁+CuA₂; RP 3 branches, MP₁₊₂ 3 branches, and MP₃₊₄ 2 branches.

Male terminalia. Pygofer (Fig. 2F, H) symmetrical, in lateral view, lateral lobes triangularly extended caudally; in ventral view, dorsal margin concave and U-shaped. Medioventral process triangular in ventral view. Anal segment (Fig. 2F, I, J) tubular, asymmetrical, widened towards apex in left side view; in right side view, left ventral margin convex and right ventral margin excavated near apex; 1.55 times longer than wide in dorsal view; anal style finger-like, beyond anal tube. Aedeagus (Fig. 2K–N) in total with 4 processes; spinose process near apex of periandrium on right side short relatively, nib-like, directed right-dorsocephalad, only a quarter length of periandrium; left side apical process of endosoma bifurcated, curved outward, rami of bifurcation asymmetrical, dorsal ramus longer and thicker, ventral ramus slender and shorter; 2 subapical spines, dorsal process long and tapering to apex, lateral margins straight, directed ventrocephalad; ventral process constricted in the middle, curved ventrocephalad. Gonostyli (Fig. 2F–H) slender, curved apically, tapering into a process, T-shaped in ventral view.

Female terminalia. Terminalia as shown in Fig. 5A ventrally. Anal segment (Fig. 5C) 1.79 times longer than wide in dorsal view. Posterior vagina (Fig. 5B) elongate, with 4 sclerites in total, dorsal sclerite tapering at the end, median and ventral sclerites long, oval and trapezoidal, respectively, left side of terminal sclerite twist into angular process with straight lateral margins.

Distribution. China (Guizhou) (Fig. 1).

Etymology. The species name is derived from the Latin adjective “*acerbus*”, referring to dorsal process of the endosoma which is pointed on the left side.

Remarks. This species is similar to *Oecleopsis wuyiensis* Guo, Wang & Feng, 2009, but differs from the latter in: (1) frons yellowish to blackish brown (frons black in *O. wuyiensis*); (2) ventral margin near base of periandrium without a spinose process (ventral margin near base of periandrium with a spinose process in *O. wuyiensis*); (3) dorsal process of endosoma directed ventrocephalad (dorsal process of endosoma directed dorsocephalad in *O. wuyiensis*); (4) ventral process of endosoma curved and rounded at apex (ventral process of endosoma straight and pointed in *O. wuyiensis*).

***Oecleopsis panxianensis* Lv & Chen, sp. nov.**

<https://zoobank.org/4A4CF424-4975-44BC-8605-DBA344D63753>

Fig. 3A–N

Type materials. Holotype: CHINA • ♂; Guizhou Province, Panxian County, Banqiao Town; 25°44'N, 104°39'E; sweeping, 2 July 2011; Zhi-Hua Fan leg.; IEGU.

Paratype: 1 ♂, same collection data as for holotype; IEGU.

Diagnosis. The salient features of the new species include: vertex (Fig. 3A, C) at least three times as long as broad; frons (Fig. 3D) yellowish brown, with brown spots; aedeagus (Fig. 3K–N) in total with 3 processes; spinose process near apex of periandrium on right side (Fig. 3K) long, half wide at base, half thinner at end; left side (Fig. 3L) apical process of endosoma bifurcated, rami long, approximately equal length; a subapical spine, lateral margins curved.

Measurements. Total length: male 7.23–7.65 mm ($n = 2$).

Description. Coloration. General color dark brown (Fig. 3A, B). Vertex blackish brown. Eyes brown, ocelli yellowish. Frons yellowish brown, with brown

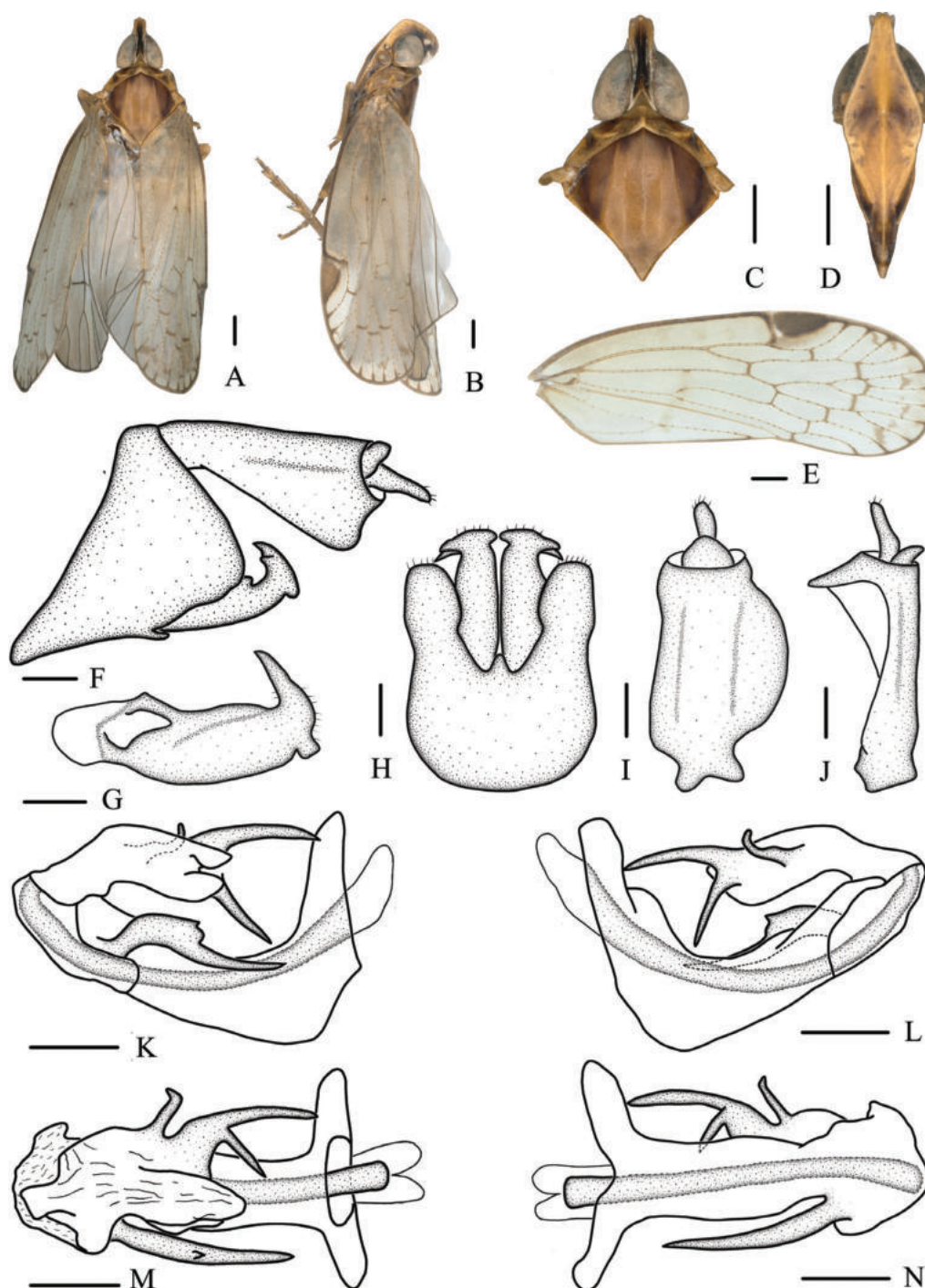


Figure 3. A–N *Oecleopsis panxianensis* sp. nov., male **A** habitus, dorsal view **B** habitus, lateral view **C** head and thorax, dorsal view **D** frons, ventral view **E** forewing **F** male terminalia, lateral view **G** gonostyli, inner lateral view **H** pygofer and gonostyli, ventral view **I** anal segment, dorsal view **J** anal segment, right lateral view **K** aedeagus, right side **L** aedeagus, left side **M** aedeagus, dorsal view **N** aedeagus, ventral view. Scale bars: 0.2 mm.

spots, carinae lighter; rostrum blackish brown. Pronotum grayish to blackish brown with carinae yellowish or light brown. Mesonotum dark brown, carinae brown. Forewings semitranslucent, light brown, with several brown markings, stigma yellowish brown. Hindwings semitransparent. Abdomen dark brown.

Head and thorax. Vertex (Fig. 3A, C) narrow, 3.23 times longer than wide. Frons (Fig. 3D) with distinct median carina, longer in middle line than wide at widest

portion (about 1.67:1). Clypeus (Fig. 3D) with distinct median and lateral carinae. Rostrum elongate, surpassing hind-coxae. Pronotum (Fig. 3C) wider than maximum width of head (including eyes) (1.60:1), lateral and median carinae present. Mesonotum (Fig. 3C) about 6.92 times longer than pronotum in midline, with 5 carinae, distal part of median carina blurry. Forewings (Fig. 3E) slender, longer than maximal width (3.01:1), with 12 apical and 6 subapical cells; fork ScP+R distal to fork CuA₁+CuA₂; RP 3 branches, MP₁₊₂ 3 branches, and MP₃₊₄ 2 branches.

Male terminalia. Pygofer (Fig. 3F, H) symmetrical, in lateral view, lateral lobes triangularly extended caudally; in ventral view, dorsal margin concave and U-shaped, middle part narrow. Medioventral process triangular in ventral view. Anal segment (Fig. 3F, I, J) tubular, asymmetrical, widened towards apex in left side view; in right side view, left ventral margin convex and right ventral margin excavated near apex; 1.68 times longer than wide in dorsal view; anal style finger-like, beyond anal tube. Aedeagus (Fig. 3K–N) in total with 3 processes; spinose process near apex of periandrium on right side long, half wide at base, half thinner at end, directed cephalically, more than 1/2 length of periandrium; left side apical process of endosoma bifurcated, rami long, approximately equal length, dorsal ramus directed cephalad, ventral ramus directed ventrocephalad; a subapical spine, lateral margins curved, curved dorsad, apical margin rounded. Gonostyli (Fig. 3F–H) slender, curved apically, tapering into a process, constricted for about 3/4 its length, T-shaped in ventral view.

Distribution. China (Guizhou) (Fig. 1).

Etymology. The new species is named after its the county in which it was collected.

Remarks. This species is similar to *Oecleopsis laminatus* Zhi & Chen, 2018, but differs from the latter in: (1) spinose process near apex of periandrium long, half wide at the base, 1/2 thinner at end (spinose process near apex of periandrium long, smoothly tapering at the end in *O. laminatus*); (2) apical process of endosoma bifurcated at base (apical process of endosoma bifurcated at apex in *O. laminatus*); (3) left side near apex of endosoma with a spiniform process, curved dorsad (left side near apex of endosoma with a large laminal process, directed cephalad in *O. laminatus*).

***Oecleopsis digitatus* Lv & Chen, sp. nov.**

<https://zoobank.org/49B9BA46-A908-44F6-8CD8-92A1373CF46C>

Figs 4A–N, 5D–F

Type materials. **Holotype:** CHINA • ♂; Sichuan Province, Dayi County, Xiling Town; 30°38'N, 103°14'E; sweeping, 20 July 2022; Sha-Sha Lv leg.; IEGU. **Paratypes:** CHINA • 6♂♂4♀♀; Sichuan Province, Dayi County, Xiling Town; 30°38'N, 103°14'E; sweeping, 20 July 2022; Sha-Sha Lv, Lan Zhang, Yong-Jin Sui & Feng-E Li leg.; IEGU.

Diagnosis. The salient features of the new species include: vertex (Fig. 4A, C) less than three times as long as broad; spinose process near apex of periandrium on right side (Fig. 4K) short and thick, finger-like; left side (Fig. 4L) apical process of endosoma bifurcated, rami short; two subapical spines long, dorsal process tapering toward the end, ventral process curved.

Measurements. Total length: male 5.8–6.4 mm ($n = 7$), female 6.8–7.5 mm ($n = 5$).

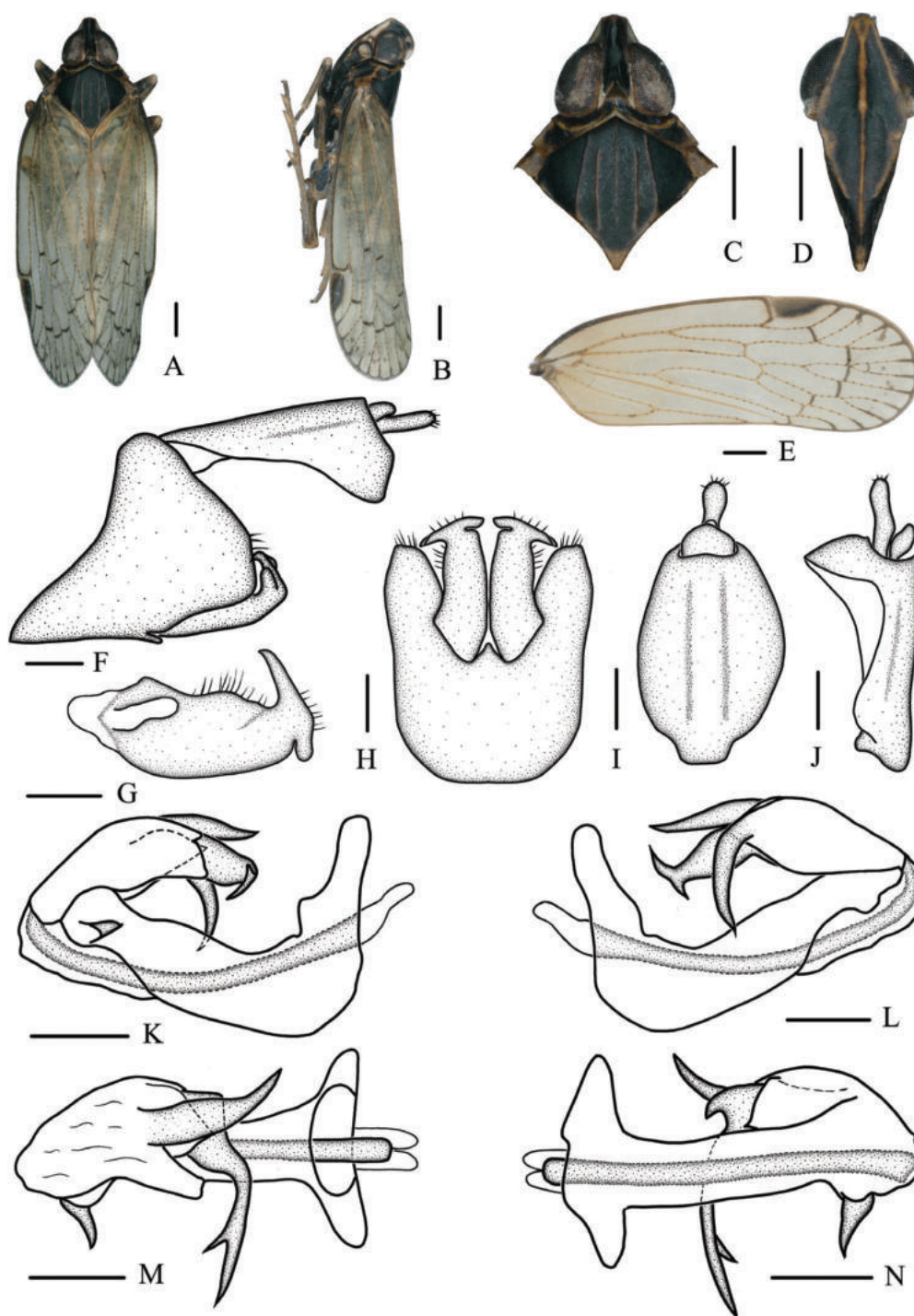


Figure 4. A–N *Oecleopsis digitatus* sp. nov., male A habitus, dorsal view B habitus, lateral view C head and thorax, dorsal view D frons, ventral view E forewing F male terminalia, lateral view G gonostyli, inner lateral view H pygofer and gonostyli, ventral view I anal segment, dorsal view J anal segment, right lateral view K aedeagus, right side L aedeagus, left side M aedeagus, dorsal view N aedeagus, ventral view. Scale bars: 0.2 mm.

Description. Coloration. General color grayish black (Fig. 4A, B). Vertex brown-black. Eyes dark brown, ocelli yellowish. Frons black, carinae yellowish brown; rostrum black. Pronotum brown-black with carinae yellowish or light brown. Mesonotum black, carinae brown. Forewings semitranslucent, yellowish brown, with several small brown markings, stigma brown. Hindwings semi-transparent. Abdomen dark brown.

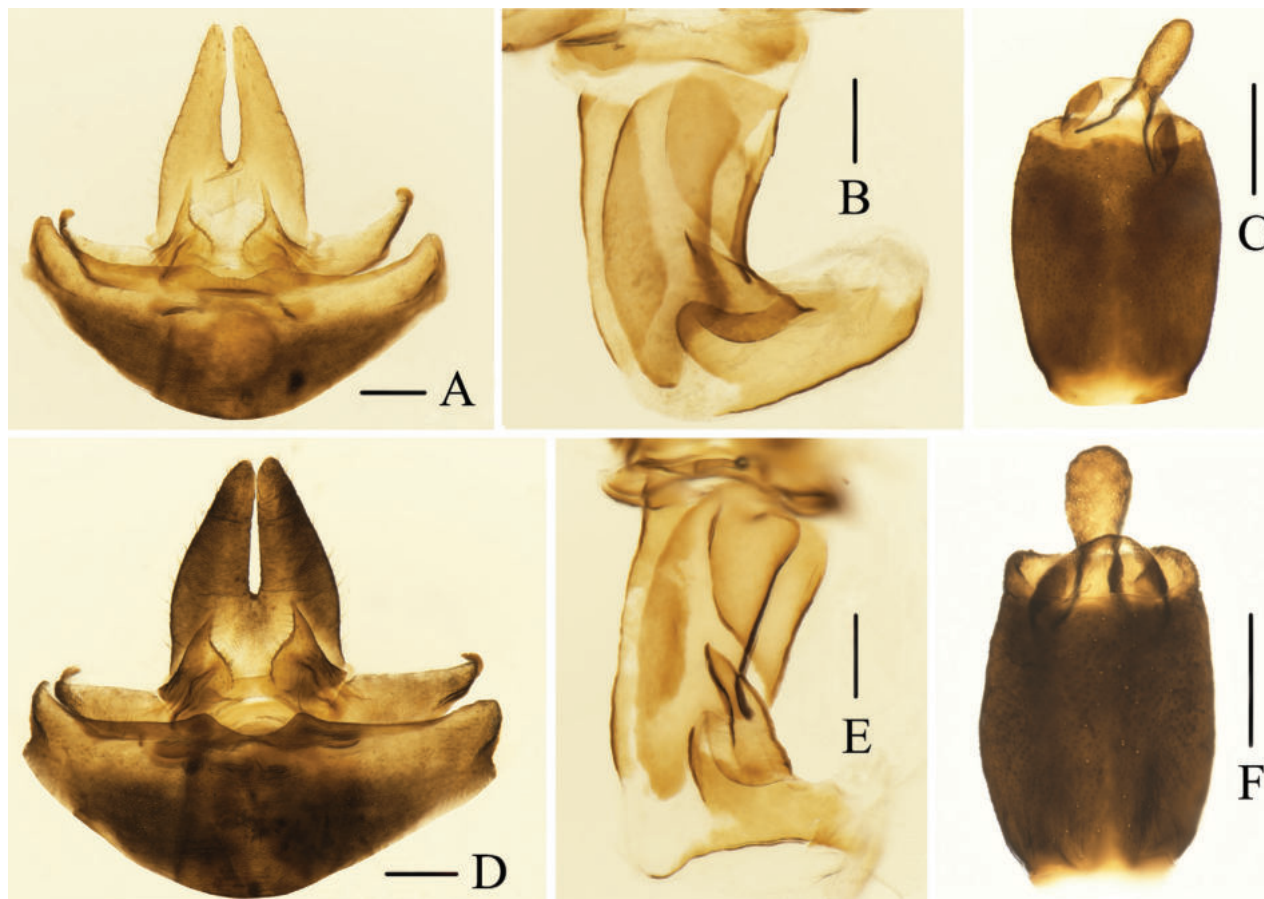


Figure 5. A–F female terminalia of *Oecleopsis* species A–C *Oecleopsis acerbus* sp. nov. D–F *Oecleopsis digitatus* sp. nov. A, D female terminalia, ventral view B, E posterior vagina, ventral view C, F anal segment, dorsal view. Scale bars: 0.2 mm.

Head and thorax. Vertex (Fig. 4A, C) narrow, 2.41 times longer than wide. Frons (Fig. 4D) with distinct median carina, longer in middle line than wide at widest portion (about 1.45:1). Clypeus (Fig. 4D) with distinct median and lateral carinae. Rostrum elongate, surpassing hind-coxae. Pronotum (Fig. 4C) wider than maximum width of head (including eyes) (1.39:1), lateral and median carinae present. Mesonotum (Fig. 4C) about 7.17 times longer than pronotum in midline, with 5 carinae, distal part of median carina blurry. Forewings (Fig. 4E) slender, longer than maximal width (2.94:1), with 12 apical and 6 subapical cells; fork ScP+R distal to fork CuA₁+CuA₂; RP 3 branches, MP₁₊₂ 3 branches, and MP₃₊₄ 2 branches.

Male terminalia. Pygofer (Fig. 4F, H) symmetrical, in lateral view, lateral lobes triangularly extended caudally; in ventral view, dorsal margin concave and U-shaped, widened towards apex. Medioventral process triangular in ventral view. Anal segment (Fig. 4F, I, J) tubular, asymmetrical, widened towards apex in left side view; in right side view, left ventral margin convex and right ventral margin excavated near apex; 1.64 times longer than wide in dorsal view; anal style finger-like, beyond anal tube. Aedeagus (Fig. 4K–N) with 4 processes in total; spinose process near apex of periandrium on right side short and thick, directed dorsocephalad, finger-like, only a 1/4 length of periandrium; left side apical process of endosoma bifurcated, curved outward, rami short, dorsal ramus directed dorsad, ventral ramus directed ventrad;

2 subapical spines long, dorsal process tapering toward end, directed cephalad; ventral process curved, curved ventrad. Gonostyli (Fig. 4F–H) slender, curved apically, tapering into a process, curved portion near right angle, T-shaped in ventral view.

Female terminalia. Terminalia, viewed ventrally, are shown in Fig. 5D. Anal segment (Fig. 5F) 1.84 times longer than wide in dorsal view. Posterior vagina (Fig. 5E) elongate, with 4 sclerites in total, dorsal sclerite tapering at the end, median and ventral sclerites long, suboblong and slender, respectively, left side of terminal sclerite twist into thick finger-like process.

Distribution. China (Sichuan) (Fig. 1).

Etymology. The species name is derived from the Latin adjective “*digitatus*”, referring to the finger-like spinose process near apex of periandrium on the right side.

Remarks. This species is similar to *Oecleopsis sinicus* (Jacobi, 1944), but differs from the latter in: (1) MP_{1+2} of forewing 3 branches (MP_{1+2} of forewing 2 branches in *O. sinicus*); (2) rami of bifurcation asymmetrical, unequal in length (rami of bifurcation symmetrical, equal in length in *O. sinicus*); (3) spinose process near apex of periandrium finger-like on right side, directed dorsocephalad (spinose process near apex of periandrium awl-shaped on right side, directed ventrocephalad in *O. sinicus*).

Discussion

Host plant information is less well documented in cixiids, especially in the genus *Oecleopsis*, where the host plants of only two species have been recorded so far. *Oecleopsis sinicus* (Jacobi, 1944) was collected on *Artemisia* L. sp. (Asteraceae) and *Zea mays* L. (Panicoidae), and *O. yoshikawai* (Ishihara, 1961) was collected on bamboo (Bambusoideae) (Zhi et al. 2018). Since these two discoveries, no additional information has been found on the ecology or behavior of any other species of *Oecleopsis*.

Based on data from published information and our field surveys, the distribution of *Oecleopsis* is restricted to the Palaearctic and Oriental regions (Fig. 1) (Holt et al. 2013), and the genus especially speciose in China where all species have been recorded to date. However, at present, it is mainly known to occur in Central, East, South, and Southwest China, but collection and survey data are still not comprehensive enough. Therefore, we believe that additional wide-ranging field surveys will find that the diversity of *Oecleopsis* in China is doubtlessly richer.

Acknowledgements

We are grateful to the specimen collectors for their hard work in the field collections. We wish to express our sincere thanks to Prof. Thierry Bourgoin for his translation of the French literature on *O. cucullatus* (Noualhier, 1896).

Additional information

Conflict of interest

The authors have declared that no competing interests exist.

Ethical statement

No ethical statement was reported.

Funding

This work was supported by the National Natural Science Foundation of China (no. 32060343), the National Key Research and Development Program (grant no. 2021YFD1601000), and the Program of Planting Management Department of the Ministry of Agriculture and Rural Affairs (grant no. 152307023).

Author contributions

SSL, LY and YBZ conceived the original idea. SSL, YZ and PZ carried out the experiment. SSL wrote the manuscript with support from LY, YBZ and XSC. SSL, YZ and PZ offered great in data analysis.


Author ORCIDs

Sha-Sha Lv  <https://orcid.org/0000-0001-5353-5082>

Lin Yang  <https://orcid.org/0000-0002-7841-5156>

Yu-Bo Zhang  <https://orcid.org/0000-0002-6118-6190>

Yan Zhi  <https://orcid.org/0000-0003-1826-8139>

Pei Zhang  <https://orcid.org/0009-0009-0251-0980>

Xiang-Sheng Chen  <https://orcid.org/0000-0001-9801-0343>

Data availability

All of the data that support the findings of this study are available in the main text.

References

- Anufriev GA, Emeljanov AF (1988) Suborder Cicadinea (Auchenorrhyncha). In: Lehr PA (Ed.) Keys to the Insects of the Far East of the USSR (Vol. 2). Homoptera and Heteroptera. Nauka Publishing House, Leningrad, 496 pp.
- Bourgoin T (1987) A new interpretation of the homologies of the Hemiptera male genitalia, illustrated by the Tettigometridae (Hemiptera, Fulgoromorpha). Proceedings 6th Auchenorrhyncha Meeting, Turin, Italy, 7–11 September, 113–120.
- Bourgoin T (1993) Female genitalia in Hemiptera Fulgoromorpha, morphological and phylogenetic data. Annales de la Société Entomologique de France 29(3): 225–244. <https://doi.org/10.1080/21686351.1993.12277686>
- Bourgoin T (2023) FLOW (Fulgoromorpha Lists On the Web): A knowledge and a taxonomy database dedicated to planthoppers (Insecta, Hemiptera, Fulgoromorpha, Fulgoroidea). Version 8, updated 06 September 2023. <https://flow.hemiptera-databases.org/flow/> [Accessed on: 6 September 2023]
- Bourgoin T, Wang RR, Asche M, Hoch H, Soulier-Perkins A, Stroiński A, Yap S, Szwedo J (2015) From micropterism to hyperpterism recognition strategy and standardized homology-driven terminology. Zoomorphology 134(1): 63–77. <https://doi.org/10.1007/s00435-014-0243-6>
- Emeljanov AF (1971) New genera of leafhoppers of the families Cixiidae and Issidae (Homoptera, Auchenorrhyncha) from the fauna of the USSR. Entomologicheskoe Obozrenie 50(3): 619–627.
- Fennah RG (1956) Fulgoroidea from Southern China. Proceedings of the California Academy of Sciences 28: 441–527.

- Guo HW, Wang YL, Feng JN (2009) Taxonomic study of the genus *Oecleopsis* Emeljanov, 1971 (Hemiptera: Fulgoromorpha: Cixiidae: Pentastirini), with descriptions of three new species from China. *Zootaxa* 2172(1): 45–58. <https://doi.org/10.11646/zootaxa.2172.1.3>
- Holt BG, Lessard JP, Borregaard MK, Fritz SA, Araújo MB, Dimitrov D, Fabre PH, Graham CH, Graves GR, Jönsson KA, Nogués-Bravo D, Wang Z, Whittaker RJ, Fjeldså J, Rahbek C (2013) An update of Wallace's zoogeographic regions of the world. *Science* 339(6115): 74–78. <https://doi.org/10.1126/science.1228282>
- Luo Y, Bourgoin T, Zhang JL, Feng JN (2022) Distribution patterns of Chinese Cixiidae (Hemiptera, Fulgoroidea), highlight their high endemic diversity. *Biodiversity Data Journal* 10: 1–81. <https://doi.org/10.3897/BDJ.10.e75303>
- Matsumura S (1914) Die Cixiinen Japans. *Annotationes Zoologicae Japonenses* 8: 393–434.
- Noualhier JM (1896) Note sur les Hémiptères récoltés en Indo-Chine et offerts au Muséum par M. Pavie. *Bulletin du Muséum d'Histoire Naturelle de Paris* 10: 251–259.
- Tsaur SC, Hsu TC, Van Stalle J (1988) Cixiidae of Taiwan, Part I. Pentastirini. *Journal of Taiwan Museum* 41(1): 35–74.
- Van Stalle J (1991) Taxonomy of Indo-Malayan Pentastirini (Homoptera, Cixiidae). *Bulletin de l'Institut Royal des Sciences Naturelles de Belgique. Entomologie* 61: 5–101.
- Zhi Y, Yang L, Zhang P, Chen XS (2018) Two new species of genus *Oecleopsis* Emeljanov from China, with descriptions of female genitalia of five species (Hemiptera, Fulgoromorpha, Cixiidae). *ZooKeys* 768: 1–17. <https://doi.org/10.3897/zookeys.768.24796>

A new species of *Lophostreptus* Cook, 1895 discovered among syntypes of *L. regularis* Attems, 1909 (Diplopoda, Spirostreptida, Spirostreptidae)

Henrik Enghoff¹, Nesrine Akkari²

¹ Natural History Museum of Denmark, University of Copenhagen, Universitetsparken 15, DK-2100 Copenhagen OE, Denmark

² Naturhistorisches Museum Wien, Burgring 7, 1010 Wien, Austria

Corresponding author: Henrik Enghoff (henghoff@snm.ku.dk)

Abstract

A new species of the genus *Lophostreptus* Cook, 1895 is described, based on specimens hidden for over a century among the syntypes of its congener *Lophostreptus regularis* Attems, 1909 housed in the Naturhistoriska Riksmuseet Stockholm (NRMS) and the Naturhistorisches Museum Wien (NHMW). A lectotype is designated for *Lophostreptus regularis* Attems, 1909 in order to stabilize its taxonomy. Updates to the millipede fauna of Mt. Kilimanjaro, Tanzania are provided.

Key words: Kilimanjaro, millipedes, natural history museums, shelf-life, Tanzania, types



Academic editor: Pavel Stoev

Received: 15 November 2023

Accepted: 4 December 2023

Published: 10 January 2024

ZooBank: <https://zoobank.org/CA455F3B-B115-4A2C-A25F-A32E5B4C8998>

Citation: Enghoff H, Akkari N (2024) A new species of *Lophostreptus* Cook, 1895 discovered among syntypes of *L. regularis* Attems, 1909 (Diplopoda, Spirostreptida, Spirostreptidae). ZooKeys 1188: 265–274. <https://doi.org/10.3897/zookeys.1188.115802>

Copyright: © Henrik Enghoff & Nesrine Akkari. This is an open access article distributed under terms of the Creative Commons Attribution License ([Attribution 4.0 International – CC BY 4.0](https://creativecommons.org/licenses/by/4.0/)).

Introduction

It quite often happens that re-examination of type material of species described by previous authors reveals that the type series includes several species. A striking myriapod example is the centipede *Lithobius lapidicola* Meinert, 1872, the type material of which turned out to include no less than nine species (Eason 1974). We are not aware of similarly impressive millipede cases, but there are several examples of millipede type series which have subsequently been shown to include more than one species. In some of these cases the type series of a species includes an additional undescribed species. Thus, Demange (1981) described *Carlogonus verhoeffi* Demange, 1981 (Harpagophoridae) from a specimen found in the presumed type series of *Indiothauma jonesi* Verhoeff, 1938, and Golovatch et al. (2017a) described *Annamina attemsi* Golovatch, Geoffroy & Akkari, 2017 (Paradoxosomatidae) from a specimen found in the type series of *A. xanthoptera* Attems, 1937.

We here put on record one more such example and describe a new species found among syntypes of *Lophostreptus regularis* Attems, 1909. This nominal species, described from Mt. Kilimanjaro in Tanzania, has long been regarded a junior subjective synonym of *L. ptilostreptoides* Carl, 1909, also from Tanzania. Recently, Enghoff et al. (in press) confirmed the suspicion of Carl (1909),

viz., that his aptly named *L. ptilostreptoides* is the same as *Ptilostreptus tersus* Cook, 1896, now valid as *Lophostreptus tersus* (Cook, 1896). Enghoff et al. (in press) examined syntypes of *L. regularis* belonging to Naturhistorisches Museum Wien (NHMW) and Naturhistoriska Riksmuseet Stockholm (NRMS) and found that one alcohol-preserved male from NRMS, as well as a set of gonopods on a slide from NHMW, belonged to an undescribed species.

In this paper we describe this new species, provide information on type material of *L. regularis*, select a lectotype of *L. regularis* in order to avoid future confusion, and give updates to the list of millipedes from Mt. Kilimanjaro by Enghoff and Frederiksen (2018).

Material and methods

The type material was obtained from Naturhistoriska Riksmuseet Stockholm (NRMS) and Naturhistorisches Museum Wien (NHMW), studied and photographed in NHMW using a Nikon DS-Ri2 camera mounted on a Nikon SMZ25 stereomicroscope or Nikon Eclipse, using NIS-Elements Microscope Imaging Software with an Extended Depth of Focus (EDF). Obtained images were edited in Adobe Photoshop 2024 and assembled in Adobe InDesign 2024. Symbols used in the description are explained in the text and in the figure legends.

Results

Taxonomy

Class Diplopoda de Blainville in Gervais, 1844

Order Spirostreptida Brandt, 1833

Family Spirostreptidae Brandt, 1833

Genus *Lophostreptus* Cook, 1895

Type species. *Glyphijulus magnus* Karsch, 1881, by original designation. Male not known.

Diagnosis. A trachystreptoform (sensu Enghoff et al. in press) genus with the anterior margin of collum unmodified, the lateroapical metaplical process (*lap*) of the gonopod coxa inclined or abruptly bent laterad, and the generally slender gonopod telopodite carrying a platelike post-torsal extension (*sf*) or at least with a marked 'knee' (*kn*) at the same place (from Enghoff et al. in press).

Other included species.

Lophostreptus armatus Pocock, 1896.

Lophostreptus bicolor Carl, 1909.

Lophostreptus cameranii Silvestri, 1896. Male not known.

Lophostreptus luridus Attems, 1934. Male not known.

Lophostreptus magombera Enghoff et al. (in press).

Lophostreptus minimus Mwabvu & VandenSpiegel, 2009.

Lophostreptus poriger Verhoeff, 1941. Male not known.

Lophostreptus similis Attems, 1914.

Lophostreptus tersus (Cook, 1896).

Lophostreptus ulopygus Attems, 1928. Male not known.

***Lophostreptus tersus* (Cook, 1896)**

Ptilostreptus tersus Cook, 1896: 57.

Lophostreptus ptilostreptoides Carl, 1909: 321, synonymized by Enghoff et al. (in press) [synonymy tentatively suggested by Carl (1909: 317)].

Lophostreptus regularis Attems, 1909: 31, synonymized with *L. ptilostreptoides* by Krabbe (1982: 258).

Lophostreptus tersus: Attems (1914: 143).

Lophostreptus malleolus Kraus, 1958: 12, synonymized with *L. ptilostreptoides* by Demange and Mauriès (1975: 79).

Lophogonus ptilostreptoides: Demange and Mauriès (1975: 78).

Material examined. Lectotype of *L. regularis* (NHMW MY8871) 1 slide with a pair of gonopods, one telopodite broken off. “1. 2. Bp cf” “*Lophostreptus/regularis/ Kibonoto*” [leg. Sjöstedt Y., 1905–1906, & don. Sjöstedt/ Attems]”. Lectotype here designated. **Paralectotypes of *L. regularis* NHRS:** 1 ♂, 6 ♀♀; Kilimandjaro, Kibonoto, Stepp-Kulturzon; 1000–1900 m a.s.l.; Oct. 1905; Y. Sjöstedt leg.; also a second ♂ of a different species, see below (NHRS-TOBI 000005480); 4 ♀♀; Kilimandjaro, Kibonoto, Massaistäppen; 1000 m a.s.l.; 23 Aug. 19905; Y. Sjöstedt leg. (NHRS-TOBI 000005478); 1 ♀; Usambara, Tanga, Jun. 1905; Y. Sjöstedt leg. (NHRS-TOBI-000005482); 4 ♀♀; Kilimandjaro, Kibonoto; Nov. 1905; Y. Sjöstedt leg.; under multnande blad i bananfarmerkulturzon (under decaying leaves in banana farm cultural zone) (NHRS-TOBI-000005476); 4 ♀♀; Kilimandjaro, Kibonoto; 1300 m a.s.l.; 1905; Y. Sjöstedt leg. I förnan under nedfallna plantanblad (in förna [plant litter] under fallen plantain leaves) (NHRS-TOBI-000005479); 1 ♀; Kilimandjaro, Kibonoto; 1905; Y. Sjöstedt leg.; Mischwald – Kulturzone (NHRS-TOBI-000005481); 4 ♀♀, 4 anamorphic juv.; Kilimandjaro, Kibonoto; Nov. 1905; Y. Sjöstedt leg.; Kulturzon (NHRS-TOBI-0000077). **NHMW:** 1 ♀ anterior body section, 1 ♀, 4 ♀♀ anterior body sections, 5 posterior body sections, 5 middle parts, 3 vials: head, collum & body segments; head & body segments (labelled “♂”); head, collum & body sections (labelled “♀”); 1 slide: three pairs of legs, antenna, gnathochilarium. Tanzania, Kilimanjaro region, Hai district, Steppe, cultivated area, mixed forest 1000–1900 m “1) *Lophostreptus regularis* Att/ Kilimandjaro, Kibonoto/ Steppe – Kulturzone 1000–1900 m/ Sjöstedt” (NHMW MY2466); 2 ♀♀, 2 ♀♀ anterior body sections, 3 juveniles, 1 juvenile anterior body section, three middle parts, three posterior body sections. Tanzania, Kilimanjaro region, Hai district, “Kibonoto” under rotten leaves, banana plantations “2) *Lophostreptus regularis/ Kilimandjaro. Kibonoto/ In Farmen unter ver-/ faulten blättern/ Sjöstedt*” (NHMW MY2467); slides “*Lophostreptus/ regularis/ Kibonoto*”, “Sjöstedt”: 1) “♂ [note in shorthand]” two pairs of legs and three single legs, 2) gonopods, one is dissected, 3) “♂ 3. 4. Sg” two segments, 4) “♀ 2. 1. 3. Bp” gnathochilarium and three pairs of legs, 5) “♀♀(KOH)” parts of segments (NHMW MY 4076). **MfN:** 10 specimens in several fragments. Although the type material is supposed to include 2 males, 5 females and 3 juveniles, we were not able to find any male among the specimens.

Remarks. This species was discussed at length by Enghoff et al. (in press). Because the type material of *Lophostreptus regularis* contains two species, we here designate a lectotype of this nominal species although it is regarded as

a junior synonym of *L. tersus*. We also provide details of the type material of *L. regularis* kept in NHMW. Further paralectotypes are housed in Naturhistoriska Riksmuseet Stockholm (NRMS) and Museum für Naturkunde Berlin (MfN) (see list of material) – to our knowledge, there are no syntypes of this species in any other collection.

***Lophostreptus neglectus* sp. nov.**

<https://zoobank.org/2BF66A14-5F02-4BEB-AE55-72AF29565ABF>

Figs 1–3

Diagnosis. Differing from all other species of *Lophostreptus* of which the male characters are known (see Remarks) by the shape of the distal part of the gonopod coxa.

Etymology. Named ‘neglectus’ (adjective) because this species remained neglected despite a slide containing its gonopods in Attems’ type material (Fig. 3C).

Material examined. Holotype. ♂, TANZANIA, Kilimandjaro, Kibonoto, Stepp-Kulturzon; 1000–1900 m a.s.l.; Oct. 1905; Y. Sjöstedt leg., NHRS-TOBI 000005630; separated from sample of 2 ♂♂, 6 ♀♀; syntypes (now paralectotypes) of *Lophostreptus regularis* (NHRS-TOBI 000005480). **Paratype.** TANZANIA, Kilimanjaro region, Hai district, “Kibonoto”, syntype of *Lophostreptus regularis* NHMW MY10381, slide “6” (ex NHMW MY 4076). “1. 2. Bp cf Kilimandjaro” gonopods and two pairs of legs. “Kibonoto” [leg. Sjöstedt Y., 1905–1906, & don. Sjöstedt/ Attems]”.

Description (holotype male). Size. Length 33 mm; midbody vertical diameter 2.4 mm; 46 podous rings, no apodous rings in front of telson.

Colour (Fig. 1A–C). After more than 100 years in alcohol overall light brown, with a darker hue along metazonital keels, posterior part of metazonites amber. Telson and legs yellowish.

Head (Fig. 1A). Vertex densely punctate, with a clearly demarcated parietal furrow. Eyes not reaching mesal of antennal socket, c. 22 ommatidia in 5–6 horizontal and c. 8 vertical rows. Antennae reaching 3rd body ring. Antennomeres 3–5 strongly narrowed at base.

Collum (Fig. 1A). Not modified for accommodation of antennae, coarsely punctate; along the posterior margin a row of quite short, weak furrows and carinae which towards the sides gradually reach further forwards. Lateral lobes much narrower than the dorsal part, not expanded, traversed by 3 anteriorly strongly ascending carinae/furrows of which the uppermost is the strongest and almost straight, reaching anterior margin above eye level, anterior corner rectangular, posterior corner more rounded, margins straight.

Body rings (Fig. 1B). Prozonites (pz) in anterior part (c. half) with very fine ring furrows which further back give place to a cell structure; posterior part (c. 20%) delimited by clear line, with a regular pattern of larger, rectangular cells. The cuticular scutes (‘cytoscutes’) of the anterior part of the prozonite are remarkable by being rounded rather than polygonal and by being arranged in an imbricate pattern, as described for several other trachystreptoform species by Enghoff et al. (in press, e.g., fig. 12G, left inset). Suture between pro- and metazonites straight, simple. Metazonites (mz) with faint constriction a little behind suture, with numerous simple keels which reach from suture, across constrict-



Figure 1. *Lophostreptus neglectus* sp. nov., holotype (NHRS-TOBI 000005630) **A** head, collum and rings 2–4, lateral view **B** midbody rings, lateral view **C** posterior rings with legs, and telson, (ventro-)lateral view **D** left leg of 1st pair, anterior view **E** the same, close-up of prefemoral lobe. For **A–C**, the specimen was superficially dried and returned to alcohol after photography. Abbreviations: av = anal valve, cxs = coxosternal setae, dps = setae of prefemoral lobe, mz = metazona, oz = ozopore, pfl = prefemoral lobe, pr = preanal ring, pz = prozona.

tion and until posterior ring margin; c. 20 keels between dorsal midline and ozopore. Ozopores (oz) small, a little in front of middle of metazonite. Sigilla not seen.

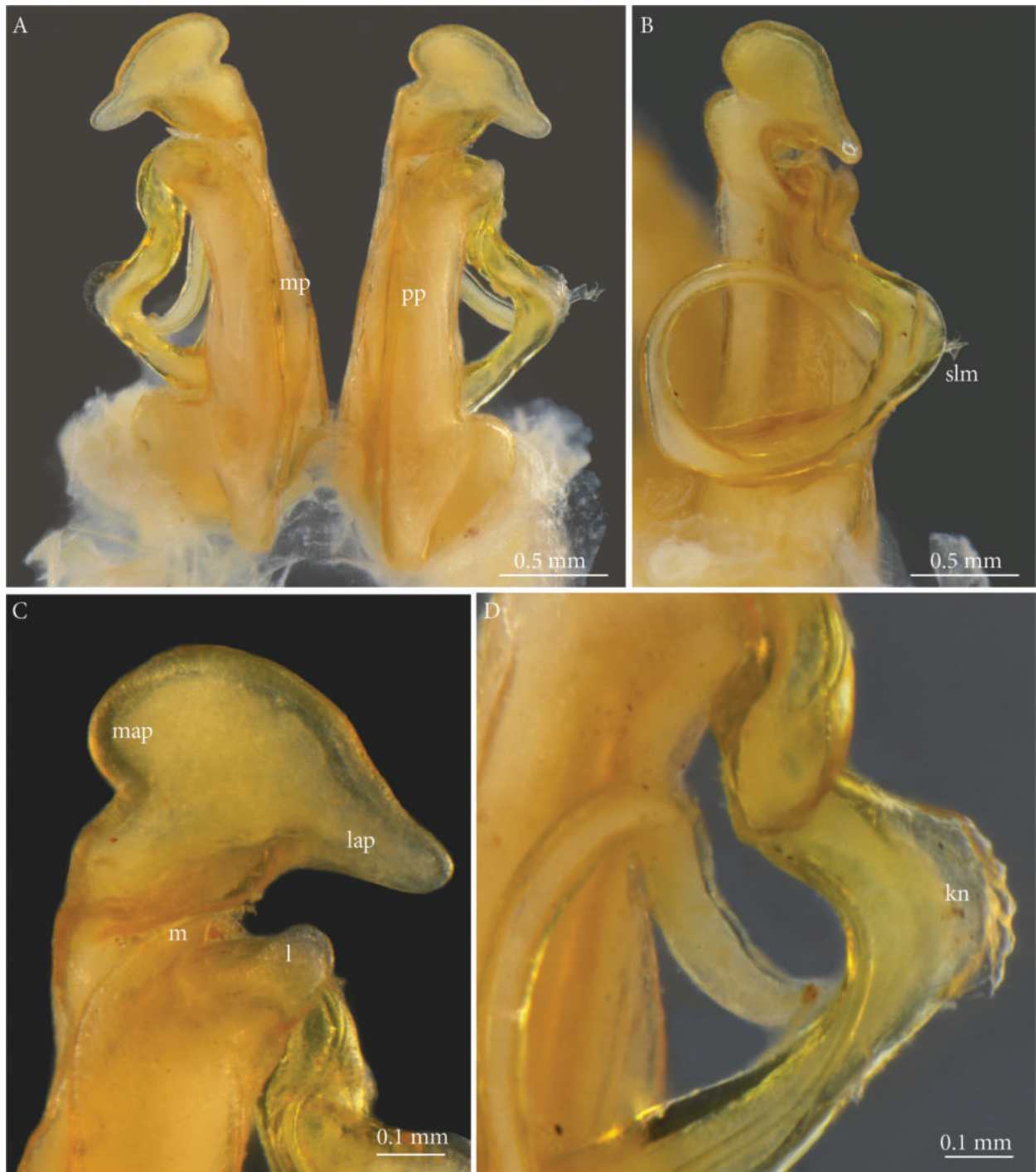


Figure 2. *Lophostreptus neglectus* sp. nov., holotype (NHRS-TOBI 000005630), gonopods **A** anterior view **B** left gonopod, posterior-lateral view **C** right gonopod, apical part, anterior view **D** telopodite. Abbreviations: *kn* = 'knee', *l* = lateral propical process, *lap* = lateroapical process, *m* = mesal propical process, *map* = mesapical process, *mp* = metaplica, *pp* = proplica, *slm* = solenomere.

Telson (Fig. 1C). Preanal ring (*pr*) regularly and densely grainy-rugose. Anal valves (*av*) overall with same sculpture, strongly vaulted, their mesal margins slightly raised as low rims, smooth, meeting in midline, paralleled more laterally by much higher lips with smooth edge; lips higher than distance between lips and mesal margin; area between mesal margin and lip with weaker sculpture than main part of valve.



Figure 3. *Lophostreptus neglectus* sp. nov. **A, B** holotype (NHRS-TOBI 000005630) **A** left gonopod telopodite, except basal part **B** distal part of telopodite, showing details of solenomere **C** paratype (NHMW MY10381). Abbreviations: *kn* = 'knee', *tf* = triangular flange, *tp* = tongue-shaped process.

Legs. Short, length c. 0.6× body diameter. No ventral pads. First pair (Fig. 1D, E): coxosternum with a few lateral setae (not evident in Fig 1D), mesally with large groups of numerous long setae (*cxs*) next to prefemoral lobes. Prefemoral lobes (*pfl*) parallel-sided, c. twice as long as broad, apically broadly rounded, with a field of long setae (*dps*) extending from tip of process almost to its base.

Gonopod coxa (Fig. 2). Proplica (*pp*) parallel-sided, apically curving slightly laterad and with a subsemicircular incision separating a broadly rounded lateral process (*l*) from a triangular mesal one (*m*). Metaplica (*mp*) with straight, only very slightly converging margins, hence almost same width throughout, subapically with mesal incision delimiting a smoothly rounded apical part with a semicircular mesapical process (*map*) and a relatively short, straight, tongue-shaped lateroapical process (*lap*).

Gonopod telopodite (Figs 2A, B, D, 3A, B). Slender, simple, with a knobby lateral 'knee' (*kn*) shortly after the emergence of the telopodite from the gonocoel, thereafter forming a full circle. Solenomere (*slm*) flanked by two triangular flanges (*tf*) and a tongue-shaped process (*tp*).

Descriptive notes on paratype. The paratype consists of a complete set of gonopods. Despite the overall poor condition of the slide, these gonopods are obviously identical to those of the holotype.

Remarks. The gonopods of *L. neglectus* sp. nov. are clearly different from those of the other *Lophostreptus* species of which the male is known. The remaining species which are currently assigned to *Lophostreptus*, but which – due to the lack of gonopod information – may just as well belong to one or more other 'trachystreptoform' genera, all seem to be bigger and/or derive from localities far away from Mt. Kilimanjaro.

Discussion

Lophostreptus neglectus sp. nov. clearly belongs to the genus *Lophostreptus* as currently (Enghoff et al. in press) understood, but future much-needed phylogenetic analyses of Spirostreptidae may well change our conception of this genus. For now, *Lophostreptus neglectus* sp. nov. should be regarded as an endemic for Mt. Kilimanjaro, and with the addition of this species, the list of millipedes known from Mt. Kilimanjaro includes 38 species. Since the review by Enghoff and Frederiksen (2018), there have been a few other changes to the list: '*Prionopetalum* n. sp. cf. *aculeatum* Attems, 1914' has been described as *Prionopetalum nessiae* Rosenmejer & Enghoff, 2021 (Rosenmejer and Enghoff 2021), '*Lophostreptus ptilostreptoides* Carl, 1909' is now *Lophostreptus tersus* (Cook, 1896) (Enghoff et al. in press), '*Proxendesmus* n. sp.' has been re-identified as *Rhododesmus mastophorus* (Gerstäcker, 1873) (HE, unpublished), and '*Procoptodesmus diffusus* Brolemann, 1920' has been transferred to the genus *Cryptocorypha* Attems, 1907 (Golovatch et al. 2017b).

Acknowledgements

We are most grateful to Tobias Malm (NRMS) and Jason Dunlop (MfN) who made type specimens of *Lophostreptus regularis* available to us for study. We thank Tarombera Mwabvu and Boyan Vagalinski for constructive criticism.

Additional information

Conflict of interest

The authors have declared that no competing interests exist.

Ethical statement

No ethical statement was reported.

Funding

The stay of Henrik Enghoff (NHMD) in Vienna in September 2023 was supported by Synthesys +.

Author contributions

Conceptualization: HE, NA. Investigation: HE, NA. Writing - original draft: HE, NA.

Author ORCIDs

Henrik Enghoff  <https://orcid.org/0000-0002-2764-8750>

Nesrine Akkari  <https://orcid.org/0000-0001-5019-4833>

Data availability

All of the data that support the findings of this study are available in the main text

References

- Attems CG (1909) Myriopoda. In: Sjöstedt Y (Ed.) Wissenschaftliche Ergebnisse der schwedischen Zoologischen Expedition nach dem Kilimandjaro, dem Meru und den Umgebenden Massaistuppen Deutsch-Ostafrikas 1905–1906, Band 19: 1–64. Stockholm.
- Attems CG (1914) Afrikanische Spirostreptiden, nebst Überblick über die Spirostreptiden orbis terrarum. Zoologica (Stuttgart) 25(65/66): 1–233.
- Carl J (1909) Reise von Dr. J. Carl im nördlichen Central-Afrikanischen Seengebiet; Diplopoden. Revue Suisse de Zoologie 17(2): 281–365. <https://doi.org/10.5962/bhl.part.75198>
- Cook OF (1896) The genera of Trachystreptidae. Brandtia 13: 55–58.
- Demange J-D (1981) Spirostreptida, Harpagophoridae (Myriapoda – Diplopoda) de Sri Lanka. Entomologica Scandinavica (Supplement 11): 63–80.
- Demange J-D, Mauriès J-P (1975) Myriapodes-Diplopes des Monts Nimba et Tonkoui (Côte d'Ivoire, Guinée) récoltés par M. Lamoote et ses collaborateurs de 1942 à 1950. Étude systématique, caractérisation des Diopsiulides Africains, révision de Trachystreptini, essai de classification des Cordyloporidae. Annales du Musée Royale de l'Arique Centrale – Tervuren, Belgique – Serie in-8° – Sciences Zoologiques 212: 1–192.
- Eason EH (1974) The type specimens and identity of the species described in the genus *Lithobius* by F. Meinert and now preserved in the Zoological Museum, Copenhagen University (Chilopoda: Lithobiomorpha). Zoological Journal of the Linnean Society 55(1): 1–52. <https://doi.org/10.1111/j.1096-3642.1974.tb01584.x>
- Enghoff H, Frederiksen S (2018) Diversity and taxonomy of millipedes from Mt Kilimanjaro. In: Hemp C, Böhning-Gaese K, Fischer M, Hemp A (Eds) The KiLi project: Kilimanjaro ecosystems under global change: linking biodiversity, biotic interactions and biogeochemical ecosystem processes. Senckenberg Gesellschaft für Naturforschung, Frankfurt/Main, 126–129. [ISBN 978-3-929907-96-4]
- Enghoff H, Ngute ASK, Kwezaura RL, Laizzer RL, Lyatuu HM, Mhagawale W, Mnenden-do HR, Marshall AR (in press) A mountain of millipedes XI. The trachystreptoform spirostreptids of the Udzungwa Mountains, Tanzania (Diplopoda, Spirostreptida, Spirostreptidae). European Journal of Taxonomy.

- Golovatch SI, Geoffroy J-J, Akkari N (2017a) Revision of the Vietnamese millipede genus *Annamina* Attems, 1937, with descriptions of three new species (Diplopoda, Polydesmida, Paradoxosomatidae). *ZooKeys* 669: 1–18. <https://doi.org/10.3897/zookeys.669.12561>
- Golovatch SI, Nzoko Fiemapong AR, VandenSpiegel D (2017b) Notes on African Pyrgodesmidae, 3 (Diplopoda: Polydesmida). *Arthropoda Selecta* 26(3): 175–215. <https://doi.org/10.15298/arthsel.26.3.01>
- Krabbe E (1982) Systematik der Spirostreptidae (Diplopoda, Spirostreptomorpha). *Abhandlungen des naturwissenschaftlichen Vereins in Hamburg, N.F.* 24: 1–476.
- Kraus O (1958) Myriapoden aus Ostafrika (Tanganjika-Territory). *Veröffentlichungen aus dem Überseemuseum Bremen (A)* 3: 1–16.
- Rosenmejer T, Enghoff H (2021) A new giant species of the millipede genus *Prionopetalum* Attems, 1909 from Mt. Kilimanjaro, Tanzania (Diplopoda, Spirostreptida, Odontopygidae). *Zootaxa* 4950(3): 561–570. <https://doi.org/10.11646/zootaxa.4950.3.8>

A new genus of soft coral (Octocorallia, Malacalcyonacea, Cladiellidae) and three new species from Indo-Pacific coral reefs

Catherine S. McFadden¹, Yehuda Benayahu², Kaveh Samimi-Namin^{3,4,5}

¹ Department of Biology, Harvey Mudd College, Claremont, CA 91711, USA

² School of Zoology, George S. Wise Faculty of Life Sciences, Tel Aviv University, Ramat Aviv, 69978, Tel Aviv, Israel

³ Marine Evolution and Ecology Group, Naturalis Biodiversity Center, P.O. Box 9517, 2300 RA Leiden, Netherlands

⁴ Department of Biology, University of Oxford, Oxfordshire, Oxford OX1 3SZ, UK

⁵ Natural History Museum, Cromwell Road, London SW7 5BD, UK

Corresponding author: Catherine S. McFadden (mcfadden@g.hmc.edu)

Abstract

Molecular systematic studies of the anthozoan class Octocorallia have revealed widespread incongruence between phylogenetic relationships and taxonomic classification at all levels of the Linnean hierarchy. Among the soft coral taxa in order Malacalcyonacea, the family Alcyoniidae and its type genus *Alcyonium* have both been recognised to be highly polyphyletic. A recent family-level revision of Octocorallia established a number of new families for genera formerly considered to belong to Alcyoniidae, but revision of *Alcyonium* is not yet complete. Previous molecular studies have supported the placement of *Alcyonium verzeveldti* (Benayahu, 1982) in family Cladiellidae rather than Alcyoniidae, phylogenetically distinct from the other three genera in that family. Here we describe a new genus, *Ofwegenum* **gen. nov.** to accommodate *O. verzeveldti* **comb. nov.** and three new species of that genus, *O. coronalucis* **sp. nov.**, *O. kloogi* **sp. nov.**, and *O. colli* **sp. nov.**, bringing the total number of species in this genus to four. *Ofwegenum* **gen. nov.** is a rarely encountered genus so far known from only a few locations spanning the Indian and western Pacific Oceans. We present the morphological characters of each species and use molecular data from both DNA barcoding and target-enrichment of conserved elements to explore species boundaries and phylogenetic relationships within the genus.

Key words: DNA barcoding, molecular phylogeny, new combination, northern Red Sea, *Ofwegenum* **gen. nov.**, Oman, Réunion, sclerites, target-enrichment, taxonomy, ultraconserved elements

Introduction

Zooxanthellate soft corals belonging to the octocorallian order Malacalcyonacea are among the most common, conspicuous, and ecologically important sessile organisms on shallow-water coral reefs throughout the Indo-Pacific; on some reefs, total percent cover of soft corals may exceed that of the reef-building scleractinian corals (Tursch and Tursch 1982; Dinesen 1983; Dai 1991; Fabricius 1997; Fabricius and Dommissé 2000). Despite their ubiquity, the taxonomy of even the most common genera of soft corals is poorly understood,



Academic editor: James Reimer

Received: 6 August 2023

Accepted: 23 November 2023

Published: 10 January 2024

ZooBank: <https://zoobank.org/528120A6-2EC0-4796-B37B-5E51FD1FE7AA>

Citation: McFadden CS, Benayahu Y, Samimi-Namin K (2024) A new genus of soft coral (Octocorallia, Malacalcyonacea, Cladiellidae) and three new species from Indo-Pacific coral reefs. ZooKeys 1188: 275–304. <https://doi.org/10.3897/zookeys.1188.110617>

Copyright: © Catherine S. McFadden et al. This is an open access article distributed under terms of the Creative Commons Attribution License ([Attribution 4.0 International – CC BY 4.0](https://creativecommons.org/licenses/by/4.0/)).

and until recently a majority of the large, fleshy, zooxanthellate genera that dominate space on shallow reefs were classified in family Alcyoniidae Lamouroux, 1812 (Fabricius and Alderslade 2001). This family, along with its type genus *Alcyonium* Linnaeus, 1758, has long been a repository for genera and species whose morphological characters do not cleanly fit the diagnoses of other families (Alderslade 2000; Williams 2000; McFadden and van Ofwegen 2013). A recent revision of class Octocorallia based on novel phylogenomic evidence has now re-circumscribed Alcyoniidae to include only azooxanthellate and mostly cold-water taxa (McFadden et al. 2022). New families have been established and previously suppressed families reinstated to accommodate the tropical genera formerly considered to be alcyoniids (McFadden et al. 2022), and some species of *Alcyonium* have been transferred to new genera and families (Alderslade 2000; Williams 2000; McFadden and Hochberg 2003; McFadden and van Ofwegen 2013, 2017). Revision of *Alcyonium* is, however, far from complete, and among the species still classified in that genus is *A. verseveldti* (Benayahu, 1982), originally described as *Metalcyonium verseveldti*, a rare species known only from a few collections in the Red Sea. Molecular phylogenetic studies suggest that this species belongs to family Cladiellidae McFadden, van Ofwegen & Quattrini, 2022, but not to any of the established genera within that family (i.e., *Cladiella* Gray, 1869, *Klyxum* Alderslade, 2000, and *Aldersladum* Benayahu & McFadden, 2011; see Benayahu et al. 2012; McFadden et al. 2022).

Pfeffer (1889) established the genus *Metalcyonium* (Octocorallia, Alcyoniidae) for two species of soft corals from South Georgia, *M. clavatum* Pfeffer, 1888 and *M. capitatum* Pfeffer, 1888, without designating a type species. His description of this genus lacked much detail, merely noting that the colonies were unbranched and club-shaped (i.e., clavate) with a distinct polyp-bearing region (polyparium) and a narrower, sterile stalk. He also observed that the polyps retracted into calyces that were distributed over the surface of the polyparium (Pfeffer 1889). He described the sclerites as warty “Doppelspindeln” (a term often used for a spindle with a median waist; Bayer et al. 1983), denser in the calyces than in the stalk, and absent from the neck of the polyp. Kükenthal (1906) concluded that in all aspects of its morphology other than the unbranched colony growth form *Metalcyonium* resembled *Alcyonium*. He relegated *Metalcyonium* to the status of a subgenus, diagnosing it succinctly as “Alcyonien von unverzweigter, walzenförmiger oder konischer Körperform” (Kükenthal 1906: 43, i.e., alcyonians with unbranched, cylindrical, or conical colony form). Subsequent authors (e.g., Thomson 1910, 1921) did not accept Kükenthal’s revision and assigned additional species of soft corals with unbranched, clavate or capitate colony forms to *Metalcyonium* throughout the early 20th century.

Utinomi (1958) further validated the genus, stating “it is undoubted that *Metalcyonium* is a unique group embracing the species which are clavate, capitate or mushroom-shaped and ordinarily unbranched in form” (1958: 110). He suggested, however, that *M. clavatum*, which he erroneously stated to be the type species of *Metalcyonium*, might belong instead to the genus *Bellonella* Gray, 1862 because its colony shape is relatively digitiform rather than capitate. In a subsequent publication, Utinomi (1964) designated *M. capitatum* as the type species of *Metalcyonium*. Williams (1986) argued that the capitate colony growth form alone did not justify the separation of the genus *Metalcyonium* from *Alcyonium* because species such as *M. patagonicum* May, 1899 and *M. variabile* J. S. Thomson, 1921 can

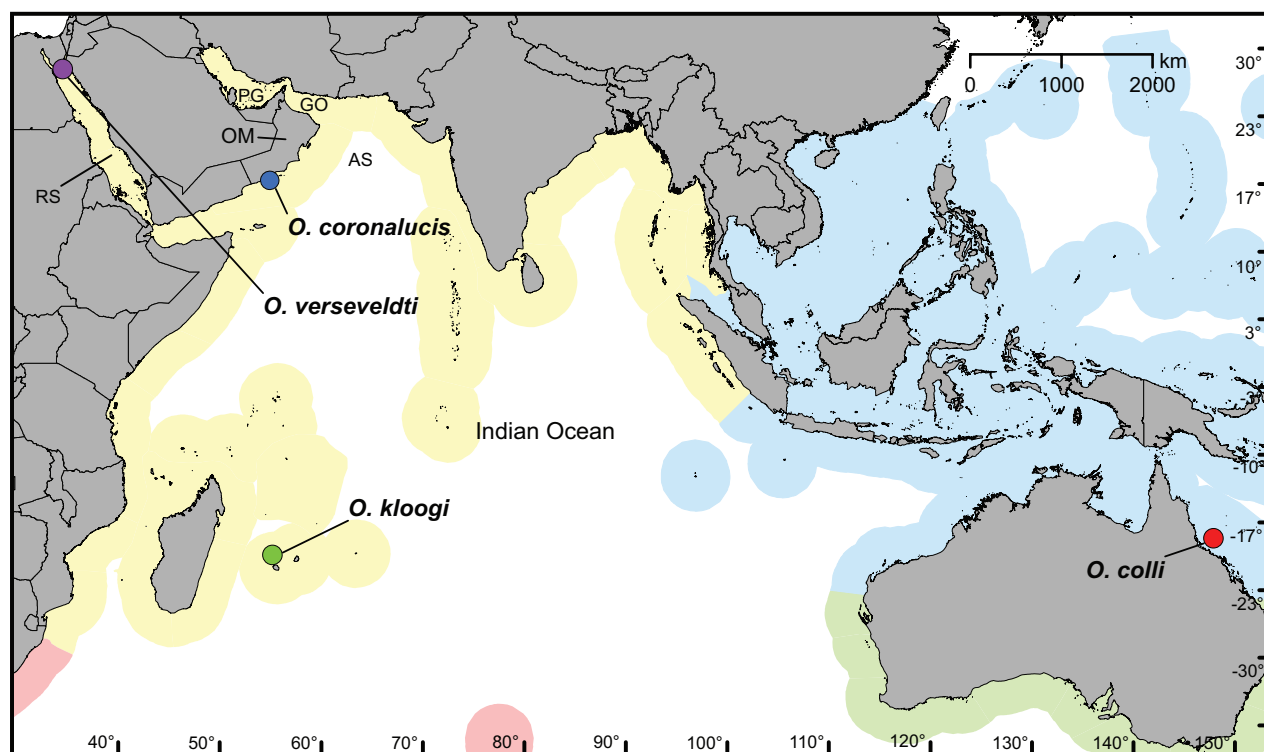


Figure 1. Distribution of the *Ofwegenium* gen. nov. species in the Indo-Pacific region. The colour shades represent the different marine realms. Yellow = West Indo-Pacific, blue = Central Indo-Pacific, red = East Africa, green = temperate Australasia; PG = Persian Gulf, AS = Arabian Sea, RS = Red Sea, GO = Gulf of Oman, OM = Oman.

exhibit a range of forms intermediate between digitiform and capitate. He transferred all capitate species of *Metalcyonium*, including the type species *M. capitatum*, to *Alcyonium*, thereby invalidating the genus. Verseveldt and Bayer (1988) then redescribed Pfeffer's original type material and moved both *M. clavatum* and *M. capitatum* to *Bellonella*, synonymising *Metalcyonium* with that genus.

Among the species of *Metalcyonium* transferred by Williams (1986) to *Alcyonium* was *M. verseveldti* Benayahu, 1982, found in the warm tropical waters of the northern Red Sea. Molecular phylogenetic analyses that have included this species place it in a clade with the tropical Indo-Pacific genera *Cladiella* Gray, 1869 and *Klyxum* Alderslade, 2000 (Benayahu et al. 2012), phylogenetically distant from *Alcyonium* (see McFadden et al. 2022).

Here, we re-examine the type material and establish a new genus for *M. verseveldti*. In addition, we describe three new species of the genus from the Indian and western Pacific Oceans (Fig. 1). We present features of the sclerites of each species and examine the genetic distinctions among species using single-locus DNA barcodes and multi-locus sequence data from target-enrichment of conserved elements (UCEs and exons).

Materials and methods

Morphological studies

The study examined the holotype and paratypes of *Metalcyonium verseveldti* Benayahu, 1982 and other relevant material deposited at the museums listed

below. Morphological features, including shape and dimensions of the preserved colonies, were recorded; terminology follows McFadden et al. (2022) and Bayer et al. (1983). To examine the sclerites, tissue samples were treated with 10% sodium hypochlorite followed by repeated rinses in distilled water. Wet preparations of the clean sclerites were examined under a Nikon Eclipse 80i light microscope at $\times 100$ –200 magnification. Scanning Electron Microscope (SEM) mounts were prepared from the sclerites. The mounts were coated with Pd/Au or Cr and viewed under a Quanta 200 FEG (Field Emission Gun) ESEM operated at 5–20 kV or Au coated and viewed under a Hitachi TM-1000 ESEM at Tel Aviv University and Jeol 6480LV SEM operated at 10 kV, with Pt coating at Naturalis Biodiversity Center, Leiden.

Abbreviations

NBC	Naturalis Biodiversity Center (formerly Rijksmuseum van Natuurlijke Historie, RMNH) Leiden, The Netherlands;
NTM	Museum and Art Gallery of the Northern Territory, Darwin, Australia;
QM	Queensland Museum, Brisbane, Australia;
SMNH-TAU	Steinhardt Museum of Natural History at Tel Aviv University, Tel Aviv, Israel;
UF	Florida Natural History Museum, Florida, United States.

Molecular phylogenetic analyses

DNA was extracted from EtOH-preserved tissue samples using a DNeasy Blood & Tissue Kit (Qiagen, Inc.). Fragments of the mitochondrial *mtMutS* and *COI* (*+igr1*) genes and nuclear *28S rDNA* were amplified by polymerase chain reaction (PCR) and sequenced using published primers and protocols (McFadden et al. 2014). New sequences were added to an alignment of family Cladiellidae analysed previously by Benayahu et al. (2012) (Table 1) that included one of the specimens described here and realigned using the L-INS-i method in MAFFT (Kato et al. 2005). Pairwise genetic distances (uncorrected p) among taxa for each gene region were determined using MEGA v.5 (Tamura et al. 2011).

Preliminary phylogenetic analyses of each gene region using PhyML (Guindon and Gascuel 2003) revealed congruence of gene trees, therefore genes were concatenated for further analyses. To minimise the effects of missing data on the analyses, a 471 bp fragment of the *mtMutS* gene was concatenated with *28S rDNA*; *COI* was not included in the concatenated alignment. Optimal models of evolution for each gene (*mtMutS*: HKY+G; *28S*: TN+G+I) were found using ModelFinder (Kalyaanamoorthy et al. 2017) and a maximum likelihood tree was constructed using IQTree v. 2.1.2 (Minh et al. 2020) with an edge-linked partition model (Chernomor et al. 2016) and 10,000 ultrafast bootstraps (Hoang et al. 2018). A partitioned analysis was run using MrBayes v. 3.2.1 (Ronquist et al. 2012), applying a HKY model to *mtMutS* and a GTR+G model to *28S rDNA*. MrBayes was run for 3,000,000 generations (until standard deviation of split partitions < 0.01) with a burn-in of 25% and default Metropolis coupling parameters.

Table 1. GenBank accession numbers for specimens of *Ofwegenum* gen. nov. and other genera of Cladiellidae included in molecular analyses (Fig. 16). Raw UCE sequence reads are deposited under project number PRJNA1035147.

Species	Museum	Locality	mtMutS	28S	COI	UCEs
<i>Ofwegenum coronalucis</i>	UF 15819	Oman	NA	OR483157	OR487130	NA
	SMNHTAU_Co_39048	Oman	OR487121	OR483155	OR487131	SAMN 38083212
	UF 17263	Oman	OR487122	OR483156	OR487134	SAMN 38083211
	UF 15877	Oman	OR487123	OR483158	OR487132	NA
	BOMAN-09174	Oman	OR487124	OR483159	NA	NA
	UF 15882	Oman	OR487125	OR483160	OR487133	NA
<i>Ofwegenum aff. coronalucis</i>	SMNHTAU_Co_38223	Aquarium trade, USA	OR487121	OR483157	OR487130	SAMN 38083213
<i>Ofwegenum verseveldti</i>	SMNHTAU_Co_33097	Israel	GU356012	JX991219	GU355978	SAMN 38083214
<i>Ofwegenum kloogi</i>	SMNHTAU_Co_34426	Reunion	OR487117	OR483152	OR487128	SAMN 38083210
	SMNHTAU_Co_38229	Reunion	OR487118	OR483153	NA	NA
<i>Ofwegenum colli</i>	NTM C13089	Australia	OR487120	NA	NA	NA
<i>Aldersladum jengi</i>	SMNHTAU_Co_33607	Taiwan	JX991144	JX991201	JX991220	NA
<i>Aldersladum sodwanum</i>	SMNHTAU_Co_31520	Kenya	JX991193	JX991213	JX991236	NA
<i>Cladiella australis</i>	SMNHTAU_Co_36313	Taiwan	MH516863	MH516878	MH516513	SAMN 38083203
	SMNHTAU_CO_36912	Taiwan	MH516570	MH516881	MH516515	SAMN 38083204
	SMNHTAU_Co_36987	Taiwan	MH516571	MH516882	MH516516	SAMN 38083205
	SMNHTAU_Co_36042	Madagascar	OR487126	OR483164	OR487135	SAMN 38083206
<i>Cladiella bottae</i>	SMNHTAU_Co_34648	Taiwan	JX991145	JX991204	JX991223	NA
<i>Cladiella kashmani</i>	SMNHTAU_Co_32334	Kenya	JX991195	JX991215	JX991238	NA
	SMNHTAU_Co_32246	Kenya	JX991194	JX991214	JX991237	NA
<i>Cladiella pachyclados</i>	SMNHTAU_Co_33604	Taiwan	JX991146	JX991206	JX991225	NA
	SMNHTAU_Co_35507	Palau	JX991197	JX991216	JX991240	NA
<i>Cladiella sphaerophora</i>	SMNHTAU_Co_34132	Israel	GQ342471	JX203653	GQ342386	NA
<i>Cladiella tuberculoides</i>	SMNHTAU_Co_34686	Taiwan	JX991227	JX991148	JX991208	NA
	SMNHTAU_Co_34642	Taiwan	JX991226	JX991147	JX991207	NA
<i>Cladiella tuberosa</i>	SMNHTAU_Co_34669	Taiwan	JX991149	JX991209	JX991228	NA
<i>Klyxum</i> sp.	UF 2684	N. Marianas	OR487127	OR483162	NA	SAMN 38083207
	QM G330915	Australia	NA	OR483163	NA	SAMN 38083208
	CKT396	Taiwan	NA	OR483161	NA	SAMN 38083209
<i>Klyxum adii</i>	SMNHTAU_Co_32636	Kenya	JX991199	JX991217	JX991242	NA
<i>Klyxum flaccidum</i>	SMNHTAU_Co_32221	Kenya	JX991200	JX991218	JX991243	NA
<i>Klyxum utinomii</i>	SMNHTAU_Co_34639	Taiwan	JX991151	JX991212	JX991232	NA
	SMNHTAU_Co_34127	Israel	GQ342476	JX203654	GQ342392	NA

Target-enrichment sequencing of conserved elements

For one or a few representatives of each species and several outgroup taxa (*Cladiella*, *Klyxum*), DNA was quantified using a Qubit 2.0 fluorometer and quality-checked (for 260:230 and 260:280 ratios) using a NanoDrop spectrophotometer. DNA samples (300–1000 ng) were sent to Arbor Biosystems (Ann Arbor, MI) for library preparation, target enrichment and sequencing. Libraries were prepared using a Kapa Hyper Prep Kit (Kapa Biosystems) with dual-indexed

iTru adaptors. myBaits protocol v. 4 (Arbor Biosystems) was used to target and enrich pools of 8 libraries using the octocoral-v. 2 bait set of Erickson et al. (2020). Enriched libraries were sequenced on one lane of Illumina HiSeq 2500 (150 bp PE reads).

Sequences were processed using the phyluce pipeline (Faircloth 2016) as outlined in Erickson et al. (2020). Briefly, reads were cleaned using illumiprocessor (Faircloth 2013) and Trimmomatic v. 0.35 (Bolger et al. 2014), then assembled into contigs using Spades v. 3.1 (Bankevich et al. 2012) with `-careful` and `-cov-cutoff 2` parameters. `phyluce_assembly_match_contigs_to_probes` was used to identify loci by matching probes to contigs with a minimum coverage of 70% and minimum identity of 70%. `phyluce_assembly_get_fastas_from_match_counts` was used to extract loci which were then aligned using MAFFT v. 7.130b (Katoh and Standley 2013). Sequences for seven outgroup taxa belonging to the genera *Cladiella* and *Klyxum* were included in the alignment. Aligned loci were edge-trimmed using `phyluce_align_seqcap_align`, and `phyluce_align_get_only_loci_with_min_taxa` was used to concatenate loci into a data matrix with 75% of taxa present for each locus. A maximum likelihood tree was constructed using IQTree v. 2.1.2 (Minh et al. 2020). ModelFinder (Kalyaanamoorthy et al. 2017) was used to select the best model of evolution (-m MFP), and an analysis was run with 1000 ultrafast bootstraps (Hoang et al. 2018) and 1000 replicates of an SH-like approximate likelihood ratio test (SH-aLRT) (Guindon et al. 2010).

Results

Systematics

Subphylum Anthozoa Ehrenberg, 1831

Class Octocorallia Haeckel, 1866

Order Malacalcyonacea McFadden, van Ofwegen & Quattrini, 2022

Family Cladiellidae McFadden, van Ofwegen & Quattrini, 2022

***Ofwegenum* gen. nov.**

<https://zoobank.org/10C92BD3-D724-42A5-A050-09F112AA33B7>

Diagnosis. Soft corals with encrusting or capitate growth forms; small (1–2 cm diameter), stalked capitula may be joined basally to form a low mat. Polyps monomorphic, non-retractile but contractile; pinnules with or without terminal branches. Coenenchymal sclerites are spindles and rods, smooth but with low, simple tubercles and areas of thickening forming concentric, raised rings. Polyp sclerites similar, usually arranged ‘en chevron’ in the polyp body, lacking a distinct collaret-and-points arrangement. Tentacles and pinnules contain numerous platelets and flattened rods (i.e., finger- biscuits, see Bayer et al. 1983) with varying features such as lateral median constrictions, side notches, or depressions at one or both ends resembling a figure-eight, arranged mostly on the aboral side of the tentacles. Some species also have tiny sclerites around the mouth. Live colonies with blue, green, or brown colouration in the coenenchyme; pinnules brown. Sclerites colourless. Zooxanthellate.

Type species. *Metalcyonium verseveldti* Benayahu, 1982: 197–201.

Etymology. The generic name *Ofwegenum* (gender: neuter) honours the late Dr. Leendert P. van Ofwegen (1953–2021), a close friend and an eminent octocoral taxonomist (Hoeksema 2021), in memory of his prolific contribution to the knowledge of this group.

Key to the species of *Ofwegenum* gen. nov.

- 1 Colonies encrusting, not capitate and without stalk..... *O. kloogi*
- Colonies capitate, with stalk..... **2**
- 2 Crosses and irregular sclerites up to 0.05 mm, around the polyp mouth....
..... *O. coronalucis*
- No sclerites around the polyp mouth..... **3**
- 3 Coenenchymal sclerites up to 0.70 mm long, tentacle sclerites mostly figure-eight platelets *O. verseveldti*
- Coenenchymal sclerites up to 0.40 mm long, tentacle sclerites mostly flattened rods or bone-shaped platelets up to 0.15 mm long..... *O. colli*

***Ofwegenum colli* sp. nov.**

<https://zoobank.org/E72328A2-B94F-4574-BBD2-BE72255AF6F6>

Figs 1, 3A, B, 4–6

Material examined. Holotype. AUSTRALIA • Queensland, N.E. Bay Great Palm Island; 18.7500°S, 146.6500°N; 6–7 m depth; 22 April 1981; coll. J. Coll; silty bottom, on a dead coral; NTM C13089.

Paratypes. AUSTRALIA • 7 colonies, same data as holotype; NTM C015578 • 5 colonies, same data as holotype; NTM C3827 • 1 colony, same data as holotype; NTM C3828 • 3 colonies, same data as holotype; May 1982; NTM C3829.

Description. The holotype is a fragment of a colony measuring 14 by 13 mm (Fig. 3A). Its polypary expands over a 2 mm thick, spreading crust-like base. The surface of the polypary features some grooves, and the contracted polyps, up to 1 mm in diameter, are visible as low mounds (Fig. 3A). The coenenchyme has sclerites in the form of spindles (with tapered ends) and rods (with blunt ends) up to 0.50 mm long, with low, simple tubercles or areas of thickening forming concentric, raised rings (Fig. 4A). The polyp body contains similar but shorter rods that appear to be arranged ‘en chevron’ when the polyps are extended. The size of the sclerites decreases along the polyp body towards the base of the tentacles (Fig. 4A).

The tentacles and pinnules contain numerous platelets and flattened rods (i.e., finger-biscuits, see Bayer et al. 1983) up to 0.10 mm long (Fig. 4B) arranged on the aboral side of the tentacles. Some of these sclerites have lateral median constrictions, side notches, or depressions at one or both ends resembling a figure-eight shape, and some have bulbous ends resembling bones (Fig. 4B).

Colour. The ethanol-preserved colony is cream.

Morphological variations. The paratype colony NTM C3829 has smoother and shorter spindles and rods compared to the holotype (0.20 vs. 0.50 mm, respectively: Figs 4A, 6A). The tentacle sclerites are up to 0.15 mm long (Fig. 6B) compared to up to 0.10 mm in the holotype (Fig. 4B). The holotype NTM C13089

has some platelets with wider ends, resembling the shape of a bone (Fig. 4B), which are not present in the other type material of this species (Figs 5B, 6B).

Remarks. This species is capitata with smaller bud-like capitula occasionally emerging from the stalk. The sclerites of the paratypes correspond to those of the holotype but differ a bit in size. This species has the largest tentacle sclerites among the congeners, up to 0.15 mm long (Figs 4–6). No information is available on the living features of this species.

Distribution. Queensland, Australia.

Etymology. The species is named after the collector of the material, Prof. John Coll of James Cook University, North Queensland, a renowned chemical ecologist who has contributed prominently to the knowledge of soft corals.

***Ofwegenum coronalucis* sp. nov.**

<https://zoobank.org/1030A306-9E82-4E0E-8565-9D3D157A5406>

Figs 1, 2A, B, 3H, I, 7–9, 10A–D, 11

Material examined. Holotype. OMAN • Dhofar, Mirbat, Michel's Reef; 16.9433°N, 54.7300°E; 25–30 m depth; 20 January 2022; coll. C.S. McFadden and K. Samimi-Namin; UF 17263 (BOMAN–08362).

Paratype. OMAN • same data as holotype; SMNHTAU_Co_39048 (BOMAN–08351).

Other material. OMAN • Dhofar, Mirbat, Frankincense; 16.9662°N, 54.6900°E; 24–30 m depth; 19 Jan 2022; coll. C.S. McFadden; UF 15819 (BOMAN–08345) • Dhofar, Mirbat, near Frankincense; 16.9688°N, 54.6877°E; 24–29 m depth; 21 Jan 2022; coll. C.S. McFadden and K. Samimi-Namin; UF15882 (BOMAN–09175) • same collection data as for preceding; UF 15877 (BOMAN–09166) • same collection data as for preceding; in situ photo, microscope slides and molecular data only; BOMAN–09174. UNKNOWN • Aquarium trade, Chicago, IL, USA; July 2013; coll. A. Parrin; SMNHTAU_Co_38223.

Description. The holotype consists of several fragments of a colony; the largest is 10 mm in diameter (Fig. 3H). The colony consists of multiple capitata polyparia on sterile stalks; side branches connect adjacent stalks to one other at the base to form an encrusting mat. Most polyps are contracted, with polyps widely set on the polyparium (Figs 3H, 9A, B).

Sclerites of the coenenchyme are spindles and rods up to 0.40 mm long with low, simple tubercles or areas of thickening forming concentric, raised rings (Fig. 7A). The polyp body contains similar but shorter rods that appear to be arranged 'en chevron' when the polyp is extended (Fig. 2A). These sclerites are usually blunt and have a crystalline texture at both ends (Fig. 7A). The length of the sclerites decreases along the polyp body towards the base of the tentacles (Fig. 7A).

The tentacles and pinnules contain numerous platelets and flattened rods (i.e., finger-biscuits) up to 0.10 mm long (Fig. 7B), arranged on the aboral side of the tentacles (Fig. 2A, B). Some of these sclerites have median constrictions, side notches, or depressions at one or both ends resembling figure-eight shapes (Fig. 7B). There are also numerous irregularly shaped platelets with side notches or side branches, up to 0.05 mm in length (Fig. 7C), that are distributed around the mouth and base of the tentacles on the oral side. These sclerites are reflective in light (Fig. 2A, B).

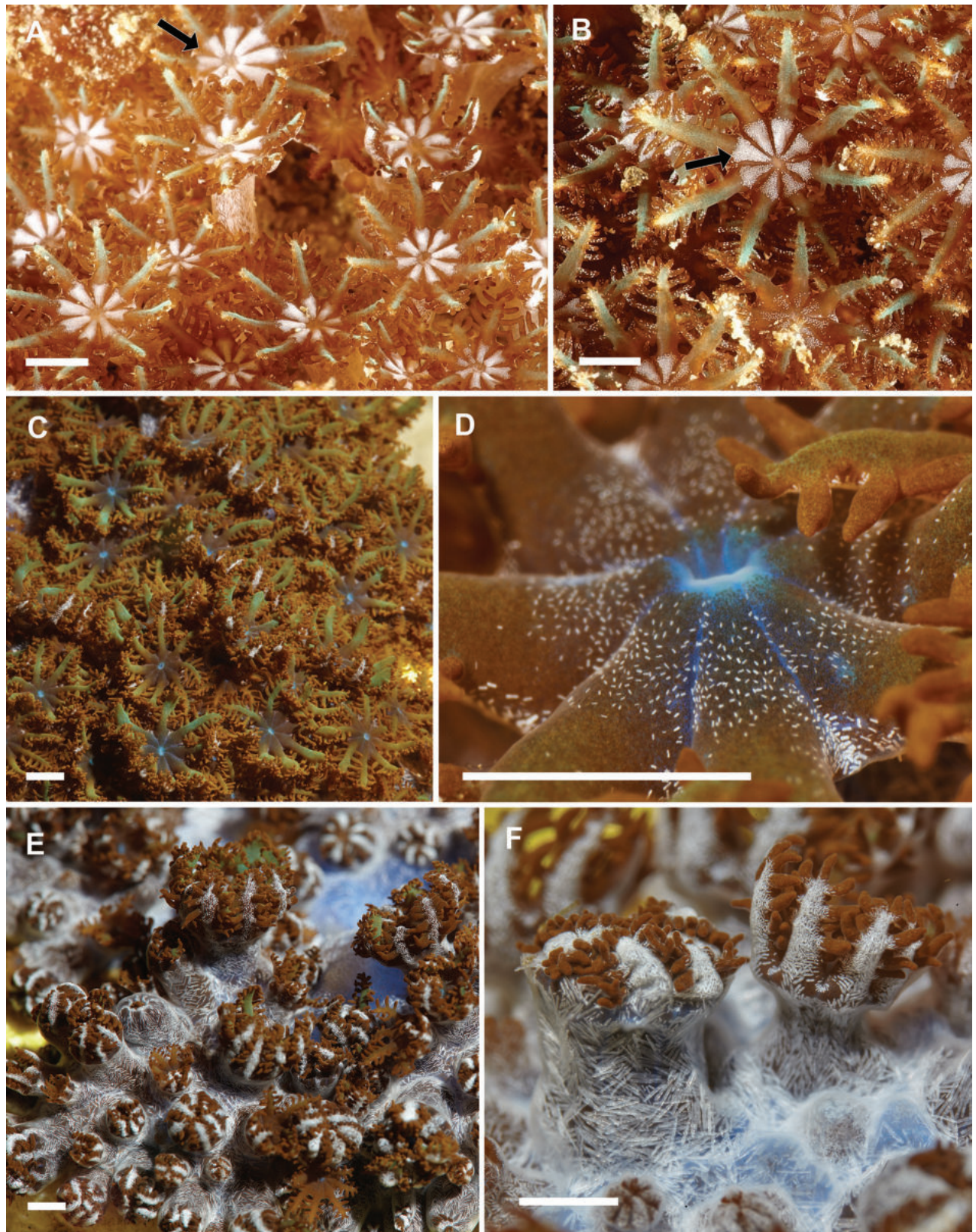


Figure 2. Morphological details of live *Ofwegenum* gen. nov. polyps **A, B** close up of *Ofwegenum coronalucis* sp. nov., holotype, UF 17263; arrows indicate the concentration of minute sclerites around the mouth opening and base of the tentacles **C–F** unknown species of *Ofwegenum* gen. nov. from the aquarium trade. Scale bars: approximately 5 mm (photographs **A, B** K. Samimi-Namin **C–F** Daniel Knop).

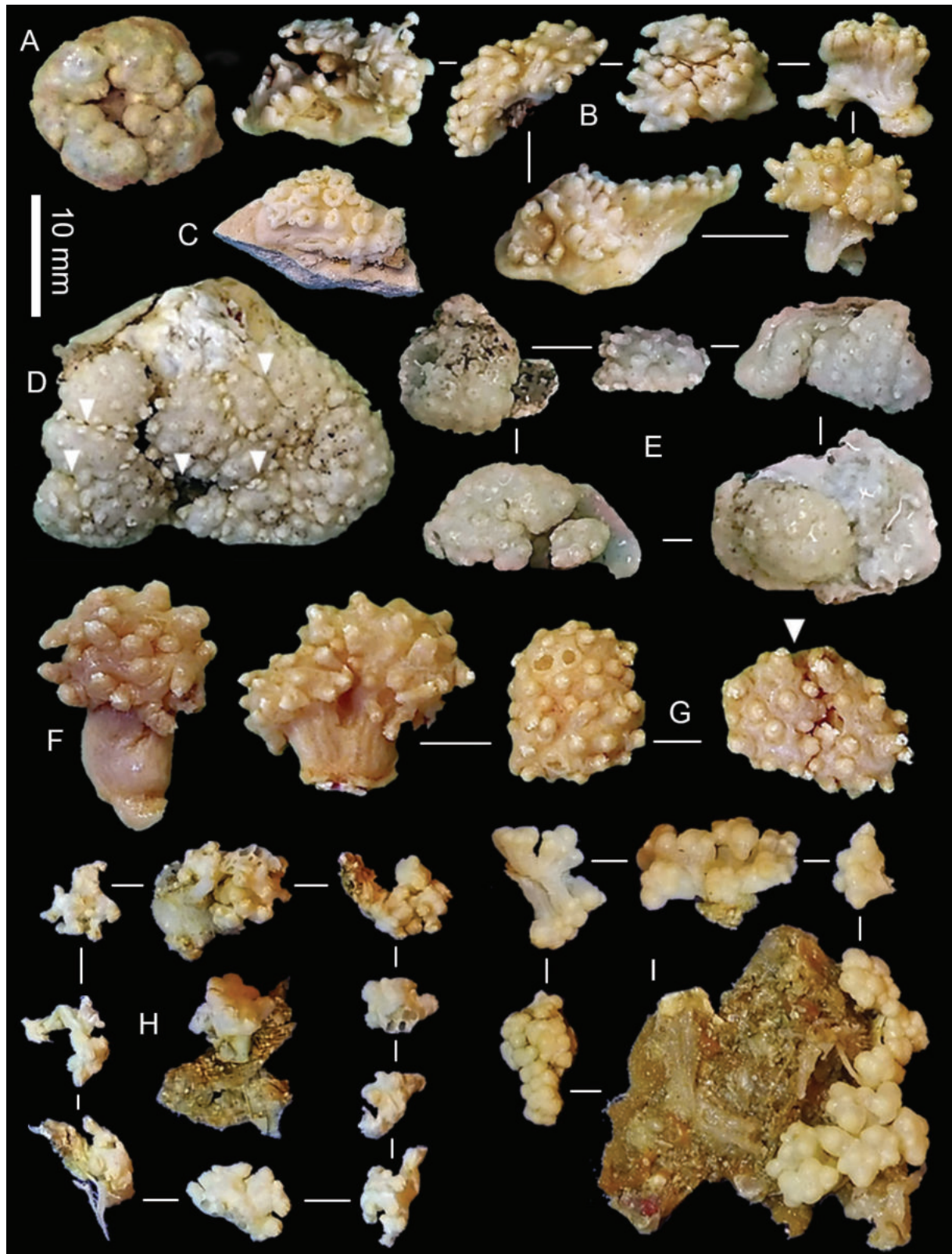


Figure 3. Preserved type colonies of *Ofwegenum* gen. nov. **A** *O. colli* sp. nov., holotype NTM C13089 **B** *O. colli* sp. nov. several paratype colonies NTM C015578 **C** *O. aff. coronalucis*, SMNHTAU_Co_38223 **D** *O. kloogi* sp. nov. holotype SMNHTAU_Co_34426, grooves on polypary are indicated by arrows, distal ends of tentacles protrude from polyp mounds **E** *O. kloogi* sp. nov., several paratype colonies SMNHTAU_Co_38299 **F** *O. verzeveldti* comb. nov., holotype SMNHTAU_Co_25554 **G** *O. verzeveldti* comb. nov., paratypes, SMNHTAU_Co_25544, grooves on polypary are indicated by arrow **H** *O. coronalucis* sp. nov., holotype, UF 17263 **I** *O. coronalucis* sp. nov., paratype SMNHTAU_Co_39048).

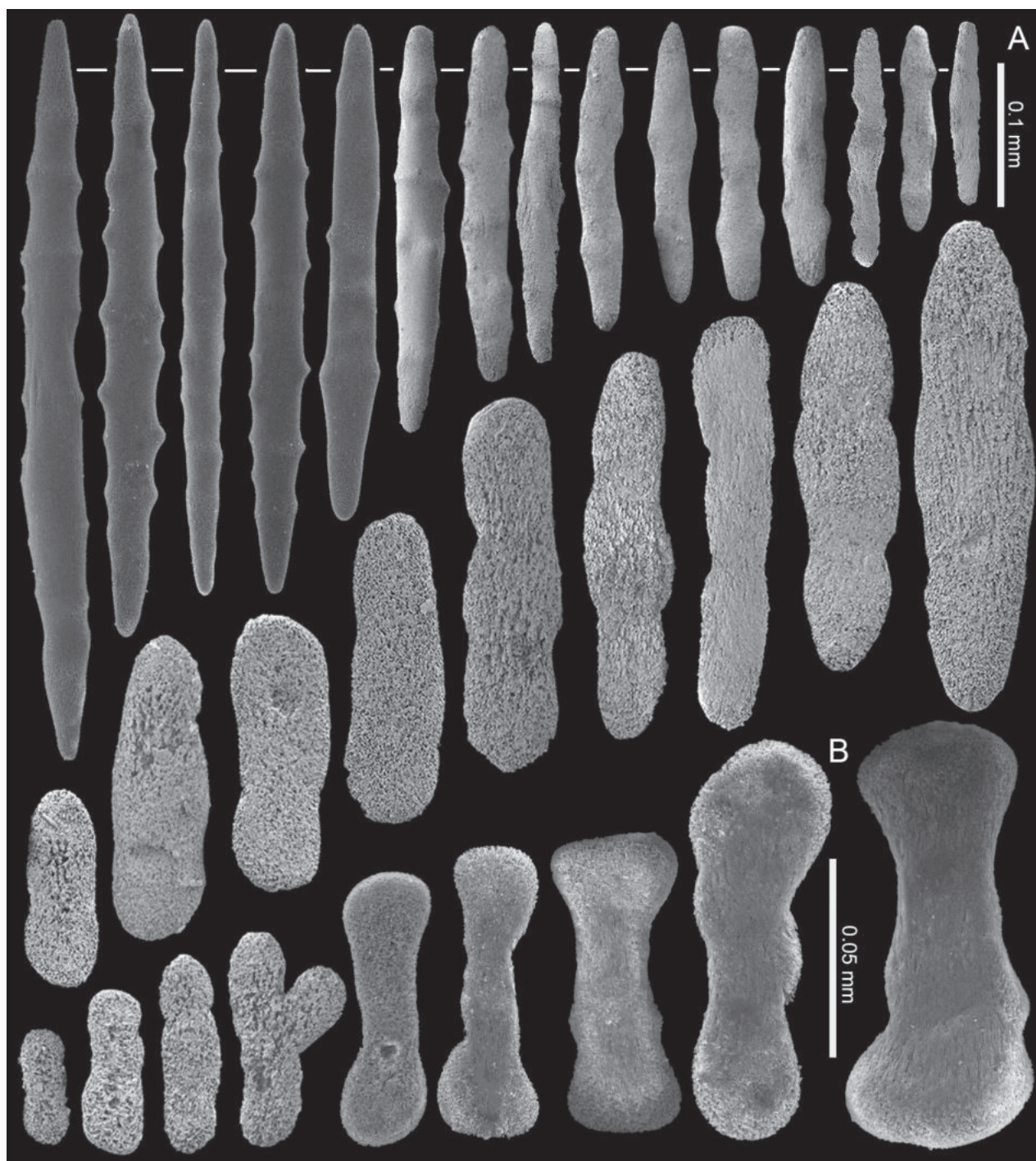


Figure 4. *Ofwegenum colli* sp. nov., holotype NTM C13089 **A** sclerites of the coenenchyme and polyp body **B** sclerites of the tentacles.

Colour. In life, colonies appear brown with blue-green tentacles. After preservation in ethanol, they are creamy white. Sclerites colourless.

Morphological variations. UF 15882 and BOMAN-09174 have slightly thinner spindles and rods both in the coenenchyme and polyp body (Fig. 8A). In addition, the polyp sclerites have fewer side notches and depressions compared to the holotype (Fig. 8B). Photos of the live specimens suggest that some of the polyps do not have the reflective sclerites around the mouth (Figs 9E, F, 10C, D).

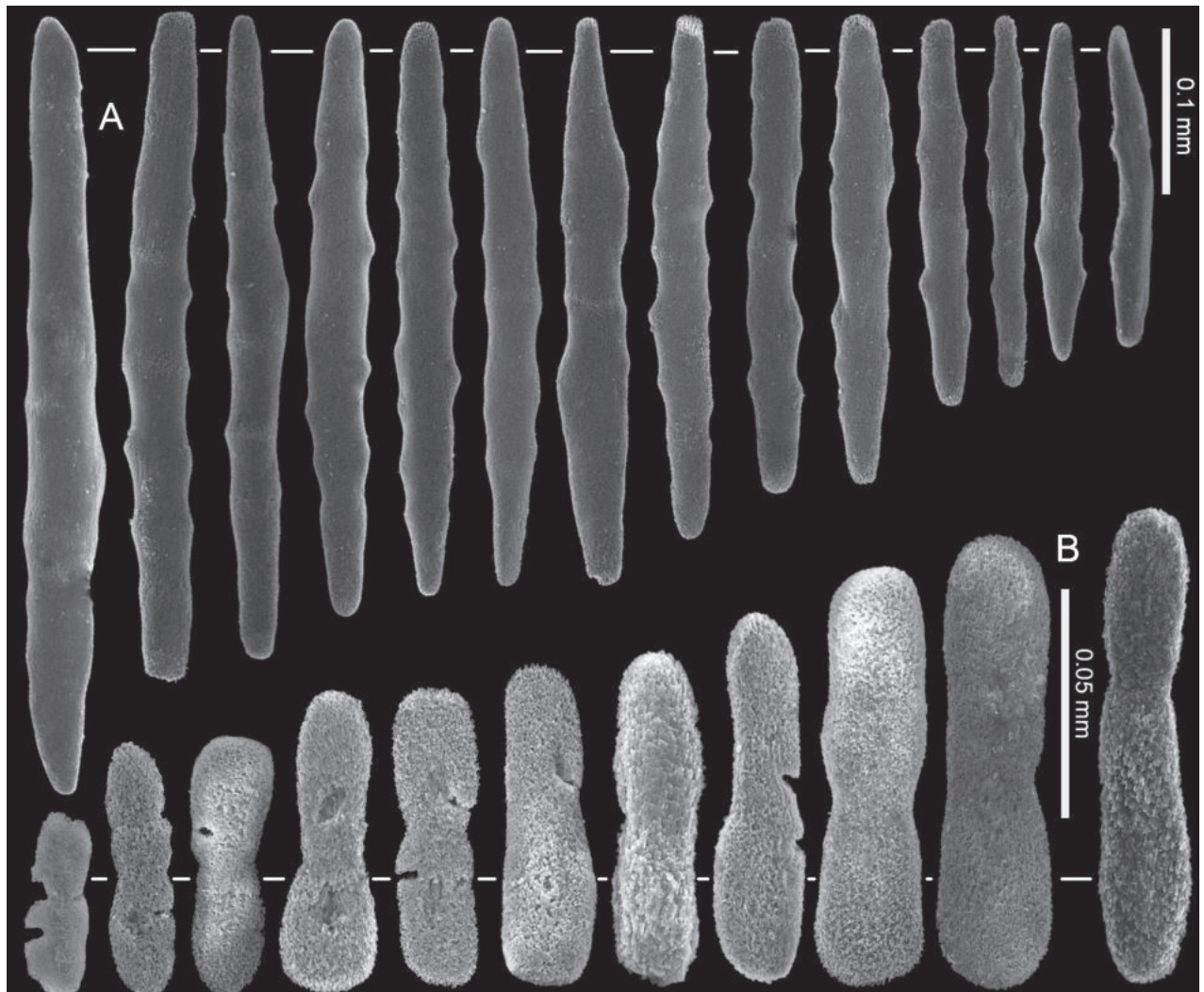


Figure 5. *Ofwegenum colli* sp. nov., paratype NTM C3827 **A** sclerites of the coenenchyme and polyp body **B** sclerites of the tentacles.

SMNH_{TAU}_Co_38223 comes from the aquarium trade in the U.S. Its commercial source is assumed to be Jakarta, Indonesia (A. Parrin, pers. comm. 12 Aug 2013), but the original collection locality remains unknown. This colony is tentatively assigned as *O. aff. coronalucis* based on its sclerite features and genetic similarity to this species (Fig. 16). However, it differs from the other material in having a blue colour in the coenenchyme and shorter tentacle sclerites up to 0.07 mm long. Such differences might be due to a prolonged exposure to the artificial aquarium environment.

Remarks. *Ofwegenum coronalucis* sp. nov. differs from its congeners in having irregularly shaped sclerites with side notches or side branches around the polyp mouth that reflect light (Figs 2A, B, 7C, 8C). Additionally, the tentacle platelets have narrow median constrictions compared to the other species (Figs 7B, 8B).

Distribution. Oman.

Etymology. The species name is from the Latin *corona* (crown) and *lucis* (of light), referring to the reflective ring of sclerites around the polyp mouth in the live specimens.

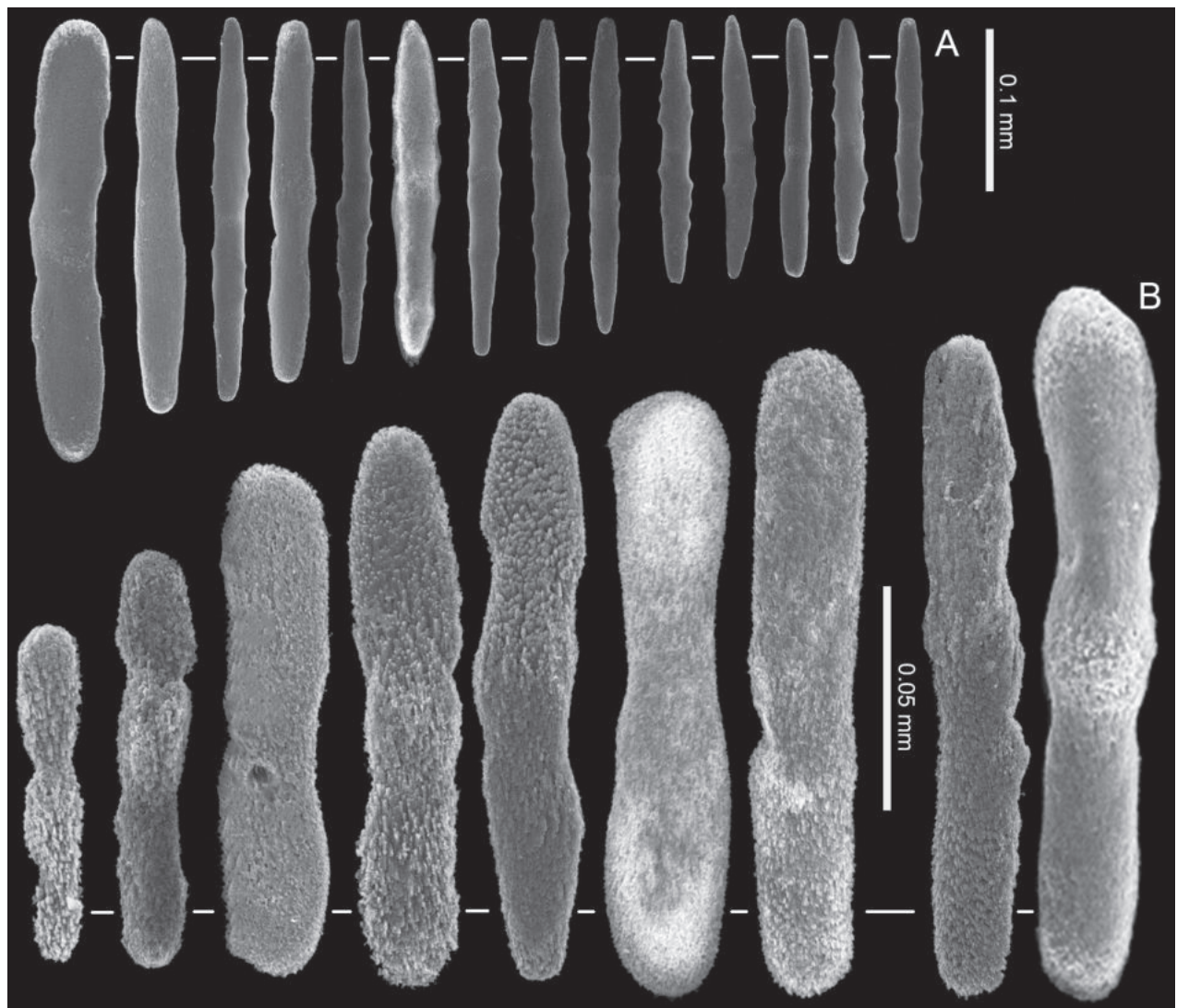


Figure 6. *Ofwegenum colli* sp. nov., paratype NTM C3829 **A** sclerites of the coenenchyme and polyp body **B** sclerites of the tentacles.

***Ofwegenum kloogi* sp. nov.**

<https://zoobank.org/F1E4D927-3C21-494B-9B53-B4EA88B49817>

Figs 1, 3D, E, 10E, 12, 13

Material examined. Holotype. LA RÉUNION • Saint-Paul, Cap la Houssaye; 21.0174°S, 55.2376°E; 17 m depth; 8 April 2008; SMNHTAU_Co_34426.

Paratype. LA RÉUNION • 13 colonies/fragments; same data as holotype; SMNHTAU_Co_38229.

Description. The holotype is an encrusting colony, measuring 28 by 25 mm, attached to a calcareous fragment by a thin spreading base (<1 mm thick). The polypary features several narrow grooves (Fig. 3D). The polyps appear as low mounds. The distal tips of the tentacles occasionally protrude from the top of the polyp mounds.

The coenenchyme sclerites are spindles and rods up to 0.50 mm long, with low, simple tubercles or areas of thickening forming concentric, raised rings (Fig. 12A). The polyp body contains shorter spindles, up to 0.30 mm long (Fig. 12A), which appear to be arranged 'en chevron' when the polyp is extend-

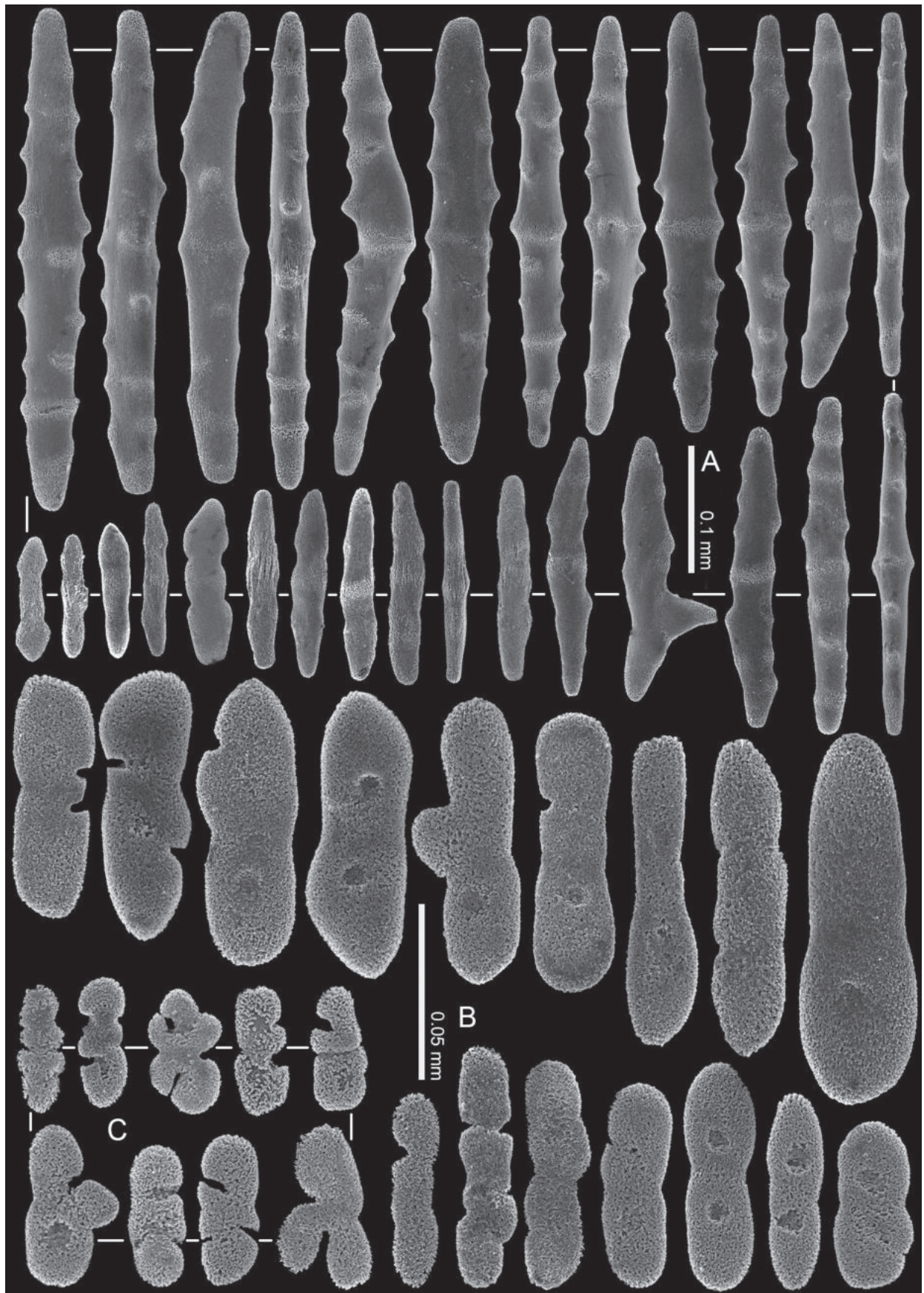


Figure 7. *Ofwegenum coronalucis* sp. nov., holotype UF 17263 **A** sclerites of the coenenchyme and polyp body **B** sclerites of the tentacles **C** sclerites around the polyp mouth opening. Scale at **B** also applies to **C**.

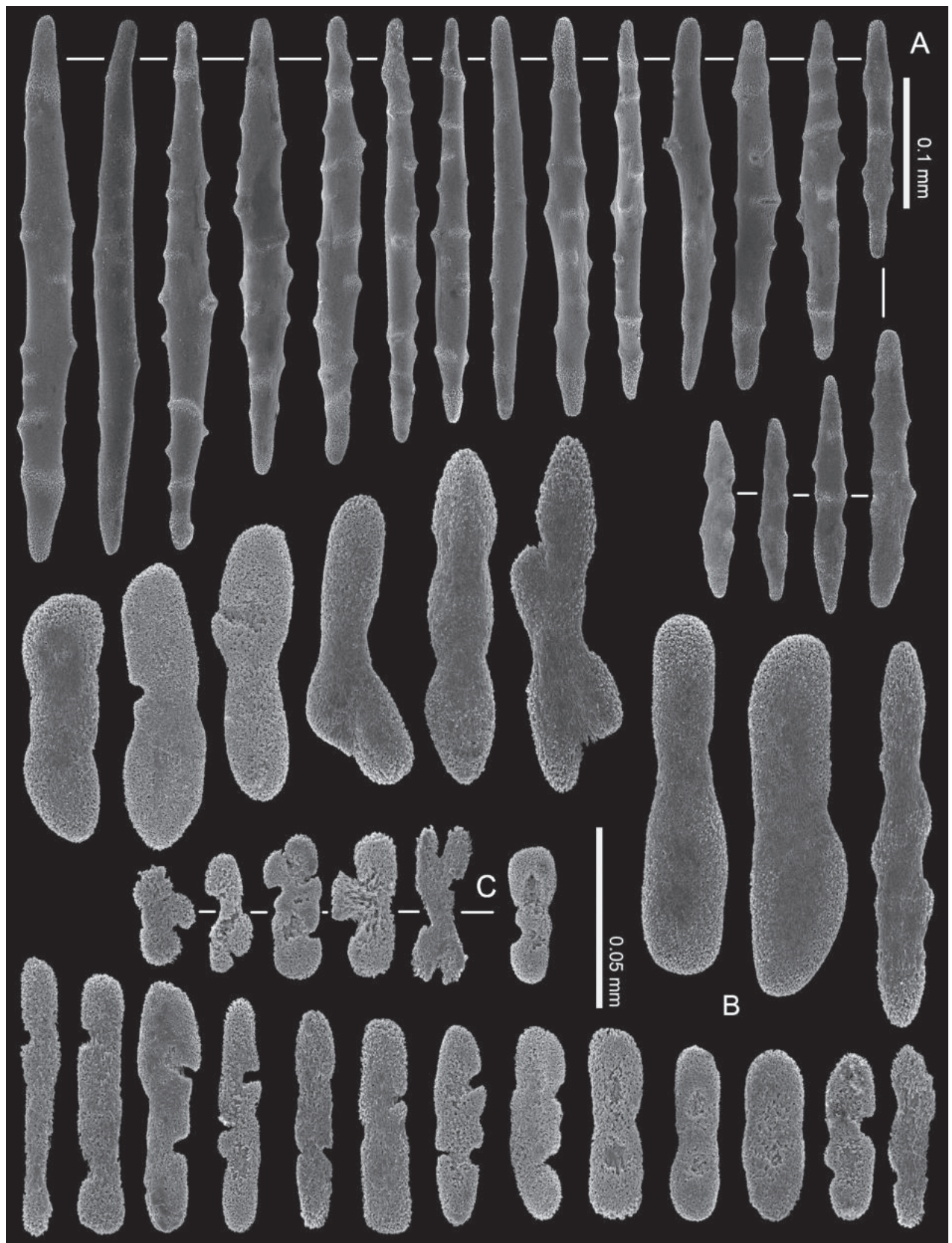


Figure 8. *Ofwegenum coronalucis* sp. nov., UF 15882 **A** sclerites of the coenenchyme and polyp body **B** sclerites of the tentacles **C** Sclerites around polyp mouth opening. Scale bars: 0.05 mm (**B**, **C**).

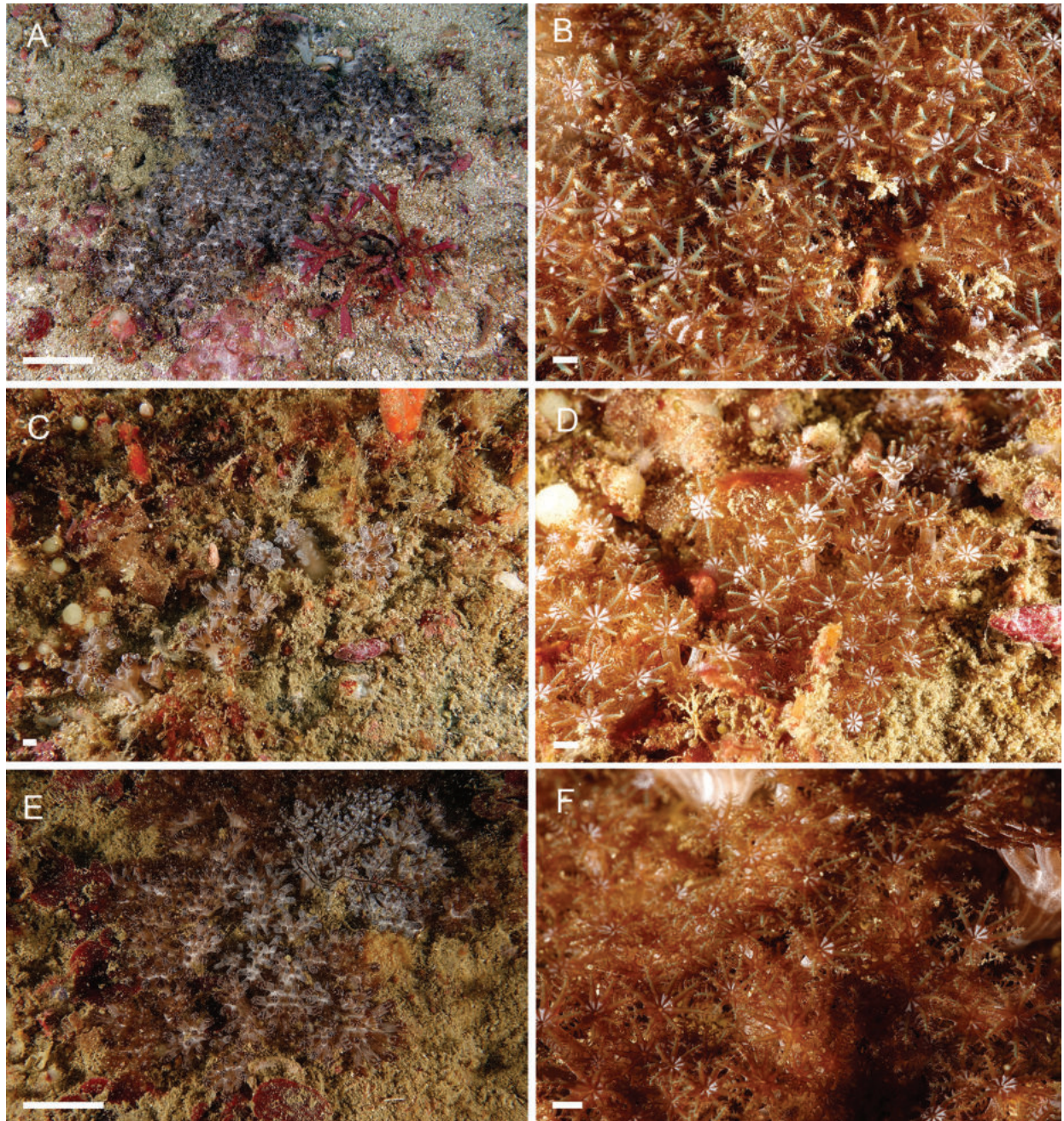


Figure 9. *Ofwegenum coronalucis* sp. nov. **A, B** colony and polyps of holotype, UF 17263 **C, D** colony and polyps of paratype, SMNHTAU_Co_39048 **E, F** colony and polyps of UF 15882. Scale bars: ~ 50 mm (**A, E**); ~ 5 mm (**B–D, F**) (photographs K. Samimi-Namin).

ed. The length of the sclerites decreases along the polyp body towards the base of the tentacles (Fig. 12A).

The tentacles and the pinnules contain numerous platelets and flattened rods (i.e., finger-biscuits) up to 0.07 mm long (Fig. 12B), arranged on the aboral side of the tentacles. Some of these sclerites have lateral median constrictions, side notches, or depressions at one or both ends (Fig. 12B).

Colour. In life the expanded tentacles are pale grey with an underlying bluish tint. The polyps have a blue mouth opening and blue line along the tentacles (Fig. 10E). The ethanol-preserved holotype is pale grey in colour.

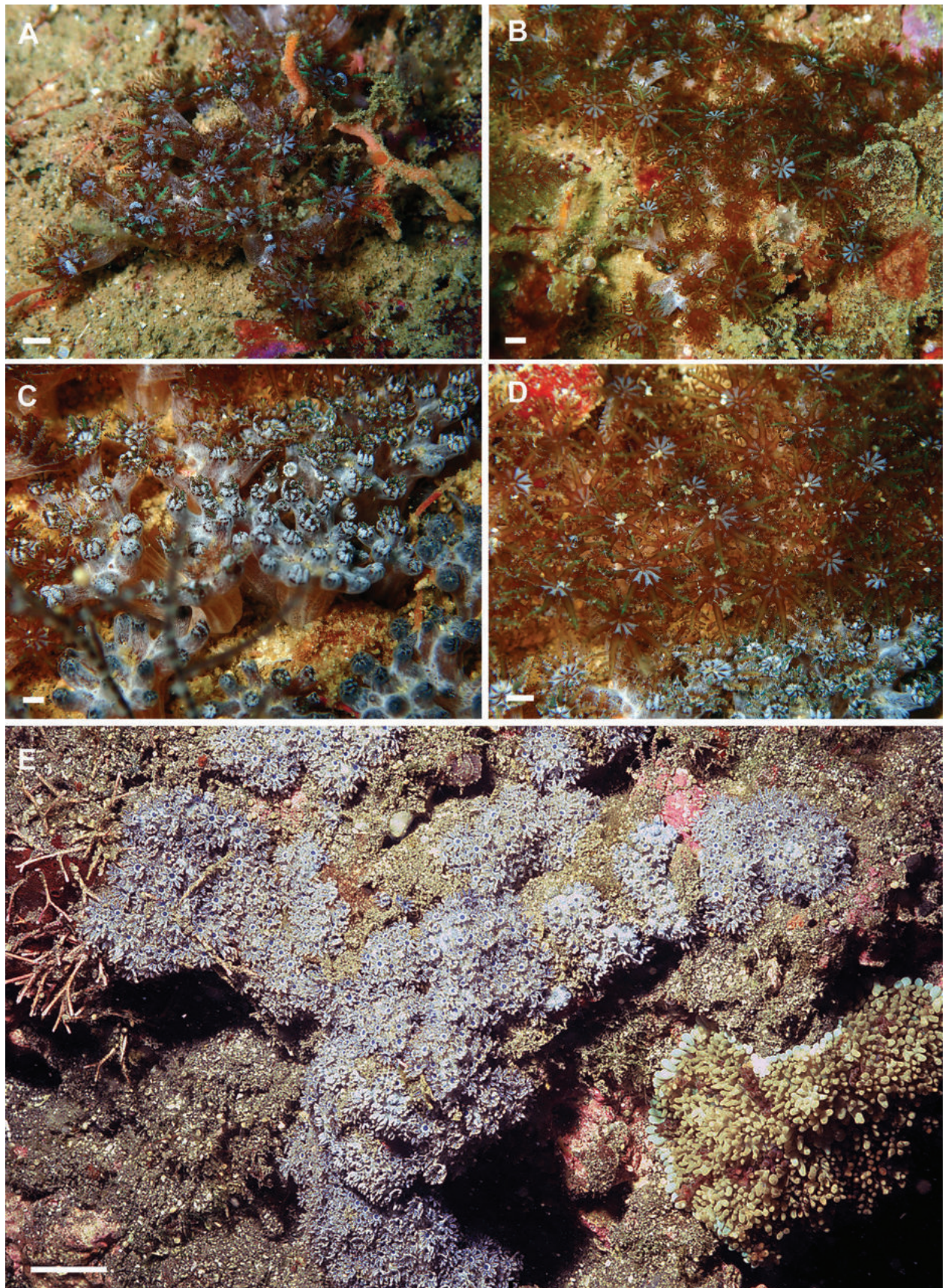


Figure 10. **A, B** *Ofwegenum coronalucis* sp. nov., UF 15877 **C, D** *Ofwegenum coronalucis* sp. nov., BOMAN-09174 **E** *Ofwegenum kloogi* sp. nov. holotype SMNHTAU_Co_34426. (Photos **A–D** C. S. McFadden **E** Y. Benayahu). Scale bars: ~ 5 mm (**A–D**); 5 cm (**E**).

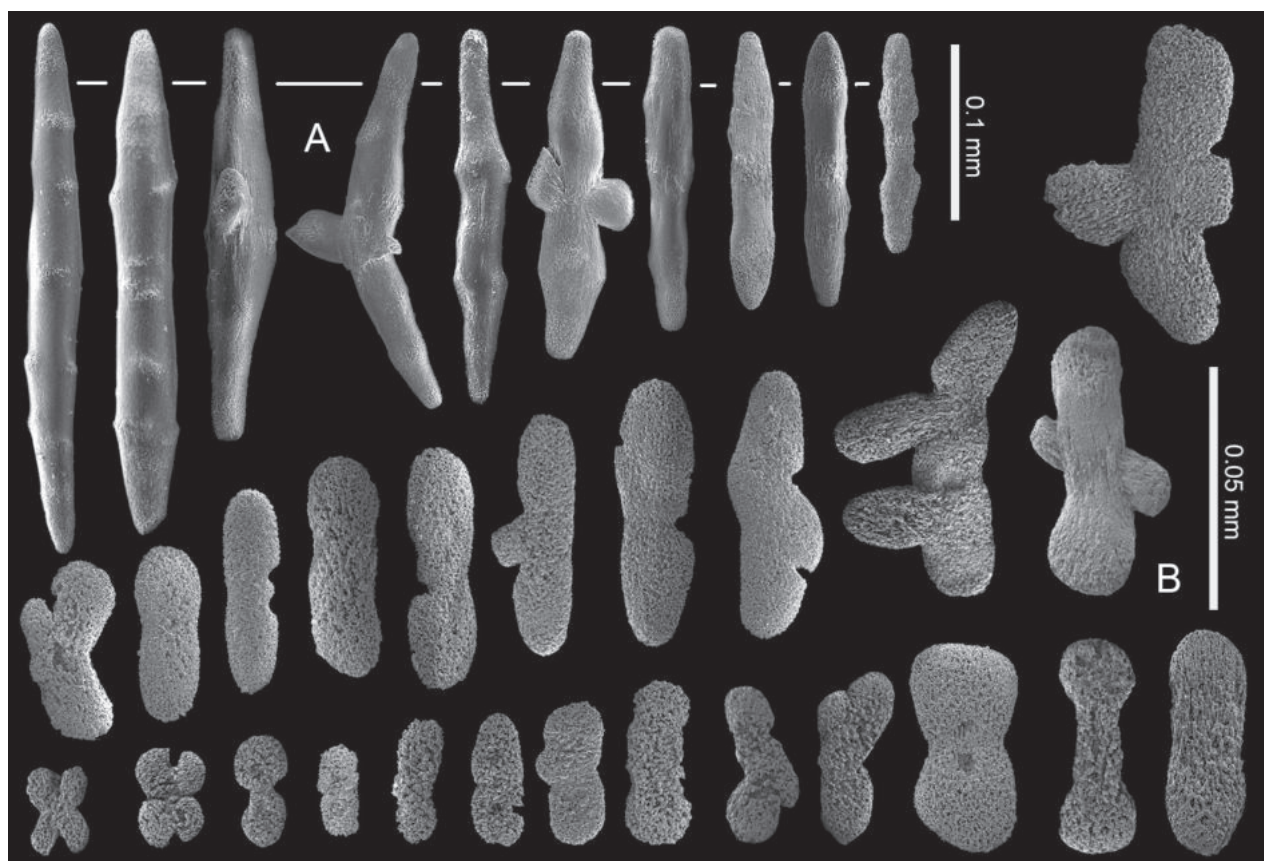


Figure 11. *Ofwegenum* aff. *coronalucis* SMNHTAU_Co_38223 **A** sclerites of the coenenchyme and polyp body **B** sclerites of the tentacles.

Morphological variations. Paratype SMNHTAU_Co_38229 has slightly longer tentacle sclerites and shorter coenenchymal sclerites compared to the holotype (Fig. 13).

Remarks. This species features a distinct encrusting growth form and surface grooves on its polypary, most probably indicating a process of colony fission (Fig. 3D, E). Its tentacle sclerites are mainly ellipsoidal platelets and flattened rods with shallow to no median constrictions (Figs 12B, 13B). The colonies grow in dense patches on the reef (Fig. 10E).

Distribution. La Réunion.

Etymology. The species is named after the late Prof. Yoel Kloog, biochemist, former Dean of the Faculty of Life Sciences, Tel Aviv University, in honour of his friendship and lifetime contributions to science.

***Ofwegenum verseveldti* (Benayahu, 1982), comb. nov.**

Figs 1, 3F, G, 14, 15

Material examined. Holotype. EGYPT • Marsa Barioka, northern Red Sea, southern tip of Sinai Peninsula; 27.7500°N, 34.2333°E; 12 m depth; 3 July 1978; coll. Y. Benayahu; SMNHTAU_Co_25554 (previously NS16770).

Paratypes. EGYPT • 33 colonies, same data as holotype; SMNHTAU_Co_25544 (previously NS16771) • same data as holotype; RMNH COEL. 13903.

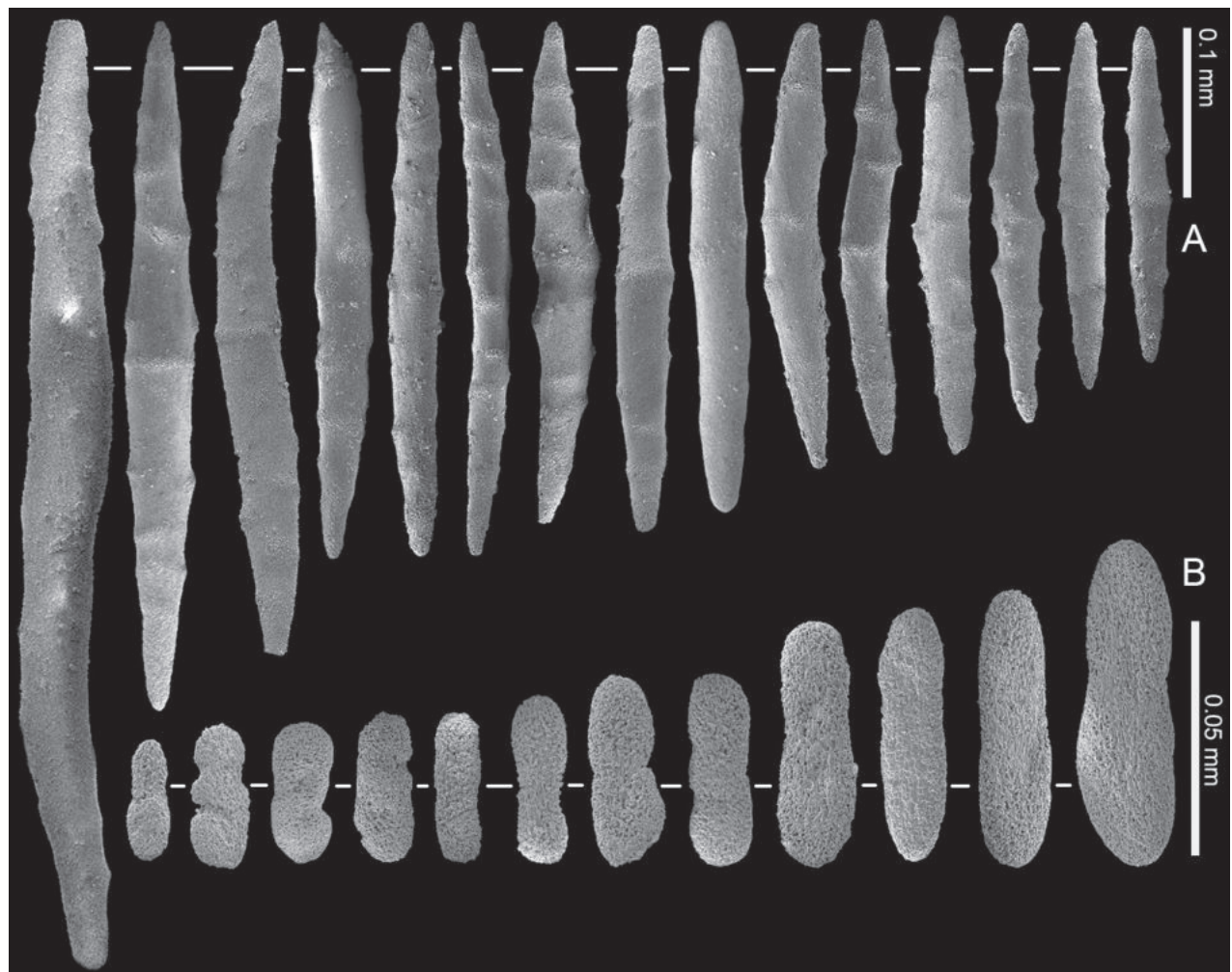


Figure 12. *Ofwegenum kloogi* sp. nov. holotype SMNHTAU_Co_34426 **A** sclerites of the coenenchyme and polyp body **B** tentacle sclerites, with ellipsoidal platelets and flattened rods with lateral notches.

Other material. ISRAEL• Eilat, northern Gulf of Aqaba, mesophotic reef across from the Inter University Institute for Marine Sciences (IUI); 60 m depth; 20 September 2005; coll. S. Eibinder; SMNHTAU_Co_33097.

Re-description (modified after Benayahu 1982). The holotype is a capitate colony, 11 mm in diameter with stalk approximately 14 mm high (Fig. 3F). The contracted polyps form conical or dome-shaped mounds, and the distal ends of some tentacles can be seen protruding from them. The coenenchyme sclerites are spindles and rods up to 0.80 mm long with low, simple tubercles or areas of thickening forming concentric, raised rings (Fig. 14A). The polyp body contains similar but shorter sclerites, up to 0.45 mm long (Fig. 14A), that appear to be arranged ‘en chevron’ when the polyp is extended. The size of the sclerites decreases along the polyp body towards the base of the tentacles.

The tentacles and pinnules include numerous crosses, flattened rods (i.e., finger-biscuits) and platelets up to 0.10 mm long (Fig. 14B), arranged on the aboral side of the tentacles. Some of these sclerites have median constrictions, side notches, or depressions at one or both ends that resemble a figure-eight shape (Fig. 14B). The platelets commonly have an asymmetrical outline and are wider at both ends (Fig. 14B).

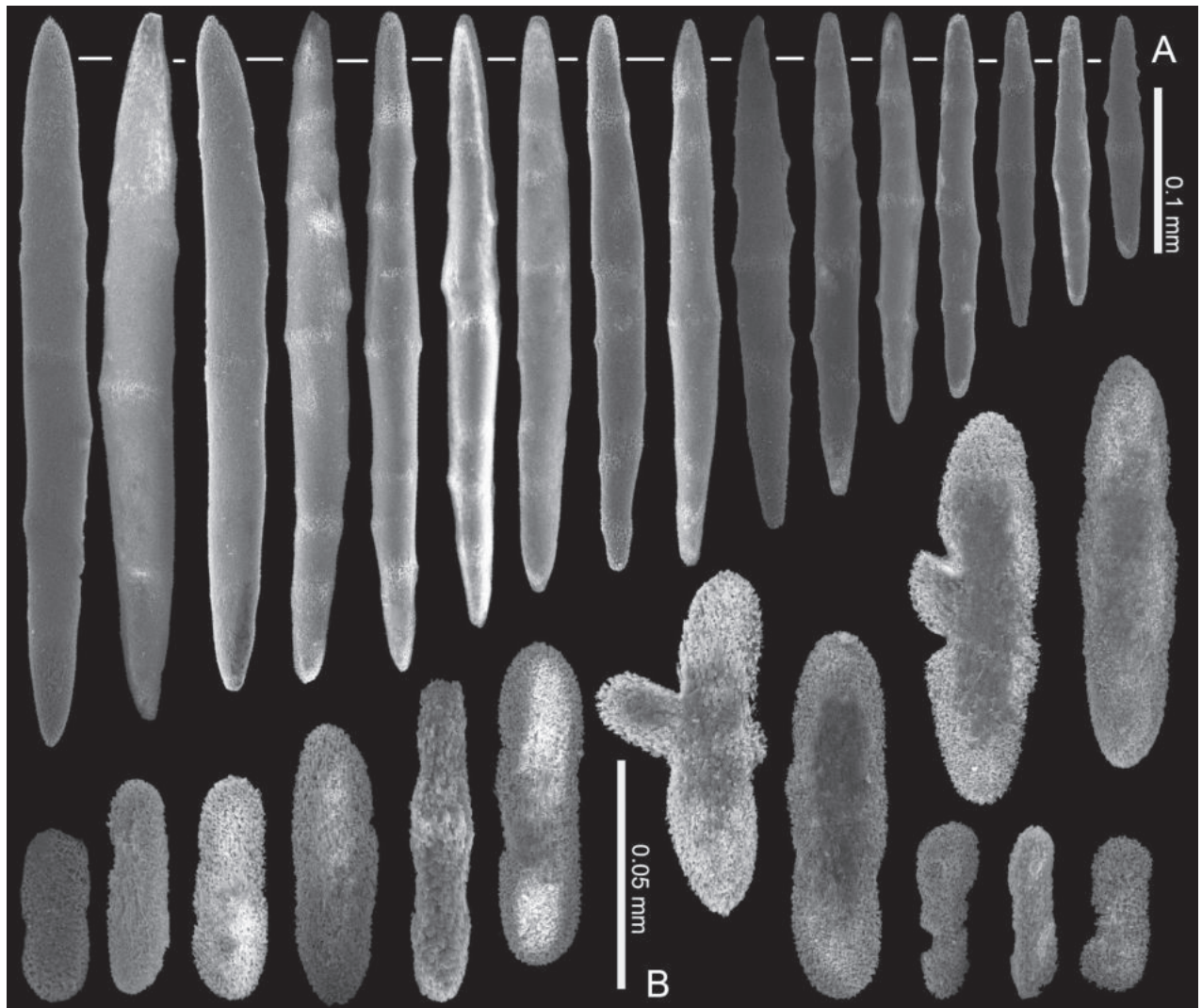


Figure 13. *Ofwegenum kloogi* sp. nov., paratype, SMNHTAU_Co_38229 **A** sclerites of the coenenchyme and polyp body **B** tentacle sclerites, with ellipsoidal platelets and flattened rods with lateral notches.

Colour. In life the coenenchyme is uniquely dark blue. The expanded polyps are pale blue, with brown pinnules that reflect the presence of symbiotic algae. The ethanol-preserved colony is creamy yellow, and the tentacles are pale cream.

Morphological variations. The paratype colonies and the other material vary in size; some colonies feature two separate polyparies on a common stalk (Fig. 3G). RMNH COEL. 13903 has smoother spindles and rods in both the coenenchyme and polyp body (Fig. 15A) and has fewer figure-eight platelets (Fig. 15B) compared to the holotype.

Remarks. *Ofwegenum verseveldti* comb. nov. is the only species with tentacle sclerites composed mainly of asymmetrical platelets resembling a figure-eight (Figs 14B, 15B). Additionally, it has the longest spindles and rods among the congeners (Figs 14A, 15A).

The current findings correspond to the original description of *M. verseveldti* (see Benayahu 1982). The new high-quality SEM images of the sclerites (Figs 14, 15) better present the species' diagnostic morphological characters. The tentacle sclerites reported as 'flattened rods with tiny pits' in the

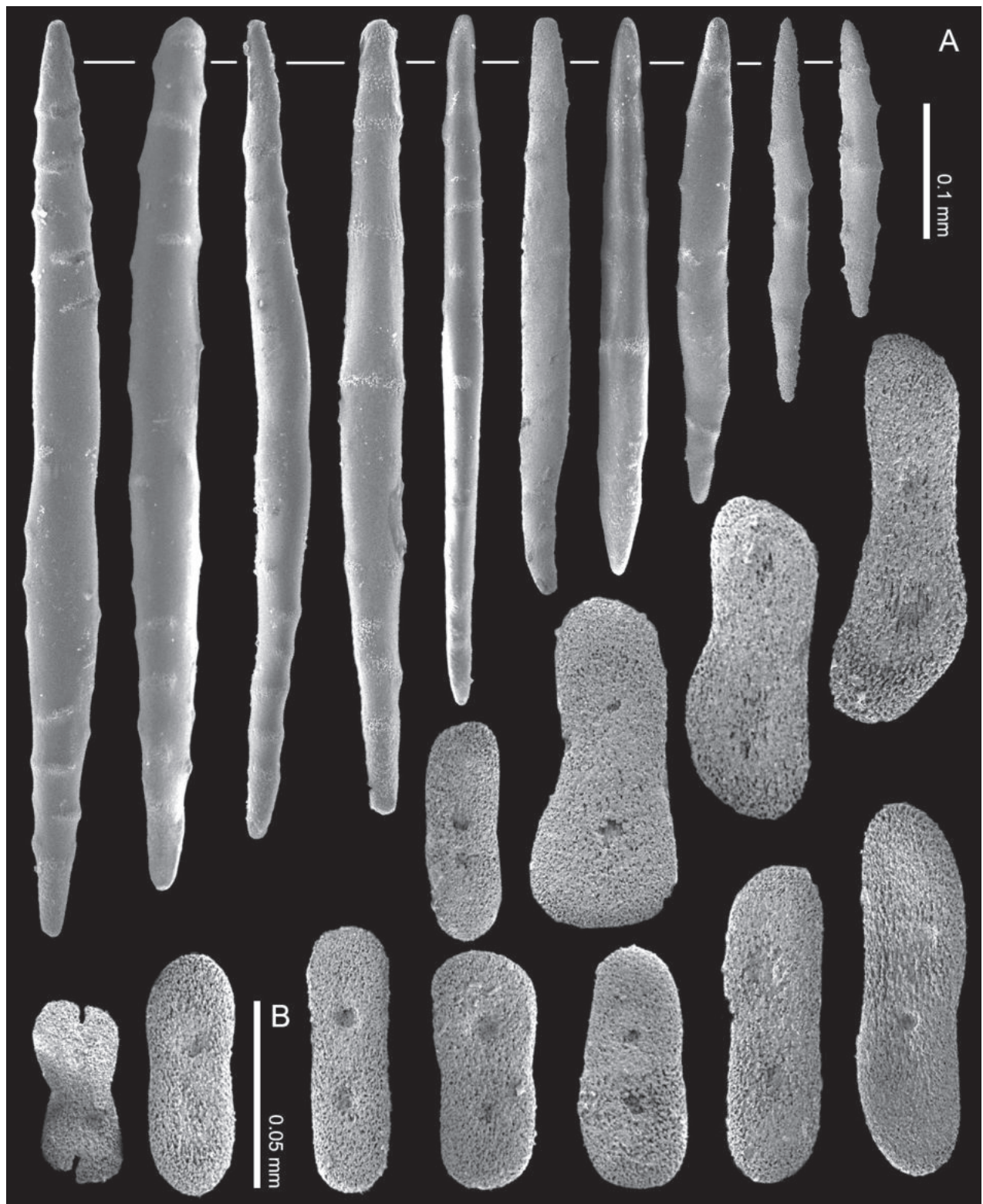


Figure 14. *Ofwegenum verseveldti* comb. nov., holotype SMNHTAU_Co_25554 **A** sclerites of the coenenchyme and polyp body **B** sclerites of the tentacles.

original description are referred to here as figure-eight platelets. The maximum length of these sclerites was erroneously presented by Benayahu (1982: 198, up to 0.19 mm) and is now corrected to be up to 0.10 mm (Fig. 14B). In the original description the species was described as having polyp sclerites

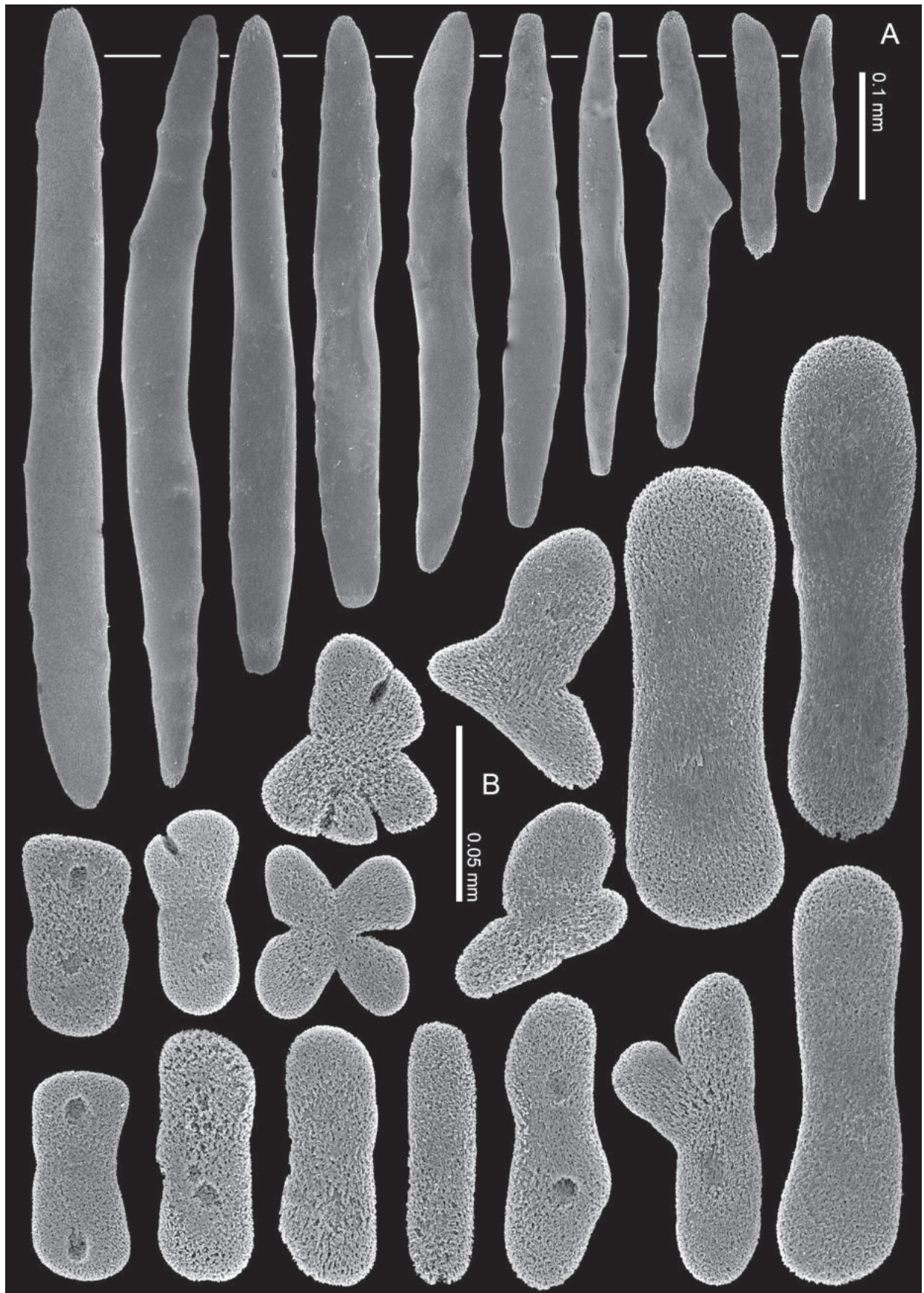


Figure 15. *Ofwegenum verseveldti* comb. nov., paratype, RMNH COEL. 13903 **A** sclerites of the coenenchyme and polyp body **B** sclerites of the tentacles.

arranged as a collaret and points, however further examination of additional material shows that is not the case. When polyps are extended the spindles and rods appear to be arranged 'en chevron'. Benayahu (1982) also did not mention anything about the presence or absence of zooxanthellae in specimens. Re-examination of the type material confirms that *O. verseveldti* is indeed zooxanthellate.

It should be noted that despite the extensive soft coral research conducted in the Gulf of Aqaba and other parts of the Red Sea, since the collection of the type material of *O. verseveldti* comb. nov. it has been found only once at a mesophotic depth on the Eilat reef (see above: SMNHTAU_Co_33097) and is also only infrequently observed by some professional divers in that region. This species should thus be considered as a rare soft coral in the Red Sea.

Distribution. Northern Red Sea.

Molecular results

DNA barcoding

Sequences for *mtMutS* (735 bp), *igr1* + *COI* (909 bp) and *28S rDNA* (800 bp) were obtained for seven specimens representing three of the four species of *Ofwegenum* plus the species from the aquarium trade (SMNHTAU_Co_38223) (Table 1). We were unable to amplify *COI* for two specimens (SMNHTAU_Co_38229, BOMAN-09174) and *mtMutS* for another (UF 15819). Only a partial fragment of *mtMutS* (450 bp) was obtained for *O. colli* sp. nov. (NTM C13089).

All phylogenetic analyses separated *Ofwegenum* gen. nov. into a well-supported clade that was sister to *Klyxum* and differed from members of that genus by mean genetic distances (uncorrected p) ranging from 1.0% ($\pm 0.06\%$ SD) at *COI* to 4.4% ($\pm 1.7\%$ SD) at *28S rDNA* (Fig. 16A). Within the *Ofwegenum* clade, however, the relationships among species were poorly resolved. All *Ofwegenum* specimens had identical *mtMutS* and *COI* sequences with the exceptions of *O. verseveldti* comb. nov., which differed by a 1 bp substitution in *mtMutS*, and *O. kloogi* sp. nov. (SMNHTAU_Co_34226) which differed by a 1 bp substitution in *COI*. The partial *mtMutS* sequence for *O. colli* sp. nov. was identical to both *O. kloogi* sp. nov. and *O. coronalucis* sp. nov. At *28S rDNA*, *O. verseveldti*, *O. kloogi* and *O. coronalucis* differed from one another by genetic distances (uncorrected p) of 0.5–0.8%. The aquarium trade specimen (SMNHTAU_Co_38223) was most similar to *O. coronalucis*, differing from the holotype UF 17263 by a 1 bp substitution. There was, however, variation among individuals of *O. coronalucis*, with two specimens from Oman (BOMAN-09174, UF 15882) differing from the others by ≤ 5 bp (uncorrected p = 0.6%). Both ML and Bayesian phylogenetic analysis of the concatenated alignment of *mtMutS* with *28S rDNA* found moderate to strong support for a clade consisting of the two specimens of *O. kloogi* and a clade of the two specimens of *O. coronalucis* with divergent *28S* sequences (BOMAN-09174, UF 15882) but did not resolve the relationships among the other taxa (Fig. 16A).

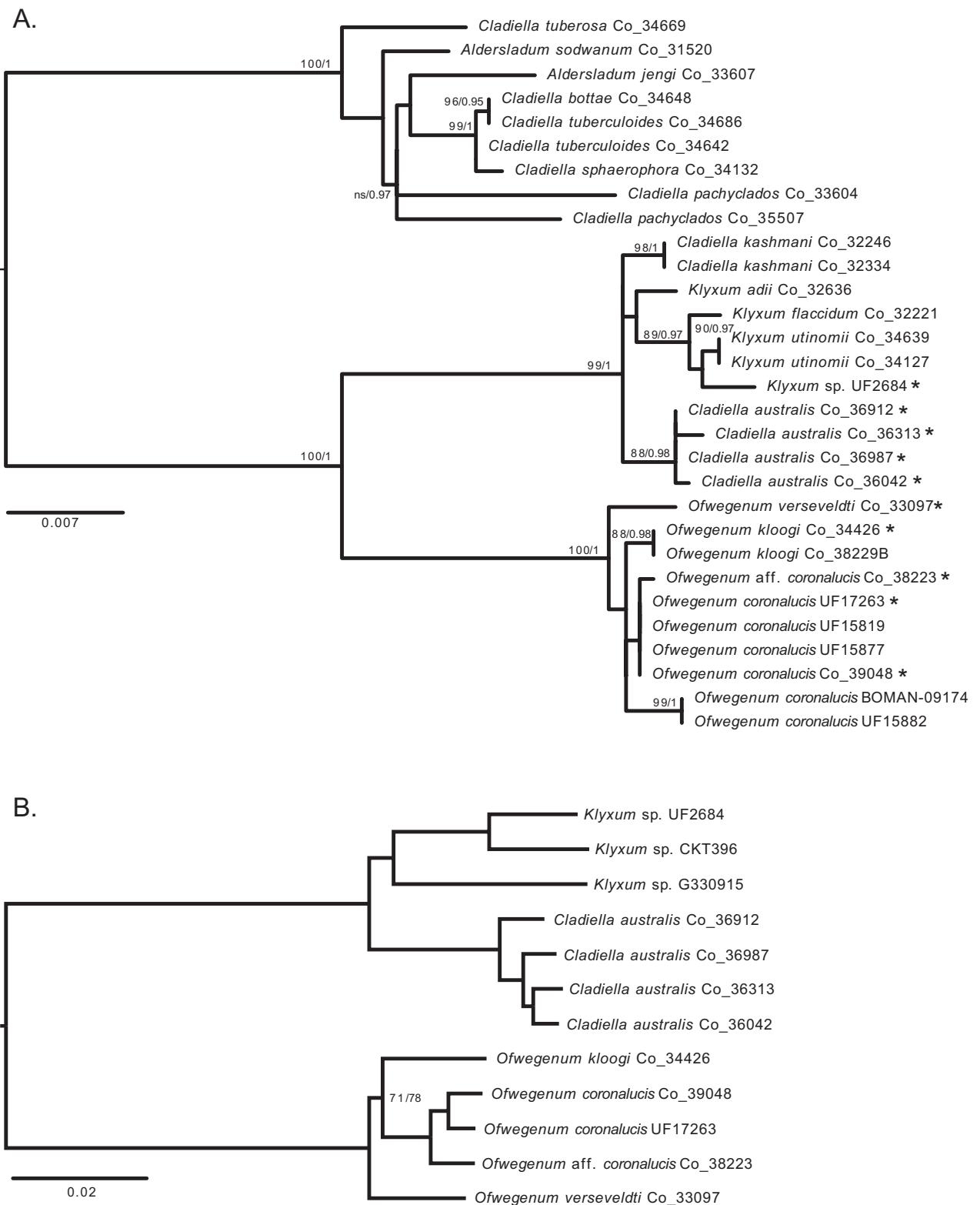


Figure 16. Phylogenetic relationships among species of *Ofwegenum* gen. nov. and other genera of the family Cladiellidae **A** maximum likelihood (ML) analysis of concatenated *mtMutS* and *28S rDNA* barcoding loci. Numbers at nodes: ML bootstrap percentage (10,000 ultrafast bootstrap replicates)/Bayesian posterior probability. Asterisks indicate samples that are included in analysis of conserved elements **B** maximum likelihood analysis of 1,213 conserved element loci (75% occupancy matrix). All nodes have 100% bootstrap support and SH-aLRT = 100 unless indicated. All Co_ numbers are SMNHTAU.

Target-capture sequencing of conserved elements

A total of 2,509 loci (out of 3,023 targeted loci) was recovered from the assembled contigs, including the seven outgroup taxa (Table 1). The mean number of loci recovered per sample was $1,747 \pm 205$ SD (range: 1,297–1,977) with a mean length of $1,247 \pm 92$ bp SD (range: 1,121–1,395 bp). The 75% complete alignment matrix included 1,213 loci for a total length of 1,511,307 nucleotides.

The maximum likelihood analysis recovered an *Ofwegenum* clade that was strongly supported and genetically distinct from the outgroup taxa (*Klyxum* spp. and *Cladiella australis*) (Fig. 16B). Within *Ofwegenum* there was strong support for a clade of *O. coronalucis* (two specimens from Oman) plus the species from the aquarium trade (SMNHATAU_Co_38223). The phylogenetic relationships among *O. verseveldti*, *O. kloogi* and *O. coronalucis*, however, remained unresolved. The single specimens of *O. verseveldti* and *O. kloogi* that were included in the analysis were equally genetically distant from *O. coronalucis*, and there was only very weak support for *O. kloogi* belonging to a clade with *O. coronalucis*.

Discussion

The phylogenetic position of *Ofwegenum* gen. nov. as sister to the genus *Klyxum* in family Cladiellidae was well supported by both single-locus mitochondrial genes as well as the multi-locus nuclear gene analysis (Fig. 16). It shares with other members of this family polyp sclerites in the form of flattened rods and small plates with a median waist that often resemble a figure-eight. The current results demonstrate the taxonomic significance of these tentacular sclerites for species delimitation within *Ofwegenum* gen. nov. Like other Cladiellidae, only a single type of sclerite is found in the coenenchyme. The form of these sclerites—smooth spindles and rods with low protuberances that may form raised concentric rings—seems, however, to be unique within the family. Its growth form, which is encrusting or consists of small stalked polyparies in the range of a centimetre in diameter joined together in a mat, is also distinct from the predominantly lobate growth forms of other Cladiellidae. Finally, the bright blue alcohol-soluble pigments that give some *Ofwegenum* species their striking blue-green colour are unique among Cladiellidae, and rare among all octocorals. Whether or not this pigment is guaiazulene, a compound that has been found in the blue gorgonian *Guaiaegorgia* and several other species (Grasshoff and Alderslade 1997) remains unknown.

Ofwegenum gen. nov. also shares with other genera of Cladiellidae a relatively invariant mitochondrial genome marked by little to no genetic differentiation among species at the loci commonly used for DNA barcoding (*mtMutS*, *COI*) (Benayahu et al. 2012). While 28S *rDNA* exhibits greater variation among species in this clade, higher levels of intraspecific variation in that gene can also confound assessment of species boundaries (McFadden et al. 2014) as observed in *O. coronalucis* (Fig. 16A). While multi-locus methods such as the target-enrichment approach employed here generally allow species to be delimited with greater confidence (Erickson et al. 2020), our analysis of *Ofwegenum* is hampered by low sample size. Only one specimen each of *O. verseveldti* and

O. kloogi and no *O. colli* yielded DNA of sufficient quantity and quality for library preparation. The absence of the latter species from our phylogeny and our inability to assess intraspecific genetic variation in the other two greatly limit the inferences we can make about the phylogenetic relationships and degree of genetic differentiation among species of *Ofwegenum*. Although increased sample sizes will be necessary to better resolve the species' relationships, the apparent rarity of this genus, with each species currently known from only 1–2 locations, may hinder future attempts to increase the phylogenetic sampling.

Although it is rarely encountered in nature, *Ofwegenum* is nonetheless present in the commercial aquarium trade. We examined and sequenced a specimen (SMNHTAU_Co_38223) obtained from a supplier in the U.S. that is genetically and morphologically most similar to *O. coronalucis* (Fig. 16). The original source location of this specimen remains unknown but was thought to be Indonesia (A. Parrin, pers. comm. 12 Aug 2013), where most of the material in the U.S. commercial trade originates (Wabnitz et al. 2003). Aquarist D. Knop shared with us photos of additional specimens sourced from Indonesia (Fig. 2C–F). Whether or not any of the species we have described (or perhaps an additional species) occurs naturally in Indonesia remains unknown. Rowlett (2020) reported that a species of *Ofwegenum* has been cultured in Queensland, Australia for exportation in the aquarium trade. Whether that species might be *O. colli* sp. nov., which occurs naturally in Queensland, or the *O. aff. coronalucis* that is found in the aquarium trade in the U.S. also remains unknown.

Conclusions

Here we established a new genus, *Ofwegenum* gen. nov., for *Metalcyonium verseveldti* Benayahu, 1982. We have redescribed the type of that species and establish it as a new combination, *O. verseveldti*. In addition, we have described three new species of *Ofwegenum* from shallow-water coral reefs in the Indo-Pacific region, bringing the total number of species in the genus to four. This genus appears to be rare on coral reefs, with each species known from only a few localities, some of which have been extensively explored. The four species have distinct, non-overlapping geographical distributions, and are currently known only from the northern Red Sea (*O. verseveldti*), Arabian Sea (*O. coronalucis*), central Indian Ocean (*O. kloogi*), and northeastern Australia (*O. colli*) (Fig. 1).

Acknowledgements

We thank Phil Alderslade, The Commonwealth Scientific and Industrial Research Organization (CSIRO), Hobart, Tasmania, Australia for providing material and S. Horner, Museum and Art Gallery of the Northern Territory, Darwin, Australia for curatorial information. We also thank the Interuniversity Institute for Marine Sciences, Eilat, Israel for use of their facilities, and S. Eibinder, Haifa University, Israel, for collecting the mesophotic samples. Collections in La Réunion were made possible due to a grant to Y. Benayahu from the “Conseil Régional de la Réunion” and “Association Parc Marin de la Réunion”. We thank E. Tessier, B. Cauvin, Y. Clain and the team of guards of the “Association Parc Marin de la Réunion” for help during the field work. We thank C. Bourmaud, J. P. Quod and M. Aknin and D. Huchon for help and advice during the La Réunion

expedition. We thank Z. Kuplik for professional curatorial skills, K. Erickson for laboratory assistance, A. Quattrini for assistance with data analysis, V. Wexler for digital editing, and N. Paz for editorial assistance. Daniel Knop provided us with high resolution photos of his aquarium specimen. Environment Authority of Oman is appreciated for granting the collection permits, and we thank M.R. Claereboudt, S. Dobretsov (Sultan Qaboos University, Oman), G. Paulay (Florida Natural History Museum) and S. Wilson (Five Oceans Environmental Services LLC) for their support in Oman. J.H. Ausubel (Rockefeller University), and L. Brown (Lounsbery Foundation) are greatly appreciated for their support and encouragement to the last author. We would like to thank O. Breedy and J. Reimer for their constructive comments and suggestions, which helped improve the manuscript.

Additional information

Conflict of interest

The authors have declared that no competing interests exist.

Ethical statement

No ethical statement was reported.

Funding

This research received support from BSF–2019624 to Y. Benayahu and NSF DEB–1929319 and DEB–1856245 to C.S. McFadden. The research at NBC and partial field-work was supported by the Richard Lounsbery Foundation grant to K. Samimi-Namin.

Author contributions

Conceptualization: YB, CSM. Formal analysis: KSN, YB, CSM. Funding acquisition: YB, CSM. Project administration: CSM. Writing – original draft: CSM, YB, KSN. Writing – review and editing: CSM, YB, KSN.

Author ORCIDs

Catherine S. McFadden  <https://orcid.org/0000-0002-8519-9762>

Yehuda Benayahu  <https://orcid.org/0000-0002-6999-0239>

Kaveh Samimi-Namin  <https://orcid.org/0000-0002-7744-9944>

Data availability

All of the data that support the findings of this study are available in the main text.

References









- Alderslade P (2000) Four new genera of soft corals (Coelenterata: Octocorallia), with notes on the classification of some established taxa. *Zoologische Mededelingen Leiden* 74: 237–249.
- Bankevich A, Nurk S, Antipov S, Gurevich A, Dvorkin M, Kulikov AS, Lesin VM, Nikolenko SI, Pham S, Prjibelski AD, Pyshkin AV, Sirotkin AV, Viahhy N, Tesler G, Alekseyev AM, Pevzner PA (2012) SPAdes: A new genome assembly algorithm and its applications to single-cell sequencing. *Journal of Computational Biology* 19(5): 455–477. <https://doi.org/10.1089/cmb.2012.0021>

- Bayer FM, Grasshoff M, Verseveldt J (1983) Illustrated Trilingual Glossary of Morphological and Anatomical Terms Applied to Octocorallia. E.J. Brill/Dr. W. Backhuys, Leiden, 75 pp. <https://doi.org/10.1163/9789004631915>
- Benayahu Y (1982) A new species of *Metalcyonium* (Octocorallia, Alcyonacea) from the Red Sea. *Zoologische Mededelingen Leiden* 56: 197–201. [pls 1–4]
- Benayahu Y, van Ofwegen LP, Soong K, Dai C-F, Jeng M-S, Schlagman A, Hsieh HJ, McFadden CS (2012) Diversity and distribution of Octocorals (Coelenterata: Anthozoa) on the coral reefs of Penghu, Taiwan. *Zoological Studies* 51: 1529–1548.
- Bolger AM, Lohse M, Usadel B (2014) Trimmomatic: A flexible trimmer for Illumina sequence data. *Bioinformatics* 30(15): 2114–2120. <https://doi.org/10.1093/bioinformatics/btu170>
- Chernomor O, von Haeseler A, Minh BQ (2016) Terrace aware data structure for phylogenomic inference from supermatrices. *Systematic Biology* 65(6): 997–1008. <https://doi.org/10.1093/sysbio/syw037>
- Dai C-F (1991) Distribution and adaptive strategies of alcyonacean corals in Nanwan Bay, Taiwan. *Hydrobiologia* 216/217(1): 241–246. <https://doi.org/10.1007/BF00026469>
- Dinesen ZD (1983) Patterns in the distribution of soft corals across the central Great Barrier Reef. *Coral Reefs* 1(4): 229–236. <https://doi.org/10.1007/BF00304420>
- Erickson KL, Pentico A, Quattrini AM, McFadden CS (2020) New approaches to species delimitation and population structure of anthozoans: Two case studies of octocorals using ultraconserved elements and exons. *Molecular Ecology Resources* 21(1): 78–92. <https://doi.org/10.1111/1755-0998.13241>
- Fabricius KE (1997) Soft coral abundance on the central Great Barrier Reef: Effects of *Acanthaster planci*, space availability, and aspects of the physical environment. *Coral Reefs* 16(3): 159–167. <https://doi.org/10.1007/s003380050070>
- Fabricius K, Alderslade P (2001) Soft Corals and Sea Fans: A Comprehensive Guide to the Tropical Shallow Water Genera of the Central-West Pacific, the Indian Ocean and the Red Sea. Australian Institute of Marine Science, Townsville, 264 pp.
- Fabricius KE, Dommissie M (2000) Depletion of suspended particulate matter over coastal reef communities dominated by zooxanthellate soft corals. *Marine Ecology Progress Series* 196: 157–167. <https://doi.org/10.3354/meps196157>
- Faircloth B (2013) illumiprocessor: A trimmomatic Wrapper for Parallel Adapter and Quality Trimming. <https://doi.org/10.6079/J9ILL>
- Faircloth BC (2016) PHYLUCE is a software package for the analysis of conserved genomic loci. *Bioinformatics* 32(5): 786–788. <https://doi.org/10.1093/bioinformatics/btv646>
- Grasshoff M, Alderslade P (1997) Gorgoniidae of Indo-Pacific reefs with description of two new genera. *Senckenbergiana Biologica* 77: 23–35.
- Guindon S, Gascuel O (2003) A simple, fast, and accurate algorithm to estimate large phylogenies by maximum likelihood. *Systematic Biology* 52(5): 696–704. <https://doi.org/10.1080/10635150390235520>
- Guindon S, Dufayard J-F, Lefort V, Anisimova M, Hordijk W, Gascuel O (2010) New algorithms and methods to assess maximum-likelihood phylogenies: Assessing the performance of PhyML 3.0. *Systematic Biology* 59(3): 307–321. <https://doi.org/10.1093/sysbio/syq010>
- Hoang DT, Chernomor O, von Haeseler A, Minh BQ, Vinh LS (2018) UFBoot2: Improving the ultrafast bootstrap approximation. *Molecular Biology and Evolution* 35(2): 518–522. <https://doi.org/10.1093/molbev/msx281>

- Hoeksema BW (2021) In memoriam: Leendert P. van Ofwegen (1953–2021), octocoral taxonomist. *ZooKeys* 1052: 157–187. <https://doi.org/10.3897/zookeys.1052.71435>
- Kalyaanamoorthy S, Minh BQ, Wong TKF, von Haeseler A, Jermini LS (2017) ModelFinder: Fast model selection for accurate phylogenetic estimates. *Nature Methods* 14(6): 587–589. <https://doi.org/10.1038/nmeth.4285>
- Katoh K, Standley DM (2013) MAFFT multiple sequence alignment software version 7: Improvements in performance and usability. *Molecular Biology and Evolution* 30(4): 772–780. <https://doi.org/10.1093/molbev/mst010>
- Katoh K, Kuma K, Toh H, Miyata T (2005) MAFFT version 5: Improvement in accuracy of multiple sequence alignment. *Nucleic Acids Research* 33(2): 511–513. <https://doi.org/10.1093/nar/gki198>
- Kükenthal W (1906) Alcyonacea. *Wissenschaftliche Ergebnisse der Deutschen Tiefsee-Expedition auf dem Dampfer "Valdivia", 1898–1899*. 13: 1–111. [pls 1–12.] <https://doi.org/10.5962/bhl.title.82676>
- McFadden CS, Hochberg FG (2003) Biology and taxonomy of encrusting alcyoniid soft corals in the northeastern Pacific Ocean with descriptions of two new genera (Cnidaria, Anthozoa, Octocorallia). *Invertebrate Biology* 122(2): 93–113. <https://doi.org/10.1111/j.1744-7410.2003.tb00076.x>
- McFadden CS, van Ofwegen LP (2013) Molecular phylogenetic evidence supports a new family of octocorals and a new genus of Alcyoniidae (Octocorallia: Alcyonacea). *ZooKeys* 346: 59–83. <https://doi.org/10.3897/zookeys.346.6270>
- McFadden CS, van Ofwegen LP (2017) Revisionary systematics of the endemic soft coral fauna (Octocorallia: Alcyonacea: Alcyoniina) of the Agulhas Bioregion, South Africa. *Zootaxa* 4363(4): 451–488. <https://doi.org/10.11646/zootaxa.4363.4.1>
- McFadden CS, Brown AS, Brayton C, Hunt CB, van Ofwegen LP (2014) Application of DNA barcoding to biodiversity studies of shallow-water octocorals: Molecular proxies agree with morphological estimates of species richness in Palau. *Coral Reefs* 33: 275–286. <https://doi.org/10.1007/s00338-013-1123-0>
- McFadden CS, van Ofwegen LP, Quattrini AM (2022) Revisionary systematics of Octocorallia (Cnidaria: Anthozoa) guided by phylogenomics. *Bulletin of the Society of Systematic Biologists* 1(3): 1–79. <https://doi.org/10.18061/bssb.v1i3.8735>
- Minh BQ, Schmidt HA, Chernomor O, Schrempf D, Woodhams MD, von Haeseler A, Lanfear R (2020) IQTree-2: New models and efficient methods for phylogenetic inference in the genomic era. *Molecular Biology and Evolution* 37(5): 1530–1534. <https://doi.org/10.1093/molbev/msaa015>
- Pfeffer G (1889) Zur Fauna von Süd-Georgien. *Jahrbuch der Hamburgischen Wissenschaftlichen Anstalten* 6: 37–55.
- Ronquist F, Teslenko M, van der Mark P, Ayres D, Darling A, Höhna S, Larget B, Liu L, Suchard MA, Huelsenbeck JP (2012) MrBayes 3.2: Efficient Bayesian phylogenetic inference and model choice across a large model space. *Systematic Biology* 61(3): 539–542. <https://doi.org/10.1093/sysbio/sys029>
- Rowlett J (2020) *Indo-Pacific Corals*. [ISBN: 9798686565975], 805 pp.
- Tamura K, Peterson D, Peterson N, Stecher G, Nei M, Kumar S (2011) MEGA5: Molecular Evolutionary Genetics Analysis using maximum likelihood, evolutionary distance and maximum parsimony methods. *Molecular Biology and Evolution* 28(10): 2731–2739. <https://doi.org/10.1093/molbev/msr121>
- Thomson JS (1910) The Alcyonaria of the Cape of Good Hope and Natal. *Alcyonacea*. *Transactions of the Royal Society of Edinburgh* 47: 549–589. [pls 1–4.] <https://doi.org/10.1017/S0080456800005032>

- Thomson JS (1921) South African Alcyonacea. Transactions of the Royal Society of South Africa 9: 149–175. [pls 5–6.] <https://doi.org/10.1080/00359192109520204>
- Tursch B, Tursch A (1982) The soft coral community on a sheltered reef quadrat at Laing Island (Papua New Guinea). Marine Biology 68(3): 321–332. <https://doi.org/10.1007/BF00409597>
- Utinomi H (1958) A revision of the genera *Nidalia* and *Bellonella* with an emendation of nomenclature and taxonomic definitions for the family Nidaliidae (Octocorallia, Alcyonacea). Bulletin of the British Museum (Natural History). Zoology 5: 101–121.
- Utinomi H (1964) Some Octocorals from the Antarctic waters off Prince Harald Coast. Memoirs of National Institute of Polar Research, Tokyo. Series E. Biology and Medical Science 23: 1–14.
- Verseveldt J, Bayer FM (1988) Revision of the genera *Bellonella*, *Eleutherobia*, *Nidalia* and *Nidaliopsis* (Octocorallia, Alcyoniidae and Nidaliidae), with descriptions of two new genera. Zoologische Verhandelingen 245: 1–131.
- Wabnitz C, Taylor M, Green E, Razak T (2003) From Ocean to Aquarium. UNEP-WCMC, Cambridge. <https://www.unep.org/resources/report/ocean-aquarium-global-trade-marine-ornamental-species>
- Williams GC (1986) Morphology, systematics, and variability of the southern African soft coral, *Alcyonium variable* (J. Stuart Thomson, 1921) (Octocorallia, Alcyoniidae). Annals of the South African Museum 96: 241–270.
- Williams GC (2000) Two new genera of soft corals (Anthozoa: Alcyoniidae) from South Africa, with a discussion of diversity and endemism in the southern African octocorallian fauna. Proceedings of the California Academy of Sciences 52: 65–75.

Scratching the tip of the iceberg: integrative taxonomy reveals 30 new species records of Microgastrinae (Braconidae) parasitoid wasps for Germany, including new Holarctic distributions

Amelie Höcherl¹, Mark R. Shaw², Caroline Boudreault³, Dominik Rabl⁴, Gerhard Haszprunar⁵, Michael J. Raupach¹, Stefan Schmidt¹, Viktor Baranov⁶, José Fernández-Triana³

¹ SNSB-Zoologische Staatssammlung München, Münchhausenstr. 21, 81247 München, Germany

² National Museums of Scotland, Chambers Street, Edinburgh EH1 1JF, UK

³ Canadian National Collection of Insects, Arachnids and Nematodes, 960 Carling Ave., Ottawa, K1A0C6, Canada

⁴ Field Station Fabriksschleichach, Department of Animal Ecology and Tropical Biology, Biocenter, University of Würzburg, Glashüttenstr. 5, Würzburg, 96181 Rauhenbrach, Germany

⁵ Department Biology II, Ludwig-Maximilians-Universität München (LMU), Großhaderner Str. 2, Martinsried, 82152 Planegg, Germany

⁶ Estación Biológica de Doñana-CSIC/Doñana Biological Station-CSIC, Seville, Spain

Corresponding author: Amelie Höcherl (amelie.hoecherl@gmail.com)

Abstract

Substantial parts of the European and German insect fauna still remain largely unexplored, the so-called “dark taxa”. In particular, midges (Diptera) and parasitoid wasps (Hymenoptera) are abundant and species-rich throughout Europe, yet are often neglected in biodiversity research. One such dark taxon is Microgastrinae wasps (Hymenoptera: Braconidae), a group of parasitoids of lepidopteran caterpillars with 252 species reported in Germany so far. As part of the German Barcode of Life Project GBOL III: Dark Taxa, reverse DNA barcoding and integrative taxonomic approaches were used to shed some light on the German Fauna of Microgastrinae wasps. In our workflow, DNA barcoding was used for molecular clustering of our specimens in a first step, morphological examination of the voucher specimens in a second step, and host data compared in a third step. Here, 30 species are reported for the first time in Germany, adding more than 10% to the known German fauna. Information for four species is provided in a new Holarctic context, reporting them for the Nearctic or, respectively, Palaearctic region, and 26 additional country records are added from sequenced material available in the collections accessible to us. Molecular clusters that show signs of discrepancies are discussed. Results show that we are just scratching the tip of the iceberg of the unexplored Microgastrinae diversity in Germany.

Key words: Dark taxa, DNA barcoding, faunistics, host-parasitoid associations, morphology, parasitoid biology

Introduction

With approximately 105,000 insect species documented (Leandro et al. 2017), the Central European fauna is one of the most comprehensively studied in the world (Hausmann et al. 2020; Ronquist et al. 2020; Wagner 2020). Therefore, many studies on insect decline focus their research on this region (Thomas et al. 2004; Hallmann et al. 2017; Seibold et al. 2019; Pilotto et al. 2020). In



This article is part of:

**Contributions to the world fauna of
Microgastrinae parasitoid wasps
(Hymenoptera, Braconidae)**

Edited by Jose Fernandez-Triana & Erinn
Fagan-Jeffries

Academic editor: Erinn Fagan-Jeffries

Received: 15 September 2023

Accepted: 24 October 2023

Published: 11 January 2024

ZooBank: <https://zoobank.org/CBA8C741-95AB-4DB5-9E80-AAAA500D3572>

Copyright: © Amelie Höcherl et al.

This is an open access article distributed under the terms of the CC0 Public Domain Dedication.

Citation: Höcherl A, Shaw MR, Boudreault C, Rabl D, Haszprunar G, Raupach MJ, Schmidt S, Baranov V, Fernández-Triana J (2024) Scratching the tip of the iceberg: integrative taxonomy reveals 30 new species records of Microgastrinae (Braconidae) parasitoid wasps for Germany, including new Holarctic distributions. ZooKeys 1188: 305–386. <https://doi.org/10.3897/zookeys.1188.112516>

Germany, in particular, where more than 33,305 insect species have been recorded (Völkl and Blick 2004), there is an exceptionally long history of insect collection, monitoring, and taxonomy (Habel et al. 2016; Hallmann et al. 2017; Jähnig et al. 2021).

However, substantial parts of the German insect fauna remain largely unexplored: the so-called “dark taxa” (Hausmann et al. 2020; Chimeno et al. 2022). This term was first used for DNA sequences with no links to previous information, such as species names, which started to accumulate in public nucleotide databases like NCBI (Page 2016). More recently, “dark taxa” has now been applied to less emblematic, hyperdiverse, and neglected taxa that are especially common in insects (Hausmann et al. 2020; Chimeno et al. 2022; Hartop et al. 2022), nematodes, or chelicerates (e.g., mites). The concept includes various groups of Diptera (flies) and Hymenoptera (bees, wasps, ants, and sawflies) – here, in particular, parasitoid wasps (Hausmann et al. 2020). Although representatives of these taxa are often very small in size, they can make up more than half of the specimens of a Malaise trap sample (Brown 2005; Karlsson et al. 2020; Wühl et al. 2022). Several factors contribute to the neglect of a taxon: First, many species descriptions in the historical literature are short, only providing inadequate or low-quality figures, and types may be lost or damaged. Second, the identification of many species relies on a combination of very subtle morphological characteristics, which are often difficult to interpret and assess, especially in closely related species or those forming part of morphologically cryptic species complexes. Third, only a comparatively small number of taxonomists focus on these groups.

As part of the German Barcode of Life Initiative, GBOL III: Dark Taxa project, we aim to change this situation by applying a reverse DNA barcoding and integrative taxonomic approach. In contrast to traditional DNA barcoding workflows, we first performed molecular analyses, tested these results via morphological comparison in a second step, and compared available host data in a third step. Our molecular work relies on DNA barcoding (Hebert et al. 2003a), a technique that uses short, standardised genetic markers such as the cytochrome c oxidase subunit I (COI) gene of the mitochondrial genome for molecular species identification (Hebert et al. 2003b). DNA barcoding has proven to be a powerful tool for valid species identification (Hebert et al. 2003a), including for many German taxa (e.g., Hausmann et al. 2011a; Raupach et al. 2014; Hendrich et al. 2015; Morinière et al. 2017). However, there are some constraints to DNA barcoding, such as introgression of mitochondrial DNA into the nuclear genome (numts) (e.g., Hebert et al. 2023), incomplete lineage sorting, recent or ongoing hybridisation events (e.g., Mutanen et al. 2016), and effects of *Wolbachia* infections (e.g., Smith et al. 2012). We aim to mitigate these by using an integrative approach that includes morphology and host information in addition to molecular evidence to support our species concepts. Especially in this dark taxa context, a reverse DNA barcoding approach has major advantages: (1) Species identification is facilitated, though still limited by significant gaps in reference libraries for dark taxa; (2) Clustering large numbers of specimens and thereby increasing the efficiency of taxonomic workflows (Brown et al. 2018; Fernandez-Triana 2022; Hartop et al. 2022); and (3) Enabling species discovery by uncovering morphologically cryptic diversity through DNA barcoding (Fernandez-Triana et al. 2014c; Smith et al. 2015; Lazarević et al. 2023).

In the last two decades, DNA barcoding and integrative taxonomy have revolutionised the study of Microgastrinae parasitoid wasps (e.g., Smith et al. 2013; Fernandez-Triana et al. 2014c; Fagan-Jeffries et al. 2018). Microgastrinae (Hymenoptera: Braconidae) is a common and highly diverse group of parasitoids of lepidopteran caterpillars, with more than 3,200 species described worldwide, but a projected diversity estimated up to 40,000–50,000 species (Fernandez-Triana et al. 2020). A total of 252 species of Microgastrinae has been recorded in Germany until now (Belokobylskij et al. 2003; Fernandez-Triana et al. 2020; Papp 1981b; Shaw 2020, 2022). Based on known host/parasitoid ratios and a host diversity of currently 3,688 established Lepidoptera species recorded from Germany (Rennwald et al. 2023), it is very likely that the officially recorded Microgastrinae fauna in the country is substantially underrepresenting the actual species-richness of this group in Germany. As a result of our approach, we report 30 species in Germany for the first time, adding more than 10% to the known German fauna. In ten cases, we link sequences to a species name for the first time and place four species in a new Holarctic context, reporting them for the Nearctic or Palaearctic regions for the first time.

Materials and methods

Specimens were collected in southern Germany (Fig. 1A) using mostly Malaise traps, but also canopy fogging. We have sampled a variety of localities and habitats from urban gardens, nature reserves and former military shooting ranges to the highest mountain in Germany, Zugspitze (Fig. 1B, C). Our dataset contains a total of 5455 specimens from Germany, of which 5364 yielded COI sequences. We also studied reared specimens from the National Museums of Scotland (**NMS**), Edinburgh, the Zoologische Staatssammlung München (**ZSM**), as well as specimens from the Canadian National Collection of Insects and Arachnids (**CNC**). We downloaded additional sequences and distribution data from the public and private data available to us in the Barcode of Life Data System (BOLD) (Ratnasingham and Hebert 2007). In accordance with our reverse DNA barcoding approach, we first used a molecular workflow for clustering, then a morphological workflow and additionally looked at host data to establish our integrative species concepts. This order of different approaches represents our workflow and does not indicate that we favoured any single one of these methods. We used molecular information as well as morphology for every single species and additionally considered biological information if available. Detailed information about these integrative species concepts is provided in the notes section of the species.

Molecular workflow

We manually size-fractionated Malaise trap bulk samples by sieving and then sorted into first-glance morphotypes, of which subsamples were chosen for sequencing. We used legs as tissue samples, depending on size of the specimen one to three legs. COI-sequencing was done at the CCDB (Canadian Centre for DNA Barcoding) using their at-the-time standard sequencing protocols and primers, which can be reviewed for each sequence in the BOLD database (www.boldsystems.org). Sequences were analysed and clustered using the

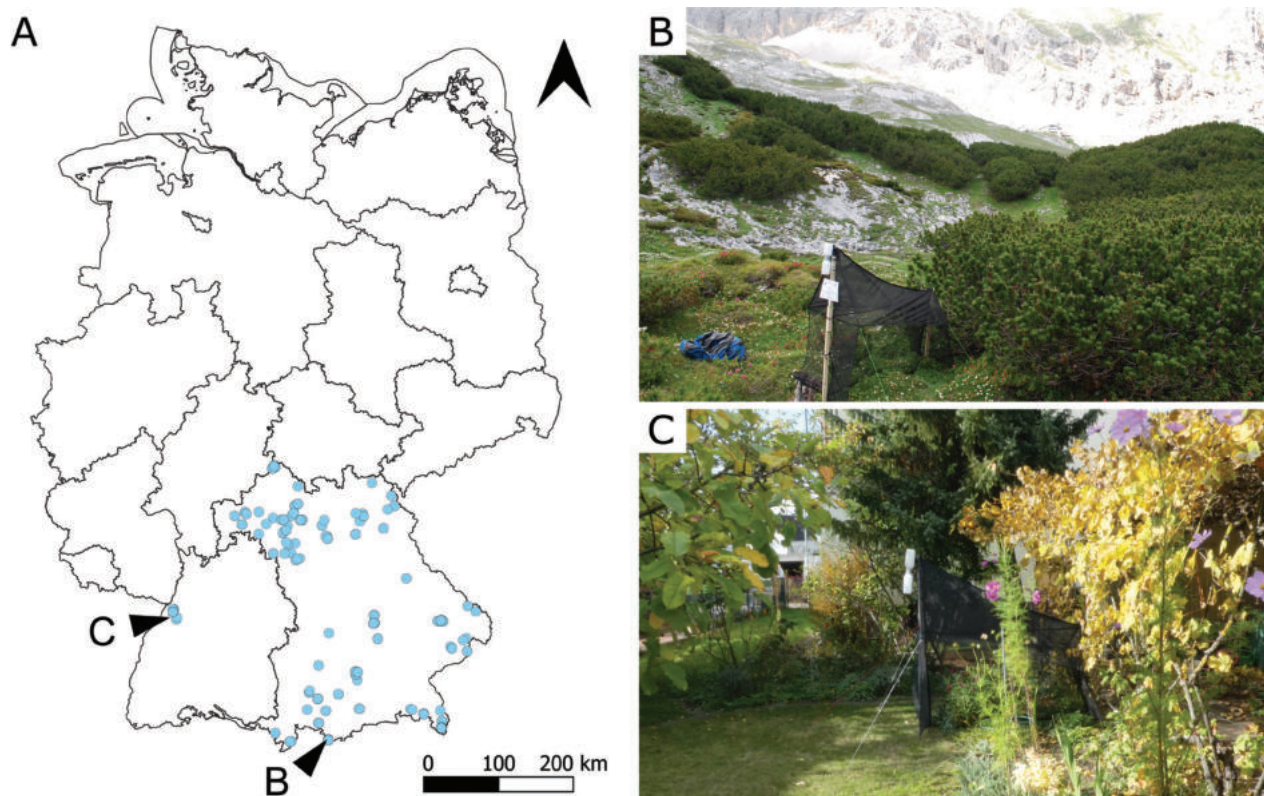


Figure 1. **A** Map showing our sampling locations in Germany, mostly in Bavaria (GeoBasis-DE / BKG 2022). The sampled habitats include a large variety from **B** the highest mountain in Germany, Zugspitze (photograph: J. Voith) to **C** an urban garden (photograph: D. Dozckal).

BOLD workbench and database (Ratnasingham and Hebert 2007). We used the Barcode Index Numbers (BINs) approach (Ratnasingham and Hebert 2013) to define molecular operational taxonomic units (MOTUs) for establishing our molecular species hypotheses. We used BIN distances from the BOLD database to identify possible BIN discrepancies and in some cases calculated distance matrices in BOLD or MEGA for intra- or interspecific distances (Kimura 2-parameter pairwise distances). For those BINs where we found possible BIN-discrepancies, we performed TCS haplotype analysis using PopART (Snell et al. 2002; Leigh and Bryant 2015) and performed clustering using ASAP (Puillandre et al. 2021). The sequences used for our analyses were selected based on sequence length and number of ambiguous characters. For haplotype network analysis, the sequence length is indicated in the description of the figures depicting the haplotype networks (Figs 14, 34, 36), sequence alignments and traits are attached in the Suppl. materials, and the ASAP partitions can be reviewed in Suppl. materials 14 and 15. BINs and BIN assignments are not static and may change as new data is added to BOLD (Ratnasingham and Hebert 2013). Our BIN assignments refer to the latest download of our dataset DS-MC-GNRECG on 9 Aug 2023. All COI sequences are attached in Suppl. material 2.

Morphological workflow

We chemically dried our voucher specimens from Germany using a modified Hexamethyldisilazane (HMDS) protocol (Heraty and Hawks 1998; Rumph and Turner 1998) and glued specimens to points using shellac gel or white glue. His-

torical specimens may have been processed differently. For morphological identification we used various identification keys by Gilbert E. J. Nixon (1965, 1968, 1970, 1972, 1973, 1974, 1976), Jenő Papp (1976a, b, 1978, 1979, 1980, 1981a, 1982, 1983, 1984a, b, 1986a, 1987, 1988, 1990), and Vladimir I. Tobias and Anatoly G. Kotenko (Tobias 1986). Material was also compared to original descriptions and to type material or authoritatively identified material stored in the collections of the CNC, ZSM, or NMS. If photographs of types or authenticated material were available due to previous work done in other institutions, we compared our specimens to these. We provide information about literature and material used for our identifications in the notes for each species. Terminology and measurements used here are explained in detail in Fernandez-Triana et al. (2014c).

Biology (host information)

We checked original descriptions for collecting any host information related to type material. The supposed host data compiled by literature abstraction, such as in the database Taxapad 2016 (Yu et al. 2016), was generally ignored due to its inherently low reliability caused by uncritically citing host associations from literature (Shaw 1994). However, we used this database to selectively track literature on host information, checked the original literature in every single case, and interpreted this information critically. Most importantly, we checked any reared and barcoded material available to us between the collections of the CNC, NMS, and ZSM. We also had access to metabarcoding data from barcoding whole caterpillars as part of the GBOL project. Host information is discussed in the notes section for each species. Synonyms and current combinations for Lepidoptera hosts were checked in Lepiforum's latest checklist for European Lepidoptera (Rennwald et al. 2023).

Additional information, abbreviations, and terminology

New information is marked by an asterisk (*). All original descriptions of the species we report here are cited in the References section. Specimens were photographed using a Keyence VHX-6000 digital microscope and panorama stacks were computed using the built-in software of the microscope. Subsequent processing and construction of image plates and figures was done using Photoshop and Inkscape. Maps were done using QGIS and Inkscape. Voucher codes that are referred to in the notes and material examined sections refer to the "SampleID" in BOLD, more information about these specimens can be retrieved from the supplementary material or from BOLD. We have, however, added MS, MRS, or MRS_JFT voucher codes for barcoded specimens housed in NMS to facilitate retrieval for further examination. Distribution data of specimens is based on the annotated world checklist, as well as abbreviations and limits for the biogeographical regions used by Fernandez-Triana et al. (2020). Abbreviations for biogeographical regions are as follows: **NEO** Neotropical, **NEA** Nearctic, **PAL** Palaearctic, **OTL** Oriental, **AFR** Afrotropical, and **AUS** Australasian and Oceanian (combined following O'Hara et al. 2009). The Holarctic includes the Nearctic and Palaearctic regions. For subsequently described or recorded species, the distribution range is based on the data provided in the respective publication (Shaw 2020, 2022, 2023). Syntax for the Material examined section is as follows: "**COUNTRY**: Province: Exact Location, coordinates in decimal degrees, elevation,

collection method/host, collection date, collector(s), voucher code". If several samples were collected at the same collecting event, several voucher codes are listed consecutively and separated by semicolons. Extrapolated information is bracketed. Different collecting events from the same location are also grouped and are separated by a semicolon. Additional information, e.g., about the sex of a specimen or the storing institution can be reviewed in the Suppl. material 1 and, if any changes happen in the future, will be updated in the BOLD database. Malaise trap specimens were collected during a period of 1–4 weeks (depending on the season: in spring and autumn collecting bottles were left for up to four weeks, and in summer (especially May, June, July, August, and even September) usually not more than two weeks. The date indicated for the collection event represents the day the bottle was collected. For a number of species collected in the former Soviet Union we were able to translate the labels and found that they were collected in countries (Armenia, Moldova, and Ukraine) that were not then formally recorded for these species, but labelled from Russia (which we mitigate here).

Results

Species recorded for Germany and other regions for the first time

Apanteles galleriae Wilkinson, 1932

Material examined. **GERMANY:** Baden-Württemberg, Malsch, Hansjakobstr. 7, Urban Garden, 48.884, 8.32, 120 m, Malaise trap, 27.ix.2020, leg. D. Doczkal, ZSM-HYM-33154-A11; ZSM-HYM-33154-A12; Bavaria: Passau, Heining, 48.583, 13.391, 432 m, Malaise trap, 13.vii.2019, leg. J. Müller, ZSM-HYM-42384-E09; **MALTA:** Zejtun, ex. *Achroia grisella*, 15.viii.2013, leg. D. Mifsud, MRS_JFT0380; **UNITED KINGDOM:** England: Battle, Sussex, 50.917489, 0.483602, ex. beehive with *Galleria mellonella*, xii.2011, leg. J. Feltwell, CNCHYM45392.

Geographical distribution. AFR, AUS, NEA, NEO, OTL, PAL.

AFR- Mauritius, Réunion; AUS- Hawaiian Islands, New Zealand; NEA- Canada (BC), United States (GA, NC, OH, SC); NEO- Argentina, Brazil (SP); OTL- China (FJ, GD, GX, GZ, HI, HN, JX, TW, ZJ), India, Pakistan; PAL- Armenia, Bulgaria, France, Greece, Germany*, Hungary, Iran, Italy, Japan, Malta, Romania, Russia (PRI), Spain, Turkey, United Kingdom.

Molecular data. BIN: BOLD:AAG1400.

Host information. Pyralidae: type reared from *Galleria mellonella* (Linnaeus, 1758) (Wilkinson 1932); also *Achroia grisella* (Fabricius, 1794), *Achroia innonata* (Walker, 1864), *Vitula edmandsii* (Packard, 1865).

Notes. Specimens in BIN BOLD:AAG1400 morphologically identified as *Apanteles galleriae* were reared from both *Galleria mellonella* (CN-CHYM45392=MRS_JFT 0107 ex. beehive with that species) and *Achroia grisella* (MRS_JFT0380). Additional host species recorded for non-type specimens are based on literature (e.g., Shimamori 1987; Watanabe 1987; Okada 1988; Whitfield and Cameron 1993); they are considered to be accurate because of the detailed evidence provided in those papers (rearing details, photos, and images), the expertise of the researchers that identified the parasitoids, and the fact that those host species are all wax moths, related to *G. mellonella*. Additional provinces for China are from Liu et al. (2020). This species is illustrated in Fig. 2.

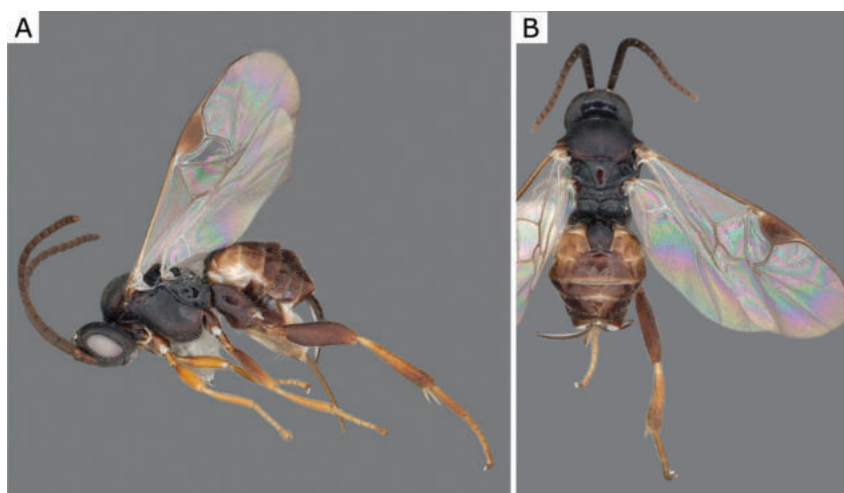


Figure 2. *Apanteles galleriae* Wilkinson, 1932, female (ZSM-HYM-42384-E09) **A** lateral and **B** dorsal views. Length of the specimen: 2.6 mm.

Apanteles kubensis Abdinbekova, 1969

Material examined. **GERMANY:** Baden-Württemberg: Malsch, Hansjakobstr. 7, Urban Garden, 48.884, 8.32, 120 m, Malaise trap, 16.viii.2020, leg. D. Doczkal, ZSM-HYM-33153-F03; Bavaria: Fabrikschleichach, close to Weilersbachtal, 49.917, 10.525, 408 m, Malaise trap, 12.vii.2019, leg. J. Müller, ZSM-HYM-42376-G08; **KOREA:** Daejon-si, Wadong; Chungnam, 36.4006, 127.444, 6.x.2006, leg. P. Tripotin, CNCH2502; CNCH2522; CNCH2526; **UKRAINE:** [translated and transcribed from Russian] Crimea, Angarskiy pass, forest, glades, 11.vii.1979, leg. A. Kotenko, CNCHYM 00136.

Geographical distribution. PAL.

PAL- Azerbaijan, Germany*, Hungary, Iran, Korea, Moldova, Mongolia, Russia (NC, S), Turkey, Ukraine*.

Molecular data. BIN: BOLD:AAH1340.

Host information. Host of type unknown (Abdinbekova 1969); also Tortricidae: *Adoxophyes orana* (Fischer von Röslerstamm, 1834).

Notes. The German specimens were compared with a specimen from Ukraine (CNCHYM 00136=CNC280641) which had been identified by Kotenko in 1981 and donated to the CNC. We also checked the information in Tobias (1986) (the key to “*Apanteles*” sensu lato species in Tobias (1986) was written in collaboration with Kotenko) and also the key in Papp (1980). Additionally, we studied CNC specimens from South Korea (CNCH2502, CNCH2522, CNCH2526) with DNA barcodes that match the sequences from German specimens and the Ukrainian specimen sent to the CNC by Kotenko. The species was recorded from Korea by Ku et al. (2001), and one of the coauthors of that paper, the Bracconidae expert Sergey Belokobylskij, works in the institution storing the type of *A. kubensis*. In BOLD there is also an additional specimen from the Primorskiy Kray, Russia (BIOUG27804-B05) that perfectly matches the German, Korean, and Ukrainian sequences; it most likely represents an additional record of the species for the Russian Far East, but we do not report it here because we could not examine the specimen. The only host reported for *A. kubensis* in the literature (Ku et al. 2001) is from Korea. The distribution in Iran was reported by Samin et al. (2020). This species is illustrated in Figs 3, 4.

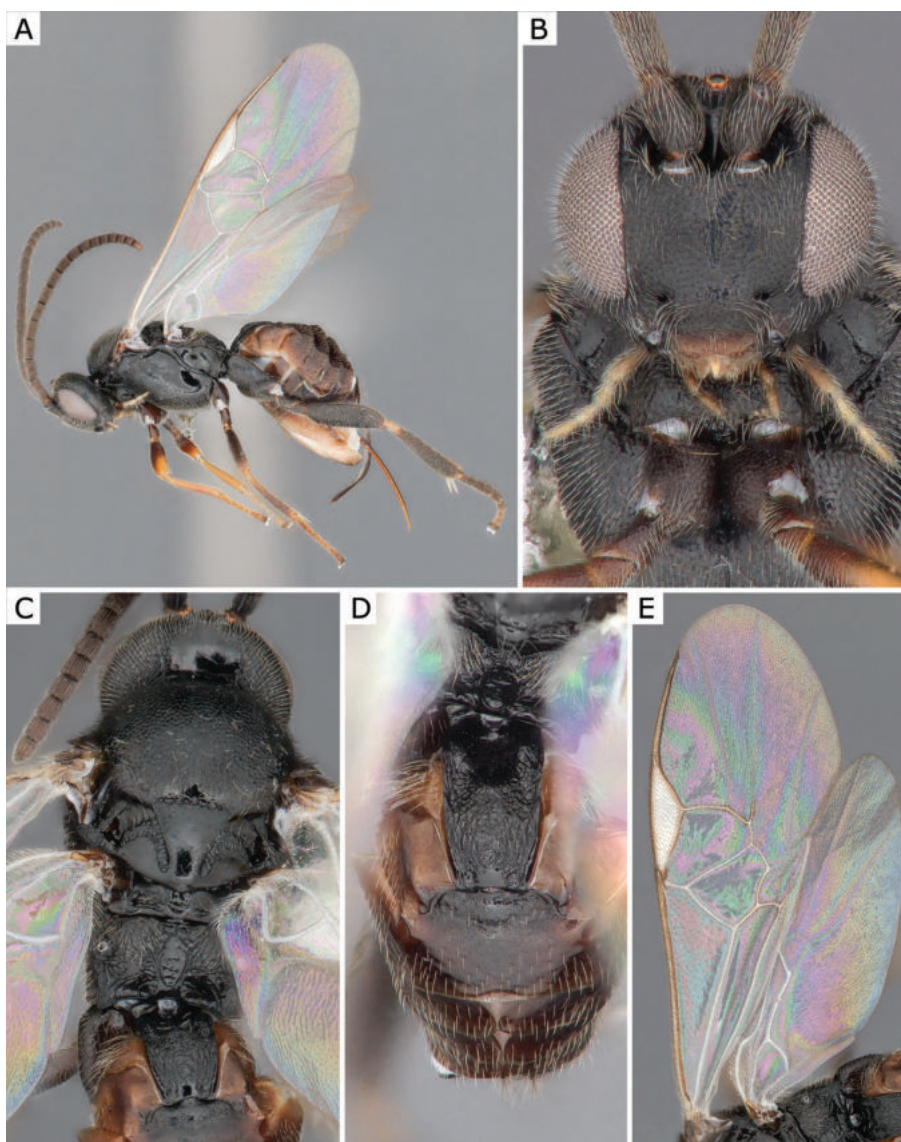


Figure 3. *Apanteles kubensis* Abdinbekova, 1969, female (ZSM-HYM-42376-G08) **A** lateral view **B** head frontal view **C** mesosoma **D** metasoma **E** wing. Length of the specimen: 3 mm.

***Choeras ciscaucasicus* (Tobias, 1971)**

Material examined. **CZECH REPUBLIC:** South Moravia, Obora Soutok, Lanzhot, 48.69, 16.945, 165 m, ex. *Sterrhopterix fusca*, 09.v.2014, leg. P. Drozd, BC-ZSM-HYM-23872-B02; **GERMANY:** Bavaria: Aub, 49.542, 10.053, 316 m, canopy fogging, 10.vii.2020, leg. B. Leroy, ZSM-HYM-42392-B10; Bad Windsheim, 49.482, 10.468, 382 m, canopy fogging, 3.vii.2019, leg. B. Leroy, ZSM-HYM-33158-H02; Iphofen, 49.646, 10.315, 355 m, canopy fogging, 2.vii.2019, leg. B. Leroy, ZSM-HYM-33158-H10; Theres, 49.997, 10.412, 275 m, canopy fogging, 2.vii.2019, leg. B. Leroy, ZSM-HYM-33159-A07.

Geographical distribution. PAL.

PAL- Czech Republic*, Germany*, Lithuania, Russia (AD, PRI).

Molecular data. BIN: BOLD:ACU3996.

Host information. Host of type unknown; also Psychidae*: *Sterrhopterix fusca** (Haworth, 1809).

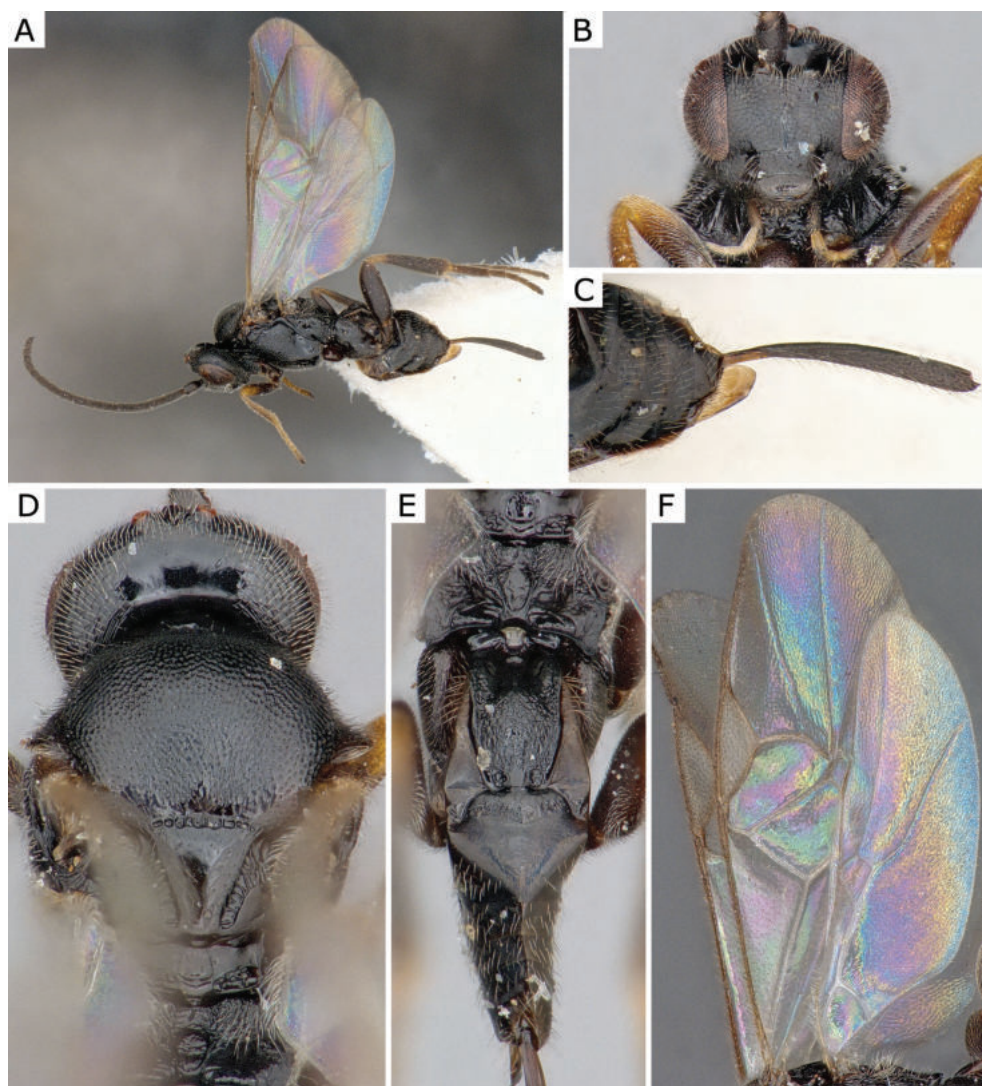


Figure 4. *Apanteles kubensis* Abdinbekova, 1969, female (CNCHYM 00136) **A** lateral view **B** head frontal view **C** hypopygium lateral view **D** mesosoma **E** metasoma **F** wing.

Notes. This species is morphologically very distinct from all other Palaearctic species of *Choeras* and can be identified by the combination of the following characters: T1 strongly narrowing; ovipositor sheaths short, $\sim \frac{1}{2}$ length of metatibia; propodeum smooth and shiny; T1 and T2 smooth, with only slight wrinkles on the posterior half of T1. Our German specimens keyed out as *Choeras ciscaucasicus* in all keys that we used (Papp 1983; Tobias 1986; van Achterberg 2002; Kotenko 2007). One Czech Republic specimen stored at the ZSM (BC-ZSM-HYM-23872-B02) was reared from *Sterrhopterix fusca* (Psychidae) and represents the first host associated with *Choeras ciscaucasicus*. This species is illustrated in Figs 5, 6.

***Choeras gnarus* (Tobias & Kotenko, 1984)**

Material examined. GERMANY: Baden-Württemberg: Gaggenau, Michelbach, 48.821, 8.388, 340 m, Malaise trap, 9.vii.2011, leg. D. Doczkal, ZSM-HYM-42398-H04; Gaggenau, Sulzbach, Querbach, 48.797, 8.378, 375 m, Malaise trap, 21.viii.2011, leg. D. Doczkal, ZSM-HYM-42323-A10; Malsch, Hansjakobstr. 7,

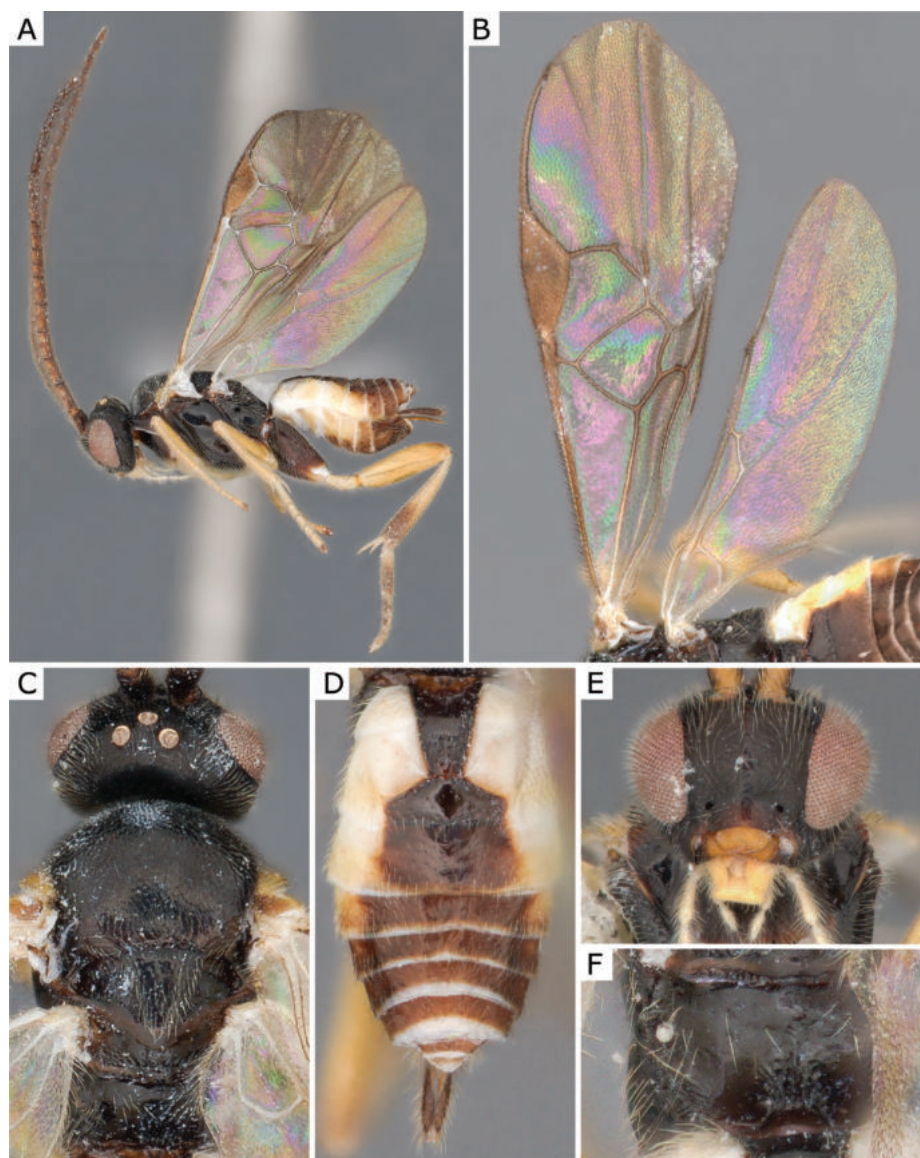


Figure 5. *Choeras ciscaucasicus* (Tobias, 1971), female (ZSM-HYM-42392-B10) **A** lateral view **B** wing **C** mesosoma **D** metasoma **E** head frontal view **F** propodeum. Length of the specimen: 2.85 mm.

Urban Garden, 48.884, 8.32, 120 m, Malaise trap, 16.viii.2020, leg. D. Doczkal, ZSM-HYM-33153-F04; 19.vii.2020, leg. D. Doczkal, ZSM-HYM-33154-G09; 2.viii.2020, leg. D. Doczkal, ZSM-HYM-33154-H03; 21.vi.2020, leg. D. Doczkal, ZSM-HYM-33152-G01; 5.vii.2020, leg. D. Doczkal, ZSM-HYM-33154-E12; Malsch, Luderbusch, 48.913, 8.332, 117 m, Malaise trap, 16.viii.2020, leg. D. Doczkal, K. Grabow, ZSM-HYM-42389-C05; 26.vii.2020, leg. D. Doczkal, K. Grabow, ZSM-HYM-42388-G07; 9.viii.2020, leg. D. Doczkal, K. Grabow, ZSM-HYM-42389-B05; Bavaria: Ammergebirge Halblech, Im Laich, gravel bar, 47.606, 10.841, 901 m, Malaise trap, 17.viii.2016, leg. D. Doczkal, J. Voith, ZSM-HYM-33166-F09; 29.vii.2016, leg. D. Doczkal, J. Voith, ZSM-HYM-33166-E07; 904 m, Malaise trap, 17.viii.2016, leg. D. Doczkal, J. Voith, ZSM-HYM-33167-C07; 29.vii.2016, leg. D. Doczkal, J. Voith, ZSM-HYM-33167-A04; ZSM-HYM-33167-A05; ZSM-HYM-33167-A07; ZSM-HYM-33167-A08; Aub, 49.542, 10.053, 316 m, fogging, 10.vii.2020, leg. B. Leroy, ZSM-HYM-42392-D03; Bamberg, Naturwaldreservat Wolfsruhe, Bruderwald, 49.856, 10.899, 282 m, Malaise trap, 13.vii.2019, leg. J. Müller, ZSM-HYM-42382-B05;

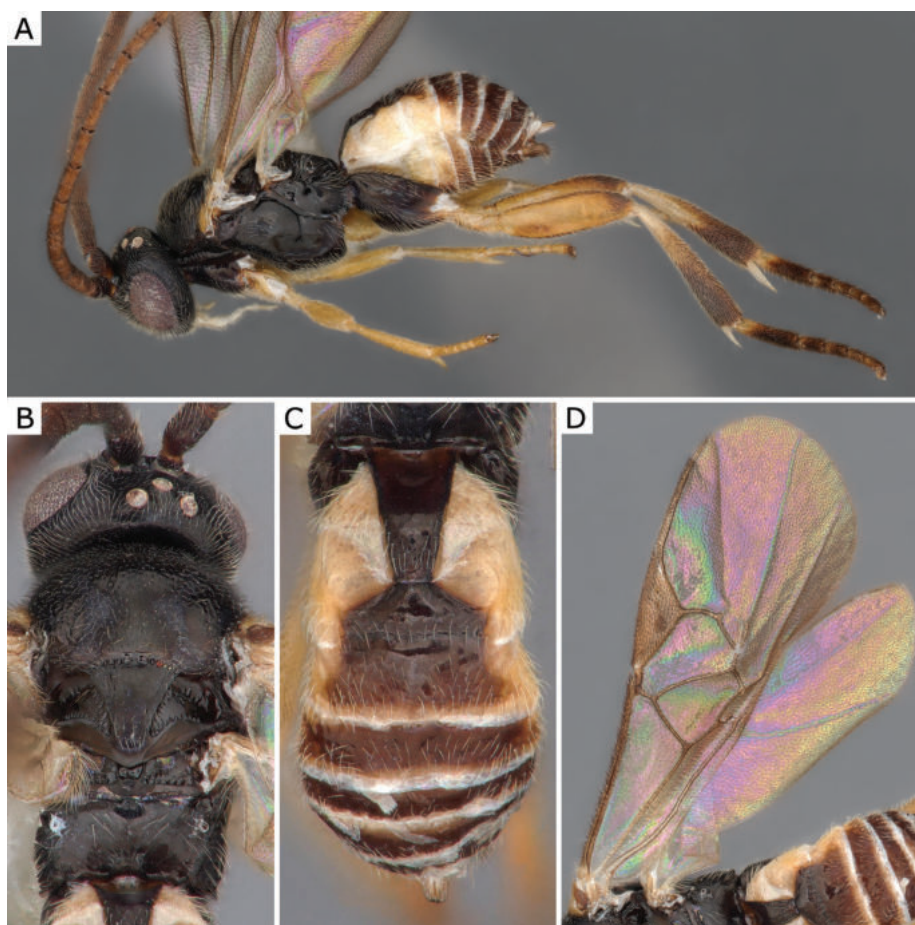


Figure 6. *Choeras ciscaucasicus* (Tobias, 1971), male (ZSM-HYM-33159-A07) **A** lateral view **B** mesosoma **C** metasoma **D** wing. Length of the specimen: 2.65 mm.

ZSM-HYM-42382-B06; Chiemgau Alps Ruhpolding, Fischbach, 47.709, 12.657, 720 m, Malaise trap, 16.viii.2016, leg. D. Doczkal, J. Voith, ZSM-HYM-33168-B02; Fabrikschleichach, close to Weilersbachtal, 49.917, 10.525, 408 m, Malaise trap, 12.vii.2019, leg. J. Müller, ZSM-HYM-42376-E07; Haselbach, Wald, 48.642, 11.019, 485 m, Malaise trap, 15.vii.2019, leg. J. Müller, ZSM-HYM-42383-A11; Jöslein, Forst Neustädtlein am Forst, 49.992, 11.482, 411 m, Malaise trap, 13.vii.2019, leg. J. Müller, ZSM-HYM-42385-F03; Lohr a. M., Romberg, 49.986, 9.59, 185 m, Malaise trap, 6.vii.2018, leg. D. Doczkal, ZSM-HYM-42323-F09; Marquartstein, close to Berg Torkopf, 47.767, 12.43, 786 m, Malaise trap, 19.vii.2019, leg. J. Müller, ZSM-HYM-42383-F04; Mauth, Naturpark Bayerischer Wald, 48.89, 13.563, 858 m, Malaise trap, 12.vii.2019, leg. J. Müller, ZSM-HYM-42381-C04; Moos, Isarmündung, 48.786, 12.959, 313 m, Malaise trap, 13.vii.2021, leg. GBOL3, R. Albrecht, ZSM-HYM-42394-F09; Moos, Isarmündung, *Molinia* meadow, 48.779, 12.95, 313 m, Malaise trap, 25.viii.2021, leg. GBOL3, R. Albrecht, ZSM-HYM-42394-E11; München, NSG Allacher Lohe, 48.201, 11.483, 499 m, Malaise trap, 21.vii.2021, leg. GBOL3, R. Albrecht, ZSM-HYM-42326-H02; Berchtesgaden National Park, Königssee, Rinnkendlsteig, 47.551, 12.964, 695 m, Malaise trap, 4.x.2017, leg. D. Doczkal, J. Voith, ZSM-HYM-33162-B10; Berchtesgaden National Park, Wald west of St. Bartholomä, 47.547, 12.965, 620 m, Malaise trap, 28.vi.2017, leg. D. Doczkal, J. Voith, ZSM-HYM-33156-G05; Oberndorf, close to Krebsbach, 49.868, 9.516, 342 m, Malaise trap, 13.vii.2019, leg. J. Müller, ZSM-

HYM-42382-H01; Willersdorf, Untere Mark, 49.733, 10.985, 292 m, Malaise trap, 12.vii.2019, leg. J. Müller, ZSM-HYM-42379-A06; München, Obermenzing, Premises of Zoologische Staatssammlung, 48.1648, 11.4849, 519 m, Malaise trap, 31.vii.2017, leg. Axel Hausman, BIOUG42697-G11; **MOLDOVA**: [translated and transcribed from Russian] Rajon Anenii Noi, Hîrbovăţ, 4.vi.1986, CNCHYM 00280; **SWEDEN**: Dalarna: Säterdalen, Näsåkerspussen; Sätters kommun, 60.366667, 15.716667, Malaise trap, 8–21.vii.2003, leg. SMTP, CNC472136; [no collection information associated] WAM 0076; Sm, Nybro kommun, Alsterbro/Alsteran., 63.122200, 15.069970, Malaise trap, 20–25.viii.2005, leg. SMTP, CNC1967347.

Geographical distribution. PAL.

PAL- Belarus, Germany*, Moldova*, Russia (NC, C), Sweden*, Ukraine.

Molecular data. BIN: BOLD:AAU6216.

Host information. Unknown.

Notes. The German specimens were compared with a specimen from Moldova (CNCHYM 00280) which had been identified by Kotenko in 1986 and donated to the CNC. We also ran our specimens through the keys of Tobias (1986), van Achterberg (2002), and Kotenko (2007) where they match *Choeras gnarus* also in accordance with Kotenko's specimen at the CNC (CNCHYM 00280). In Abdoli et al. (2019), some of our specimens match *Choeras formosus* Abdoli & Fernandez-Triana, 2019 from Iran, based on the presence of a well-defined median carina on the propodeum. However, this character is variable in our specimens ranging from irregular rugosities to an incomplete to clearly defined median carina (see Fig. 8). In addition to morphology, our barcodes match a barcoded specimen from Moldova (CNCHYM 00280) by 100%, authoritatively identified by A. Kotenko, who is an author of the species. The presence/absence of a median carina as a character to identify species of *Choeras* may have to be reassessed in the future. This species is illustrated in Figs 7–9.

***Cotesia coryphe* (Nixon, 1974)**

Material examined. **AUSTRIA**: Hinterreit, Gemeinde Großgmain, 47.75, 12.946, 493 m, ex. *Hemaris fuciformis*, 22.vi.2021, leg. W. Langer, ZSM-HYM-ZLAB01-E11; **GERMANY**: Baden-Württemberg: Malsch, Hansjakobstr. 7, Urban Garden, 48.884, 8.32, 120 m, Malaise trap, 2.viii.2020, leg. D. Doczkal, ZSM-HYM-33154-H02; Bavaria: Arnstein, Rieden, 49.938, 10.051, 260 m, Malaise trap, 16.vii.2019, leg. J. Müller, ZSM-HYM-42385-H08; Bad Königshofen, 50.292, 10.484, 274 m, Malaise trap, 16.vii.2019, leg. J. Müller, ZSM-HYM-42384-E11; Forchheim, Untere Mark close to Willersdorf, 49.739, 10.969, 261 m, Malaise trap, 12.vii.2019, leg. J. Müller, ZSM-HYM-42377-E08; Isarmündung, Magerrasen, swampy, 48.78, 12.966, 313 m, sweeping, 30.vi.2021, leg. A. Höcherl, ZSM-HYM-ZLAB01-C05; Lkr. Kelheim Abensberg-Sandharlanden, NSG Sandharlandener Heide, 48.845, 11.801, 376 m, Malaise trap, 3.viii.2017, leg. D. Doczkal, J. Voith, ZSM-HYM-33157-E11; ZSM-HYM-33157-G09; ZSM-HYM-33157-G10; ZSM-HYM-33157-G11; ZSM-HYM-33157-G12; 8.ix.2017, leg. D. Doczkal, J. Voith, ZSM-HYM-33157-H07; Moos, Isarmündung, Magerrasen, swampy, 48.78, 12.966, 313 m, Malaise trap, 25.viii.2021, leg. GBOL3, R. Albrecht, ZSM-HYM-42396-F08; München, NSG Allacher Lohe, 48.199, 11.475, 502 m, Malaise trap, 21.vii.2021, leg. GBOL3, R. Albrecht, ZSM-HYM-42326-D06; 23.vi.2021, leg. GBOL3, R. Al-

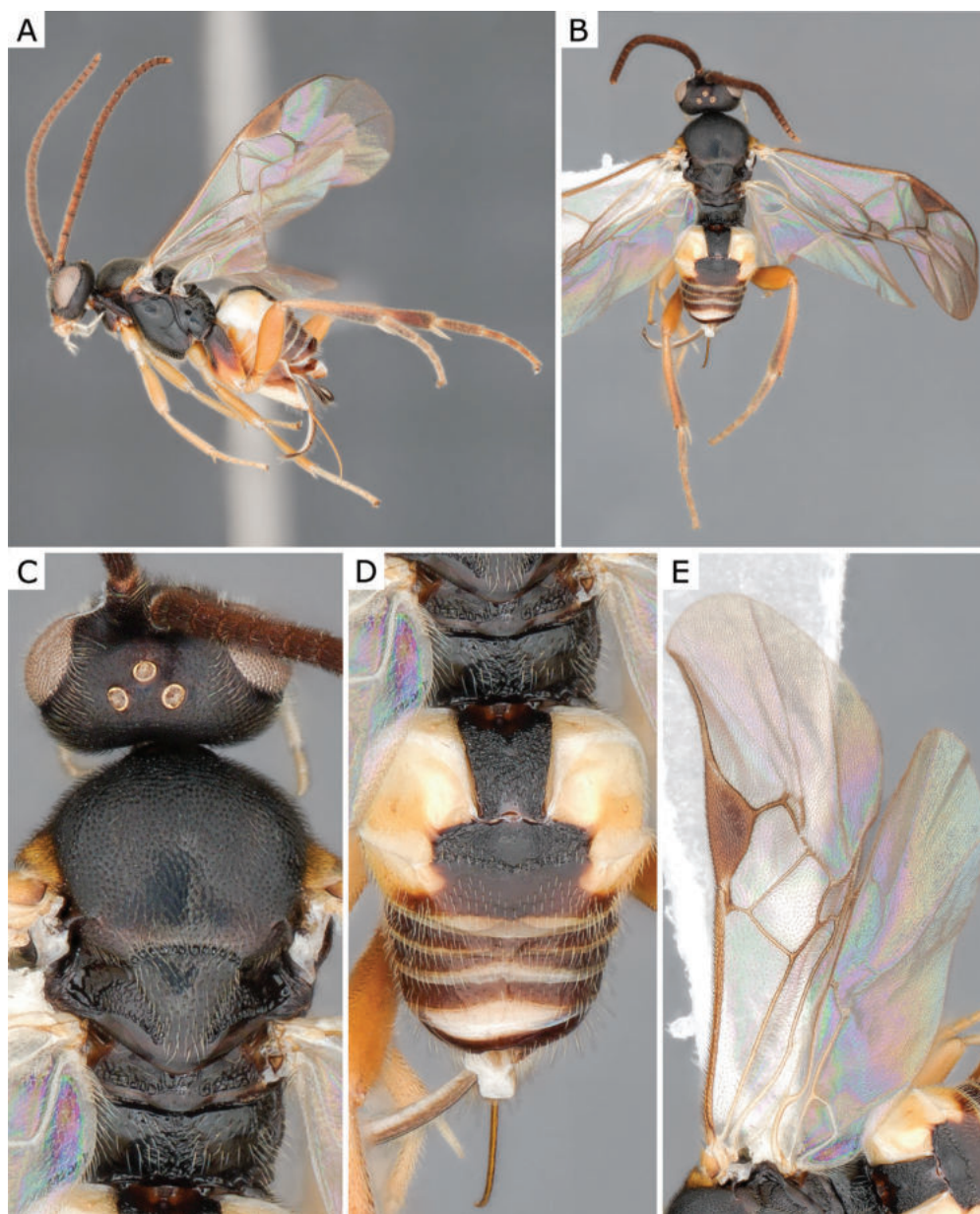


Figure 7. *Choeras gnarus* (Tobias & Kotenko, 1984), female (ZSM-HYM-33167-A07) **A** lateral view **B** dorsal view **C** mesosoma **D** metasoma **E** wing. Length of the specimen: 3.35 mm.

brecht, ZSM-HYM-42326-B06; Berchtesgaden National Park, Königssee, Rinnkendlsteig, 47.553, 12.964, 775 m, Malaise trap, 30.vii.2017, leg. D. Doczkal, J. Voith, ZSM-HYM-33161-B03; Oberndorf, close to Krebsbach, 49.868, 9.516, 342 m, Malaise trap, 13.vii.2019, leg. J. Müller, ZSM-HYM-42382-G12; Oberstdorf, Oytal, rubble cone east of Gleitweg, 47.389, 10.348, 1200 m, 16.vi.2014, leg. D. Doczkal, S. Schmidt, J. Voith, ZSM-HYM-33420-A03; Sielstetten, östlich Grafendorfer Forst, 48.578, 11.863, 520 m, Malaise trap, 16.vii.2019, leg. J. Müller, ZSM-HYM-42383-A01; München, Obermenzing, Premises of Zoologische Staatssammlung, 48.1648, 11.4849, 519 m, Malaise trap, 31.vii.2017, leg. Axel Hausmann, BIOUG42687-C04; BIOUG42697-G07; **NETHERLANDS:** Noord Holland, duinreservaat Egmond aan Zee, ex. *Hemaris fuciformis*, 17.vii.2016, leg. M. R. Shaw, MRS_JFT0691; **UNITED KINGDOM:** England: Wiltshire, Bentley Woods, ex. *Hemaris tityus*, 26.vi.2011, leg. M. Townesend, CNCHYM45325.

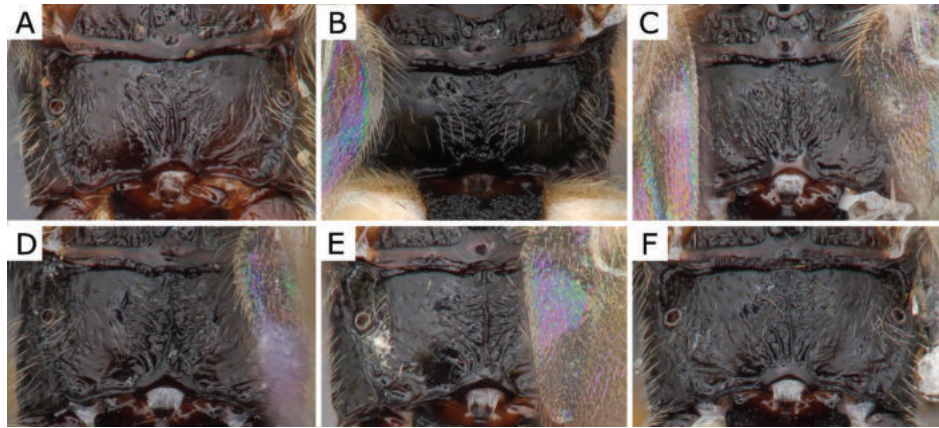


Figure 8. *Choeras gnarus* (Tobias & Kotenko, 1984) female propodeum **A** CNCHYM 00280 (Moldova) **B** ZSM-HYM-33167-A07 (Germany) **C** ZSM-HYM-42379-A06 (Germany) **D** CNC472136 (Sweden) **E** ZSM-HYM-33162-B10 (Germany) **F** ZSM-HYM-33167-A04 (Germany).

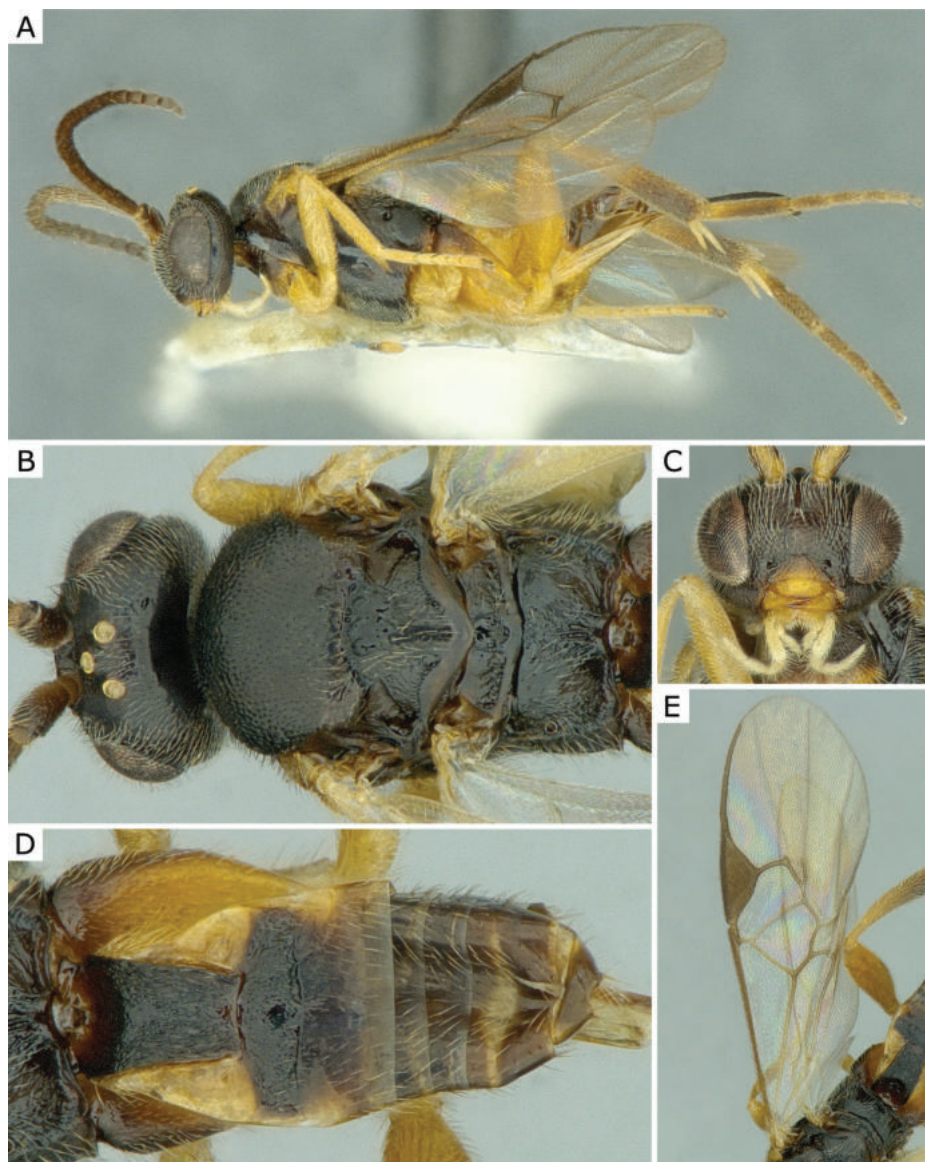


Figure 9. *Choeras gnarus* (Tobias & Kotenko, 1984), female (CNCHYM 00280) identified by A. Kotenko **A** lateral view **B** mesosoma **C** head frontal view **D** metasoma **E** wing. Length of the specimen: 2.95 mm.

Geographical distribution. PAL.

PAL: Austria*, Germany*, Netherlands*, United Kingdom.

Molecular data. BIN: partially BOLD:AAA7143.

Host information. Sphingidae: type reared from *Hemaris fuciformis* (Linnaeus, 1758); also *Hemaris tityus** (Linnaeus, 1758).

Notes. The German specimens were identified using Nixon (1974). Our sequences of this species were formerly part of BIN BOLD:ABY6805 and merged into BOLD:AAA7143 in February 2023. This BIN includes many clearly different species of *Cotesia*; see discussion below about this “megaBIN”. ASAP clustering resolves this species as a single cluster. One of the specimens that we examined (ZSM-HYM-ZLAB01-E11) and another specimen in this cluster (MRS_JFT0691) were reared from *Hemaris fuciformis*, which is congruent with the host information given in the original description of the species (Nixon 1974). A specimen from the United Kingdom (CNCHYM45325=MRS_JFT 0223) reared from *Hemaris tityus* represents an additional host record for *Cotesia coryphe*. This species is illustrated in Fig. 10.

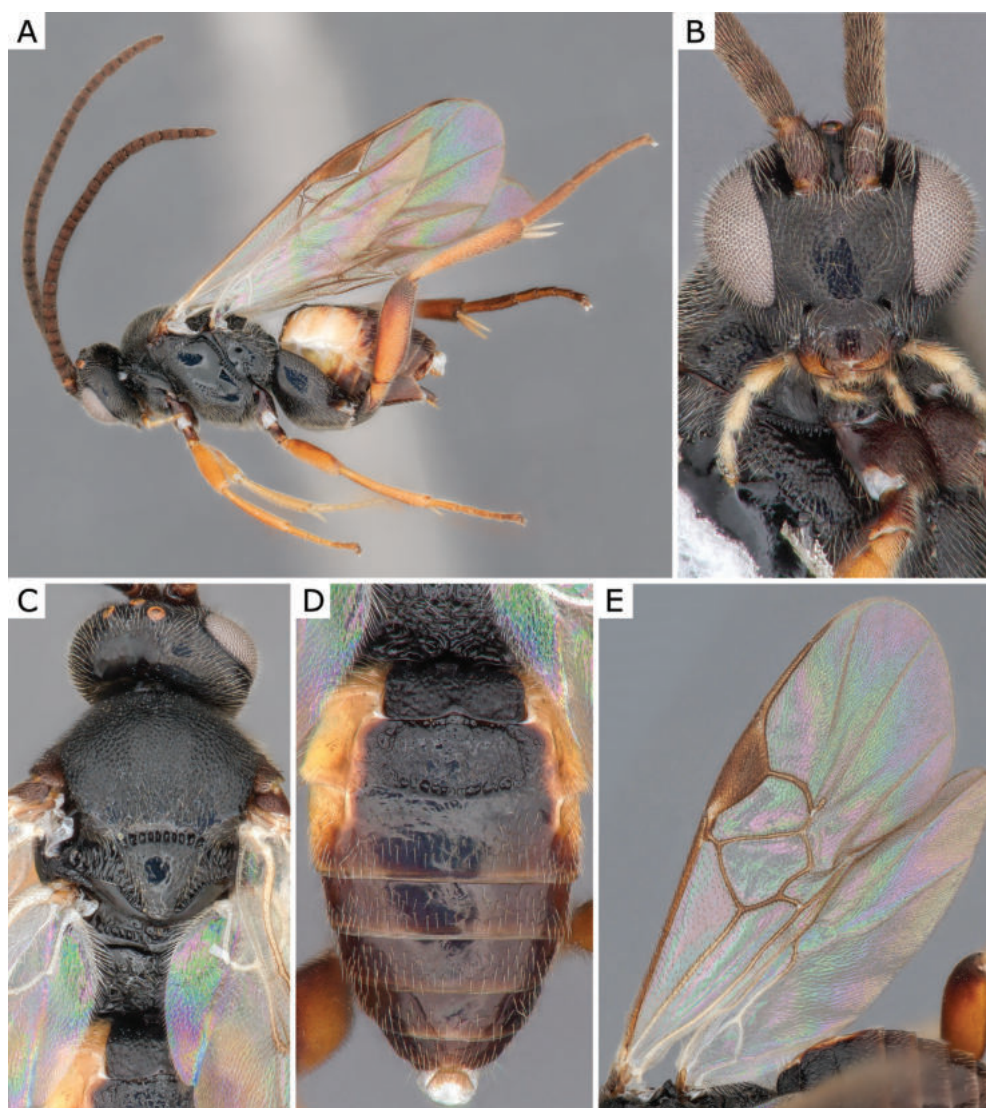


Figure 10. *Cotesia coryphe* (Nixon, 1974), female (ZSM-HYM-33157-E11) **A** lateral view **B** head frontal view **C** mesosoma **D** metasoma **E** wing. Length of the specimen: 2.85 mm.

***Cotesia eunomia* Shaw, 2009**

Material examined. **BELGIUM:** Luxembourg, Pisserotte, ex. *Boloria eunomia*, vi.2004, leg. J. Choutt, individuals from separate gregarious broods, MS 106; MS 107; MS 108; **FINLAND:** Janakkala, ex. *Boloria eunomia*, 14.vi.1992, leg. M. R. Shaw, MRS-JFT 0655; MRS-JFT 0656; **FRANCE:** Pyrénées-Orientales, Porte, ex. *Boloria eunomia*, 30.v.2001, leg. T. Lafranchis, MRS_JFT 0118; **GERMANY:** Bavaria: Rhön, Hausen, Kleines Moor, 50.487, 10.039, 890 m, Malaise trap, 11.vii.2018, leg. D. Doczkal, ZSM-HYM-33165-E05.

Geographical distribution. PAL.

PAL- Belgium, Finland*, France*, Germany*.

Molecular data. BIN: BOLD:AAV9098.

Host information. Nymphalidae: type reared from *Boloria eunomia* (Esper, 1800).

Notes. Our specimen from Germany matches the original description and clusters very closely (max. p-dist 0.34%) with six specimens (MRS-JFT 0655, MRS-JFT 0656, MS 106, MS 107, MS 108, MRS_JFT0118) reared from *Boloria eunomia*, the host of the holotype (Shaw 2009). This wasp species appears to be completely specialised to *Boloria eunomia*, which is classified as a highly endangered species in Bavaria and Germany (Reinhardt and Bolz 2011; Voith et al. 2016). As our German specimens are not reared, we checked the platform iNaturalist (<https://www.inaturalist.org/>) to verify whether this rather rare host occurs in this area. In a 5 km radius of our sampling site we found eight observations of *B. eunomia*. All these observations were confirmed by a lepidopterist via photos uploaded to iNaturalist. This species is illustrated in Fig. 11.

***Cotesia inducta* Papp, 1973**

Material examined. **GERMANY:** Bavaria: Oberstdorf, Oytal, rubble cone east of Gleitweg, 47.389, 10.348, 1200 m, Malaise trap, 16.vi.2014, leg. D. Doczkal, S. Schmidt, J. Voith, ZSM-HYM-33420-A02; **SPAIN:** Córdoba, Huerta El Caño, ex. *Leptotes pirithous*, 15.vi.2012, leg. R. Obregón, MRS_JFT0268; Córdoba, Los Ídolos, ex. *Leptotes pirithous*, 5.xii.2013, leg. R. Obregón, MRS_JFT0425; **UNITED KINGDOM:** England: Biggleswade, ex. *Satyrion w-album*, 01.vi.2005, leg. R. Revels, MS 005.

Geographical distribution. PAL.

PAL- Bulgaria, Germany*, Hungary, Ireland, Israel, Korea, Moldova, Russia (KDA, PRI), Slovakia, Spain, Turkey, Ukraine, United Kingdom, Uzbekistan.

Molecular data. BIN: BOLD:AAV9096.

Host information. Host of type unknown; also Lycaenidae: *Callophrys avis* Chapman, 1909, *Celastrina argiolus* (Linnaeus, 1758), *Glaucopsyche melanos* (Boisduval, 1828), *Leptotes pirithous** (Linnaeus, 1767), *Satyrion w-album* (Knoch, 1782), *Tomares ballus* (Fabricius, 1787).

Notes. German specimens were compared with the description and keys in Papp (1973, 1986a, 1987) and Shaw (2007). No host was mentioned in the original description (Papp 1973) nor in later mentions of this species by its author (cf. Papp 1990). For more detailed and updated information on hosts and distribution of this species see Shaw (2007). Two specimens reared from *Leptotes pirithous* (MRS_JFT0268, MRS_JFT0425) represent a new host record and cluster in the same BIN as our German specimens. This species is illustrated in Fig. 12.

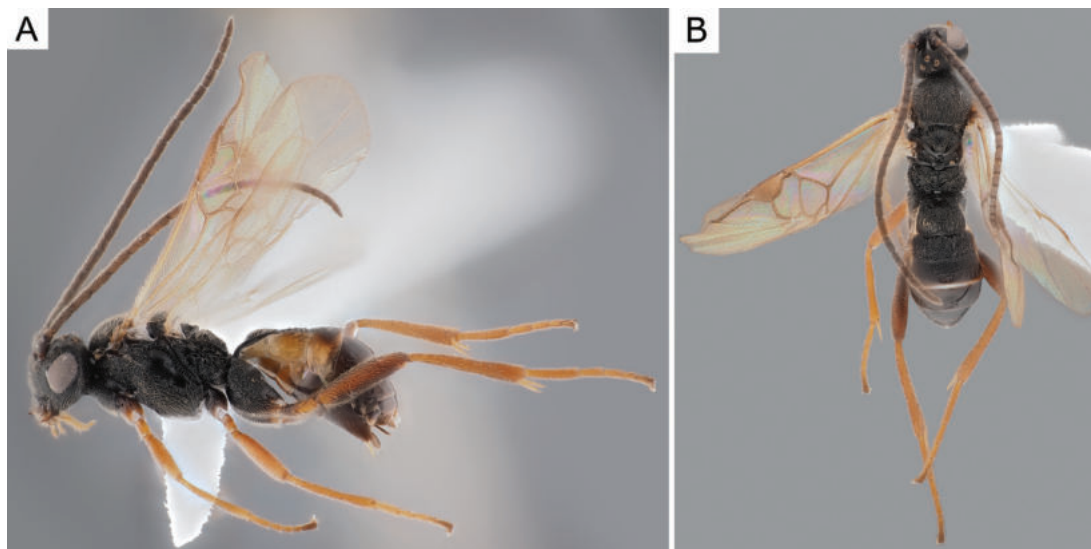


Figure 11. *Cotesia eunomiae* Shaw, 2009, female (ZSM-HYM-33165-E05) **A** lateral and **B** dorsal views. Length of the specimen: 2.9 mm.

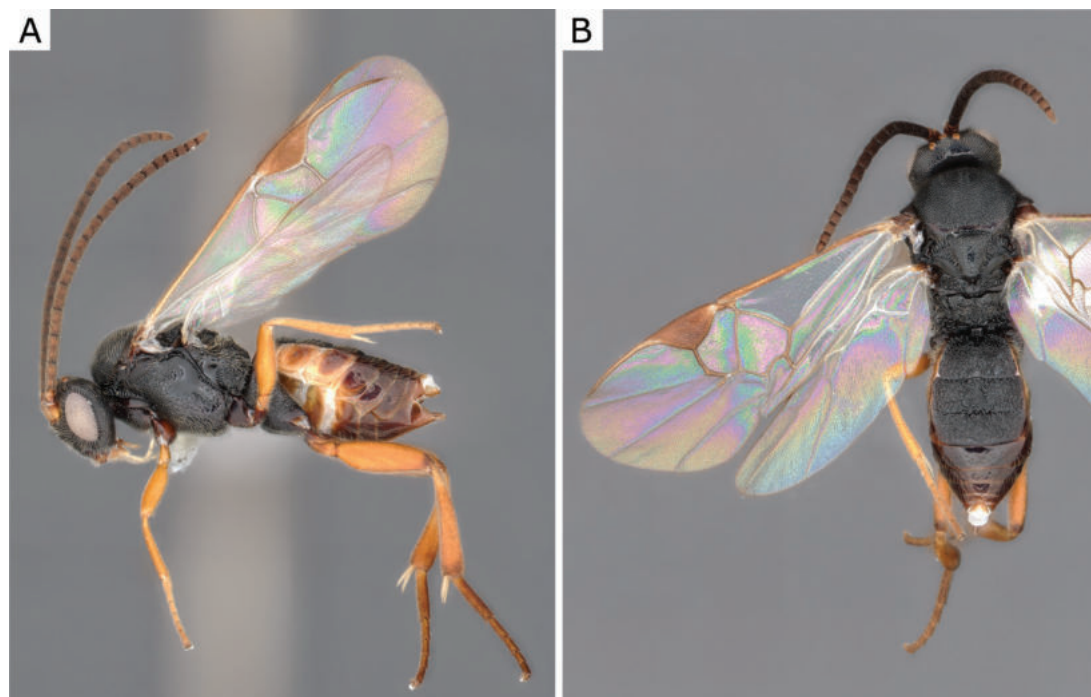


Figure 12. *Cotesia inducta* Papp, 1973, female (ZSM-HYM-33420-A02) **A** lateral and **B** dorsal views. Length of the specimen: 2.9 mm.

***Cotesia mendicae* (Tobias, 1986)**

Material examined. **AUSTRIA:** Lower Austria, Raglitz, ex. *Phragmatobia fuliginosa*, 06.viii.2006, leg. J. Connell, MS 055; **GERMANY:** Bavaria: Balderschwang, Leiterberg, 47.489, 10.088, 1600 m, Malaise trap, 21.ix.2017, leg. D. Doczkal, J. Voith, ZSM-HYM-42326-A10.

Geographical distribution. PAL.

PAL: Austria*, Germany*, Kazakhstan, Russia (VOR).

Molecular data. BIN: partially BOLD:AAA7143.

Host information. Host of (para-)type *Diaphora mendica* (Clerck, 1759); also Erebidae: *Phragmatobia fuliginosa** (Linnaeus, 1758).

Notes. Specimens were compared with the information provided in Tobias (1986) and Papp (1990). The specimen from Austria (MS 055) was compared to a paratype and reared from the same host group as the paratype. The COI barcode sequences of the Austrian and German specimens match 100% over a length of 616 bp and the specimens are very similar in morphology. This BIN includes many clearly different species of *Cotesia*; see discussion below about this “megaBIN”. ASAP clustering resolves the sequences of this species as a single cluster. No host is mentioned in the original description (Tobias 1986) but the paratype seen by Mark Shaw is labelled as from “*S.*” *mendica* [*Diaphora mendica* (Clerck, 1759)]. Here we present a related host record from *Phragmatobia fuliginosa* based on a gregarious brood from Austria (MS 055). Our sequences of this species are part of BIN BOLD:AAA71433. This species is illustrated in Fig. 13.

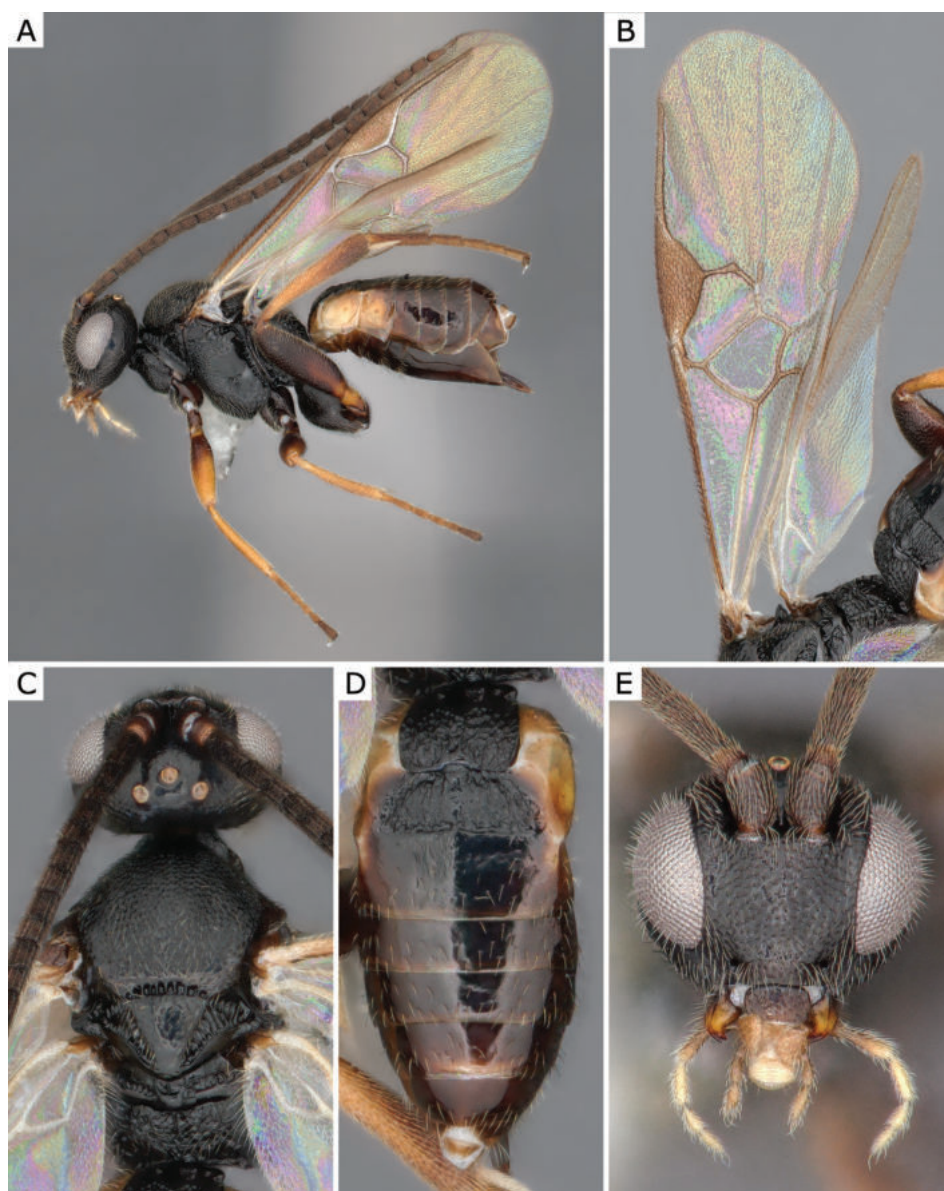


Figure 13. *Cotesia mendicae* (Tobias, 1986), female (ZSM-HYM-42326-A10) **A** lateral view **B** wing **C** mesosoma **D** metasoma **E** head frontal view. Length of the specimen: 2.85 mm.

***Cotesia risilis* (Nixon, 1974)**

Material examined. **FINLAND:** Uusimaa: Helsinki, Kaisaniemi Botanic Garden, 60.175700, 24.944700, Malaise trap, 29.viii-5.ix.2018, leg. J. Paukkunen, CNC1182785; **FRANCE:** Var, Callas, ex. *Satyrium w-album*, 5.v.2015, leg. P. Kan, B. Kan, MRS-JFT 0604; **GERMANY:** Baden-Württemberg: Malsch, Luderbusch, 48.913, 8.332, 117 m, Malaise trap, 26.vii.2020, leg. D. Doczkal, K. Grabow, ZSM-HYM-42388-G06; Bavaria: Bad Tölz, forest close to Isarstausee, 47.77, 11.547, 652 m, Malaise trap, 16.vii.2019, leg. J. Müller, ZSM-HYM-42378-F10; Chiemgau Alps, Ruhpolding, Fischbach, 47.709, 12.657, 720 m, Malaise trap, 30.viii.2016, leg. D. Doczkal, J. Voith, ZSM-HYM-33168-B10; Moos, Isarmündung, Magerrasen, swampy, 48.78, 12.966, 313 m, Malaise trap, 29.vii.2021, leg. GBOL3, R. Albrecht, ZSM-HYM-42396-E05; Moos, Isarmündung, 48.792, 12.968, 312 m, Malaise trap, 30.vi.2021, leg. GBOL3, R. Albrecht, ZSM-HYM-42395-B05; München, Fasanerie, Feldmoching, close to the train tracks, 48.193, 11.517, 509 m, Malaise trap, 9.vii.2019, leg. J. Müller, ZSM-HYM-42379-C09; Berchtesgaden National Park, Königssee, Rinnkendlsteig, 47.553, 12.964, 775 m, Malaise trap, 30.vii.2017, leg. D. Doczkal, J. Voith, ZSM-HYM-33161-B04; ZSM-HYM-33161-B05; 47.555, 12.965, 750 m, Malaise trap, 9.viii.2017, leg. D. Doczkal, J. Voith, ZSM-HYM-33161-H08; Neu-Geusmanns, Wald, 49.76, 11.48, 474 m, Malaise trap, 13.vii.2019, leg. J. Müller, ZSM-HYM-42378-B07; ZSM-HYM-42378-B08; **SPAIN:** Barcelona, Valles Oriental, St Pere de Vilamajor, ex. *Gonepteryx* cf. *ramni*, 21.vi.2009, leg. C. Stefanescu, MS 095.

Geographical distribution. PAL.

PAL- Finland*, France, Germany*, Greece, Hungary, Iran, Italy, Mongolia, Montenegro, Netherlands, Romania, Slovakia, Spain, Sweden, Turkey, United Kingdom.

Molecular data. BIN: partially BOLD:AAA6099.

Host information. Pieridae: type reared from *Gonepteryx ramni* (Linnaeus, 1758); also Lycaenidae: *Satyrium w-album* (Knoch, 1782).

Notes. Barcoding cluster BIN BOLD:AAA6099 currently includes 155 sequences which have been assigned seven species names: *Cotesia risilis*, *C. saltatoria* (+ *C. cf. saltatoria*), *C. amesis*, *C. ancilla*, *C. cyaniridis*, *C. kazak*, and *C. flaviconchae*. The barcoding cluster also includes a large number of specimens from the Nearctic currently labelled as “*Cotesia jft09*”. Many of these species names are represented by reared material and, based on morphology and biology, clearly represent different species. They are all parasitoids of Pieridae and Lycaenidae with the exception of *C. kazak* (which might have been a misidentification) and possibly *C. flaviconchae*.

We performed a Haplotype Network analysis including most sequences in this BIN (excluding specimens CNCHYM00406 (*C. cyaniridis*) and DQ538819 (*C. flaviconchae*) due to the sequences being significantly shorter than the other available sequences and with incomplete collection data). Our German material clusters in eight different haplotypes (Fig. 14) that include at least three different species identifications. However, we observed that some of our sequences (all voucher codes in material section of this species) are separated by at least four mutations from all other sequences in this BIN and 100% match the sequence of a specimen from Spain (MS 095) identified as *C. risilis* reared from *Gonepteryx* cf. *ramni*, the host of the holotype. Morphological examination confirmed that our voucher specimens match the species concept of *C. risilis*

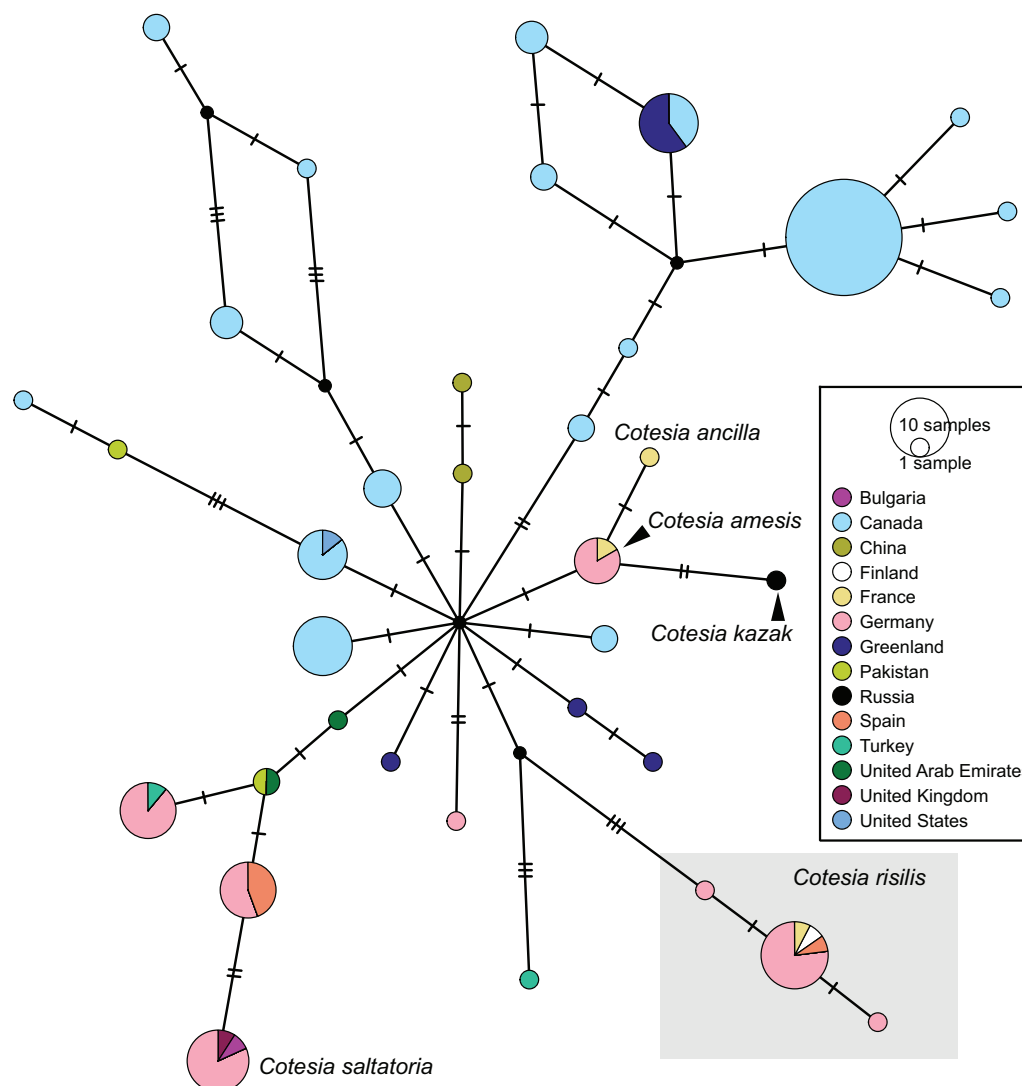


Figure 14. TCS haplotype network of BIN BOLD:AAA6099, sequence length for analysis: 504 bp. The haplotypes morphologically identified as *Cotesia risilis* as part of this project are marked by a box. Each hatch mark in the network represents a single mutational change; small black dots at nodes indicate missing haplotypes. The diameter of the circles is proportional to the number of haplotypes sampled and the countries are colour-coded. The aligned sequences and traits can be reviewed in Suppl. materials 8, 9.

(Nixon 1974). Distance matrix analysis of these specimens showed 0.31% intraspecific p-distance for *C. risilis*. Another specimen identified as *C. risilis* from France (the sequence of which is also part of this *C. risilis* haplotype) was reared from *Satyrion w-album* (MRS-JFT 0604). A host record from *Gonepteryx cleopatra* (Linnaeus, 1767) in Spain is called into doubt by Shaw and Colom (2023) as probably *G. rhamni*. This species is illustrated in Fig. 15.

Cotesia selenevora Shaw, 2009

Material examined. **BELGIUM:** Luxembourg: Libin, ex. *Boloria selene*, 01.vi.2008, leg. J. Choutt, MRS-Cot-cal [paratype]; **GERMANY:** Bavaria: Lkr. Kelheim, Siegenburg, Bombodrom, 48.755, 11.791, 411 m, Malaise trap, 8.ix.2017, leg. D. Doczkal, J. Voith, ZSM-HYM-33169-A02.

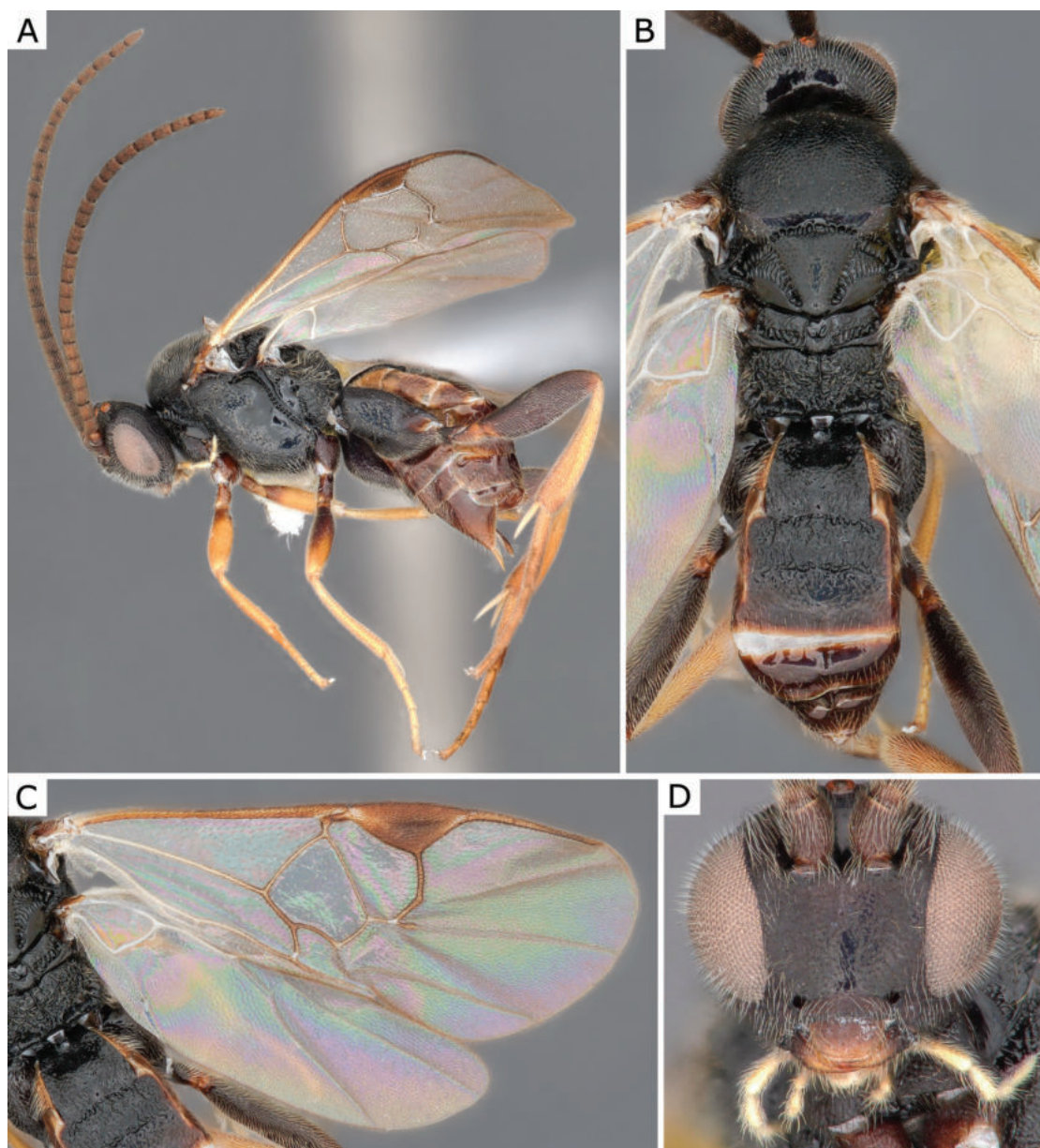


Figure 15. *Cotesia risilis* (Nixon, 1974), female (ZSM-HYM-33161-B04) **A** lateral view **B** meso- and metasoma **C** wing **D** head frontal view. Length of the specimen: 3.35 mm.

Geographical distribution. PAL.

PAL- Belgium, Finland, Germany*, Sweden.

Molecular data. BIN: partially BOLD:AAA7143.

Host information. Nymphalidae: type reared from *Boloria selene* (Denis & Schiffermüller, 1775).

Notes. Our sequences of this species were formerly part of BIN BOLD:AAA9381 and merged into BOLD:AAA7143 in February 2023. This BIN includes many clearly different species of *Cotesia*; see discussion below about this “megaBIN”. ASAP clustering resolves this species as a single cluster, including a specimen reared from *Boloria selene* (Denis & Schiffermüller, 1775) and part of the type series (MRS-Cot-cal=MS 075). Our German specimen matches the barcode of the paratype 100% and also matches the species morphologically, based on Shaw (2009). This species is illustrated in Fig. 16.

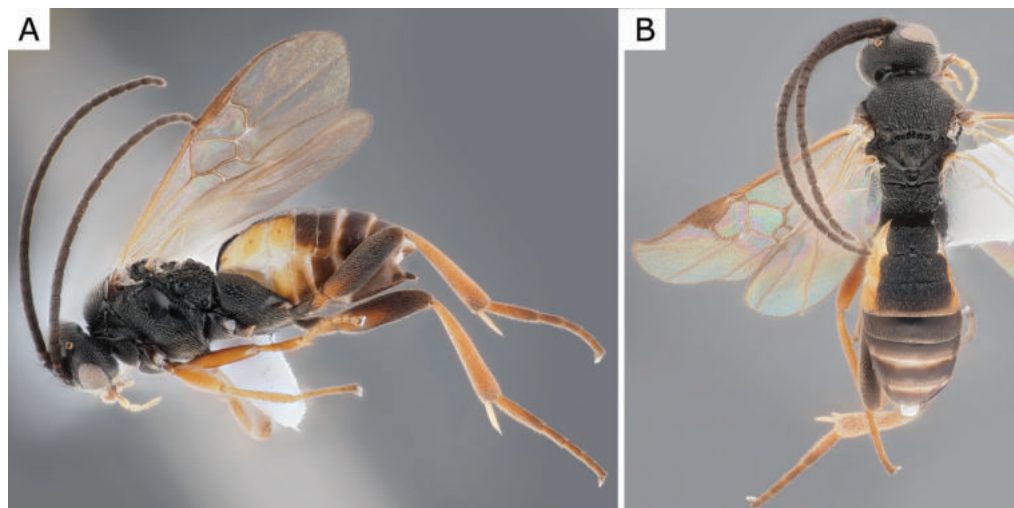


Figure 16. *Cotesia selenevora* Shaw, 2009, female (ZSM-HYM-33169-A02) **A** lateral and **B** dorsal views. Length of the specimen: 3.0 mm.

***Cotesia subordinaria* (Tobias, 1976)**

Material examined. **GERMANY:** Bavaria: Plattling, Isarmündung, renat. gravel bar, 48.781, 12.906, 317 m, Malaise trap, 30.vi.2021, leg. GBOL3, R. Albrecht, ZSM-HYM-42393-H02; Waldbrunn, Stadtfurst, 49.762, 9.803, 299 m, Malaise trap, 13.vii.2019, leg. J. Müller, ZSM-HYM-42385-G03; **POLAND:** Biebrza National Park, 53.473694, 22.65675, ex. *Rivula sericealis*, 15.vi.2014, leg. M. R. Shaw, MRS_JFT0436; **UNITED KINGDOM:** England: Gloucestershire, Eastleach, ex. *Rivula sericealis*, 20.vii.2009, leg. M. R. Shaw, MS 082; 01.viii.2009, leg. M. R. Shaw, MS 102.

Geographical distribution. PAL.

PAL: Azerbaijan, Georgia, Germany*, Netherlands, Poland*, Russia (NC), United Kingdom.

Molecular data. BIN: partially BOLD:ACO3220.

Host information. Host of type unknown; also Erebidae: *Rivula sericealis* (Scopoli, 1763).

Notes. German specimens were identified using the keys of Tobias (1986) and Papp (1986a). Sequences of three reared and identified specimens ex. *Rivula sericealis* detailed in Shaw (2012a, b) match our sequences from Germany at 0.16% max. p-distance: MRS_JFT0436, MS 082, MS 102. Our sequences of this species were formerly part of BIN BOLD:ACO3220 and merged into BOLD:AAA7143 in February 2023. This BIN includes many clearly different species of *Cotesia*; see discussion below about this “megaBIN”. ASAP clustering resolves this species as a single cluster. No host is mentioned in the original description (Tobias 1976), but we follow Shaw (2012a, 2012b) and the host data associated with those barcoded specimens. This species is illustrated in Fig. 17.

***Deuterixys plugarui* (Tobias, 1975)**

Material examined. **GEORGIA:** Kakheti: Lagodekhi reserve, Mt Kudigora, 41.855850, 46.292733, 847 m, Malaise trap, 25.viii-4.ix.2014, leg. G. Japoshvili, CNC506818; **GERMANY:** Bavaria: Bad Windsheim, Rappenau, 49.482, 10.468,

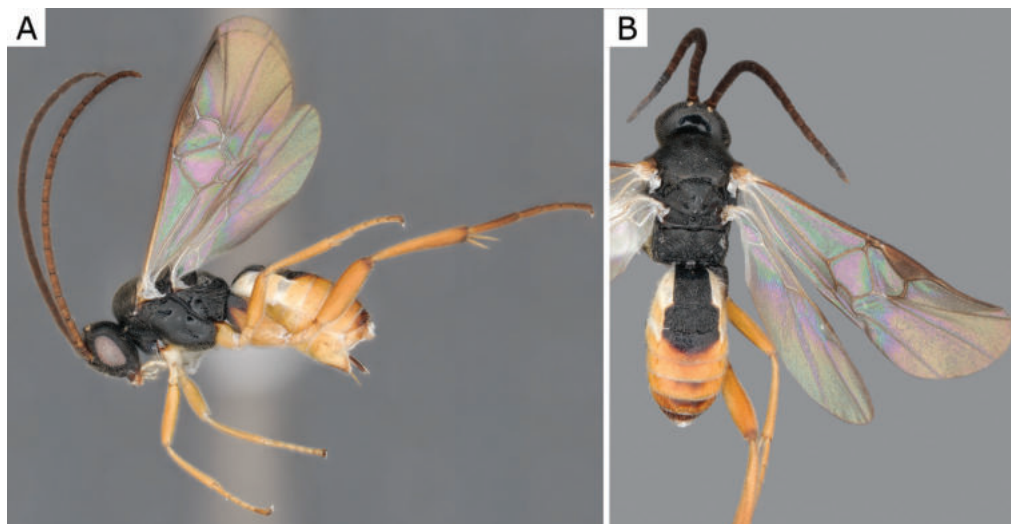


Figure 17. *Cotesia subordinaria* (Tobias, 1976), female (ZSM-HYM-42393-H02) **A** lateral and **B** dorsal views. Length of the specimen: 3.1 mm.

382 m, canopy fogging, 9.vii.2020, leg. B. Leroy, ZSM-HYM-42392-G03; Bad Windsheim, 49.47, 10.446, 400 m, fogging, 19.v.2020, leg. B. Leroy, ZSM-HYM-42392-B01; ZSM-HYM-42392-B02; 49.488, 10.513, 411 m, canopy fogging, 20.v.2020, leg. B. Leroy, ZSM-HYM-42392-A10; Bibart, 49.657, 10.435, 325 m, canopy fogging, 7.vii.2020, leg. B. Leroy, ZSM-HYM-42392-D02; Schonungen, 50.075, 10.426, 341 m, canopy fogging, 20.v.2020, leg. B. Leroy, ZSM-HYM-42392-B06; Uffenheim, 49.544, 10.252, 357 m, canopy fogging, 3.vii.2019, leg. B. Leroy, ZSM-HYM-33159-B05; Wiesentheid, 49.803, 10.277, 216 m, canopy fogging, 2.vi.2019, leg. B. Leroy, ZSM-HYM-33158-E09; Wonfurt, 49.994, 10.408, 264 m, canopy fogging, 2.vii.2019, leg. B. Leroy, ZSM-HYM-33159-H10; **NETHERLANDS:** Gelderland: Otterlo, Hoge Veluwe NP, ex. *Bucculatrix ulmella*, 16.viii.2019, leg. M. R. Shaw, MRS_JFT0823; 24.viii.2019, leg. M. R. Shaw, MRS_JFT0826.

Geographical distribution. PAL.

PAL- Georgia*, Germany*, Hungary, Moldova, Netherlands*, Russia (S), Ukraine, United Kingdom.

Molecular data. BIN: BOLD:AEJ7518.

Host information. Bucculatricidae: type reared from *Bucculatrix ulmella* Zeller, 1848.

Notes. German specimens were identified using the keys and information provided in Papp (1983), Tobias (1986), and especially Zeng et al. (2011). This species is matched with a DNA barcode for the first time. The only known host data is from the original description (Tobias 1975). Two specimens reared from *Bucculatrix ulmella* were also available to us (MRS_JFT0823, MRS_JFT0826); they match our morphological concept of this species and were reared from the same host as the type, but have not yet been sequenced. This species is illustrated in Figs 18, 19.

***Dolichogenidea cerialis* (Nixon, 1976)**

Material examined. GERMANY: Baden-Württemberg: Malsch, Hansjakobstr. 7, Urban Garden, 48.884, 8.32, 120 m, Malaise trap, 13.ix.2020, leg. D. Doczkal,

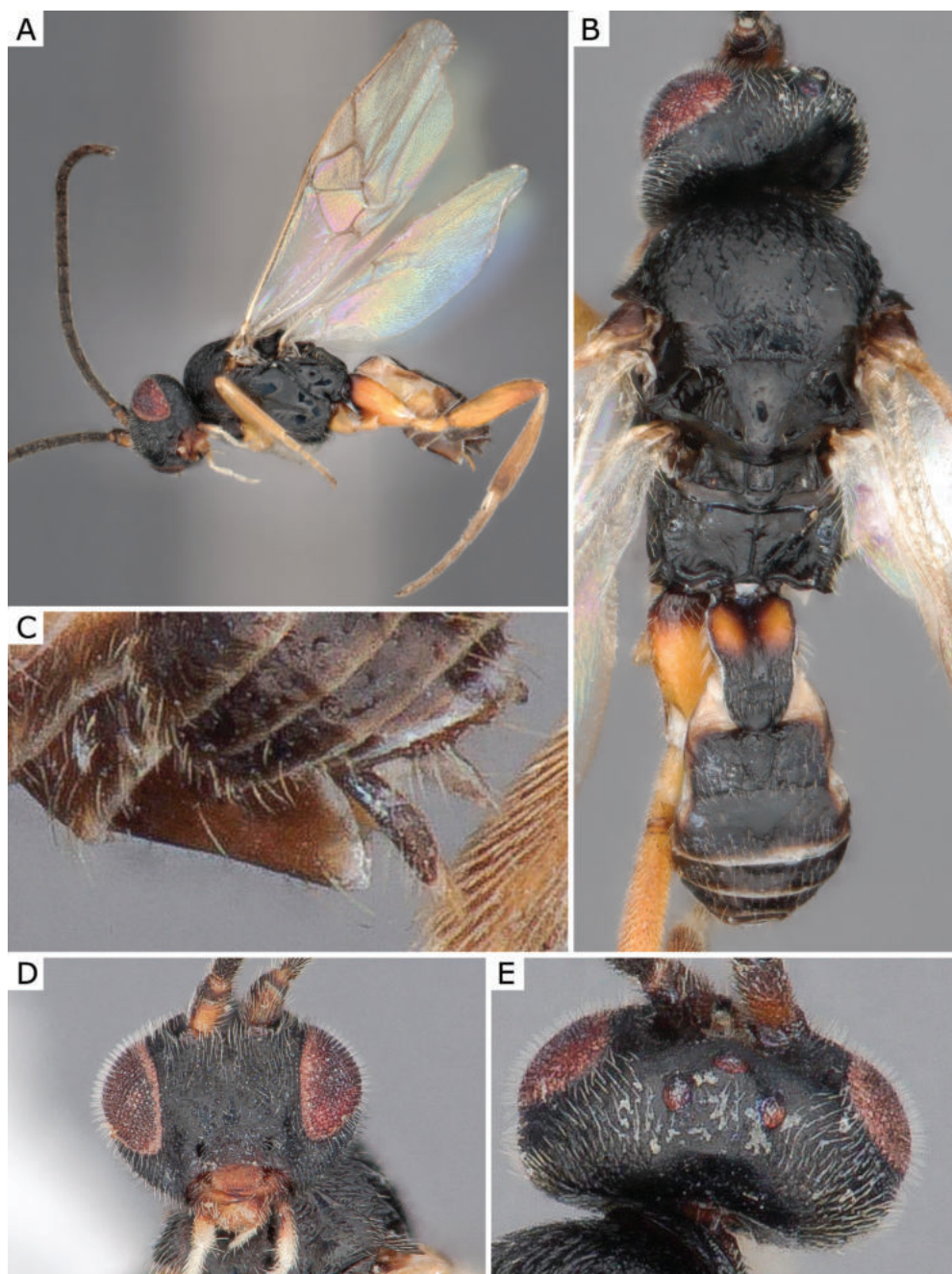


Figure 18. *Deuterixys plugarui* (Tobias, 1975), female (ZSM-HYM-42392-D02) **A** lateral view **B** meso- and metasoma **C** hypopygium lateral view **D** head frontal and **E** head dorsal views. Length of the specimen: 1.65 mm.

ZSM-HYM-33154-A05; Malsch, Luderbusch, 48.913, 8.332, 117 m, Malaise trap, 2.viii.2020, leg. D. Doczkal, K. Grabow, ZSM-HYM-42389-A11; 26.vii.2020, leg. D. Doczkal, K. Grabow, ZSM-HYM-42388-G11; ZSM-HYM-42388-H01; **UKRAINE:** [translated and transcribed from Russian] Kaniv Nature Reserve, Shlehiv island, 4.ix.1991, leg. A. Kotenko, CNCHYM 01013.

Geographical distribution. PAL.

PAL- Bulgaria, Germany*, Hungary, Israel, Italy, Kazakhstan, Russia (S), Spain, Ukraine*.

Molecular data. BIN: BOLD:AAZ9570.

Host information. Host of type unknown.

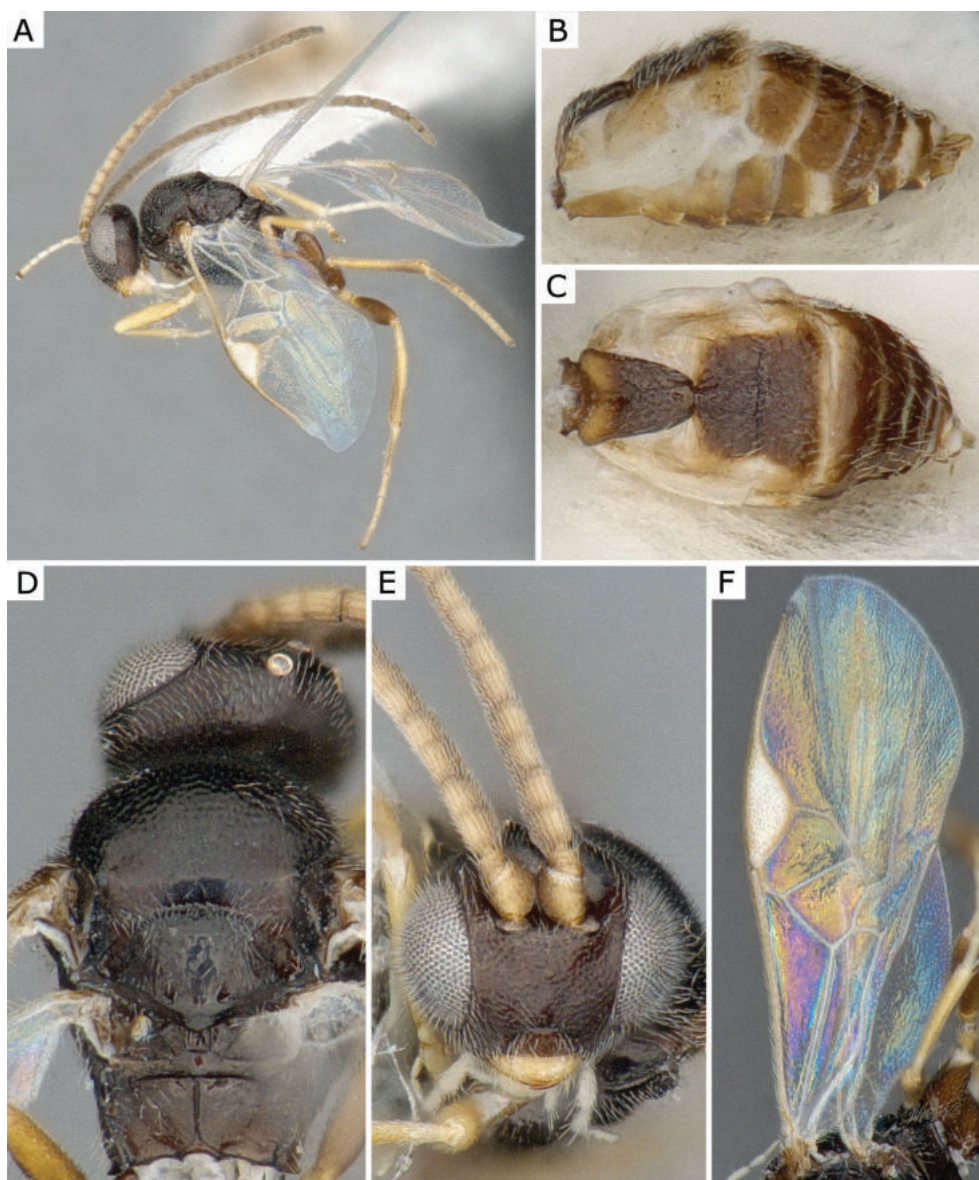


Figure 19. *Deuterixys plugarui* (Tobias, 1975), male (CNC506818) **A** lateral view **B** metasoma lateral view **C** metasoma dorsal view **D** mesosoma **E** head frontal view **F** wing.

Notes. The sequences of our German specimens match that of a specimen from Ukraine, identified by Kotenko and stored in the CNC collection (CNCHYM 01013); we studied both the German and the Ukrainian specimens and they match the morphological characters described by Nixon (1976), particularly the apical segment of the fore tarsus with a distinctive spine, the very short ovipositor sheaths (those two characters are very unusual in Dolichogenidea) but also leg colour, weak pale basal spot on pterostigma, anteromesoscutum punctuation, scutellum sculpture, propodeum areolation, hind spurs size, shape of T1 and T2. Nixon (1976) mentioned *Ascotis selenaria* (Denis & Schiffermüller, 1775) as host of additional non-type specimens from Israel which he identified as *Dolichogenidea cerialis*, but at the same time noted that these reared specimens differed slightly in morphology from the type series. These specimens might represent a different species, so we consider this as a questionable host record for *D. cerialis*. This species is illustrated in Figs 20, 21.

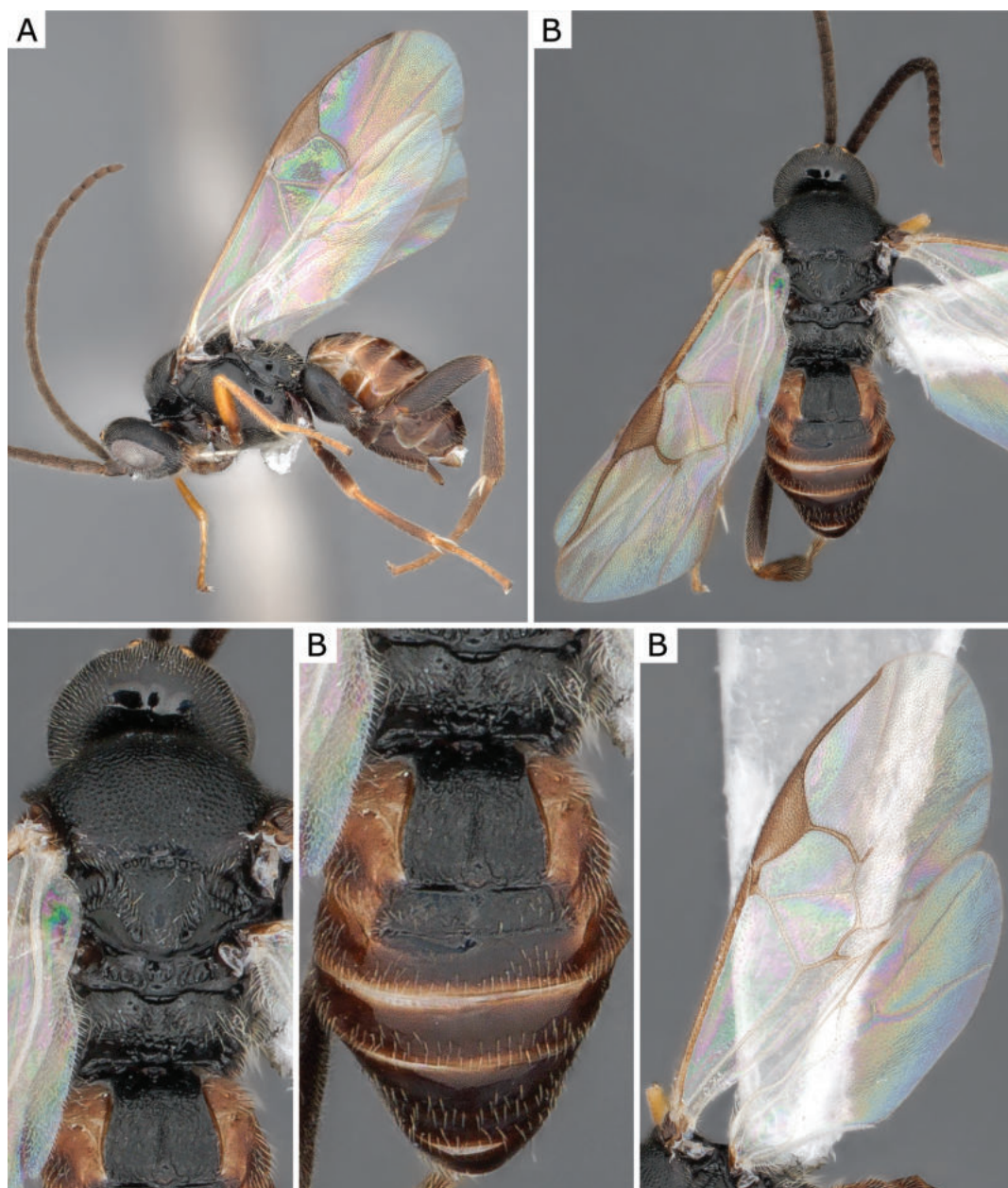


Figure 20. *Dolichogenidea cerialis* (Nixon, 1976), female (ZSM-HYM-42388-G11) **A** lateral view **B** dorsal view **C** mesosoma **D** metasoma **E** wing. Length of the specimen: 2.4 mm.

Dolichogenidea cheles (Nixon, 1972)

Material examined. **GERMANY:** Baden-Württemberg: Malsch, Hansjakobstr. 7, Urban Garden, 48.884, 8.32, 120 m, Malaise trap, 19.vii.2020, leg. D. Doczkal, ZSM-HYM-33154-G12; 5.vii.2020, leg. D. Doczkal, ZSM-HYM-33152-H03; ZSM-HYM-33152-H05; Bavaria: Moos, Isarmuendung, Hartholzauwald, 48.786, 12.959, 313 m, Malaise trap, 13.vii.2021, leg. GBOL3, R. Albrecht, ZSM-HYM-42394-F11; ZSM-HYM-42394-F12; 29.vii.2021, leg. GBOL3, R. Albrecht, ZSM-HYM-42394-G09; Sielstetten, östlich Grafendorfer Forst, 48.578, 11.863, 520 m, Malaise trap, 16.vii.2019, leg. J. Müller, ZSM-HYM-42383-A03.

Geographical distribution. PAL.

PAL- Finland, Germany*, Hungary, Poland, Russia (NW), Sweden, Turkey.

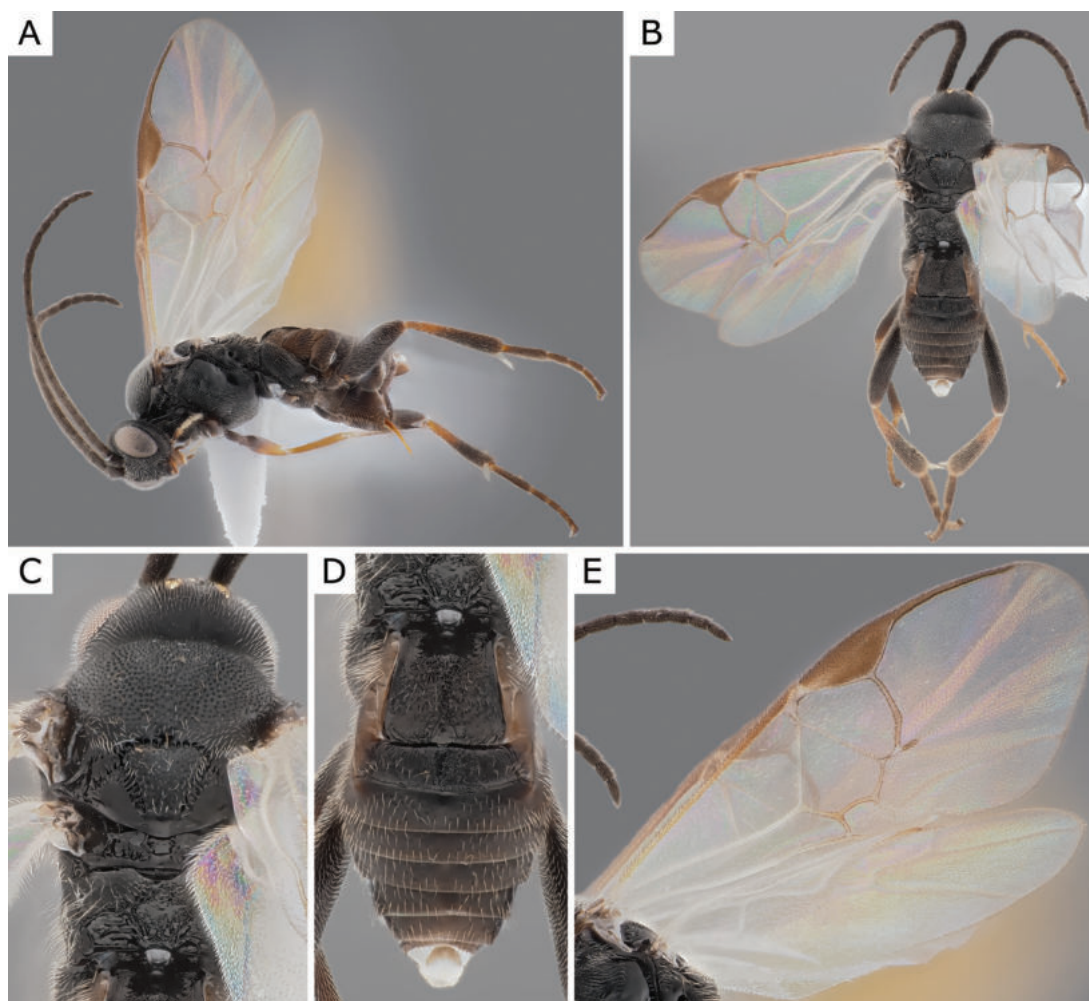


Figure 21. *Dolichogenidea cerialis* (Nixon, 1976), female (ZSM-HYM-33154-A05) **A** lateral view **B** dorsal view **C** mesosoma **D** metasoma **E** wing. Length of the specimen: 2.4 mm.

Molecular data. BIN: BOLD:ACQ9527.

Host information. Host of type unknown. Other host associations in need of verification.

Notes. German specimens were compared with the original description (Nixon 1972) as well as the works of Papp (1978) and Tobias (1986), and they match perfectly the characters provided in Nixon's original description, particularly: colour of legs, tegula, pterostigma, flagellomeres (more or less, the paler areas in flagellomeres are present but not as sharp as described by Nixon), ocelli in very low triangle, anteromesoscutum and scutellum sculpture, propodeum sculpture (lack of carinae, as described by Nixon), metatibial spurs, density and shape of spines on outer surface of metatibia, T1 and T2 shape and sculpture, length of ovipositor sheaths, partial widening of sheaths towards posterior end, and down-curved ovipositor. The hosts that in the past have been associated with this species are not from the type material and comprise two different Lepidoptera families: Tortricidae – *Acleris holmiana* (Linnaeus, 1758) (Papp 1988), and Gracillariidae – *Caloptilia rufipennella* (Hübner, 1796) (Papp 1988) and *Caloptilia fribergensis* (Fritzsche, 1871) (Marczak and Buszko 1993); therefore, we consider supposed hosts in need of verification. This species is illustrated in Fig. 22.

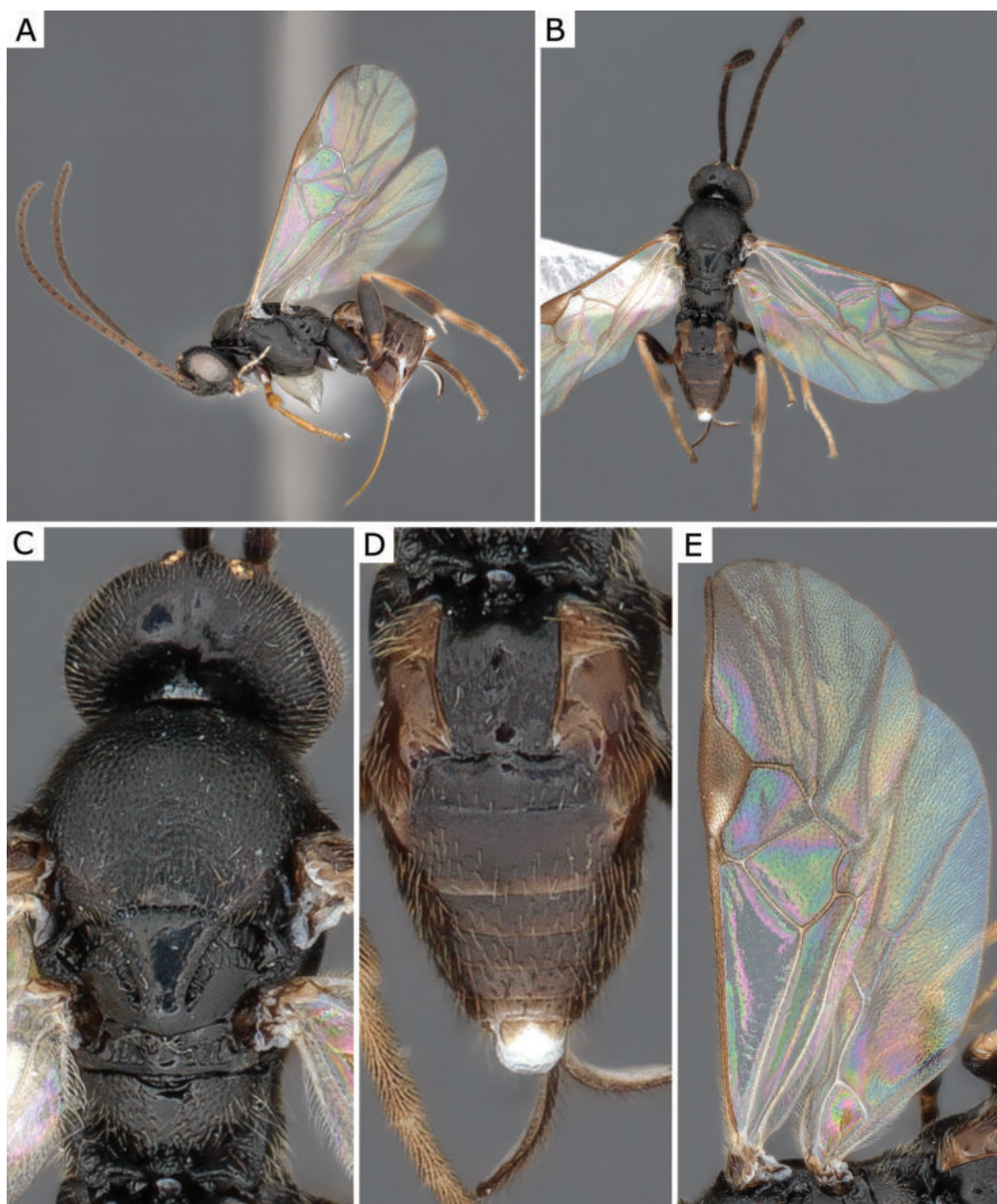


Figure 22. *Dolichogenidea cheles* (Nixon, 1972), female (ZSM-HYM-33152-H03) **A** lateral view **B** dorsal view **C** mesosoma **D** metasoma **E** wing. Length of the specimen: 2.3 mm.

***Dolichogenidea coleophorae* (Wilkinson, 1938)**

Material examined. **CANADA:** Newfoundland and Labrador: 2 miles west of Gambo, 48.789478, -54.261043, 19.vi.1975, leg. A. G. Raske, J. D. Rowe, ex. *Coleophora serratella*, CNCHYM 01020; Gambo, 48.786481, -54.215467, 27.vii.1985, CNCHYM 01019; **GERMANY:** Baden-Württemberg: Malsch, Luderbusch, 48.912, 8.332, 112 m, Malaise trap, 24.v.2020, leg. D. Doczkal, K. Grabow, ZSM-HYM-42386-G05; Bavaria: Forchheim, Untere Mark bei Willersdorf, 49.739, 10.969, 261 m, Malaise trap, 12.vii.2019, leg. J. Müller, ZSM-HYM-42377-D11; [exact location unknown], 13.viii.1975, CNCHYM 01021; **SWITZERLAND:** Aigle, 46.319083, 6.970444, 9.viii.1973, CNCHYM 01024; **UNITED KINGDOM:** England: [exact location unknown], 15.iii.1938, ex. *Coleophora serratella*, CNCHYM 01023.

Geographical distribution. NEA, PAL.

NEA: Canada (NL); PAL: Azerbaijan, Finland, Germany*, Hungary, Poland, Romania, Russia (KHA, VOR, YAR), Slovakia, Switzerland, Tajikistan, Tunisia, Turkey, United Kingdom, Uzbekistan.

Molecular data. BOLD: AEO8197.

Host information. Coleophoridae: type reared from *Coleophora serratella* (Linnaeus, 1761); also possibly *Coleophora ?ibipennella* Zeller, 1849; *Coleophora ?lusciniaepennella* (Treitschke, 1833); *Coleophora ?obducta* (Meyrick, 1931); *Coleophora ?tadzhikiella* Danilevsky, 1955.

Notes. Several Canadian (CNCHYM 01019, CNCHYM 01020) and European specimens at the CNC (CNCHYM 01021 from Germany, CNCHYM 01023 from United Kingdom, CNCHYM 01024 from Switzerland) were reared from the host of the type or the synonym *Coleophora fuscadinella* Zeller, 1849 and identified as *D. coleophorae*. We compared our material collected in Germany with those reared specimens collected in Canada and Europe as well as the original description and the works of Nixon (1976), Papp (1981a) and Tobias (1986). Our freshly collected material from Germany morphologically matches the reared specimens as well as the literature. All specimens we examined are associated with sequences, except for CNCHYM 01023 which was collected in 1938. The barcode sequences of the reared specimens are short (107 bp) and all of these specimens were collected between 1973 and 1985. They do not 100% match our sequences (3 bp difference). However, since the COI sequences of the historical material are very short, the species occurs in several neighbouring countries of Germany, the host is widely distributed in Europe and occurs in Germany, and our specimens match the morphological concept of the species, we conclude that our specimens fit our current concept of this species despite the currently somewhat conflicting DNA barcodes. In the historical literature there are other host records from several additional species of *Coleophora*, which may be correct but are here cited as questionable. Other literature host records from different Lepidoptera families are much less probable and we do not consider them here. This species is illustrated in Fig. 23.

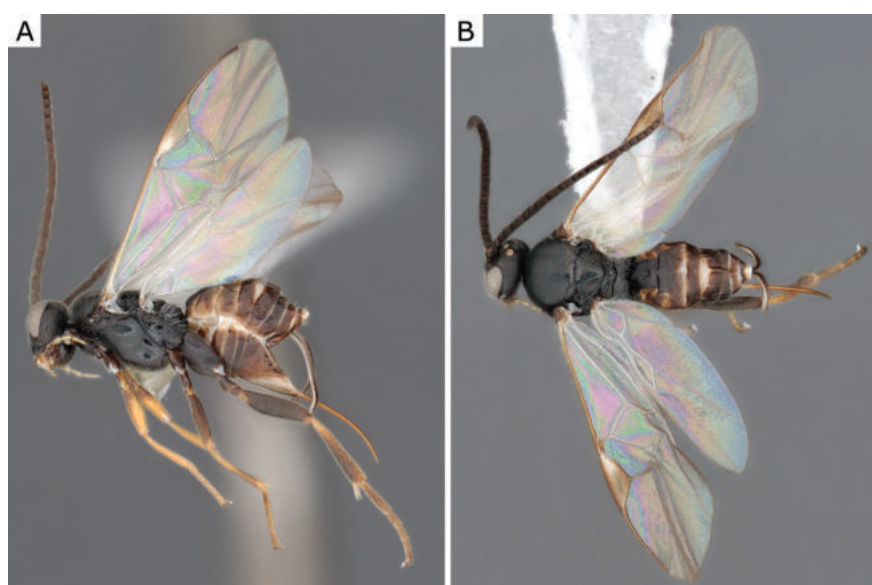


Figure 23. *Dolichogenidea coleophorae* (Wilkinson, 1938), female (ZSM-HYM-42377-D11) **A** lateral and **B** dorsal views. Length of the specimen: 2.25 mm.

***Glyptapanteles indiensis* (Marsh, 1979)**

Material examined. **CZECH REPUBLIC:** South Moravia: Obora Soutok, Lanžhot, 48.69, 16.945, 165 m, 14.v.2013, leg. P. Drozd, BC-ZSM-HYM-23872-A04; ex. *Alsophila auscularia*, 05.v.2015, leg. M. Sigut, BC-ZSM-HYM-27569-F09; ex. *Operophtera brumata*, 08.v.2015, leg. P. Drozd, BC-ZSM-HYM-23872-F08; **GERMANY:** Baden-Württemberg: Malsch, Hansjakobstr. 7, Urban Garden, 48.884, 8.32, 120 m, Malaise trap, 11.x.2020, leg. D. Doczkal, ZSM-HYM-33154-B09; Bavaria: Markt Nordheim, Kehrenberg, 49.547, 10.366, 419 m, canopy fogging, 10.vii.2020, leg. B. Leroy, ZSM-HYM-42393-B07; Rhön Fladungen, NSG Schwarzes Moor, Kermi-Hochmoor, 50.512, 10.069, 780 m, Malaise trap, 23.viii.2017, leg. D. Doczkal, ZSM-HYM-33165-A08; Rhön Hausen, Eisgraben, basalt block heap at forest edge, 50.503, 10.09, 735 m, Malaise trap, 23.vii.2018, leg. D. Doczkal, ZSM-HYM-33166-C03; 9.viii.2018, leg. D. Doczkal, ZSM-HYM-33166-D10; Südpark, 48.103, 11.509, 550 m, ex. *Operophtera brumata*, 28.v.2021, leg. W. Langer, ZSM-HYM-ZLAB01-F05; **INDIA:** Kashmir Sprinagar, ex. *Lymantria obfuscata*, [collector unknown], 2.v.1977, CNCHYM 03231; CNCHYM 03232; **JAPAN:** Aichi: Mt. Chausu, 35.2275 137.655558, 1300 m, 9.vii.1995, leg. K. Yamagishi, JMIC 0011.

Geographical distribution. NEA, OTL, PAL.

NEA: USA (PA), OTL: India, PAL: Czech Republic*, Germany*, Japan*.

Molecular data. BOLD:ABY2372.

Host information. Erebidae: type reared from *Lymantria obfuscata* (Marsh, 1979); also *Lymantria dispar* (Linnaeus, 1758); Geometridae*: *Operophtera brumata** (Linnaeus, 1758).

Notes. We record *G. indiensis* for the first time in the Palaearctic region, based on specimens from Germany, Japan and Czech Republic. This species is morphologically similar, especially in habitus, to several *Glyptapanteles* species. Our identification was therefore based on a careful study (detailed below) which included a combination of morphology (see Figs 25, 26, both examination of authenticated specimens and consulting original descriptions and other relevant papers (e.g., Muesebeck 1928; Nixon 1973; Marsh 1979; Papp 1983)), DNA barcodes (available for all species discussed below, see Suppl. materials and Fig. 24) and hosts (available for most species mentioned above, except for *G. popovi*). The German, Japanese (JMIC 0011) and Czech specimens (BC-ZSM-HYM-23872-A04, BC-ZSM-HYM-23872-F08, BC-ZSM-HYM-27569-F09) were identified by morphological comparison with two paratypes of *G. indiensis* deposited in the CNC as well as information from the original description (Marsh 1979). One of those paratypes (a male specimen (CNCHYM 03232) reared from *Lymantria obfuscata* in India, apparently part of the same brood as the female paratype deposited at the CNC (CNCHYM 03231)) was successfully barcoded and the 455 bp sequence matches the remaining sequences in this BIN by 99.5%. *Glyptapanteles indiensis* is known to parasitise *Lymantria obfuscata* in India and *Lymantria dispar* (at least in the laboratory), and therefore is of interest as a biocontrol agent (Marsh 1979), although we are not aware of published data confirming the parasitisation of *L. dispar* by *G. indiensis* in the wild. However, we have additional data from a metabarcoding study in Germany including caterpillars that were collected as part of a canopy fogging project. There, seven individual caterpillars of *L. dispar* had more than 30 reads of sequences that match the barcoding cluster that we associated with *G. indiensis*.

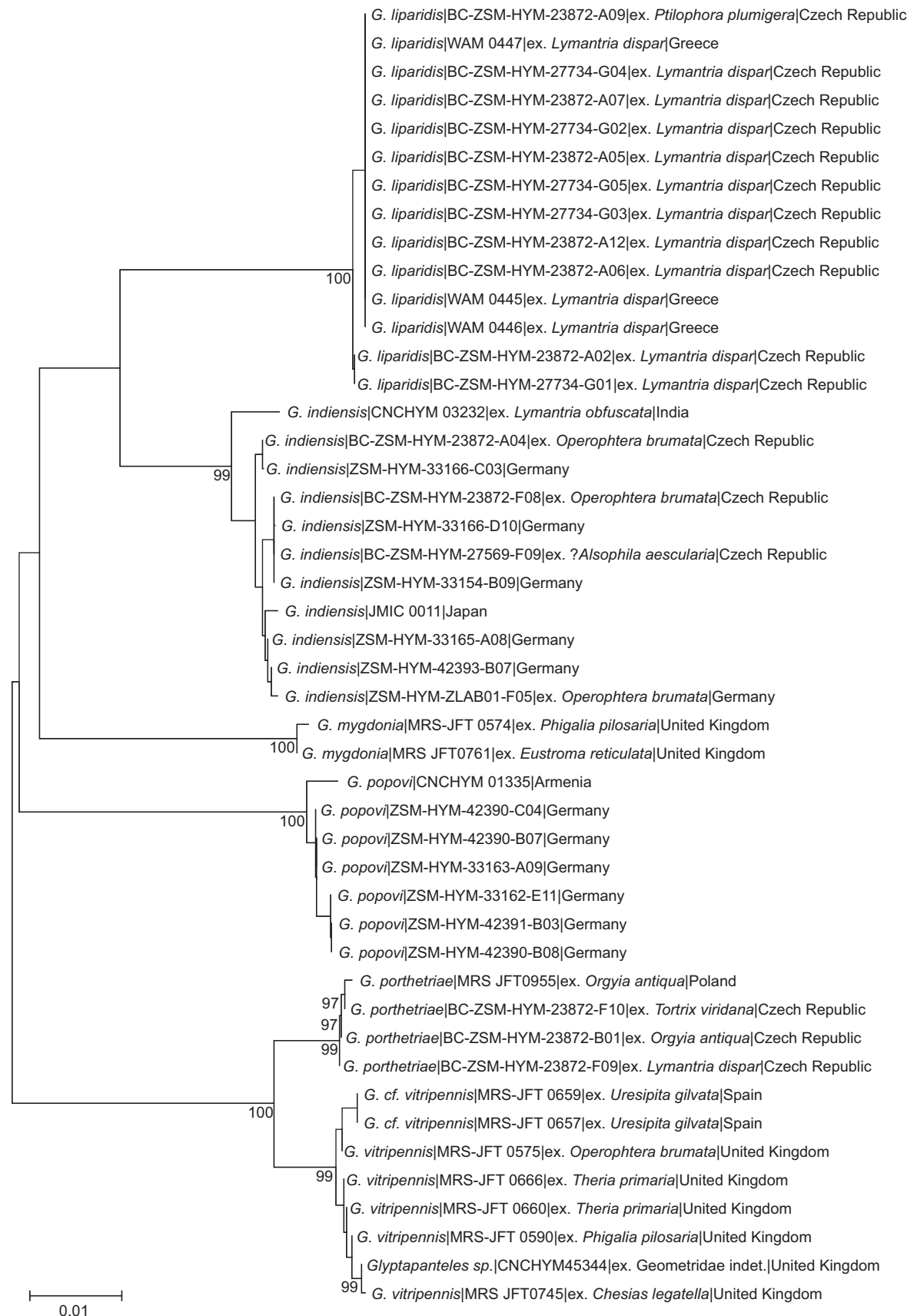


Figure 24. Neighbour-joining topology of the COI barcoding region of *Glyptapanteles indiensis*, *G. popovi* and morphologically similar species, based on Kimura 2-parameter distances. Numbers next to nodes represent non-parametric bootstrap values > 90% (1,000 replicates). The aligned sequences and N-J topology can be reviewed in Suppl. materials 6, 7.

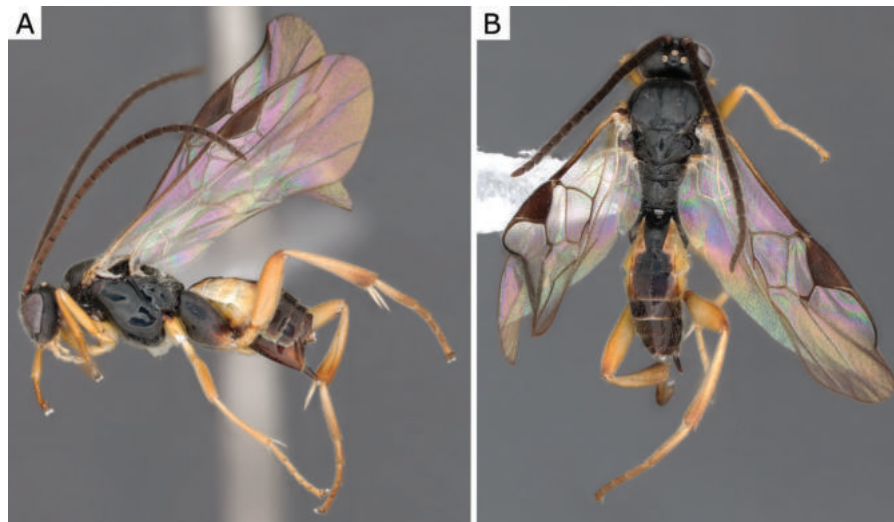


Figure 25. *Glyptapanteles indiensis* (Marsh, 1979), female (ZSM-HYM-33154-B09) **A** lateral and **B** dorsal views. Length of the specimen: 3.5 mm.

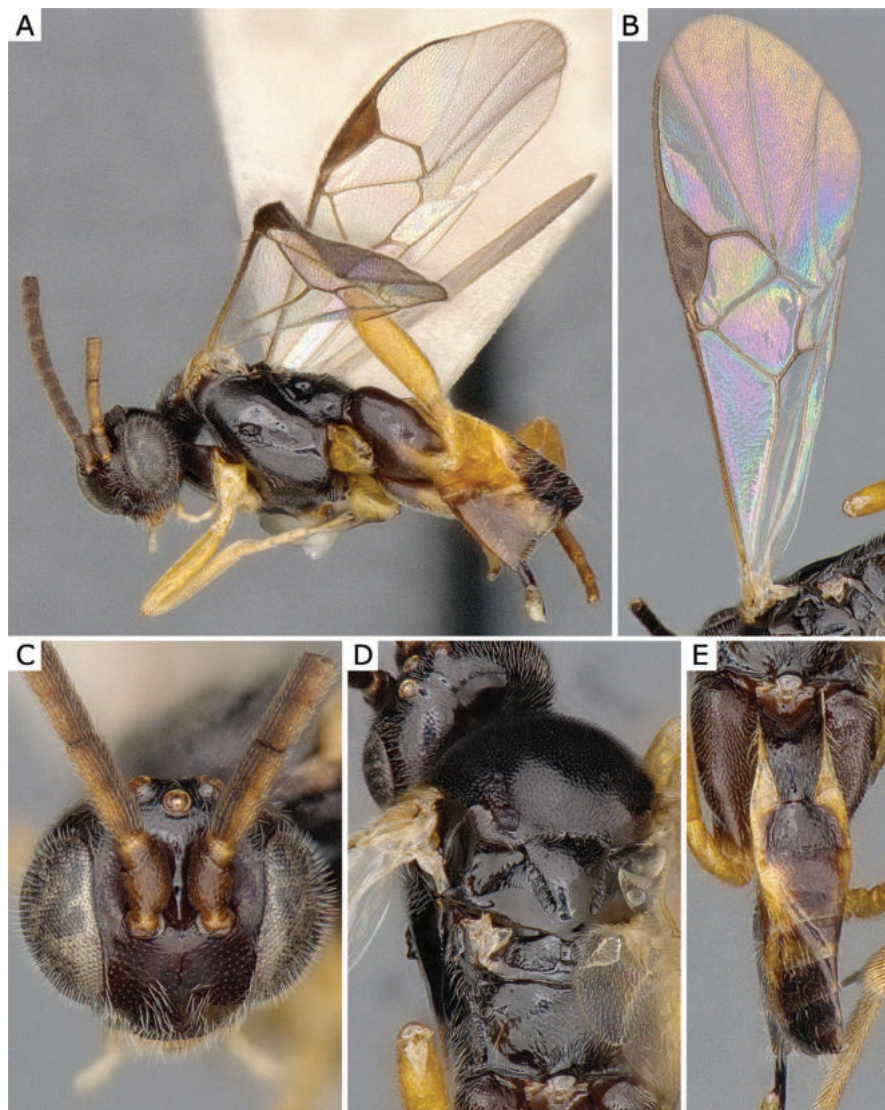


Figure 26. *Glyptapanteles indiensis* (Marsh, 1979), female paratype (CNCHYM 03231) **A** lateral view **B** forewing **C** head frontal view **D** mesosoma **E** metasoma.

(99.6–100% bp similarity), therefore providing at least an indirect confirmation of the parasitisation of *L. dispar* in the wild by this wasp species. Additionally, we examined two specimens (ZSM-HYM-ZLAB01-F05 and BC-ZSM-HYM-23872-F08) which were reared from the Geometridae *Operophtera brumata* and represent a new host family record for this species. The aforementioned metabarcoding data suggests that there might be additional hosts for this species; however, this would need to be confirmed by rearing.

Other species of *Glyptapanteles* parasitising *Lymantria dispar* are *Glyptapanteles liparidis* (BOLD:AAV2164, including several reared specimens from this host such as WAM 0445=MRS_JFT 0028, BC-ZSM-HYM-23872-A02, BC-ZSM-HYM-23872-A05) and *Glyptapanteles porthetriae* (BOLD:ACL7229, including a reared specimen from this host: BC-ZSM-HYM-23872-F09). The many available barcodes from both *G. porthetriae* and *G. liparidis* are very distinct and clearly separated from those of *G. indiensis* (> 3.5% K2P-distance, see Fig. 24), and there are also morphological differences between these three species as detailed in Marsh (1979).

The known hosts of *G. mygdonia* include *Operophtera brumata* and the multiple hosts recorded for *G. vitripennis* in the literature (many of them likely incorrect) include both *O. brumata* and *L. dispar*. The many available sequences of *G. mygdonia* (BOLD:AAU5027) and *G. vitripennis* (BOLD:AAA7148) are also very distinctive and far apart from those of *indiensis* [The sequences of *G. vitripennis* and *G. liparidis* are relatively very close (2.13% p-distance); furthermore, *G. vitripennis* seems to include a complex of species that remains unresolved, but that is beyond the scope of the present paper]. There are also morphological differences between these species and *G. indiensis* (Nixon 1973). Two characters we found were useful are the relative length of the ovipositor sheaths, which is much longer in *G. indiensis* as compared to the other two species and the lack of a curved spine on the fore tarsus for *G. indiensis* (present in both *G. mygdonia* and *G. vitripennis*).

The last species we compared to *G. indiensis* was *G. popovi*, which is much less understood. Until now, *G. popovi* was only known from Turkey and Turkmenistan (Fernandez-Triana et al. 2020) and there is no host known for this species. Based on information from Telenga (1955), Tobias (1986), and the study of a specimen of *G. popovi* from Armenia (CNCHYM 01335) identified by Kotenko in 1981 and deposited in the CNC these two species are different. Analyses of available DNA sequences strongly support that (these two species are clearly apart by more than 5% K2P-distance, compare Fig. 25). We found German specimens from both species and thus both species are recorded from Germany in this paper (see also comments below, under *G. popovi*). *Glyptapanteles indiensis* is illustrated in Figs 25, 26.

***Glyptapanteles popovi* (Telenga, 1955)**

Material examined. ARMENIA: [translated and transcribed from Russian] Khosrov Forest State Reserve, Vediiskii reservoir sector (of reserve), montane forest, 30.vi.1981, CNCHYM 01335; **GERMANY:** Bavaria: Garmisch-Partenkirchen, Zugspitze, Platt, 47.406, 11.009, 1965 m, Malaise trap, 11.ix.2018, leg. D. Doczkal, J. Voith, ZSM-HYM-33163-A09; 47.407, 11.006, 2030 m, Malaise trap, 11.ix.2018, leg.

D. Doczkal, J. Voith, ZSM-HYM-42391-B03; 47.407, 11.008, 2005 m, Malaise trap, 11.ix.2018, leg. D. Doczkal, J. Voith, ZSM-HYM-42390-B07; ZSM-HYM-42390-B08; 9.x.2018, leg. D. Doczkal, J. Voith, ZSM-HYM-42390-C04; 47.412, 11.007, 2210 m, Malaise trap, 2.viii.2018, leg. D. Doczkal, J. Voith, ZSM-HYM-33162-E11.

Geographical distribution. PAL.

PAL- Armenia*, Germany*, Turkey, Turkmenistan.

Molecular data. BIN: BOLD:AEJ4298.

Host information. Host unknown.

Notes. Our specimens were identified morphologically using keys and information in Telenga (1955), Papp (1983), and Tobias (1986) as well as comparison with a specimen from Armenia (CNCHYM 01335) identified by Kotenko in 1981 and deposited in the CNC. The German and Armenian specimens also share similar DNA barcodes (99.5% overlap, sequence length of Armenian specimen is 425 bp). See also comments under *G. indiensis* above. Our material of this species was collected only in an alpine habitat (> 1900 m, Zugspitze). This species is illustrated in Figs 27, 28.

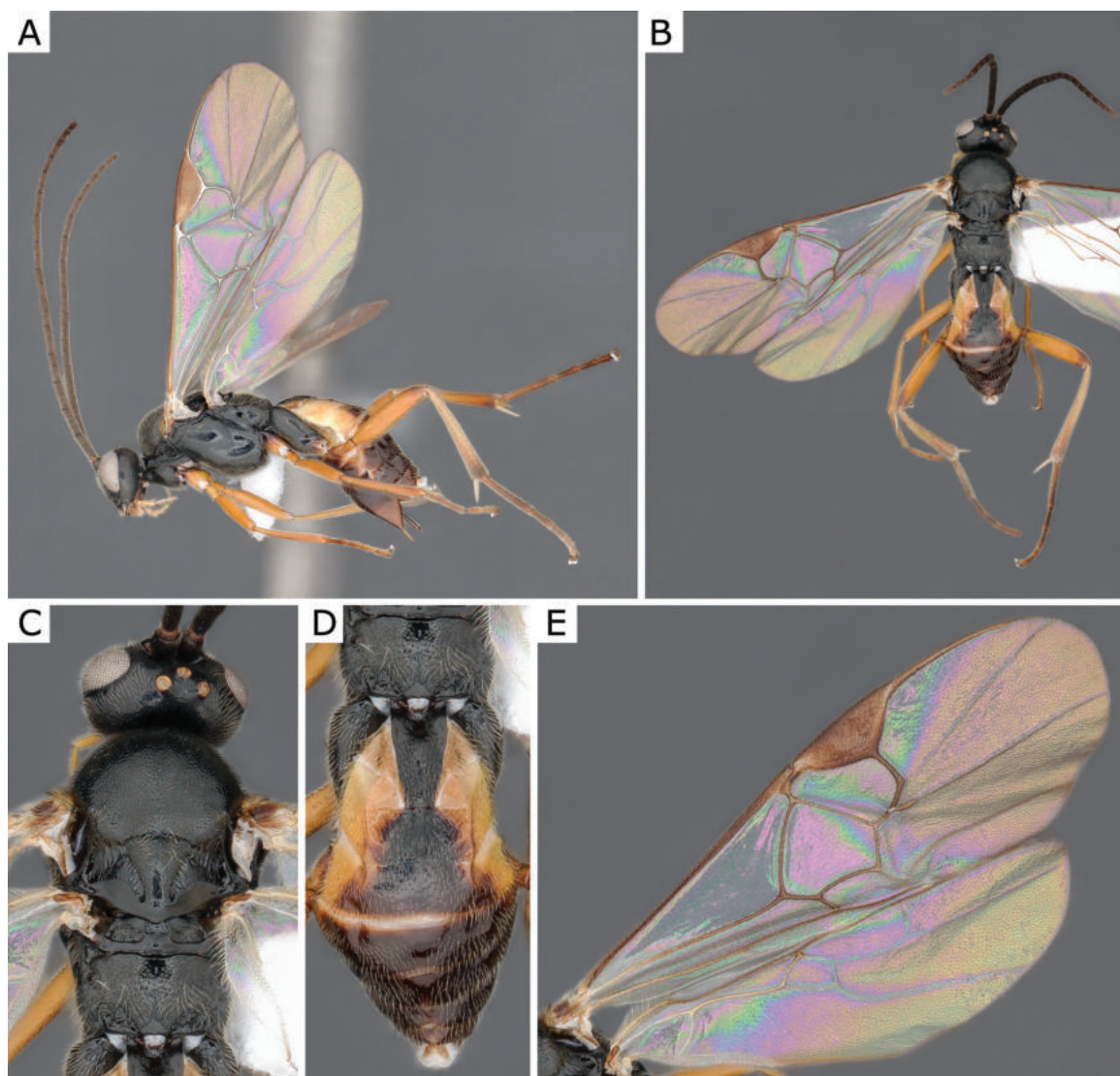


Figure 27. *Glyptapanteles popovi* (Telenga, 1955), female (ZSM-HYM-33163-A09) **A** lateral view **B** dorsal view **C** mesosoma **D** metasoma **E** wing. Length of the specimen: 4.0 mm.

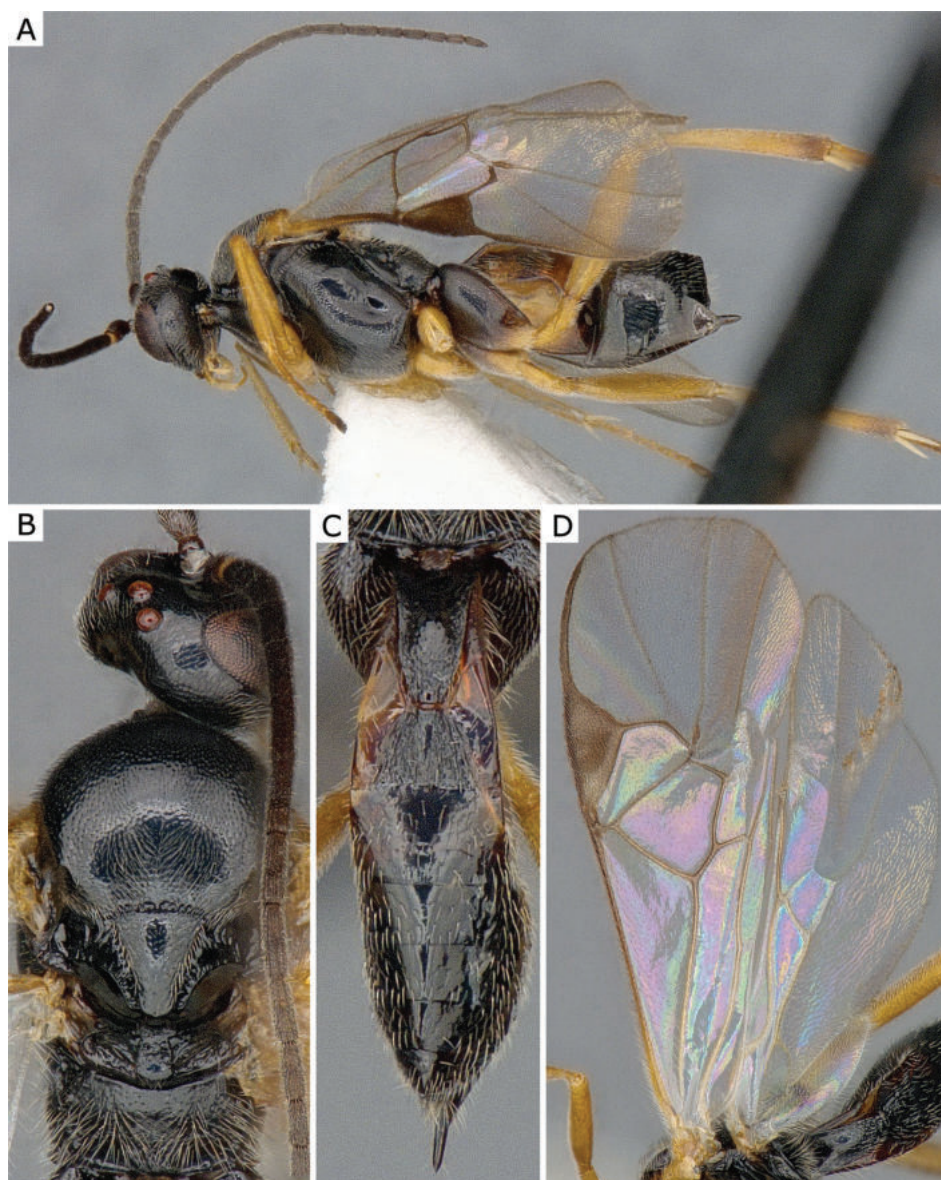


Figure 28. *Glyptapanteles popovi* (Telenga, 1955), female (CNCHYM 01335=CNC280989) **A** lateral view **B** mesosoma **C** metasoma **D** wing.

Illidops cloelia (Nixon, 1965)

Material examined. GERMANY: Bavaria: Garmisch-Partenkirchen, Zugspitze, Platt, 47.407, 11.008, 2005 m, Malaise trap, 2.viii.2018, leg. D. Doczkal, J. Voith, ZSM-HYM-42389-G08.

Geographical distribution. PAL.

PAL- Austria, Germany*, Hungary, Korea, Russia (E, NC), Slovakia, Switzerland, Tajikistan, former Yugoslavia.

Molecular data. BIN: BOLD: AEO8223.

Host information. Host unknown.

Notes. The German specimen was identified by comparison with the keys and details from the works of Nixon (1965, 1976), Papp (1973, 1981a), and Tobias (1986). Our material of this species was collected only in an alpine habitat (> 2000 m, Zugspitze). This species is illustrated in Fig. 29.

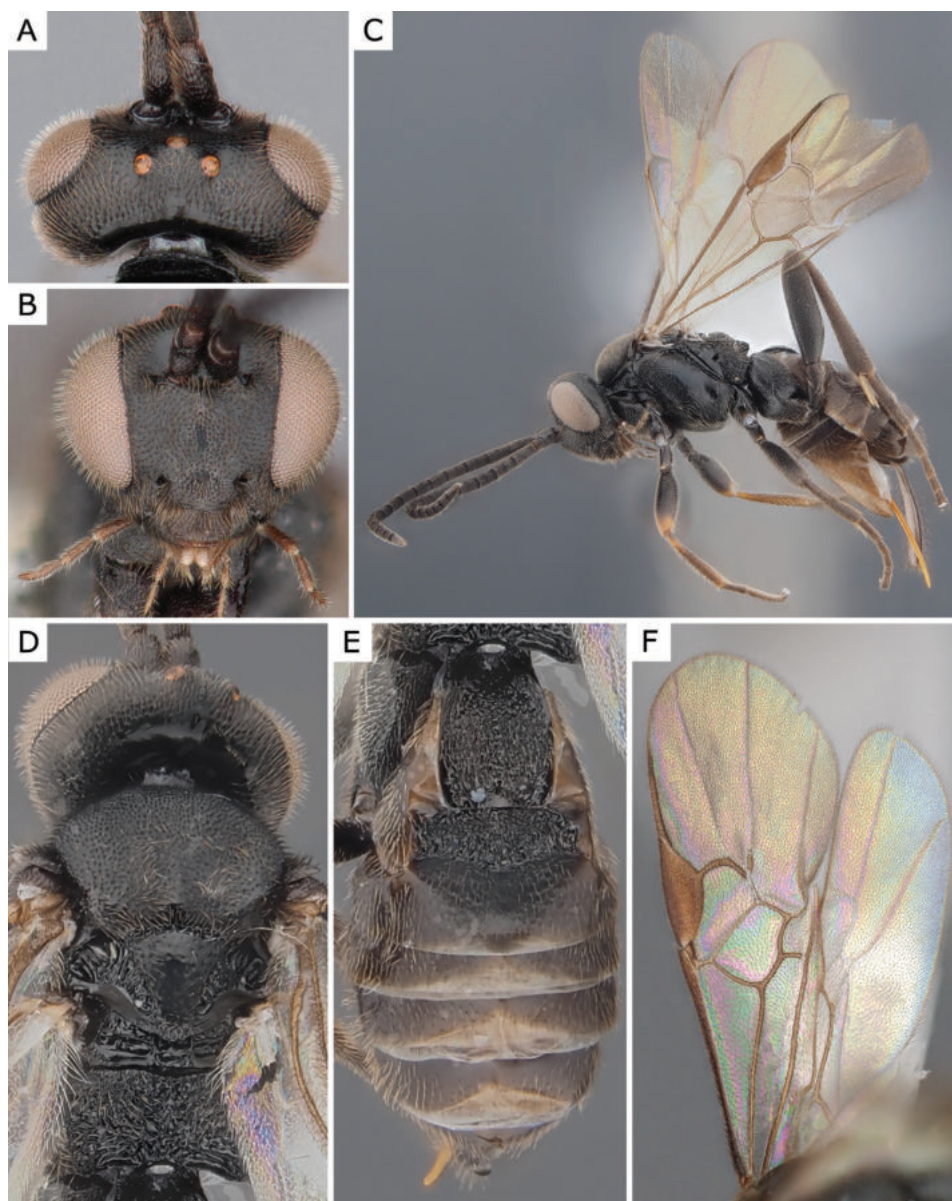


Figure 29. *Illidops cloelia* (Nixon, 1965), female (ZSM-HYM-42389-G08) **A** head dorsal view **B** head frontal view **C** lateral view **D** mesosoma **E** metasoma **F** wing. Length of the specimen: 2.75 mm.

***Illidops splendidus* (Papp, 1974)**

Material examined. **GERMANY:** Bavaria: Lkr. Kelheim Siegenburg, Bombodrom, 48.755, 11.791, 411 m, Malaise trap, 26.v.2017, leg. D. Doczkal, J. Voith, ZSM-HYM-33168-H06.

Geographical distribution. PAL.

PAL- Germany*, Hungary, Russia (C).

Molecular data. BIN: BOLD:AEJ7519.

Host information. Host unknown.

Notes. The German specimen was identified by comparison with the keys of Papp (1974, 1981a) and Tobias (1986) and the original description by Papp (1974). The single specimen available to us was collected in a rare sand-dune habitat close to Siegenburg in Bavaria. This species is illustrated in Fig. 30.

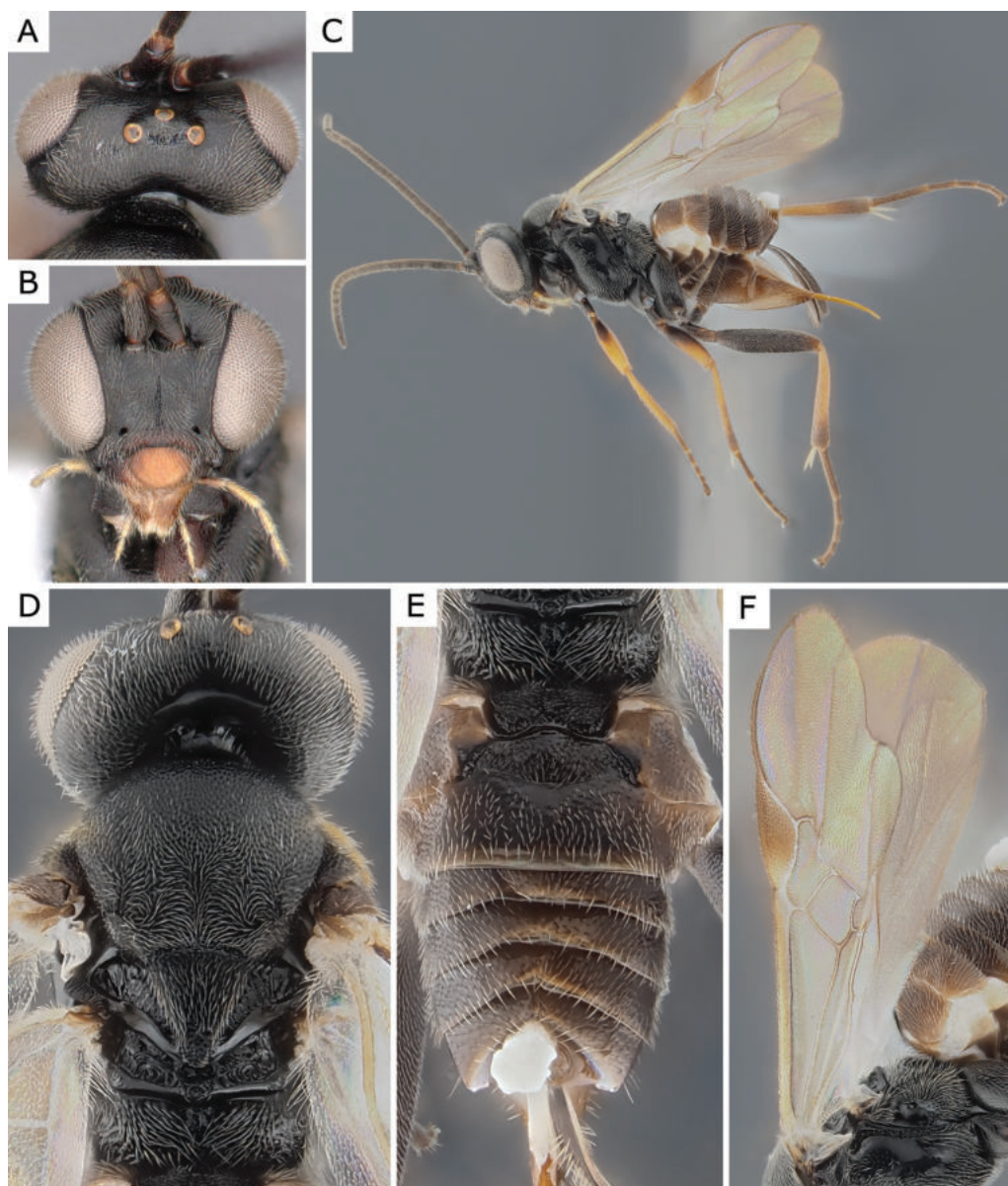


Figure 30. *Illidops splendidus* (Papp, 1974), female (ZSM-HYM-33166-H06) **A** head dorsal view **B** head frontal view **C** lateral view **D** mesosoma **E** metasoma **F** wing. Length of the specimen: 2.75 mm.

***Microgaster arctostaphylica* Shaw, 2012**

Material examined. **GERMANY:** Bavaria: Bad Tölz, forest close to Isarstausee, 47.77, 11.547, 652 m, Malaise trap, 16.vii.2019, leg. J. Müller, ZSM-HYM-42378-F09; Berchtesgaden National Park, Königssee, Rinnkendlsteig, 47.553, 12.964, 775 m, Malaise trap, 14.vi.2017, leg. D. Doczkal, J. Voith, ZSM-HYM-33160-F10; ZSM-HYM-33160-F12; Oberndorf, close to Krebsbach, 49.868, 9.516, 342 m, Malaise trap, 13.vii.2019, leg. J. Müller, ZSM-HYM-42325-C09; Rhön Fladungen, NSG Schwarzes Moor, Kermi-Hochmoor, 50.512, 10.069, 780 m, Malaise trap, 18.vii.2017, leg. D. Doczkal, ZSM-HYM-33164-G03; **SWEDEN:** Gotland: Roleks; Gotlands kommun, 57.536783, 18.337883, Malaise trap, 17.vii-9.viii.2005, leg. SMTP, CNC471954; **UNITED KINGDOM:** Scotland: Inverness-shire, Tulloch Moor, ex. *Argyroploce arbutella*/*Stictea mygindiana*, 30.iv.2016, leg. R.

J. Heckford, MRS_JFT0770; Morayshire, Boat of Garton NH9319, ex. ?*Stictea mygdeana*, 20.v.2014, leg. R. J. Heckford, MRS-JFT 0640.

Geographical distribution. PAL.

PAL- Germany*, Sweden*, United Kingdom.

Molecular data. BIN: BOLD:AAH1039.

Host information. Tortricidae: type reared from *Argyroploce arbutella* (Linnaeus, 1758); also *Epinotia nemorivaga* (Tengström, 1848), *Stictea mygindiana* (Denis & Schiffermüller, 1775).

Notes. German specimens were identified by comparison with the original description and specimens from that paper (Shaw 2012a); all specimens we examined except for one had the orange (paler) tip of mesofemur that is considered one of the diagnostic features. The species can be confused with *Microgaster messoria* Haliday, 1834. However, *M. messoria* clusters in BIN BOLD:AAV2150 (including a reared specimen ex. *Aspilapteryx tringipennella* (Zeller, 1839) in the BOLD database, one of the hosts that Nixon based his concept on (of *Microgaster tibialis* Nees, 1834, a synonym of *M. messoria*)). It is well separated from the BIN that contains our sequences of *M. arctostaphylica* (BOLD:AAV2150: within-BIN max. p-distance: 0.86%, Nearest-Neighbour minimum p-distance: 2.31%). Based on publicly available data in BOLD, *M. arctostaphylica* also could be present in Turkey (CGTURK-1139) but we could not examine that specimen. This BIN is quite variable (2.25% max. within-BIN max. p-distance and 2.69% min. p-distance to the Nearest-Neighbor). There is a single specimen (ZSM-HYM-42325-C09) that is 2.3% apart from the other German material and clusters with the specimen from Turkey; except for some minor differences in colouration it matches our morphological concept of the species. Future analyses and study of more specimens might provide support to consider this a complex of species, but for the time being we consider all of them to belong to *Microgaster arctostaphylica*. This wasp species is known to parasitise several Tortricidae hosts, all of which were collected feeding on *Arctostaphylos uva-ursi* (Shaw, 2012). Two reared specimens from Scotland were sequenced and clustered in the same BIN (BOLD:AAH1039), one from ?*Stictea mygindiana* (MRS-JFT 0640), and one from *Argyroploce arbutella*/ *Stictea mygindiana* (MRS_JFT0770). This species is illustrated in Fig. 31.

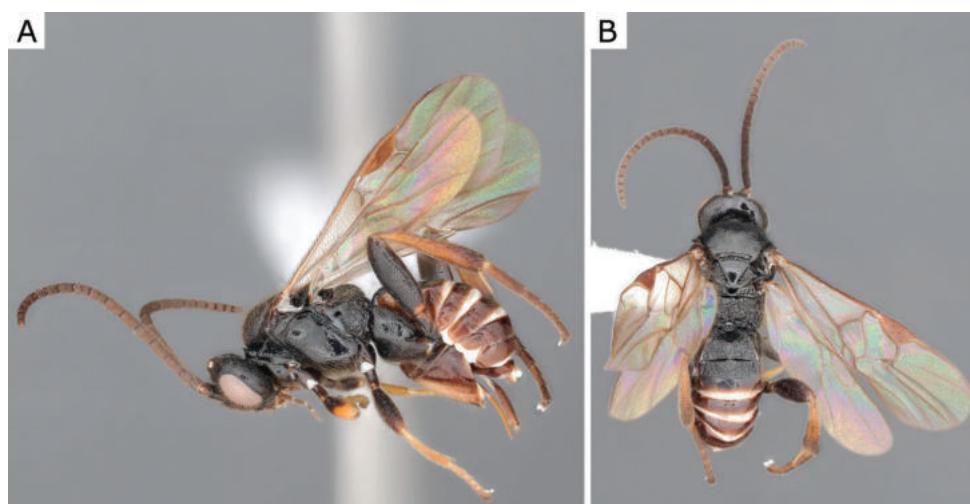


Figure 31. *Microgaster arctostaphylica* Shaw, 2012, female (ZSM-HYM-33160-F12) **A** lateral and **B** dorsal views. Length of the specimen: 3.45 mm.

***Microgaster caris* Nixon, 1968**

Material examined. GERMANY: Bavaria: Allgäu, Oberstdorf, Oytal Magerweide östlich Oytalhaus, 47.388, 10.344, 1056 m, 1.vi.2014, leg. D. Doczkal, S. Schmidt, J. Voith, BC-ZSM-HYM-24118-E02; Atzmansberg, Hessenreuther und Atzmansberger Forst, 49.825, 11.963, 550 m, Malaise trap, 11.vii.2019, leg. J. Müller, ZSM-HYM-42384-B05; Bad Toelz, forest close to Isarstausee, 47.77, 11.547, 652 m, Malaise trap, 16.vii.2019, leg. J. Müller, ZSM-HYM-42378-G03; Berchtesgaden, Bischofswiesener Ache, 47.629, 12.975, 597 m, Malaise trap, 20.vii.2019, leg. J. Müller, ZSM-HYM-42375-F10; Berchtesgaden, Königssee, Wald west of St. Bartholomae, 47.547, 12.965, 620 m, Malaise trap, 14.vii.2017, leg. D. Doczkal, J. Voith, ZSM-HYM-42323-C08; Dienhausen, 47.886, 10.827, 724 m, Malaise trap, 15.vii.2019, leg. J. Müller, ZSM-HYM-42380-A03; Fabrikschleichach, close to Weilersbachtal, 49.917, 10.525, 408 m, Malaise trap, 12.vii.2019, leg. J. Müller, ZSM-HYM-42376-D12; Ketterschwang, Wald, 47.963, 10.676, 650 m, Malaise trap, 16.vii.2019, leg. J. Müller, ZSM-HYM-42381-F10; Marktoberdorf, nördlich von Rieder, 47.76, 10.643, 769 m, Malaise trap, 15.vii.2019, leg. J. Müller, ZSM-HYM-42384-H07; Moos, Isarmündung, Hartholzauwald, 48.786, 12.959, 313 m, Malaise trap, 25.viii.2021, leg. GBOL3, R. Albrecht, ZSM-HYM-42395-A10; Moos, Isarmündung, Mager-rasen, swampy, 48.78, 12.966, 313 m, Malaise trap, 12.viii.2021, leg. GBOL3, R. Albrecht, ZSM-HYM-42396-E09; 25.viii.2021, leg. GBOL3, R. Albrecht, ZSM-HYM-42396-F07; Moos, Isarmündung, *Molinia* meadow, 48.779, 12.95, 313 m, Malaise trap, 12.viii.2021, leg. GBOL3, R. Albrecht, ZSM-HYM-42394-H03; 13.vii.2021, leg. GBOL3, R. Albrecht, ZSM-HYM-42394-B03; 16.vi.2021, leg. GBOL3, R. Albrecht, ZSM-HYM-42391-D03; 25.viii.2021, leg. GBOL3, R. Albrecht, ZSM-HYM-42394-E10; 29.vii.2021, leg. GBOL3, R. Albrecht, ZSM-HYM-42394-C09; 30.vi.2021, leg. GBOL3, R. Albrecht, ZSM-HYM-42391-E09; ZSM-HYM-42391-E10; Moos, Isarmündung, Weichholz Auwald, 48.792, 12.968, 312 m, Malaise trap, 13.vii.2021, leg. GBOL3, R. Albrecht, ZSM-HYM-42395-B12; 25.viii.2021, leg. GBOL3, R. Albrecht, ZSM-HYM-42395-C01; Berchtesgaden National Park, Wald west of St. Bartholomä, 47.547, 12.965, 620 m, Malaise trap, 21.viii.2017, leg. D. Doczkal, J. Voith, ZSM-HYM-33156-F04; ZSM-HYM-33156-F05; Neu-Geusmanns, Wald, 49.76, 11.48, 474 m, Malaise trap, 13.vii.2019, leg. J. Müller, ZSM-HYM-42378-B05; Plattling, Isarmündung, renat. gravel bar, 48.781, 12.906, 317 m, Malaise trap, 25.viii.2021, leg. GBOL3, R. Albrecht, ZSM-HYM-42391-B11; ZSM-HYM-42391-B12; 30.vi.2021, leg. GBOL3, R. Albrecht, ZSM-HYM-42393-H01; Rothenbuch, 49.963, 9.389, 346 m, Malaise trap, 15.vii.2019, leg. J. Müller, ZSM-HYM-42382-C02; ZSM-HYM-42382-C03; Ruhpolding, Fischbach, 47.709, 12.657, 720 m, Malaise trap, 4.vii.2016, leg. D. Doczkal, J. Voith, ZSM-HYM-42398-C10; 47.716, 12.658, 710 m, Malaise trap, 13.ix.2016, leg. D. Doczkal, J. Voith, ZSM-HYM-42323-A03; Siegenburg, 48.755, 11.791, 411 m, Malaise trap, 13.vii.2017, leg. D. Doczkal, J. Voith, ZSM-HYM-42324-D06; Wimmelbach, close to Untere Mark, pond edge, 49.71, 10.994, 290 m, Malaise trap, 12.vii.2019, leg. J. Müller, ZSM-HYM-42381-C12.

Geographical distribution. PAL.

PAL- Austria, China (JL), Czech Republic, Germany*, Hungary, Russia (C, PR), Slovakia, Switzerland.

Molecular data. BIN: BOLD:ACN6851.

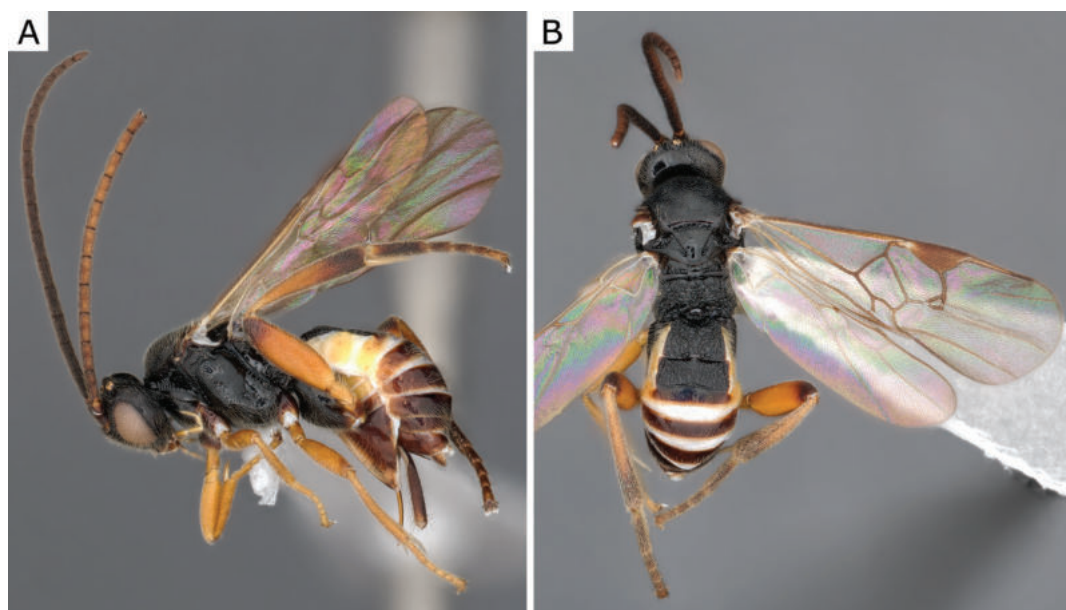


Figure 32. *Microgaster caris* Nixon, 1968, female (ZSM-HYM-33156-F04) **A** lateral and **B** dorsal views. Length of the specimen: 3.55 mm.

Host information. Host of type unknown. Other host associations in need of verification.

Notes. The German specimens were identified by comparison with the original description (Nixon 1968) as well as information from Papp (1976a). The host data associated with this wasp species (?Gelechiidae: ?*Anacampsis populella* (Clerck, 1759); ?Tortricidae: ?*Archips rosana* (Linnaeus, 1758)) was reported in later publications without enough detail and thus it is here considered to be questionable. This species is illustrated in Fig. 32.

***Microgaster nervosae* Shaw, 2023**

Material examined. **GERMANY:** Baden-Württemberg: Malsch, Luderbusch, 48.912, 8.332, 114 m, Malaise trap, 12.iv.2020, leg. D. Doczkal, K. Grabow, ZSM-HYM-42386-G09; Bavaria: Bodenwöhr, Truppenübungsplatz, 49.264, 12.358, 395 m, Malaise trap, 22.v.2016, leg. D. Doczkal, J. Voith, ZSM-HYM-42397-H05; ZSM-HYM-42397-H06; Lkr. Kelheim Siegenburg, Bombodrom, 48.755, 11.791, 411 m, Malaise trap, 26.v.2017, leg. D. Doczkal, J. Voith, ZSM-HYM-33168-H04; ZSM-HYM-33168-H05; 48.759, 11.809, 407 m, Malaise trap, 26.v.2017, leg. D. Doczkal, J. Voith, ZSM-HYM-33168-E09; ZSM-HYM-33168-E10; Siegenburg, Bombodrom, 48.755, 11.791, 411 m, Malaise trap, 14.vi.2017, leg. D. Doczkal, J. Voith, ZSM-HYM-42324-C06; **UNITED KINGDOM:** Scotland: Edinburgh, Blackford Hill, ex. *Agonopterix nervosa*, 23.iv.2019, leg. M. R. Shaw, MRS_JFT0801 [paratype]; 01.v.2019, leg. M. R. Shaw, MRS_JFT0802 [paratype].

Geographical distribution. PAL.

PAL- Germany*, United Kingdom.

Molecular data. BIN: BOLD:ACR4142.

Host information. Depressariidae: type reared from *Agonopterix nervosa* (Haworth, 1811); also *Agonopterix umbellana* (Fabricius, 1794).

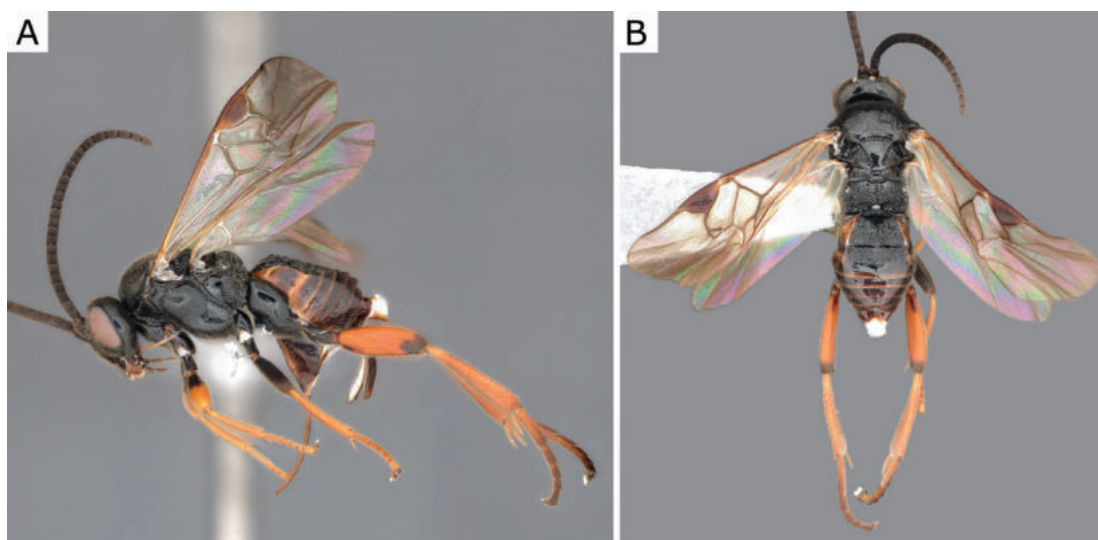


Figure 33. *Microgaster nervosae* Shaw, 2023, female (ZSM-HYM-33168-E09) **A** lateral and **B** dorsal views. Length of the specimen: 4.0 mm.

Notes. This species was very recently described from Britain (Shaw 2023) and German specimens were compared morphologically with the description. Our sequences 100% match the sequences of two paratypes reared from *Agonopterix nervosa* (MRS_JFT0801, MRS_JFT0802). This species is illustrated in Fig. 33.

***Microgaster nixalebion* Shaw, 2004**

Material examined. **AUSTRIA:** Lower Austria: Opponitz, ex. *Patania ruralis*, vi.2007, leg. J. Connell, MRS_JFT0934; **GERMANY:** Baden-Württemberg: Malsch, Hansjakobstr. 7, Urban Garden, 48.884, 8.32, 120 m, Malaise trap, 13.ix.2020, leg. D. Doczkal, ZSM-HYM-33153-H06; Malsch, Hardtwald NE Kieswerk Glaser, 48.915, 8.313, 125 m, Malaise trap, 9.vii.2011, leg. D. Doczkal, ZSM-HYM-42323-D11; Malsch, Luderbusch, 48.913, 8.332, 117 m, Malaise trap, 2.viii.2020, leg. D. Doczkal, K. Grabow, ZSM-HYM-42389-A08; 26.vii.2020, leg. D. Doczkal, K. Grabow, ZSM-HYM-42388-F12; Bavaria: Böbing, Ammertal, 47.747, 10.965, 686 m, 14.vii.2013, leg. D. Doczkal, ZSM-HYM-33420-D06; Dienhausen, 47.886, 10.827, 724 m, Malaise trap, 15.vii.2019, leg. J. Müller, ZSM-HYM-42325-C12; ZSM-HYM-42325-D01; ZSM-HYM-42380-A05; ZSM-HYM-42380-A06; ZSM-HYM-42380-A07; ZSM-HYM-42380-A08; Fabrikschleichach, Lichtung, 49.918, 10.56, 366 m, Malaise trap, 12.vii.2019, leg. J. Müller, ZSM-HYM-42382-F04; ZSM-HYM-42382-F05; Fabrikschleichach, close to Weilersbachtal, 49.917, 10.525, 408 m, Malaise trap, 12.vii.2019, leg. J. Müller, ZSM-HYM-42376-D10; ZSM-HYM-42376-D11; ZSM-HYM-42376-E01; Gütersleben, Gramschatzer Wald, 49.873, 9.932, 272 m, Malaise trap, 12.vii.2019, leg. J. Müller, ZSM-HYM-42379-F08; Lkr. Kelheim Abensberg-Sandharlanden, NSG Sandharlandener Heide, 48.845, 11.801, 376 m, Malaise trap, 3.viii.2017, leg. D. Doczkal, J. Voith, ZSM-HYM-33157-F07; Lkr. Kelheim Siegenburg, Bombodrom, 48.755, 11.791, 411 m, Malaise trap, 8.ix.2017, leg. D. Doczkal, J. Voith, ZSM-HYM-33168-H09; Lohr am Main, Beilstein, Weinberg Waldrand, 50.003, 9.563, 195 m, Malaise trap, 14.vii.2018, leg. D. Doczkal, ZSM-HYM-33156-A01;

3.vi.2018, leg. D. Doczkal, ZSM-HYM-33155-E07; Moos, Isarmündung, *Molinia* meadow, 48.779, 12.95, 313 m, Malaise trap, 30.vi.2021, leg. GBOL3, R. Albrecht, ZSM-HYM-42391-E06; Moos, Isarmündung, Stromtalwiese, 48.777, 12.994, 310 m, Malaise trap, 13.vii.2021, leg. GBOL3, R. Albrecht, ZSM-HYM-42395-E03; München, NSG Allacher Lohe, 48.199, 11.475, 502 m, Malaise trap, 19.viii.2021, leg. GBOL3, R. Albrecht, ZSM-HYM-42326-F04; 23.vi.2021, leg. GBOL3, R. Albrecht, ZSM-HYM-42326-B01; Berchtesgaden National Park, Königssee, Rinnkendlsteig, 47.551, 12.964, 695 m, Malaise trap, 9.viii.2017, leg. D. Doczkal, J. Voith, ZSM-HYM-33162-B05; Berchtesgaden National Park, Wald west of St.Bartholomä, 47.547, 12.965, 620 m, Malaise trap, 28.vi.2017, leg. D. Doczkal, J. Voith, ZSM-HYM-33156-D11; ZSM-HYM-33156-D12; ZSM-HYM-33156-E01; ZSM-HYM-33156-E02; Rhön Fladungen, NSG Schwarzes Moor, Kermi-Hochmoor, 50.512, 10.069, 780 m, Malaise trap, 9.viii.2017, leg. D. Doczkal, ZSM-HYM-33165-A02; Rhön Hausen, Kleines Moor, 50.487, 10.039, 890 m, Malaise trap, 25.vii.2018, leg. D. Doczkal, ZSM-HYM-33165-F06; Sankt Wolfgang, Wald, 48.466, 13.146, 474 m, Malaise trap, 13.vii.2019, leg. J. Müller, ZSM-HYM-42384-A03; Schärding, 48.436, 13.41, 304 m, Malaise trap, 13.vii.2019, leg. J. Müller, ZSM-HYM-42325-D06; ZSM-HYM-42325-D07; ZSM-HYM-42375-E09; Selb, Schönwald, 50.187, 12.1, 675 m, Malaise trap, 14.vii.2019, leg. J. Müller, ZSM-HYM-42381-F04; Siegenburg, Bombodrom, 48.755, 11.791, 411 m, Malaise trap, 13.vii.2017, leg. D. Doczkal, J. Voith, ZSM-HYM-42324-D04; 23.viii.2017, leg. D. Doczkal, J. Voith, ZSM-HYM-42324-G09; 29.vi.2017, leg. D. Doczkal, J. Voith, ZSM-HYM-42324-E12; Thiersheim, Karlmühle, 50.075, 12.152, 517 m, Malaise trap, 15.vii.2019, leg. J. Müller, ZSM-HYM-42381-A02; ZSM-HYM-42381-A05; Volkach, Kolitzheim, 49.922, 10.234, 229 m, Malaise trap, 16.vii.2019, leg. J. Müller, ZSM-HYM-42378-D02; Wimmelbach, close to Untere Mark, pond edge, 49.71, 10.994, 290 m, Malaise trap, 12.vii.2019, leg. J. Müller, ZSM-HYM-42381-C10; München, Obermenzing, Premises of Zoologische Staatssammlung, 48.1648, 11.4849, 519 m, Malaise trap, 31.vii.2017, leg. Axel Hausman, BIOUG42788-F01; **SERBIA**: Southwestern Serbia, 2.3 km SE of Nova Varoš, along Creek, 43.443, 19.853, 1014 m, 14.vi.2009, leg. J. Skevington, CNCH1019; **SPAIN**: Can Liro; Barcelona, Catalonia, ex. *Vanessa atalanta*, 12.v.2006, leg. C. Stefanescu, WAM 0444; Catalonia, El Puig, ex. *Vanessa cardui* on *Echium* sp., 15.vi.2016, leg. C. Stefanescu, MRS_JFT0714; **UNITED KINGDOM**: England, Beetham, Cumbria, ex. *Anthophila fabriciana*, 15.viii.2013, leg. M. R. Shaw, MRS_JFT0342.

Geographical distribution. PAL.

PAL- Austria*, Belgium, France, Germany*, Greece, Serbia*, Spain*, United Kingdom.

Molecular data. BIN: BOLD:ABY6385.

Host information. Choerutidae: type reared from *Anthophila fabriciana* (Linnaeus, 1767); also *Prochoreutis myllerana* (Fabricius, 1794); Nymphalidae: *Aglais urticae* (Linnaeus, 1758), *Vanessa atalanta* (Linnaeus, 1758); *Vanessa cardui** (Linnaeus, 1758); Pyralidae: *Patania ruralis* (Scopoli, 1763).

Notes. German specimens were identified by comparing with the information in the original description (Shaw 2004) as well as specimens deposited in the CNC. Our sequences from German specimens are a 100% match for barcode sequences of several reared specimens: two specimens identified as *M. nixalebion*, one reared from *Patania ruralis* (MRS_JFT0934), one from

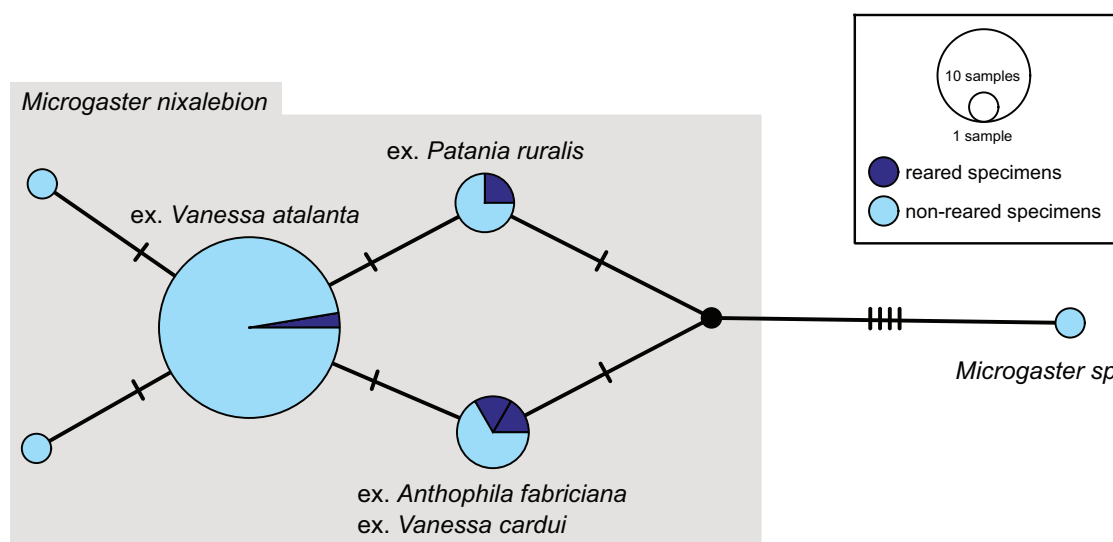


Figure 34. TCS haplotype network of BIN BOLD:ABY6385, sequence length for analysis: 392 bp to accommodate MRS_JFT0342=MARKB109-21 ex. *Anthophila fabriciana* from the United Kingdom. The haplotypes morphologically identified as *Microgaster nixalebion* as part of this project are marked by a grey background. Each hatch mark in the network represents a single mutational change; small black dots at nodes indicate missing haplotypes. The diameter of the circles is proportional to the number of haplotypes sampled (see legend). The aligned sequences and traits can be reviewed in Suppl. materials 10, 11.

Vanessa atalanta (WAM 0444=MRS_JFT 0029). There are two more reared specimens in this barcoding cluster, both males and initially determined only to genus, one from *Vanessa cardui* (Linnaeus, 1758) (MRS_JFT0714) and one from *Anthophila fabriciana*, the host of the holotype (MRS_JFT0342). A single specimen in this barcoding cluster differs by several mutations from the other sequences; until more specimens for morphological study are available we keep it as *Microgaster* sp. (ZSM-HYM-42325-G10) (see Fig. 34). This species is illustrated in Fig. 35.

Microgaster raschkiellae Shaw, 2012

Material examined. GERMANY: Bavaria: Rhön Hausen, Eisgraben, basalt block heap at forest edge, 50.503, 10.09, 735 m, Malaise trap, 23.vii.2018, leg. D. Doczkal, ZSM-HYM-33166-C08; Rhön Hausen, Kleines Moor, 50.487, 10.039, 890 m, Malaise trap, 25.vii.2018, leg. D. Doczkal, ZSM-HYM-33165-G04; **UNITED KINGDOM:** Scotland: Armadale, Skye, ex. *Mompha raschkiella*, 4.vii.2012, leg. M. R. Shaw, CNCHYM45380.

Geographical distribution. NEA, PAL.

NEA: Canada (MB); PAL: Germany*, United Kingdom.

Molecular data. BOLD:AAC9130.

Host information. Momphidae: type reared from *Mompha raschkiella* (Zeller, 1839).

Notes. German specimens were identified by comparing to the original description (Shaw 2012a). BIN BOLD:AAC9130 probably includes more than one species. This BIN includes two haplotype clusters (Fig. 36) separated by seven mutations. Cluster A includes specimens from the United Kingdom identified

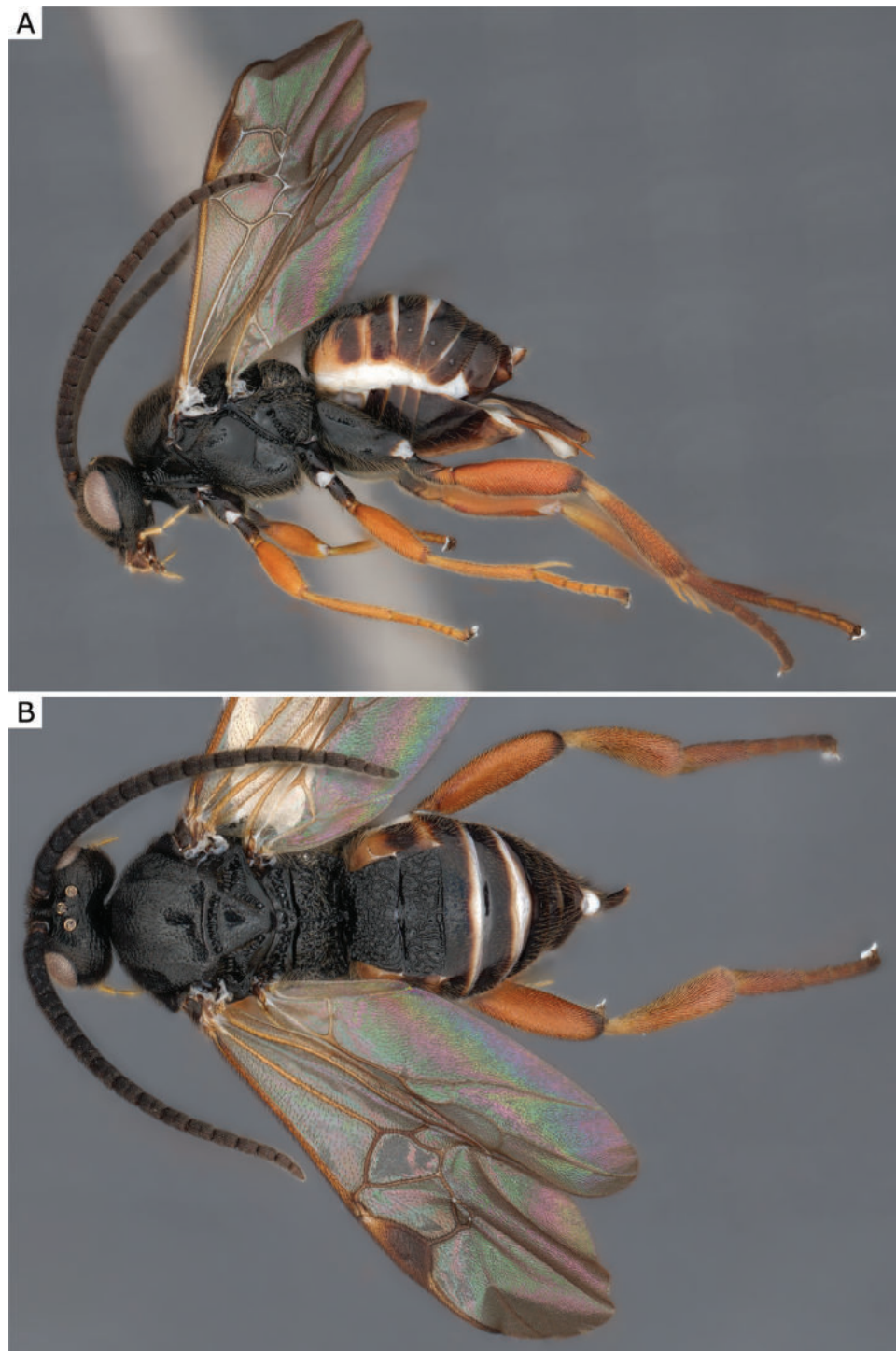


Figure 35. *Microgaster nixalebion* Shaw, 2004, female (ZSM-HYM-42380-A06) **A** lateral and **B** dorsal views. Length of the specimen: 4.25 mm.

by the original author of the species and reared from the same host as the holotype (CNCHYM45380=MRS_JFT0192). Our specimens collected from Germany cluster with these authoritatively identified specimens and match the species morphologically with some minor differences. We consider them *Microgaster raschkiellae* and report this species for Germany for the first time. Cluster B likely represents a different species from the Nearctic, but exploring this further is beyond the scope of this project. This species is illustrated in Fig. 37.

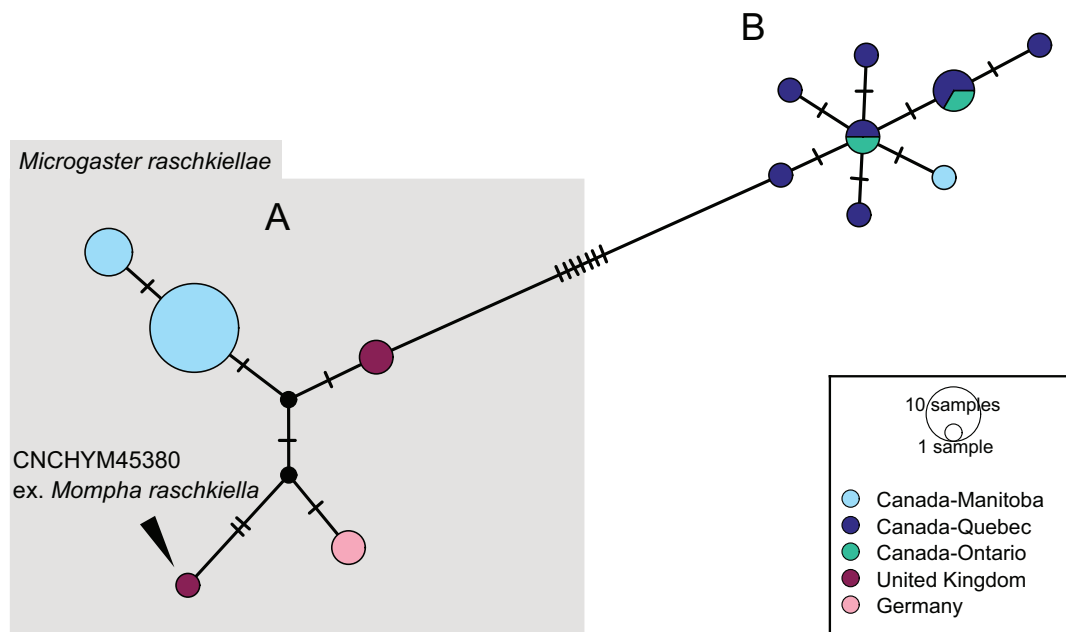


Figure 36. TCS haplotype network of BIN BOLD:AAC9130, the haplotypes morphologically identified as *Microgaster raschkiellae* as part of this project are in cluster A and marked by a grey background. Each hatch mark in the network represents a single mutational change; small black dots at nodes indicate missing haplotypes. The diameter of the circles is proportional to the number of haplotypes sampled (see legend). The aligned sequences and traits can be reviewed in Suppl. materials 12, 13.

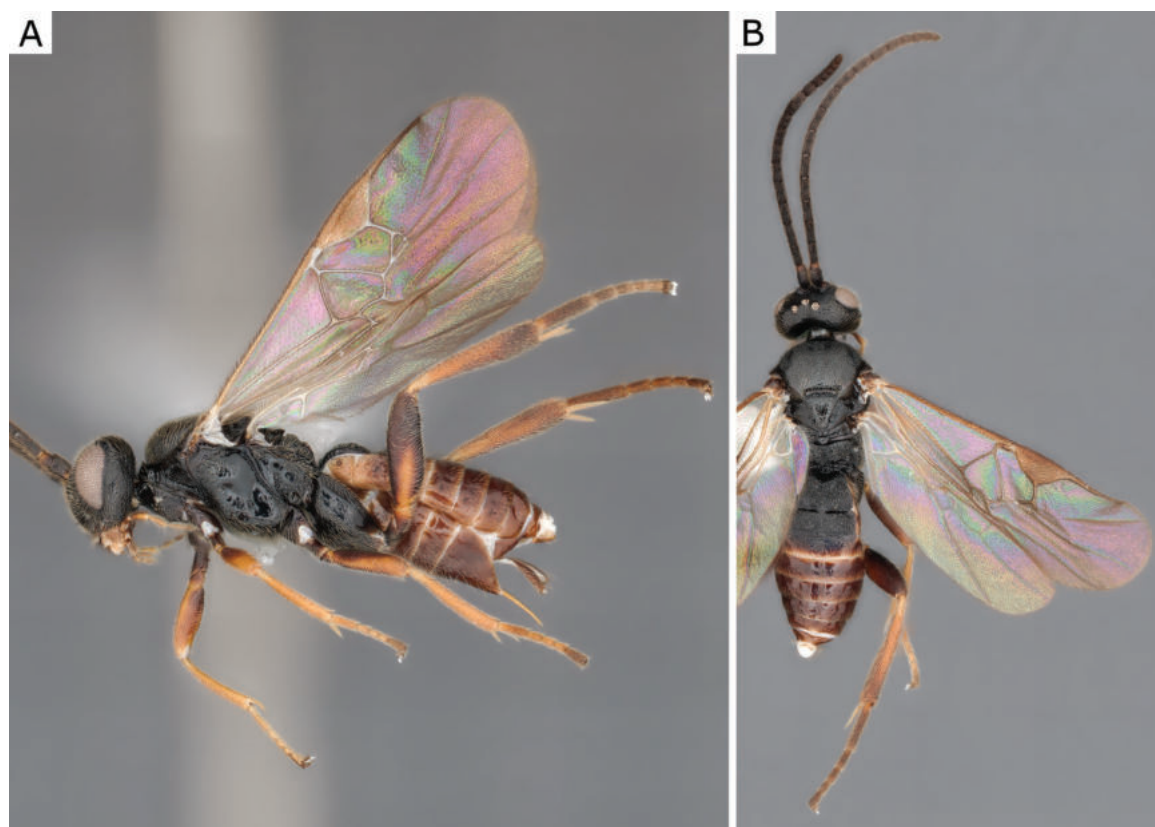


Figure 37. *Microgaster raschkiellae* Shaw, 2012, female (ZSM-HYM-33165-G04) **A** lateral and **B** dorsal views. Length of the specimen: 3.0 mm.

***Microplitis coactus* (Lundbeck, 1896)**

Material examined. **CANADA:** Newfoundland and Labrador: Saglek, Torngat Mountains NP, Base Camp south of park, 58.451, -62.798, 5 m, 01.viii.2014, leg. D. Whitaker, BIOUG18647-F03; Nunavut: Ellesmere Island, Hazen Camp, 81.816667, -71.300000, [date unknown, leg. unknown], CNC497575; **GERMANY:** Bavaria: Atzmannsberg, Hessenreuther and Atzmannsberger Forst, 49.825, 11.963, 550 m, Malaise trap, 11.vii.2019, leg. J. Müller, ZSM-HYM-42384-B08; St. Oswald, National Park Bayerischer Wald, 48.9509, 13.422, 842 m, Malaise trap, 20.vi.2012, leg. G. Sellmayer, BIOUG05949-B01.

Geographical distribution. NEA, PAL.

NEA- Canada (NL*, NU), Greenland; PAL- Germany*, Iceland.

Molecular data. BIN: BOLD:ACA4555.

Host information. Host of type unknown; also Noctuidae.

Notes. German specimens were identified by comparison with many specimens at the CNC (see Figs 38, 39) and by checking the keys and information in Papp (1984b) and van Achterberg (2006) and the original description (Lundbeck 1896). The associated host information is taken from the original description of the species (Lundbeck 1896, 244) which stated that (loose translation from Danish follows): “there were nine specimens from earlier dates without a

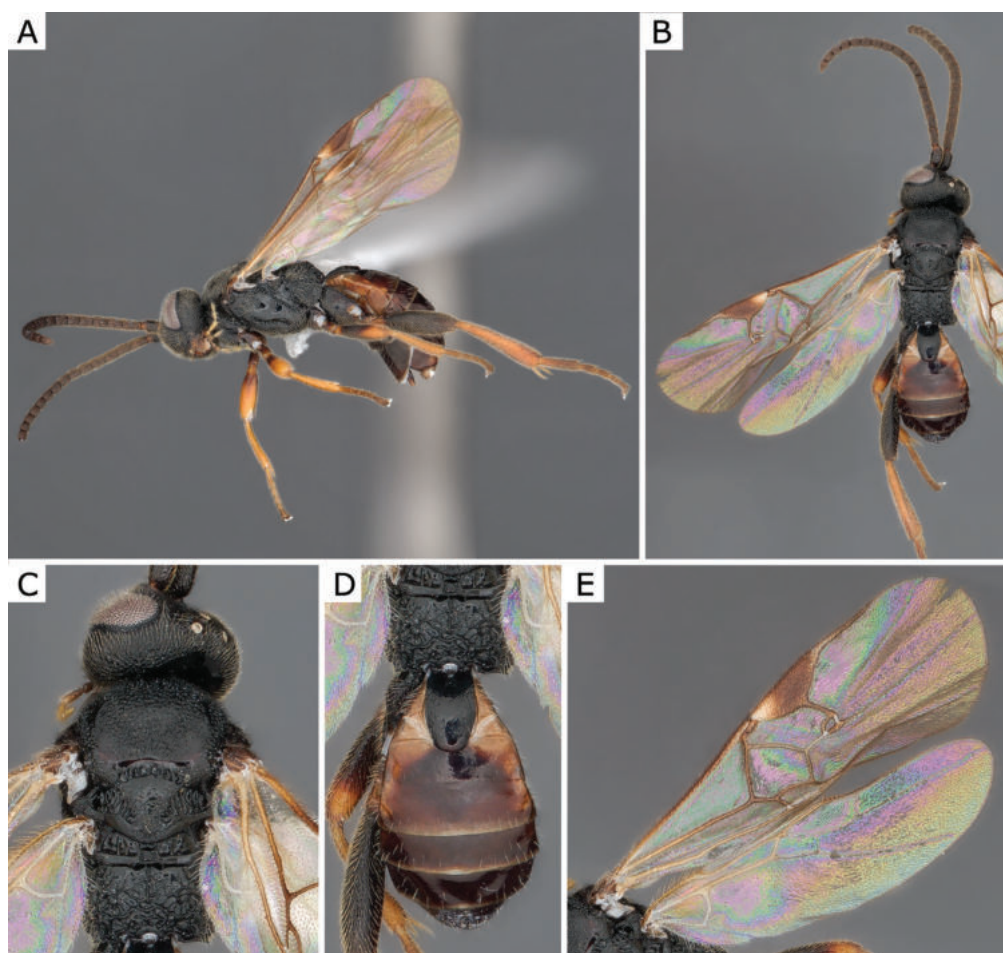


Figure 38. *Microplitis coactus* (Lundbeck, 1896), female (ZSM-HYM-42384-B08) **A** lateral view **B** dorsal view **C** mesosoma **D** metasoma **E** wing. Length of the specimen: 2.6 mm.

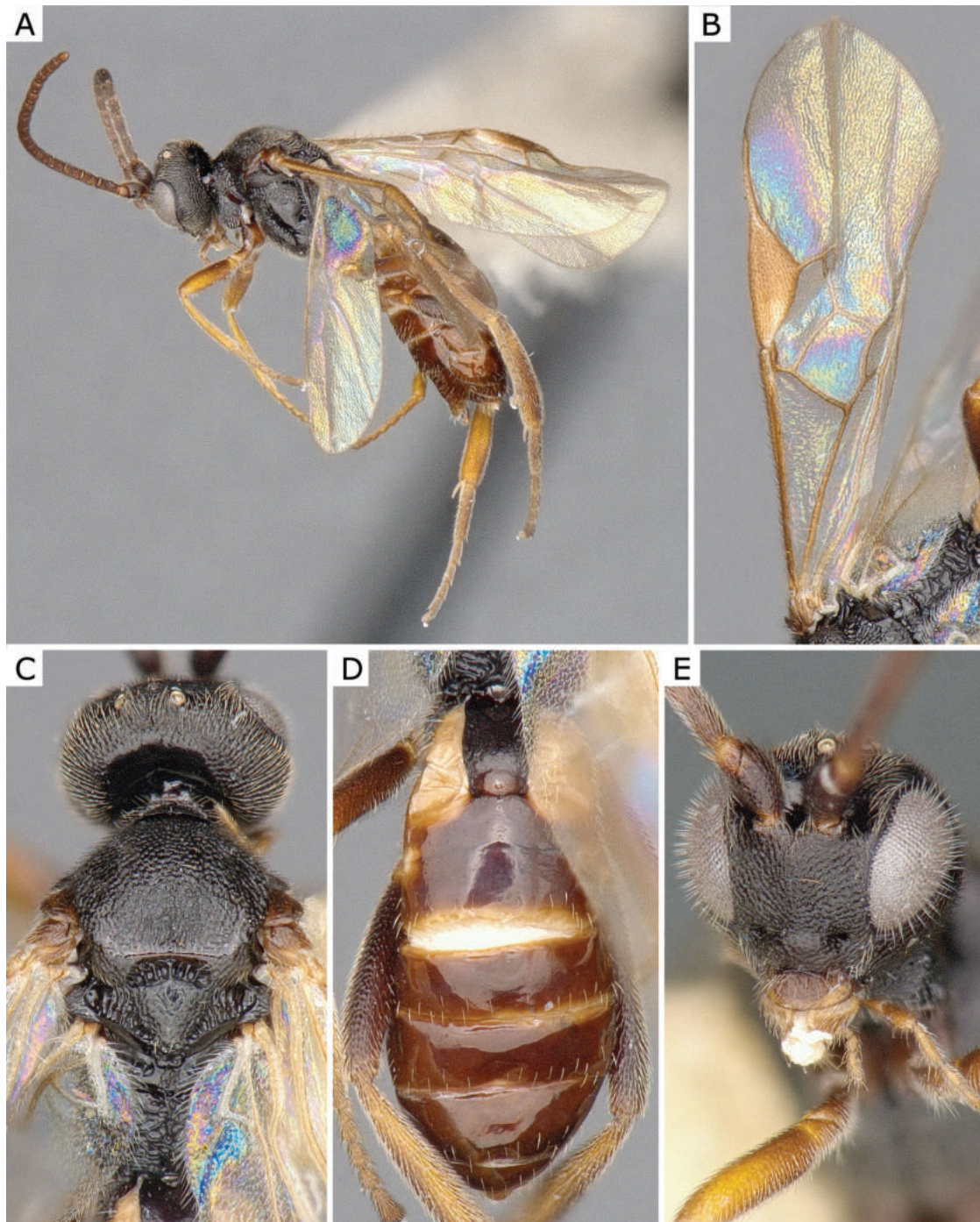


Figure 39. *Microplitis coactus* (Lundbeck, 1896), female (CNC497575) **A** lateral view **B** forewing **C** mesosoma **D** metasoma **E** head frontal view.

specific locality, all females; according to the inscription, they hatched from a *Noctua* species [this would refer just to a noctuid = Noctuidae at that time]. [...] The wasp cocoons seem to form a hollow ball and were found under rocks in several places in both northern and southern Greenland”. This is the first record of the species outside the Nearctic and Iceland. The sequences from Germany match well (0.31% p-distance) with the sequences from Greenland available in BOLD, and the corresponding BIN is fairly cohesive (average of 0.58% of bp difference within BIN and 0.96% max. p-distance within the BIN) and compara-

tively very well differentiated from any other BIN currently in BOLD (nearest BIN is at 3.57% p-distance), therefore confirming also from a molecular perspective the presence of this species in Europe. This species is illustrated in Figs 38, 39.

***Microplitis kewleyi* Muesebeck, 1922**

Material examined. GERMANY: Bavaria: Ammergebirge Halblech, Im Laich, gravel bar, 47.606, 10.841, 904 m, Malaise trap, 16.ix.2016, leg. D. Doczkal, J. Voith, ZSM-HYM-33167-F01; Forchheim, Untere Mark bei Willersdorf, 49.739, 10.969, 261 m, Malaise trap, 12.vii.2019, leg. J. Müller, ZSM-HYM-42377-F06; Lkr. Kelheim Abensberg-Sandharlanden, NSG Sandharlandener Heide, 48.845, 11.801, 376 m, Malaise trap, 3.viii.2017, leg. D. Doczkal, J. Voith, ZSM-HYM-33157-E03; Marquartstein, close to Rathaus, 47.759, 12.462, 543 m, Malaise trap, 19.vii.2019, leg. J. Müller, ZSM-HYM-42380-C10; Plattling, Isarmündung, renat. gravel bar, 48.781, 12.906, 317 m, Malaise trap, 25.viii.2021, leg. GBOL3, R. Albrecht, ZSM-HYM-42391-B09; Siegenburg, Bombodrom, 48.76, 11.807, 410 m, Malaise trap, 23.viii.2017, leg. D. Doczkal, J. Voith, ZSM-HYM-42324-C05; Sielstetten, östlich Grafendorfer Forst, 48.578, 11.863, 520 m, Malaise trap, 16.vii.2019, leg. J. Müller, ZSM-HYM-42383-A06; Willersdorf, Untere Mark, 49.733, 10.985, 292 m, Malaise trap, 12.vii.2019, leg. J. Müller, ZSM-HYM-42379-A12.

Geographical distribution. NEA, PAL.

NEA- Canada (AB, MB, NB, NL, NS, ON, PE, QC), United States (CA, DC, IA, MD, MI, NJ, NY, WI); PAL*- Germany*.

Molecular data. BIN: BOLD:AAB8493.

Host information. Noctuidae: type reared from *Euxoa* sp.; also *Agrotis ipsilon* (Hufnagel, 1766), *Euxoa ochrogaster* (Guenée, 1852), *Pseudohermonassa bicarnea* (Guenée, 1852).

Notes. German specimens were identified by comparison with many specimens in the CNC and by checking the keys and information in Muesebeck (1922). This is the first record of the species outside the Nearctic. A few described species in the Palearctic share some characteristics with *M. kewleyi* (and other Nearctic species), particularly the short antenna, large pale spot anteriorly on pterostigma, and relatively small body size (e.g., see couplet 21 in Nixon (1970) and Papp (1984b)). However, *M. kewleyi* can be distinguished from *M. spectabilis* based on shape of T1 and darker colour of anterior flagellomeres; from *M. tristis* because wings are not infumated, shorter inner spur of metatibia, and thinner femora; from *M. pallidipennis* based on shape and sculpture of T2; from *M. steinbergi* because of thinner metafemur and metatibia; and from *M. heterocerus* because of a much larger pale spot on pterostigma, different leg colouration and thinner femora. Eight sequences from Germany match 100% with the many sequences from Canada and the USA available in BOLD, and the corresponding BIN is very cohesive (average of 0.03% of bp difference within BIN members) and very apart from any other BIN currently in BOLD (nearest BIN is 5.77% different), therefore confirming also from a molecular perspective the presence of this species in Europe (Germany). There are also two sequences from Bulgaria, two from Pakistan, and one from Tanzania, but those specimens are from different institutions which we were not able to examine, and no photographs were available for them in BOLD either. Therefore, those countries are

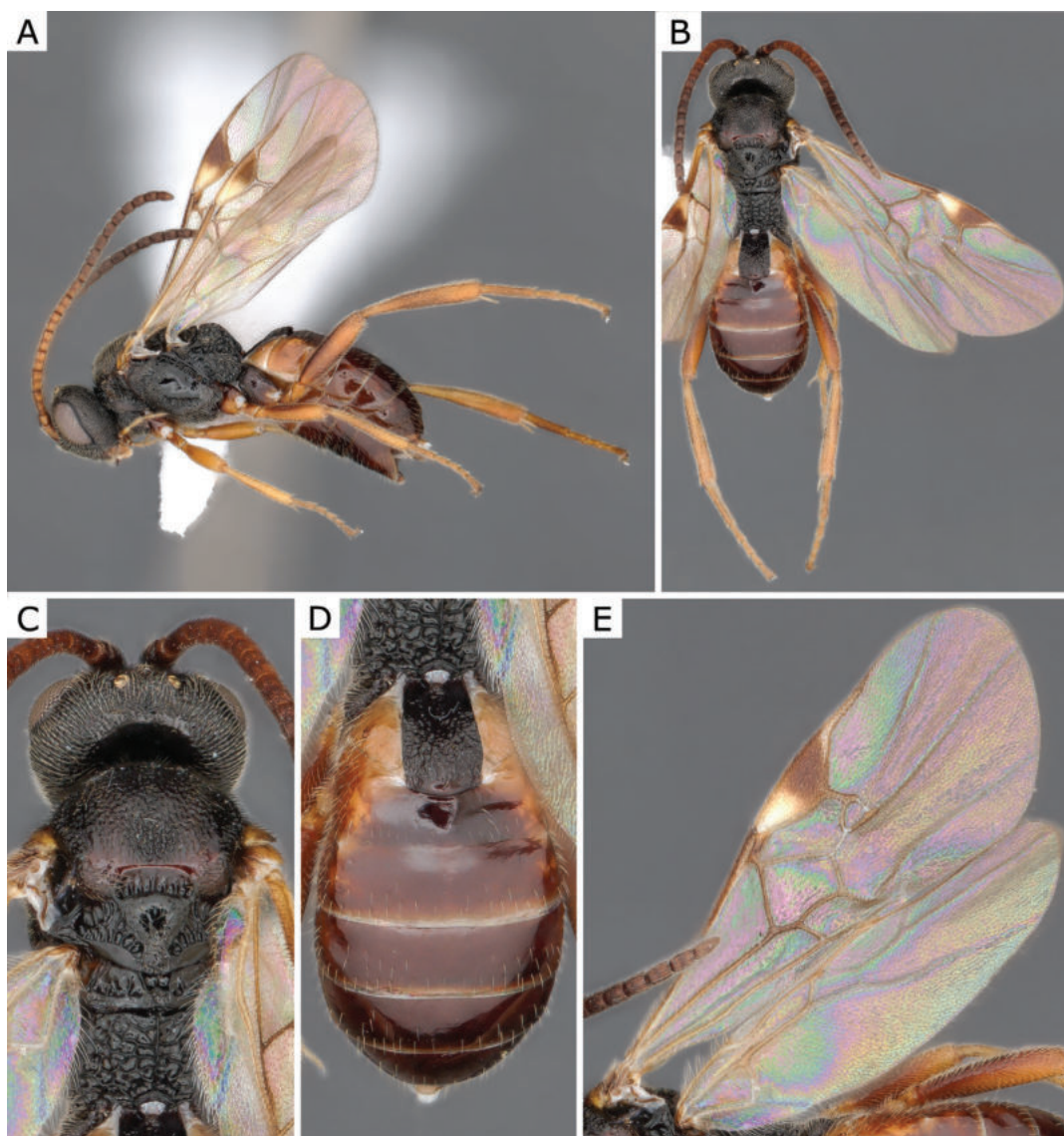


Figure 40. *Microplitis kewleyi* Muesebeck, 1922, female (ZSM-HYM-33157-E03). **A** lateral view, **B** dorsal view, **C** mesosoma, **D** metasoma, **E** wing. Length of the specimen: 2.35 mm.

not recorded for the species here, even if the DNA barcode evidence indicates a reasonable chance that *M. kewleyi* could also be present there. Two of the hosts associated with this species were recorded by Muesebeck, who had described the wasp species and are therefore considered to be accurate. A third host, *Euxoa ochrogaster*, is within the same genus as the host of the type and it is also considered to be reliable. Only one host record from the literature is here considered to be questionable, as it comes from a compilation of information without any supporting evidence. This species is illustrated in Fig. 40.

***Microplitis naenia* Nixon, 1970**

Material examined. **CZECH REPUBLIC:** South Moravia: Obora Soutok, Lanžhot, 48.69, 16.945, 165 m, ex. *Orthosia cruda*, 14.v.2013, leg. P. Drozd, BC-ZSM-HYM-23873-E06; **GERMANY:** Bavaria: Grettstadt, 49.963, 10.372, 248 m, can-

opy fogging, 28.v.2021, leg. B. Leroy, ZSM-HYM-42393-D05; Iphofen, 49.646, 10.315, 355 m, canopy fogging, 2.v.2019, leg. B. Leroy, ZSM-HYM-33158-A10; Prichsenstadt, 49.855, 10.304, 258 m, canopy fogging, 1.v.2019, leg. B. Leroy, ZSM-HYM-33158-A09; Schonungen, 50.077, 10.429, 359 m, canopy fogging, 23.v.2019, leg. B. Leroy, ZSM-HYM-33158-E05; ZSM-HYM-33158-E06; Wiesenheid, 49.803, 10.277, 216 m, canopy fogging, 1.v.2019, leg. B. Leroy, ZSM-HYM-33158-B02; ZSM-HYM-33158-B03; Thüringen: Neubrunn, 50.511, 10.457, 448 m, canopy fogging, 29.v.2021, leg. D. Rabl, ZSM-HYM-42447-D08.

Geographical distribution. PAL.

PAL- Czech Republic*, Germany*, Hungary, Russia (C, NW), Slovakia, Turkey, United Kingdom.

Molecular data. BINs: BOLD:ABV9098, BOLD:AEK2564.

Host information. Host of type unknown; also Noctuidae: *Cosmia trapezina* (Linnaeus, 1758), *Conistra vaccinii* (Linnaeus, 1761), *Eupsilia transversa* (Hufnagel, 1766), *Orthosia cruda* (Denis & Schiffermüller, 1775), *Orthosia cerasi* (Fabricius, 1775), *Rileyiana fovea* (Treitschke, 1825).

Notes. The morphology of our material (see Fig. 41) matches the species described in Nixon (1970), as well as the keys in Papp (1984b), Tobias (1986), and

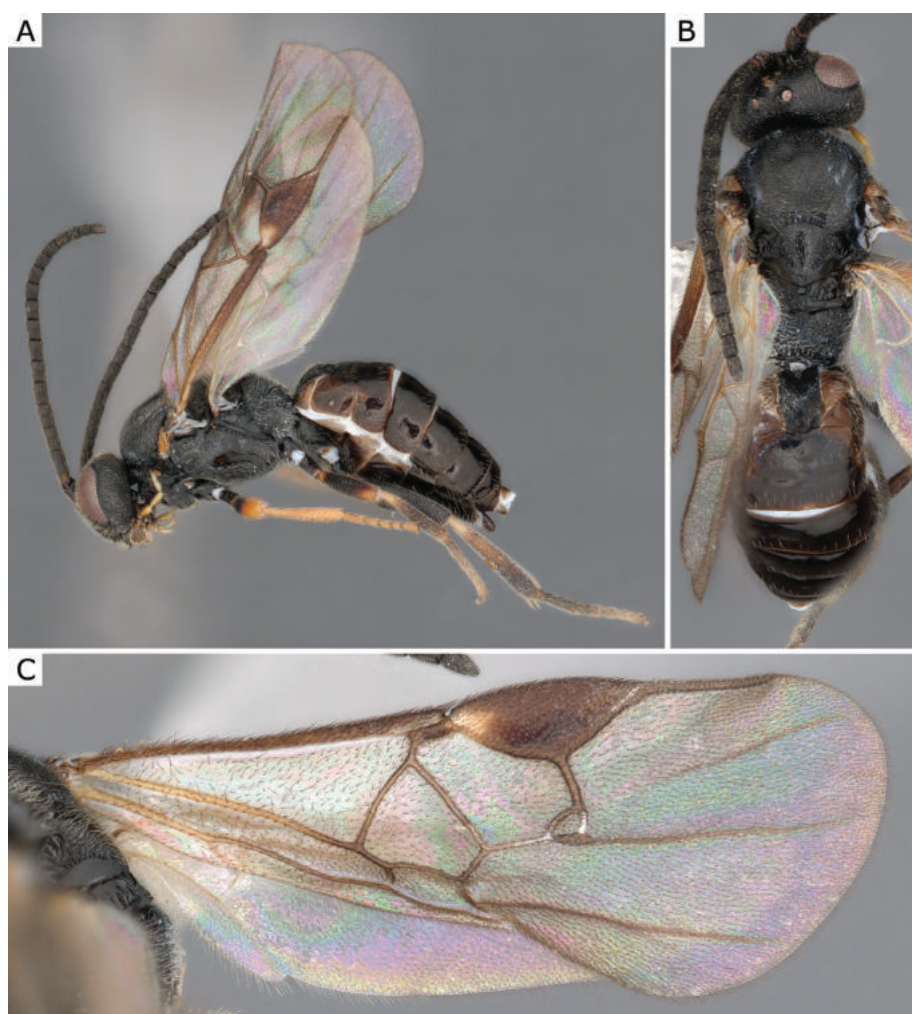


Figure 41. *Microplitis naenia* Nixon, 1970, female (ZSM-HYM-42447-D08) **A** lateral view **B** meso- and metasoma **C** wing. Length of the specimen: 3.5 mm.

Kotenko (2007). There are two BINs which we associate with this species. Our specimens show some intraspecific morphological variability, which matches what Nixon mentioned in the original description of the species. Specimens of both barcoding clusters parasitise the same host, *Orthosia cruda*, from which two of Nixon's paratypes were reared. One specimen from BOLD:ABV9098 (BC-ZSM-HYM-23873-E06) was reared from this species, and we have metabarcoding data that strongly indicates that members of BOLD:AEK2564 parasitise the same host species. Metabarcoding of 22 individual caterpillars of *O. cruda* resulted in more than 100 reads per caterpillar of sequences that match this BIN. With this information, we consider our specimens of both barcoding clusters to represent members of *M. naenia*. BIN BOLD:ABV9098 and BOLD:AEK2564 are separated by 1.71% p-distance and the species has an intraspecific variability of 2.63% (p-distance). The hosts associated with this wasp species were reported either by Nixon (1970), as part of the original description, or by Capek (1972) and Capek et al. (1982); we consider both to be reliable because some of the material reported by Nixon (1970) came from Capek. This species is illustrated in Fig. 41.

***Pholetesor bedelliae* (Viereck, 1911)**

Material examined. **CANADA:** New Brunswick: Fredericton, 45.963487, -66.6442, 9.vii.1970, leg. C. M. Yoshimoto, CNCHYM 03145 [paratype]; **GERMANY:** Bavaria: Bayreuth, Gemein, Trebgast, 49.989, 11.603, 348 m, Malaise trap, 11.vii.2019, leg. J. Müller, ZSM-HYM-42385-C09; Volkach, Stammheim am Main, 49.92, 10.192, 215 m, Malaise trap, 16.vii.2019, leg. J. Müller, ZSM-HYM-42380-E08.

Geographical distribution. AUS, NEA, NEO, PAL.

AUS: Hawaiian Islands; NEA: Canada (AB, BC, MB, NB, NS, ON, QC, SK), USA (AK, AZ, AR, CA, CT, DC, FL, IL, IA, KA, LA, MO, NJ, NY, OR, VA); NEO: Bermuda, Peru; PAL: Finland, Germany*.

Molecular data. BIN: BOLD:AAA9172.

Host information. Types reared from *Bedellia* sp. At least 21 host species within seven families of Lepidoptera have been recorded as hosts of this wasp species (Yu et al. 2016), but many may be incorrect and thus are not cited here.

Notes. We compared our specimens to a paratype and many other Nearctic specimens stored at the CNC (such as CNCHYM 03145), as well as the comprehensive description in Whitfield (2006). Morphologically, this species is somewhat similar to *Pholetesor maritimus* (Wilkinson, 1941), which is also recorded from Europe (Fernandez-Triana et al. 2020). However, the characters used by Nixon (1973) do not work in all cases to separate these species, as some specimens of *Pholetesor bedelliae* have coarse/strong sculpture (of T1, T2, and anteromesoscutum) that approaches or is very similar to the sculpture described for *P. maritimus*. DNA barcodes unequivocally show that the two species are far apart and that the German specimens clearly cluster with many specimens identified by us of *P. bedelliae* from Canada and USA. All these sequences are separated by ~ 5% p-distance from the sequences of *P. maritimus* currently available in BOLD (MRS_JFT0464, MRS_JFT0471). Many hosts associated with *P. bedelliae* in the historical literature are probably incorrect, due to problems identifying both the wasp and caterpillar species (e.g., see Whitfield 2006); solving this problem is beyond the scope of this paper. This species is illustrated in Fig. 42.

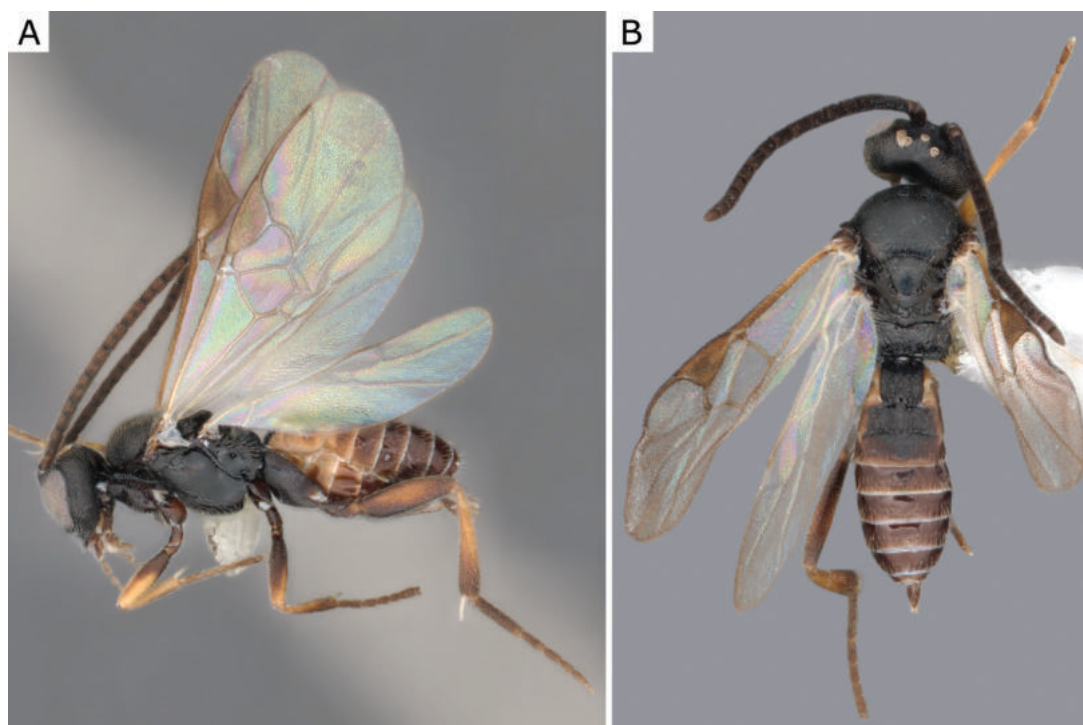


Figure 42. *Pholetesor bedelliae* (Viereck, 1911), female (ZSM-HYM-42380-E08) **A** lateral and **B** dorsal view. Length of the specimen: 2.15 mm.

***Protopanteles endemus* (Nixon, 1965)**

Material examined. **FRANCE:** Jura, Ounans, ex. *Thyatira batis*, 25.vii.2013, leg. M. R. Shaw, MRS_JFT0355; **GERMANY:** Baden-Württemberg: Malsch, Hansjakobstr. 7, Urban Garden, 48.884, 8.32, 120 m, Malaise trap, 30.viii.2020, leg. D. Doczkal, ZSM-HYM-33153-G08; Malsch, Luderbusch, 48.913, 8.332, 117 m, Malaise trap, 19.vii.2020, leg. D. Doczkal, K. Grabow, ZSM-HYM-42388-D09; **POLAND:** Biebrza National Park, cocoons on *Ribes nigrum* with *Abraxas grossulariata*, leg. M. R. Shaw, MRS_JFT0444.

Geographical distribution. PAL.

PAL: France, Germany*, Hungary, Kazakhstan, Poland*, Russia (ZAB, SPE), Switzerland, Ukraine, United Kingdom.

Molecular data. BIN: BOLD:AEI1558.

Host information. Geometridae: Type reared from *Abraxas grossulariata* (Linnaeus, 1758); also Drepanidae*: *Thyatira batis** (Linnaeus, 1758).

Notes. The German specimens were identified based on information from the original description (Nixon 1965) as well as subsequent papers (Nixon 1976; Papp 1984a). Our German sequences 99.7–100% match two identical sequences of specimens with some host relations: one was collected as a cocoon from *Ribes* sp. with *Abraxas grossulariata* (MRS_JFT0444), the Geometrid species the holotype was reared from (Nixon 1965). Another specimen was reared from *Thyatira batis* (MRS_JFT0355), a rather novel host and member of Drepanidae. We propose here that an additional host record from the literature is excluded: Tobias (1971: 246) had recorded *Autographa gamma* (Linnaeus, 1758) Noctuidae as a host of *Protopanteles endemus* in the St. Petersburg (as Leningrad) region; however, a subsequent paper from the same author (Tobias

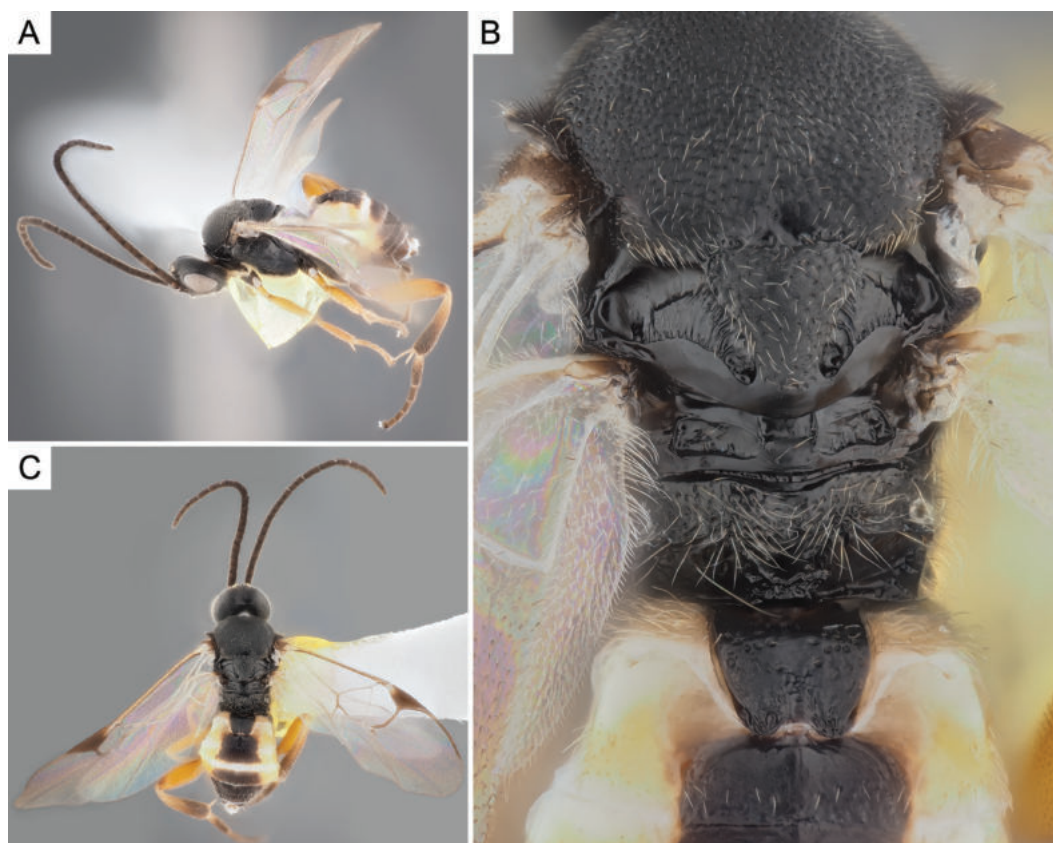


Figure 43. *Protapanteles endemus* (Nixon, 1965), female (ZSM-HYM-33153-G08) **A** lateral view **B** mesosoma, T1, and T2 **C** dorsal view. Length of the specimen: 2.5 mm.

1986: 661) ignored that host record and even the record of the wasp species from that region (it only recorded *P. endemus* from a much more southern region of the former Soviet Union, now Ukraine). It is likely that either the wasp, the host or both were misidentified in the 1971 paper and therefore this record must be removed (unless additional data in the future confirms that association). This species is illustrated in Fig. 43.

***Rasivalva desueta* Papp, 1989**

Material examined. **GERMANY:** Bavaria: Bayernwald National Park, Schöberg, ex. *Eilema depressa*, 16.vi.2015, leg. M. R. Shaw, MRS-JFT 0582; Berchtesgaden National Park, Königssee, Rinnkendlsteig, 47.555, 12.965, 750 m, Malaise trap, 21.viii.2017, leg. D. Doczkal, J. Voith, ZSM-HYM-33162-A05; **SWEDEN:** Öland: Gamla Skogsby (Kalkstad); Mörbylånga kommun, 56.616700, 16.507617, Malaise trap, 17.vii-7.viii.2003, leg. SMTP, CNC602554.

Geographical distribution. PAL.

PAL- Germany*, Sweden*, Switzerland.

Molecular data. BIN: BOLD:ADE2589.

Host information. Host of type unknown. Other host associations in need of verification.

Notes. The non-reared German specimen was identified as *Rasivalva desueta* by comparing it with the detailed original description (Papp 1989) and

Oltra-Moscardó and Jiménez-Peydró (2005). One male specimen (MRS-JFT 0582) in this cluster, also from Germany, was possibly reared from *Eilema depressa* (Esper, 1787) which would represent the first host record for this wasp species. However, the wasp cocoon could not be associated unequivocally with host remains and hence the host association needs to be confirmed. We also report Sweden as a new country record based on a male specimen we examined (CNC602554), which is morphologically similar to the German female (except for darker metafemur and less broad T1 and T2, in agreement with the original description of a male paratype) as well as matching DNA barcode sequences. This species is illustrated in Figs 44, 45.

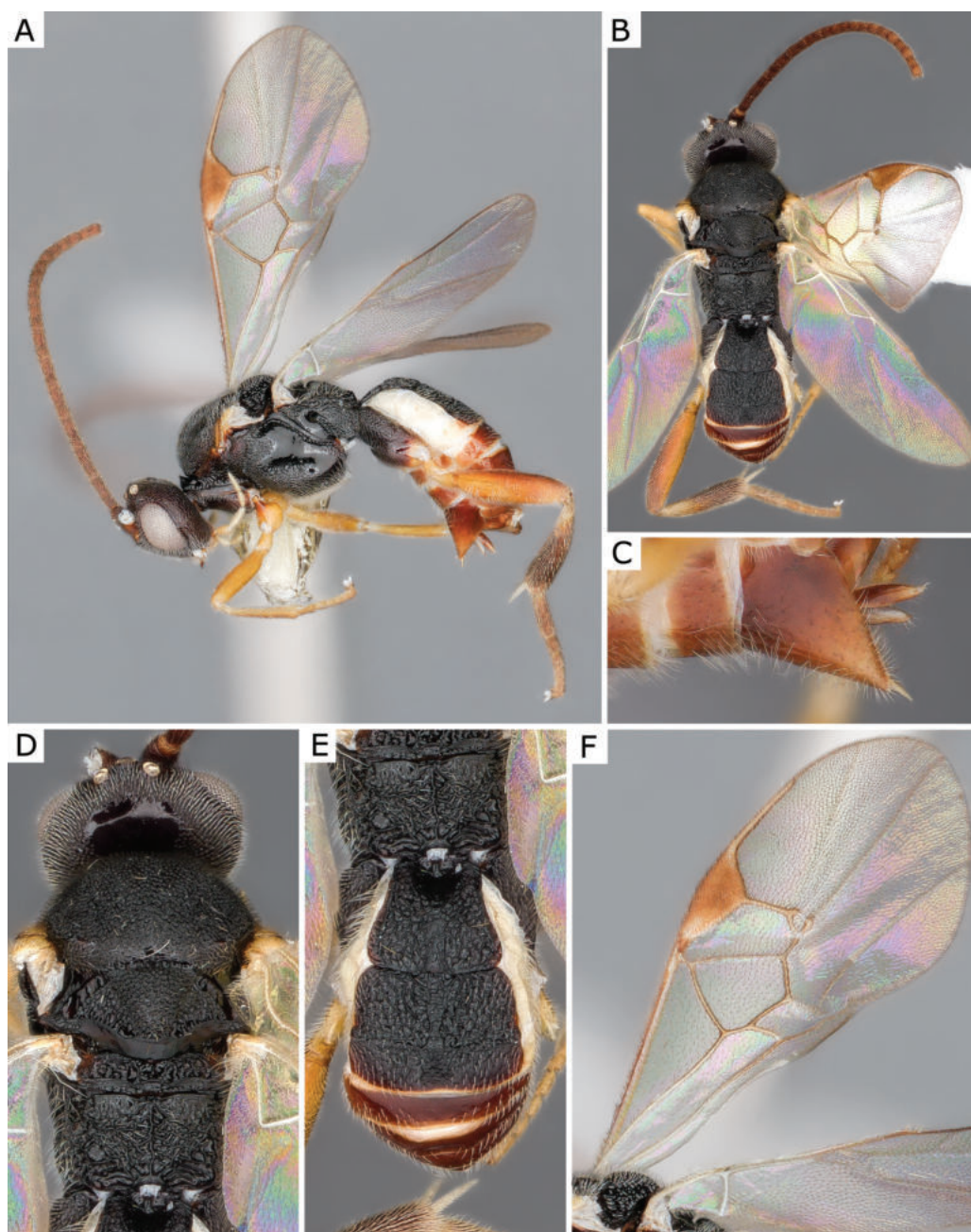


Figure 44. *Rasivalva desueta* Papp, 1989, female (ZSM-HYM-33162-A05) **A** lateral view **B** dorsal view **C** hypopygium lateral view **D** mesosoma **E** metasoma **F** forewing. Length of the specimen: 3.3 mm.

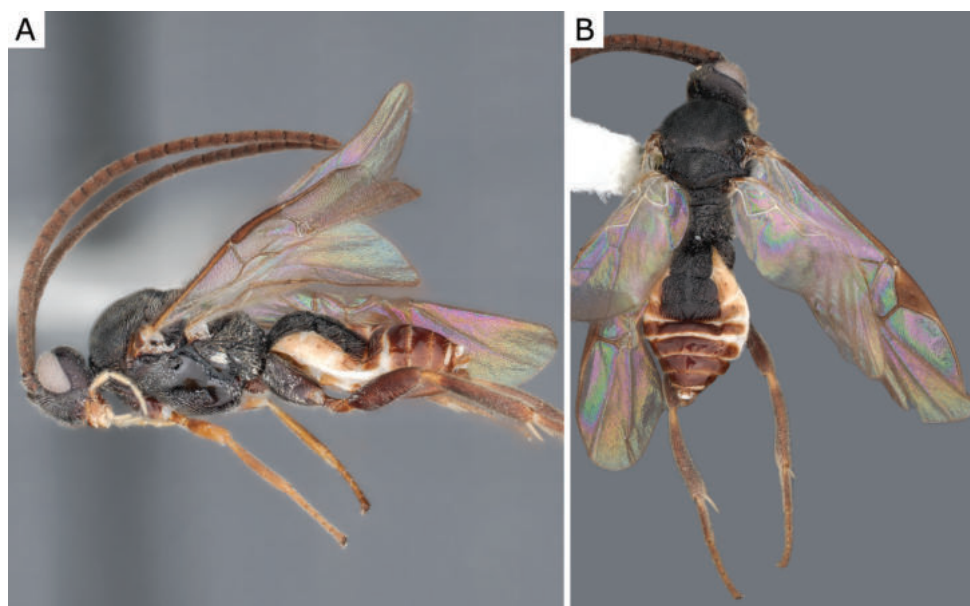


Figure 45. *Rasivalva desueta* Papp, 1989, male (CNC602554) **A** lateral and **B** dorsal views.

Additional species

Cotesia eulipis (Nixon, 1974)

Material examined. **CANADA:** British Columbia: Winfield, 50.061, -119.431, [450m], ex. *Operophtera bruceata*, 17.v.2001, leg. K. Deglow, CNCHYM 00330; CNCHYM 00331; Prince Edward Island: Brackley Beach, Prince Edward Island National Park, 46.431111, -63.216111, ex. *Rheumaptera hastata*, 10.viii.1940, leg. G.S. Walley, CNC1447813; Yukon: Top of the World Highway km 82, 64.09, -140.951, 19.vii.2006, leg. H. Goulet, C. Boudreault, HYM00001784; **FINLAND:** Lapland: Utsjoki, Kevo, ex. *Operophtera brumata*, 28.vi.2010, leg. K. Ruohomaki, MRS 0049; MRS_JFT0049; Utsjoki, Vetsikko, ex. *Operophtera brumata*, 28.vi.2010, leg. K. Ruohomaki, MRS 0050; **GERMANY:** Bavaria; St. Oswald, National Park Bayerischer Wald, 48.951, 13.422, 842 m, Malaise trap, 25.vii.2012, leg. G. Sellmayer, BIOUG07768-G08; **NORWAY:** Rogaland, Hana, ex. *Operophtera brumata*, 28.vi.2010, leg. K. Ruohomaki, MRS 0048; **UNITED KINGDOM:** Scotland: Argyll, Scotnish Farm, ex. *Rheumaptera hastata*, 25.iv.1990, leg. K. P. Bland, CNCHYM49288.

Geographical distribution. NEA, PAL.

NEA*- Canada* (BC, PE, YT); PAL- Bulgaria, Finland, Germany, Greece, Hungary, Norway*, Sweden, United Kingdom.

Molecular data. BIN: BOLD:ACZ1254.

Host information. Geometridae: type reared from *Rheumaptera hastata* (Linnaeus, 1758); also *Operophtera bruceata** (Hulst, 1886), *Operophtera brumata** (Linnaeus, 1758).

Notes. Barcoding cluster BOLD:ACZ1254 includes sequences of specimens from Finland, Germany, Norway, United Kingdom, and Canada. Specimens in this cluster from both sides of the Atlantic were reared from *Rheumaptera hastata* (the host of the holotype): from the United Kingdom (CNCHYM49288=MRS_JFT 0154) and from Canada (CNC1447813). Morphological examination resulted in some differences in leg colouration between Canadian and European specimens available to us (see Figs 46, 47). However, T1–T3 shape and

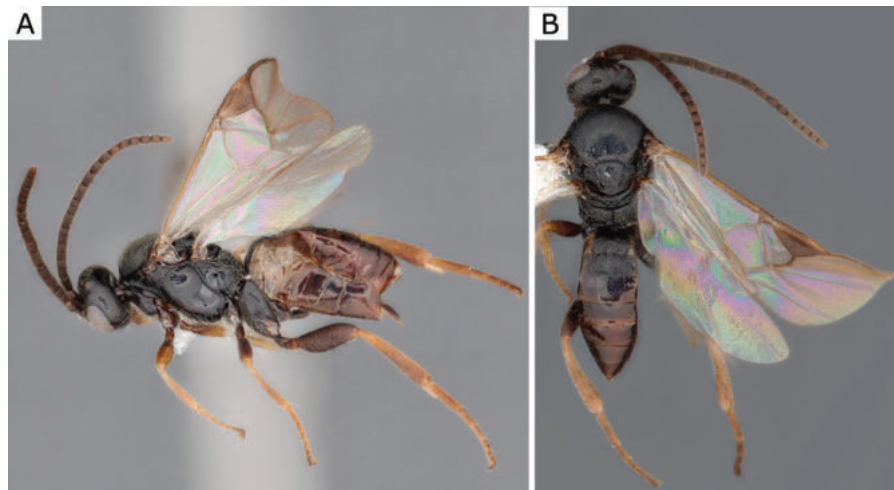


Figure 46. *Cotesia eulipis* (Nixon, 1974), female (BIOUG07768-G08) **A** lateral and **B** dorsal views. Length of the specimen: 2.75 mm.

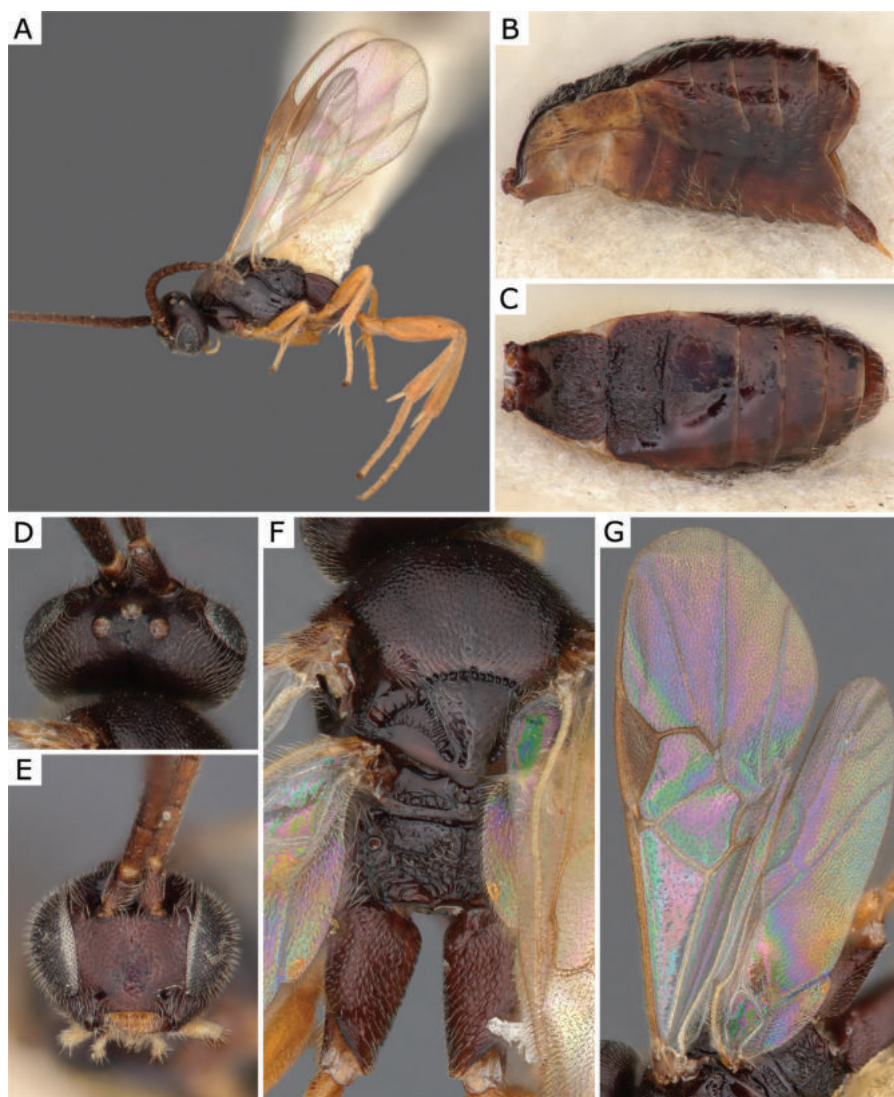


Figure 47. *Cotesia eulipis* (Nixon, 1974), female (CNC1447813) **A** lateral view **B** metasoma lateral view **C** metasoma dorsal view **D** head dorsal view **E** head frontal view **F** mesosoma dorsal view **G** wing. Length of the specimen: head + mesosoma 1.5 mm, metasoma 1.0 mm.

structure are similar and the host information and DNA barcoding also point towards all of our specimens representing one species. Based on this integrative species concept from studying specimens from German as well as some Canadian and European material, and considering the hosts of this species, we here consider BIN BOLD:ACZ1254 to represent *C. eulipis* and report this species for the Nearctic for the first time. Other specimens in this BIN were reared from *Operophtera brumata* (MRS 0048=MRS_JFT0048, MRS 0049=MRS_JFT0049, MRS 0050=MRS_JFT0050) in Finland and Norway and from *Operophtera bruceata* (CNCHYM 00330, CNCHYM 00331) in Canada. There is another specimen from Austria (CNC990841=MRS_JFT0743) that morphologically matches *C. eulipis*, yet clusters in a different BIN (BOLD:AEV7769) which has a p-distance of 1.9% to all other specimens that we identified as *C. eulipis* and is reared from *Hydria cervinalis* (Scopoli, 1763), a host so far not reported for this species. Resolving this goes beyond the scope of this paper, for the purpose of this manuscript we prefer to retain this specimen as “*Cotesia* cf. *eulipis*”. This species is illustrated in Figs 46, 47.

***Cotesia tetrica* (Reinhard, 1880)**

Material examined. **AUSTRIA:** Lower Austria, Raglitz, ex. *Aphantopus hyperantus*, 04.v.2011, leg. J. Connell, MRS 0054; **GERMANY:** Bavaria: Allgäu, Oberstdorf, Oytal, Schochen, alpine meadow, 47.392, 10.37, 1930 m, 6.viii.2014, leg. D. Doczkal, S. Schmidt, J. Voith, BC-ZSM-HYM-24109-E04; Balderschwang, Leiterberg, 47.486, 10.09, 1290 m, Malaise trap, 25.viii.2017, leg. D. Doczkal, J. Voith, ZSM-HYM-42325-F05; Garmisch-Partenkirchen, Zugspitze, Platt, 47.405, 11.009, 1980 m, Malaise trap, 2.viii.2018, leg. D. Doczkal, J. Voith, ZSM-HYM-42390-G12; Lkr. Weilheim, Pähl, Hartschimmelhof Niedermoor west of Goasl, 47.942, 11.182, 713 m, Malaise trap, 18.viii.2021, leg. GBOL3, R. Albrecht, ZSM-HYM-42398-E12; Rhön Hausen, Kleines Moor, 50.487, 10.039, 890 m, Malaise trap, 25.vii.2018, leg. D. Doczkal, ZSM-HYM-33165-G09.

Geographical distribution. PAL.

PAL- Austria*, Germany, Montenegro, Serbia, United Kingdom.

Molecular data. BIN: BOLD:AAV9103.

Host information. Host of type unknown; also Nymphalidae: Satyrinae*: *Lasiommata megera* (Linnaeus, 1767), *Maniola jurtina* (Linnaeus, 1758); *Aphantopus hyperantus** (Linnaeus, 1758).

Notes. This species was previously recorded from Germany (Belokobylskij et al. 2003). Germany was also mentioned as the type locality in the world checklist (Fernandez-Triana et al. 2020); however, the country was not added to the distribution range of that species by error, so we confirm it here. Other specimens morphologically identified as *Cotesia tetrica* clustering in this BIN were reared from *Aphantopus hyperantus* in Austria (MRS 0054, CNC990821, CNC990822), and there are barcoded specimens in NMS from several identified European species of *Erebia* (M. Rindos and MRS pers. obs) in the same BIN. Host records in the historical literature from other Lepidoptera families are incorrect, and Wilkinson (1945: 84) had already advised against reporting those records. The distribution in Serbia is based on Žikić et al. (2021). This species is illustrated in Fig. 48.

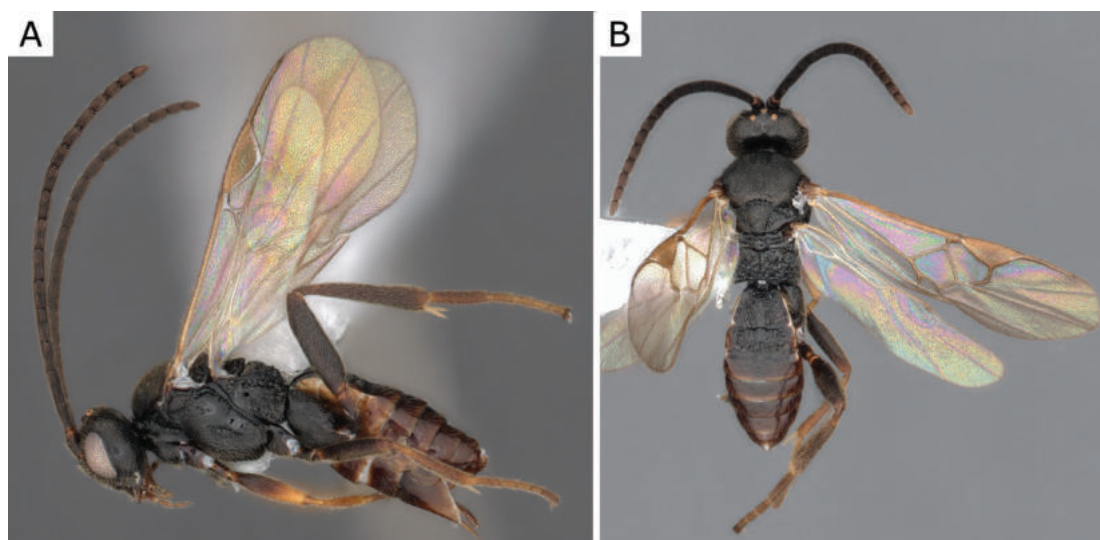


Figure 48. *Cotesia tetrica* (Reinhard, 1880), female (ZSM-HYM-42325-F05) **A** lateral and **B** dorsal views. Length of the specimen: 2.55 mm.

***Diolcogaster claritibia* (Papp, 1959)**

Material examined. **CANADA:** Ontario: Ottawa, Central Experimental Farm, DBM Field Cage Trials, 45.389959, -75.711949, 23.vi.2010, leg. P. Mason, S. Girardoz, CNCHYM 01692; CNCHYM 01693; CNCHYM 01694; **CYPRUS:** Amathus, 21-iv-1966, leg. Mavromoustakis, CNCHYM 00892; **FRANCE:** Languedoc-Roussillon: Baillargues, Herault, 43.662, 4.014, 3-vi-1995, leg. P. Mason, CNCH1127; Bel Air, Herault, 43.639, 3.75, 5-vi-1995, leg. P. Mason, CNCH1126; **GERMANY:** Baden-Württemberg: Malsch, Hansjakobstr. 7, Urban Garden, 48.884, 8.32, 120 m, Malaise trap, 19.vii.2020, leg. D. Doczkal, ZSM-HYM-33154-G11; 5.vii.2020, leg. D. Doczkal, ZSM-HYM-33152-H07; Bavaria: Bayreuth, Laineck, 49.959, 11.618, 358 m, Malaise trap, 11.vii.2019, leg. J. Müller, ZSM-HYM-42375-C09; ZSM-HYM-42375-C10; ZSM-HYM-42375-D01; ZSM-HYM-42375-D03; Bobingen, cemetery, 48.272, 10.84, 524 m, Malaise trap, 16.vii.2019, leg. J. Müller, ZSM-HYM-42385-C11; Forkendorf, close to Thiergarten, 49.903, 11.555, 423 m, Malaise trap, 10.vii.2019, leg. J. Müller, ZSM-HYM-42385-D06; Hassfurt, Mechenried, 50.096, 10.483, 254 m, Malaise trap, 12.vii.2019, leg. J. Müller, ZSM-HYM-42383-C09; ZSM-HYM-42383-C10; Iphofen, Mönchsondheim, 49.668, 10.28, 263 m, Malaise trap, 16.vii.2019, leg. J. Müller, ZSM-HYM-42384-E02; Volkach, Kolitzheim, 49.922, 10.234, 229 m, Malaise trap, 16.vii.2019, leg. J. Müller, ZSM-HYM-42378-D08; Wimmelbach, close to Untere Mark, pond edge, 49.71, 10.994, 290 m, Malaise trap, 12.vii.2019, leg. J. Müller, ZSM-HYM-42381-D01; Wunsiedel, Waldrand SW von Wintersreuth, 50.035, 12.039, 538 m, Malaise trap, 16.vii.2019, leg. J. Müller, ZSM-HYM-42380-B06; **JORDAN:** East Jordan: Wadi Schaib, 9-ii-1968, leg. J.S. Klapperich, CNCHYM 00893; **NETHERLANDS:** Gelderland: Wageningen, ex *Plutella xylostella*, 2012, leg. J. Harvey, CNCHYM45357.

Geographical distribution. NEA, PAL.

NEA- Canada (AB, MB, ON); PAL- Afghanistan, Armenia, Austria, Azerbaijan, Belarus, Cyprus, Finland, France, Georgia, Germany, Greece, Hungary, Italy, Iran, Jordan, Kazakhstan, Lithuania, Macedonia, Moldova, Netherlands,

Russia (ZAB, KDA), Spain, Syria, Tunisia, Turkey, Turkmenistan, Ukraine, former Yugoslavia.

Molecular data. BIN: BOLD:AAH1034, BOLD:AEV8838.

Host information. Host of type unknown; also Plutellidae: *Plutella armoraciae* Busck, 1912, *Plutella xylostella* (Linnaeus, 1758).

Notes. German specimens were identified based on the detailed species concept in Fernandez-Triana et al. (2014b). One of the hosts currently associated with this species, *Plutella xylostella*, has been widely reported in the literature (e.g., Papp 1981b; Fernandez-Triana et al. 2014a) and the wasp is commonly reared from it. Our sequences match specimens reared from *P. xylostella* (CNCHYM 01692, CNCHYM 01693, CNCHYM 01694) in Canada and a sequence from another specimen from the Netherlands (CNCHYM45357=MRS_JFT0220) also reared from the same host; the maximum p-distance for those specimens and the German material is 0.82%. Specimens of this species cluster in two BINs which are separated by 2.14% but also show a high within-BIN variability of 2.28% and 2.64%. A second host species, *Plutella armoraciae*, has been recently recorded for this wasp in Canada (Abram et al. 2022). The reared wasps are not yet sequenced. Whether *D. claritibia* represents a single species or a complex of morphologically cryptic species is beyond the scope of the present paper and will need further study including more (reared) specimens from both the Palearctic and the Nearctic. The hosts were first recorded by Papp (1981b) and Abram et al. (2022). The distribution of this species in Germany was mentioned by Papp (1981b), but to our knowledge not cited in literature since, so we confirm it here. Additionally, we add the distribution for Syria, which was also mentioned by Papp (1981b), but not cited since. Finally, we correct the distribution from the world checklist and add the records from Cyprus, France, Italy, Jordan, and the Netherlands reported by Fernandez-Triana et al. (2014b). This species is illustrated in Fig. 49.

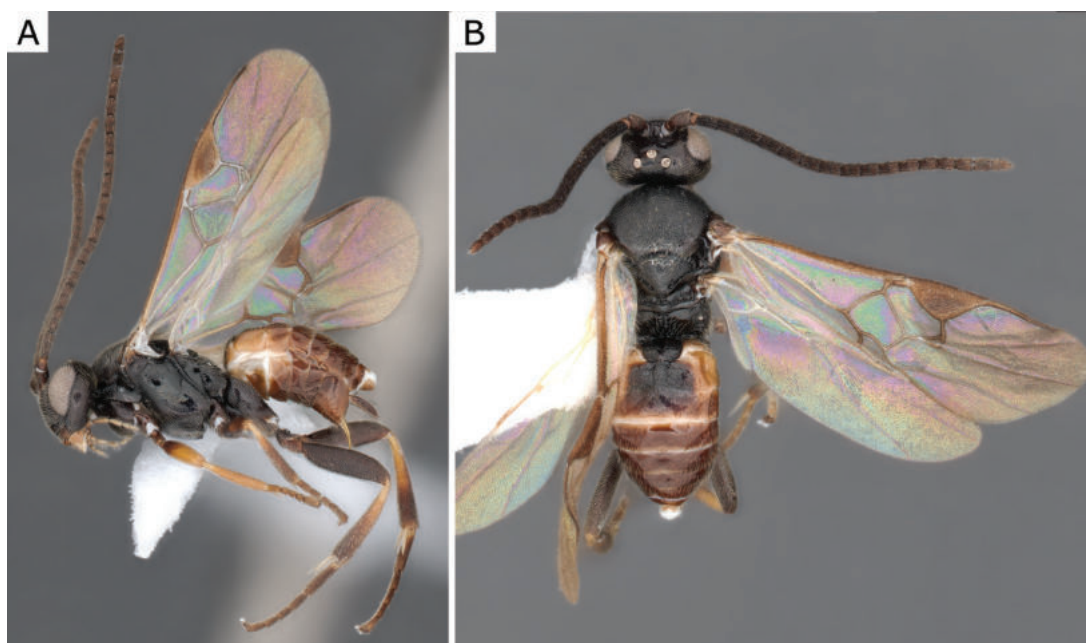


Figure 49. *Diolcogaster claritibia* (Papp, 1959), female (ZSM-HYM-33152-H07) **A** lateral and **B** dorsal views. Length of the specimen: 2.25 mm.

***Microgaster procera* Ruthe, 1860**

Material examined. **CANADA:** Prince Edward Island: Near Georgetown; Georgetown, 46.417, -62.667, 8 m, 31.vii.2005, leg. M. Sharkey, WMIC 0244; WMIC 0245; **GERMANY:** Bavaria: Berchtesgaden National Park, Königssee, Rinnkendlsteig, 47.553, 12.964, 775 m, Malaise trap, 30.vii.2017, leg. D. Doczkal, J. Voith, ZSM-HYM-33160-F06; Berchtesgaden National Park, Wald west of St.Bartholomä, 47.547, 12.965, 620 m, Malaise trap, 28.vi.2017, leg. D. Doczkal, J. Voith, ZSM-HYM-33156-E05; ZSM-HYM-33156-E06; ZSM-HYM-33156-E07; Schmelzenholzham, Waldrand, 48.488, 13.124, 468 m, Malaise trap, 12.vii.2019, leg. J. Müller, ZSM-HYM-42325-B01; Siegenburg, Bombodrom, 48.755, 11.791, 411 m, Malaise trap, 13.vii.2017, leg. D. Doczkal, J. Voith, ZSM-HYM-42324-D03.

Geographical distribution. NEA, PAL.

NEA*- Canada* (PE); PAL- Austria, Finland, Germany, Hungary, Ireland, Mongolia, Netherlands, Poland, Romania, Russia (SPE), Spain, Ukraine.

Molecular data. BIN: BOLD:AAA9548.

Host information. Host of type unknown. Shaw (2012a) gives tentative hosts of some British specimens (see below).

Notes. This is not a new record for Germany, but morphological examination of German material and assignment of the species name to a barcoding cluster allow us to record the species in the Nearctic for the first time. The Canadian specimens were compared to the European material and all sequences in this barcoding cluster have a maximum pairwise-distance of just 0.15%. The host information for this species must be considered as mostly unreliable; based on a recent discussion (Shaw 2012a: 194) it seems as though the crambid *Anania hortulata* could be the most trustable record, but even that needs verification. This species is illustrated in Figs 50, 51.

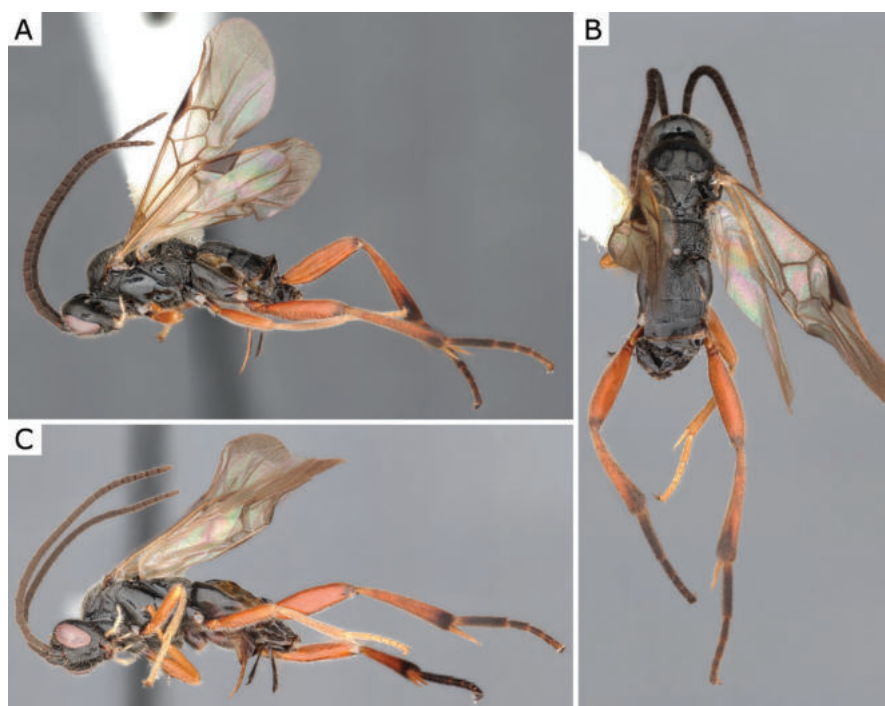


Figure 50. *Microgaster procera* Ruthe, 1860, female (WMIC0245) **A** lateral view **B** dorsal view **C** lateroventral view. Length of the specimen: 4.15 mm.

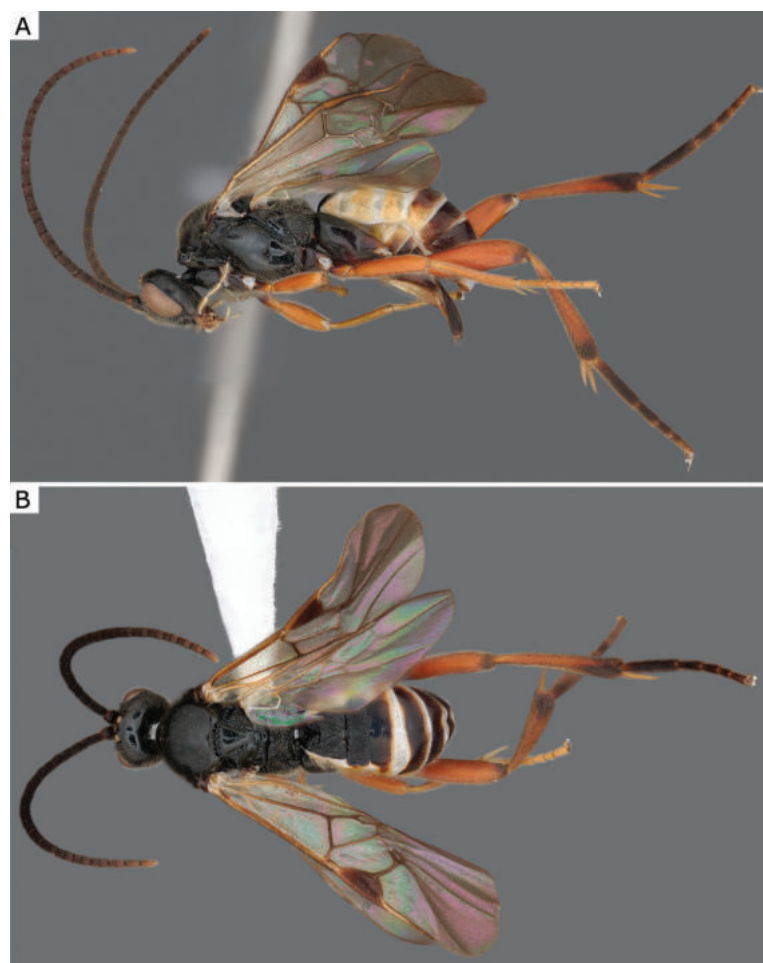


Figure 51. *Microgaster procera* Ruthe, 1860, female (ZSM-HYM-33160-F06) **A** lateral and **B** dorsal views. Length of the specimen: 5.25 mm.

Discussion

DNA Barcoding

Processing 5364 specimens in this reversible DNA barcoding approach combined with integrative taxonomy enabled us to gather many new distributions as well as much biological data in a relatively short time frame. We were able to report 30 species for Germany for the first time, four species as occurring in the Holarctic for the first time and, by also taking into account material already determined in NMS and CNC collection, publish 26 additional country records, disclose ten new host-parasitoid associations (five of which are new host families), link ten species with DNA barcodes for the first time, and, based mainly on recently collected German material, illustrate many species for which photographs were not previously available. We were also able to link males and females in a few cases (*Choeras ciscaucasicus*, *Rasivalva desueta*), although we mostly selected female specimens for examination. We increased the known German fauna of Microgastrinae by more than 10% from 252 species (Papp 1981b; Belokobylskij et al. 2003; Fernandez-Triana et al. 2020; Shaw 2020, 2022) to 282 species and provide a first step towards a comprehensive barcode library for German Microgastrinae.

We used the framework of the BOLD workbench and database as it already includes more than 65,000 sequences of Microgastrinae worldwide (www.boldsystems.org).

boldsystems.org, accessed on 20 Aug 2023) and has been used as a main molecular analysis tool in Microgastrinae taxonomy in the past (Smith et al. 2013; Fernandez-Triana et al. 2014c; Fagan-Jeffries et al. 2018). It is important to note that all this barcoding data available for Microgastrinae wasps is still very much under-representing the molecular diversity of the group and hence molecular species hypotheses might change in the future. We critically tested all our molecular species hypotheses by using morphology and biology in our integrative species concepts.

We investigated BINs that had high within-BIN maximum p-distances ($> 2.2\%$) (Ratnasingham and Hebert 2013) and BINs with low p-distances to their Nearest Neighbour ($< 2.2\%$) (Raupach et al. 2020). Using this as a rough method for screening our molecular clusters, we found several cases of BIN discrepancies. In one case a species was represented by more than one BIN (= over-splitting: *Microplitis naenia* BOLD:ABV9098 and BOLD:AEK2564, potentially *Diolcogaster claritibia* BOLD:AAH1034 and BOLD:AEV8838). This does not represent a major problem for molecular species identifications as long as the multiple BINs would be associated with a single taxon. In fact, the two BINs that represent *M. naenia* are Nearest Neighbours (NN) and separated only by a minimum NN p-distance of 1.70%. This case of over-splitting probably represents intraspecific variation and, once more haplotypes are sampled, those barcoding clusters might eventually merge. There are other BINs that are close (p-dist $< 2.2\%$) to their Nearest Neighbour: *Cotesia eulipis* BOLD:ACZ1254, *Dolichogenidea cerialis* BOLD:AAZ9570, *Microgaster caris* BOLD:ACN6851. Those clusters could potentially be problematic; however, in those cases, the within-BIN maximum p-distance is much lower than the minimum NN p-distance. Meanwhile, cases of BIN-sharing represent a problem for DNA-based species identification: In those cases, a BIN includes several species (= BIN-sharing: e.g., *Cotesia risilis* in BIN BOLD:AAA6099).

BOLD:AAA7143 is an even more extreme case of BIN-sharing, it includes four species of *Cotesia* treated in this paper: *C. coryphe*, *C. mendicae*, *C. selenevora*, and *C. subordinaria*. When starting our analyses in 2022, each of these species was part of a separate BIN but merged into this “megaBIN” in early 2023. In Table 1, the previous BINs are included in brackets below the current BIN. This cluster includes a total of 1772 members (last updated 07 Aug 2023) and several possibly misidentified families, subfamilies, and genera. We performed ASAP clustering for a subset of sequences: this revealed 163 clusters in the first partition (ASAP score 3.99) and 141 clusters in the second partition (ASAP score 6.50). Our subset includes 1471 sequences, 100 interim species identifications (indicating different morphotypes), and 26 species. This “mega-BIN” is clearly not useful in clustering these species of *Cotesia*. This problem is likely temporary as it only appeared by spring 2023 and might be resolved, e.g., by removing some sequences that might be causing these problems.

Overall, a more general observation from discussing integrative species concepts in our dataset is that the distances between barcoding clusters can vary substantially between genera. We were able to observe several cases of lumping (or BIN-sharing) in *Cotesia* with p-distances of ~ 1.0 – 1.5% between morphologically and biologically well-established species. We had to exclude some species from this paper because the situation turned out to be more complex than previously expected (e.g., *Cotesia euchloeovora* Shaw, 2020 and *Cotesia pilicornis* (Thomson, 1895); see discussion of these two species in Shaw and Fernandez-Triana 2020). Other genera such as *Illidops* or *Deuterixys* were not affected by this and showed

Table 1. P-distances and member counts of the BINs treated in this paper, retrieved on 8 Aug 2023. Single asterisks (*) mark each species name that was matched to a BIN for the first time, Double asterisks (**) mark each species that was sequenced for the first time. A BIN in parentheses shows that the BIN represents more than one species and cannot be used for molecular identification of the species. A BIN in brackets shows the previous BIN before February 2023. If the minimum NN p-distance is < 2.2% or within BIN maximum p-distance > 2.2%, then the within-BIN max. p-distance and minimum NN-p-distance are in bold font.

Species names	BIN(s)	Members (BIN)	BIN-compliant members	within- BIN average p-dist	within-BIN max. p-dist	min. NN p-dist
<i>Apanteles galleriae</i>	BOLD:AAG1400	25	13	0.38%	1.17%	2.36%
<i>Apanteles kubensis</i>	BOLD:AAH1340	7	5	0.14%	0.32%	5.61%
<i>Choeras ciscaucasicus</i> *	BOLD:ACU3996	5	1	0.22%	0.48%	6.78%
<i>Choeras gnarus</i> *	BOLD:AAU6216	41	12	0.08%	0.52%	2.23%
<i>Cotesia coryphe</i>	(BOLD:AAA7143) [BOLD:ABY6805]	1772 [25]	859 [5]	3.85% [0.16%]	7.61% [0.71%]	2.21% [1.50%]
<i>Cotesia eulipis</i>	BOLD:ACZ1254	16	4	0.29%	0.59%	1.18%
<i>Cotesia eunomia</i>	BOLD:AAV9098	6	0	0.18%	0.34%	7.68%
<i>Cotesia inducta</i>	BOLD:AAV9096	4	1	0.22%	0.34%	2.48%
<i>Cotesia mendicae</i>	(BOLD:AAA7143) [BOLD:ABY8119]	1772 [N/A]	859 [N/A]	3.85% [N/A]	7.61% [N/A]	2.21% [N/A]
<i>Cotesia risilis</i>	(BOLD:AAA6099)	182	105	1.25%	2.87%	1.12%
<i>Cotesia selenevora</i>	(BOLD:AAA7143) [BOLD:AAA9381]	1772 [23]	859 [6]	3.85% [0.62%]	7.61% [2.84%]	2.21% [1.40%]
<i>Cotesia subordinaria</i>	(BOLD:AAA7143) [BOLD:ACO3220]	1772 [5]	859 [0]	3.85% [0.07%]	7.61% [0.19%]	2.21% [1.44%]
<i>Cotesia tetrica</i>	BOLD:AAV9103	25	17	0.29%	0.66%	2.84%
<i>Deuterixys plugarui</i> **	BOLD:AEJ7518	9	0	0.54%	0.96%	5.83%
<i>Diolcogaster claritibia</i>	BOLD:AAH1034	95	73	0.34%	2.28%	2.14%
	BOLD:AEV8838	16	8	0.66%	2.64%	2.14%
<i>Dolichogenidea cerialis</i>	BOLD:AAZ9570	8	5	0.28%	0.49%	1.28%
<i>Dolichogenidea cheles</i> *	BOLD:ACQ9527	10	5	0.57%	1.42%	3.33%
<i>Dolichogenidea coleophorae</i> **	BOLD:AE08197	2	0	0.00%	0.00%	2.72%
<i>Glyptapanteles indiensis</i>	BOLD:ABY2372	16	8	0.31%	0.81%	3.52%
<i>Glyptapanteles popovi</i>	BOLD:AEJ4298	7	0	0.23%	0.64%	3.25%
<i>Illidops cloelia</i> **	BOLD:AE08223	2	0	0.00%	0.00%	4.81%
<i>Illidops splendidus</i> **	BOLD:AEJ7519	1	0	N/A	N/A	6.58%
<i>Microgaster arctostaphylica</i>	BOLD:AAH1039	12	7	0.93%	2.25%	2.68%
<i>Microgaster caris</i>	BOLD:ACN6851	66	4	0.17%	0.72%	1.60%
<i>Microgaster nervosae</i>	BOLD:ACR4142	11	3	0.35%	0.82%	2.72%
<i>Microgaster nixalebion</i>	BOLD:ABY6385	62	12	0.20%	1.48%	0.97%
<i>Microgaster procera</i> *	BOLD:AAA9548	8	3	0.04%	0.16%	5.33%
<i>Microgaster raschkiellae</i>	BOLD:AAC9130	36	25	0.91%	2.26%	1.93%
<i>Microplitis coactus</i>	BOLD:ACA4555	6	4	0.58%	0.96%	3.57%
<i>Microplitis kewleyi</i>	BOLD:AAB8493	127	53	0.03%	0.80%	5.77%
<i>Microplitis naenia</i>	BOLD:ABV9098	18	17	0.35%	1.28%	1.70%
	BOLD:AEK2564	9	2	0.36%	0.64%	1.70%
<i>Pholetesor bedelliae</i>	BOLD:AAA9172	74	55	0.46%	1.62%	3.29%
<i>Protapanteles endemus</i> *	BOLD:AEI1558	2	1	0.17%	0.17%	7.64%
<i>Rasivalva desueta</i> *	BOLD:ADE2589	4	2	0.08%	0.17%	3.04%

p-distances of ~ 4–10% between species in our larger dataset (pers. obs.). This has been documented and discussed for other taxa (e.g., Schütte et al. 2023). For now, we recommend that barcoding data for Microgastrinae wasps should be critically analysed, also from a genus-specific point of view.

So far, barcoding has worked well for the majority of Microgastrinae species and has been an essential tool in advancing the study of Microgastrinae diversity (Smith et al. 2013; Fernandez-Triana et al. 2014c; Fagan-Jeffries et al. 2018). Cases of BIN-discrepancies, depending on the case, may or may not cause problems for identifying species by DNA barcoding. Still, barcoding works very well for a large proportion of species (90–99%) in various insect taxa

(Hausmann et al. 2011a, b; Hendrich et al. 2015; Schmidt et al. 2015; Schmid-Egger et al. 2019; Raupach et al. 2020), and less well in others, such as Orthoptera (Hawlitschek et al. 2017). At this point, it is difficult to evaluate the level of agreement between molecular species hypotheses (in our case BINs) and morphological and biological species concepts in Microgastrinae. The ideal case would be a 1:1 match between molecular clusters (BINs) and morphological (or biological) species. Although we conclude that barcoding data needs to be interpreted carefully in Microgastrinae wasps and should be paired with other methods, it also made this study possible in the first place. DNA barcoding enabled us to tackle this dark taxon at such a scale in a short time by clustering large amounts of sequences linked to thousands of specimens. We could link our material to previously barcoded material in the databases that provided additional information about (1) species identification (often narrowing down possible identifications), (2) biological interactions (even if hosts were parasitised by solitary males – information that is otherwise potentially lost as males can usually not be identified by morphology alone), (3) geographical distribution (especially important as some species have wide distribution ranges and may not always be included in the keys traditionally used for Western Europe), (4) phenology, and (5) sexes not available in our material, etc. DNA barcoding gave us access to these different aspects of our integrative species concepts.

Fig. 52 provides a Neighbour-Joining topology for our dataset, providing a first-glance impression of sample size and sequence divergence of the species treated here. In addition, our dataset is linked to the information about BIN distances of more than 65,000 sequences of Microgastrinae registered in the BOLD database, which is represented via colouration of the triangles: orange triangles indicate species with a minimum p-distance to the Nearest Neighbour < 2.2%, blue triangles indicate species that cluster in BINs with a maximum within-BIN distance > 2.2%. This N-J topology is not representative of any fauna as it only includes a few selected species per genus (here compared to the number of species reported for Germany): *Apanteles* (2/12), *Choeras* (2/9), *Cotesia* (9/62), *Deuterixys* (1/3), *Diolcogaster* (1/9), *Dolichogenidea* (3/45), *Glyptapanteles* (2/24), *Illidops* (2/4), *Microgaster* (6/32), *Microplitis* (3/39), *Pholetesor* (1/11), *Protapanteles* (1/12), and *Rasivalva* (1/3).

Distribution in Europe and the Holarctic region

The known distribution in Europe of some species is significantly expanded: *Choeras ciscaucasicus* was previously only known from Russia and Lithuania; in this case the new record from Germany expands this species' range to the western part of Europe. *Microgaster arctostaphylica* and *Microgaster nervosae*, two recently described species (Shaw 2012a, 2023) are recorded outside of the United Kingdom for the first time. *Microplitis coactus* has been known to be distributed in the Nearctic, except for Iceland (PAL). Our record from Germany presents a major expansion of the known range of this species.

A main result of this study is that four species were recorded for the first time for the Palaearctic (*Glyptapanteles indiensis*, *Microplitis kewleyi*) and Nearctic regions (*Cotesia eulipis*, *Microgaster procera*). According to the supplementary material of the world checklist published in 2020, only 5% (56) of the 1,178 Holarctic species of Microgastrinae are shared between the Nearctic and Palaearctic re-

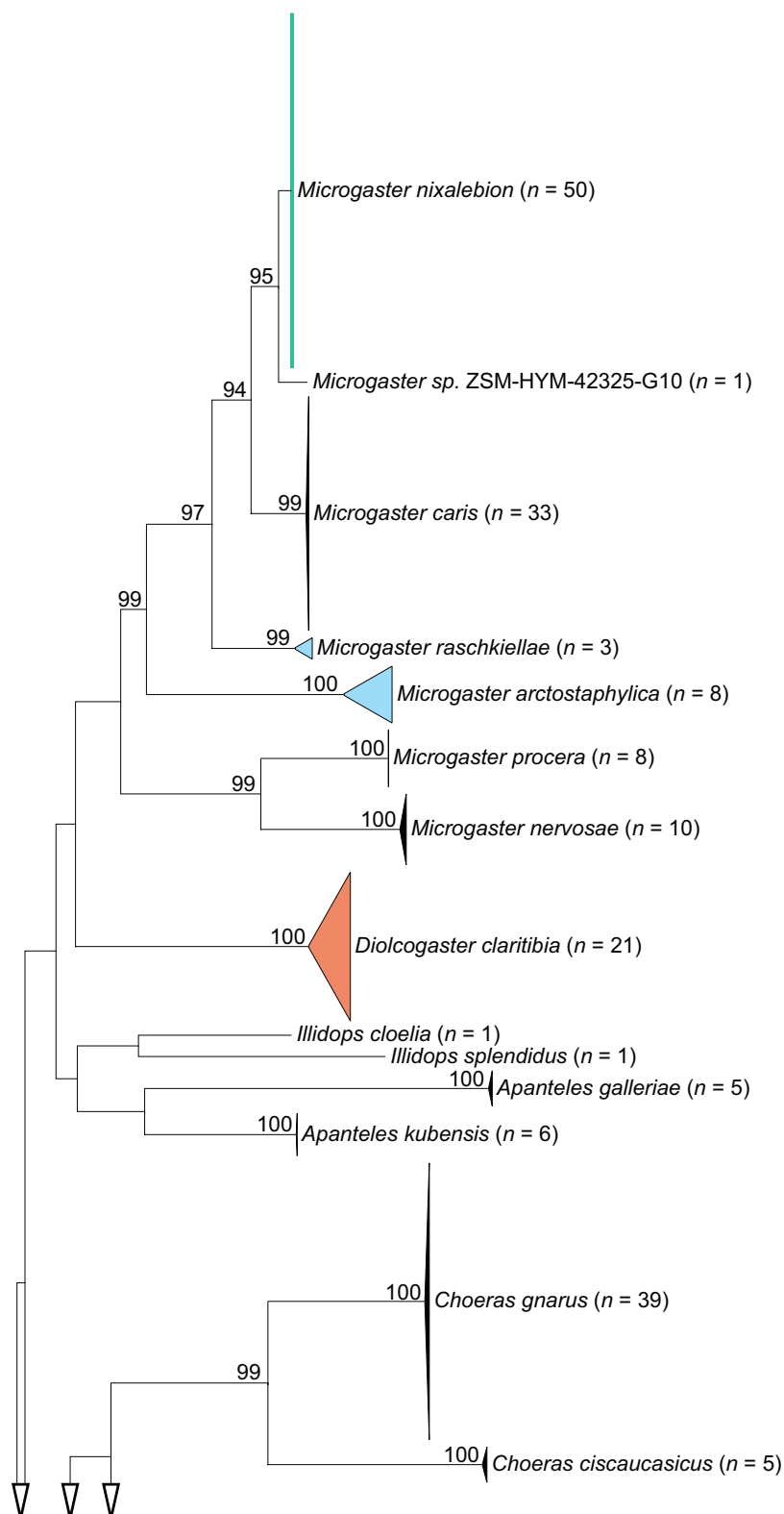


Figure 52. Neighbour-joining topology of the barcoding region of our dataset of the analysed species based on Kimura 2-parameter distances. Triangles show the relative number of individuals sampled (height) and sequence divergence (width). Pale blue colouration indicates species associated with BINs that have a maximum within-BIN distance > 2.2%. Green colouration indicates species associated with BINs that have a higher within-BIN p-distance compared to NN p-distance. Orange colouration indicates species with “BIN-sharing”. Numbers next to nodes represent non-parametric bootstrap values > 90% (1,000 replicates). Sequences shorter than 400 bp were excluded from this analysis. The aligned sequences and N-J topology can be reviewed in Suppl. materials 3, 4.

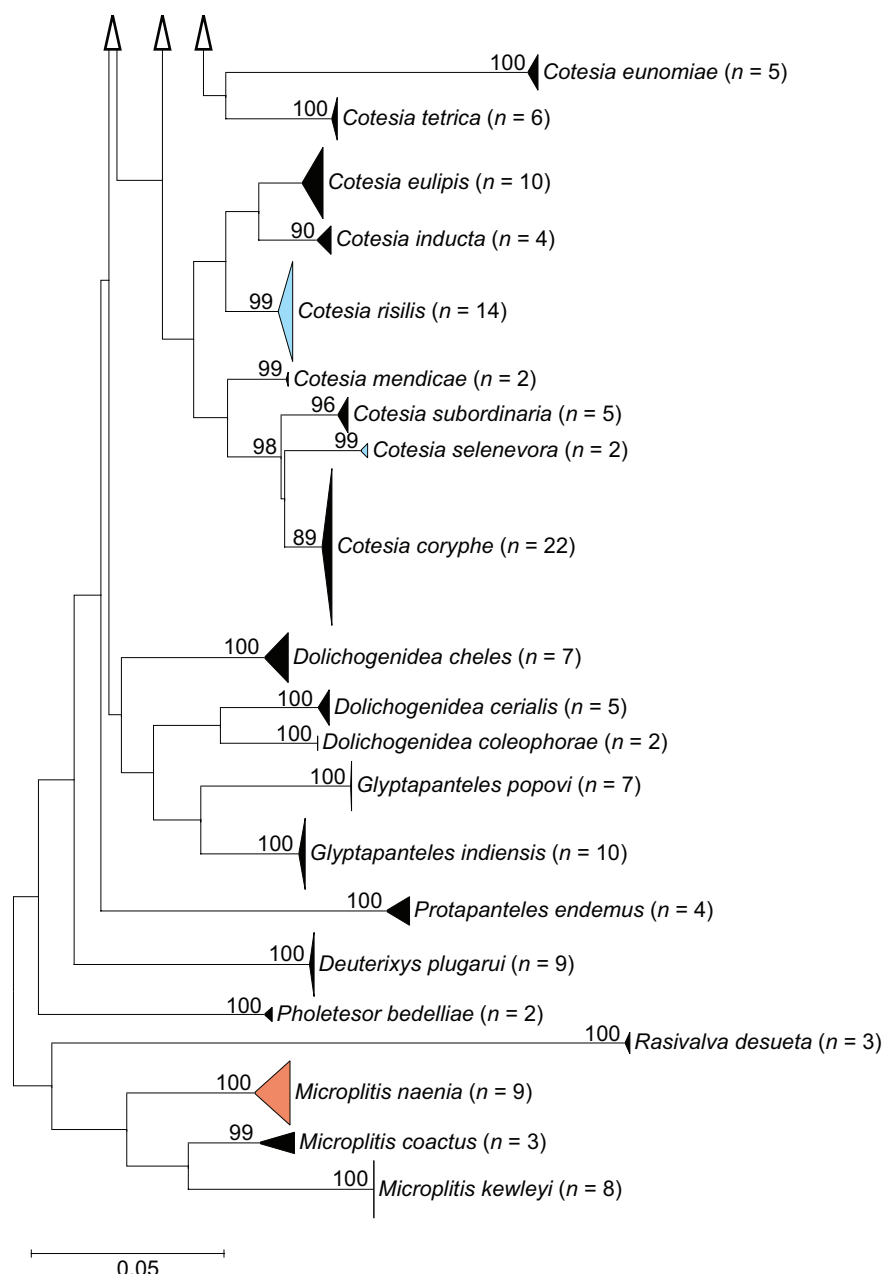


Figure 52. Continued.

gions. Of these 56 species, 29 have an exclusively Holarctic distribution (Fernandez-Triana et al. 2020) whereas the remaining species have a wider distribution, partly due to parasitising pests or species otherwise spread by human activity (such as *Apanteles galleriae* which parasitises wax moths commonly found in beehives). These relatively low percentages of shared species are misleading, as most studies available (identification keys and taxonomic revisions) usually cover only the Nearctic or the Palearctic region, but rarely both (the exceptions are smaller genera which are revised at wider range (e.g., Papp 1986b; Whitfield and Oltra Moscardó 2004; Fernandez-Triana et al. 2014c; Fujie et al. 2021). With DNA barcoding and the use of international databases and collaborations, we now have efficient tools at our hands to make more of these transatlantic and world-wide connections. For some species discussed here (Fig. 53) we already know that their distribution exceeds even the Holarctic region: the molecular cluster

that we consider to represent *Microplitis kewleyi* also has members in Bulgaria and Pakistan (which is part of the Oriental region following O'Hara et al. 2009). This is based on publicly available data and shows a much wider distribution range compared to what we formally report here (as we were not able to observe the specimens). *Glyptapanteles indiensis* is another more widely distributed species which was first described from the Oriental region. All four species in Fig. 53 show somewhat patchy distributions, which likely do not represent the actual range of these species, but rather point out sampling bias. Most sequences in the BOLD database are from either North America or Western Europe. For Microgastrinae specifically, the countries with the most entries are Costa Rica (25512), Canada (14256), Germany (5650), United States (2453), and Australia (1781). Other than these, Holarctic countries with most entries are Turkey (433), Norway (361),

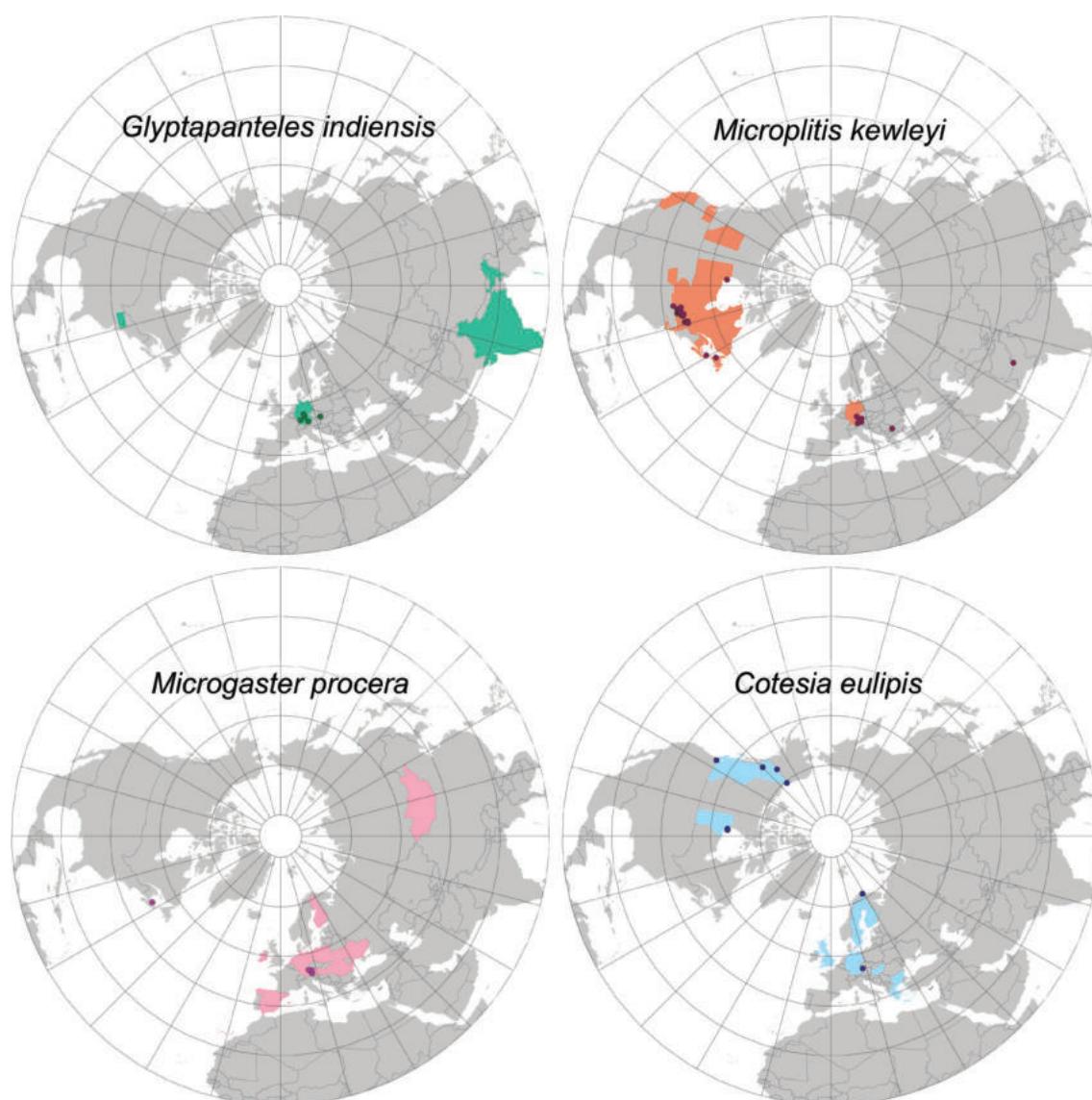


Figure 53. Distribution maps for the four newly recorded Holarctic species. Coloured countries/states show the known distribution as in Fernandez-Triana et al. (2020) with confirmed additional data from this study. Dots show sampling locations of the species from our dataset and mined public data from the matching BINs from BOLD. In these cases, the countries/states were not coloured because we were not able to confirm this by studying the specimens. The coordinates used for the distributions can be reviewed in Suppl. material 5.

Japan (258), United Kingdom (257), and Sweden (243) (<https://www.boldsystems.org/>, accessed 18 Aug 2023). Accounting for previously known distribution ranges and historical data (represented by the coloured countries/states) somewhat mitigates this, but sampling is still a significant source of bias in the species distributions that might also influence our current species concepts. With more international collaborations and as DNA barcoding becoming more accessible in the future, sampling might hopefully become more equally distributed.

Acknowledgments

We would like to acknowledge Wolfgang Langer, Ingrid Langer, and Pavel Drozd for reared specimens, and Benjamin Leroy, Dieter Doczkal, Johannes Voith, Jörg Müller, and the Swedish Malaise Trap Project for numerous bulk samples. The GBOL3-Team at ZSM, namely Caroline Chimeno, Jeremy Hübner, and Rosa Albrecht, helped with fractioning and sorting the numerous Malaise trap bulk samples. Andreas Segerer and Mario Harzheim contributed identification and expertise on Lepidoptera.

Additional information

Conflict of interest

The authors have declared that no competing interests exist.

Ethical statement

No ethical statement was reported.

Funding

Funding was provided by the Bundesministerium für Bildung und Forschung (BMBF) of Germany, through the project “German Barcode of Life III: Dark Taxa” (FKZ 16LI1901C).

Author contributions

Conceptualization: AH, JLFT. Data curation: AH, JLFT, MRS, CB, DR. Formal analysis: AH, JLFT, MRS. Funding acquisition: SS. Investigation: AH, JLFT, MRS. Project administration: AH. Resources: SS. Supervision: JLFT, GH, MJJR, SS. Visualization: AH, CB. Writing – original draft: AH, JLFT. Writing – review and editing: AH, JLFT, MRS, VAB, CB, MJJR, SS, GH.

Author ORCIDs

Amelie Höcherl  <https://orcid.org/0009-0007-4211-7468>

Mark R. Shaw  <https://orcid.org/0000-0002-6651-8801>

Caroline Boudreault  <https://orcid.org/0000-0002-4511-2626>

Dominik Rabl  <https://orcid.org/0000-0002-0613-7804>

Michael J. Raupach  <https://orcid.org/0000-0001-8299-6697>

Stefan Schmidt  <https://orcid.org/0000-0001-5751-8706>

Viktor Baranov  <https://orcid.org/0000-0003-1893-3215>

José Fernández-Triana  <https://orcid.org/0000-0003-0425-0309>

Data availability

All of the data that support the findings of this study are available in the main text or Supplementary Information.

References

- Abdinbekova A (1969) New braconid wasps (Hymenoptera, Braconidae) in the fauna of Azerbaijan. *Doklady Akademii Nauk Azerbaidzhanskoi SSR* 25: 72–77.
- Abdoli P, Talebi A, Farahani S, Fernandez-Triana JL (2019) Three new species of the genus *Choeras* Mason, 1981 (Hymenoptera: Braconidae, Microgastrinae) from Iran. *Zootaxa* 4545(1): 77–92. <https://doi.org/10.11646/zootaxa.4545.1.4>
- Abram PK, Thiessen J, Clarke P, Gillespie DR, Fernández-Triana JL, Bennett AMR, Gibson GAP, Huber JT, Mason PG, Landry J-F (2022) Natural History of *Plutella armoraciae* Busck, 1912, A Sympatric Congener of the Diamondback Moth, *Plutella xylostella* (L., 1758), in Southwestern Canada. *Journal of the Lepidopterists Society* 76(1): 25–39. <https://doi.org/10.18473/lepi.76i1.a4>
- Belokobylskij SA, Taeger A, van Achterberg C, Haeselbarth E, Riedel M (2003) Checklist of the Braconidae of Germany (Hymenoptera). *Beiträge zur Entomologie = Contributions to Entomology* 53: 341–435. <https://doi.org/10.21248/contrib.entomol.53.2.341-435>
- Brown BV (2005) Malaise trap catches and the crisis in neotropical dipterology. *American Entomologist* 51(3): 180–183. <https://doi.org/10.1093/ae/51.3.180>
- Brown BV, Borkent A, Adler PH, Amorim D de S, Barber K, Bickel D, Boucher S, Brooks SE, Burger J, Burington ZL, Capellari RS, Costa DNR, Cumming JM, Curler G, Dick CW, Epler JH, Fisher E, Gaimari SD, Gelhaus J, Grimaldi DA, Hash J, Hauser M, Hippa H, Ibáñez-Bernal S, Jaschhof M, Kameneva EP, Kerr PH, Korneyev V, Korytkowski CA, Kung G-A, Kvifte GM, Lonsdale O, Marshall SA, Mathis W, Michelsen V, Naglis S, Norrbom AL, Paiero S, Pape T, Pereira-Colavite A, Pollet M, Rochefort S, Rung A, Runyon JB, Savage J, Silva VC, Sinclair BJ, Skevington JH, Stireman III JO, Swann J, Thompson FC, Vilkamaa P, Wheeler T, Whitworth T, Wong M, Wood DM, Woodley N, Yau T, Zavortink TJ, Zumbado MA (2018) Comprehensive inventory of true flies (Diptera) at a tropical site. *Communications Biology* 1(1): 1–8. <https://doi.org/10.1038/s42003-018-0022-x>
- Capek M (1972) [Verzeichnis der aus Schädlinginsekten erzogenen Parasiten. Teil V. – Die Brackwespen (Braconidae, Hymenoptera)]. *Entomologické problémy* 10: 125–140.
- Capek M, Hladil J, Sedivy J (1982) [Verzeichnis der aus verschiedenen Insekten erzogenen parasitischen Hymenopteren – Teil VI.]. *Entomologické problémy* 17: 325–371.
- Chimeno C, Hausmann A, Schmidt S, Raupach MJ, Doczkal D, Baranov V, Hübner J, Höcherl A, Albrecht R, Jaschhof M, Haszprunar G, Hebert PDN (2022) Peering into the darkness: DNA barcoding reveals surprisingly high diversity of unknown species of Diptera (Insecta) in Germany. *Insects* 13(1): 1–82. <https://doi.org/10.3390/insects13010082>
- Fagan-Jeffries EP, Cooper SJB, Bertozzi T, Bradford TM, Austin AD (2018) DNA barcoding of microgastrine parasitoid wasps (Hymenoptera: Braconidae) using high-throughput methods more than doubles the number of species known for Australia. *Molecular Ecology Resources* 18(5): 1132–1143. <https://doi.org/10.1111/1755-0998.12904>
- Fernandez-Triana JL (2022) Turbo taxonomy approaches: Lessons from the past and recommendations for the future based on the experience with Braconidae (Hymenoptera) parasitoid wasps. *ZooKeys* 1087: 199–220. <https://doi.org/10.3897/zookeys.1087.76720>
- Fernandez-Triana J, Shaw MR, Cardinal S, Mason P (2014a) Contributions to the study of the Holarctic fauna of Microgastrinae (Hymenoptera, Braconidae). I. Introduction and first results of transatlantic comparisons. *Journal of Hymenoptera Research* 37: 61–76. <https://doi.org/10.3897/jhr.37.7186>
- Fernandez-Triana J, Shaw MR, Cardinal S, Dosdall L, Mason P (2014b) First Nearctic record of *Diolcogaster claritibia* (Hymenoptera: Braconidae: Microgastrinae), with

- notes on taxonomic status and natural history. *Canadian Entomologist* 146(6): 609–620. <https://doi.org/10.4039/tce.2014.16>
- Fernandez-Triana J, Whitfield J, Rodriguez J, Smith MA, Janzen D, Hallwachs W, Hajibabaei M, Burns J, Solis A, Brown J, Cardinal S, Goulet H, Hebert P (2014c) Review of *Apanteles sensu stricto* (Hymenoptera, Braconidae, Microgastrinae) from Area de Conservación Guanacaste, northwestern Costa Rica, with keys to all described species from Mesoamerica. *ZooKeys* 383: 1–565. <https://doi.org/10.3897/zookeys.383.6418>
- Fernandez-Triana J, Shaw MR, Boudreault C, Beaudin M, Broad GR (2020) Annotated and illustrated world checklist of Microgastrinae parasitoid wasps (Hymenoptera, Braconidae). *ZooKeys* 920: 1–1089. <https://doi.org/10.3897/zookeys.920.39128>
- Fujie S, Japoshvili G, Fernandez-Triana J (2021) Review of the world species of *Paroplitis* Mason, 1981 (Hymenoptera, Braconidae, Microgastrinae), with description of three new species. *Deutsche Entomologische Zeitschrift* 68(1): 33–43. <https://doi.org/10.3897/dez.68.59641>
- Habel JC, Segerer A, Ulrich W, Torchik O, Weisser WW, Schmitt T (2016) Butterfly community shifts over two centuries. *Conservation Biology* 30(4): 754–762. <https://doi.org/10.1111/cobi.12656>
- Hallmann CA, Sorg M, Jongejans E, Siepel H, Hofland N, Schwan H, Stenmans W, Müller A, Sumser H, Hörren T, Goulson D, de Kroon H (2017) More than 75 percent decline over 27 years in total flying insect biomass in protected areas. *PLoS ONE* 12(10): e0185809. <https://doi.org/10.1371/journal.pone.0185809>
- Hartop E, Srivathsan A, Ronquist F, Meier R (2022) Towards Large-Scale Integrative Taxonomy (LIT): Resolving the Data Conundrum for Dark Taxa. [Dayrat B (Ed.)] *Systematic Biology* 71(6): 1404–1422. [syac033] <https://doi.org/10.1093/sysbio/syac033>
- Hausmann A, Haszprunar G, Hebert PDN (2011a) DNA Barcoding the Geometrid Fauna of Bavaria (Lepidoptera): Successes, Surprises, and Questions. *PLoS ONE* 6(2): e17134. <https://doi.org/10.1371/journal.pone.0017134>
- Hausmann A, Haszprunar G, Segerer AH, Speidel W, Behounek G, Hebert PDN (2011b) Now DNA-barcoded: The butterflies and larger moths of Germany. *Spixiana* 34: 47–58.
- Hausmann A, Krogmann L, Peters R, Rduch V, Schmidt S (2020) GBOL III: Dark Taxa. *iBOL Barcode Bulletin*. <https://ibol.org/barcodebulletin/research/gbol-iii-dark-taxa/> [August 25, 2022]
- Hawllitschek O, Morinière J, Lehmann GUC, Lehmann AW, Kropf M, Dunz A, Glaw F, Decharoen M, Schmidt S, Hausmann A, Szucsich NU, Caetano-Wyler SA, Haszprunar G (2017) DNA barcoding of crickets, katydids and grasshoppers (Orthoptera) from Central Europe with focus on Austria, Germany and Switzerland. *Molecular Ecology Resources* 17(5): 1037–1053. <https://doi.org/10.1111/1755-0998.12638>
- Hebert PDN, Ratnasingham S, de Waard JR (2003a) Barcoding animal life: Cytochrome c oxidase subunit 1 divergences among closely related species. *Proceedings of the Royal Society of London, Series B, Biological Sciences* 270(suppl_1): S96–S99. <https://doi.org/10.1098/rsbl.2003.0025>
- Hebert PDN, Cywinska A, Ball SL, deWaard JR (2003b) Biological identifications through DNA barcodes. *Proceedings of the Royal Society of London, Series B, Biological Sciences* 270(1512): 313–321. <https://doi.org/10.1098/rspb.2002.2218>
- Hebert PDN, Bock DG, Prosser SWJ (2023) Interrogating 1000 insect genomes for NUMTs: A risk assessment for estimates of species richness. *PLoS ONE* 18(6): e0286620. <https://doi.org/10.1371/journal.pone.0286620>
- Hendrich L, Morinière J, Haszprunar G, Hebert PDN, Hausmann A, Köhler F, Balke M (2015) A comprehensive DNA barcode database for Central European beetles with

- a focus on Germany: Adding more than 3500 identified species to BOLD. *Molecular Ecology Resources* 15(4): 795–818. <https://doi.org/10.1111/1755-0998.12354>
- Heraty J, Hawks D (1998) Hexamethyldisilazane – A chemical alternative for drying Insects. *Entomological News* 109: 1–4.
- Jähnig SC, Baranov V, Altermatt F, Cranston P, Friedrichs-Manthey M, Geist J, He F, Heino J, Hering D, Hölker F, Jourdan J, Kalinkat G, Kiesel J, Leese F, Maasri A, Monaghan MT, Schäfer RB, Tockner K, Tonkin JD, Domisch S (2021) Revisiting global trends in freshwater insect biodiversity. *WIREs. Water* 8(2): e1506. <https://doi.org/10.1002/wat2.1506>
- Karlsson D, Hartop E, Forshage M, Jaschhof M, Ronquist F (2020) The swedish malaise trap project: a 15 year retrospective on a countrywide insect inventory. *Biodiversity Data Journal* 8: e47255. <https://doi.org/10.3897/BDJ.8.e47255>
- Kotenko A (2007) Microgastrinae. In: Lelej A (Ed.) *Neuropteroidea, Mecoptera, Hymenoptera. Key to the Insects of Russia Far East*. Dalnauka, Vladivostok, 134–192.
- Ku D, Belokobylskij S, Cha J (2001) Hymenoptera (Braconidae). *Economic Insects of Korea* 16. *Insecta Koreana*. Supplement 23. Junghaengsa, Suwon, 283 pp.
- Lazarević M, Stanković SS, van Achterberg C, Marczak D, Modić Š, Ilić Milošević M, Trajković A, Žikić V (2023) Morphological and genetic variability of *Cotesia tibialis* species complex (Hymenoptera: Braconidae: Microgastrinae). *Zoologischer Anzeiger* 302: 58–66. <https://doi.org/10.1016/j.jcz.2022.10.007>
- Leandro C, Jay-Robert P, Vergnes A (2017) Bias and perspectives in insect conservation: A European scale analysis. *Biological Conservation* 215: 213–224. <https://doi.org/10.1016/j.biocon.2017.07.033>
- Leigh JW, Bryant D (2015) PopART: Full-feature software for haplotype network construction. *Methods in Ecology and Evolution* 6(9): 1110–1116. <https://doi.org/10.1111/2041-210X.12410>
- Liu Z, He J-H, Chen X-X, Gupta A (2020) The *ater*-group of the genus *Apanteles* Foerster (Hymenoptera, Braconidae, Microgastrinae) from China with the descriptions of forty-eight new species. *Zootaxa* 4807(1): 1–205. <https://doi.org/10.11646/zootaxa.4807.1.1>
- Lundbeck W (1896) Hymenoptera groenlandica. *Videnskabelige Meddelelser fra den Naturhistoriske Forening i Kjøbenhavn* 58: 220–251.
- Marczak P, Buszko J (1993) Braconid wasps (Hymenoptera, Braconidae) reared from mining Lepidoptera. *Wiadomosci Entomologiczne* 12: 259–272.
- Marsh PM (1979) The Braconid (Hymenoptera) Parasites of the Gypsy Moth, *Lymantria dispar* (Lepidoptera: Lymantriidae). *Annals of the Entomological Society of America* 72(6): 794–810. <https://doi.org/10.1093/aesa/72.6.794>
- Morinière J, Hendrich L, Balke M, Beermann AJ, König T, Hess M, Koch S, Müller R, Leese F, Hebert PDN, Hausmann A, Schubart CD, Haszprunar G (2017) A DNA barcode library for Germany's mayflies, stoneflies and caddisflies (Ephemeroptera, Plecoptera and Trichoptera). *Molecular Ecology Resources* 17(6): 1293–1307. <https://doi.org/10.1111/1755-0998.12683>
- Muesebeck C (1922) A revision of the North American ichneumon-flies, belonging to the subfamilies Neoneurinae and Microgasterinae. *Proceedings of the United States National Museum* 61(2436): 1–76. <https://doi.org/10.5479/si.00963801.61-2436.1>
- Muesebeck C (1928) A new European species of *Apanteles* parasitic on the gypsy moth. *Proceedings of the Entomological Society of Washington* 30: 8–9.
- Mutanen M, Kivelä SM, Vos RA, Doorenweerd C, Ratnasingham S, Hausmann A, Huemer P, Dincă V, van Nieukerken EJ, Lopez-Vaamonde C, Vila R, Aarvik L, Decaëns T, Efetov KA, Hebert PDN, Johnsen A, Karsholt O, Pentinsaari M, Rougerie R, Segerer A, Tarmann G, Zahiri R, Godfray HCJ (2016) Species-level para- and polyphyly in DNA

- barcode gene trees: Strong operational bias in european Lepidoptera. *Systematic Biology* 65(6): 1024–1040. <https://doi.org/10.1093/sysbio/syw044>
- Nixon G (1965) A reclassification of the tribe Microgasterini (Hymenoptera: Braconidae). *Bulletin of the British Museum (Natural History). Entomology* 2(Supplement 2): 1–284. <https://doi.org/10.5962/p.144036>
- Nixon G (1968) A revision of the genus *Microgaster* Latreille (Hymenoptera: Braconidae). *Bulletin of the British Museum (Natural History). Entomology* 22: 31–72. <https://doi.org/10.5962/bhl.part.9950>
- Nixon G (1970) A revision of the N. W. European species of *Microplitis* Forster (Hymenoptera: Braconidae). *Bulletin of the British Museum (Natural History). Entomology* 25: 1–30.
- Nixon G (1972) A revision of the north-western European species of the *laevigatus*-group of *Apanteles* Förster (Hymenoptera, Braconidae). *Bulletin of Entomological Research* 61(4): 701–743. <https://doi.org/10.1017/S0007485300047544>
- Nixon G (1973) A revision of the north-western European species of the *vitripennis*, *pallipes*, *octonarius*, *triangulator*, *fraternus*, *formosus*, *parasitellae*, *metacarpalis* and *circumscripatus*-groups of *Apanteles* Förster (Hymenoptera, Braconidae). *Bulletin of Entomological Research* 63(2): 169–230. <https://doi.org/10.1017/S0007485300039006>
- Nixon GEJ (1974) A revision of the north-western European species of the *glomeratus* group of *Apanteles* Förster (Hymenoptera, Braconidae). *Bulletin of Entomological Research* 64(3): 453–524. <https://doi.org/10.1017/S0007485300031333>
- Nixon G (1976) A revision of the north-western European species of the *merula*, *lacteus*, *vipio*, *ultor*, *ater*, *butalidis*, *popularis*, *carbonarius* and *validus*-groups of *Apanteles* Förster (Hymenoptera, Braconidae). *Bulletin of Entomological Research* 65(4): 687–735. <https://doi.org/10.1017/S0007485300006386>
- O'Hara JE, Shima H, Zhang C (2009) Annotated catalogue of the Tachinidae (Insecta: Diptera) of China. *Zootaxa* 2190(1): 1–236. <https://doi.org/10.11646/zootaxa.2190.1.1>
- Okada I (1988) Three species of wax moths in Japan. *Mitsubachi Kagaku* 9: 145–149.
- Oltra-Moscardó MT, Jiménez-Peydró R (2005) The taxon *Rasivalva* (Hymenoptera: Braconidae) in the Palaearctic region and description of *Rasivalva pyrenaica* new species from Andorra. *Journal of Entomological Science* 40(4): 438–445. <https://doi.org/10.18474/0749-8004-40.4.438>
- Page RDM (2016) DNA barcoding and taxonomy: Dark taxa and dark texts. *Philosophical Transactions of the Royal Society of London, Series B, Biological Sciences* 371(1702): 1–7. <https://doi.org/10.1098/rstb.2015.0334>
- Papp J (1959) The *Microgaster* Latr., *Microplitis* Först., and *Hygroplitis* Thoms. species of the Carpathian Basin (Hymenoptera, Braconidae). *Annales Historico-Naturales Musei Nationalis Hungarici* 51: 397–413.
- Papp J (1973) New *Apanteles* Först. species from Hungary (Hymenoptera, Braconidae: Microgasterinae), II. *Annales Historico-Naturales Musei Nationalis Hungarici* 65: 287–304.
- Papp J (1974) New *Apanteles* Först. species from Hungary (Hymenoptera, Braconidae: Microgasterinae), III. *Annales Historico-Naturales Musei Nationalis Hungarici* 66: 325–337.
- Papp J (1976a) A survey of the European species of *Apanteles* Först. (Hymenoptera, Braconidae: Microgasterinae) I. The species-groups. *Annales Historico-Naturales Musei Nationalis Hungarici* 68: 251–274.
- Papp J (1976b) Key to the European *Microgaster* Latr. species, with a new species and taxonomical remarks (Hymenoptera: Braconidae; Microgasterinae). *Acta Zoologica Academiae Scientiarum Hungaricae* 22: 97–117.

- Papp J (1978) A survey of the European species of *Apanteles* Först. (Hymenoptera, Braconidae: Microgasterinae) II. The *laevigatus*-group, I. Annales Historico-Naturales Musei Nationalis Hungarici 70: 265–301.
- Papp J (1979) A survey of the European species of *Apanteles* Först. (Hymenoptera, Braconidae: Microgasterinae) III. The *laevigatus*-group, 2. Annales Historico-Naturales Musei Nationalis Hungarici 71: 235–250.
- Papp J (1980) A survey of the European species of *Apanteles* Först. (Hymenoptera, Braconidae: Microgasterinae) IV. The *lineipes*-, *obscurus*- and *ater*-group. Annales Historico-Naturales Musei Nationalis Hungarici 72: 241–272.
- Papp J (1981a) A survey of the European species of *Apanteles* Först. (Hymenoptera, Braconidae: Microgastrinae), V. The *lacteus*-, *longipalpis*-, *ultor*-, *butalidis*- and *vipio*-group. Annales Historico-Naturales Musei Nationalis Hungarici 73: 263–291.
- Papp J (1981b) Contributions to the Braconid fauna of Hungary, III. Opiinae and Microgasterinae (Hymenoptera: Braconidae). Folia Entomologica Hungarica 42: 127–141.
- Papp J (1982) A Survey of the European species of *Apanteles* Först. (Hymenoptera, Braconidae: Microgastrinae), VI. The *laspeyresiella*-, *merula*-, *falcatus*- and *validus*-group. Annales Historico-Naturales Musei Nationalis Hungarici 74: 255–267.
- Papp J (1983) A survey of the European species of *Apanteles* Först. (Hymenoptera, Braconidae: Microgastrinae), VII. The *carbonarius*-, *circumscriptus*-, *fraternus*-, *pallipes*-, *parasitellae*-, *vitripennis*-, *liparidis*-, *octonarius*- and *thompsoni*-group. Annales Historico-Naturales Musei Nationalis Hungarici 75: 247–283.
- Papp J (1984a) A survey of the European species of *Apanteles* Först. (Hymenoptera, Braconidae: Microgastrinae), VIII. The *metacarpalis*-, *formosus*-, *popularis*- and *suevus*-group. Annales Historico-Naturales Musei Nationalis Hungarici 76: 265–295.
- Papp J (1984b) Palaearctic species of *Microgaster* Latreille (= *Microplitis* Förster) with description of seven new species (Hymenoptera, Braconidae, Microgastrinae). Entomologische Abhandlungen 47: 95–140.
- Papp J (1986a) A survey of the European species of *Apanteles* Först. (Hymenoptera, Braconidae: Microgastrinae) IX. The *glomeratus*-group, 1. Annales Historico-Naturales Musei Nationalis Hungarici 78: 225–247.
- Papp J (1986b) First survey of the *Glabromicroplitis* Papp species of the Holarctic Region, with taxonomical remarks of three *Microgaster* Latreille species (Hymenoptera, Braconidae: Microgastrinae). Annales Historico-Naturales Musei Nationalis Hungarici 78: 249–253.
- Papp J (1987) A survey of the European species of *Apanteles* Först. (Hymenoptera, Braconidae: Microgastrinae), X. The *glomeratus*-group 2 and the *cultellatus*-group. Annales Historico-Naturales Musei Nationalis Hungarici 79: 207–258.
- Papp J (1988) A survey of the European species of *Apanteles* Först. (Hymenoptera, Braconidae: Microgastrinae) XI. “Homologization” of the species-group of *Apanteles* s. l. with Mason’s generic taxa. Checklist of genera. Parasitoid host list 1. Annales Historico-Naturales Musei Nationalis Hungarici 80: 145–175.
- Papp J (1989) Three new braconid species from Central Switzerland (Hymenoptera, Braconidae). Journal of the Swiss Entomological Society 62: 269–278. <https://doi.org/10.5169/seals-402353>
- Papp J (1990) A survey of the European species of *Apanteles* Först. (Hymenoptera, Braconidae: Microgastrinae) XII. Supplement to the key of the *glomeratus*-group. Parasitoid/host list 2. Annales Historico-Naturales Musei Nationalis Hungarici 81: 159–203.
- Pilotto F, Kühn I, Adrian R, Alber R, Alignier A, Andrews C, Bäck J, Barbaro L, Beaumont D, Beenaerts N, Benham S, Boukal DS, Bretagnolle V, Camatti E, Canullo R, Cardoso

- PG, Ens BJ, Everaert G, Evtimova V, Feuchtmayr H, García-González R, Gómez García D, Grandin U, Gutowski JM, Hadar L, Halada L, Halassy M, Hummel H, Huttunen K-L, Jaroszewicz B, Jensen TC, Kalivoda H, Schmidt IK, Kröncke I, Leinonen R, Martinho F, Meesenburg H, Meyer J, Minerbi S, Monteith D, Nikolov BP, Oro D, Ozoliņš D, Padedda BM, Pallett D, Pansera M, Pardal MÂ, Petriccione B, Pipan T, Pöyry J, Schäfer SM, Schaub M, Schneider SC, Skuja A, Soetaert K, Sprinĝe G, Stanchev R, Stockan JA, Stoll S, Sundqvist L, Thimonier A, Van Hoey G, Van Ryckegem G, Visser ME, Vorhauser S, Haase P (2020) Meta-analysis of multidecadal biodiversity trends in Europe. *Nature Communications* 11(1): e3486. <https://doi.org/10.1038/s41467-020-17171-y>
- Puillandre N, Brouillet S, Achaz G (2021) ASAP: Assemble species by automatic partitioning. *Molecular Ecology Resources* 21(2): 609–620. <https://doi.org/10.1111/1755-0998.13281>
- Ratnasingham S, Hebert PDN (2007) BOLD: The Barcode of Life Data System (<http://www.barcodinglife.org>). *Molecular Ecology Notes* 7(3): 355–364. <https://doi.org/10.1111/j.1471-8286.2007.01678.x>
- Ratnasingham S, Hebert PDN (2013a) A DNA-Based Registry for All Animal Species: The Barcode Index Number (BIN) System. *PLoS ONE* 8(7): e66213. <https://doi.org/10.1371/journal.pone.0066213>
- Ratnasingham S, Hebert PDN (2013b) A DNA-Based Registry for All Animal Species: The Barcode Index Number (BIN) System. *PLoS ONE* 8(7): e66213. <https://doi.org/10.1371/journal.pone.0066213>
- Raupach MJ, Hendrich L, K  chler SM, Deister F, Morini  re J, Gossner MM (2014) Building-Up of a DNA Barcode Library for True Bugs (Insecta: Hemiptera: Heteroptera) of Germany Reveals Taxonomic Uncertainties and Surprises. *PLoS ONE* 9(9): e106940. <https://doi.org/10.1371/journal.pone.0106940>
- Raupach MJ, Hannig K, Morini  re J, Hendrich L (2020) A DNA barcode library for ground beetles of Germany: The genus *Pterostichus* Bonelli, 1810 and allied taxa (Insecta, Coleoptera, Carabidae). *ZooKeys* 980: 93–117. <https://doi.org/10.3897/zookeys.980.55979>
- Reinhard H (1880) Beitr  ge zur Kenntniss einiger Braconiden-Gattungen. F  nftes St  ck. XVI. Zur Gattung *Microgaster*, Latr. (*Microgaster*, *Microplitis*, *Apanteles*). *Deutsche Entomologische Zeitschrift* 24: 353–370. <https://doi.org/10.1002/mmnd.4800240215>
- Reinhardt R, Bolz R (2011) Rote Liste und Gesamtartenliste der Tagfalter (Rhopalocera) (Lepidoptera: Papilionoidea et Hesperioidea) Deutschlands. *Naturschutz und Biologische Vielfalt* 3: 167–194.
- Rennwald E, Rodeland J, Guggemoos T (2023) Lepiforum’s Checklist of European Lepidoptera. https://lepiforum.org/wiki/page/Downloads#Lepiforums-Europaliste_der_Schmetterlinge-Lepiforums_Checklist_of_European_Lepidoptera [July 21, 2023]
- Ronquist F, Forshage M, H  ggqvist S, Karlsson D, Hovm  ller R, Bergsten J, Holston K, Britton T, Abenius J, Andersson B, Buhl PN, Coulianos C-C, Fjellberg A, Gertsson C-A, Hellqvist S, Jaschhof M, Kj  randsen J, Klopstein S, Kobro S, Liston A, Meier R, Pollet M, Riedel M, Roh   ek J, Schuppenhauer M, Stigenberg J, Struwe I, Taeger A, Ulefors S-O, Varga O, Withers P, G  rdenfors U (2020) Completing Linnaeus’s inventory of the Swedish insect fauna: Only 5,000 species left? *PLoS ONE* 15(3): e0228561. <https://doi.org/10.1371/journal.pone.0228561>
- Rumph JA, Turner WJ (1998) Alternative to critical point drying for soft-bodied insect larvae. *Annals of the Entomological Society of America* 91(5): 693–699. <https://doi.org/10.1093/aesa/91.5.693>
- Ruthe J (1860) Deutsche Braconiden. Erstes St  ck. *Deutsche Entomologische Zeitschrift* 4: 105–160.

- Samin N, Chelav HS, Ahmad Z, Penteado-Dias AM, Samiuddin A (2020) A faunistic study on the family Braconidae (Hymenoptera: Ichneumonoidea) from Iran. *Scientific Bulletin of the Uzhhorod University* 48: 14–19. <https://doi.org/10.24144/1998-6475.2020.48.14-19>
- Schmid-Egger C, Straka J, Ljubomirov T, Blagoev GA, Morinière J, Schmidt S (2019) DNA barcodes identify 99 per cent of apoid wasp species (Hymenoptera: Ampulicidae, Crabronidae, Sphecidae) from the Western Palearctic. *Molecular Ecology Resources* 19(2): 476–484. <https://doi.org/10.1111/1755-0998.12963>
- Schmidt S, Schmid-Egger C, Morinière J, Haszprunar G, Hebert PDN (2015) DNA barcoding largely supports 250 years of classical taxonomy: Identifications for Central European bees (Hymenoptera, Apoidea partim). *Molecular Ecology Resources* 15(4): 985–1000. <https://doi.org/10.1111/1755-0998.12363>
- Schütte A, Stüben P, Astrin J (2023) Molecular Weevil Identification Project: A thoroughly curated barcode release of 1300 Western Palearctic weevil species (Coleoptera, Curculionidae). *Biodiversity Data Journal* 11: e96438. <https://doi.org/10.3897/BDJ.11.e96438>
- Seibold S, Gossner MM, Simons NK, Blüthgen N, Müller J, Ambarlı D, Ammer C, Bauhus J, Fischer M, Habel JC, Linsenmair KE, Nauss T, Penone C, Prati D, Schall P, Schulze E-D, Vogt J, Wöllauer S, Weisser WW (2019) Arthropod decline in grasslands and forests is associated with landscape-level drivers. *Nature* 574(7780): 671–674. <https://doi.org/10.1038/s41586-019-1684-3>
- Shaw MR (1994) Parasitoid host ranges. In: Hawkins BA, Sheehan W (Eds) *Parasitoid Community Ecology*. Oxford University Press, Oxford, 111–144. <https://doi.org/10.1093/oso/9780198540588.003.0007>
- Shaw MR (2004) *Microgaster alebion* Nixon and its “var A”: Description of a new species and biological notes (Hymenoptera: Braconidae, Microgastrinae). *Entomologist's Gazette* 55: 217–224.
- Shaw MR (2007) The species of *Cotesia* Cameron (Hymenoptera: Braconidae: Microgastrinae) parasitising Lycaenidae (Lepidoptera) in Britain. *British Journal of Entomology and Natural History* 20: 255–267.
- Shaw MR (2009) *Cotesia* Cameron (Hymenoptera: Braconidae: Microgastrinae) parasitoids of Heliconiinae (Lepidoptera: Nymphalidae) in Europe, with description of three new species. *British Journal of Entomology and Natural History* 22: 133–146.
- Shaw M (2012a) Notes on some European Microgastrinae (Hymenoptera: Braconidae) in the National Museums of Scotland, with twenty species new to Britain, new host data, taxonomic changes and remarks, and descriptions of two new species of *Microgaster* Latreille. *Entomologist's Gazette* 63: 173–201.
- Shaw MR (2012b) Larval parasitoids of *Rivula sericealis* (Scopoli) (Lepidoptera: Noctuidae) in Britain, including notes on the biology of *Cotesia subordinaria* (Tobias) (Hymenoptera: Braconidae, Microgastrinae), a solitary-cum-gregarious parasitoid. *Entomologist's Gazette* 63: 251–257.
- Shaw MR (2020) Discovery of the genus *Venanides* Mason 1981 (Hymenoptera: Braconidae, Microgastrinae) in Europe, with description of a new species parasitizing *Carcina quercana* (Fabricius) (Lepidoptera: Peleopodidae). *Entomologist's Gazette* 71(1): 45–57. <https://doi.org/10.31184/G00138894.711.1755>
- Shaw MR (2022) Rearings of four European Microgastrinae (Hymenoptera: Braconidae), three new to Britain including a new species of *Cotesia* Cameron, 1891. *Entomologist's Gazette* 73(3): 165–175. <https://doi.org/10.31184/G00138894.733.1853>
- Shaw MR (2023) Two new species of European *Microgaster* Latreille, 1804 (Hymenoptera: Braconidae, Microgastrinae), with host data on some further

- species. *Entomologist's Gazette* 73(4): 219–232. <https://doi.org/10.31184/G00138894.734.1867>
- Shaw MR, Colom P (2023) Notes on the three species of *Cotesia* Cameron, 1891 (Hymenoptera: Braconidae, Microgastrinae) parasitizing *Gonepteryx* [Leach, 1815] species (Lepidoptera: Pieridae) in Europe, with description of a new species from the Balearic Islands. *Entomologist's Gazette* 73(4): 253–260. <https://doi.org/10.31184/G00138894.734.1872>
- Shaw MR, Fernandez-Triana JL (2020) Two new European species of *Cotesia* Cameron, 1891 (Hymenoptera: Braconidae, Microgastrinae) parasitizing butterflies (Lepidoptera: Papilionoidea), and an unrelated synonymy in the genus. *Entomologist's Gazette* 71(3): 181–195. <https://doi.org/10.31184/G00138894.713.1768>
- Shimamori K (1987) On the biology of *Apanteles galleriae*, a parasite of the two species of wax moths. *Mitsubachi Kagaku* 8: 107–112.
- Smith MA, Bertrand C, Crosby K, Eveleigh ES, Fernandez-Triana J, Fisher BL, Gibbs J, Hajibabaei M, Hallwachs W, Hind K, Hrcek J, Huang D-W, Janda M, Janzen DH, Li Y, Miller SE, Packer L, Quicke D, Ratnasingham S, Rodriguez J, Rougerie R, Shaw MR, Sheffield C, Stahlhut JK, Steinke D, Whitfield J, Wood M, Zhou X (2012) Wolbachia and DNA Barcoding Insects: Patterns, Potential, and Problems. *PLoS ONE* 7(5): e36514. <https://doi.org/10.1371/journal.pone.0036514>
- Smith AM, Fernández-Triana JL, Eveleigh E, Gómez J, Guclu C, Hallwachs W, Hebert PDN, Hrcek J, Huber JT, Janzen D, Mason PG, Miller S, Quicke DLJ, Rodriguez JJ, Rougerie R, Shaw MR, Várkonyi G, Ward DF, Whitfield JB, Zaldívar-Riverón A (2013) DNA barcoding and the taxonomy of Microgastrinae wasps (Hymenoptera, Braconidae): Impacts after 8 years and nearly 20 000 sequences. *Molecular Ecology Resources* 13(2): 168–176. <https://doi.org/10.1111/1755-0998.12038>
- Smith MA, Whitfield JB, Fernandez-Triana JL, Kula RR, Hallwachs W, Janzen DH (2015) Revision of the genera *Microplitis* and *Snellenius* (Hymenoptera, Braconidae, Microgastrinae) from Area de Conservacion Guanacaste, Costa Rica, with a key to all species previously described from Mesoamerica. *Deutsche Entomologische Zeitschrift* 62(2): 137–201. <https://doi.org/10.3897/dez.62.5276>
- Snell Q, Walker P, Posada D, Crandall K (2002) TCS: Estimating Gene Genealogies. International parallel and distributed processing symposium 2: 184–191.
- Telenga N (1955) Braconidae, subfamily Microgasterinae, subfamily Agathinae. *Fauna USSR* 5(4): 1–311.
- Thomas JA, Telfer MG, Roy DB, Preston CD, Greenwood JJD, Asher J, Fox R, Clarke RT, Lawton JH (2004) Comparative losses of british butterflies, birds, and plants and the global extinction crisis. *Science* 303(5665): 1879–1881. <https://doi.org/10.1126/science.1095046>
- Tobias V (1971) Review of the Braconidae (Hymenoptera) of the U.S.S.R. *Trudy Vsesoyuznogo Entomologicheskogo Obshchestva* 54: 156–268.
- Tobias V (1975) Two new species of braconids from the genus *Apanteles* Forst. (Hymenoptera, Braconidae) parasites of the moth *Bucculatrix ulmella* Z. *Izvestiia Akademii nauk Moldavskoi SSR: seriia biologicheskikh i khimicheskikh nauk* 3: 60–63.
- Tobias V (1976) Braconids of the Caucasus (Hymenoptera, Braconidae). *Opred. Faune SSSR*: 1–286.
- Tobias V (1986) Subfamily Microgasterinae. Key to the Insects of the European Part of the USSR III. 4. Institute of Zoology, Academy of Sciences of the USSE, Leningrad, 605–815.

- Tobias V, Kotenko A (1984) Three new species of genus *Apanteles* Foerster of the *parasitellae*-group (Hymenoptera, Braconidae). *Taxonomy and Zoogeography of Insects*. Kiev, 61–66.
- van Achterberg C (2002) *Apanteles* (*Choeras*) *gielisi* spec. nov. (Hymenoptera: Braconidae: Microgastrinae) from The Netherlands and the first report of Trichoptera as host of Braconidae. *Zoologische Mededelingen Leiden* 72: 53–60.
- van Achterberg C (2006) The Braconidae (Hymenoptera) of Greenland. *Zoologische Mededelingen* 80: 1–179.
- Viereck HL (1911) Descriptions of six new genera and thirty-one new species of ichneumon flies. *Proceedings of the United States National Museum* 40(1812): 173–196. <https://doi.org/10.5479/si.00963801.1812.173>
- Voith J, Bräu M, Dolek M, Nunner A, Wolf W (2016) Rote Liste und Gesamtartenliste der Tagfalter (Lepidoptera: Rhopalocera) Bayerns.
- Völkl W, Blick T (2004) Die quantitative Erfassung der rezenten Fauna von Deutschland. *BfN-Skripten* 117: 1–85.
- Wagner DL (2020) Insect Declines in the Anthropocene. *Annual Review of Entomology* 65(1): 457–480. <https://doi.org/10.1146/annurev-ento-011019-025151>
- Watanabe C (1987) Occurrence of *Apanteles galleriae* (Hymenoptera, Braconidae), parasite of wax moth, in Japan. *Kontyu* 55: 3–94.
- Whitfield J (2006) Revision of the Nearctic species of the genus *Pholetesor* Mason (Hymenoptera: Braconidae). *Zootaxa* 1144(1): 3–94. <https://doi.org/10.11646/zootaxa.1144.1.1>
- Whitfield J, Cameron S (1993) Comparative notes on Hymenopteran parasitoids in bumble bee and honey bee colonies (Hymenoptera, Apidae) reared adjacently. *Entomological News* 104: 240–248.
- Whitfield JB, Oltra Moscardó MTO (2004) The neotropical species of *Deuterixys* Mason (Hymenoptera: Braconidae). *Journal of Hymenoptera Research* 13: 134–148.
- Wilkinson DS (1932) Four new *Apanteles* (Hym., Brac.). *Proceedings of the Royal Entomological Society of London, Series B, Taxonomy* 1(6): 139–144. <https://doi.org/10.1111/j.1365-3113.1932.tb01372.x>
- Wilkinson DS (1938) On a Further Two New Palaearctic Species of *Apanteles* (Hym. Brac.). *Proceedings of the Royal Entomological Society of London, Series B, Taxonomy* 7(10): 222–227. <https://doi.org/10.1111/j.1365-3113.1938.tb01231.x>
- Wilkinson D (1945) Description of Palaearctic species of *Apanteles* (Hymen., Braconidae). *Transactions of the Royal Entomological Society of London* 95(3): 35–226. <https://doi.org/10.1111/j.1365-2311.1945.tb00436.x>
- Wühl L, Pylatiuk C, Giersch M, Lapp F, von Rintelen T, Balke M, Schmidt S, Cerretti P, Meier R (2022) DiversityScanner: Robotic handling of small invertebrates with machine learning methods. *Molecular Ecology Resources* 22(4): 1626–1638. <https://doi.org/10.1111/1755-0998.13567>
- Yu D, van Achterberg C, Horstmann K (2016) Taxapad 2016, Ichneumonoidea 2015. Nepean, Ontario. <http://www.taxapad.com>
- Zeng J, He J-H, Chen X (2011) The genera *Deuterixys* Mason, 1981 and *Wilkinsonellus* Mason, 1981 (Hymenoptera, Braconidae, Microgastrinae) from China, with description of two new species. *ZooKeys* 120: 27–40. <https://doi.org/10.3897/zookeys.120.891>
- Žikić V, Lazarević M, Ilić Milošević M, Trajković A, Hric B, Stanković SS (2021) Diversity of the Genus *Cotesia* Cameron (Braconidae: Microgastrinae) in Serbia. *Acta Entomologica Serbica* 26: 27–35. <https://doi.org/10.5281/zenodo.5704966>

Supplementary material 1

Specimen Data Spreadsheet (BOLD) for DS-MCGNRECS

Author: Amelie Höcherl

Data type: xlsx

Explanation note: This table includes all relevant data associated with specimens that are included in our BOLD dataset (341 specimens).

Copyright notice: This dataset is made available under the Open Database License (<http://opendatacommons.org/licenses/odbl/1.0/>). The Open Database License (ODbL) is a license agreement intended to allow users to freely share, modify, and use this Dataset while maintaining this same freedom for others, provided that the original source and author(s) are credited.

Link: <https://doi.org/10.3897/zookeys.1188.112516.suppl1>

Supplementary material 2

COI-Sequences for DS-MCGNRECS

Author: Amelie Höcherl

Data type: fas

Explanation note: Includes all COI sequences used in our interactive species concepts.

Copyright notice: This dataset is made available under the Open Database License (<http://opendatacommons.org/licenses/odbl/1.0/>). The Open Database License (ODbL) is a license agreement intended to allow users to freely share, modify, and use this Dataset while maintaining this same freedom for others, provided that the original source and author(s) are credited.

Link: <https://doi.org/10.3897/zookeys.1188.112516.suppl2>

Supplementary material 3

Alignment used for NJ-topology of DS-MCGNRECS

Author: Amelie Höcherl

Data type: fasta

Explanation note: Includes the alignment and all sequences used for the NJ-topology in Fig. 52, sequences > 400 bp.

Copyright notice: This dataset is made available under the Open Database License (<http://opendatacommons.org/licenses/odbl/1.0/>). The Open Database License (ODbL) is a license agreement intended to allow users to freely share, modify, and use this Dataset while maintaining this same freedom for others, provided that the original source and author(s) are credited.

Link: <https://doi.org/10.3897/zookeys.1188.112516.suppl3>

Supplementary material 4

NJ-topology of DS-MCGNRECS

Author: Amelie Höcherl

Data type: nwk

Copyright notice: This dataset is made available under the Open Database License (<http://opendatacommons.org/licenses/odbl/1.0/>). The Open Database License (ODbL) is a license agreement intended to allow users to freely share, modify, and use this Dataset while maintaining this same freedom for others, provided that the original source and author(s) are credited.

Link: <https://doi.org/10.3897/zookeys.1188.112516.suppl4>

Supplementary material 5

Coordinates for Holarctic distribution maps

Author: Amelie Höcherl

Data type: csv

Explanation note: Includes the coordinates used for the distribution maps in Fig. 53.

Copyright notice: This dataset is made available under the Open Database License (<http://opendatacommons.org/licenses/odbl/1.0/>). The Open Database License (ODbL) is a license agreement intended to allow users to freely share, modify, and use this Dataset while maintaining this same freedom for others, provided that the original source and author(s) are credited.

Link: <https://doi.org/10.3897/zookeys.1188.112516.suppl5>

Supplementary material 6

Glyptapanteles indiensis and related species sequences

Author: Amelie Höcherl

Data type: fasta

Explanation note: All sequences used for NJ-topology in Fig. 24.

Copyright notice: This dataset is made available under the Open Database License (<http://opendatacommons.org/licenses/odbl/1.0/>). The Open Database License (ODbL) is a license agreement intended to allow users to freely share, modify, and use this Dataset while maintaining this same freedom for others, provided that the original source and author(s) are credited.

Link: <https://doi.org/10.3897/zookeys.1188.112516.suppl6>

Supplementary material 7

***Glyptapanteles indiensis* and related species NJ-topology**

Author: Amelie Höcherl

Data type: nwk

Explanation note: NJ-topology in Fig. 24.

Copyright notice: This dataset is made available under the Open Database License (<http://opendatacommons.org/licenses/odbl/1.0/>). The Open Database License (ODbL) is a license agreement intended to allow users to freely share, modify, and use this Dataset while maintaining this same freedom for others, provided that the original source and author(s) are credited.

Link: <https://doi.org/10.3897/zookeys.1188.112516.suppl7>

Supplementary material 8

BOLD:AAA6099 sequences

Author: Amelie Höcherl

Data type: nexus

Explanation note: Sequences in BIN BOLD:AAA6099 used for haplotype network in Fig. 14 for *Cotesia risilis*.

Copyright notice: This dataset is made available under the Open Database License (<http://opendatacommons.org/licenses/odbl/1.0/>). The Open Database License (ODbL) is a license agreement intended to allow users to freely share, modify, and use this Dataset while maintaining this same freedom for others, provided that the original source and author(s) are credited.

Link: <https://doi.org/10.3897/zookeys.1188.112516.suppl8>

Supplementary material 9

BOLD:AAA6099 traits

Author: Amelie Höcherl

Data type: txt

Explanation note: Amelie Höcherl Traits (countries) for BIN BOLD:AAA6099 used for haplotype network in Fig. 14 for *Cotesia risilis*.

Copyright notice: This dataset is made available under the Open Database License (<http://opendatacommons.org/licenses/odbl/1.0/>). The Open Database License (ODbL) is a license agreement intended to allow users to freely share, modify, and use this Dataset while maintaining this same freedom for others, provided that the original source and author(s) are credited.

Link: <https://doi.org/10.3897/zookeys.1188.112516.suppl9>

Supplementary material 10

BOLD:ABY6385 sequences

Author: Amelie Höcherl

Data type: nexus

Explanation note: Sequences in BOLD:ABY6385 used for haplotype network in Fig. 34 for *Microgaster nixalebion*.

Copyright notice: This dataset is made available under the Open Database License (<http://opendatacommons.org/licenses/odbl/1.0/>). The Open Database License (ODbL) is a license agreement intended to allow users to freely share, modify, and use this Dataset while maintaining this same freedom for others, provided that the original source and author(s) are credited.

Link: <https://doi.org/10.3897/zookeys.1188.112516.suppl10>

Supplementary material 11

BOLD:ABY6385 traits

Author: Amelie Höcherl

Data type: txt

Explanation note: Traits (hosts) for BIN BOLD:ABY6385 used for haplotype network in Fig. 34 for *Microgaster nixalebion*.

Copyright notice: This dataset is made available under the Open Database License (<http://opendatacommons.org/licenses/odbl/1.0/>). The Open Database License (ODbL) is a license agreement intended to allow users to freely share, modify, and use this Dataset while maintaining this same freedom for others, provided that the original source and author(s) are credited.

Link: <https://doi.org/10.3897/zookeys.1188.112516.suppl11>

Supplementary material 12

BOLD:AAC9130 sequences

Author: Amelie Höcherl

Data type: nexus

Explanation note: Sequences in BIN BOLD:AAC9130 used for haplotype network in Fig. 36 for *Microgaster raschkiellae*.

Copyright notice: This dataset is made available under the Open Database License (<http://opendatacommons.org/licenses/odbl/1.0/>). The Open Database License (ODbL) is a license agreement intended to allow users to freely share, modify, and use this Dataset while maintaining this same freedom for others, provided that the original source and author(s) are credited.

Link: <https://doi.org/10.3897/zookeys.1188.112516.suppl12>

Supplementary material 13

BOLD:AAC9130 traits

Author: Amelie Höcherl

Data type: txt

Explanation note: Traits (hosts) for BIN BOLD:AAC9130 used for haplotype network in Fig. 36 for *Microgaster raschkiellae*.

Copyright notice: This dataset is made available under the Open Database License (<http://opendatacommons.org/licenses/odbl/1.0/>). The Open Database License (ODbL) is a license agreement intended to allow users to freely share, modify, and use this Dataset while maintaining this same freedom for others, provided that the original source and author(s) are credited.

Link: <https://doi.org/10.3897/zookeys.1188.112516.suppl13>

Supplementary material 14

ASAP partition 1 of BOLD:AAA7143

Author: Amelie Höcherl

Data type: csv

Explanation note: Sequences downloaded 7th of august, 2023, ASAP score 3.99.

Copyright notice: This dataset is made available under the Open Database License (<http://opendatacommons.org/licenses/odbl/1.0/>). The Open Database License (ODbL) is a license agreement intended to allow users to freely share, modify, and use this Dataset while maintaining this same freedom for others, provided that the original source and author(s) are credited.

Link: <https://doi.org/10.3897/zookeys.1188.112516.suppl14>

Supplementary material 15

ASAP partition 2 of BOLD:AAA7143

Author: Amelie Höcherl

Data type: csv

Explanation note: Sequences downloaded 7th of august, 2023, ASAP score 6.50.

Copyright notice: This dataset is made available under the Open Database License (<http://opendatacommons.org/licenses/odbl/1.0/>). The Open Database License (ODbL) is a license agreement intended to allow users to freely share, modify, and use this Dataset while maintaining this same freedom for others, provided that the original source and author(s) are credited.

Link: <https://doi.org/10.3897/zookeys.1188.112516.suppl15>